Copyright © by

ANDREA DE MARI

1968

ACCURATE NUMERICAL STEADY-STATE AND TRANSIENT ONE-DIMENSIONAL SOLUTIONS OF SEMICONDUCTOR DEVICES

Thesis by

Andrea De Mari

In Partial Fulfillment of the Requirements

For the Degree of

Doctor of Philosophy

California Institute of Technology

Pasadena, California

1968

(Submitted October 16, 1967)

ACKNOWLEDGEMENTS

I am very much indebted and grateful to Professor R. D. Middlebrook for his help and guidance. This work was in part supported by the U.S. Navy through Contracts N123(60530)51608A, N123(60530)54694A, N00123-67-C-1187, and partially conducted with the assistance of a General Telephone and Electronics Fellowship, for which I am grateful.

The patience and skillful typing of Mrs. Doris A. Schlicht is very much appreciated.

ABSTRACT

Numerical iterative methods of solution of the one-dimensional basic two-carrier transport equations describing the behavior of semiconductor junctions under both steady-state and transient conditions are presented. The methods are of a very general character: none of the conventional assumptions and restrictions are introduced, and freedom is available in the choice of the doping profile, generation-recombination law, mobility dependencies, injection level, and boundary conditions applied solely at the external contacts. For a specified arbitrary input signal of either current or voltage (as a function of time) the solution yields terminal properties and all the quantities of interest in the interior of the device, such as carrier densities, electric field, electrostatic potential, particle and displacement currents, as functions of position (and time).

The work is divided into two parts. In Part I a numerical method of solution of the steady-state problem, already available in the literature, is improved and extended, and is applied to a two-contact and a three-contact device. The analytical formulation of the original method is shown to be unsuitable for generating a sound numerical algorithm sufficiently accurate and valid for high reverse bias conditions. Difficulties and limitations are exposed and overcome by an improved formulation extended to any bias condition. As a simple application of the improved formulation, "exact" and first-order theory results for an idealized N-P structure are presented and compared. The poorness of some of the basic assumptions of the conventional first-order theory is exposed, in spite of a satisfactory agreement between the exact and

first-order results of the terminal properties for particular bias conditions. Results for an N-P-N transistor are also reported and the inadequacy of the one-dimensional model discussed.

The time-dependent analysis of the problem is presented in Part II. The fundamental equations are rearranged to an equivalent set of three non-linear partial differential equations more suitable for numerical methods. A highly non-uniform two-dimensional mesh, subject to maintenance of constant truncation errors in both spatial and time domains of certain pointwise operations, is chosen for the discretization of the problem, in view of the variation of most quantities over extreme ranges within short regions. Consequently an implicit discretization scheme is selected for the second-order partial differential equations of the parabolic type in order to avoid restrictions on the mesh size, without endangering numerical stability. An iterative procedure is necessary at each instant of time to cope with the several non-linearities of the problem and to achieve consistency between the internal distributions and the generating equations. This procedure is easily generalized to incorporate equations pertinent to networks of passive elements and ideal generators connected to the semiconductor device. Results for a particular single-junction structure under typical time-dependent excitations of external current and terminal voltage, and for an N-P diode interacting with an external resistor under switching conditions, are reported and discussed in detail.

Considerable attention is focused on the numerical analysis of the steady-state and transient problems in order to achieve a numerical algorithm sufficiently sound and efficient to cope with the several

difficulties of the problem, such as the small differences between nearly equal numbers, the variation of most quantities over extremely wide ranges in short regions, and the stability conditions related to the discretization of partial differential equations of the parabolic type.

TABLE OF CONTENTS

INTRODUCTION 1

PART I

CHAPTER I OUTLINE OF THE METHOD FOR THE SOLUTION OF THE DIRECT PROBLEM $(V_A \rightarrow J)$ FOR A TWO CONTACT DEVICE 8

1.1. Physical and mathematical model 8

1.1.1. Fundamental equations 8
1.1.2. Normalization of the fundamental equations 14
1.1.3. Boundary conditions 17

1.2. Derivation of the reduced set of equations 19

1.3. Iterative procedure of solution 22

1.3.1. Two special cases 25

1.4. Conclusion 27

CHAPTER II IMPROVED ANALYTICAL FORMULATION AND NUMERICAL TECHNIQUES 29

2.1. Generalities 30

2.2. Improved analytical formulation 31

2.2.1. Small differences between nearly equal numbers 31
2.2.2. Extension to high reverse bias conditions 35

2.3. Numerical techniques 41

2.3.1. Automatically adjustable non-uniform step distribution 41
2.3.2. Numerical integration and differentiation 62
2.3.3. Numerical solution of Poisson's equation 65

2.4. Computer program for a special case 72

2.5. Conclusion 72

CHAPTER III TWO SIMPLE APPLICATIONS OF THE BASIC DIRECT PROGRAM 75

3.1. Generalities 75

3.2. Computation of the total incremental capacitance 75

3.3. A solution for the reverse problem $(J \rightarrow V_A)$ 77

3.3.1. Description of the method 78
3.3.2. Results 82

3.4. Conclusion 83

CHAPTER IV EXTENSION OF THE METHOD TO THE SOLUTION OF THE TRANSISTOR 84

4.1. Mathematical model and boundary conditions 84

4.2. Analytical formulation 88

4.3. Iterative procedure for the direct and reverse problem 92

4.4. Conclusion 95

CHAPTER V ON THE ACCURACY OF THE NUMERICAL RESULTS 97

5.1. Generalities 97

5.2. Sources of error 98

5.2.1. Discretization error 98
5.2.2. Numerical error 99
5.2.3. Physical model discretization error 99

5.3. Influence and control of the errors 99

5.3.1. Discretization error 99
5.3.2. Numerical error 102
5.3.3. Physical model discretization error 104

5.4. Testing criteria of the accuracy of the results 104

5.5. Conclusion 107

CHAPTER VI RESULTS 109

6.1. Generalities 109

6.2. A two-contact device: the N-P diode 110

6.2.1. External contacts of the ohmic type 111
6.2.2. A finite value of surface recombination velocity at one external contact 141

6.3. A three-contact device: the N-P-N transistor 148

6.4. Conclusion 177

PART II

CHAPTER VII ANALYTICAL FORMULATION OF THE CURRENT-DRIVEN TRANSIENT PROBLEM FOR A TWO-CONTACT DEVICE 180

7.1. Generalities 180

7.2. Physical and mathematical model 182

7.2.1. Normalized fundamental equations 182
7.2.2. Boundary and initial conditions 183

7.3. Derivation of the reduced set of equations 186

7.4. Iterative method of solution 188

7.5. Conclusion 190

CHAPTER VIII DISCRETIZATION OF THE ANALYTICAL FORMULATION FOR THE CURRENT-DRIVEN TRANSIENT 193

8.1. Selection of the discretization scheme 193

8.2. Discretization by implicit schemes 197

8.2.1. Generalized pure implicit scheme 198
8.2.2. Generalized Crank-Nicholson scheme 207

8.3. Detailed iterative procedure of solution 211

8.4. Automatically adjustable non-uniform discretization mesh 218

8.5. Conclusion 223

CHAPTER IX VOLTAGE-DRIVEN TRANSIENT 225

9.1. Generalities 225

9.2. Voltage-driven transient: outline of the method 227

9.3. A compatible steady-state solution 234

9.4. Time-dependent solutions for the combination of an active device with a network of passive circuit elements 237

9.5. Conclusion 241

CHAPTER X ON THE ACCURACY OF THE TRANSIENT SOLUTIONS 242

10.1. Generalities 242

10.2. Discretization error in the time domain 243

10.3. Numerical error and its growth in the time domain 246

10.3.1. Iteration error 247
10.3.2. Inaccuracy of the initial conditions 250
10.3.3. Tolerance on the specified excitation in the voltage-driven transient 251

10.4. Conclusion 252

CHAPTER XI RESULTS 253

11.1. Generalities 253

11.2. The N-P diode driven by ideal current and voltage sources 257

11.2.1. Excitation: a low current step 259
11.2.2. Excitation: a high current step 271

11.2.3. Excitation: a spike of current 281
11.2.4. Excitation: a low voltage step 287

11.3. The interaction of the N-P diode and an external resistor under switching conditions 298

11.4. Conclusion 313

CHAPTER XII CONCLUSIONS 314

APPENDIX A SOME RESULTS OF THE CONVENTIONAL FIRST-ORDER THEORY FOR THE N-P JUNCTION IN STEADY-STATE 320

APPENDIX B NUMERICAL INTEGRATION AND DIFFERENTIATION

APPENDIX C COMPUTER PROGRAM FOR THE DIRECT STEADY-STATE PROBLEM

APPENDIX D COMPUTER PROGRAM FOR THE CALCULATION OF THE TOTAL INCREMENTAL CAPACITANCE

APPENDIX E COMPUTER PROGRAM FOR THE REVERSE STEADY-STATE PROBLEM

APPENDIX F ON THE NUMERICAL SOLUTION OF SECOND ORDER PARTIAL DIFFERENTIAL EQUATIONS OF THE PARABOLIC TYPE

APPENDIX G COMPUTER PROGRAM FOR THE TRANSIENT DIRECT AND REVERSE PROBLEMS

LIST OF PRINCIPAL SYMBOLS

REFERENCES

INTRODUCTION

Basic concepts in the theory of the P-N junction were first presented in Shockley's fundamental paper [1] with an approximate solution for the low-level injection case, and many authors presented in the following years extensions, corrections and refinements in the search for a generalized solution to the problem. A comprehensive bibliography is given by Moll [2], Pritchard [3], and Matz [4], and more recent considerations have been presented by Middlebrook [5], Van Vliet [6], and Sah [7]. Only partial success has so far been achieved; this is due mainly to serious difficulties in the analytical solution of the pertinent set of equations that describe mathematically even the simplest physical model.

In order to achieve analytical results in closed form, a number of assumptions in the model and of approximations in the set of equations has been consistently introduced; several "first-order" results, valid in certain ranges of the relevant quantities and for a limited number of specialized structures, have been obtained. Some of these assumptions for the one-dimensional model (to which attention will be limited in this paper) are the following:

(a) separation of the structure into regions with sharp boundaries, either fully depleted of mobile carriers, or space-charge neutral;

(b) postulation of explicit boundary conditions on the relevant quantities in the interior of the device, at the interfaces between the depleted and neutral regions of assumption (a); limited choice of boundary conditions at the external contacts;

(c) limitation of the doping profile to very special cases (mostly

step and linear distributions) and to particular quantitative values (either symmetric or highly asymmetric impurity distributions);

(d) simplification of the dependence of the carrier mobilities upon electric field, doping and scattering phenomena;

(e) limitation of carrier recombination laws to the low-level linear case.

The most unsatisfactory of the above assumptions is certainly the first, which is definitely in error at high injection levels, highly questionable near equilibrium, and probably only slightly inaccurate in high reverse bias cases.

Numerical methods, with the aid of high-speed digital computers, represent an alternative approach to the problem, the final aim being the achievement of an "exact" solution of the most general character with none of the conventional assumptions. This also allows comparison with the classical first-order theory results so that the goodness (or poorness) of the numerous conventional assumptions may be judged.

Serious difficulties are also present in a numerical investigation, and have prevented most of the currently available numerical solutions from having the general character desired. These difficulties arise already in the much simpler metal-semiconductor junction case treated by Macdonald [8], and are responsible for the acceptance of some of the conventional assumptions in the P-N junction case. Lawrence and Warner [9] and Breitschwerdt [10] present a numerical integration of Poisson's equation in the fully-depleted region for various doping profiles; Sparkes [11] gives the complete, partially

numerical, solution for the abrupt P-N junction in equilibrium in steady-state; van der Maesen [12], Lieb et al. [13], Kano and Reich [14], and Chang [15] restrict the analysis to the injection region only in the charge-neutrality approximation with the low-level recombination law for the case of an asymmetric abrupt junction. Fulkerson and Nussbaum [16] and Sanchez [17] present a complete steady-state solution, again for the asymmetric abrupt case (with ohmic contacts, constant mobilities, uniform doping); their method implies, though, the reduction of the two-boundary problem to an initial-value problem very much sensitive, for the case under consideration, to the several required guesses of slopes at the boundaries. This guesswork is likely to become critical in most instances. In addition the method described in Ref. 16 is based upon the separation of the interior of the device into several regions and the iterative solution of various sets of approximate equations, specialized for each region, matched by boundary conditions at the interfaces.*

The only comprehensive and general numerical procedure for the steady-state problem is presented by Gummel [18], and is applied to the solution of the transistor. The method allows for arbitrary impurity distribution, recombination law, mobility dependencies, injection level, and boundary conditions. Hypothetical regions in the interior of the device are not assumed, and the problem is tackled exclusively with the postulation of boundary conditions at the external

---

* As a direct consequence of the method, questionable results are obtained near the internal interfaces.

contacts for a set of basic equations valid throughout the whole interior. Although Gummel's iterative scheme is of a very general character, its analytical formulation is unsuitable for generating a sound numerical algorithm sufficiently accurate and valid for high reverse-bias conditions.

It is the purpose of the present work to present an improved and extended analytical formulation of Gummel's original steady-state scheme, to present a numerical method of solution of the P-N junction under arbitrary transient conditions, to expose the difficulties of both fundamental and practical nature arising in the numerical analysis of the problems, and to illustrate results for particular structures under both steady-state and transient conditions.

The presentation is divided into two parts: the first is restricted to the steady-state analysis and illustrates solutions obtained with the improved formulation based on Gummel's original iterative scheme; the second is mostly concerned with the analysis of the problem in transient conditions.

In Part I, Chapter I describes the physical model adopted for a two-contact device, the fundamental equations and boundary conditions that determine mathematically the steady-state problem, an alternative derivation of Gummel's relations featuring a more convenient choice of unknowns, and the overall iterative scheme for the "direct problem" (the terminal voltage is specified). Chapter II exposes the difficulties of the original formulation arising in the numerical analysis of the problem, describes an improved and extended formulation, treats the discretization problem in detail, and illustrates appropriate

numerical techniques. Chapter III presents two applications of the basic program for the direct problem: the computation of the total incremental capacitance of the device as obtained by two successive steady-state solutions, and a method of solution of the "reverse" problem (the total current is specified). Chapter IV extends the steady-state solution to the transistor, on the basis of Gummel's general lines, discusses the inadequacy of the one-dimensional model, and analyzes the effects of an alternative boundary condition for the base contact. Chapter V discusses the various sources of errors and the accuracy of the final results, tested with several sets of relations, derived from the fundamental equations and suitable to expose discretization and numerical errors. Chapter VI presents steady-state results for a few special structures: terminal properties and quantities in the interior of the device are illustrated for an abrupt N-P diode and N-P-N transistor; "exact" and approximate conventional "first-order" results are compared and discrepancies are exposed.

In Part II, Chapter VII presents an analytical formulation suitable for the achievement of numerical transient solutions for excitations of external current for a two-contact device; boundary and initial conditions are chosen. The problem of the selection of sound discretization schemes, featuring numerical stability, is analyzed in Chapter VIII; discretized formulations are given in detail for two implicit schemes; the overall iterative procedure of solution is illustrated and a simple method for an automatic time step selection is described. In Chapter IX a method of solution for the voltage-driven transient is presented, and an alternative procedure

to achieve steady-state solutions is described; the time-dependent algorithm for the analysis of an isolated device driven by ideal generators is extended to incorporate a general network of circuit elements. Chapter X completes the discussion, initiated in Chapter V, of the overall accuracy of the results; the various contributions to the discretization and numerical errors in the time domain are identified, and techniques to estimate and control the accuracy of the results are described. As an example of numerical calculations, time-dependent solutions are illustrated in Chapter XI for a particular structure of an N-P diode under various excitations of current and voltage, and for the combination of an N-P diode and an external resistor under switching from a forward to a reverse bias condition. The potential of the basic tool developed throughout the present investigation is underlined in Chapter XII; some of the several immediate applications for the analysis of devices under more general conditions and the possibilities of extensions to more complex situations are briefly discussed.

In the Appendices (A to G) are gathered the conventional first-order theory steady-state results, discretized formulations suitable for numerical integration and differentiation, basic concepts and conclusions available from the theory of numerical analysis on the discretization of partial differential equations of the parabolic type, and the FORTRAN programs for both the steady-state and transient algorithms.

PART I

STEADY-STATE ANALYSIS

CHAPTER I

OUTLINE OF THE METHOD FOR THE SOLUTION OF THE DIRECT PROBLEM ($V_A \rightarrow J$) FOR A TWO CONTACT DEVICE

In this Chapter the physical model and corresponding fundamental two-carrier transport equations describing the behavior of semiconductor junction devices are presented, then specialized and normalized for the one-dimensional steady-state case. Boundary conditions of a very general character for a two-contact device, are given to complete the mathematical description of the problem. The basic equations are then rearranged to an equivalent reduced set, more appropriate to an iterative type of procedure. Only the "direct" problem (the applied voltage is specified, the total current unknown) is considered; the analysis of the "reverse" problem (the total current is specified, the terminal voltage unknown) is postponed to a later chapter. Schematic block diagrams illustrate the procedure in the general and particular cases.

1.1. Physical and mathematical model.

1.1.1. Fundamental equations.

The following assumptions are introduced:

(a) non-degenerate conditions (for validity of the Boltzmann statistics)

(b) constant temperature

(c) time-independent impurity distribution

(d) full ionization of the impurities

Phenomena occurring in the interior of the device may be interpreted with the aid of the Boltzmann transport equation supplemented

by quantum mechanics. The conventional stage of approximation (see, for example, Moll [19] pp. 62-67) of the Boltzmann equation treats electron and hole currents as a sum of a diffusion component proportional to the carrier density gradient and a drift component representing Ohm's law. Such a simplified form of the current flow equations, together with Poisson's equation and the continuity equations for the mobile carriers, are here taken as the mathematical description of the behavior of the device. Generation-recombination processes are assumed to be satisfactorily described by an additive expression solely in the continuity equations for electron and hole densities. For the present purposes this expression is permitted to assume the most general form in terms of the quantities of interest, and will be left unspecified.

Although more general and complete formulations of the problem may be devised, solutions of the simplified set of equations, presented below, will be here referred to as "exact" solutions.

Maxwell's equations

$$j(\underset{\sim}{r},t) = j_n(\underset{\sim}{r},t) + j_p(\underset{\sim}{r},t) - \varepsilon \frac{\partial}{\partial t} \nabla\psi(\underset{\sim}{r},t) \tag{1.1}$$

$$\nabla \cdot j(\underset{\sim}{r},t) = 0 \tag{1.1a}$$

show the solenoidal character of the total current density* j

* Current densities have the dimension of current/area. For simplicity, in the following context the term "current" will be consistently used to denote "current density".

expressed as sum of the electron and hole particle currents j_n, j_p and the displacement current in terms of the electrostatic potential ψ and the dielectric constant ε. The current flow equations for electrons and holes:

$$j_n(\underset{\sim}{r}, t) = -e\mu_n(\underset{\sim}{r})\, n(\underset{\sim}{r}, t)\, \nabla\psi(\underset{\sim}{r}, t) + eD_n(\underset{\sim}{r})\, \nabla n(\underset{\sim}{r}, t) \tag{1.2}$$

$$j_p(\underset{\sim}{r}, t) = -e\mu_p(\underset{\sim}{r})\, p(\underset{\sim}{r}, t)\, \nabla\psi(\underset{\sim}{r}, t) - eD_p(\underset{\sim}{r})\, \nabla p(\underset{\sim}{r}, t) \tag{1.3}$$

express the electron and hole currents as sums of their drift and diffusion components, in terms of the electron charge $-e$, electron and hole concentrations n, p, mobilities μ_n, μ_p, and diffusion constants D_n, D_p.

Poisson's equation

$$\nabla^2\psi(\underset{\sim}{r}, t) = \frac{e}{\varepsilon}\,[n(\underset{\sim}{r}, t) - p(\underset{\sim}{r}, t) - N(\underset{\sim}{r})] \tag{1.4}$$

with $N(\underset{\sim}{r}) = N_D(\underset{\sim}{r}) - N_A(\underset{\sim}{r})$ relates the electrostatic potential to the net spatial electric charge in terms of the mobile carrier densities and the fixed net impurity atom concentration N, which is the difference between the donor and acceptor contributions N_D, N_A.

The continuity equations for electrons and holes

$$\frac{\partial n(\underset{\sim}{r}, t)}{\partial t} = -U(\underset{\sim}{r}, t) + \frac{1}{e}\,\nabla\cdot j_n(\underset{\sim}{r}, t) \tag{1.5}$$

$$\frac{\partial p(\underset{\sim}{r}, t)}{\partial t} = -U(\underset{\sim}{r}, t) - \frac{1}{e}\,\nabla\cdot j_p(\underset{\sim}{r}, t) \tag{1.6}$$

state the equality between the time variation of the carrier concentrations in a certain region and the flow out of such a region subtracted from the internal net generation-recombination term described by U.

It is of interest to observe that only six of the above equations are independent. Equations (1.1a), (1.4), (1.5) and (1.6) are related: any one of these may be obtained from the remaining three (and the knowledge of $N(\underset{\sim}{r})$ if Poisson's equation is omitted).

If $E(\underset{\sim}{r},t)$ is the electric field, k the Boltzmann constant, T the absolute temperature, $V_t \triangleq kT/e$ the thermal voltage, then the following subsidiary relations are valid:

$$E(\underset{\sim}{r},t) = -\nabla\psi(\underset{\sim}{r},t)$$

$$D_n(\underset{\sim}{r}) = \mu_n(\underset{\sim}{r})\, V_t$$

$$D_p(\underset{\sim}{r}) = \mu_p(\underset{\sim}{r})\, V_t$$

The one-dimensional structure of Fig. 1.1 is considered, in which x represents the position coordinate, 0 and L the external contacts, and M the metallurgical interface between the N-material and P-material. The fundamental equations, specialized for the one-dimensional steady-state case, assume the simpler forms:

$$j = j_n(x) + j_p(x) \tag{1.7}$$

$$\frac{dj}{dx} = 0 \tag{1.7a}$$

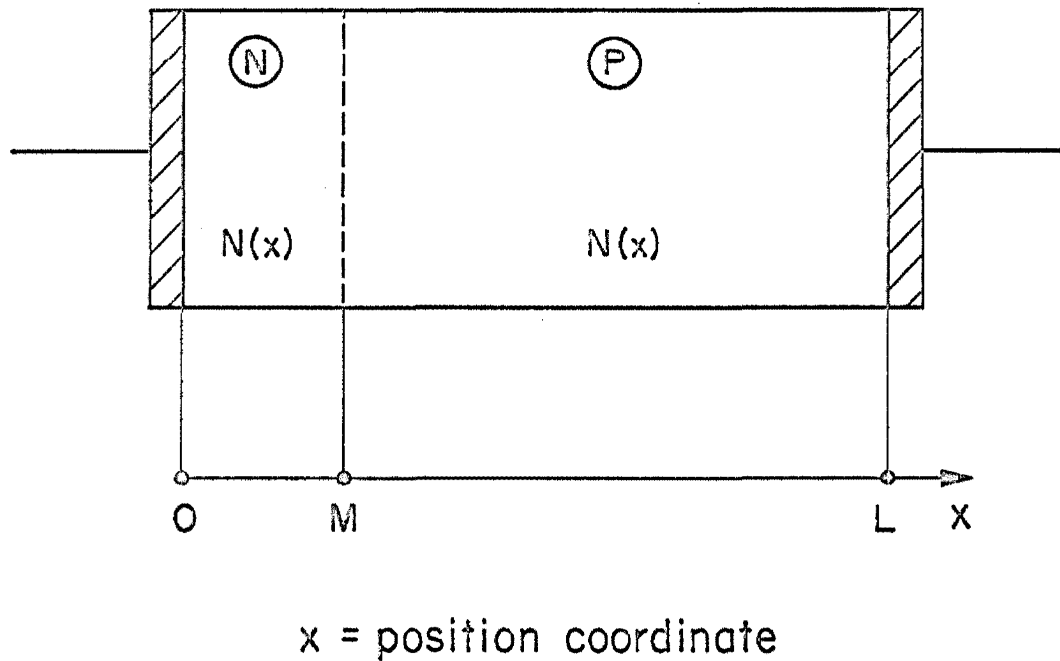

Fig. 1.1. One-dimensional N-P diode structure.

$$j_n(x) = - e\mu_n(x)\ n(x)\ \frac{d\psi(x)}{dx} + eD_n(x)\ \frac{dn(x)}{dx} \tag{1.8}$$

$$j_p(x) = - e\mu_p(x)\ p(x)\ \frac{d\psi(x)}{dx} - eD_p(x)\ \frac{dp(x)}{dx} \tag{1.9}$$

$$\frac{d^2\psi(x)}{dx^2} = \frac{e}{\varepsilon}\ [n(x) - p(x) - N(x)] \tag{1.10}$$

$$\frac{dj_n(x)}{dx} = eU(x) \tag{1.11}$$

$$\frac{dj_p(x)}{dx} = - eU(x) \tag{1.12}$$

with the subsidiary relations:

$$E(x) = - \frac{d\psi(x)}{dx} \quad , \quad N(x) = N_D(x) - N_A(x)$$

$$D_n(x) = \mu_n(x)\ V_t \quad , \quad D_p(x) = \mu_p(x)\ V_t$$

$$\varphi_n(x) \triangleq \psi(x) - V_t \ln \frac{n(x)}{n_I} \tag{1.13}$$

$$\varphi_p(x) \triangleq \psi(x) + V_t \ln \frac{p(x)}{n_I} \tag{1.14}$$

$$\sigma(x) = e\mu_n n(x) + e\mu_p p(x) \tag{1.15}$$

where n_I is the intrinsic carrier concentration and $\sigma(x)$ is the conductivity of the material.

Equations (1.13) and (1.14) may be taken as definitions of the electron and hole quasi Fermi levels φ_n, φ_p introduced originally by Shockley [1].

1.1.2. Normalization of the fundamental equations.

It is very convenient at this stage to express the relevant quantities in dimensionless form; the set of normalization constants is chosen with the criterion of achieving the highest simplification in the relations of interest. The list of normalization factors is given in Table 1.1.

The signs of j_n and j_p were originally chosen positive in the positive x direction (Eqs.(1.8) and (1.9)); in order to obtain positive currents in the forward bias case for the structure under consideration, a negative normalization factor is chosen for the current. Normalized electron, hole and total current densities will then be indicated by $J_n(x)$, $J_p(x)$, J. Hole and electron diffusion constants are normalized in a symmetric fashion with the introduction of an arbitrary diffusion constant D_o; for convenience in the normalized context, the following dimensionless quantities will be used

$$\gamma_n(x) = D_o/D_n(x) \qquad ; \qquad \gamma_p(x) = D_o/D_p(x)$$

With the exception of the above, symbols adopted for the unnormalized quantities will also be used for the normalized ones. For the remainder of this work, all symbols will consistently refer to normalized quantities, unless otherwise indicated.

The fundamental equations may be written in normalized terms as:

$$J = J_n(x) + J_p(x) \tag{1.16}$$

DESCRIPTION	NORMALIZED QUANTITY	NORMALIZATION FACTOR	
		symbol	numerical value
position coordinate	x	$L_D \triangleq \sqrt{\epsilon V_t / e n_I}$	9.56685×10^{-5} cm
time coordinate	t	L_D^2 / D_o	9.15246×10^{-9} sec
electrostatic potential	ψ	V_t	0.025875 volt
quasi-Fermi levels	φ_n, φ_p	V_t	"
applied (or terminal) voltage	V_A	V_t	"
diffusion (or barrier) potential	V_d	V_t	"
electric field	E	V_t / L_D	270.465 volt/cm
carrier densities	n, p	n_I	2.5×10^{13} cm^{-3}
net impurity, donor, and acceptor densities	N, N_D, N_A	n_I	"
total, electron, and hole current densities	J, J_n, J_p	$- e D_o n_I / L_D$	$-$ 0.0418649 ampere/cm^2
generation-recombination rate	U	$D_o n_I / L_D^2$	2.73151×10^{21} cm^{-3} sec^{-1}
carrier diffusion constants	γ_n^{-1}, γ_p^{-1}	D_o	1 cm^2/sec
carrier mobilities	γ_n^{-1}, γ_p^{-1}	D_o / V_t	38.6473 cm^2/volt-sec
conductivity	σ	$e n_I D_o / V_t$	1.54789×10^{-4} $(\Omega \text{ cm})^{-1}$
capacitance/unit area	C	ϵ / L_D	1.48084×10^{-8} farad/cm^2

Table 1.1. List of normalization factors for the quantities of interest.

$$\frac{dJ}{dx} = 0 \tag{1.16a}$$

$$J_n(x) = \frac{1}{\gamma_n(x)} \left[n(x) \frac{d\psi(x)}{dx} - \frac{dn(x)}{dx} \right] \tag{1.17}$$

$$J_p(x) = \frac{1}{\gamma_p(x)} \left[p(x) \frac{d\psi(x)}{dx} + \frac{dp(x)}{dx} \right] \tag{1.18}$$

$$\frac{d^2\psi(x)}{dx^2} = n(x) - p(x) - N(x) \tag{1.19}$$

$$\frac{dJ_n(x)}{dx} = - U(x) \tag{1.20}$$

$$\frac{dJ_p(x)}{dx} = U(x) \tag{1.21}$$

with the subsidiary relations

$$E(x) = - \frac{d\psi(x)}{dx} \tag{1.22}$$

$$N(x) = N_D(x) - N_A(x) \tag{1.23}$$

$$\gamma_n(x) = \frac{1}{\mu_n(x)} \quad , \quad \gamma_p(x) = \frac{1}{\mu_p(x)}$$

$$\varphi_n(x) = \psi(x) - \ln n(x) \tag{1.24}$$

$$\varphi_p(x) = \psi(x) + \ln p(x) \tag{1.25}$$

$$\sigma(x) = \frac{n(x)}{\gamma_n(x)} + \frac{p(x)}{\gamma_p(x)} \tag{1.26}$$

Equations (1.16) and (1.17) to (1.21) represent a set of six independent equations in the six unknowns $n(x)$, $p(x)$, $\psi(x)$, $J_n(x)$, $J_p(x)$, J. Equation (1.16a) follows directly from Eqs.(1.16), (1.20), (1.21) and will be considered as the dependent equation of the set.

1.1.3. Boundary conditions.

It is apparent from the nature of the fundamental set of ordinary differential equations that six conditions at the boundaries are necessary. These are chosen as the carrier concentrations

$$n(0), \quad p(0), \quad n(L), \quad p(L)$$

and the electrostatic potential

$$\psi(0), \quad \psi(L)$$

at the external contacts 0 and L. Either of the boundary conditions on the electrostatic potential may be taken as a reference value, the other being directly related to the externally applied voltage V_A and the diffusion potential V_d:

$$\psi(0) - \psi(L) = V_d - V_A \tag{1.27}$$

The boundary conditions on the carrier densities are in general given by relationships involving the currents at the external contacts; since explicit forms of such relationships are not essential for the present purposes, only their functional dependence will be indicated:

$$\left.\begin{aligned} n(0) &= f_{n0}[J_n(0),\ J_p(0)] \\ p(0) &= f_{p0}[J_n(0),\ J_p(0)] \\ n(L) &= f_{nL}[J_n(L),\ J_p(L)] \\ p(L) &= f_{pL}[J_n(L),\ J_p(L)] \end{aligned}\right\} \qquad (1.28)$$

The above relations assume the simplest form for contacts of the ohmic type, defined by:

$$\left.\begin{aligned} n(0) &= n_N \quad ; \quad n(L) = n_P \\ p(0) &= p_N \quad ; \quad p(L) = p_P \end{aligned}\right\} \qquad (1.29)$$

where n_N and p_N (n_P and p_P) are the electron and hole equilibrium densities at the external contact of the N-material (P-material) respectively. An equivalent definition requires charge neutrality at the contacts

$$\left.\begin{aligned} n(0) - p(0) - N(0) &= 0 \\ n(L) - p(L) - N(L) &= 0 \end{aligned}\right\} \qquad (1.30)$$

and coincidence of the quasi-Fermi levels at the contacts

$$\left.\begin{aligned} \varphi_n(0) &= \varphi_p(0) \\ \varphi_n(L) &= \varphi_p(L) \end{aligned}\right\} \qquad (1.31)$$

With the aid of Eqs. (1.30), (1.31), (1.24) and (1.25) the carrier density boundary values are readily obtained, for this special case, in terms of the doping concentrations:

$$\begin{aligned}
n(0) &= n_N = \sqrt{\left[\frac{N(0)}{2}\right]^2 + 1} + \frac{N(0)}{2} \quad ; \qquad [N(0) > 0] \\
p(0) &= p_N = 1/n_N \\
n(L) &= n_P = 1/p_P \\
p(L) &= p_P = \sqrt{\left[\frac{N(L)}{2}\right]^2 + 1} - \frac{N(L)}{2} \quad ; \qquad [N(L) \leq 0]
\end{aligned} \tag{1.32}$$

1.2. Derivation of the reduced set of equations.

It is convenient to rearrange Eqs.(1.17) to (1.21) in a form more appropriate for numerical methods.

Equations (1.17) and (1.18), rewritten as

$$\frac{dn(x)}{dx} + E(x)\, n(x) = -\, \gamma_n(x)\, J_n(x)$$

$$\frac{dp(x)}{dx} - E(x)\, p(x) = \gamma_p(x)\, J_p(x) \quad ,$$

may be treated as two independent first-order linear differential equations in the unknowns $n(x)$ and $p(x)$, respectively, if the other quantities are considered as non-constant coefficients. Analytic solutions are straightforward:

$$n(x) = e^{-\int E(x)dx} \left[- \int \gamma_n(x)\, J_n(x)\, e^{\int E(x)dx}\, dx + C_n \right]$$

$$p(x) = e^{\int E(x)dx}\left[\int \gamma_p(x)\ J_p(x)\ e^{-\int E(x)dx}\ dx + C_p\right]$$

C_n and C_p being integration constants. A more definite form is obtained if x and L are taken as limits of integrations, and if C_n and C_p are expressed in terms of the boundary conditions at the point L:

$$n(x) = e^{\psi(x)}\left[\int_x^L \gamma_n(x')\ J_n(x')\ e^{-\psi(x')}\ dx' + n(L)\ e^{-\psi(L)}\right] \tag{1.33}$$

$$p(x) = e^{-\psi(x)}\left[-\int_x^L \gamma_p(x')\ J_p(x')\ e^{\psi(x')}\ dx' + p(L)\ e^{\psi(L)}\right] \tag{1.34}$$

The current densities J_n, J_p may be expressed in terms of $U(x)$ and $\psi(x)$. Integration of Eqs.(1.20) and (1.21) yields:

$$J_n(x) = -\int_0^x U(x')\ dx' + K_n \tag{1.35}$$

$$J_p(x) = \int_0^x U(x')\ dx' + K_p \tag{1.36}$$

The constants of integration K_n, K_p are readily obtained by inserting Eqs.(1.35), (1.36) respectively into Eqs.(1.33), (1.34) evaluated at $x = 0$:

$$n(0) = e^{\psi(0)}\left[\int_0^L \gamma_n(x)e^{-\psi(x)}\left(-\int_0^x U(x')dx' + K_n\right)dx + n(L)e^{-\psi(L)}\right] \tag{1.37}$$

$$p(0) = e^{-\psi(0)}\left[-\int_0^L \gamma_p(x)e^{\psi(x)}\left(\int_0^x U(x')dx' + K_p\right)dx + p(L)e^{\psi(L)}\right] \tag{1.38}$$

The expressions for K_n and K_p found from Eqs.(1.37), (1.38) can be inserted into Eqs.(1.35), (1.36) to give the final results for the current densities in terms of the potential distributions:

$$J_n(x) = -\int_0^x U(x')dx' + \frac{n(0)e^{-\psi(0)} - n(L)e^{-\psi(L)} + \int_0^L \gamma_n(x)e^{-\psi(x)}\left[\int_0^x U(x')dx'\right]dx}{\int_0^L \gamma_n(x)e^{-\psi(x)}dx} \tag{1.39}$$

$$J_p(x) = \int_0^x U(x')dx' + \frac{p(L)e^{\psi(L)} - p(0)e^{\psi(0)} - \int_0^L \gamma_p(x)e^{\psi(x)}\left[\int_0^x U(x')dx'\right]dx}{\int_0^L \gamma_p(x)e^{\psi(x)}dx} \tag{1.40}$$

Gummel's relations are essentially contained in the above and have been here derived directly from the basic equations, rather than through the introduction of a set of identities [18].

The five basic equations (1.17) to (1.21) have been rearranged to a reduced set of three equations [Eq.(1.19) and Eqs.(1.33), (1.34) combined with relations (1.39), (1.40)] with the boundary conditions (1.27), (1.28). In this new formulation of the problem the electrostatic potential ψ, the electron density n and the hole density p are chosen as the independent quantities and represent the unknowns of the reduced set of equations.

If generation-recombination processes are neglected $[U(x) = 0]$, Eqs.(1.39) and (1.40) assume the simpler forms:

$$J_n = \frac{n(0)\ e^{-\psi(0)} - n(L)\ e^{-\psi(L)}}{\int_0^L \gamma_n(x)\ e^{-\psi(x)}\ dx} \tag{1.41}$$

$$J_p = \frac{p(L)\ e^{\psi(L)} - p(0)\ e^{\psi(0)}}{\int_0^L \gamma_p(x)\ e^{\psi(x)}\ dx} \tag{1.42}$$

which clearly shows the solenoidal character of each current throughout the interior of the device in this special case.

1.3. Iterative procedure of solution.

An iterative procedure may now be employed to cope with the several nonlinearities of the problem. For this purpose it is convenient to rearrange Poisson's Eq.(1.19) in a more appropriate form, in terms of a quantity with zero boundary values. The correction $\delta^{(j+1)}(x)$ between the electrostatic potential distributions obtained by consecutive iterations $(j+1)$ and (j) is introduced, and defined as:

$$\delta^{(j+1)}(x) \triangleq \psi^{(j+1)}(x) - \psi^{(j)}(x) \quad ; \quad j = 1,\ 2,\ 3,\ \cdots$$

where $\psi^{(j)}(x)$ and $\psi^{(j+1)}(x)$ are the potential distributions at the completion of the $(j)^{th}$ and $(j+1)^{th}$ iterations respectively. It is readily verified that:

$$\delta^{(j)}(0) = \delta^{(j)}(L) = 0 \quad ; \quad j = 1,\ 2,\ 3,\ \cdots \tag{1.43}$$

as desired. Poisson's Eq.(1.19) may be written, in terms of the quasi-Fermi levels (1.24), (1.25), for the $(j+1)^{th}$ iteration as:

$$\frac{d^2\psi^{(j+1)}(x)}{dx^2} = e^{\psi^{(j+1)}(x) - \varphi_n^{(j)}(x)} - e^{\varphi_p^{(j)}(x) - \psi^{(j+1)}(x)} - N(x) \tag{1.44}$$

or

$$\frac{d^2\delta^{(j+1)}(x)}{dx^2} - \delta^{(j+1)}(x)\left[\overset{(j)}{n}(x) + \overset{(j)}{p}(x)\right] = -\frac{d^2\overset{(j)}{\psi}}{dx^2} + \overset{(j)}{n}(x) - \overset{(j)}{p}(x) - N(x) \tag{1.45}$$

if terms of order $\left[\delta^{(j+1)}(x)\right]^2$ and higher are neglected.*

Equation (1.45) represents a second-order linear differential equation in the unknown $\delta^{(j+1)}(x)$, with boundary conditions (1.43), if the remaining quantities are available after the completion of the $(j)^{th}$ iteration.

The complete iteration scheme for the general case is shown in Fig. 1.2. The applied voltage V_A is specified, a trial potential distribution is chosen, and absence of recombination is assumed in order to start the first cycle of the main iteration loop (labeled "j"). The electric field $E(x)$ and the mobilities $\gamma_n^{-1}(x)$, $\gamma_p^{-1}(x)$, in general dependent upon the electric field, are computed as functions of position. If relations (1.28), that specify the boundary values of the mobile carrier densities, combined with Eqs.(1.39), (1.40) may not be reduced to an explicit form for the currents at the boundaries in terms of $\psi(x)$ and $U(x)$, a preliminary iteration loop (labeled "h") is required. An initial guess on the current boundary values (for example zero) is inserted in Eq.(1.28) to compute preliminary carrier density boundary values, which in turn are inserted in Eqs.(1.39), (1.40) specialized at $x = 0$ and $x = L$ respectively, to compute new current boundary values, and the "h" loop is repeated until the desired accuracy is reached. Eqs.(1.39), (1.40) yield then the electron and

---

* This is not related to the accuracy of the final results if convergence of the iterative scheme occurs, i.e. $\delta^{(j)}(x) \to 0$ ($0 \le x \le L$) for large enough j.

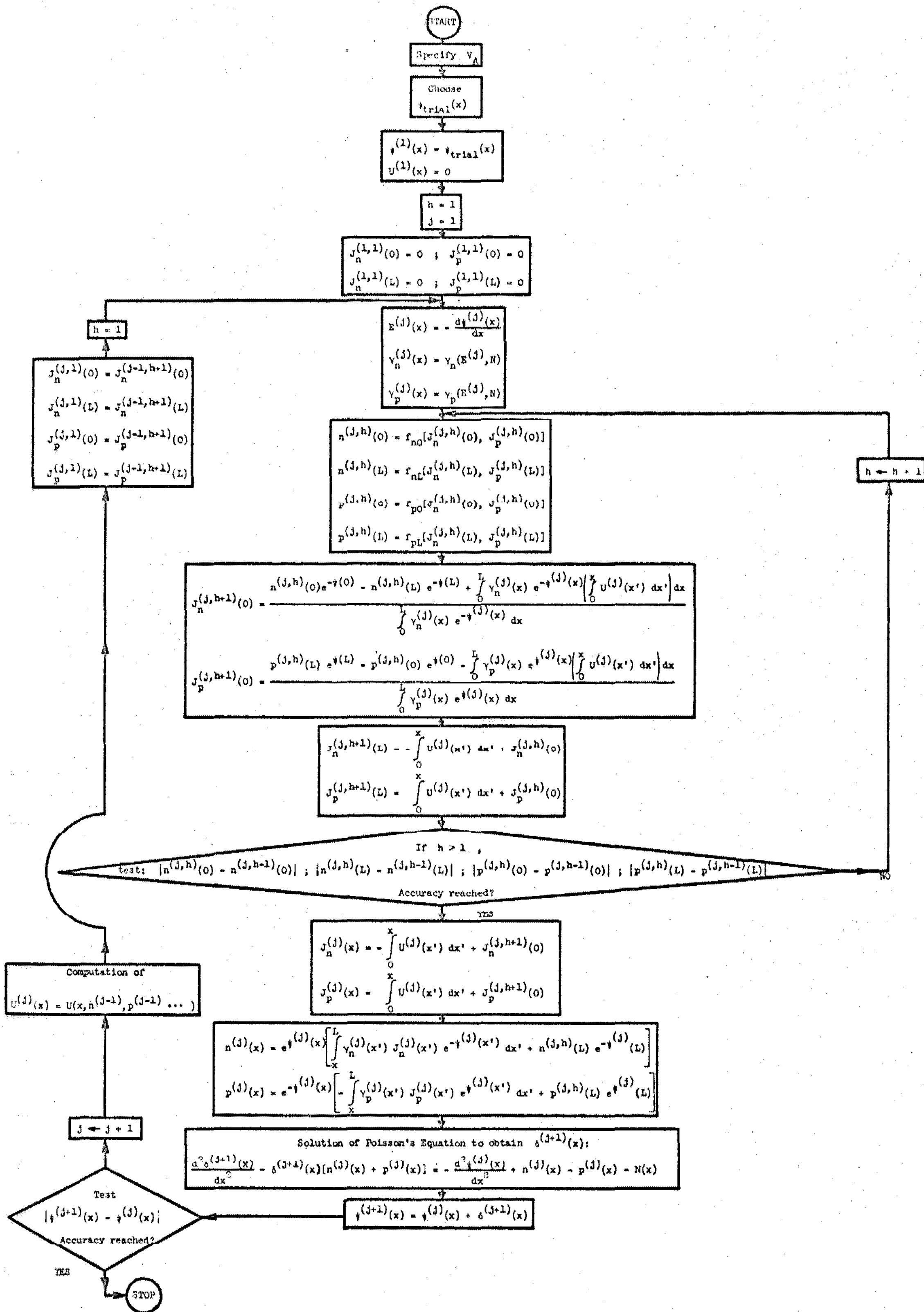

Fig. 1.2. Block diagram of the iterative procedure for the general case.

hole current distributions $J_n(x)$ and $J_p(x)$, which, inserted in Eqs.(1.33), (1.34), allow the computation of the carrier densities $n(x)$ and $p(x)$ as functions of position. The solution of Poisson's Eq.(1.45) yields then an improved potential distribution, and the generation-recombination term may be computed with the aid of the quantities already available. The "j" cycle, with inclusion of the "h" loop, may now be repeated to the desired accuracy.

The generality of the method is apparent. Complete freedom is available in the choice of the impurity distribution, the carrier boundary conditions at the external contacts, the dependence of the mobilities on the electric field and doping, the generation-recombination law, and the injection level. If the applied voltage V_A is specified, the method solves for the total current J and all the quantities of interest in the interior of the device as functions of position. This is referred to as the "direct problem", as opposed to the "reverse problem" of specifying the total current J and solving for the terminal voltage V_A.

1.3.1. Two special cases.

If the combination of Eqs.(1.39), (1.40) and the relations (1.28), that specify the boundary conditions on the carrier densities, allows explicit solutions for both the carrier densities and the currents at the contacts, the secondary "h" loop and the initial guess on the current boundary values is unnecessary. This is certainly the case for contacts of the ohmic type, defined in Subsection 1.1.3. The iteration scheme is then simplified, with the aid of relations (1.29), as shown in Fig. 1.3.

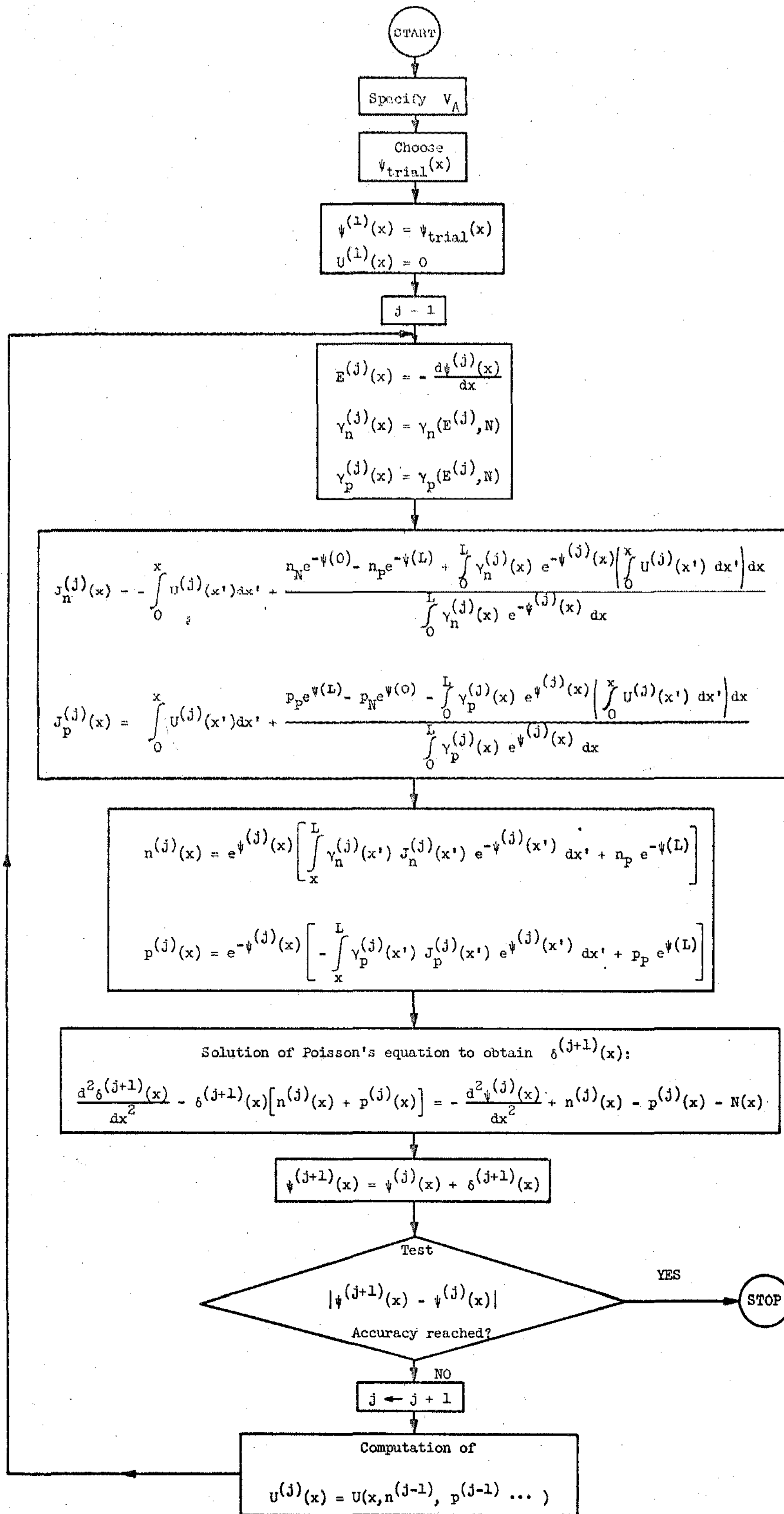

Fig. 1.3. Block diagram of the iterative procedure for a special case characterized by ohmic contacts.

A further simplification is achieved if recombination in the interior of the device is neglected $[U(x) = 0]$ and mobilities are considered constant. The electrostatic potential may be considered in this case as the only independent unknown of the problem, since every quantity may be expressed solely in terms of $\psi(x)$ and assigned constants. Equations (1.41) and (1.42) apply in this case, and the iteration scheme is shown in Fig. 1.4.

1.4. Conclusion.

The basic two-carrier transport equations describing the behavior of semiconductor junction devices have been stated, specialized for the one-dimensional steady-state case, and normalized in dimensionless form. The fundamental set of equations has been applied to a two-contact device and boundary conditions of a general nature have been specified to complete the mathematical formulation of the problem. An equivalent reduced set of relations has been derived directly from the fundamental set, and an iterative scheme suitable to generate solutions under general conditions has been illustrated.

However, basic limitations of most currently available digital computers prevent achievement of solutions of such general character and sufficient accuracy if the described formulation (originally presented by Gummel [18] in a slightly different form) is taken to generate the numerical algorithm. These difficulties are exposed and overcome in the following Chapter.

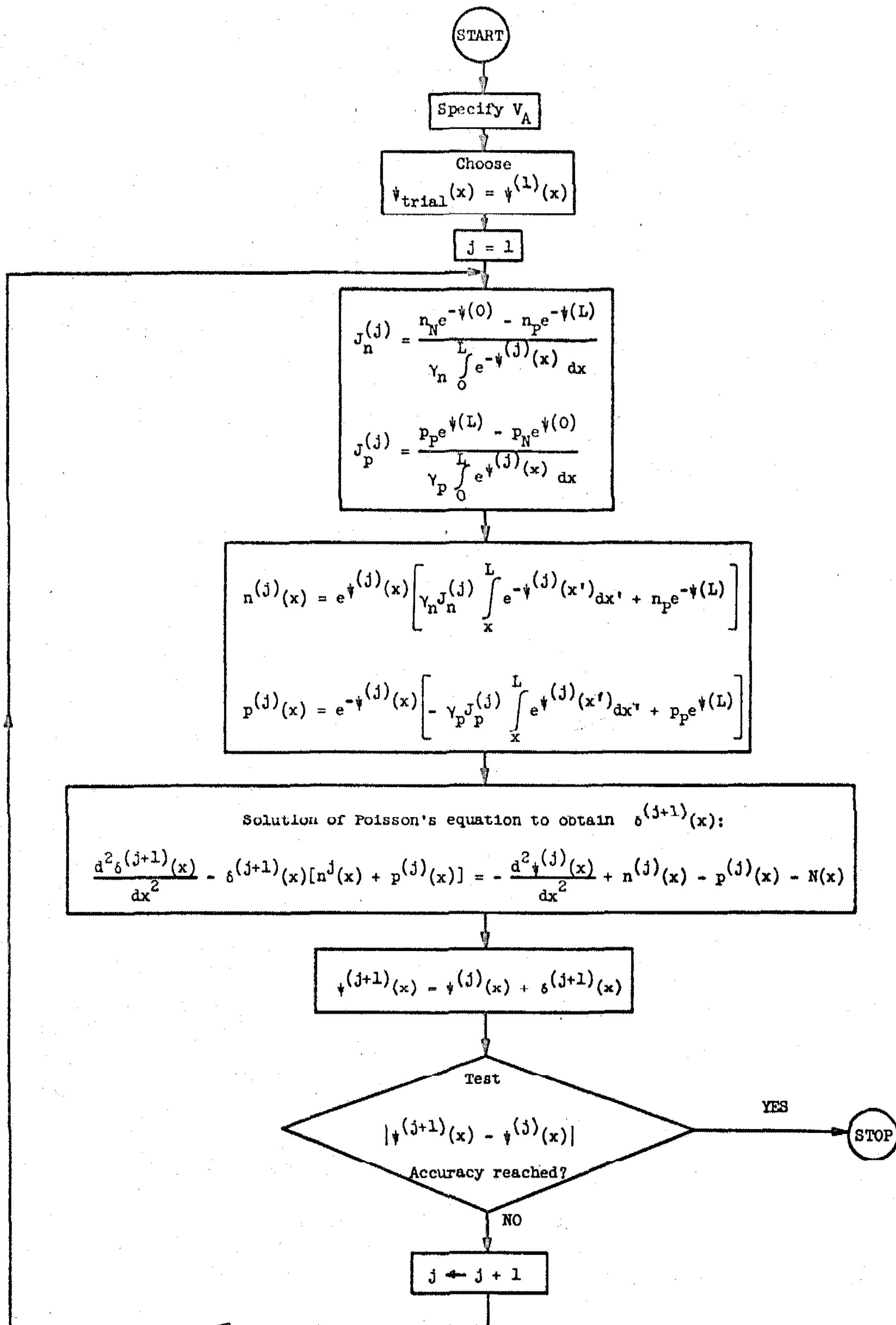

Fig. 1.4. Block diagram of the iterative procedure for a special case characterized by ohmic contacts, absence of recombination in the interior, constant mobilities.

CHAPTER II

IMPROVED ANALYTICAL FORMULATION AND NUMERICAL TECHNIQUES

In this Chapter the method of solution, outlined in Chapter I, is analyzed from a numerical point of view, to expose serious difficulties of fundamental and practical nature that arise if the described analytical formulation is taken to generate the numerical algorithm. Small differences between nearly equal numbers and quantities exceeding in magnitude the range permitted by most digital machines are recognized to occur in certain conditions. An improved and extended analytical formulation that overcomes these hindrances is presented.

The discretization problem is discussed in detail, and criteria for the selection of a non-uniform step distribution automatically adjusted by the computer during the entire solution are given.

Numerical techniques for the evaluation of numerical integrations and differentiations, and for the solution of Poisson's equation are illustrated. The non-uniform character of the step distribution suggests a finite difference scheme for the numerical solution of Poisson's equation to reduce the problem to the solution of a system of simultaneous linear algebraic equations. A direct method, rather than an iterative one, is preferred to solve such a system, in consideration of the triple-diagonal character of the corresponding matrix. A very interesting feature is the conservation of the same triple-diagonal matrix for any order of finite difference scheme employed.

A detailed illustration of the alternatives chosen in the computer program, reported in an appendix, concludes this Chapter.

2.1. Generalities.

Serious hindrances arise in the numerical analysis of the problem if the analytical formulation, described in the previous Chapter, is used to generate the numerical algorithm. These difficulties are related to basic limitations of the digital machines available, such as the finite number of significant digits and the limited range of the magnitude of the quantities that may be accommodated, and the finite memory size. Each of these three constraints is responsible, in the problem under consideration, for a major difficulty that deserves particular attention, and therefore is analyzed separately in this Chapter. Small differences between nearly equal numbers generate, in certain conditions, highly inaccurate results, and the tendency of several terms of the relevant expressions to exceed in magnitude the permissible range restricts the solutions to forward and to low reverse-bias cases. To overcome these major restrictions an improved analytical formulation is necessary. In addition, variations of most quantities over wide ranges in short regions require an appropriate discretization technique to contain truncation errors within acceptable limits.

A simplified model, characterized by ohmic contacts, absence of recombination in the bulk $[U(x) = 0]$, and constant mobilities, is considered throughout this Chapter. These restrictions contribute to expose (rather than alleviate) the basic difficulties in a clearer context stripped of several cumbersome details. These can then be readily filled in, once the basic hindrances have been overcome, to generalize fully the procedure, if so desired. The original formulation that applies to such a simplified model is illustrated in Fig. 1.4, and the

iterative scheme is described in Section 1.3.

2.2. Improved analytical formulation.

2.2.1. Small differences between nearly equal numbers.

The computation of the difference between nearly equal quantities, whose accuracy is specified by a finite number of exact significant digits, yields a considerably less accurate result. This difficulty is already present in the basic Eqs.(1.17), (1.18), and arises, in the described method of solution, when the computation of the mobile carrier densities is attempted through the combination of Eqs.(1.39), (1.40) with Eqs.(1.33), (1.34) respectively. Equations (1.33), (1.34) with the aid of Eqs.(1.39), (1.40), specialized according to the simplified model (ohmic contacts, absence of recombination in the interior, constant mobilities), may be rewritten as:

$$n(x) = e^{\psi(x)-\psi(0)}\left[n_N \frac{F_{In}(x)}{F_{In}(0)} - n_P \frac{F_{In}(x)}{F_{In}(0)} e^{\psi(0)-\psi(L)} + n_P e^{\psi(0)-\psi(L)}\right] \quad (2.1)$$

$$p(x) = e^{\psi(0)-\psi(x)}\left[p_N \frac{F_{Ip}(x)}{F_{Ip}(0)} - p_P \frac{F_{Ip}(x)}{F_{Ip}(0)} e^{\psi(L)-\psi(0)} + p_P e^{\psi(L)-\psi(0)}\right] \quad (2.2)$$

where:

$$F_{In}(x) \triangleq \int_x^L e^{-\psi(x')}\, dx'$$

$$F_{Ip}(x) \triangleq \int_x^L e^{\psi(x')}\, dx'$$

The differences appearing in the square brackets of Eqs.(2.1), (2.2) may represent sources of excessive numerical errors, and therefore are

highly undesirable. For example, in Eq.(2.2), throughout part of the quasi-neutral N-region, the second term within the square brackets is nearly equal to the third; their subtraction introduces a large error which, if comparable to the first term, is responsible for a highly inaccurate hole distribution in that region. The higher the applied voltage (in the forward bias direction), the higher the influence of such error. This is certain to reach prohibitive limits at high injection levels. A similar situation arises in Eq.(2.1).

These difficulties may be overcome at once with the introduction of the new integrals

$$F_n(x) \triangleq \int_0^x e^{-\psi(x')}\, dx'$$

$$F_p(x) \triangleq \int_0^x e^{\psi(x')}\, dx'$$

(to be evaluated numerically directly from the integrands*) and a rearrangement of Eqs.(2.1), (2.2) to the following form:

$$n(x) = \left[F_n(x) + \frac{n_N\, p_P}{e^{\psi(0)-\psi(L)}}\; F_{In}(x) \right] \frac{e^{\psi(x)-\psi(L)}}{p_P\, F_n(L)} \qquad (2.3)$$

---

* That is, not by using the relations

$$F_n(x) = F_{In}(0) - F_{In}(x)$$

$$F_p(x) = F_{Ip}(0) - F_{Ip}(x)$$

$$p(x) = \left[F_{Ip}(x) + \frac{n_N\ p_P}{e^{\psi(0)-\psi(L)}}\ F_p(x) \right] \frac{e^{\psi(0)-\psi(x)}}{n_N\ F_{Ip}(0)} \qquad (2.4)$$

Extension of the above expressions to the more general case is straightforward. For example, if generalized boundary conditions on the mobile carriers are specified, the electron and hole densities are given by:

$$n(x) = \left[F_n(x) + \frac{n(0)}{n(L)\ e^{\psi(0)-\psi(L)}}\ F_{In}(x) \right] \frac{n(L)\ e^{\psi(x)-\psi(L)}}{F_n(L)} \qquad (2.5)$$

$$p(x) = \left[F_{Ip}(x) + \frac{p(L)}{p(0)\ e^{\psi(0)-\psi(L)}}\ F_p(x) \right] \frac{p(0)\ e^{\psi(0)-\psi(x)}}{F_{Ip}(0)} \qquad (2.6)$$

In particular, the values of the minority carrier densities at each external contact may be determined by a finite surface recombination velocity, and the majority carrier density by the requirement of charge neutrality at the contact:

$$\begin{cases} p(0) - p_N = \dfrac{J_p}{s_0} \\ p(0) - n(0) + N_D = 0 \end{cases} \qquad \begin{cases} n(L) - n_P = \dfrac{J_n}{s_L} \\ p(L) - n(L) - N_A = 0 \end{cases} \qquad (2.7)$$

where s_0 and s_L are the surface recombination velocities at the contacts 0 and L respectively. In this case explicit expressions for the current densities may be found by combining relations (2.7) with Eqs.(1.41), (1.42):

$$J_n = \frac{\gamma_p F_{Ip}(0)\left[n_N e^{-\psi(0)} - n_P e^{-\psi(L)}\right] + \left[p_P e^{\psi(L)-\psi(0)} - n_P e^{\psi(0)-\psi(L)} + N_D\right]/s_0}{\left[\gamma_p F_{Ip}(0) + e^{\psi(0)}/s_0\right]\left[\gamma_n F_n(L) + e^{-\psi(L)}/s_L\right] - e^{\psi(L)-\psi(0)}/(s_0 s_L)} \tag{2.8}$$

$$J_p = \frac{\gamma_n F_n(L)\left[p_P e^{\psi(L)} - p_N e^{\psi(0)}\right] + \left[n_N e^{\psi(L)-\psi(0)} - p_N e^{\psi(0)-\psi(L)} + N_A\right]/s_L}{\left[\gamma_p F_{Ip}(0) + e^{\psi(0)}/s_0\right]\left[\gamma_n F_n(L) + e^{-\psi(L)}/s_L\right] - e^{\psi(L)-\psi(0)}/(s_0 s_L)} \tag{2.9}$$

Equations (2.3), (2.4) (or alternatively Eqs.(2.5), (2.6)) are numerically accurate expressions for the electron and hole distributions, provided that each single term, or combination thereof, does not exceed in magnitude the maximum range that the particular computer available may accommodate.* This is usually the case for forward and for low reverse bias cases, so that the above relations will be restricted to such conditions. The high reverse bias case is discussed in the following Section.

The expression for the net charge in Poisson's Eq.(1.19) also exhibits small differences in the quasi-neutral regions of the device. However, these may well be tolerated, since the only consequence is a very small absolute error in the curvature of the electrostatic potential in such regions.

---

* The permissible range on the IBM 7094/7040, on which actual calculations were performed, is the following: $10^{\mp 38}$ for real numbers in single precision (8 significant digits), $> 10^{-29}$, $< 10^{38}$ for real numbers in double precision (16 significant digits).

2.2.2. Extension to high reverse-bias conditions.

When the applied voltage exceeds a few volts in the reverse direction, several terms of Eqs.(1.33), (1.34), (1.39), (1.40) exceed in magnitude the range permitted by most digital computers.* A new set of relations is therefore required to allow the computation of the mobile carrier densities in high reverse-bias conditions. This may be achieved by dividing the electrostatic potential range $\psi(0) - \psi(L)$ into several cells defined as follows:

1st cell	$\psi(L) \leq \psi(x) < \psi_1$	$(x_0 \triangleq L \geq x > x_1)$
2nd cell	$\psi_1 \leq \psi(x) < \psi_2$	$(x_1 \geq x > x_2)$
. . .	. . .	. . .
rth cell	$\psi_{r-1} \leq \psi(x) < \psi_r$	$(x_{r-1} \geq x > x_r)$
. . .	. . .	. . .
mth cell	$\psi_{m-1} \leq \psi(x) \leq \psi_m \geq \psi(0)$	$(x_{m-1} \geq x \geq x_m \triangleq 0)$

where

$$\left.\begin{aligned} &\psi_1 - \psi(L) = R \\ &\psi_i - \psi_{i-1} = 2R \quad , \quad i = 2, 3, \cdots m \end{aligned}\right\} \qquad (2.10)$$

---

* The permissible range of the applied reverse bias may be doubled by taking the value $[\psi(0) + \psi(L)]/2$ as origin for the electrostatic potential in Eqs.(1.33), (1.34), (1.39), (1.40).

and R must be chosen small enough to limit the magnitude of the quantities

$$(L\, n_N\, e^R)^{\mp 1} \quad , \quad (L\, p_P\, e^R)^{\mp 1}$$

within the allowed range. The situation is illustrated in Fig. 2.1.

The following quantities are then defined

$$\begin{aligned} \psi_{O1} &\triangleq \psi(L) \\ \psi_{Or} &\triangleq \frac{\psi_r + \psi_{r-1}}{2} , \quad r = 2, 3, \cdots m \end{aligned} \tag{2.11}$$

and are treated as scale factors to allow in each cell r the numerical computation of the integral

$$F_{pr}(x) \triangleq \int_x^L e^{\psi(x')-\psi_{Or}}\, dx' \quad , \quad r = 1, 2, \cdots m \tag{2.11a}$$

for $x_{r-1} \geq x > x_r$. If the following quantities are defined as:

$$\begin{aligned} \theta &\triangleq \frac{n_N\, p_P}{e^{\psi(0)-\psi(L)}} \\ Y_{pr} &\triangleq \left[\frac{F_{pm}(0)}{e^{\psi(0)-\psi_{om}}}\right] e^{\psi(L)-\psi_{Or}}\, n_N\, p_P \quad , \quad r = 1, 2, \cdots m \\ Z_p &\triangleq \left[\frac{F_{pm}(0)}{e^{\psi(0)-\psi_{Om}}}\right] n_N \end{aligned} \tag{2.12}$$

Eq.(2.2) may then be rewritten as:

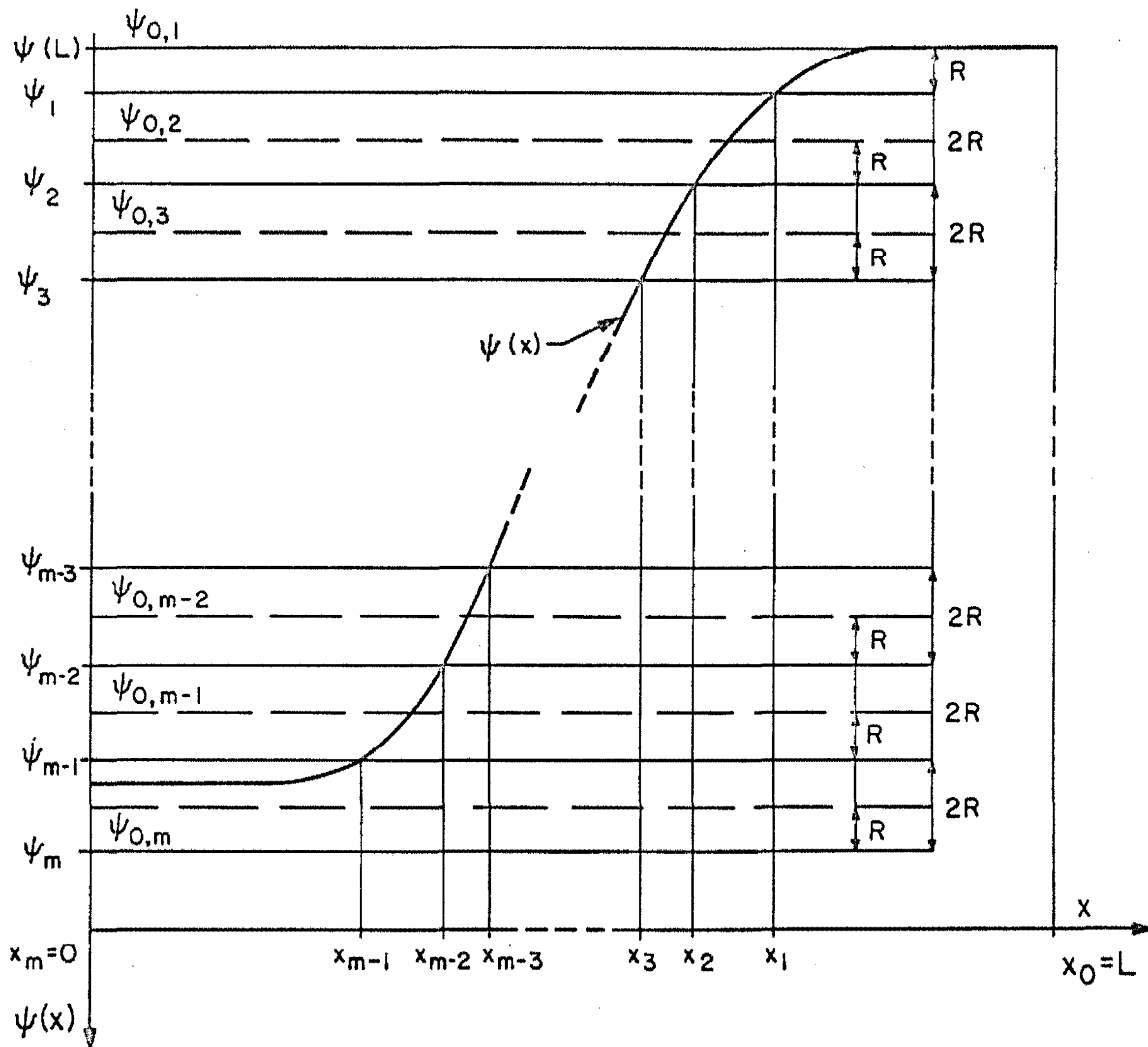

Fig. 2.1. Separation of the electrostatic potential range $\psi(0) - \psi(L)$ into m cells, and definition of the scale factors ψ_{0r} ($r = 1, 2, \ldots m$).

$$p(x) = \left[(1-\theta)\ F_{pr}(x) + Y_{pr}\right] / \left[Z_p e^{\psi(x)-\psi_{Or}}\right] \qquad (2.13)$$

for $x_{r-1} \geq x > x_r$, $r = 1, 2, \cdots m$

where ψ_{Or} is selected as the scale factor corresponding to the rth cell in which the particular value of x [or $\psi(x)$] is located. It is readily verified that $p(x)$ is scale factor independent, as desired.

The quantities θ and Y_{pr} $(r = 2, 3, \cdots m)$ still exceed the permitted range for an applied voltage V_A such that

$$\psi(0) - \psi(L) > R \quad , \quad \text{i.e.} \quad V_A < V_d - R$$

However, for large enough R^*, the following inequalities are valid:

$$Y_{pr} \ll F_{pr}(x) \qquad \text{if} \qquad x \leq x_1 \ , \quad \text{i.e.} \quad r > 1$$

$$\theta \ll 1 \qquad \text{if} \qquad \psi(0) - \psi(L) > R$$

Moreover, it can be observed that, for a given r, $\theta\ F_{pr}(x)$ is either negligible with respect to Y_{pr}, or else comparable to Y_{pr}, in which case if $\psi(0) - \psi(L) > R$ then $x \leq x_1$.

The above considerations lead to the following rules:

---

* A value of $R \geq 50$ is usually sufficient. Currently available digital machines allow a considerably larger value.

(1) for $0 > V_A \geq V_d - R$, i.e. low reverse bias, one cell only is present $(m = 1)$, the parameters Y_{p1} and θ are sufficiently large and equation (2.13) may be computed in its complete form.

(2) for $V_A < V_d - R$ the quantity θ is ignored, and its computation is not attempted; the parameter Y_{pr} is calculated only in the first cell $(r = 1)$ since it becomes insignificant elsewhere.

With the aid of the above rules, Eq.(2.13) is suitable for an accurate numerical computation of $p(x)$, for an arbitrary reverse bias condition.

A similar procedure leads to an expression extended to high reverse bias cases for the electron density. The electrostatic potential range $\psi(0) - \psi(L)$ is divided into cells defined by:

1st cell	$\psi(0) > \psi(x) > \psi'_1$	$(x'_0 \triangleq 0 \leq x < x'_1)$
rth cell	$\psi'_{r-1} \geq \psi(x) > \psi'_r$	$(x'_{r-1} \leq x < x'_r)$, $r = 2, 3, \cdots m-1$
mth cell	$\psi'_{m-1} \geq \psi(x) \geq \psi'_m \leq \psi(L)$	$(x'_{m-1} \leq x \leq x'_m \triangleq L)$

where

$$\left.\begin{aligned} &\psi(0) - \psi'_1 = R \\ &\psi'_{r-1} - \psi'_r = 2R \quad , \quad r = 2, 3, \cdots m \end{aligned}\right\} \qquad (2.14)$$

With the aid of the scale factors

$$\left.\begin{aligned} \psi'_{01} &\triangleq \psi(0) \\ \psi'_{0r} &= \frac{\psi'_r + \psi'_{r-1}}{2} \quad , \quad r = 2, 3, \cdots m \end{aligned}\right\} \tag{2.15}$$

the corresponding modified integral

$$F_{nr}(x) \triangleq \int_0^x e^{\psi'_{0r} - \psi(x')} dx' \quad , \quad x'_{r-1} \le x < x'_r \quad , \quad r = 1, 2, \cdots m \tag{2.15a}$$

may be inserted in Eq.(2.1) to obtain the final expression:

$$n(x) = \left[(1-\theta)\ F_{nr}(x) + Y_{nr}\right] / \left[Z_n e^{\psi'_{0r} - \psi(x)}\right] \tag{2.16}$$

for $\qquad x'_{r-1} \le x < x'_r \quad , \quad r = 1, 2, \cdots m$

where:

$$Y_{nr} \triangleq \left[\frac{F_{nm}(L)}{e^{\psi'_{0m} - \psi(L)}}\right] e^{\psi'_{0r} - \psi(0)}\ n_N\ p_P$$

$$Z_n \triangleq \frac{F_{nm}(L)}{e^{\psi'_{0m} - \psi(L)}}\ p_P$$

and θ is given by relation (2.12).

Considerations similar to those presented in connection with Eq. (2.13) lead to the same rules concerning here the parameters Y_{nr} and θ in Eq.(2.16).

Equations (2.3) and (2.4), or alternatively Eqs.(2.5) and (2.6) for forward bias, and Eqs.(2.13) and (2.16) for any reverse bias condition, represent the improved analytical expressions for the mobile

carrier densities and complete the formulation of the "direct" problem of specifying the applied voltage and solving for the total current and the relevant distributions as functions of position.

The improved formulation for the simplified model is summarized in Table 2.1.

2.3. Numerical techniques.

Once a satisfactory analytical formulation of the problem is achieved, the following phase toward a numerical solution is the discretization of the relevant quantities at a finite number of points. This involves the problem of the distribution of such points throughout the interior of the device, or, in equivalent terms, the determination at each point of the step, defined as the distance between two consecutive points. In addition, appropriate numerical techniques must be devised to approximate the analytical integrations and differentiations of the relevant expressions, and to solve the second order linear differential Eq.(1.45) (essentially Poisson's equation). These topics are analyzed in the following subsections.

2.3.1. Automatically adjustable non-uniform step distribution.

It is quite clear from the expected distributions of most quantities throughout the interior of the device that the choice of a uniform step would hardly be satisfactory. To yield comparable accuracy in the process of discretization, the rapidly varying distributions near the metallurgical interface require a step much smaller than that needed in the quasi-neutral regions. An algorithm capable of an automatic step selection, subject to a preassigned condition, is therefore highly desirable.

FORWARD BIAS

$$n(x) = [F_n(x) + \theta F_{In}(x)] \frac{e^{\psi(x)-\psi(L)}}{p_P F_n(L)} \tag{2.3}$$

$$p(x) = [F_{Ip}(x) + \theta F_p(x)] \frac{e^{\psi(0)-\psi(x)}}{n_N F_{Ip}(0)} \tag{2.4}$$

where: $F_{In}(x) \triangleq \int_x^L e^{-\psi(x')} dx'$; $F_{Ip}(x) \triangleq \int_x^L e^{\psi(x')} dx'$

$F_n(x) \triangleq \int_0^x e^{-\psi(x')} dx'$; $F_p(x) \triangleq \int_0^x e^{\psi(x')} dx'$

$$\theta \triangleq \frac{n_N p_P}{e^{\psi(0)-\psi(L)}} \tag{2.12}$$

REVERSE BIAS

$$n(x) = [(1-\theta)F_{nr}(x) + Y_{nr}]/[Z_n e^{\psi'_{Or}-\psi(x)}] \tag{2.16}$$

$$p(x) = [(1-\theta)F_{pr}(x) + Y_{pr}]/[Z_p e^{\psi(x)-\psi_{Or}}] \tag{2.13}$$

where: $F_{nr}(x) \triangleq \int_0^x e^{\psi'_{Or}-\psi(x')} dx'$; $F_{pr}(x) \triangleq \int_x^L e^{\psi(x')-\psi_{Or}} dx'$

$$Y_{nr} = \begin{cases} \left[\dfrac{F_{nm}(L)}{e^{\psi'_{Om}-\psi(L)}}\right] n_N p_P e^{\psi'_{Or}-\psi(0)} & \text{if} \quad r = 1 \\ 0 & \text{if} \quad r \neq 1 \end{cases}$$

$$Y_{pr} = \begin{cases} \left[\dfrac{F_{pm}(0)}{e^{\psi(0)-\psi_{Om}}}\right] n_N p_P e^{\psi(L)-\psi_{Or}} & \text{if} \quad r = 1 \\ 0 & \text{if} \quad r \neq 1 \end{cases}$$

$$\theta = \begin{cases} \dfrac{n_N p_P}{e^{\psi(0)-\psi(L)}} & \text{if} \quad 0 > V_A \geq V_d - R \\ 0 & \text{if} \quad V_A < V_d - R \end{cases}$$

$Z_n = \left[\dfrac{F_{nm}(L)}{e^{\psi'_{Om}-\psi(L)}}\right] p_P$; $Z_p = \left[\dfrac{F_{pm}(0)}{e^{\psi(0)-\psi_{Om}}}\right] n_N$

ψ_{Or} and ψ'_{Or}, $r = 1, 2, \cdots m$ are scale factors given by relations (2.10), (2.11), and (2.14), (2.15). R is chosen as the largest number that allows $[L\, n_N\, e^R]^{\mp 1}$ and $[L\, p_P\, e^R]^{\mp 1}$ within the permissible range.

Table 2.1. Improved and extended analytical formulation for the simplified model (ohmic contacts, absence of recombination, constant mobilities).

It is apparent from Fig. 1.4 and Table 2.1 that two main operations are present in the iterative scheme: the integration of the functions $e^{\mp \psi(x)}$ and the solution of Poisson's equation. In consideration of the accumulative type of error propagation in the execution of a pointwise integration, the former operation is chosen to dictate the criterion responsible for the selection of the step distribution.

The integration, in the discretized context, will be performed as a sum of a finite number of terms, each computed with the use of an interpolation technique; an error will be introduced in each of such terms, depending upon the magnitude of the step at the correspondent point for a chosen order of interpolating curve. It is of interest to consider the relative error ε_S pertinent to each term, defined as:

$$\varepsilon_S \triangleq \text{relative error of a single term} \triangleq \frac{\text{absolute error}}{\text{magnitude of term}}$$

A step distribution will be considered optimum if it yields the same relative error for each single term; the whole integral will then suffer from the same relative error. If this is specified the correspondent optimum step distribution can be determined by the procedure illustrated schematically in Fig. 2.2. An upper bound S_{Mx} for the step together with the parameter RATIO, the step modifier, may be initially fixed. Starting with the step at its upper bound at the boundary on the left, $(x = 0)$ the whole region is scanned to adjust at each point the step according to the result of the comparison between the actual relative error and the specified one ε_S. When the boundary on the right $(x = L)$ is reached, the step distribution and the total

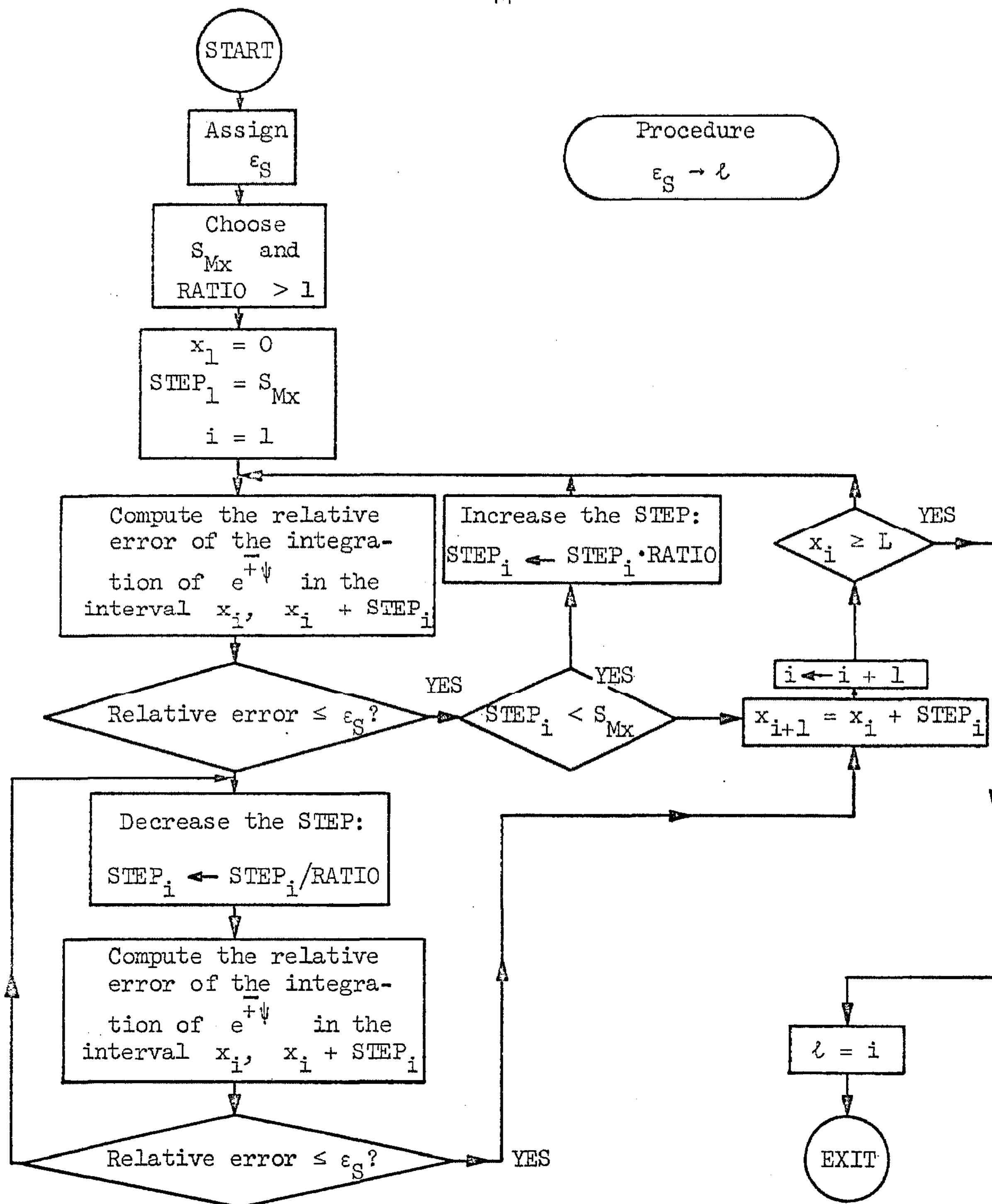

Fig. 2.2. Procedure suitable to obtain the step distribution and the total number of points ℓ, if ε_S is specified.

number of points is obtained.

The two integrands $e^{\mp\psi(x)}$ will in general generate two different step distributions; it is appropriate to choose at each point the most severe step requirement featured by the two distributions.

It is very convenient to proceed one stage further by linking, in reverse order, the relative error ε_S with the desired total number of points ℓ. This latter parameter is directly related to the storage capability of the particular machine available (and to the actual computation time), therefore it may be inserted externally as input DATA to suit the particular needs of the programmer. When ℓ is specified, the problem consists in determining ε_S, which allows then the generation of the step distribution with the aid of the procedure discussed above. This can be achieved with an interpolation scheme of the type illustrated in Fig. 2.3. A few trials with suitable values of ε_S will determine the correspondent ℓ values to surround the required number of points ℓ_R by two ℓ values; at this point successive Lagrangian interpolations may be used on the curve $\varepsilon_S = \varepsilon_S(\ell)$ to complete the search of the relative error $(\varepsilon_S)_R$ correspondent to ℓ_R.

Two different approaches may be taken for the actual pointwise computation of the relative error to be compared with the specified ε_S, depending upon the availability of the function $\psi(x)$ in discretized or analytical form.

(a) The function $\psi(x)$ is available in discretized form only.

At the completion of the jth principal iteration cycle (Fig. 1.2) the electrostatic potential $\psi^{(j+1)}(x)$ is known only at a finite number of points determined by the previous step distribution required by

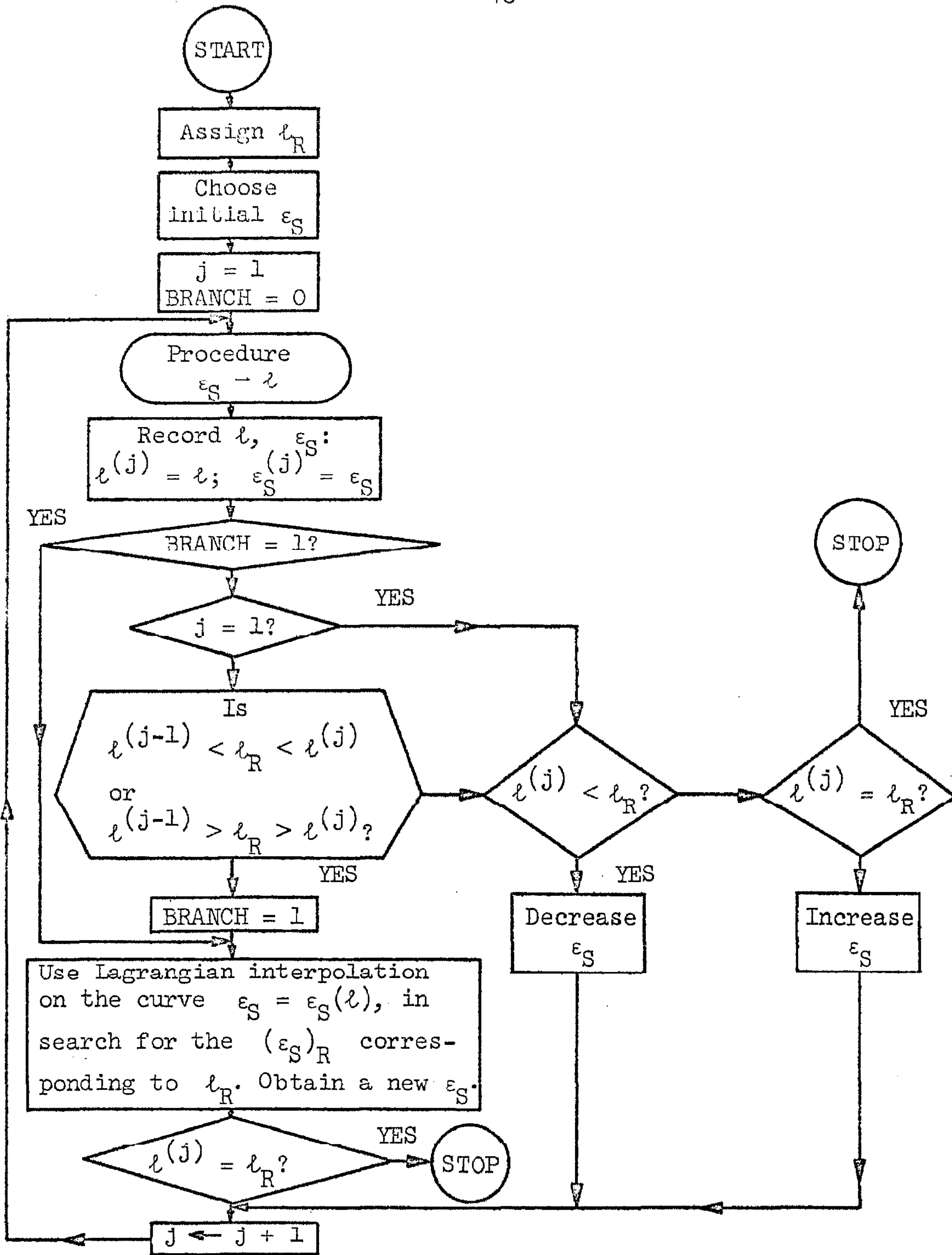

Fig. 2.3. Procedure suitable to obtain the step distribution and the relative error ε_S, if the total number of points ℓ_R is specified.

$\psi^{(j)}(x)$. If the correction $\delta^{(j+1)}(x)$ is significant, a new step distribution may be desirable. In this case the following algorithm may be used to obtain the relative error at each point.

Let S_i be the step at the point of abscissa x_i, defined as

$$S_i \triangleq x_{i+1} - x_i > 0 \quad , \quad i = 1, 2, 3, \cdots \ell-1$$

where $x_1 = 0$, $x_\ell = L$. In the execution of one sweep from 0 to L the steps

$$S_r \quad , \quad r = 1, 2, \cdots i-1$$

are supposed already adjusted to the proper value; the adjustment of the step S_i is sought. Moreover, for simplicity, let the trapezoidal rule be chosen for the numerical integration of the function $f(x)$; an elementary contribution amounts, in the present case, to the area between points x_i, x_{i+1} under the curve $f(x)$ (see Fig. 2.4). This value must be compared with the exact one, which, for all practical purposes, may be computed with the use of a higher order interpolating curve, for example by tracing a cubic through the points f_{i-1}, f_i, f_{i+1}, f_{i+2}, and by integrating it between x_i and x_{i+1} (see Appendix B for explicit relations). Result of the comparison may cause a shift in x_{i+1} to a new position x'_{i+1}; the correspondent value $f'_{i+1} \simeq f(x'_{i+1})$ may then be recovered on the same cubic already employed. A new comparison between linear and cubic integration between the points x_i, x'_{i+1} may now be performed in the search for the step at the point

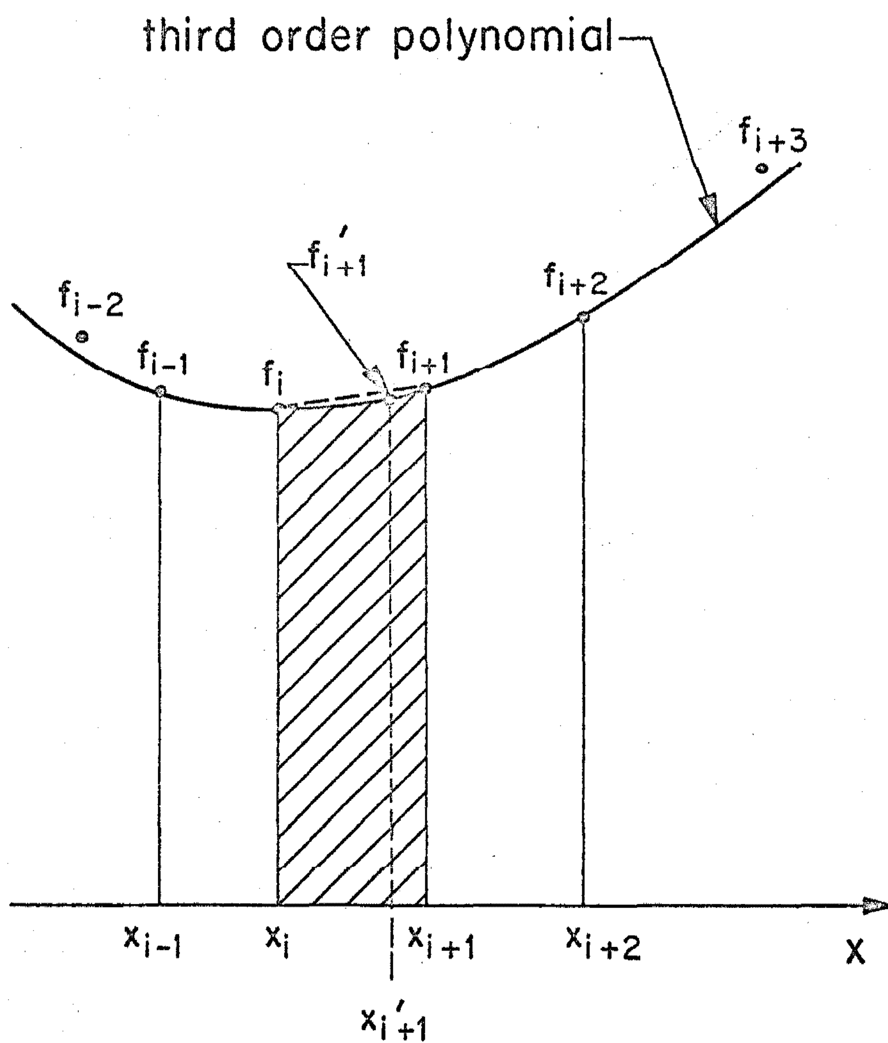

Fig. 2.4. Shift of the point x_{i+1} to achieve the required integration error and determine the step size at the point x_i.

x_i that will yield a relative error approximately equal to the one specified. Once this is achieved, the new point x_{i+1} is determined and the procedure may continue to adjust the next step S_{i+1}.

The scheme may be extended easily to interpolating functions of order higher than linear and cubic, if so desired.

Alternatively it may be more convenient to approximate with an interpolating polynomial directly $\psi(x)$, rather than the functions $e^{\mp \psi(x)}$; this would indeed be the case for a structure close to that considered in Appendix A, which displays a first-order parabolic distribution of $\psi(x)$ in the transition region. The above procedure requires then only a minor alteration.

(b). <u>The function $\psi(x)$ is available in analytical form.</u>

If the trial potential function is chosen in analytical form and the selection of the optimum step distribution is performed only once, before the first iteration, the costly procedure discussed in the previous Section may be considerably simplified. It is then implicitly assumed that the corrections $\delta^{(j)}(x)$ obtained after each Poisson's iteration will not be of such magnitude to require a significant alteration in the original step distribution.

To illustrate an example, let the trial potential function be represented by the first-order potential distribution for an abrupt N-P asymmetric junction with uniform doping (see Appendix A). Such a trial function will then display the square-law spatial dependence of Eqs.(A-36), (A-37) (of Appendix A) in the transition region, logarithmic dependence in the neutral region in the low conductivity side and constancy in the neutral region in the high conductivity side.

Let the relative radius of curvature of a function $f(x)$ at a point x_0 be:

$$R_{curv,rel}(x_0) \triangleq \frac{f(x_0)}{\left.\frac{d^2f(x)}{dx^2}\right|_{x=x_0}}$$

From an intuitive point of view it is clear that the relative radius of curvature of the functions $e^{\mp\,\psi(x)}$ is somehow related to the required step distributions: the smaller the relative radius of curvature at a particular point, the smaller must there be the step. It would be desirable to find an explicit relationship between the two quantities.

Let the transition region be considered first. With reference to Fig. A-1, the functions of interest are given by Eqs.(A-36), (A-37) as:

$$f_N^{\mp} \triangleq e^{\mp\,\psi} = \exp\left\{\mp\left[-\frac{N_D z^2}{2} + \psi(M_N)\right]\right\} \quad ; \quad z \triangleq x - M_N > 0$$

in the N transition region, and

$$f_P^{\mp} \triangleq e^{\mp\,\psi} = \exp\left\{\mp\left[\frac{N_A y^2}{2} + \psi(M_P)\right]\right\} \quad ; \quad y \triangleq M_P - x > 0$$

in the P transition region. From these one obtains:

$$\frac{d^2 f_N^{\mp}}{dz^2} = N_D(N_D z^2 \pm 1)\, f_N^{\mp}$$

$$\frac{d^2 f_P^{\mp}}{dy^2} = N_A(N_A y^2 \mp 1)\, f_P^{\mp}$$

and:

$$R^{\mp}_{curv,rel,N} \triangleq \frac{f_N^{\mp}}{\frac{d^2 f_N^{\mp}}{dz^2}} = \frac{1}{N_D(N_D z^2 \pm 1)} \tag{2.17}$$

$$R^{\mp}_{curv,rel,P} \triangleq \frac{f_P^{\mp}}{\frac{d^2 f_P^{\mp}}{dy^2}} = \frac{1}{N_A(N_A y^2 \mp 1)} \tag{2.18}$$

The functions with the smallest relative radius of curvature in each region are then:

$$f_N^{-} = e^{-\psi} = \exp\left[\frac{N_D}{2} z^2 - \psi(M_N)\right] \tag{2.19}$$

$$f_P^{+} = e^{+\psi} = \exp\left[\frac{N_A}{2} y^2 + \psi(M_P)\right] \tag{2.20}$$

Let the step S_i at point i be tested with the comparison between trapezoidal and Simpson's rules for the computation of the ith term Q_i in the pointwise execution of the integral $\int_0^{x_i} f(x)\,dx$. With reference to Fig. 2.5 one obtains:

$$(Q_i)_{trapezoidal} = (f_i + f_{i+1})\, S_i/2 \tag{2.21}$$

$$(Q_i)_{Simpson} = (f_i + 4f_{i+1/2} + f_{i+1})\, S_i/6 \tag{2.22}$$

After completion of the adjustment of the step S_i to meet the

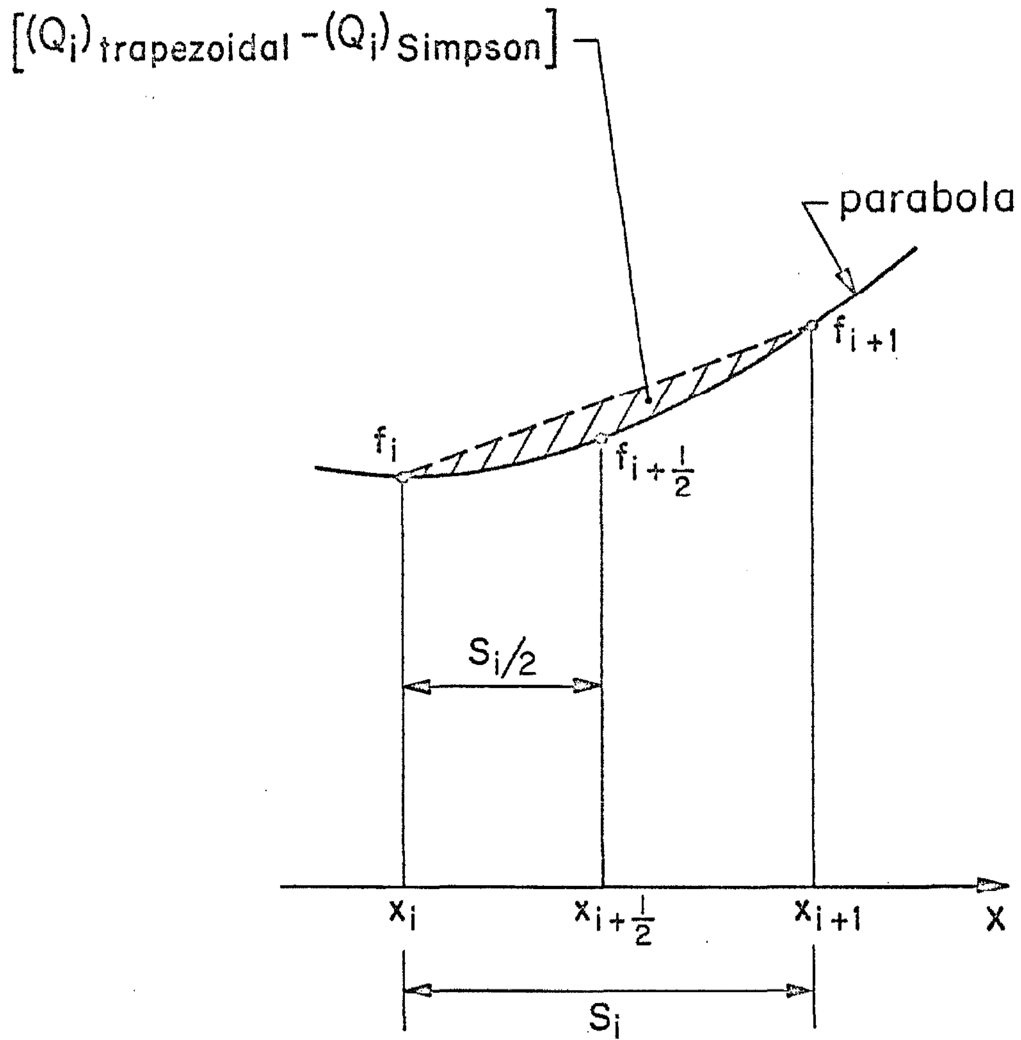

Fig. 2.5. Determination of the error of the pointwise integration of an elementary interval.

requirement dictated by the specified relative error ε_S, the following relation will be valid:

$$\varepsilon_S = \left| \frac{(Q_i)_{trapezoidal} - (Q_i)_{Simpson}}{(Q_i)_{trapezoidal}} \right| =$$

$$= \frac{2}{3} \frac{f_i - 2 f_{i+1/2} + f_{i+1}}{f_i + f_{i+1}} \qquad (2.23)$$

where relations (2.21), (2.22) have been used.

Otherwise, if the simple three-point formula to approximate the curvature at the point $x_{i+1/2}$ is chosen,

$$R_{curv,rel}\Big|_{x=x_{i+1/2}} = \frac{f_{i+1/2}}{\left.\frac{d^2f}{dx^2}\right|_{x=x_{i+1/2}}} = \frac{f_{i+1/2}}{f_i - 2 f_{i+1/2} + f_{i+1}} \left(\frac{S_i}{2}\right)^2$$

which may be inserted in Eq.(2.23) to obtain

$$S_i = \sqrt{6 \ \varepsilon_S \cdot (R_{curv,rel})_{i+1/2} \ \frac{f_i + f_{i+1}}{f_{i+1/2}}} \qquad (2.24)$$

Moreover, for a function of the type

$$f(u_i) = \exp(K \ u_i^2 + \text{constant}) \quad ; \quad K = \text{constant} > 0 \quad , \quad u_i > 0$$

and for $S_i = u_{i+1} - u_i > 0$ the following holds:

$$\frac{f_i + f_{i+1}}{f_{i+1/2}} = \frac{\exp[Ku_i^2] + \exp[K(u_i + S_i)^2]}{\exp[K(u_i + S_{i/2})^2]} = \exp\left[-\frac{KS_i^2}{4} - KS_iu_i\right] +$$

$$+ \exp[\tfrac{3}{4} KS_i^2 + KS_iu_i] > \exp[- KS_iu_i] + \exp[+ KS_iu_i] >$$

$$> (1 - KS_iu_i) + (1 + KS_iu_i) = 2 \qquad (2.25)$$

If the above result is applied to Eqs.(2.19), (2.20) it may be observed that the first inequality of relation (2.25) becomes, for all practical purposes, an equality in most of the transition region (where $u_i \gg S_i$), with exception of a short region near the origin $u = 0$ where S_i becomes comparable to u_i. The second inequality also reduces essentially to an equality if the following condition is satisfied:

$$(KS_iu_i)^2 \ll 1 \qquad (2.26)$$

If this is the case, then with the aid of relations (2.17), (2.18), (2.24), (2.25) (replacing $R_{curv,rel}\Big|_{x=x_{i+1/2}}$ with $R_{curv,rel}\Big|_{x=x_i}$) one obtains:

$$\text{N transition region:} \quad S_i = \left[\frac{12\ \varepsilon_S}{N_D(N_D z_i^2 + 1)}\right]^{1/2} ; \quad (z_i = x_i - M_N) \qquad (2.27)$$

$$\text{P transition region:} \quad S_i = \left[\frac{12\ \varepsilon_S}{N_A(N_A y_i^2 + 1)}\right]^{1/2} ; \quad (y_i = M_P - x_i) \qquad (2.28)$$

The condition (2.26), with the aid of relations (2.27), (2.28) and with the substitution

$$K = \begin{cases} N_{D}/2 & \text{in the } N \text{ region} \\ N_{A}/2 & \text{in the } P \text{ region} \end{cases}$$

may be written as:

$$\varepsilon_S \ll \frac{1}{3} + \frac{1}{6Ku^2}$$

which is certainly satisfied, since reasonable values of ε_S are several orders of magnitude below unity.

Equations (2.27), (2.28) yield then an explicit expression for the step distribution in the transition region in terms of the relative error ε_S. This relationship was derived with the implicit agreement of accepting a slightly more severe requirement for a few steps near the points M_N, M_P (in virtue of the first inequality of relation (2.25)), which is certainly a negligible drawback.

From Eqs. (2.27), (2.28) it can easily be observed that the smallest step in each region occurs at the metallurgical interface M. With the aid of relations (A-38), (A-39), the step values at $x = M$, approached by both regions, are obtained as:

$$(S_M)_{N\text{-region}} = \left[6\varepsilon_S \cdot \left(\frac{\psi(M_P) - \psi(0)}{\frac{1}{N_D} + \frac{1}{N_A}} + \frac{N_D}{2} \right)^{-1} \right]^{1/2} \qquad (2.29)$$

$$(S_M)_{P\text{-region}} = \left[6\varepsilon_S \cdot \left(\frac{\psi(M_P) - \psi(0)}{\frac{1}{N_A} + \frac{1}{N_D}} + \frac{N_A}{2} \right)^{-1} \right]^{1/2} \qquad (2.30)$$

which locate the smallest step at the interface M on the side of higher impurity concentration.

Similar considerations may be applied to the low conductivity neutral region, where Eq.(A-16) is valid. The functions of interest will then be:

$$F_P^{\mp} \triangleq e^{\mp\psi} = \left[e^{\psi(L)} (1 + \beta v_i) \right]^{\pm 1}$$

where

$$\beta \triangleq \frac{\chi - n_P^2}{L - M_P} \quad ; \quad \chi \triangleq \frac{n(M_P)}{p_P} \quad \text{(injection parameter)}$$

$$v_i \triangleq L - x_i$$

The relative ratios of curvature become:

$$R_{curv,rel,P} = \frac{F_P^{\mp}}{\frac{d^2 F_P^{\mp}}{dv^2}} = \begin{cases} \infty \\ \frac{(1 + \beta v_i)^2}{2\beta^2} \end{cases} \qquad (2.31)$$

so that only the function $e^{+\psi}$ deserves further attention. Moreover:

$$\frac{(F_P^+)_i + (F_P^+)_{i+1}}{(F_P^+)_{i+1/2}} = \frac{\frac{1}{1+\beta v_i} + \frac{1}{1+\beta(v_i+S_i)}}{\frac{1}{1+\beta(v_i+\frac{S_i}{2})}} =$$

$$= 2\left[1 + \frac{\left(\frac{\beta S_i}{2}\right)^2}{(1+\beta v_i)^2 + \beta S_i(1+\beta v_i)}\right] > 2 \tag{2.32}$$

It may be observed that if the condition

$$(\beta S_i)^2 \ll 1 \tag{2.33}$$

is valid, the inequality (2.32) becomes essentially an equality throughout the entire region. In this case, with aid of relations (2.24), (2.31), (2.32) an explicit expression for the step distribution may be obtained:

$$(S_i)_{\substack{\text{neutral}\\ \text{P-region}}} = \sqrt{6\varepsilon_S} \cdot \left(\frac{1}{\beta} + v_i\right) \quad ; \quad v_i = L - x_i \tag{2.34}$$

The inequality (2.33) may now be verified, with aid of Eq.(2.34). The relation

$$(\beta S_i)^2 \leq (\beta S_i)^2_{x_i = M_P} = 6\varepsilon_S \cdot [1 + (\chi - n_P^2)]^2$$

leads to

$$\varepsilon_S \ll \frac{1}{6} \cdot [s + (\chi - n_P^2)]^{-2}$$

which is usually satisfied.

For a given bias condition, the step increases linearly, in the low conductivity neutral region, from the minimum value

$$(S_i)_{x=L} = \frac{\sqrt{6\varepsilon_S}}{\beta} \tag{2.35}$$

at $x = L$, to the maximum

$$(S_i)_{x=M_P^+} = \sqrt{6\varepsilon_S}\,(\frac{1}{\beta} + L - M_P)$$

at $x = M_P$ (at the neutral region side). The above quantity may be compared to the corresponding value in the transition region, given by Eq.(2.28) as

$$(S_i)_{x=M_P^-} = \sqrt{6\varepsilon_S}\sqrt{\frac{2}{N_A}} ,$$

to observe that, for usual structure parameters*, the step at the transition region side of the boundary $x = M_P$ is considerably lower than that at the neutral region side. It may also be observed from relation (2.35) that the step at the external contact $x = L$ is inversely proportional to the injection parameter, in forward bias condition.

In the high conductivity neutral region the assumed constancy of $\psi(x)$ would generate a step of infinite magnitude, which would also

---

* With exception of extremely narrow low conductivity neutral regions or conductivities close to the intrinsic value.

occur in the low conductivity neutral region for small enough injection parameter. This situation is of course taken care of by establishing an upper bound for the step. An upper bound on the ratio of consecutive steps may also be introduced to limit the loss of accuracy due to the various interpolations involved in the discretization process of the pertinent integrations and differentiations.

The foregoing results suggest then the scheme shown in Fig. 2.6, suitable to obtain the optimum step distribution and the total number of points, for a specified relative error ε_s. For illustration purposes the structure of Fig. A-1 is chosen, with the N-region on the left and $N_D \gg N_A$. The metallurgical interface M is the starting point, where relation (2.29) furnishes the initial step value. The scanning is performed first in the N region toward the external boundary 0. The determination of the step in the transition region by relation (2.27) is followed by the test on the ratio of consecutive steps. If such a ratio exceeds the maximum allowed RATMX, the step will be modified to suit this additional requirement; such modification will always result in a step decrease, since the generating functions (2.27) and (2.28) are monotonically increasing with $|x - M|$. Comparison with the upper bound S_{Mx} is then performed, before the step is permitted to modify the x coordinate; the cycle may now be repeated until the boundary 0 is reached. The same scheme is used in the P-transition starting again at $x = M$, with the same initial value for the step previously employed (Eq.(2.29)). When either the upper bound for the step or the external contact L is reached, a similar procedure starts at $x = L$ to scan backwards the P-neutral region and to provide proper matching of the

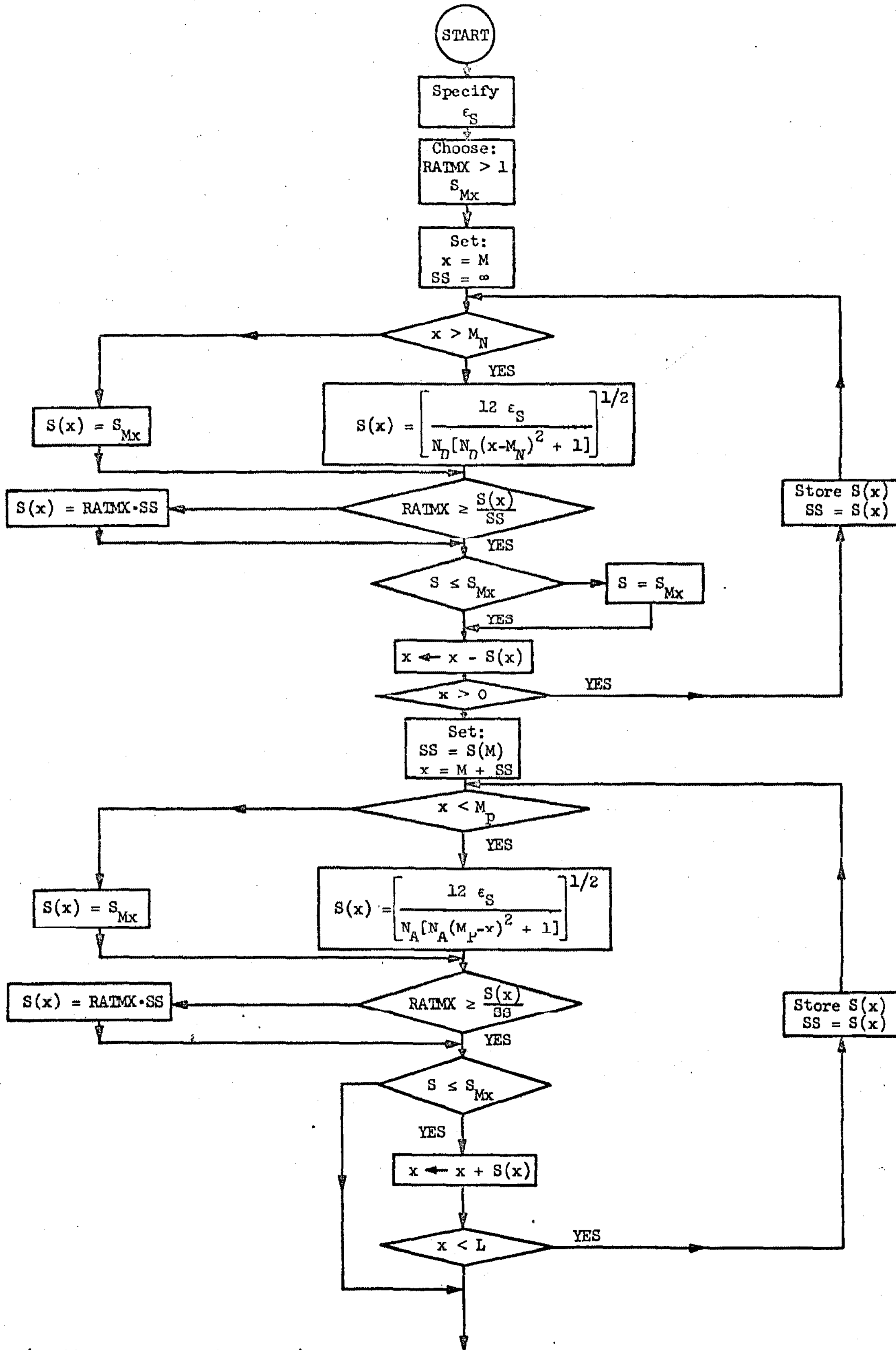

(Continued on following page.)

(Continued from previous page.)

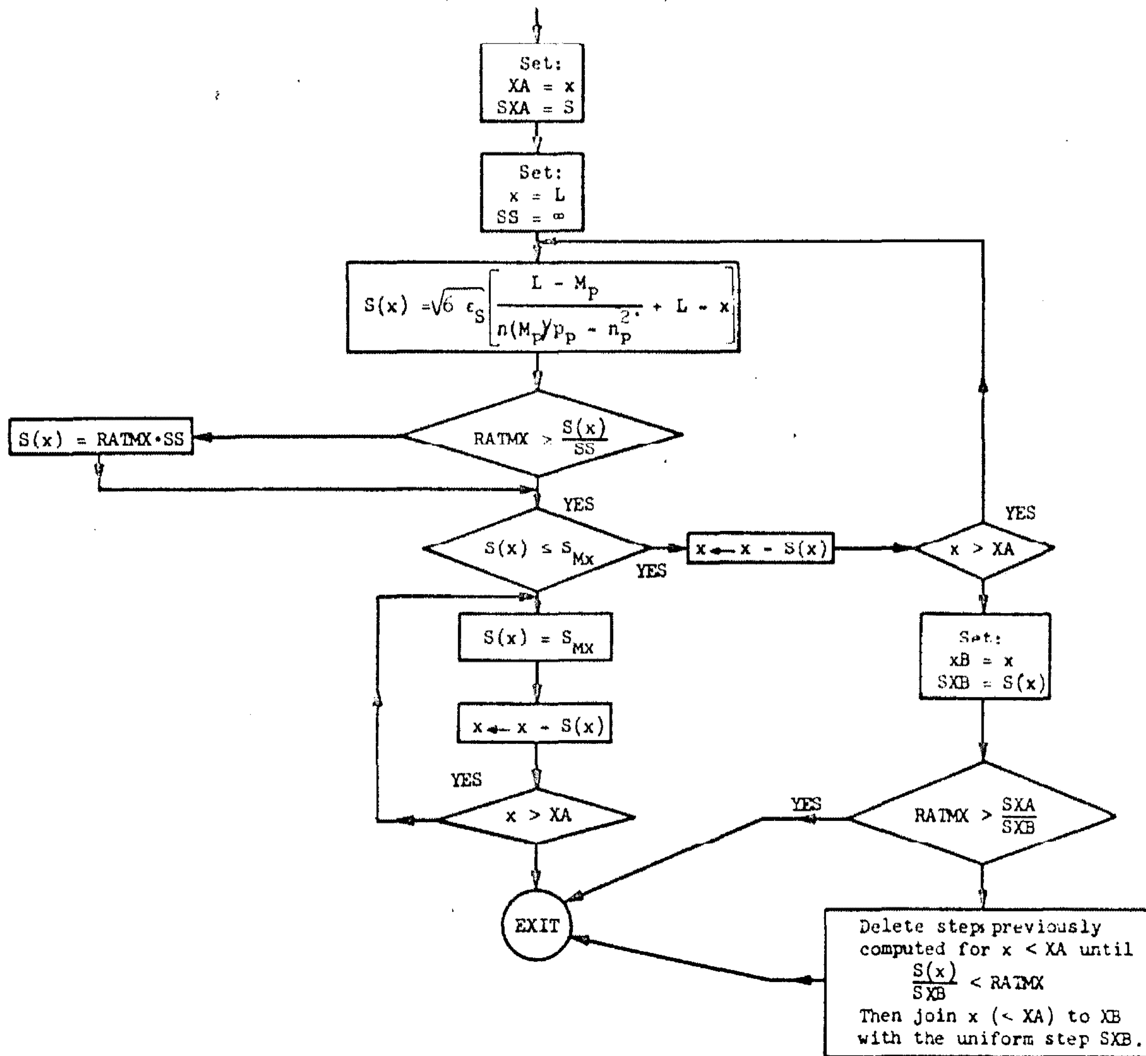

Fig. 2.6. Procedure suitable to obtain the step distribution for a specified error ϵ_S, on the basis of a trial potential function given in analytical form for a special case.

step distributions in the transition and neutral regions, subject to the requirement dictated by the upper bound of the ratio between consecutive steps.

An example displaying the result of the above procedure is illustrated in Fig. 2.7 for a highly asymmetric abrupt N-P junction with uniform doping under a high injection condition (number of points specified $\ell = 1000$, RATMX = 1.05, $S_{Mx} = L/200$). The step distribution (in semi-logarithmic axis) and the trial potential function are shown as functions of position x. The various regions are readily recognizable; the variation of the step size over a wide range throughout the entire device is enlightening.

The above procedure represents an example of how the rather lengthy scheme required for case (a) may be reduced to a much simpler one, with a resulting decrease in computation time of one or more orders of magnitude. This is achieved with the agreement of selecting only once the step distribution on the trial potential function, which is supposed to be given in analytical form and reasonably close to the exact one.

2.3.2. Numerical integration and differentiation.

Now that the criteria for the selection of the automatically adjustable non-uniform step distribution throughout the interior of the device have been stated, the problem of choosing suitable numerical techniques to approximate the analytical integrations and differentiations of interest is considered. In the numerical execution of such operations an error is usually introduced, which often arises from truncating an infinite series at a convenient point. Therefrom this

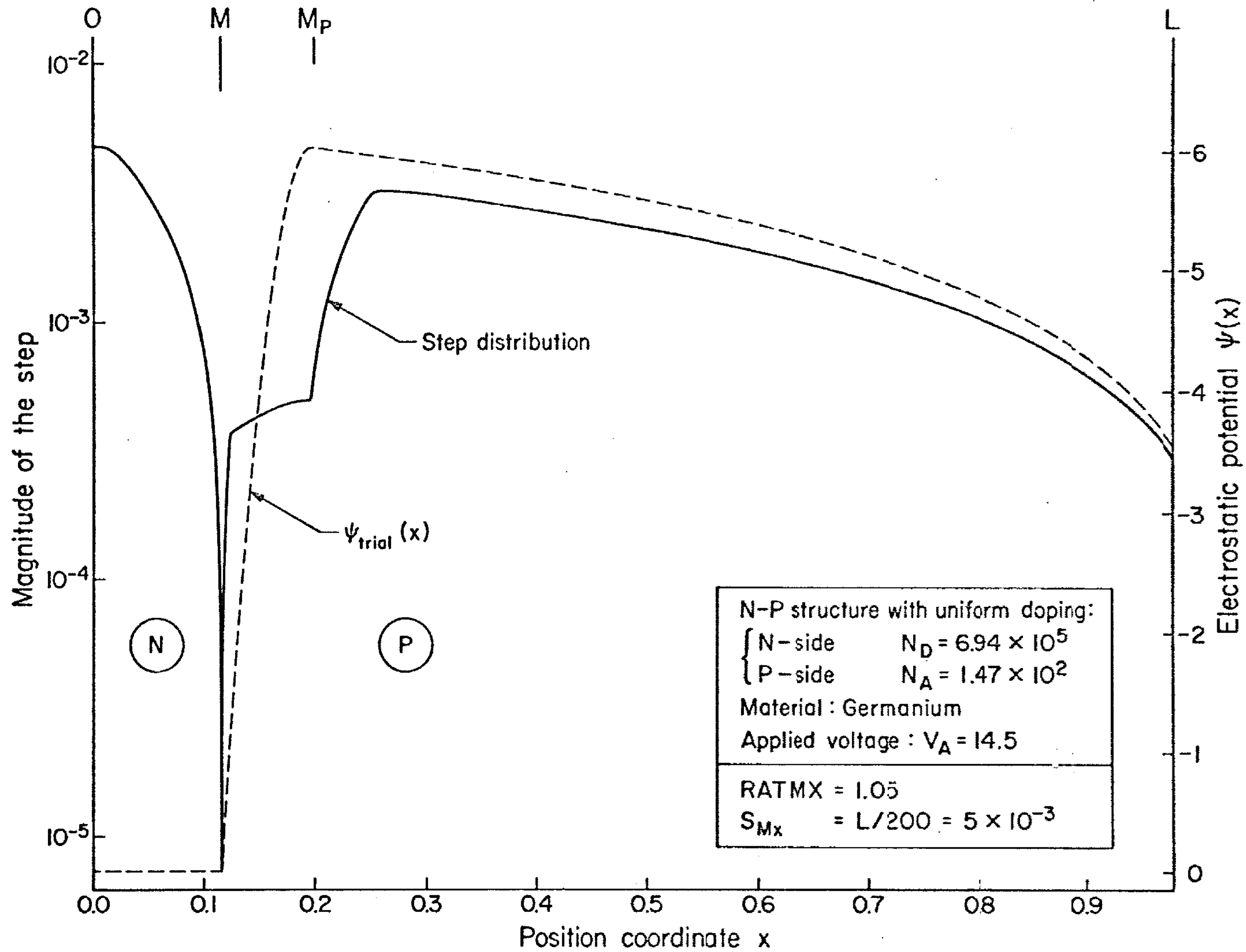

Fig. 2.7. A typical spatial step distribution generated by a trial potential function $\psi_{trial}(x)$ available in analytical form, for a special case.

error is referred to as "truncation error" or, more generally, "discretization error." This is very much dependent upon the value of higher derivatives, very sensitive, in the problem under consideration, to the abruptness of the junction, i.e. the specified doping profile. It is therefore desirable to employ an algorithm, for the numerical integrations and differentiations, of a considerable degree of flexibility, to permit a significant control of the discretization error once the device parameters, the total number of points, and the criteria for the step selection are specified.

Also in consideration of the availability of the relevant quantities solely in a discretized form with a non-uniform step distribution, a simple but efficient numerical technique based on a Lagrangian interpolation scheme is chosen. This determines numerically a polynomial of appropriate degree that approximates locally the quantities available at an unequally spaced array of points; the integrated or differentiated analytical form of this polynomial is then readily computed. Higher order interpolating schemes may be selected to reduce the discretization error within certain limits. Since the numerical error (mostly introduced by the usual problem of small differences between nearly equal numbers arising in any finite difference.algorithm) increases for increasing order of the interpolation scheme, a compromise must be usually reached. Another limitation is represented by the rapid increase in the number of elementary operations (or computation time) for an increase of the order of interpolating scheme.

Details of the algorithm are reported in Appendix B for various orders of interpolating schemes of practical interest.

It may also be observed that the use of different interpolating functions (other than a polynomial, for instance exponentials), although of great interest, is likely to require prohibitive computation times, if a sufficient number of points in the interior of the device is employed.

2.3.3. Numerical solution of Poisson's equation.

Poisson's equation in the original form (1.19) has been rearranged to Eq.(1.45), in terms of the correction $\delta(x)$ for the electrostatic potential distribution.

To solve the second order linear differential Eq.(1.45) in the unknown $\delta^{(j+1)}(x_i)$, with boundary conditions

$$\delta^{(j)}(0) = \delta^{(j)}(L) = 0 \quad , \tag{2.36}$$

several numerical techniques are available. The method of approximating the analytical derivatives with a finite difference scheme, followed by the solution of a system of linear algebraic equations, applies in a straightforward fashion to the present case in which the relevant quantities are already discretized with a non-uniform step distribution. Equation (1.45) may be rewritten for the internal point i as:

$$\left.\frac{d^2\delta}{dx^2}\right|_{x=x_i} - \delta_i(n_i + p_i) = -\left.\frac{d^2\psi}{dx^2}\right|_{x=x_i} + n_i - p_i - N_i \tag{2.37}$$

where the iteration index (j) has been omitted for conciseness. The second derivative of ψ with respect to x, at the point i, may be computed numerically with one of the finite difference schemes

illustrated in Appendix B (3-point, or higher order formulae) so that the right hand side of Eq.(2.37) at an internal point i may be considered numerically known.

If the second derivative of the unknown δ is expressed with the 3-point finite difference formula B-12, Eq.(2.37) at the point i reduces to:

$$\alpha_i \delta_{i-1} - [(\alpha_i + 1) + \eta_i(n_i + p_i)] \; \delta_i + \delta_{i+1} = d_i \qquad (2.38)$$

where:

$$S_i \triangleq x_{i+1} - x_i \quad ; \quad \alpha_i \triangleq S_i/S_{i-1} \quad ; \quad \eta_i \triangleq S_i(S_i + S_{i-1})/2$$

$$d_i \triangleq \left\{ - \left[\frac{d^2\psi}{dx^2} \right]_{x=x_i} + n_i - p_i - N_i \right\} \cdot \eta_i$$

The ensemble of Eqs.(2.38) written at each internal point

$$i = 2, 3, 4, \cdots \ell\text{-}1$$

represents a system of $\ell-2$ linear algebraic equations in the $\ell-2$ unknowns δ_i, with the additional conditions at the boundaries:

$$\delta_1 = \delta_\ell = 0$$

In vector notation:

$$T \; \delta = d \qquad (2.39)$$

where:

$$\delta \triangleq \begin{pmatrix} \delta_2 \\ \delta_3 \\ \cdot \\ \cdot \\ \cdot \\ \delta_{\ell-1} \end{pmatrix} \quad \text{is the unknown vector}$$

$$d \triangleq \begin{pmatrix} d_2 \\ d_3 \\ \cdot \\ \cdot \\ \cdot \\ d_{\ell-1} \end{pmatrix} \quad \text{is the known vector}$$

and

$$T = \begin{pmatrix} [(\alpha_2+1) + \eta_2(n_2+p_2)] \, , \, 1, \, 0, \, 0 \cdots \\ \cdots\cdots \\ \cdots \, 0, \, 0, \, \alpha_i \, , \, -[(\alpha_i+1) + \eta_i(n_i+p_i)] \, , \, 1, \, 0, \, 0 \cdots \\ \cdots\cdots \\ \cdots \quad 0, \, 0, \, \alpha_{\ell-1} \, , \, -[(\alpha_{\ell-1}+1) + \eta_{\ell-1}(n_{\ell-1}+p_{\ell-1})] \end{pmatrix}$$

is a triple-diagonal matrix of dimension $(\ell-2)$ with known entries.

The numerical solution of the system of Eq.(2.39) may be achieved with two basically different methods: direct or iterative. The former is based on Gaussian elimination and back-substitution, the latter on the successive correction of an initial trial solution with an iterative scheme. Although several iterative methods are available featuring a very fast convergence and allowing a precise control of the accuracy desired, the direct method is preferred in the present case, in

consideration of the sparse character of the matrix T (purely triple-diagonal) and of the small error introduced in such an operation (mostly round-off) which is certainly not the dominant error of the whole solution.*

For a tridiagonal matrix the direct method reduces to the very simple and elegant algorithm summarized below [see, for instance, Ref. 20 pp.101-103]. Let the set of linear algebraic equations be represented as

$$a_i \, \delta_{i-1} + b_i \, \delta_i + c_i \, \delta_{i+1} = d_i \quad , \quad i = 2, 3, \cdots \ell-1 \qquad (2.40)$$

with boundaries $\delta_1 = \delta_\ell = 0$. The solution of such a system of difference equations is uniquely determined if two values of δ_i are given (for example the values at the boundaries). It will therefore be pertinent to seek two quantities g_i, h_i such that

$$\delta_i = g_i - h_i \, \delta_{i+1} \quad , \quad i = \ell-1, \ell-2, \cdots 1 \qquad (2.41)$$

Application of the first boundary, $\delta_1 = 0$, yields

$$g_1 = h_1 = 0 \qquad (2.42)$$

---

* Computation time and availability of core memory in the machine are certainly in favor of the direct method.

Substitution of

$$\delta_{i-1} = g_{i-1} - h_{i-1}\,\delta_i$$

in the difference Eq.(2.40) yields:

$$\delta_i = \frac{d_i - a_i\, g_{i-1}}{b_i - a_i\, h_{i-1}} - \frac{c_i}{b_i - a_i\, h_{i-1}}\ , \quad i = \ell-1,\ \ell-2 \cdots 2$$

so that it is immediately possible to identify

$$\left.\begin{aligned} g_i &= \frac{d_i - a_i\, g_{i-1}}{b_i - a_i\, h_{i-1}} \\ h_i &= \frac{c_i}{b_i - a_i\, h_{i-1}} \end{aligned}\right\} \quad i = 2,\ 3,\ \cdots\ \ell-1 \qquad (2.43)$$

Recursively then, the quantities g_i, h_i may be determined from relations (2.42), (2.43), to compute subsequently all the unknowns δ_i with the aid of Eq.(2.41).

Moreover, for the present case, the following inequalities hold:

$$a_i > 0\ ,\quad b_i < 0\ ,\quad c_i > 0\quad ,\quad i = 2,\ 3,\ \cdots \ell-1$$

$$|b_i| > a_i + c_i$$

with:

$$a_i = S_i \quad , \quad c_i = S_{i-1}$$

$$b_i = -\,[(S_i+S_{i-1}) + \eta_i(n_i+p_i)]\quad ;$$

it may then be shown that the quantities g_i, h_i very conveniently stay in scale.

For the special case of a tridiagonal matrix with the upper diagonal elements equal to unity (this is indeed the case for the matrix T of Eq.(2.39)) the above scheme may be reduced to the following:

solution of $a_i \delta_{i-1} + b_i \delta_i + \delta_{i+1} = d_i$, $i = 2, 3, \cdots \ell-1$ (2.44)

with boundaries $\delta_1 = \delta_\ell = 0$

given by

$$\begin{cases} h_2' = b_2 \quad , \quad g_2 = \dfrac{d_2}{b_2} \\ \left.\begin{aligned} h_i' &\triangleq b_i - a_i/h_{i-1}' \\ g_i &= (d_i - a_i\, g_{i-1})/h_{i-1}' \end{aligned}\right\} \quad i = 3, 4, \cdots \ell-1 \\ \delta_i = g_i - \delta_{i+1}/h_i' \quad , \quad i = \ell-1, \ell-2, \cdots 2 \end{cases} \quad (2.45)$$

The efficiency of the method is apparent: only four multiplications (or divisions) per point are required, and only three vectors of dimensions ℓ are needed for storage if the coefficients a_i, b_i, d_i need not be conserved.*

Once δ has been obtained with the direct method described, the error introduced may be easily tested, for example by comparison of the

---

* This may be achieved, for instance, by assigning the same storage locations to δ_i, d_i, g_i and to b_i, h_i'.

vector $T\delta$ with the known vector d. Whenever the entity of such error becomes significant*, an iterative method may be easily inserted in the program (see Appendix C) to replace the direct one.

It is important to observe that the discretization error pertinent to the solution of Poisson's equation is solely related to the order of the finite difference formula that approximates the quantity

$$\left[\frac{d^2\psi(x)}{dx^2}\right]_{x=x_i}$$

of Eq.(2.37), and is not connected in any way to the truncation error introduced by the numerical evaluation of

$$\left[\frac{d^2\delta(x)}{dx^2}\right]_{x=x_i}$$

for small enough δ. This is indeed the case if convergence of the iterative scheme occurs (and this is the prime requirement for the validity of the whole procedure), in which case $\delta_i \to 0$ at each point i, for a large enough number of iterations. It may be concluded that the choice of a 3-point formula to approximate the curvature of the unknown δ is in no way restrictive, so that the triple-diagonal structure of the matrix T may be conserved if higher order finite difference schemes are employed for the computation of $d^2\psi(x)/dx^2$, in order to reduce the truncation error.

---

* This has never been observed to be the case.

In consideration of the much heavier computational load involved in the handling of a band matrix wider than a triple-diagonal, the above feature acquires particular value.

2.4. Computer program for a special case.

Several alternatives have been presented in Chapter I regarding the physical model on which various schemes of solutions are based; other alternatives have been discussed in the previous sections concerning the numerical aspect of the solution of the relevant equations.

Choices between the various possibilities have been made to construct a program and perform a series of illuminating calculations on a digital computer. Table 2.2 is intended to summarize all the alternatives mentioned, and to indicate clearly those chosen to be incorporated in the program reported in Appendix C (coded in Fortran IV, version 4).

A special effort has been made in sectioning the program, in the coded context, into several subdivisions or subprograms, each featuring a set of operations logically separated from the remainder. Such a modular characteristic offers several programming advantages; among them the possibility of performing substitutions of one or more subprograms, if alternatives other than the chosen are desired.

Results of calculations performed on an IBM shared file system, which includes the computers 7094 and 7040, will be presented in a later chapter.

2.5. Conclusion.

Difficulties of fundamental and practical nature, arising in the numerical analysis of the original formulation of Chapter I, have been

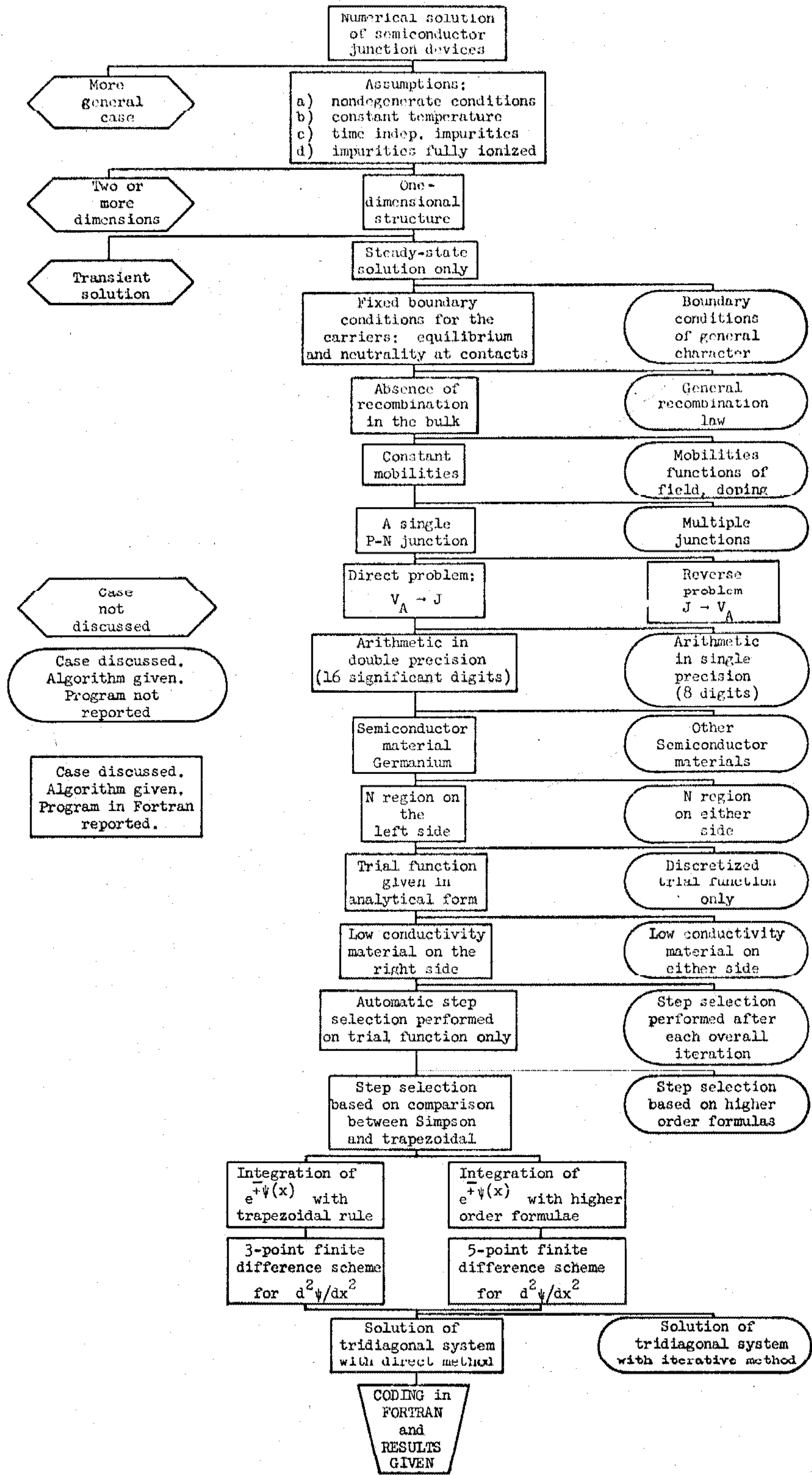

Table 2.2. Illustration of the various alternatives: the central column displays those actually incorporated in the program reported in Appendix C.

exposed and overcome by an improved and extended analytical formulation.

Numerical techniques suitable for the discretization of the problem have been discussed. Criteria for the selection of an automatically adjustable non-uniform step distribution, numerical methods for the execution of integrations and differentiations and for the solution of Poisson's equation have been presented.

A satisfactory rate of convergence to the exact solution for successive iterations is clearly the prime requirement for the success of the described procedure. In all cases tested on the computer, for a wide range of structure parameters and injection levels, a good convergence rate has been observed, even for quite poor trial potential functions.

A basic program, written in a highly modular fashion for a special structure, has been reported*; its flexibility allows prompt alterations in case incorporation of different numerical schemes or extension to more general cases are desired.

As an example, the use of the basic program in two different applications will be described in the following Chapter: the computation of the total incremental capacitance of the device, and a solution for the reverse problem $(J \rightarrow V_A)$.

---

* The organization of the program and coding details are gathered in Appendix C.

CHAPTER III

TWO SIMPLE APPLICATIONS OF THE BASIC DIRECT PROGRAM

3.1. Generalities.

In Chapters II and III an iterative scheme for the direct problem has been described and a basic computer program has been written to achieve the complete solution of the junction for a specified applied voltage.

As an example of the application of the basic program in two slightly more intricate schemes, an algorithm for the computation of the total incremental capacitance of the device is illustrated, and a solution for the "reverse" problem is presented (the terminal voltage and quantities in the interior of the device are sought for a specified total current). The former task requires two successive solutions for slightly different values of applied voltage, the latter is solved with the combination of the basic direct program and an interpolation scheme on the exact current-voltage characteristic.

3.2. Computation of the total incremental capacitance.

If Q is the total charge (of one polarity, per unit area) in the device, the incremental capacitance C (per unit area) at a specified voltage $V = V_A$ may be defined as:

$$C\Big|_{V=V_A} = \frac{dQ}{dV}\Big|_{V=V_A} \tag{3.1}$$

The neutrality condition on the entire device implies the presence of sheets of charge at the external contacts if the interior exhibits an overall unbalance of charges. Poisson's Eq.(1.19) written in integral

form in terms of the electric field at the contacts

$$\int_0^L [p(x)-n(x)+N(x)]dx = E(L) - E(0)$$

may be differentiated with respect to the applied voltage, to obtain

$$\left[\frac{d}{dV}\int_0^L p(x)dx\right]_{V=V_A} - \left[\frac{d}{dV}\int_0^L n(x)dx\right]_{V=V_A} = \left\{\frac{d}{dV}\,[E(L) - E(0)]\right\}_{V=V_A} \qquad (3.2)$$

The term on the right side of Eq.(3.2) represents the contribution of the surface charge at the terminals to the total capacitance. If this term may be neglected* the relation (3.1) becomes:

$$C\Big|_{V=V_A} = \left[\frac{d}{dV}\int_0^L p(x)dx\right]_{V=V_A} = \left[\frac{d}{dV}\int_0^L n(x)dx\right]_{V=V_A} \qquad (3.3)$$

If a two-point formula is chosen for the discretization of the above derivatives, one obtains:

$$C\Big|_{V=V_A} = \int_0^L \frac{p'(x)-p(x)}{V_A' - V_A}\,dx = \int_0^L \frac{n'(x)-n(x)}{V_A' - V_A}\,dx \qquad (3.4)$$

where $n'(x)$ and $p'(x)$ are the electron and hole densities corresponding to the applied voltage V_A' slightly incremental with respect to the applied voltage V_A, which generates $n(x)$ and $p(x)$.

---

* This is indeed a very common case, with the exception of structures with extremely short neutral regions or at extremely high injection levels.

Of course, higher order finite difference schemes may be employed to approximate the derivatives of relations (3.3); additional solutions for incremented applied voltages are then required.

The modular organization of the basic direct program of Appendix C requires only a variation of the main program to incorporate the algorithm for the computation of the total incremental capacitance. An example of such a modified main program, with the coding details, is reported in Appendix D.

Although the validity of the definition (3.1) of the incremental capacitance C may be questioned, it is very much of interest to obtain "exact" results on the basis of such a definition, since this is the only calculation that steady-state considerations permit, and is therefore conventionally accepted. A more appropriate definition relates solely terminal properties and is in general a function of frequency f, for a small increment of applied sinusoidal voltage $v(f)$ about the value V_A:

$$C(f)\Big|_{V_A} = \Big\{[J(f)]_{reactive} \,/\, [2\pi f\, v(f)]\Big\}_{V_A} \qquad (3.5)$$

Comparison between results furnished by the two definitions is of considerable interest and requires the availability of solutions for transient conditions.

3.3. A solution for the reverse problem $(J \rightarrow V_A)$.

It is desired to solve numerically the fundamental Eqs.(1.16) to (1.21), subject to the boundary conditions (1.28) on the mobile carrier densities, for a specified value of total current J. Accurate

solutions for all the quantities of interest in the interior of the device and the terminal voltage are sought. To achieve this, a rearrangement of the fundamental equations may be attempted in the search for a suitable new formulation. This approach will be discussed in Part II, Section 9.3.

An alternative procedure, which employs the basic direct program, is illustrated below.

3.3.1. Description of the method.

The quasi-linear local feature of the current-voltage characteristic in semilogarithmic axes, together with the availability of the basic program, suggests a successive approximation procedure based on a Lagrangian interpolation scheme.

The discussion will be restricted to the case, of practical interest, of forward bias. Positive currents are then assumed.

The following notation is introduced:

J = variable representing total current on the exact current-voltage characteristic

V_A = variable representing the voltage at the terminals* on the exact current-voltage characteristic

J_S = specified value of total current

V_{AS} = voltage at the terminals correspondent to J_S

H = $\ln(J)$

H_S = $\ln(J_S)$

---

* In the following context for "voltage at the terminals", or briefly "voltage", the difference of the electrostatic potential at the external contacts subtracted from the diffusion potential will be intended [i.e. $V_A = V_d + \psi(L) - \psi(0)$].

Were V_{AS} known, then the direct program would readily give the sought complete solution of the basic equations. The problem is therefore to determine V_{AS} once the current J_S is specified.

To achieve this, H_S is first surrounded by two points H_1, H_2 on the curve $H = f(V_A)$ such that:

$$H_1 \leq H_S \leq H_2 \quad \text{or} \quad H_1 \geq H_S \geq H_2 \tag{3.6}$$

The exact current values H_1 and H_2 may be obtained merely by guessing two values of applied voltage V_{A1}, V_{A2} (or better, by use of the first-order theory, if applicable) and determining the correspondent values of currents with use of the basic program. Subsequently successive Lagrangian interpolations on the function $V_A = g(H)$, with the aid of the basic program, are suitable to refine the search of the quantity V_{AS} to the desired accuracy.

If the general first-order theory results are used to obtain V_{A1} and V_{A2}, a preliminary successive approximation scheme must be employed to solve the implicit system of Eqs.(A-13) and (A-41) for the applied voltage, for a given total current $J = J_n$.

The whole procedure is illustrated in Fig. 3.1. The current J_S is specified together with a tolerance ERRJ such that any value of voltage, yielding an exact current J satisfying the relation

$$\frac{|J_S - J|}{J_S} < \text{ERRJ} \quad , \tag{3.7}$$

will be accepted as the solution of the problem. A first value V_{A1}

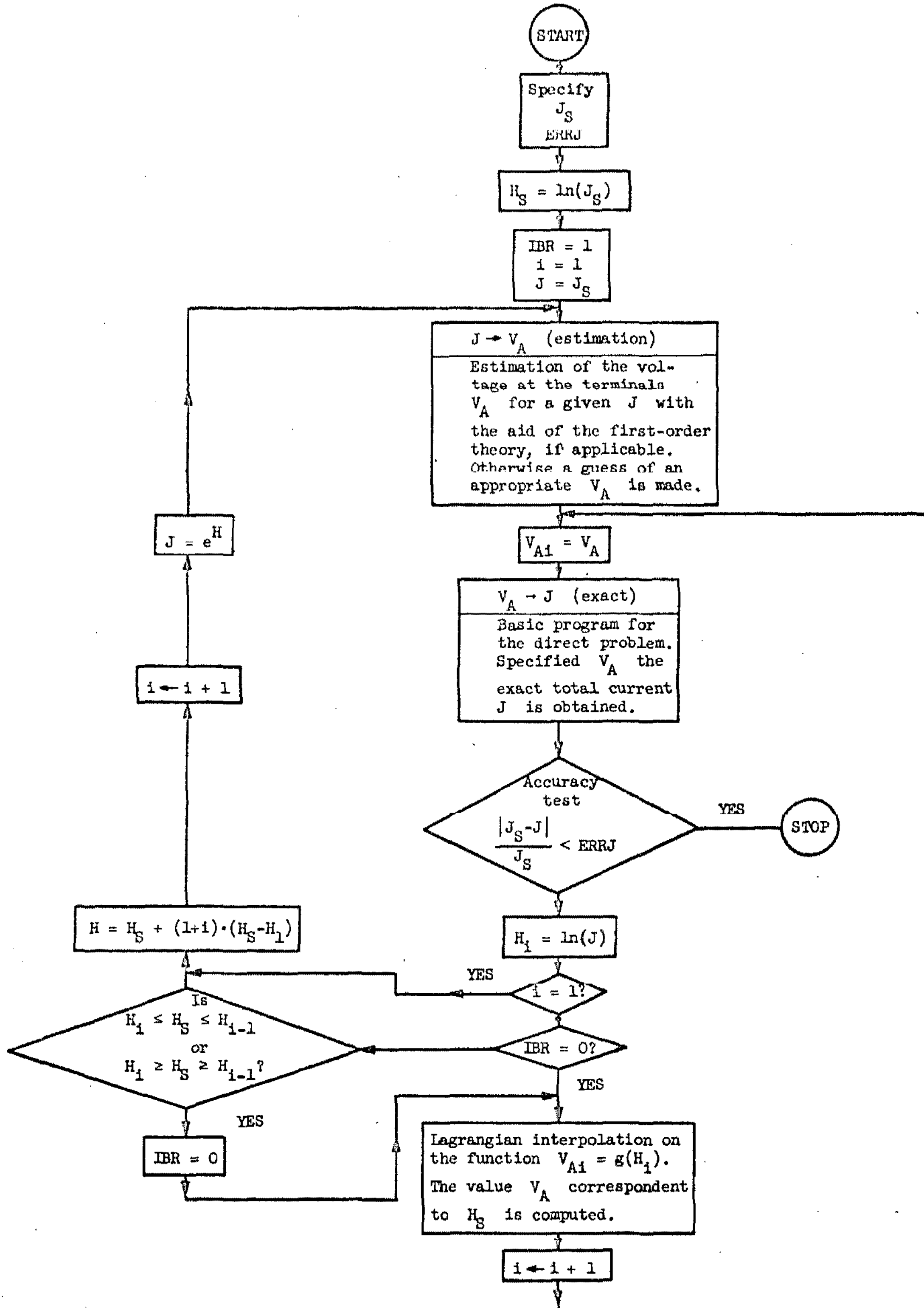

Fig. 3.1. Schematic block diagram illustrating a successive approximation scheme for the solution of the reverse problem.

is sought, approximately correspondent to a current value $J_1' = J_S$, and obtained by use of the first-order theory, if applicable. The basic direct program will then yield the exact current J_1 correspondent to V_{A1}. Failure of the accuracy test of Eq.(3.7) is followed by the estimation of a value of current J_2' with the aid of the relation

$$H = H_S + (1+i) \cdot (H_S - H_1) \qquad (i = 1) \qquad (3.8)$$

with $\quad H_1 = \ln J_1$

and $\quad J_2' = \exp(H)$

The above is then repeated: an approximate voltage V_{A2} is computed to enter once more the basic program and obtain the exact current J_2 to perform the test on the condition (3.6). A negative outcome reiterates the cycle with the parameter i of Eq.(3.8) increased each time by unity. A very few iterations will generally satisfy the condition (3.6) so that a Lagrangian interpolation on the function

$$V_{Am} = g(H_m) \qquad m = 1,\ 2,\ \cdots\ i$$

may be successfully used to obtain a new (and considerably more accurate) value of $V_{A,\,i+1}$ to be fed into the basic direct program and obtain the correspondent exact current J_{i+1}, or H_{i+1}. Successive applications of the interpolation operation and of the basic program will then lead to the desired value V_{AS} with the specified accuracy.

The Lagrangian interpolation procedure involves the solution of a system of linear algebraic equations, which may be reduced to a matrix

form, and treated with one of the conventional methods available from numerical analysis. A protection feature must then be incorporated in the program to cope with the unfortunate situation of the matrix becoming ill-conditioned for the method of solution chosen. This circumstance may occur in the present procedure if too small a tolerance parameter ERRJ is specified.

3.3.2. Results.

The computer program for the solution of the reverse problem features only a slight alteration of the main program of Appendix C and a mere addition to the basic direct program of a subroutine to execute the interpolation procedure. The organization of the program with the coding details is shown in Appendix E.

Several test calculations have been performed on the computer for various structures, total number of points, specified current ranges, for several current tolerance parameters. The results obtained may be summarized in the following: three to five iteration cycles (i.e. calls of the basic direct program) are sufficient to satisfy a tolerance parameter ERRJ $= 10^{-5}$, whereas four to seven iteration cycles are usually required if a tolerance parameter ERRJ $= 10^{-7}$ is specified; however, a very few isolated cases feature an ill-conditioned matrix before reaching the latter value if single precision arithmetic is used. Interruption of the procedure at an appropriate point,* yields for these singular cases results satisfying a tolerance ERRJ $\cong 10^{-6}$ which is still to be considered well acceptable from any practical point of view.

---

* The protection feature incorporated in the program may very well take care of this.

Alternatively double precision arithmetic may be used, if a more severe tolerance is desired.

3.4. Conclusion.

Two simple examples of the application of the basic direct program in slightly more intricate schemes have been illustrated. The total incremental capacitance has been obtained from two successive steady-state solutions for different values of applied voltage, and a method of solution of the fundamental transport equations for a specified total current has been described.

The highly modular organization of the basic direct program requires only slight variations of the main program and the addition of one subroutine to incorporate the new features.

CHAPTER IV

EXTENSION OF THE METHOD TO THE SOLUTION OF THE TRANSISTOR

Although the method of solution described in the previous chapters for a two-contact device allows for doping profiles generating multiple junctions, additional boundary conditions are required if a multiple-contact device is analyzed. As an example, the extension of the method to the solution of the transistor is discussed in this Chapter. The general lines of Gummel's original procedure [18] are followed, the inadequacy of the one-dimensional model to implement a realistic representation of the base contact (other than, perhaps, in the low injection case) is recognized, and a slightly different approach is suggested as an alternative to the original procedure. Details of the modifications introduced by the additional boundary conditions in the analytical formulation and in the overall iterative scheme are illustrated.

4.1. Mathematical model and boundary conditions.

Under the same assumptions stated in Subsection 1.1.1 the equations that describe the behavior of the transistor are given by the fundamental set of Eqs.(1.16) to (1.21). These are here applied to the one-dimensional N-P-N structure of Fig. 4.1, in which O, B, and L represent the external contacts of the emitter, base, and collector respectively, and M and M_C the metallurgical interfaces of the emitter-base and base-emitter junctions, respectively. The impurity density $N(x)$ as a function of position x may be again expressed in terms of the donor and acceptor contributions as

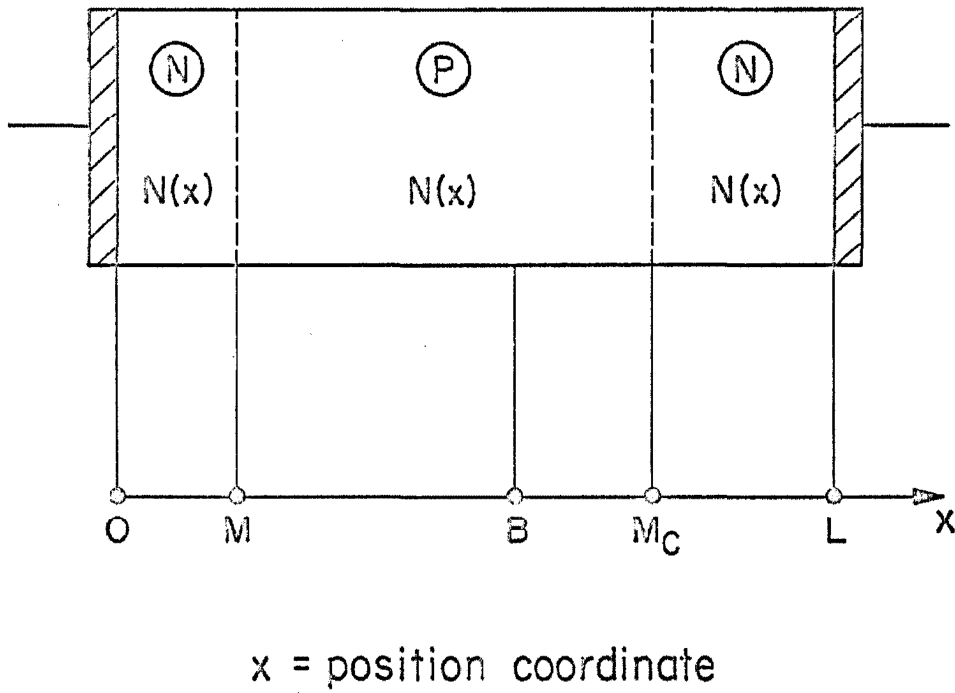

Fig. 4.1. One-dimensional N-P-N transistor structure.

$$N(x) = N_D(x) - N_A(x)$$

and is assumed consistent with the N-P-N device configuration.

The same boundary conditions for the carrier densities discussed in Subsection 1.1.3 may be specified for the emitter and collector external contacts 0 and L, whereas the base contact must be treated differently. This is a consequence of the one-dimensional model, certainly inadequate to represent with comparable degree of realism and generality the position and property of the third contact for the device under consideration. If Gummel's general lines [18] are followed, the value of the majority carrier (hole) quasi-Fermi level at the position of the base contact is chosen as the additional boundary condition according to the relation:

$$\varphi_p(B) - \varphi_p(0) = V_{BE} \tag{4.1}$$

or

$$\varphi_p(B) - \varphi_p(L) = V_{BC}$$

where V_{BO} and V_{BL} are the voltage differences applied between the base contact and the emitter contact, and between the base contact and the collector contact respectively. This choice was originally justified by the observation that the majority-carrier quasi-Fermi level is essentially constant throughout the base and that the position of the base contact is not critical. Although this may be well acceptable in low-injection cases, it is reasonable to expect, in the one-dimensional model under consideration, both internal and terminal properties to

become highly dependent upon the position of the base contact in high injection conditions. This is a consequence of the significant conductivity modulation in the base, which is responsible for considerably different potential drops in the emitter side and collector side of the "neutral" base for given total currents, or alternatively different total currents for specified voltage differences at the contacts. It is apparent that, in these conditions, the choice of the position of the base contact becomes highly critical.

Although the basic inadequacies of the one-dimensional model can not be entirely resolved, the choice of a more realistic boundary condition may be attempted by specifying the position of the base contact at the point* where the majority carrier density, or in essentially equivalent terms the conductivity, assumes the value one would specify as a boundary condition at the base external contact in a realistic three-dimensional model. In this case the position of the base contact must be determined by a successive approximation method,** as a consequence of the additional requirement introduced. The lack of freedom in the choice of the position of the base contact in the one-dimensional model, for a specified boundary condition of the described type, is of insignificant importance, since there is very little relation between the position of the base contact in the one-dimensional model and the actual position in the real three-dimensional device. Results of calculations, illustrating the importance of the choice of the position of the base contact, are reported in a later chapter.

---

* In the base at the collector side, for normal transistor operation.
** An automatic procedure may be easily incorporated in the computer program as part of the solution.

It is also of interest to observe, as a direct consequence of the dependence of the boundary condition at the base contact solely on the majority carrier (hole) quasi-Fermi level, that the external base current is only generated by the difference between the majority carrier currents at the emitter and collector side of the base contact, and not by the minority carrier (electron) current, continuous at the position of the base contact.

Two boundary conditions on the electrostatic potential, chosen as the values at the emitter and collector external contacts, complete the mathematical formulation of the problem. Either of these boundary values may be taken as a reference value, the other being directly related to the externally applied voltages V_{BE} and V_{BC} and the diffusion potentials V_{dE} and V_{dC} of the emitter and collector junctions respectively:

$$\psi(L) - \psi(0) = V_{BE} - V_{BC} - V_{dE} + V_{dC} \qquad (4.2)$$

4.2. Analytical formulation.

The same procedure employed for a two-contact device to rearrange the fundamental Eqs.(1.16) to (1.21) to the reduced set of Eqs.(1.39), (1.40) (with (1.33), (1.34)), (1.19) and subsequently to the improved form of Eqs.(2.5), (2.6), (2.11), (2.12) may be used here for the transistor, with provision for the additional boundary condition at the base contact. This leads to only slight modifications in the final form of the analytical formulation concerning the hole density distribution and the terminal properties.

It is appropriate to define two domains in the interior of the device:

emitter domain for $0 \leq x \leq B$

collector domain for $B \leq x \leq L$

At the interface of the two domains the hole quasi-Fermi level is specified by the condition (4.1), which, with the aid of the definition (1.25), may also be rewritten as:

$$p(B) = \exp[\varphi_p(B)-\psi(B)] = \exp[\varphi_p(0)+V_{BE}-\psi(B)] = p(0)\ \exp[\psi(0)+V_{BE}-\psi(B)] \tag{4.3}$$

to give a boundary condition on the hole density at the base contact in terms of the hole density and the electrostatic potential at the emitter contact, the base to emitter external voltage and the electrostatic potential at the domain interface. The hole density and hole current distributions in the two domains assume the following form (which corresponds to Eqs.(1.34) and (1.40) for the two contact device):

$$p(x) = e^{-\psi(x)}\left[-\int_x^B \gamma_p(x')\ J_p(x')\ e^{\psi(x')}\ dx' + p(B)\ e^{\psi(B)}\right]$$

$$J_p(x) = \int_0^x U(x')\ dx' + \frac{p(B)\ e^{\psi(B)} - p(0)\ e^{\psi(0)} - \int_0^B \gamma_p(x)\ e^{\psi(x)}\left(\int_0^x U(x')dx'\right)dx}{\int_0^B \gamma_p(x)\ e^{\psi(x)}\ dx} \tag{4.4}$$

for $0 \leq x \leq B$, and

$$p(x) = e^{-\psi(x)}\left[-\int_x^L \gamma_p(x')\, J_p(x')\, e^{\psi(x')}\, dx' + p(L)\, e^{\psi(L)}\right]$$

$$J_p(x) = \int_B^x U(x')\, dx' + \frac{p(L)e^{\psi(L)} - p(B)e^{\psi(B)} - \int_B^L \gamma_p(x)e^{\psi(x)}\left(\int_B^x U(x')dx'\right)dx}{\int_B^L \gamma_p(x)\, e^{\psi(x)}\, dx} \qquad (4.5)$$

for $B \le x \le L$, and $p(B)$ is given by the condition (4.3). Expressions for the electron density and electron current distributions valid throughout the whole interior of the device $(0 \le x \le L)$ are still given by Eqs.(1.33) and (1.39).

The same considerations of Section 2.2 lead in each domain to improved analytical formulations for the hole density essentially equivalent to those presented for a two-contact device. For example, for the simplified case characterized by absence of recombination $[U(x) = 0]$ and constant mobilities, the following relations apply for forward and moderate reverse-bias conditions at either junction. The electron density throughout the entire device

$$n(x) = \left\{\left[F_{In}^{(T)}(x) + e^{\frac{\psi(0)-\psi(L)}{2}}\left(\theta_n F_n^{(T)}(x)\right)\right]\left[\frac{n(0)e^{\psi_{BL}-\psi(0)}}{F_n^{(T)}(L)}\right]\right\} e^{\psi(x)-\psi_{BL}} \qquad (4.6)$$

is valid for $0 \le x \le L$, with

$$F_{In}^{(T)}(x) = \int_L^x e^{\psi_{BL}-\psi(x')}dx' \quad , \quad F_n^{(T)}(x) = \int_0^x e^{\psi_{BL}-\psi(x')}dx'$$

$$\theta_n = \frac{n(L)e^{\frac{\psi(0)-\psi(L)}{2}}}{n(0)} \quad , \quad \psi_{BL} = \frac{\psi(B) + \psi(L)}{2}$$

The hole density throughout the emitter domain

$$p(x) = \left\{ \left[F_{Ipe}(x) + e^{\frac{\psi(B)-\psi(0)}{2}} \left(\theta_e F_{pe}(x) \right) \right] \left[\frac{p(0) e^{\psi(0)-\psi_{OB}}}{F_{pe}(B)} \right] \right\} e^{\psi_{OB}-\psi(x)} \tag{4.7}$$

is valid for $0 \le x \le B$, with

$$F_{pe}(x) = \int_0^x e^{\psi(x')-\psi_{OB}}\, dx' \quad , \quad F_{Ipe}(x) = \int_x^B e^{\psi(x')-\psi_{OB}}\, dx'$$

$$\theta_e = \frac{p(B) e^{\frac{\psi(B)-\psi(0)}{2}}}{p(0)} \quad , \quad \psi_{OB} = \frac{\psi(0) + \psi(B)}{2}$$

The hole density throughout the collector domain

$$p(x) = \left\{ \left[F_{pc}(x) + e^{\frac{\psi(B)-\psi(L)}{2}} \left(\theta_c F_{Ipc}(x) \right) \right] \left[\frac{p(L) e^{\psi(L)-\psi_{BL}}}{F_{pc}(L)} \right] \right\} e^{\psi_{BL}-\psi(x)} \tag{4.8}$$

is valid for $B \le x \le L$, with

$$F_{pc}(x) = \int_B^x e^{\psi(x)-\psi_{BL}}\, dx \quad ; \quad F_{Ipc}(x) = \int_x^L e^{\psi(x)-\psi_{BL}}\, dx$$

$$\theta_c = \frac{p(B) e^{\frac{\psi(B)-\psi(L)}{2}}}{p(L)} \quad ; \quad \psi_{BL} = \frac{\psi(B) + \psi(L)}{2}$$

The introduction of the scale factors ψ_{BL} and ψ_{OB}, together with the additional rearrangement of terms, extends the range of numerical application of the above relations to moderate reverse bias, according to the restrictions:

$$V_{BE} \geq R - V_{dE}$$

$$V_{BC} \geq 2R - V_{dC}$$

where R is the parameter defined in Subsection 2.2.2, and V_{BE}, V_{BC} and V_{dE}, V_{dC} are the normalized applied voltages and diffusion potentials defined in Section 4.1. Considerations similar to those presented in Subsection 2.2.2 lead to the corresponding relations for the carrier density distributions at any reverse-bias condition.

Terminal currents are, in the general case, easily recovered with the aid of Eqs.(1.39), (4.4) and (4.5). For instance, the base current J_B is given, as the difference between the emitter current J_E and collector current J_C, by:

$$J_B = J_E - J_C = [J_n(x) + J_p(x)]_{\substack{x \text{ in emitter} \\ \text{domain}}} - [J_n(x) + J_p(x)]_{\substack{x \text{ in collector} \\ \text{domain}}} =$$

$$= \int_0^B U(x)dx + \frac{p(B)e^{\psi(B)} - p(0)e^{\psi(0)} - \int_0^B \gamma_p(x)e^{\psi(x)}\left(\int_0^x U(x')dx'\right)dx}{\int_0^B \gamma_p(x)e^{\psi(x)}\,dx}$$

$$- \frac{p(L)e^{\psi(L)} - p(B)e^{\psi(B)} - \int_B^L \gamma_p(x)\,e^{\psi(x)}\left(\int_B^x U(x')dx'\right)dx}{\int_B^L \gamma_p(x)e^{\psi(x)}\,dx} \qquad (4.9)$$

The sign convention for the external currents is shown in Fig. 4.2

4.3. Iterative procedure for the direct and reverse problem.

The same iterative scheme described in Section 1.3 for a two-contact device is applicable to the transistor, for the solution of the

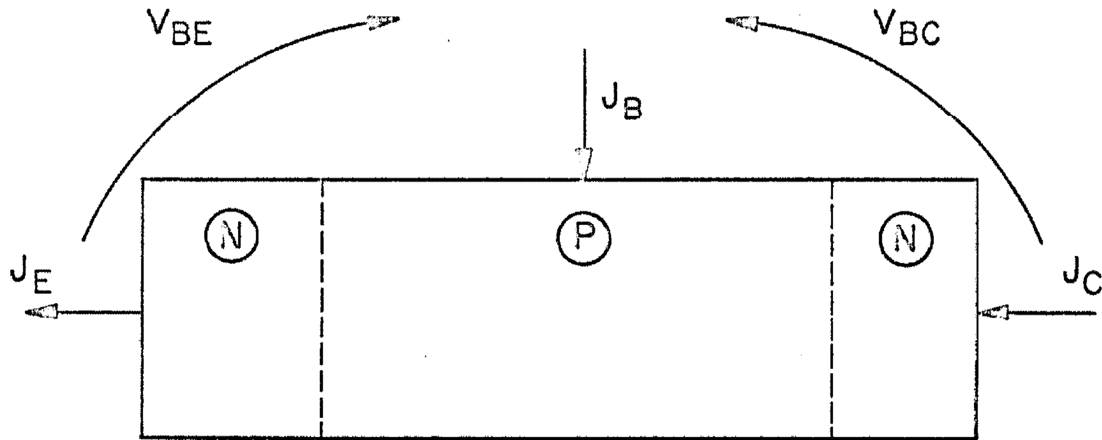

V_{BE} = base-to-emitter voltage (positive for forward-biased emitter junction)

V_{BC} = base-to-collector voltage (positive for forward-biased collector junction)

Fig. 4.2. Sign convention for the applied voltages and external currents: currents are positive if flowing in the indicated directions.

direct problem. The emitter to base and collector to base voltage differences are specified, a trial potential function is chosen (consistent with the boundary condition (4.2)), and the recombination-generation term is set to zero for the first cycle. The values of the mobile carrier densities at the emitter and collector external contacts are determined, in the general case, by the combination of relations (1.28) with Eqs.(1.39) and (4.4) specialized at the emitter external contact and with Eqs.(1.39) and (4.5) specialized at the collector external contact, with the aid of a secondary iteration loop if necessary. Mobile carrier density distributions are given by Eqs.(4.6), (4.7), (4.8) for the constant mobility, absence of recombination case (or by their generalized equivalent if required). The same procedure, formulation, and numerical techniques described in Subsection 2.3.3 may be used for the solution of Poisson's equation (1.45) with boundary conditions (1.43), to obtain an improved potential distribution and restart the cycle.

The combination of the described iterative scheme for the direct problem with an interpolating procedure of the type described in Subsection 3.3.1 may be used for the solution of the reverse problem on either junction or both simultaneously (that is, for the case that either one external current and one voltage difference between terminals or two external currents are specified).

4.4. Conclusion.

Since freedom is available in the choice of the doping profile in the method presented in Chapters I and II for a two-contact device, the numerical solution of multiple-junction two-contact devices does not require any variation in the previously described formulation. If a three-contact device is considered, such as the bipolar transistor examined in this Chapter, additional boundary conditions are necessary fully to determine the mathematical problem.

The implementation in the one-dimensional model of realistic boundary conditions has been shown to be a difficult task. As an alternative to Gummel's original method [18], a more realistic representation of the boundary condition on the external base contact has been attempted through a slightly different approach. The position of the external base contact in the one-dimensional model has been treated as a parameter dependent upon additional properties imposed on the mathematical base contact, rather than as an independent parameter [18]. One motivation for this choice is the little relation between the position of the base contact in the one-dimensional model and the actual one in the three-dimensional device.

Minor rearrangements in the analytical formulation discussed for a two-contact device and in the iteration scheme to incorporate the additional boundary conditions have been presented to extend the method to the transistor. Results for a particular structure, under various bias conditions, (obtained with a slightly modified version of the computer program of Appendix C) illustrate both internal distributions and terminal properties, and are reported in a later chapter.

Further extensions to more complex multiple-junctions and multiple-contact devices may be attained by the same procedure. However, for such cases it would be desirable, as has been made apparent by the example of the bipolar transistor, to allow more realistic models through development of multidimensional solutions.

CHAPTER V

ON THE ACCURACY OF THE NUMERICAL RESULTS

In this Chapter the sources of error are individually analyzed and their influence on the final results is examined. Techniques suitable to control the magnitude of such errors are discussed, and a realistic criterion for the evaluation of the consistency of the results achieved is described and accepted as a satisfactory means of accuracy estimation.

5.1. Generalities.

One of the most delicate problems of the numerical solutions presented is indeed related to the accuracy of the results obtained. This peculiarity is to be consistently expected in most problems involving the solution of the bipolar transport equations applied to semiconductor junctions and must be regarded as a feature inherent in the pertinent expressions which suffer from serious hindrances, such as the variation of the relevant quantities over extremely wide ranges and small differences between nearly equal numbers.

The ideal approach to this problem consists in the determination of the single errors (or proper bounds) introduced by each elementary operation to achieve an estimation of the total error for a particular algorithm chosen. An alternative method may restrict the evaluation of the accuracy solely to the final results by testing their consistency with an appropriate set of relations. These "testing relations" must then feature finite difference schemes and numerical errors different from those exhibited by the actual expressions which originally genera-

ted such results and must conveniently expose the discrepancies, which will then serve as a measure of the accuracy achieved.

Preference will be given, in the following context, to the latter approach, rather than to the former more rigorous one, whose difficulties seem to prevent a sufficiently realistic estimation of the total error. The problem may then be considered threefold:

(a) searching all the single sources of error present in the procedure

(b) analyzing the influence of each error on the accuracy of the final results and devising techniques to minimize such influence

(c) constructing an appropriate set of "testing relations" to evaluate the consistency of the results.

These three aspects of the problem will be considered separately in the following sections.

5.2. Sources of error.

5.2.1. Discretization error.

The exact analytical formulation, describing mathematically the physical phenomena, is approximated by a discretized formulation, which evaluates and recognizes the quantities at a finite number of points only. An error may then be introduced whenever an operation is performed on a discretized function; the magnitude of such error depends on the order of approximation used. Two basic operations are of interest in the present context:

(a) quadratures of functions of the type $e^{\mp\,\psi(x)\,+\,\text{constant}}$

(b) computation of the first and second spatial derivatives of the

electrostatic potential.

5.2.2. Numerical error.

The denomination "numerical error" is usually given to any departure of the actual numerical result from the exact solution of the discretized formulation. The following sources of inaccuracies will be considered in this class of errors:

(a) round-off errors

(b) quantities exceeding the allowed range

(c) small differences between nearly equal numbers

(d) interruption of the overall iteration scheme (iteration error).

5.2.3. Physical model discretization error.

If the exact representation in the discretized context of an abrupt impurity distribution were attempted, a spatial step of zero magnitude would be required at the metallurgical interface. The impossibility of realizing this condition introduces an error in the discretized physical model furnished to the digital machine.

5.3. Influence and control of the errors.

5.3.1. Discretization error.

(a) Quadratures.

Particular care must be exerted in the evaluation of the integrals of functions such as $e^{\mp \psi(x) + \text{constant}}$, especially in the transition region, in which $\psi(x)$ is forced to a considerable variation in both magnitude and derivatives. The problem has been examined in detail in Section 2.3 and treated by the automatic selection of a non-uniform step distribution, based on the criterion of achieving constant accuracy at each step in the pointwise integration throughout the interior of

the device. The magnitude of the error may be specified a priori, its lower limit being determined by the maximum number of points the program allows for. Alternatively, the total number of points may be specified, with reference to the storage capabilities of the machine, computer time the programmer is willing to accept, and accuracy in the final results. A further reduction of the truncation error may be successfully achieved, for a specified number of points, by adopting higher order discretization schemes, for instance of the type shown in Section B-1 (Appendix B).

(b) Differentiation.

The iterative procedure described requires two differentiations in the solution of Poisson's equation: the second derivative of the electrostatic potential $\psi(x)$ and of the correction $\delta(x)$. It has already been observed (Subsection 2.3.3) that the truncation error pertinent to the latter quantity is by no means connected to the error of the final results, if convergence occurs. Since the step size is already determined by the quadrature requirements, the truncation error introduced in the differentiation of $\psi(x)$ may be solely controlled by the order of the finite-difference scheme employed. A successful improvement of the accuracy is then strictly dependent upon a "well-behaved" shape of the function $\psi(x)$ and its derivatives. This is indeed the case in the problem under consideration, with the exception of a short region about the metallurgical interface, where the curvature of the electrostatic potential (i.e. the net charge density) undergoes a variation of several orders of magnitude. This peculiarity is certainly enhanced by an abrupt impurity distribution, in which case the

entire variation occurs, in the discretized model, in one step length. The higher order derivatives become extremely large there, causing a huge truncation error in the computation of $\frac{d^2\psi(x)}{dx^2}$ at the points close to the metallurgical interface, for any finite difference scheme. For the abrupt case, since the problem is particularly serious, an extrapolation technique on the discretized $\psi(x)$, on both sides of the interface, has been attempted. This procedure, which indeed would have considerably lessened the difficulty, had to be discarded, since it impaired beyond tolerance the overall convergence of the iterative scheme. However, the disturbance created at the interface by the discontinuity of the higher derivatives of $\psi(x)$ may be confined to a very narrow region if the step is there further reduced* by one or more orders of magnitude. Such additional constraint is then relaxed away from the interface, to allow the step to resume the appropriate magnitude previously selected. This "step-compression technique", merely a palliative, has proven to succeed in localizing the disturbance on the internal distributions to a region as short as 10^{-5} x the transition region length. Also in consideration of the insignificant effect of such error on the terminal properties of the device, this solution is to be considered acceptable for any practical purpose.

If the electric field distribution throughout the device is also desired, the above may be applied also to the computation of the first derivative of $\psi(x)$.

---

* The smallest step, according to the selection described in Subsection 2.3.1, is usually located at the interface.

Several finite-difference schemes are reported in Appendix B, suitable for the computation of the first and second derivatives of a function available in discretized form at unevenly spaced points.

5.3.2. Numerical error.

(a) Round-off error.

A round-off error in introduced, in general, at the execution of any elementary operation on quantities represented with a finite number of digits. This type of error is then strictly dependent upon the machine employed; in the present case a choice on either 8 (single-precision arithmetic) or 16 (double-precision arithmetic) significant digits is available.

Also in consideration of the significant exposure of the round-off error caused by the presence of unfortunate conditions (such as small differences between nearly equal numbers), double precision arithmetic is certainly required whenever good accuracy (5-6 exact significant digits) in the final results is desired. The round-off error will then certainly be negligible when compared to other types of error, and does not deserve any further attention. On the other hand, the adoption of single-precision arithmetic in a sound algorithm will be responsible for round-off errors comparable to low-order truncation errors and will still lead in most cases to reasonably accurate results (2-4 exact significant digits).*

---

* The total number of points is also limited in this case by the round-off errors on the smallest step.

(b) Quantities exceeding in magnitude the allowed range.

The range of the numbers a digital machine is capable of handling is usually limited and may not satisfy the requirements of certain formulations. This has been indeed the case in the problem under consideration: an appropriate numerical formulation has therefore been devised (Subsection 2.2.2) to avoid gross errors leading to meaningless results.

(c) Small differences between nearly equal numbers.

This problem arose in Subsection 2.2.1, where its influence on the computation of the electron and hole distributions was discussed. A rearrangement of the algorithm succeeded in eliminating such sources of error from the relevant expressions. This is indeed the ideal approach for this kind of problem, since, in general, increasing the number of significant digits is not an acceptable solution. A similar, but less serious problem, is also present in the right-hand side of Poisson's equation (Eq.(1.19)). A considerable relative error may be introduced in the computation of the net charge, in the highly neutral regions of the device; this may well be tolerated, since the only consequence is an insignificant absolute error in the second derivative of the electrostatic potential.

(d) Iteration error.

The interruption of the overall iteration scheme after a finite number of cycles introduces an error. In consideration of the fast convergence observed,* it seems reasonable to accept as a measure of

---

* 8-15 iteration cycles reach a correction $\delta(x) \leq 10^{-7} \cdot V_d$ for an abrupt junction, with first-order theory trial potential function, for low and moderate injection. More iterations are required for very high injection cases.

such "iteration error" the largest correction $\delta(x)$ for the electrostatic potential, over all x, achieved at the last cycle. The magnitude of the iteration error may then be specified by the programmer and inserted as DATA to interrupt the iterative procedure.

The magnitude of the dominant error in the entire procedure may serve as a convenient guide for the most economical choice of iteration error.

5.3.3. Physical model discretization error.

Limiting factors such as the upper bound for the ratio of consecutive steps, the total number of points, and the round-off error determine the minimum step size. The discretization of an ideal abrupt impurity distribution, useful for comparison with the first-order theory results, may therefore not be realized exactly. However, only discrepancies of insignificant amount, and confined to an extremely narrow region about the metallurgical interface, are thus introduced. A reduction of this error is in any case obtained with the "step compression" technique mentioned in Subsection 5.3.1 (b).

5.4. Testing criteria of the accuracy of the results.

Same quantities may be expressed in terms of various analytically equivalent formulations, whose numerical counterparts display errors of quite different nature and magnitude. These may be used to expose the inaccuracy of the results. From the fundamental equations (1.16) to (1.21), and subsidiary relation (1.22), specialized for simplicity for the zero-recombination case, the following set of relations may be obtained.

(a) Electric field:

$$E(x) = -\frac{d\psi(x)}{dx} \tag{5.1}$$

$$E(x) = \int_0^x [p(x')-n(x') + N(x')]\, dx' + E(0) \tag{5.2}$$

$$E(x) = \int_L^x [p(x')-n(x') + N(x')]\, dx' + E(L) \tag{5.3}$$

(b) Currents:

$$J_n = \frac{n(0)\, e^{-\psi(0)} - n(L)\, e^{-\psi(L)}}{\int_0^L \gamma_n(x)\, e^{-\psi(x)}\, dx} \tag{5.4}$$

$$J_n = -\frac{1}{\gamma_n(x)} \left[n(x) \cdot E(x) + \frac{dn(x)}{dx} \right] \tag{5.5}$$

$$J_n = \frac{n(x)}{\gamma_n(x)} \frac{d\varphi_n(x)}{dx} = -\frac{e^{\psi(x)}}{\gamma_n(x)} \frac{de^{-\varphi_n(x)}}{dx} \tag{5.6}$$

$$J_n = \frac{-1/L}{\int_0^L \gamma_n(x) dx} \left[\int_0^L E(x) \cdot n(x)\, dx - n(L) + n(0) \right] \tag{5.7}$$

$$J_p = \frac{p(L)\, e^{\psi(L)} - p(0)\, e^{\psi(0)}}{\int_0^L \gamma_p(x)\, e^{\psi(x)}\, dx} \tag{5.8}$$

$$J_p = \frac{1}{\gamma_p(x)} \left[-p(x) \cdot E(x) + \frac{dp(x)}{dx} \right] \tag{5.9}$$

$$J_p = \frac{p(x)}{\gamma_p(x)} \frac{d\varphi_p(x)}{dx} = \frac{e^{-\psi(x)}}{\gamma_p(x)} \frac{de^{\varphi_p(x)}}{dx} \tag{5.10}$$

$$J_p = \frac{-1/L}{\int_0^L \gamma_p(x) dx} \left[\int_0^L E(x) \cdot p(x)\, dx - p(L) + p(0) \right] \tag{5.11}$$

Equations (5.4), (5.8) are the actual expressions used in the numerical solution to compute the total current; the identity of Eqs.(5.6) and (5.10) with Eqs.(5.5) and (5.9), respectively, is easily verified with the aid of the definitions (1.24) and (1.25); Eqs.(5.7), (5.11) are readily obtained by integration of Eqs.(5.5), (5. 9) respectively.

(c) Consistency of Poisson's equation:

$$\varepsilon_{Ps}(x) \triangleq \left[p(x) - n(x) + N(x) + \frac{d^2\psi(x)}{dx^2}\right] \Big/ [p(x) - n(x) + N(x)] \qquad (5.12)$$

$$\varepsilon'_{Ps}(x) \triangleq \left[p(x) - n(x) + N(x) - \frac{dE}{dx}\right] \Big/ [p(x) - n(x) + N(x)] \qquad (5.13)$$

(d) Incremental surface charge:

$$\frac{d(\sigma_L - \sigma_0)}{dV_A} = - \frac{d[E(L) - E(0)]}{dV_A} \qquad (5.14)$$

$$\frac{d(\sigma_L - \sigma_0)}{dV_A} = \int_0^L \frac{dn(x)}{dV_A}\, dx - \int_0^L \frac{dp(x)}{dV_A}\, dx \qquad (5.15)$$

The consistency of the final distributions of $\psi(x)$, $n(x)$, $p(x)$ may be evaluated first by comparing the discrepancies on the electric field at each point obtained from relations (5.1) to (5.3). Such discrepancies will be exposed by relations (5.5), (5.6), (5.7), and (5.9), (5.10), (5.11), if compared to relations (5.4) and (5.8), respectively. The usual small differences between nearly equal numbers are present in the former set and are in this instance usefully exploited. Equations (5.5), (5.6), (5.9), and (5.10) conveniently expose the error at each point in the interior of the device, leaving to Eqs.(5.7), (5.11)to

show the overall effects of the various internal inconsistencies on the terminal properties. The relative error $\varepsilon_{Ps}(x)$ given by relation (5.12) is directly dependent upon the specified iteration error [Subsection 5.3.2 (d)] if $\frac{d^2\psi(x)}{dx^2}$ is computed with the same finite-difference scheme.

The consistency of Poisson's equation in terms of the electric field may then be tested with the aid of relation (5.13) and comparison of the two relative errors $\varepsilon'_{Ps}(x)$ and $\varepsilon_{Ps}(x)$.

Relations (5.14) and (5.15) yield an indication of the accuracy of the incremental capacitance by comparing the incremental surface charge at the external boundaries evaluated first in terms of the field variation at the contacts and second in terms of the incremental net charge in the interior of the device.

5.5. Conclusion.

Several types of errors arising in the numerical solution under consideration have been described, their importance and influence on the overall accuracy has been illustrated, means to control within limits the magnitude of such errors have been suggested, and criteria suitable to evaluate the accuracy of the final results have been stated. The abruptness of the assigned doping profile has been recognized as a determinant factor for the overall accuracy, since it affects very much the magnitude of the truncation errors of the numerical operations. The step distribution for the impurity density represents the worst case numerically, since it maximizes discretization errors. This ideal situation, although unrealistic from a technological point of view, has

been selected to perform a series of actual numerical calculations also in order to test severely the accuracy of the solution under extreme conditions. Some of the results obtained for such ideal structures are discussed in the next Chapter.

CHAPTER VI

RESULTS

Solutions obtained with the numerical procedure described in the previous chapters are presented for a few special structures. A narrow-base abrupt asymmetric N-P diode and an N-P-N transistor, with external contacts of the ohmic type, are considered. The effect of a finite surface recombination velocity at the external contact of the high-conductivity side of the diode is also analyzed. Distributions of electrostatic potential and quasi-Fermi levels, mobile carrier and net electric charge densities, and increments of mobile carrier densities for a small increment of applied voltage are shown as functions of position throughout the interior of the device. Terminal properties including currents and total incremental capacitance versus applied voltage are illustrated. "Exact" and conventional approximate analytical results are compared, and discrepancies are exposed.

6.1. Generalities.

In the previous chapters a numerical method of solution of the one-dimensional two-carrier transport equations describing the behavior of semiconductor junction devices has been described in detail. Difficulties arising in the numerical analysis of the problem have been exposed and overcome; criteria for the evaluation of the accuracy of the final results have been stated.

Although both method of solution and numerical techniques allow for arbitrary doping profiles, recombination-generation law, boundary conditions at the external contacts, and mobility dependencies, results

for a special type of idealized structure are presented as an example of numerical computation for a two-contact and a three-contact device. Absence of recombination in the interior of the device $[U(x) = 0]$, abrupt asymmetric impurity distribution, and constant mobilities are assumed. The analysis is restricted to "short" structures (with respect to diffusion lengths) so that recombination effects other than at the contacts may be neglected. The choice of abrupt doping profiles has two motivations:

(a) the achievement of an extensive analysis for the numerically worst case represented by abrupt variations,

(b) the comparison between "exact" and approximate analytical solutions only available for idealized structures.

Motivation (b) also justifies the selection of appropriate constant values for the carrier mobilities.

Results, obtained for an idealized two-contact, single-junction device and a three-contact double-junction device, are presented and discussed in the following sections.

6.2. A two-contact device: the N-P diode.

A short N-P structure of the type illustrated in Fig. 1.1 is considered first. Absence of generation-recombination in the interior of the device $[U(x) = 0]$, highly asymmetric step distribution for the impurity density, and constant mobilities are assumed. The device will be examined under two different types of external contacts.

6.2.1. External contacts of the ohmic type.

In addition to the above assumptions, external contacts of the ohmic type (Eq.(1.32)) are specified for the N-P device under consideration. The physical parameters characterizing the structure are listed in Table 6.1.

For various applied voltages the electrostatic potential ψ and the quasi-Fermi levels φ_n, φ_p are shown in Fig. 6.1 as functions of position, the mobile carrier densities n, p and the net charge ρ in Fig. 6.2 (semi-logarithmic scales) and in Fig. 6.3 (linear scales), and the increments of mobile carriers Δn, Δp for a small increment of applied voltage (0.1% of the potential drop across the transition region), in Fig. 6.4. A dashed vertical line indicates the position of the metallurgical interface at $x = 0.2$. Terminal properties (current-voltage characteristic, and total incremental capacitance versus voltage) are depicted in Figs. 6.5 and 6.6. Quantities are displayed in normalized form; currents and capacitances are given per unit cross-sectional area. Both exact and first-order results (identified by the superscript "f") are displayed wherever appropriate (the first-order net charge density is not shown in the high-conductivity side because of the narrowness of its depleted region); the carrier and net charge densities are compared at the same value of total current, and the electrostatic potential and quasi-Fermi levels at the same value of applied voltage.

The first-order results displayed are generated by the simple conventional formulation briefly summarized in Appendix A. The electrostatic potential distribution $\psi^{(f)}$ is given in the various regions by

Parameter	Value
Material:	germanium (relative permittivity = 16)
Temperature:	$300^{\circ}K$
Doping:	N-side, $N(x) = N_D = 10^4$ (or 2.5×10^{17} cm^{-3}) P-side, $-N(x) = N_A = 10^2$ (or 2.5×10^{15} cm^{-3})
Length:	N-side, M-0 = 0.2 (or 0.1913×10^{-4} cm) P-side,* forward bias L-M = 1.4 (or 1.339×10^{-4} cm) P-side,* reverse bias L-M = 3.0 (or 2.870×10^{-4} cm)
Carrier mobilities:	electron, $\gamma_n^{-1} = 93$ (or $\simeq 3600$ cm^2/volt-sec) hole, $\gamma_p^{-1} = 44$ (or $\simeq 1700$ cm^2/volt-sec)

Table 6.1. The physical parameters characterizing the N-P structure, analyzed under steady-state conditions for various applied voltages.

---

* Consistency with the first-order theory model requires a slightly longer structure in reverse-bias cases. Boundary effects not accounted for by the first order theory, such as the contribution to the total incremental capacitance of the sheet of charge at the external contacts, are then negligible.

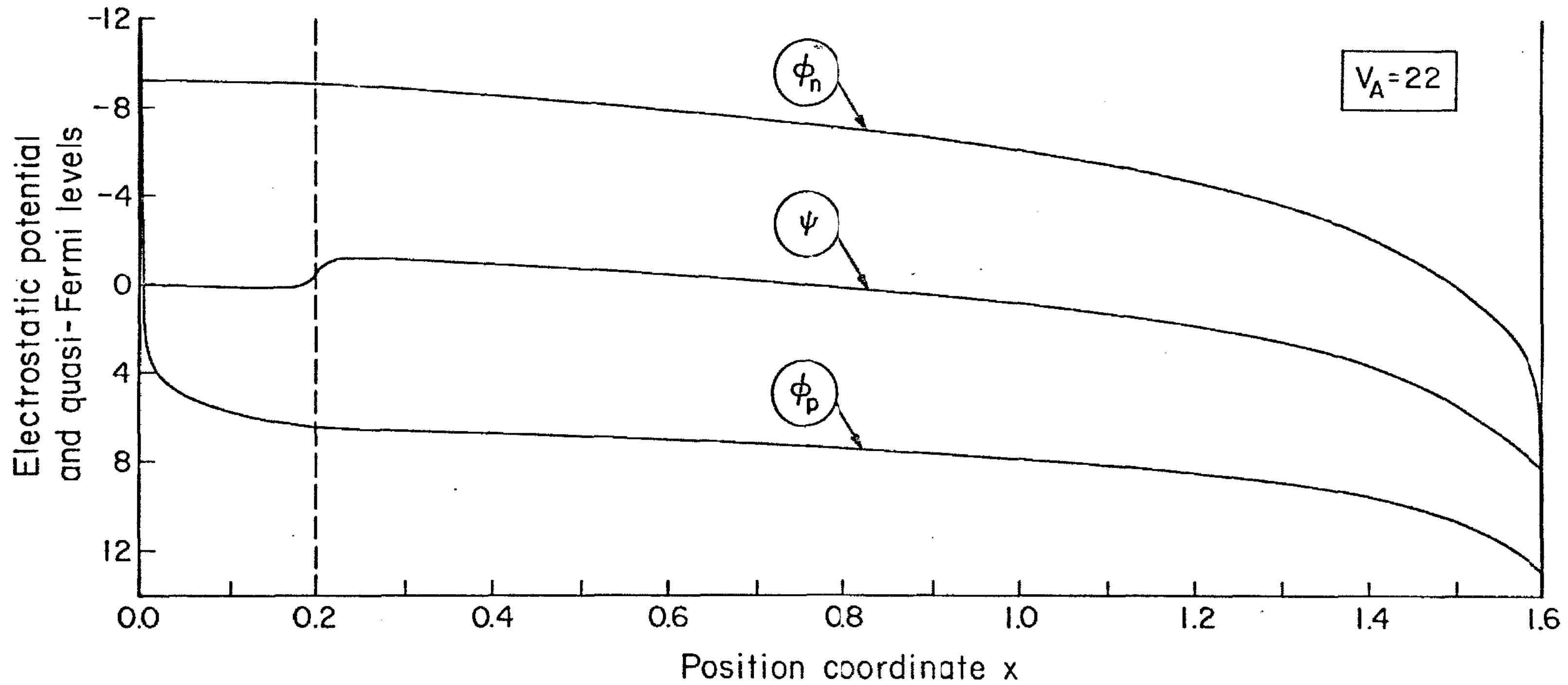

Fig. 6.1a. Structure of Fig. 1.1; parameters of Table 6.1; boundary conditions (1.32). Electrostatic potential and quasi-Fermi levels as functions of position. High forward bias case ($V_A = 22$).

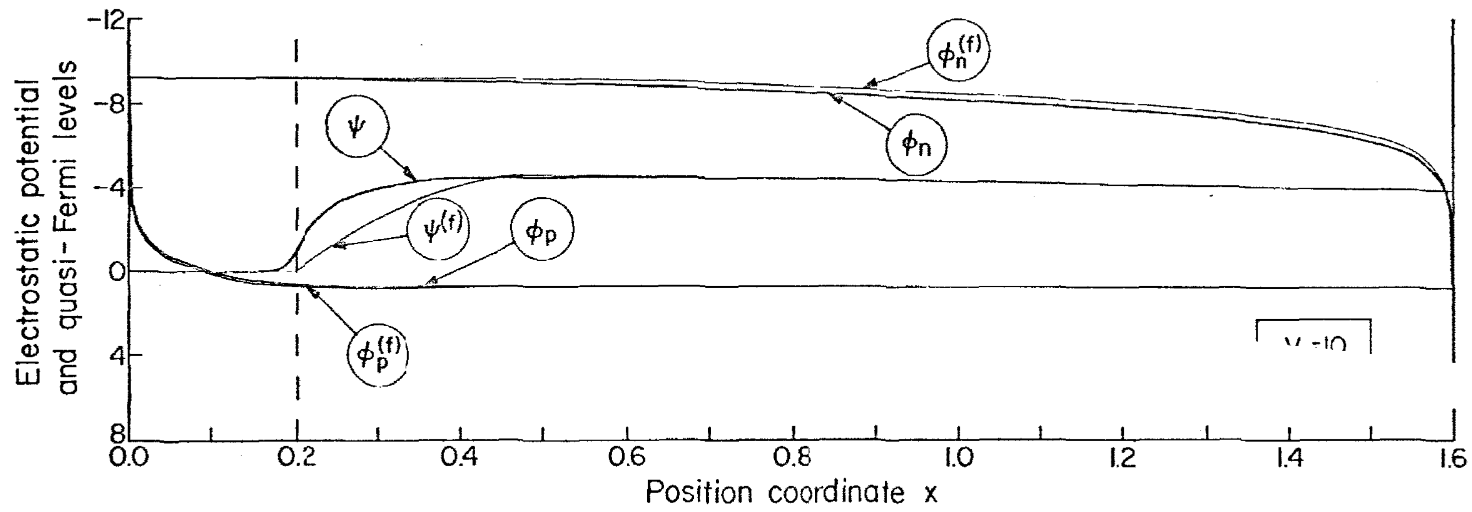

Fig. 6.1b. Device as in Fig. 6.1a. Electrostatic potential and quasi-Fermi levels as functions of position. Moderate forward bias case ($V_A = 10$).

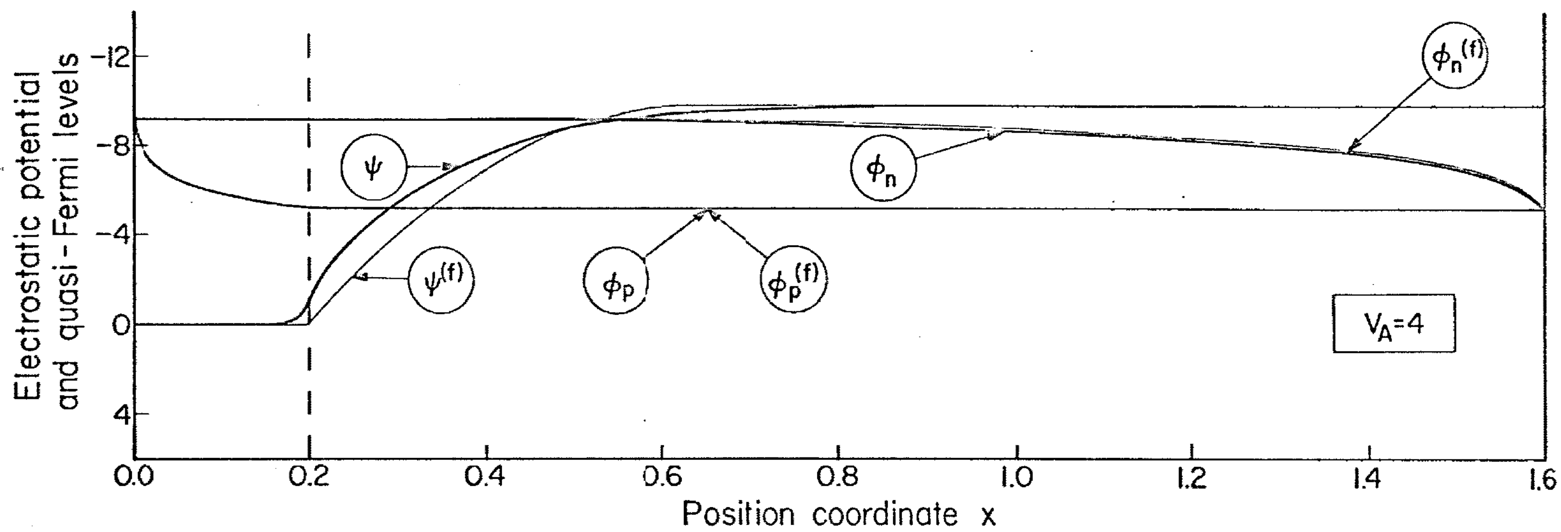

Fig. 6.1c. Device as in Fig. 6.1a. Electrostatic potential and quasi-Fermi levels as functions of position. Low forward bias case ($V_A = 4$).

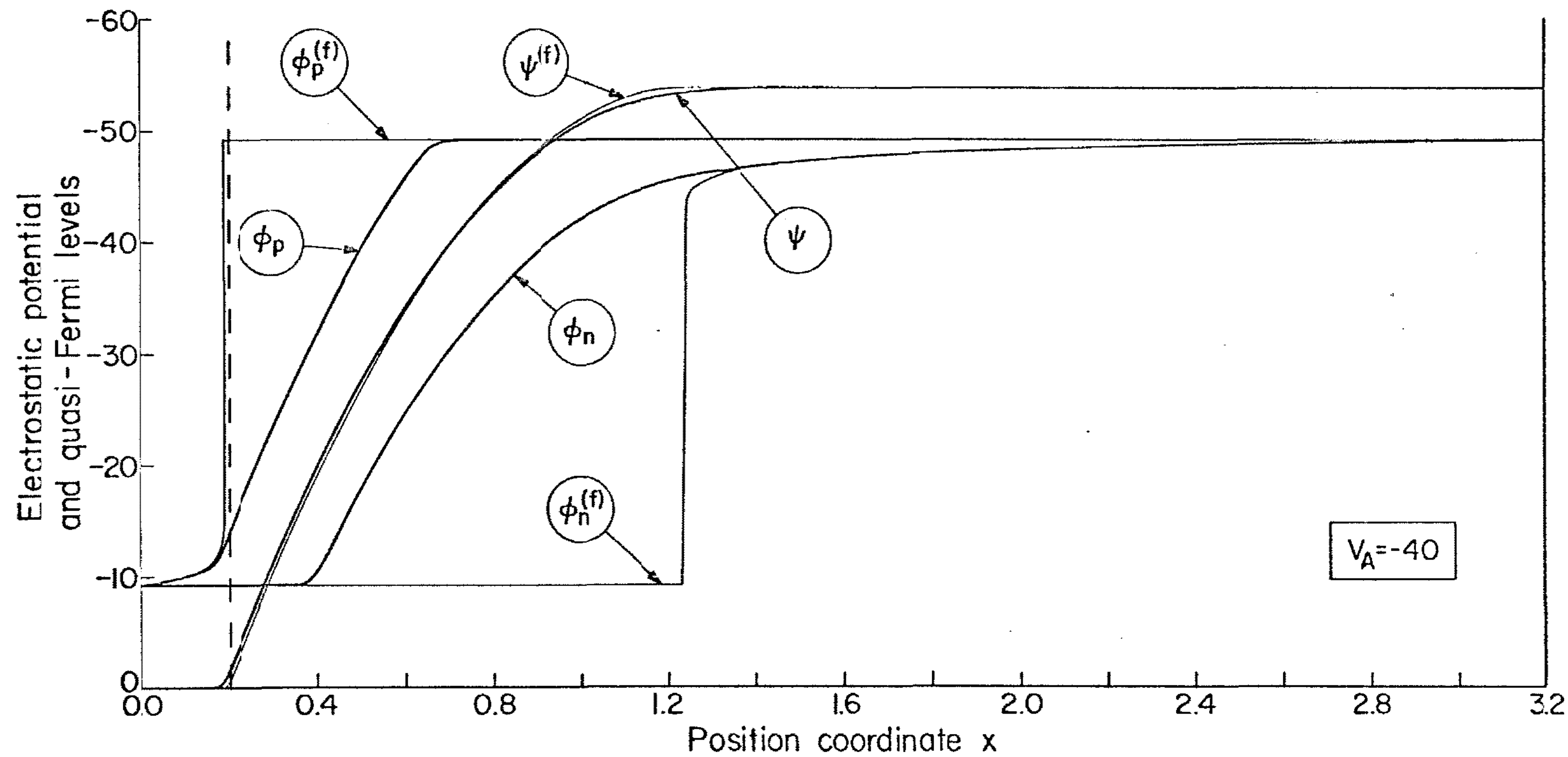

Fig. 6.1d. Device as in Fig. 6.1a. Electrostatic potential and quasi-Fermi levels as functions of position. Low reverse bias case ($V_A = -40$).

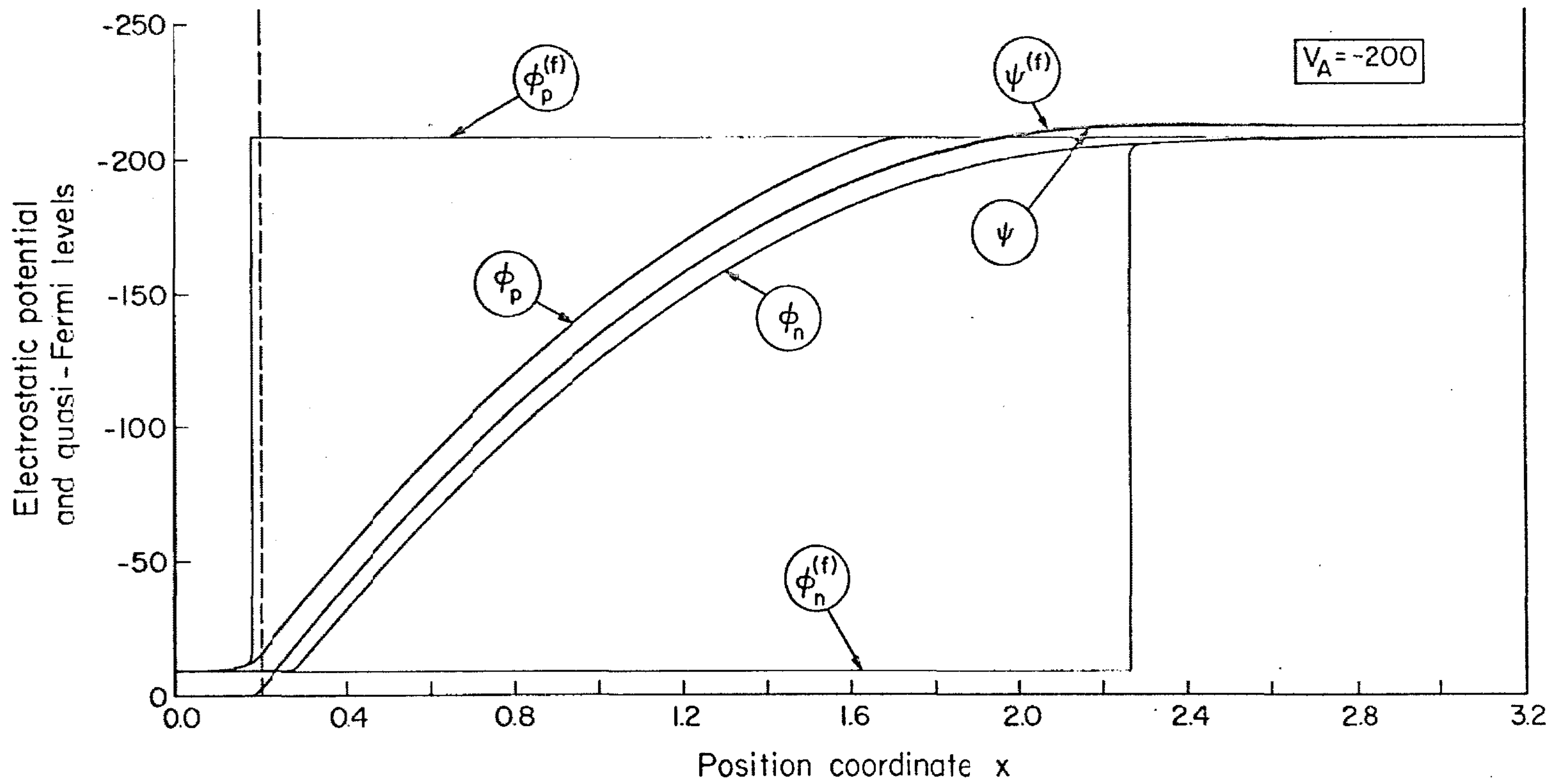

Fig. 6.1e. Device as in Fig. 6.1a. Electrostatic potential and quasi-Fermi levels as functions of position. Moderate reverse bias case ($V_A = -200$).

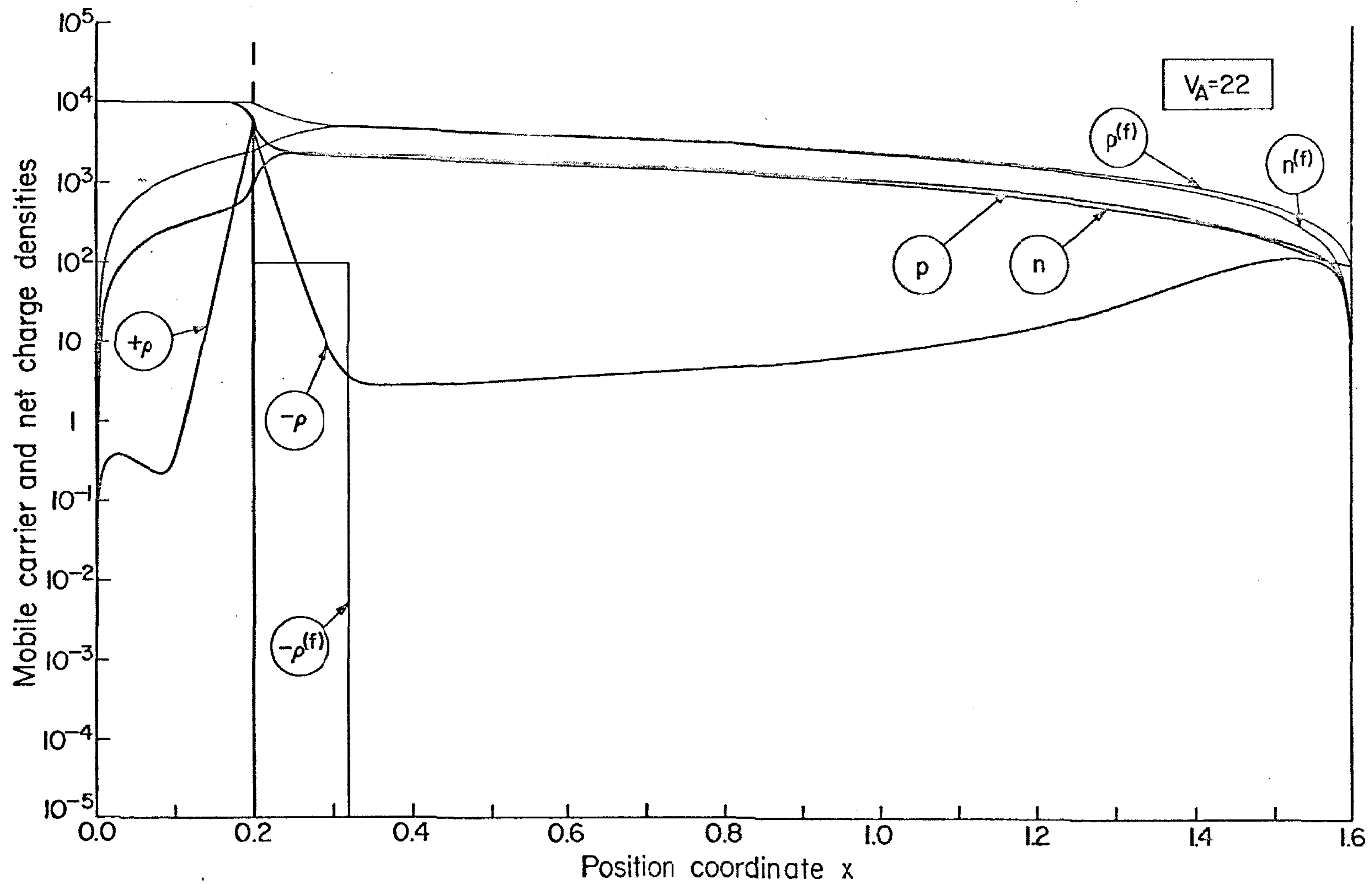

Fig. 6.2a. Device as in Fig. 6.1a. Mobile carrier and net charge densities as functions of position (semi-logarithmic scales). High forward bias case (V_A = 22).

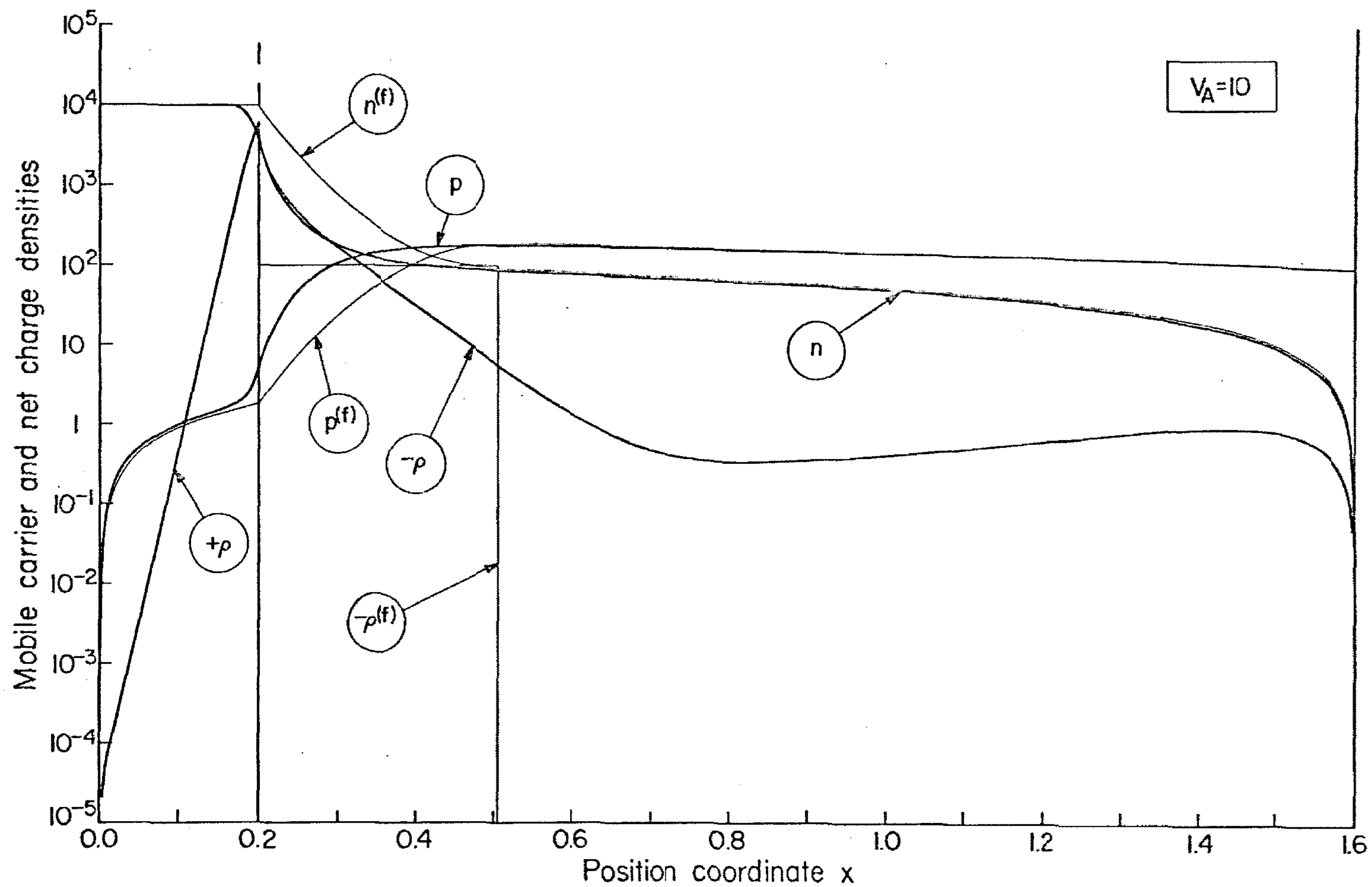

Fig. 6.2b. Device as in Fig. 6.1a. Mobile carrier and net charge densities as functions of position (semi-logarithmic scales). Moderate forward bias case (V_A = 10).

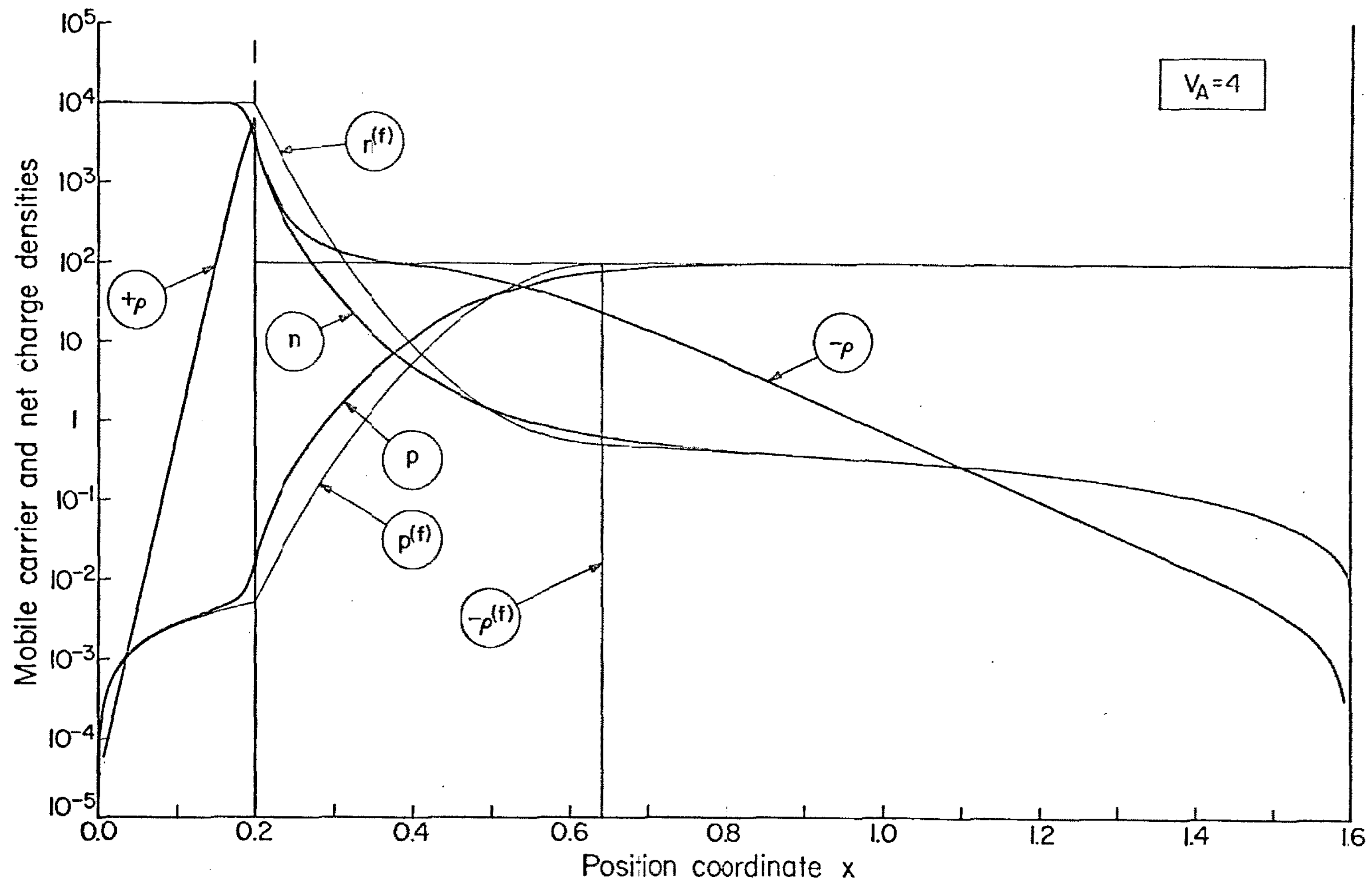

Fig. 6.2c: Device as in Fig. 6.1a. Mobile carrier and net charge densities as functions of position (semi-logarithmic scales). Low forward bias case ($V_A = 4$).

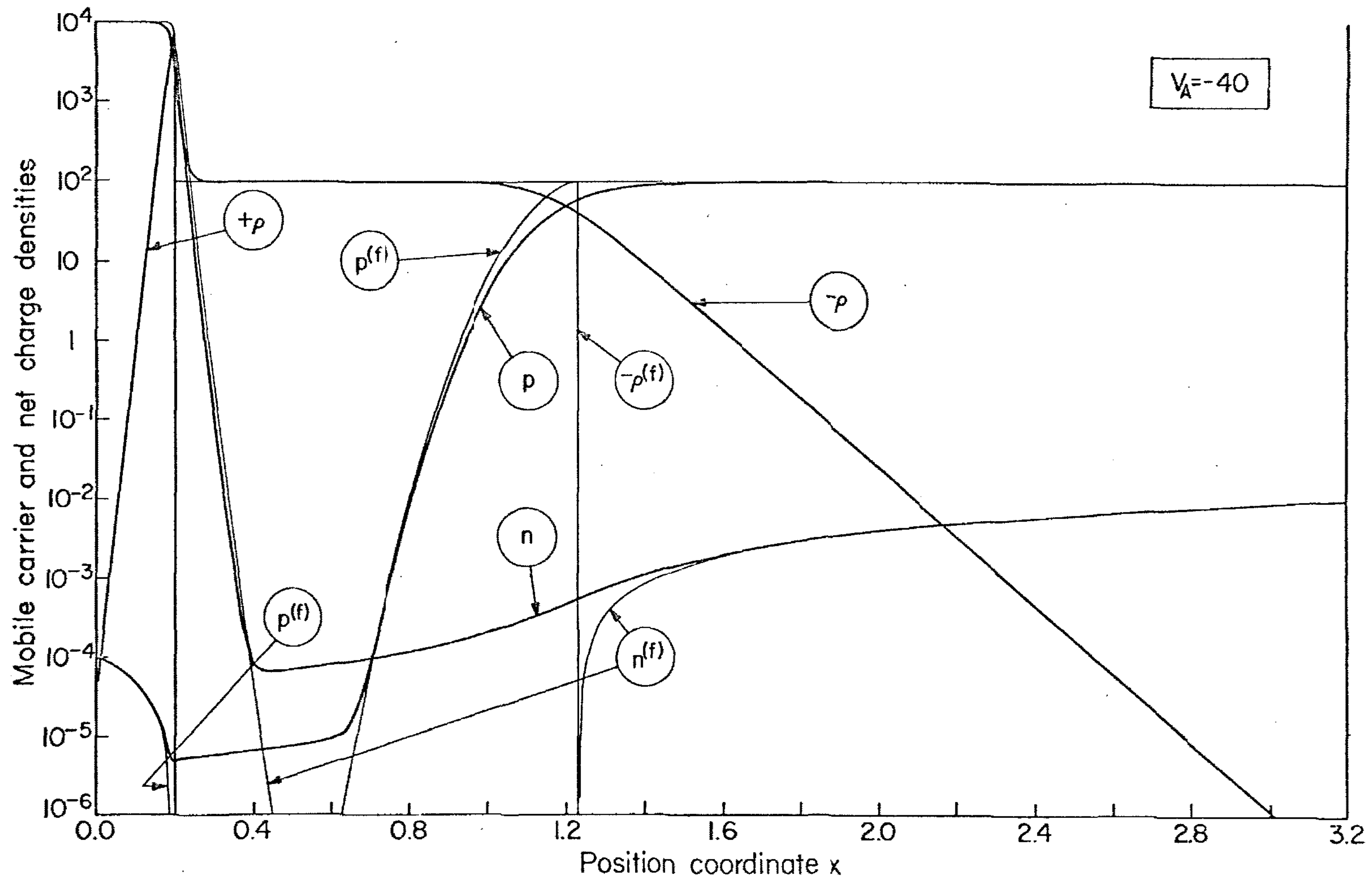

Fig. 6.2d. Device as in Fig. 6.1a. Mobile carrier and net charge density as functions of position (semi-logarithmic scales). Low reverse bias case (V_A =-40).

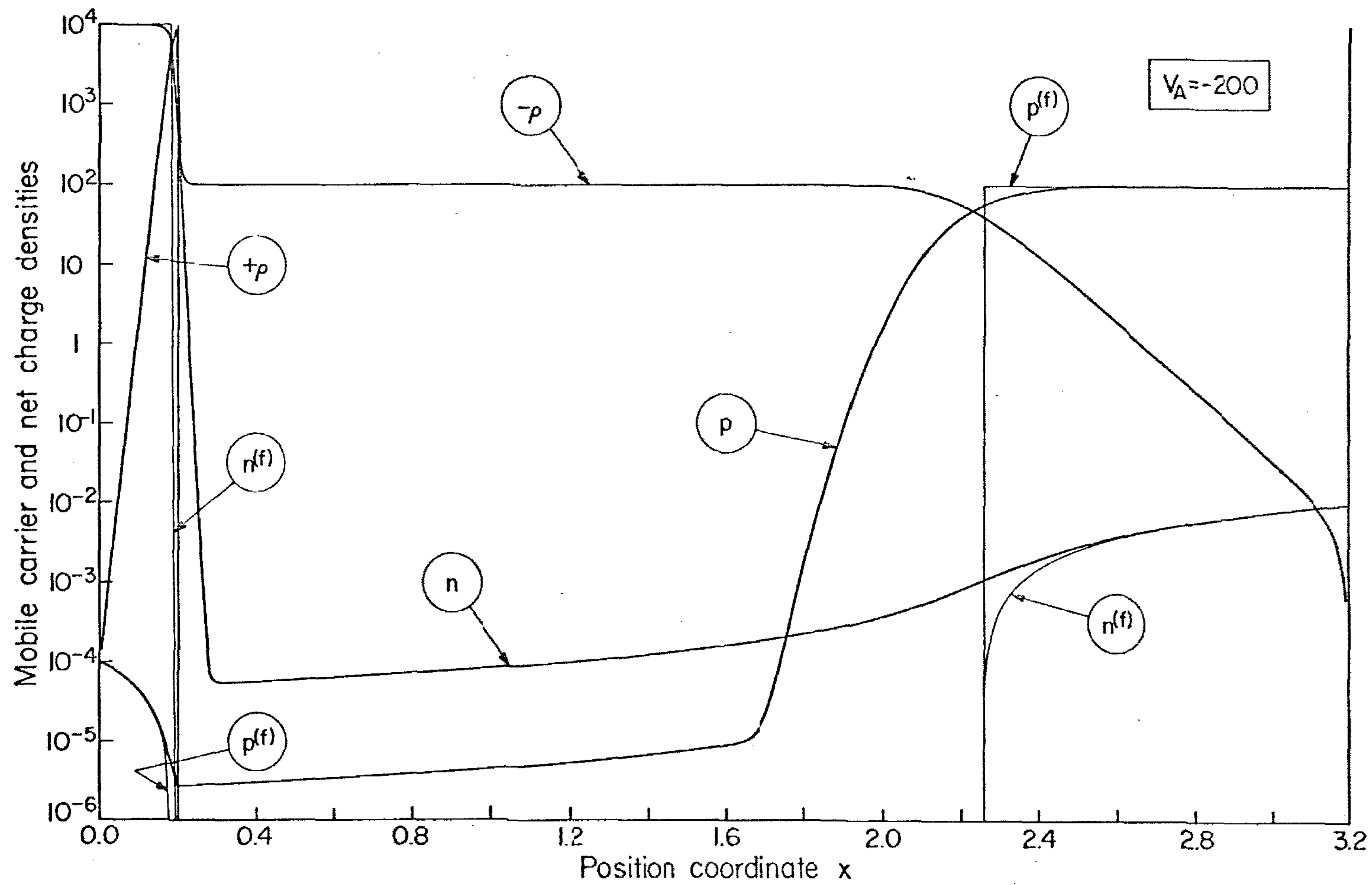

Fig. 6.2e. Device as in Fig. 6.1a. Mobile carrier and net charge densities as functions of position (semi-logarithmic scales). Moderate reverse bias case (V_A = -200).

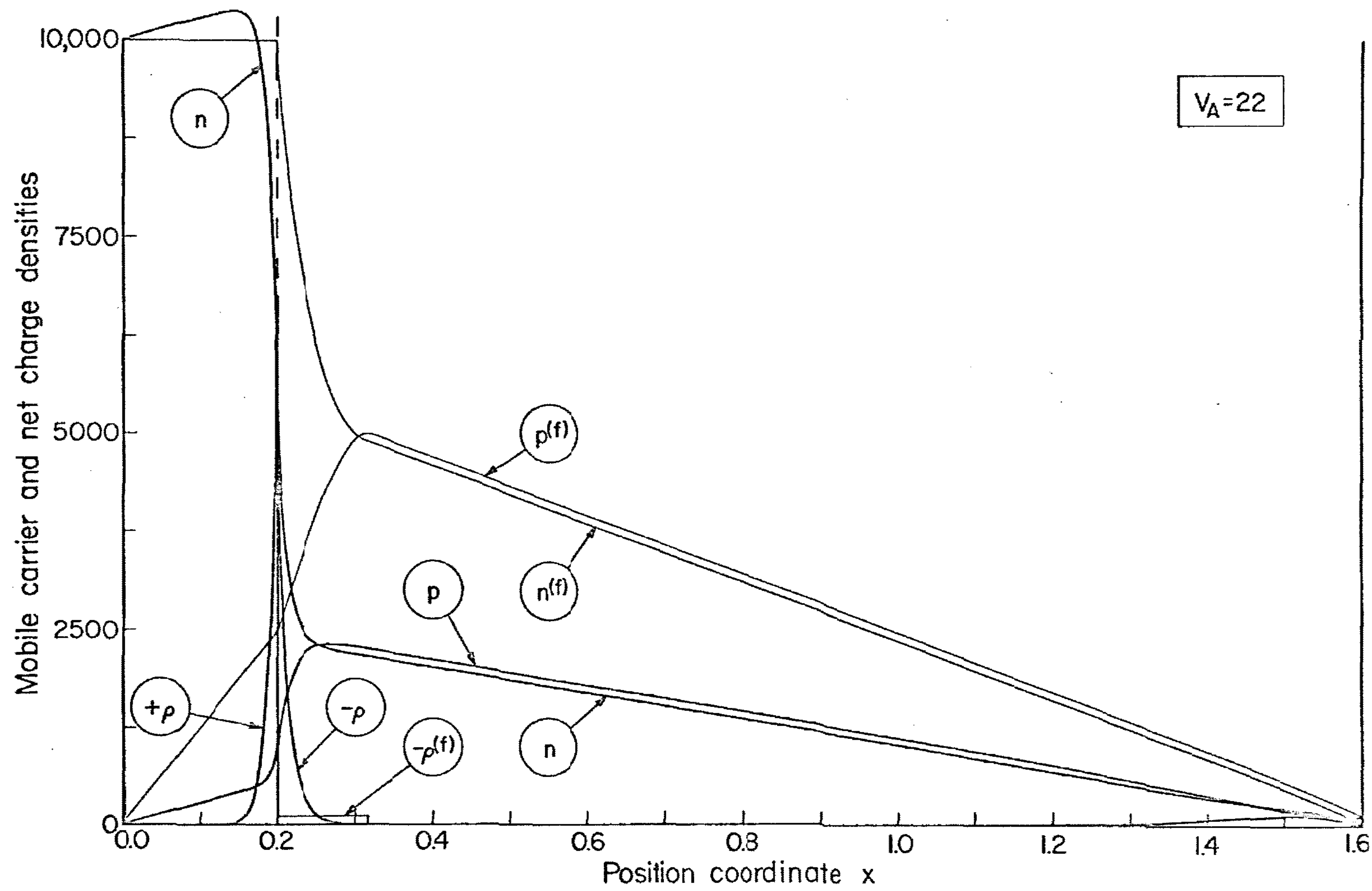

Fig. 6.3a. Device as in Fig. 6.1a. Mobile carrier and net charge densities as functions of position (linear scales). High forward bias case (V_A = 22).

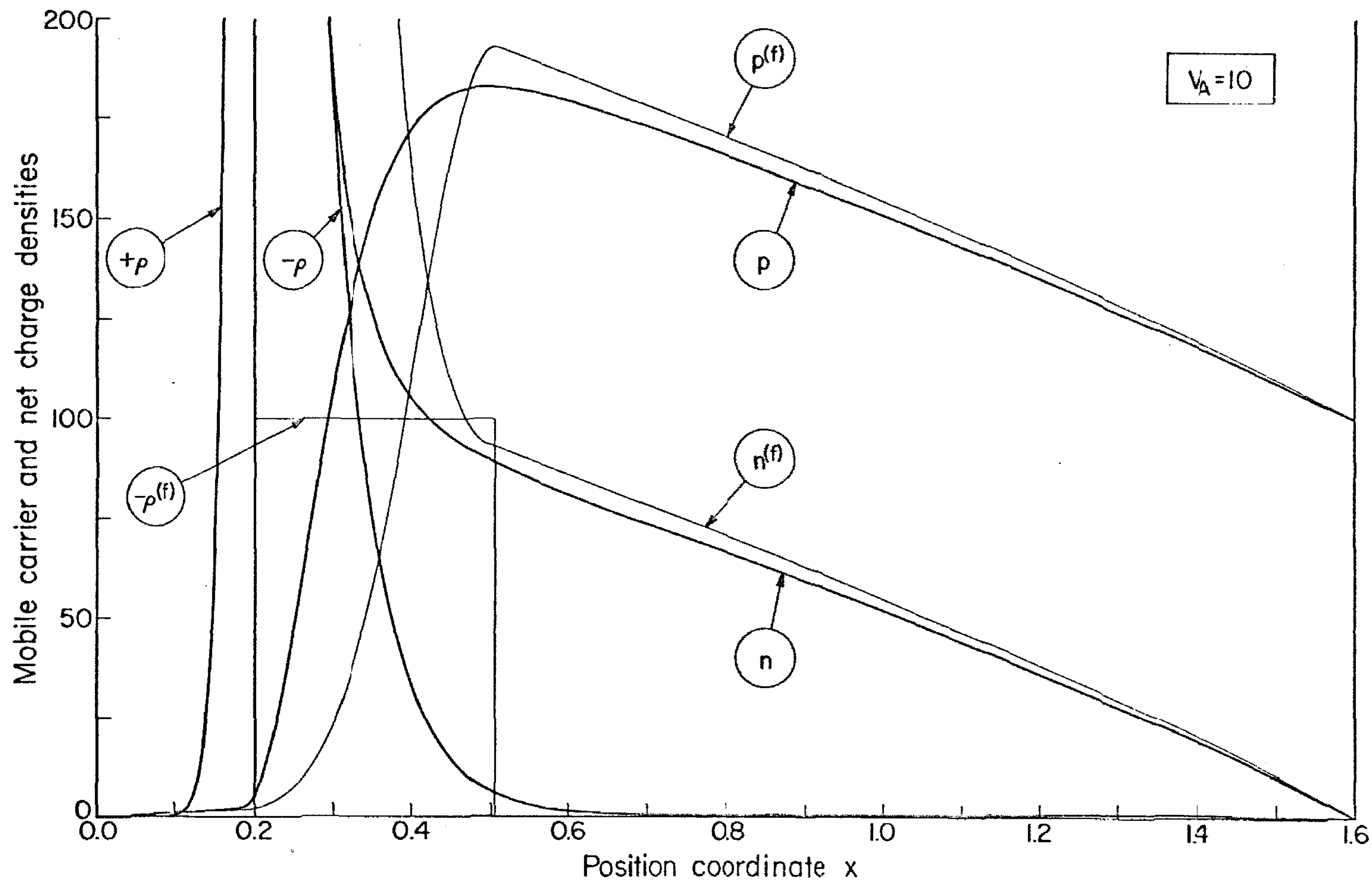

Fig. 6.3b. Device as in Fig. 6.1a. Mobile carrier and net charge densities as functions of position (linear scales). Moderate forward bias case ($V_A = 10$).

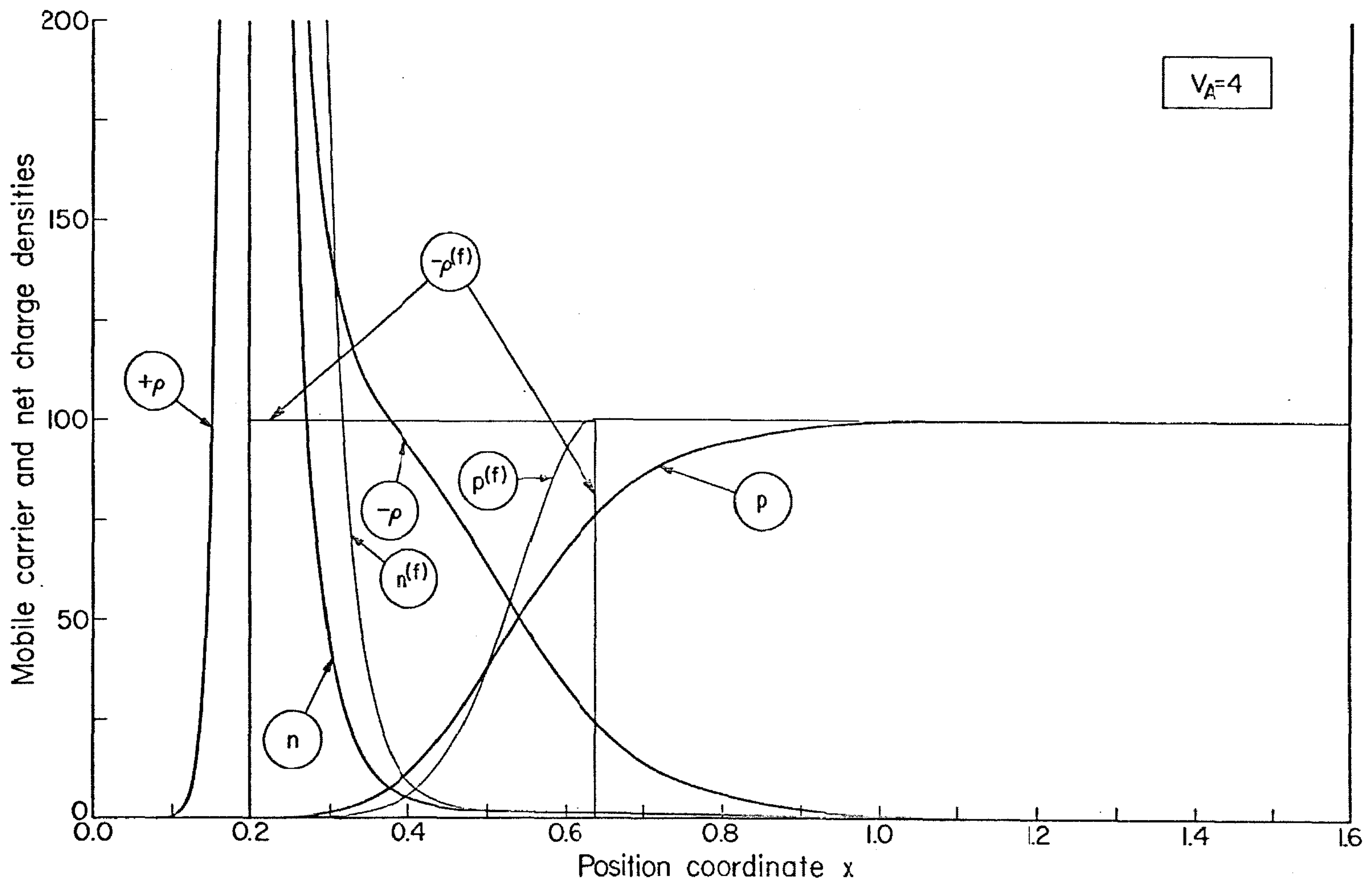

Fig. 6.3c$_1$. Device as in Fig. 6.1a. Mobile carrier and net charge densities as functions of position (linear scales). Low forward bias case (V_A = 4).

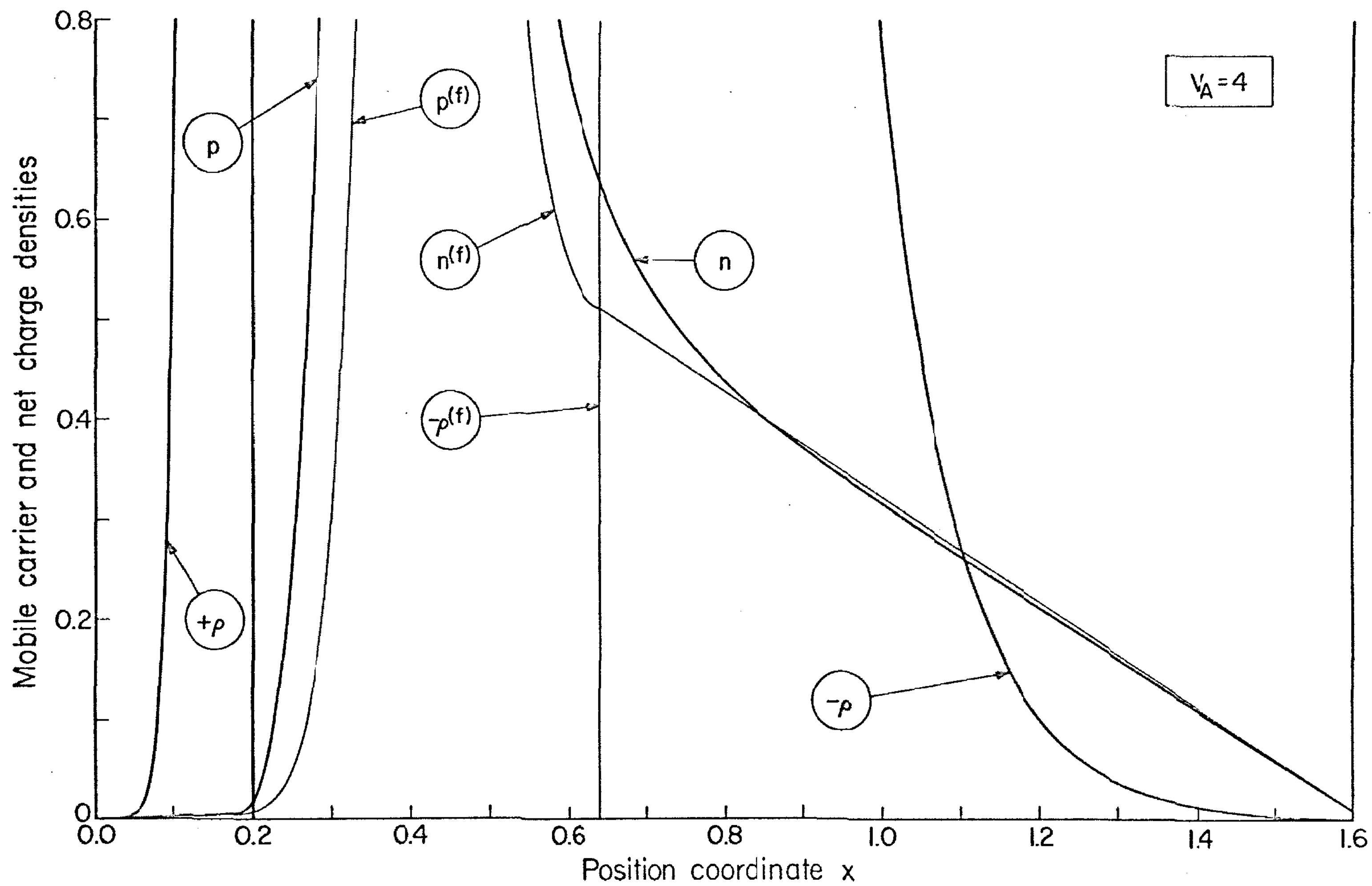

Fig. 6.3c$_2$. Device as in Fig. 6.1a. Mobile carrier and net charge densities as functions of position (linear scales). Low forward bias case ($V_A = 4$).

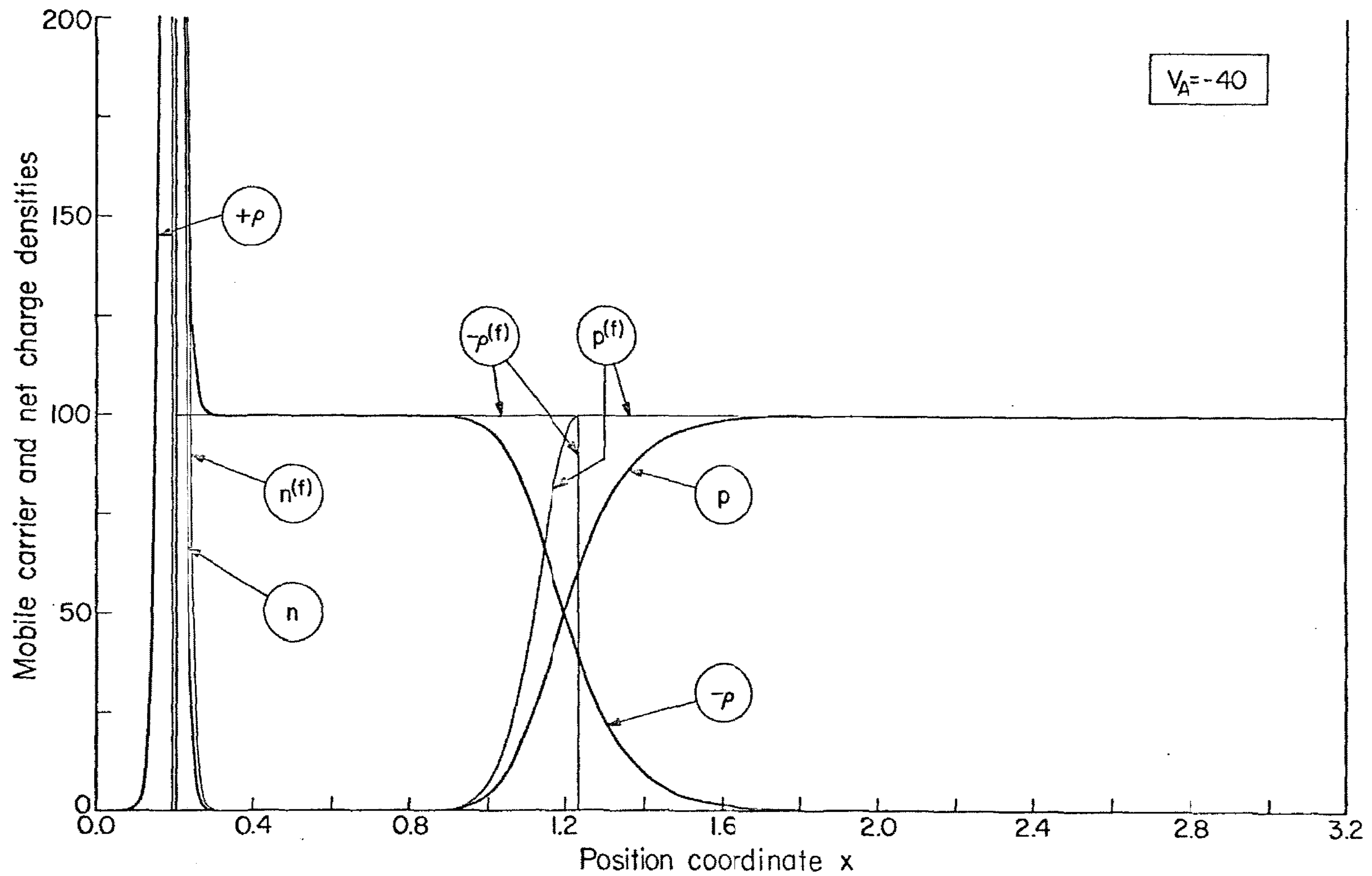

Fig. 6.3d. Device as in Fig. 6.1a. Mobile carrier and net charge densities as functions of position (linear scales). Low reverse bias case (V_A = -40).

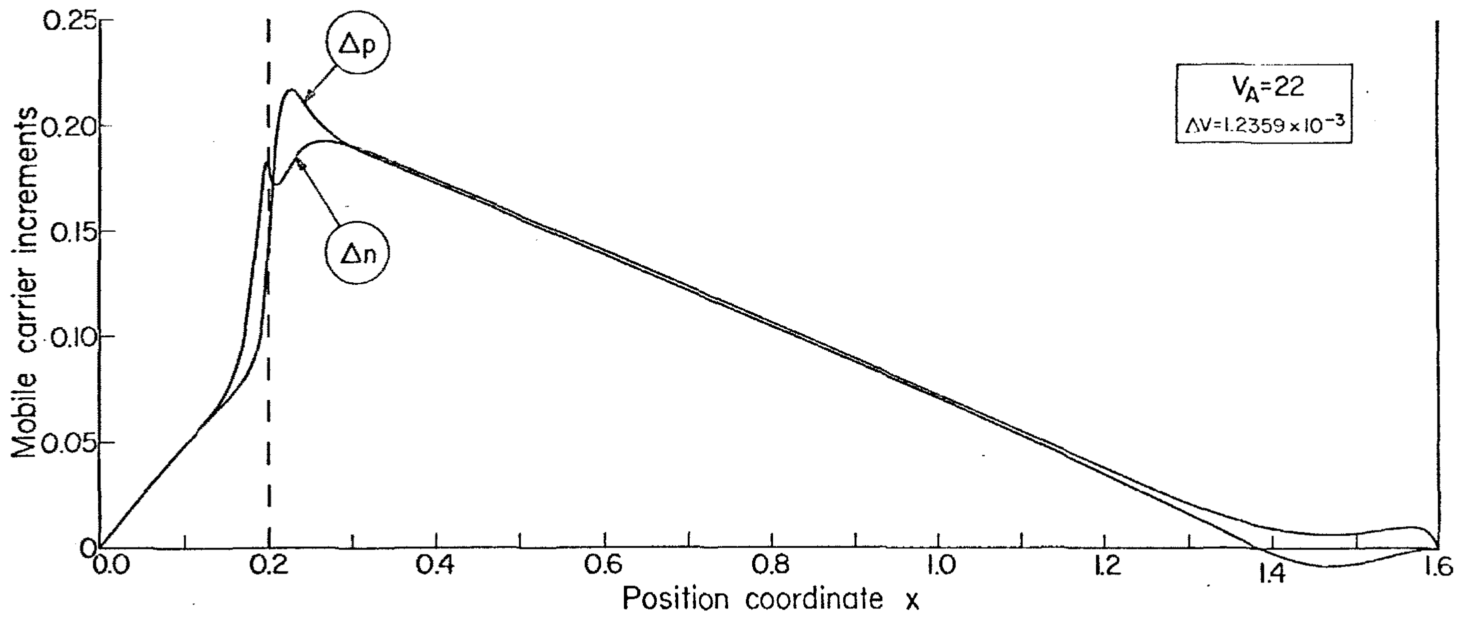

Fig. 6.4a. Device as in Fig. 6.1a. Mobile carrier density increments as functions of position, for a small increment ΔV of applied voltage (linear scales). High forward bias case (V_A = 22).

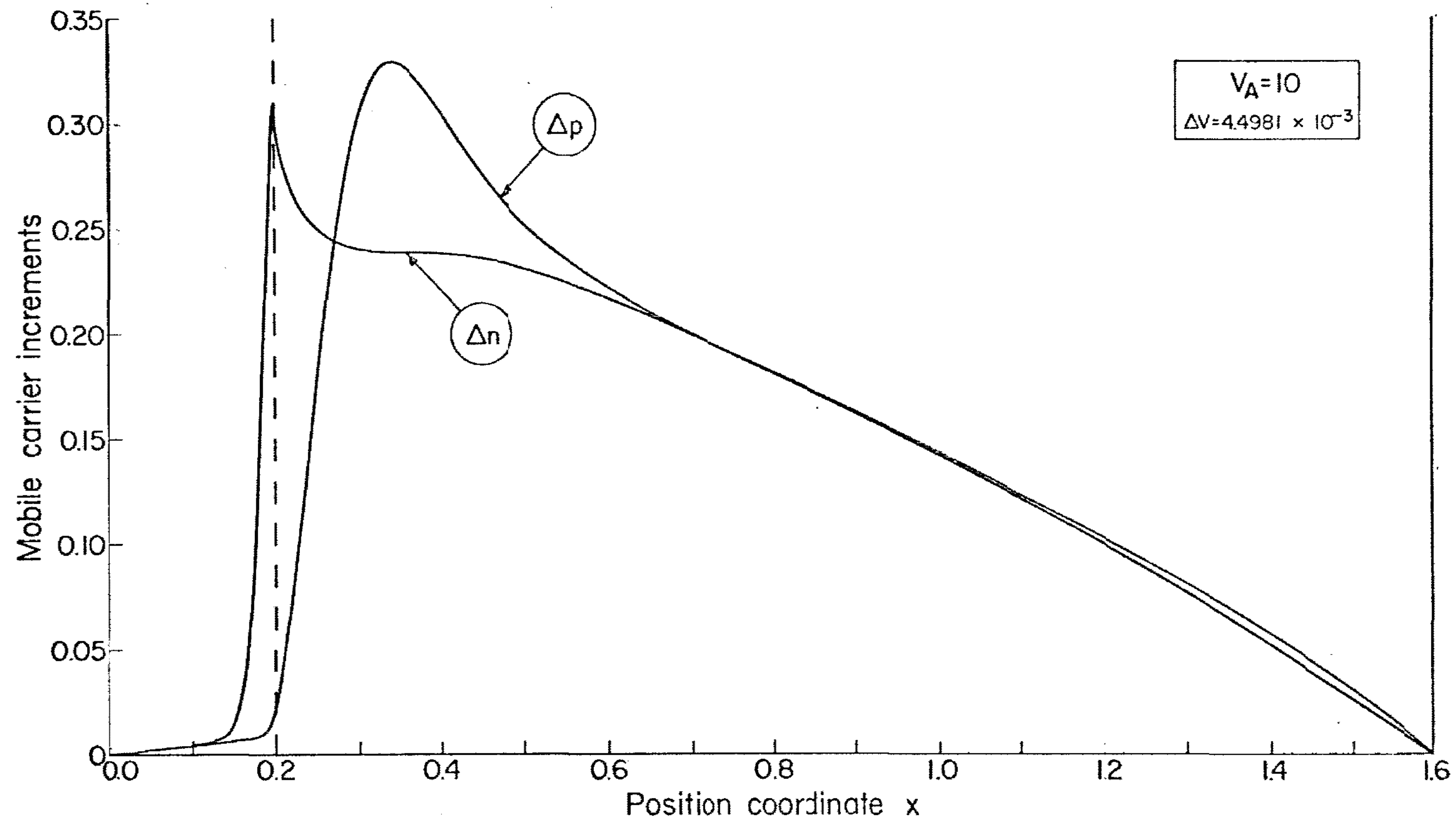

Fig. 6.4b. Device as in Fig. 6.1a. Mobile carrier density increments as functions of position, for a small increment ΔV of applied voltage (linear scales). Moderate forward bias case ($V_A = 10$).

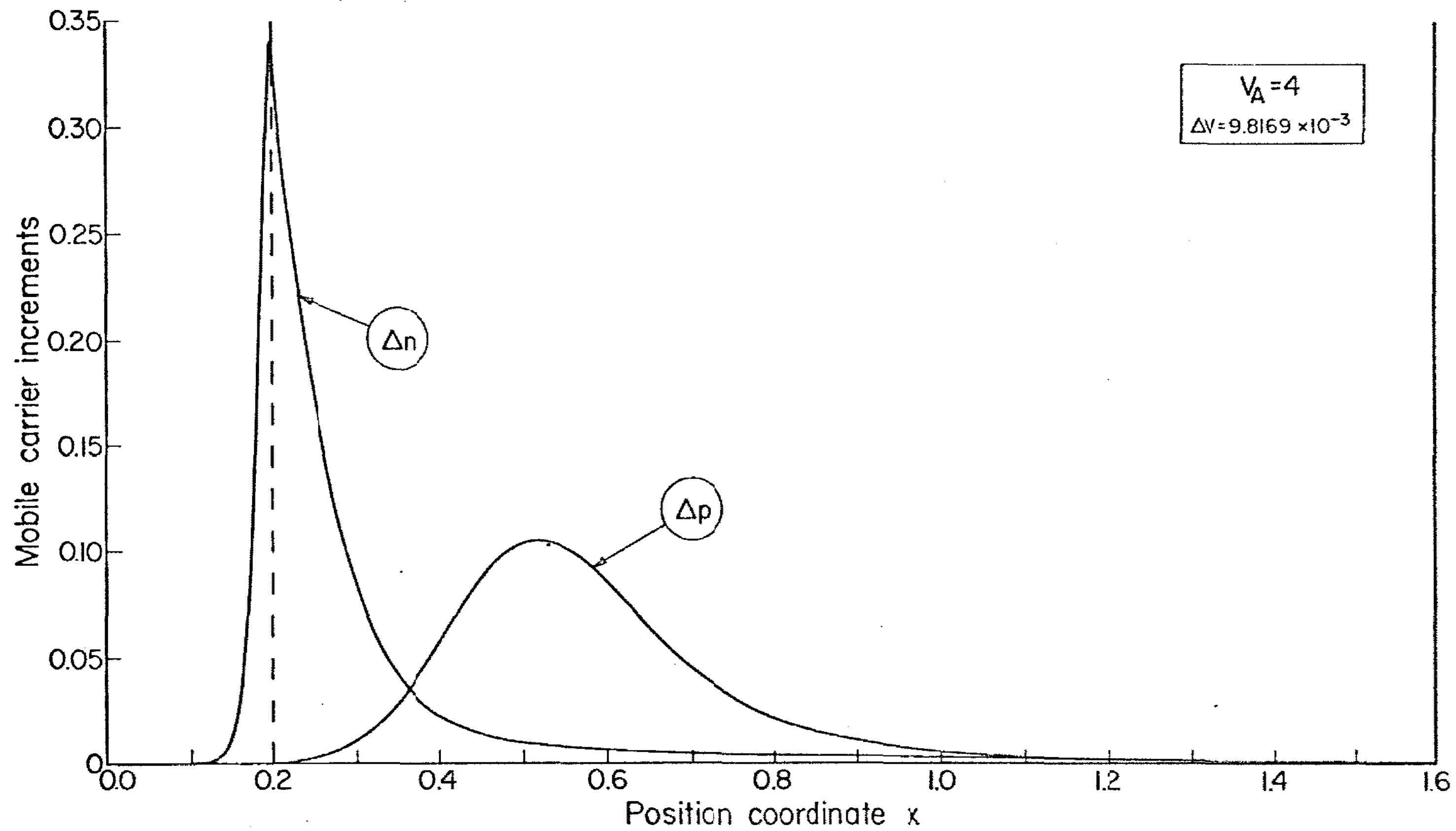

Fig. 6.4c. Device as in Fig. 6.1a. Mobile carrier density increments as functions of position, for a small increment ΔV of applied voltage (linear scales). High forward bias case. ($V_A = 4$).

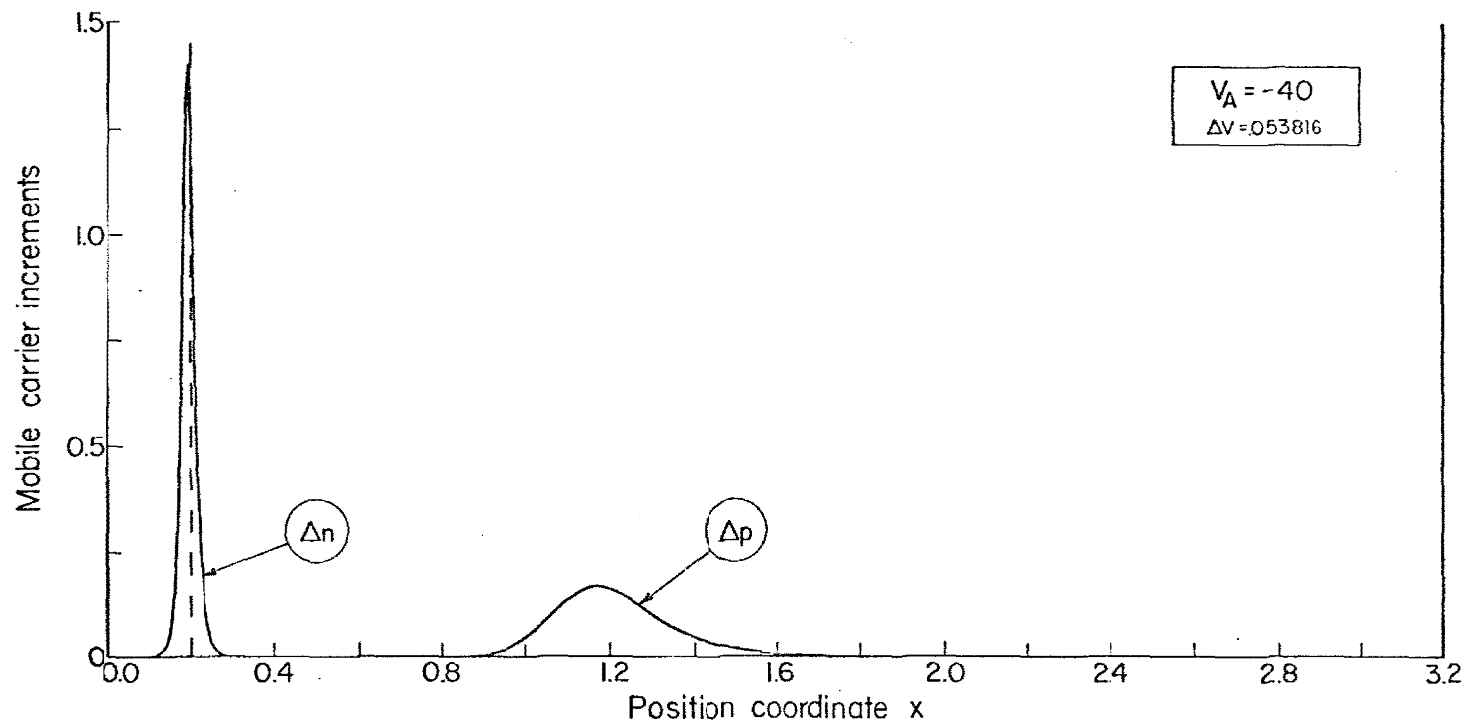

Fig. 6.4d. Device as in Fig. 6.1a. Mobile carrier density increments as functions of position, for a small increment ΔV of applied voltage (linear scales). Low reverse bias case ($V_A = -40$).

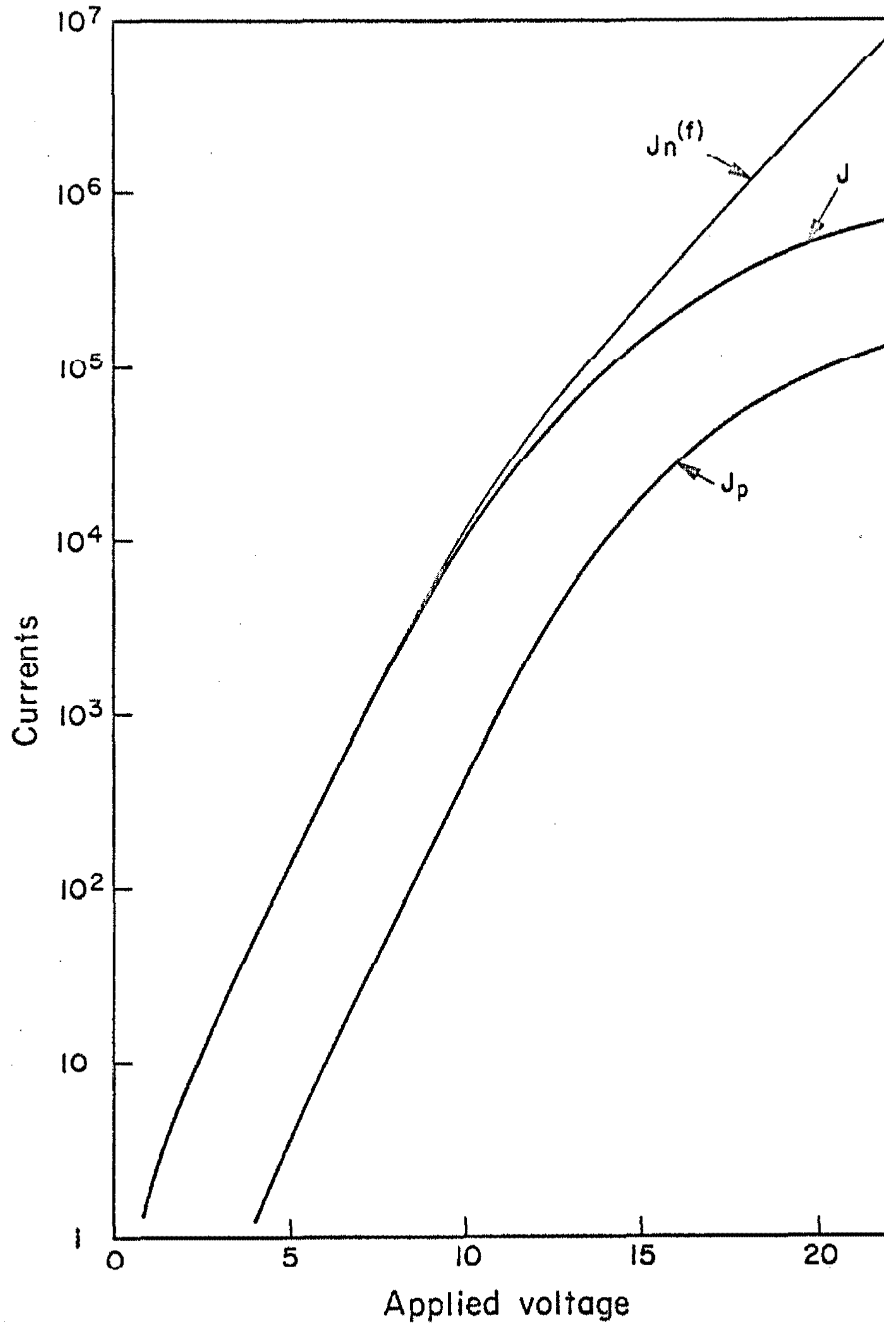

Fig. 6.5a. Device as in Fig. 6.1a. Current densities as functions of applied voltage. Forward bias.

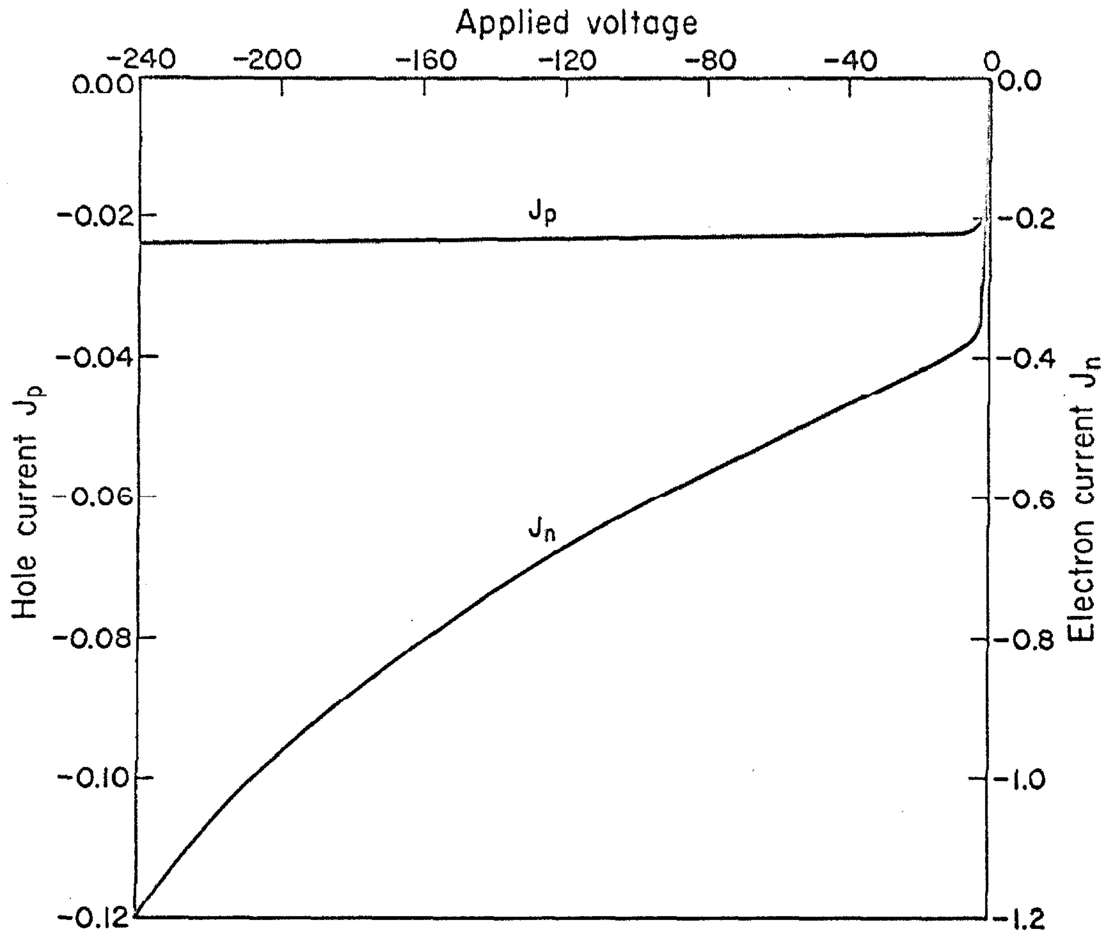

Fig. 6.5b. Device as in Fig. 6.1a. Current densities as functions of applied voltage. Reverse bias.

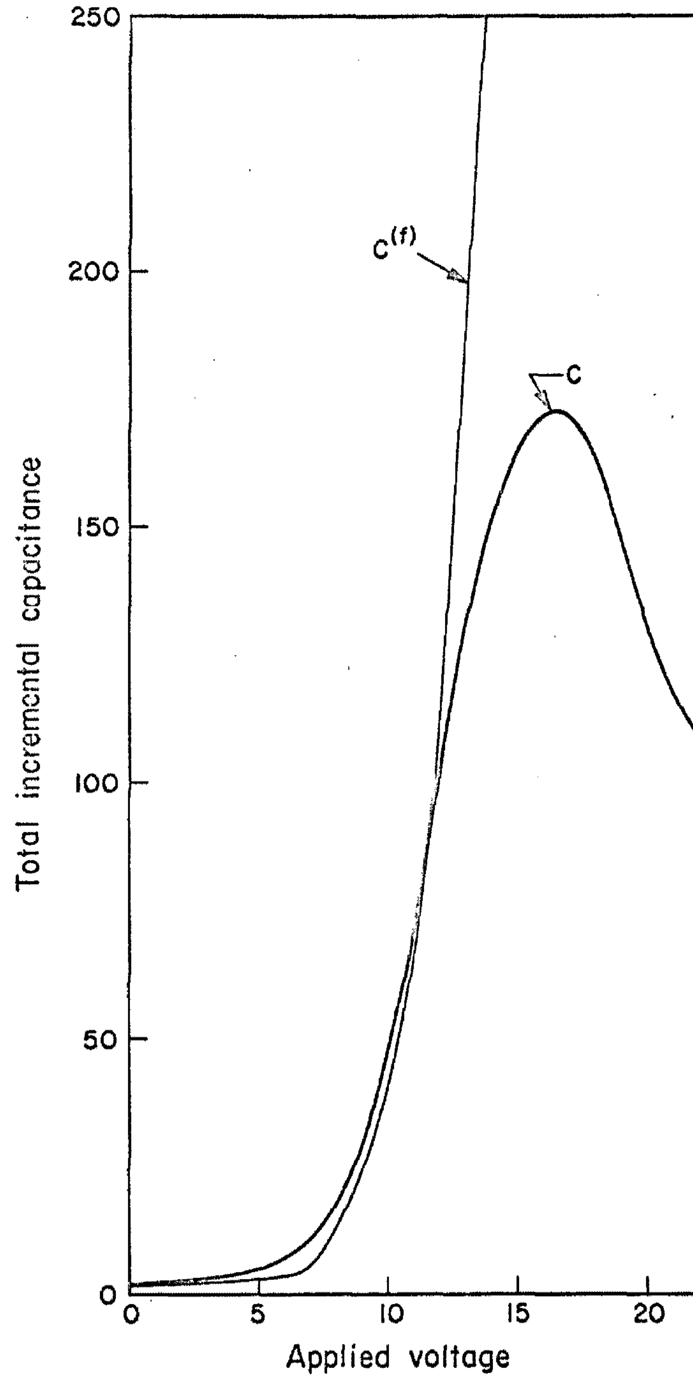

Fig. 6.6a Device as in Fig. 6.1a. Total incremental capacitance (per unit area) as a function of applied voltage. Forward bias.

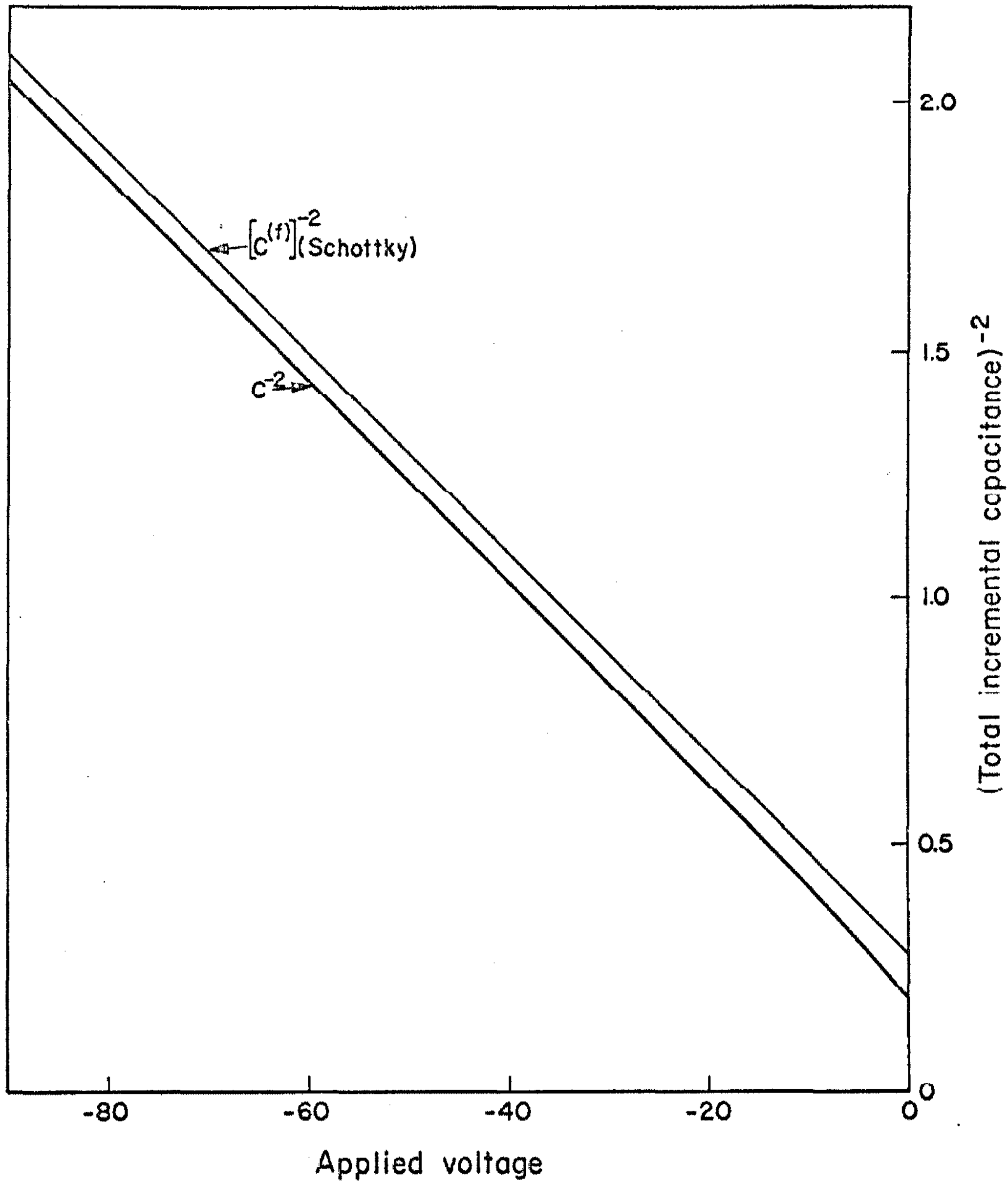

Fig. 6.6b. Device as in Fig. 6.1a. Reciprocal of the square of the total incremental capacitance (per unit area) as a function of applied voltage. Reverse bias.

Eqs.(A-21), (A-36), (A-37), (A-42) and by the combination of Eqs. (A-12) and (A-15); the electron density distribution $n^{(f)}$ by Eqs. (A-20), (A-30), and (A-12); the hole density distribution $p^{(f)}$ by Eqs.(A-19), (A-35), and (A-9). Relations (A-6a), (A-6b) yield then the quasi-Fermi level distributions $\varphi_n^{(f)}$, $\varphi_p^{(f)}$, and the right-hand side of Poisson's equation (A-4), together with the assumption of fully-depleted transition region, yields the net electric charge $\rho^{(f)}$. The current-voltage relationship $J_n^{(f)} = J_n^{(f)}(V_A)$ is given by the combination of Eq.(A-13) with Eq.(A-41), and the total incremental capacitance $C^{(f)}$ by the sum of the expressions (A-54) and (A-55).

The poorness of the first-order theory assumptions of sharp boundaries between the depleted and neutral regions is evident in Fig. 6.2 and particularly in the linear expansions of Fig. 6.3: with exception of the reverse-bias cases, the net charge density distribution has little resemblance to the first-order idealization. Moreover, the concept of a depleted region appears to be highly unrealistic even at moderate injection levels.

On the other hand, neutrality is well conserved far from the transition region, with the exception of a narrow region near the external contact on the P-side at high injection levels. The "ohmic" contact prevents the conductivity of such a narrow region from being significantly modulated, so that the large current causes a high voltage drop, or, in equivalent terms, a strong (negative) electric field near the terminal. Holes tend then to be expelled from this region and electrons attracted, the consequence being a local alteration of the neutrality balance. This effect is particularly evident in the very high injection

case depicted in Fig. 6.2a, which shows how the electron density is forced to become greater than the hole density in a short region near the external contact in the low conductivity P-side.

Although the positions of the boundaries of the transition region are not well defined, it may be observed (Figs. 6.2, 6.3) that the exact distributions indicate, at high injection levels, a width of the "depleted region" significantly smaller than that predicted by the first-order theory.

On the contrary, the Boltzmann relation for injected minority carriers, in terms of the exact potential drop across the transition region, agrees well with the exact equivalent in forward bias. This may also be verified from the constancy of the exact quasi-Fermi levels in the transition region. In reverse bias (Fig. 6.2d, e) the Boltzmann relation is in error by many orders of magnitude in predicting the minority carrier density at the edges of the transition region. This discrepancy may be related to Middlebrook's detailed treatment [5] of the transition region properties of a reverse-biased P-N junction under various conditions of current injection.

The monotonic character of the exact quasi-Fermi levels throughout the entire length of the device, for any forward bias condition, reaffirms the inequality

$$p(x) \cdot n(x) \leq e^{V_A}$$

between the hole-electron product and the externally applied voltage V_A. This is in agreement with Gummel's recent numerical results [21]

for a slightly different structure.

The distributions of the injected minority carriers (Fig. 6.3) are closely linear in forward bias and would agree well with the first-order results were the boundary values at the edges of the transition region predicted correctly.

In spite of the serious disagreement between the distributions of the relevant quantities in the interior of the device, the first-order terminal properties are close to the exact ones with the exception of the very high injection range. The discrepancy in the current-voltage characteristic (Fig. 6.5a) at high injection is generated mainly by the properties of the external contact of the ohmic type in the N-side and by the particular structural parameters chosen. The equilibrium carrier boundary condition at the external contact of the high conductivity N-side, together with the narrowness of the N-material, tend to oppose the conductivity modulation of the P-material at the transition region edge. This effect becomes already significant at high injection levels and is responsible for a smaller current and a higher potential drop across the transition region, for a given applied voltage, than predicted by the first-order theory which does not account for this phenomenon. A far better agreement is observed if the external boundary condition of the high conductivity side is modified by the introduction of a finite surface recombination velocity, with conservation of charge neutrality. The hole density at the contact is thus permitted to increase by several orders of magnitude, with the consequence of a significant decrease of the hole current and increase of the total current. This effect is considered in detail in the following

Section.

The decrease of emitter efficiency (i.e. the ratio between the injected minority current in the low-conductivity side and the total current) for increasing applied voltage may be explained as follows. The quasi-neutral region in the low-conductivity side (P-side), with exception of the regions adjacent to the boundaries, is considered. In such a region, at low injection, the electron current (i.e. the minority current) is essentially diffusion current, whereas both drift and diffusion are responsible for the hole current. In any forward bias case the electron current is given by the arithmetic sum of the drift and diffusion terms, and the hole current is given by the arithmetic difference between the two components. In addition, for any forward bias case, the hole diffusion component and electron diffusion component are essentially equal* (this is a consequence of electric charge neutrality in the region considered), and the magnitude of the hole drift current is always larger than the magnitude of the hole diffusion current. At high injection the electron density is essentially equal to the hole density, so that the electron and hole drift components are essentially equal.* It may also be observed, as a consequence of the essentially linear distribution of the mobile carriers, that the value of the electron and hole densities n and p increases, for an increase of applied voltage V_A, with the same rate as the respective slopes $\frac{dn}{dx}$ and $\frac{dp}{dx}$. Since also the electric field increases for

---

* The difference in electron and hole mobilities, or diffusion constants, is unimportant for the present reasoning. It is also recalled that both J_n and J_p are independent of position throughout the entire device.

increasing V_A, it may be concluded that, for both electron and hole currents, the magnitude of the drift terms increases faster than the magnitude of the respective diffusion terms, for an increase of V_A. It is then apparent that the ratio

$$\frac{J_n}{J_p} = \left| \frac{|(J_n)_{drift}| + |(J_n)_{diffusion}|}{|(J_p)_{drift}| - |(J_p)_{diffusion}|} \right| ,$$

and consequently also the emitter efficiency, decreases with increasing applied voltage.

The first-order dominant current is not shown in the reverse current-voltage characteristic (Fig. 6.5b) since its magnitude is approximately only 1% larger than the exact equivalent. Both minority and majority currents are highly dependent upon the structural parameters, through the length of the respective quasi-neutral regions.

The tendency of the device to behave inductively at very high injection is apparent in Fig. 6.6a, which exhibits a decrease of total incremental capacitance C for increasing applied voltage. Although the graph of $1/C^2$ versus reverse voltage (Fig. 6.6b) is closely linear, it is slightly displaced from the straight line representing Schottky's capacitance. This discrepancy is responsible for a significant error ($\simeq$ 25% in the present case) in the evaluation of the barrier potential by extrapolation of capacitance measurements, and is related to the inaccuracy of the first-order theory model in assuming depleted regions with sharp boundaries, as discussed above. Chang's approximate treatment [22] of the total incremental capacitance, based (although not explicitly stated) on the constancy of the quasi-Fermi levels in

the transition region, leads to results in good agreement with the exact ones (Fig. 6.6b). This is once more indicative of the little effect on the terminal properties of drastic first-order assumptions in reverse-bias conditions, in spite of the serious departure of the exact quasi-Fermi levels from the constant first-order value in the transition region (Fig. 6.1d, e).

The computer program used for this set of calculations is reported in Appendix C and D.

6.2.2. A finite value of surface recombination velocity at one external contact.

In the previous Subsection the discrepancy between the exact and first-order current-voltage characteristic at high injection levels (Fig. 6.5a) was exposed. This effect was attributed to the imposed equilibrium boundary condition at the external contact of the high-conductivity side, the narrowness of which enhances the phenomenon. This situation is examined in detail in this Subsection, by analyzing the effects introduced by modified boundary conditions on the mobile carrier densities in the high-conductivity side.

A model characterized by absence of recombination in the interior of the device, abrupt asymmetric impurity distribution, and constant mobilities is still assumed. The same physical parameters of the structure considered in the previous Subsection, and listed in Table 6.1, are specified, with exception of the doping ratio between the N-side and P-side, to better expose the effects of interest. The impurity step distribution is quantitatively defined by:

$$\left.\begin{array}{lll} \text{N-side:} & N(x) = N_D = 10^6 & (\text{or } 2.5 \times 10^{19} \text{ cm}^{-3}) \\ \text{P-side:} & -N(x) = N_A = 10^2 & (\text{or } 2.5 \times 10^{15} \text{ cm}^{-3}) \end{array}\right\} \quad (6.1)$$

With reference to Eq.(2.7), the following boundary conditions on the mobile carrier densities are imposed at the external contacts:

$$\left.\begin{array}{ll} \text{N-side} \quad (x = 0) & \left\{\begin{array}{l} \text{a finite value of surface recombination} \\ \text{velocity } s_0 \text{ for the minority carrier density,} \\ \text{electric charge neutrality at the contact;} \end{array}\right. \\ \\ \text{P-side} \quad (x = L) & \left\{\begin{array}{l} \text{contact of the ohmic type, i.e. } s_L = \infty \text{ and} \\ \text{electric charge neutrality at the contact.} \end{array}\right. \end{array}\right\} (6.2)$$

The analytical formulation applicable to the case under consideration, is given by Eqs.(2.8), (2.9), and (2.37).

Exact total currents and hole currents corresponding to different values of s_0 (∞, 150, 10) and the first-order dominant current ($s_0 = \infty$ only) are displayed versus forward applied voltage in Fig. 6.7. Exact electron and hole distributions for a high-injection case are shown as functions of position in Fig. 6.8, for the same values of s_0.

As briefly mentioned in the previous Section, the modified boundary condition permits a considerable increase of the hole density at the external contact of the N-side, with a consequent increase of the mobile carrier distributions throughout the interior of the device. Whereas for low to moderate injection cases the total current (essentially electron current) is unaffected by a change in s_0, at high injection levels the total current increases significantly, as s_0 decreases, toward the first-order dominant current ($s_0 = \infty$). The hole current, instead, decreases for decreasing s_0 for any injection level up to

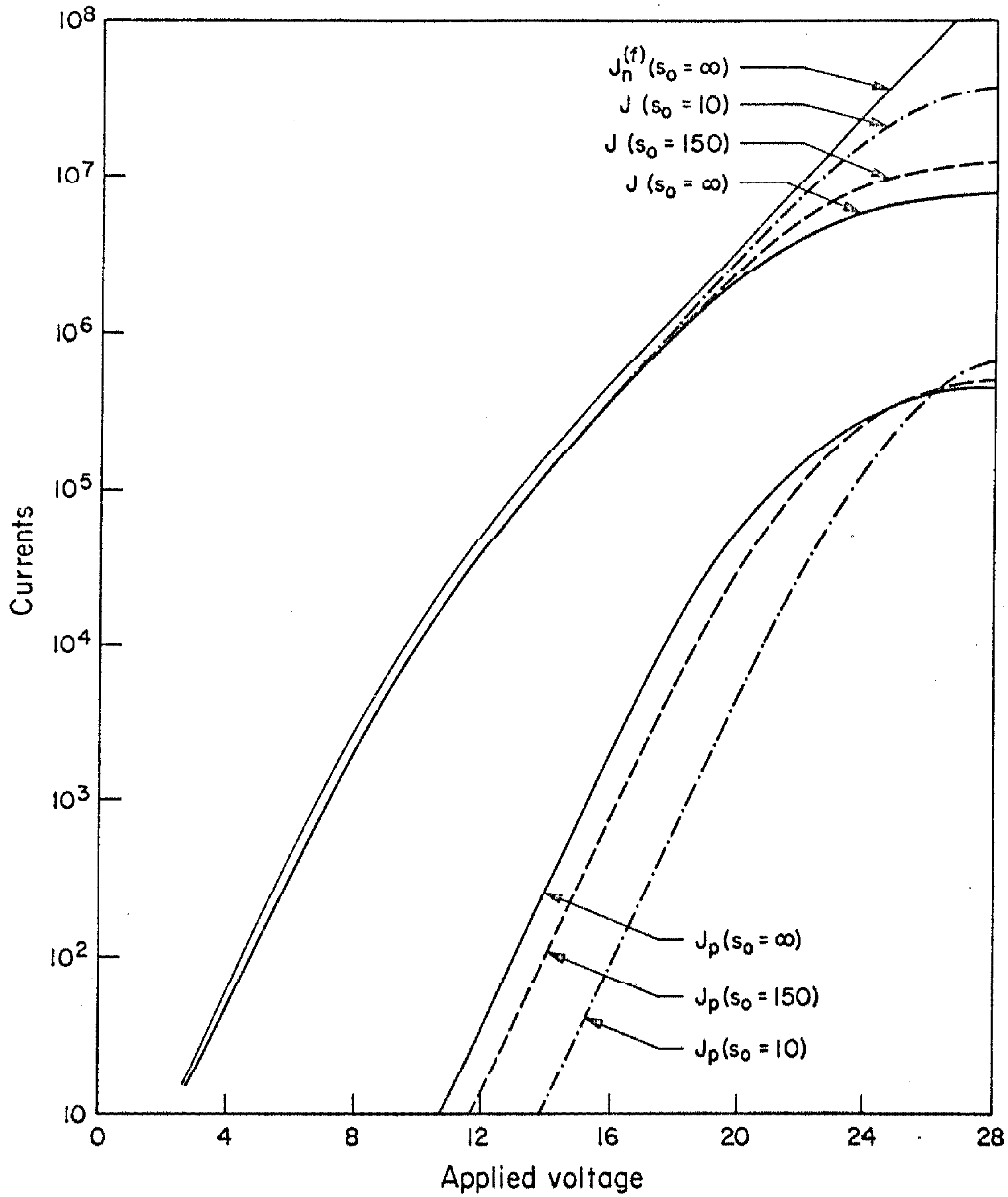

Fig. 6.7. Structure of Fig. 1.1; parameters of table 6.1 with doping profile (6.1); boundary conditions (6.2). Current densities as functions of applied voltage for various values of surface recombination velocity $s_0 = \infty$, 150, 10). Forward bias.

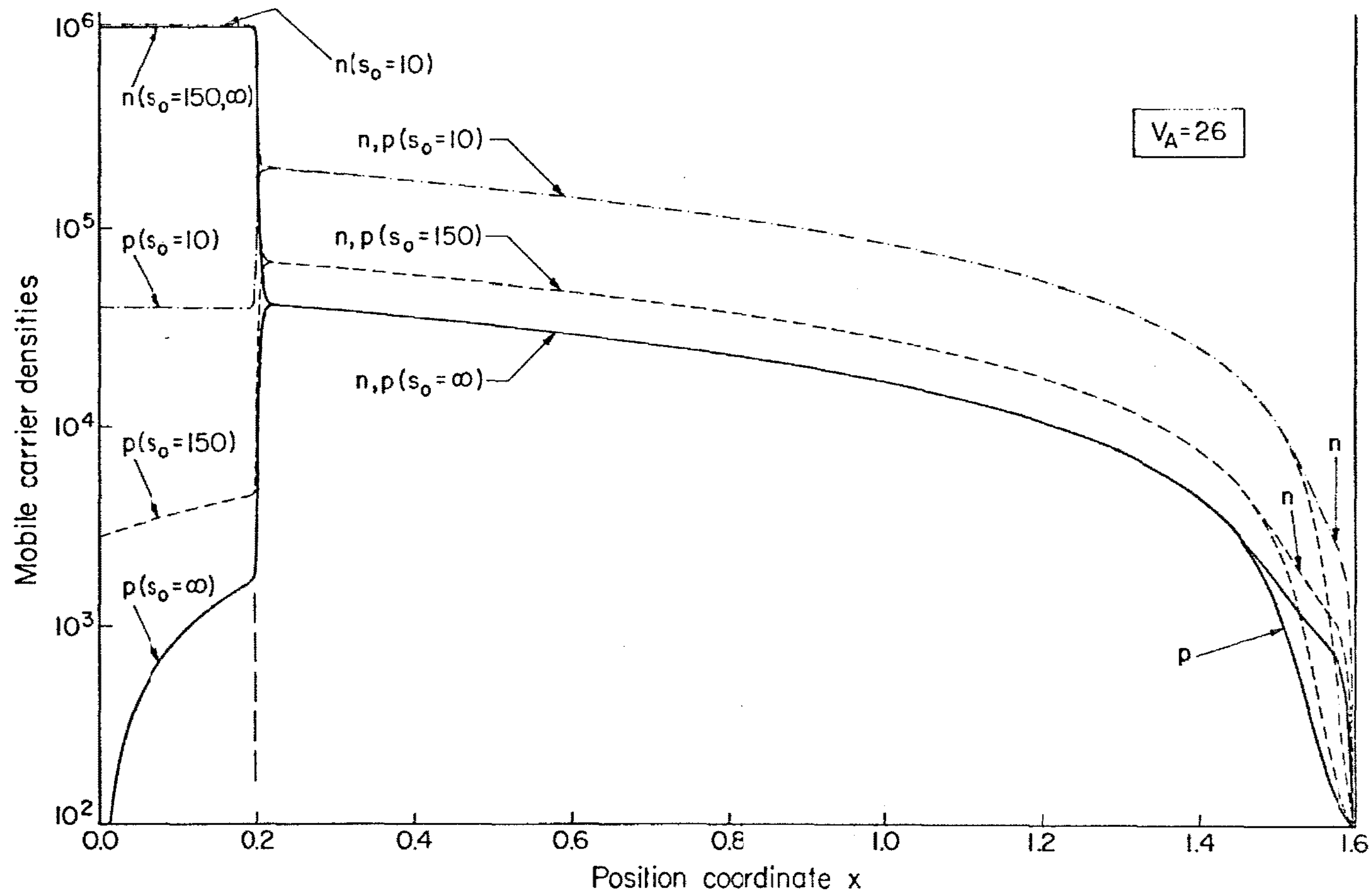

Fig. 6.8. Device as in Fig. 6.7. Mobile carrier densities as functions of position for various values of surface recombination velocity s_0 ($s_0 = \infty$, 150, 10). High forward bias case ($V_A = 26$).

very high values ($V_A \cong 26$), above which the dependence of J_p upon s_0 is inverted. At thermal equilibrium, of course, the value of the surface recombination velocity becomes irrelevant (see Eqs.(2.7)), since both J_n and J_p are zero. The peculiar terminal characteristics of Fig. 6.7 are interpreted below, by analyzing the effect of the modified boundary condition on the internal distributions.

The quasi-neutral region of the high-conductivity side is considered first. As a consequence of the high doping ratio between the N-side and the P-side, the high conductivity side operates generally under low-injection conditions, with exception of extremely high bias conditions combined with extremely low values of the surface recombination velocity s_0. For the case $s_0 = \infty$, and any forward-bias condition, the electron current J_n is given by the arithmetic difference between drift and diffusion components, whereas the hole current J_p is given by the arithmetic sum between the corresponding two components. In addition, the magnitude of the electron drift component is larger than the magnitude of the diffusion component, and the hole drift component is negligible with respect to the hole diffusion component. If s_0 is now decreased, and the applied voltage V_A is fixed, the magnitude of the diffusion components (essentially equal for electric charge neutrality) decreases (with exception of cases combining small values of s_0 with very high bias conditions, in which the diffusion term inverts sign and increases in magnitude) and the drift component increases. At low and moderate bias conditions J_p will then decrease, for decreasing s_0, since the diffusion process dominates, whereas at very high bias levels and for small s_0 the hole drift component becomes

dominant, so that the dependence of J_p upon s_0 inverts direction. This is apparent in Fig. 6.7 which indicates the normalized voltage $V_A \simeq 26$ as the point of inversion. Since the electron drift component always dominates, inversion for the electron current does not occur, so that, as shown in Fig. 6.7, J_n increases as s_0 decreases for any forward-bias condition. This effect becomes significant only for high current values, at which variations of the hole distribution, for a variation of s_0, require a significant variation either in the electric field or in the electron density distribution.

A different situation occurs in the quasi-neutral region of the low-conductivity side (P-side), which is now considered with exception of the regions adjacent to the boundaries. The electron current (minority current) is given by the arithmetic sum between drift and diffusion components and the hole current by the arithmetic difference between the corresponding two components. The applied voltage V_A is considered fixed and s_0 is varied. With exception of extremely high injection levels, the mobile carrier distributions are essentially linear so that n and p increase with the same rate of $\frac{dn}{dx}$ and $\frac{dp}{dx}$ (again essentially equal for electric charge neutrality) as s_0 decreases. Since the mobile carrier densities at the edges of the transition region increase for decreasing s_0 (and fixed V_A), the electrostatic potential drop on the transition region decreases (also in view of the Boltzmann relation), so that the (positive) electric field in the transition region decreases. As a consequence, the magnitude of the (negative) electric field in the quasi-neutral region under consideration also decreases, in order to maintain the constancy of the

integral

$$\int_0^L E(x)\,dx$$

required by the assumed fixed V_A. This is also related to the higher rate of increase of the conductivity compared to the rate of increase of the current, for decreasing s_0 and fixed V_A. It may be concluded that, as s_0 decreases, the drift components increase slower than the respective diffusion components, so that the net hole current decreases as shown in Fig. 6.7, with exception of very high injection levels ($V_A \gtrsim 26$). In those conditions the assumption of linearity in the mobile carrier distributions becomes invalid: the distributions display a negative curvature consistent with the considerable variation of the drift components upon position. As s_0 decreases, n and p increase faster than the respective slopes dn/dx and dp/dx, so that, in spite of the decrease of the electric field, the drift components increase faster than the diffusion components. This is consistent with the inversion of the dependence of J_p upon s_0 occurring for $V_A \gtrsim 26$. On the other hand, the electron current J_n, as an arithmetic sum of two increasing quantities, always increases as s_0 decreases.

The mobile carrier distributions for the high-injection case of Fig. 6.8 clearly show, in the region adjacent to the external contact of the P-side, the unbalance of net electric charge, mentioned in the previous Subsection. This was attributed to the effect of the strong electric field near the contact generated by the high current. The action of the field upon the mobile carriers attracts electrons and

expells holes from this region, forcing the minority (electron) carrier density to exceed the majority carrier density.

6.3. A three-contact device: the N-P-N transistor.

As an example of one-dimensional solutions for a three-contact device, results for a narrow-base N-P-N transistor are presented in this Section. The special case already discussed for the diode in Subsection 6.2.1, and characterized by absence of generation-recombination processes in the interior of the device $[U(x) = 0]$, constant mobilities, abrupt doping profile, is here considered and equally motivated. Emitter and collector external contacts of the ohmic type and boundary conditions, at the position of the external base contact, of the type discussed in Chapter IV are specified. The analytical formulation that applies in such a case has been described in Section 4.2.

The physical parameters characterizing the structure, schematically indicated in Fig. 4.1, are listed in Table 6.2. The values chosen for the impurity density, with the specified carrier mobilities, yield N-material with a (thermal equilibrium) conductivity of 10^4 $(\Omega\ cm)^{-1}$ and P-material with a (thermal equilibrium) conductivity of 1 $(\Omega\ cm)^{-1}$.

For a fixed position of the external base contact $(B = 1.2)$ in the quasi-neutral region of the base, and for various bias conditions, the "exact" and first-order electrostatic potential ψ and $\psi^{(f)}$ and the "exact" quasi-Fermi levels φ_n, φ_p are shown in Figs. 6.9a to 6.17a as functions of position, and the "exact" mobile carrier and net electric charge densities n, p, ρ in Figs. 6.9b to 6.17b. Terminal characteristics are displayed in Fig. 6.18 and 6.19. The effects of modified

Material:	germanium (relative permittivity = 16)
Temperature:	300° K
Doping:	emitter (N-type), $N(x) = N_D$ = 69,467 (or 1.7367×10^{19} cm^{-3})
	base (P-type), $-N(x) = N_A$ = 146.85 (or 3.6712×10^{15} cm^{-3})
	collector(N-type), $N(x) = N_D$ = 69,467 (or 1.7367×10^{19} cm^{-3})
Length:	emitter, $M - 0 = 0.1164$ (or 1.1136×10^{-5} cm)
	base, $M_C - M = 2.9672$ (or 2.8387×10^{-4} cm)
	collector, $L - M_C = 0.1164$ (or 1.1136×10^{-5} cm)
	total, $L - 0 = 3.2$ (or 3.0614×10^{-4} cm)
Carrier mobilities:	electron, $\gamma_n^{-1} = 93$ (or $\simeq 3600$ cm^2/volt-sec)
	hole, $\gamma_p^{-1} = 44$ (or $\simeq 1700$ cm^2/volt-sec)

Table 6.2. The physical parameters characterizing the N-P-N structure, analyzed under steady-state conditions for various applied voltages.

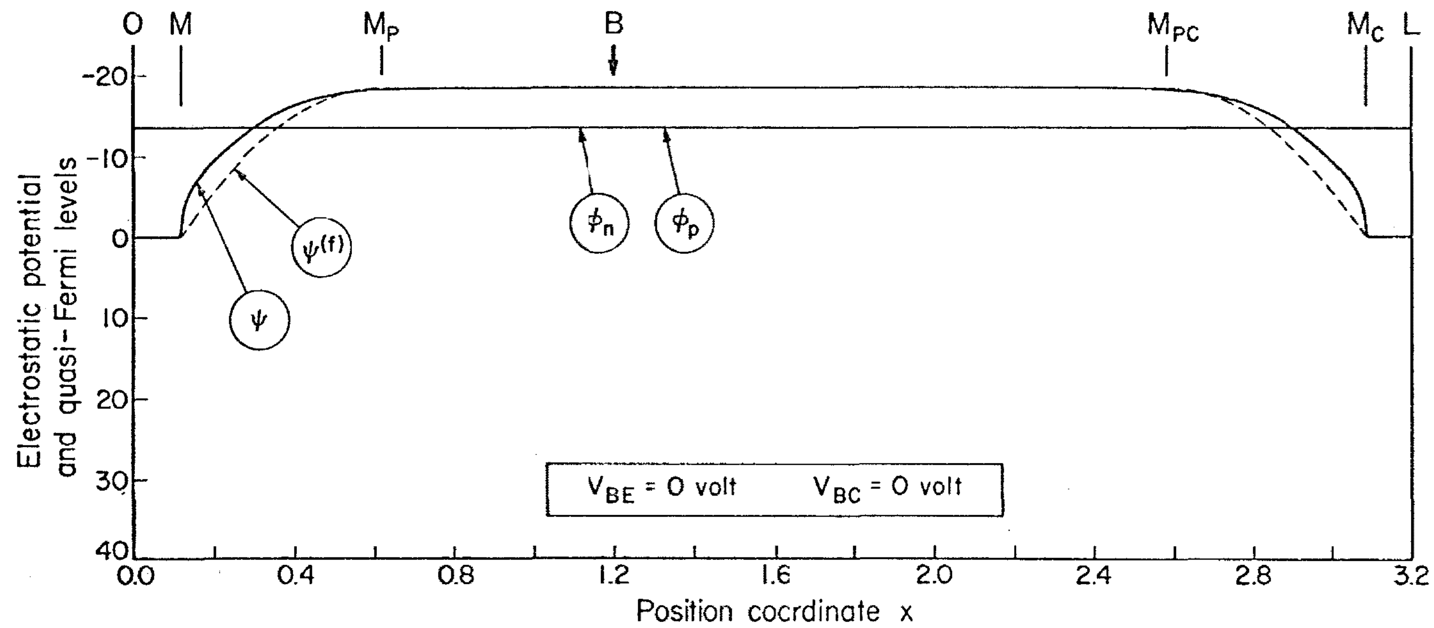

Fig. 6.9a. Structure of Fig. 4.1; parameters of Table 6.2; boundary conditions (1.32) for the emitter and collector external contacts and (4.1) for the base external contact located at B = 1.2. Electrostatic potential and quasi-Fermi levels as functions of position. Thermal equilibrium.

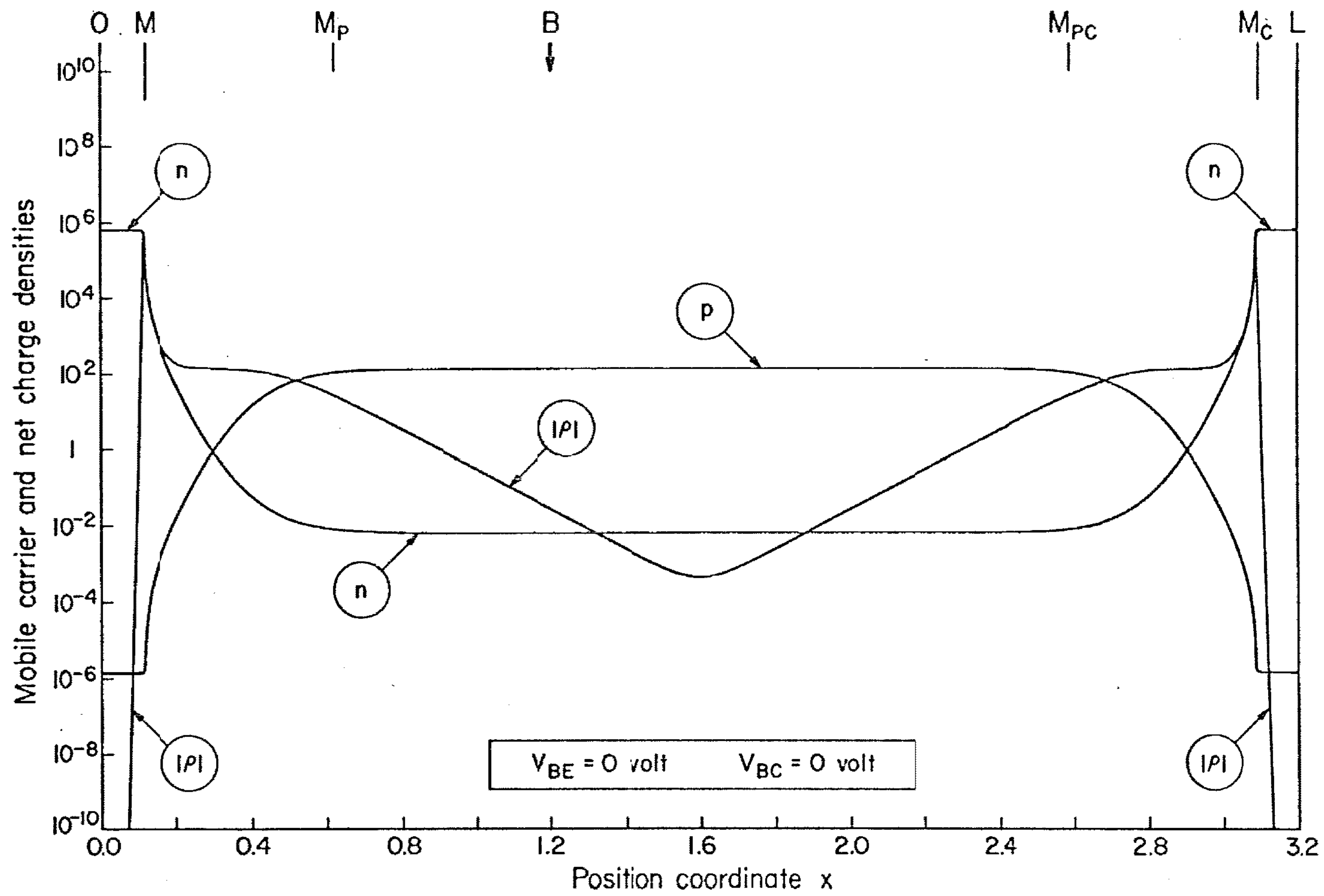

Fig. 6.9b. Device as in Fig. 6.9a. Mobile carrier and net charge densities as functions of position. Thermal equilibrium.

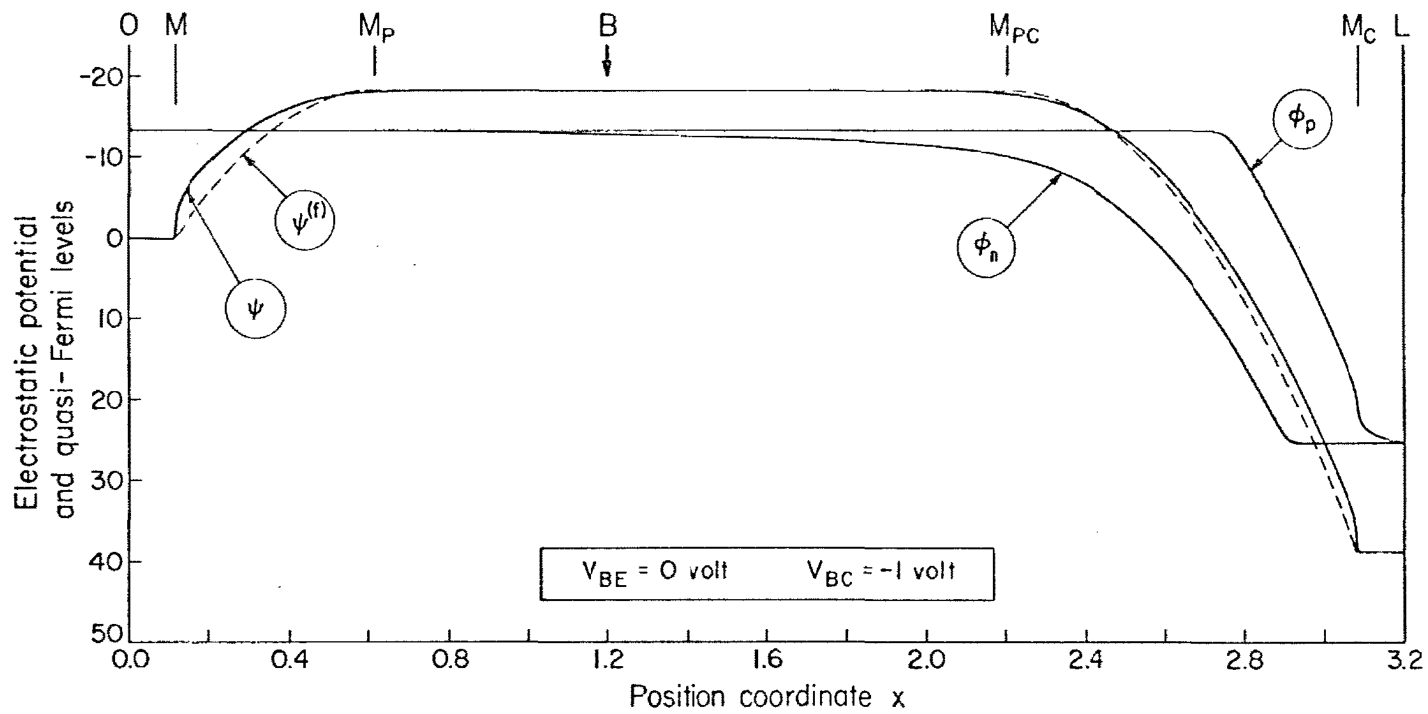

Fig. 6.10a. Device as in Fig. 6.9a. Electrostatic potential and quasi-Fermi levels as functions of position. Base-to-emitter voltage V_{BE} = 0 volt, base-to- collector voltage V_{BC} = -1 volt.

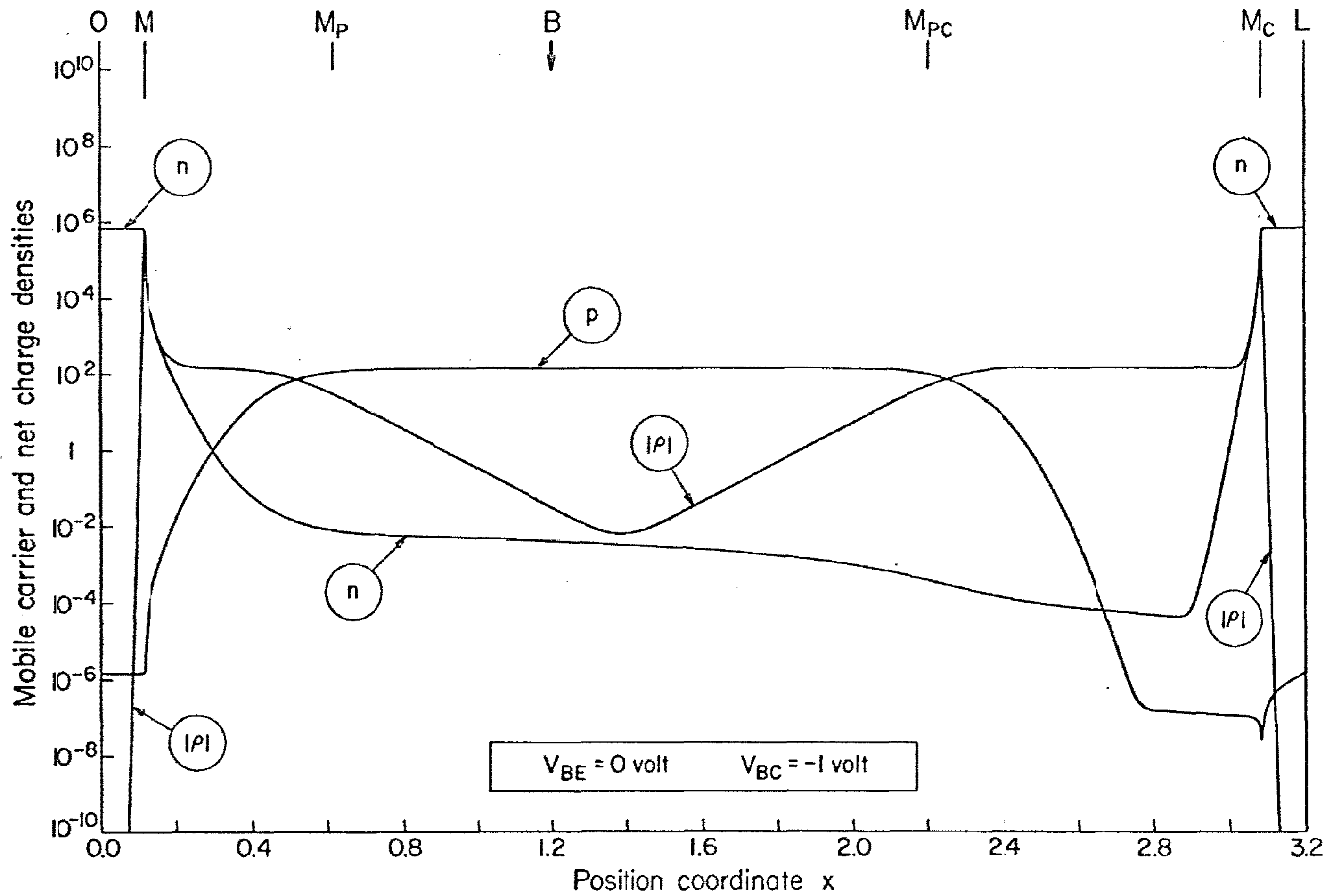

Fig. 6.10b. Device as in Fig. 6.9a. Mobile carrier and net charge densities as functions of position. Base-to-emitter voltage V_{BE} = 0 volt, base-to-collector voltage V_{BC} = -1 volt.

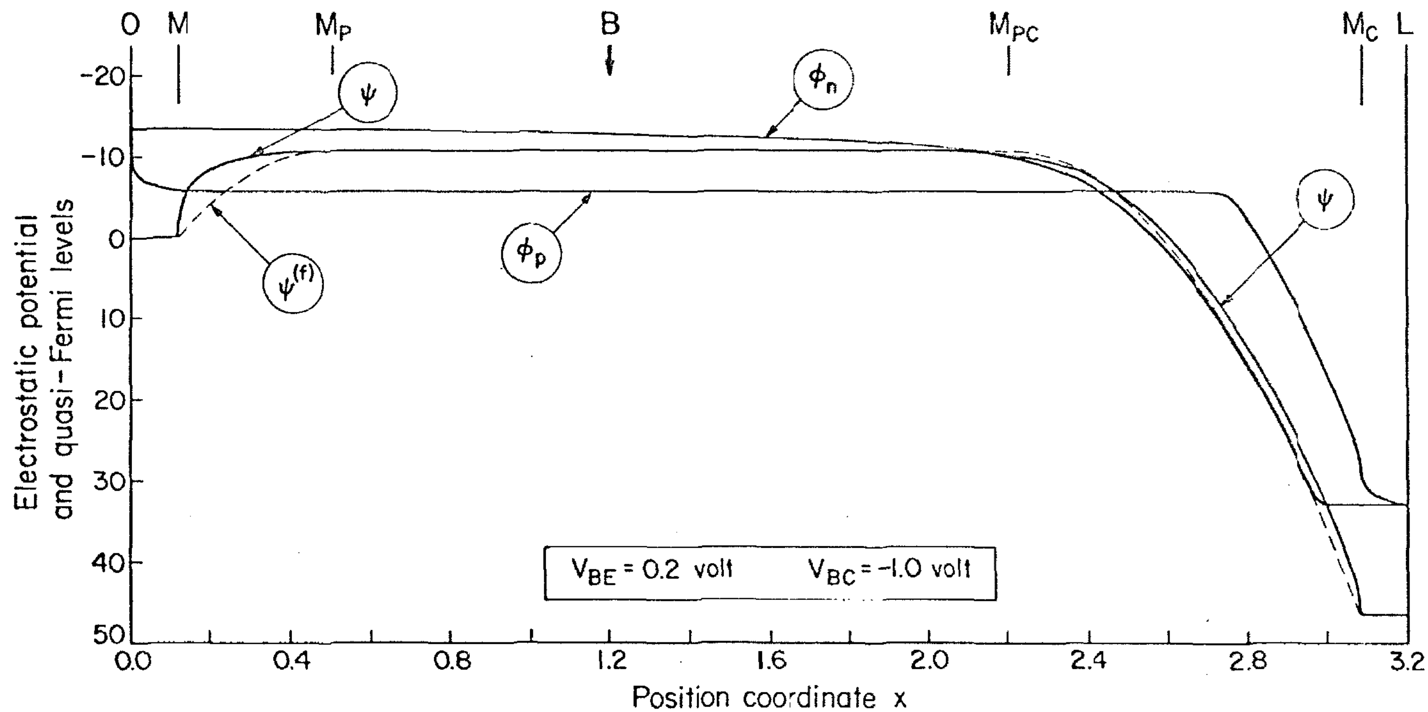

Fig. 6.11a. Device as in Fig. 6.9a. Electrostatic potential and quasi-Fermi levels as functions of position. Base-to-emitter voltage $V_{BE} = 0.2$, base-to-collector voltage $V_{BC} = -1$ volt.

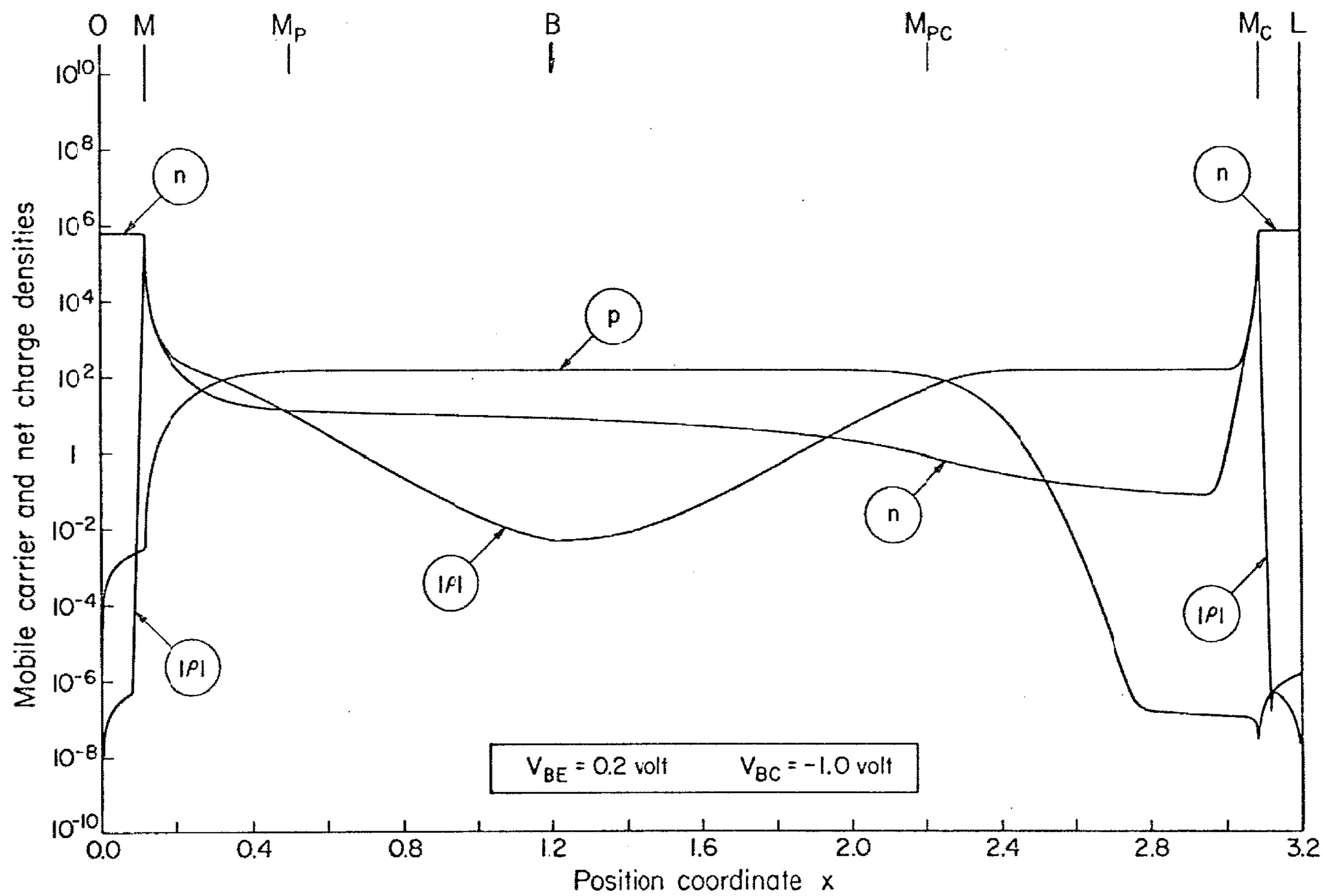

Fig. 6.11b. Device as in Fig. 6.9a. Mobile carrier and net charge densities as functions of position. Base-to-emitter voltage V_{BE} = 0.2 volt, base-to-collector voltage V_{BC} = -1 volt.

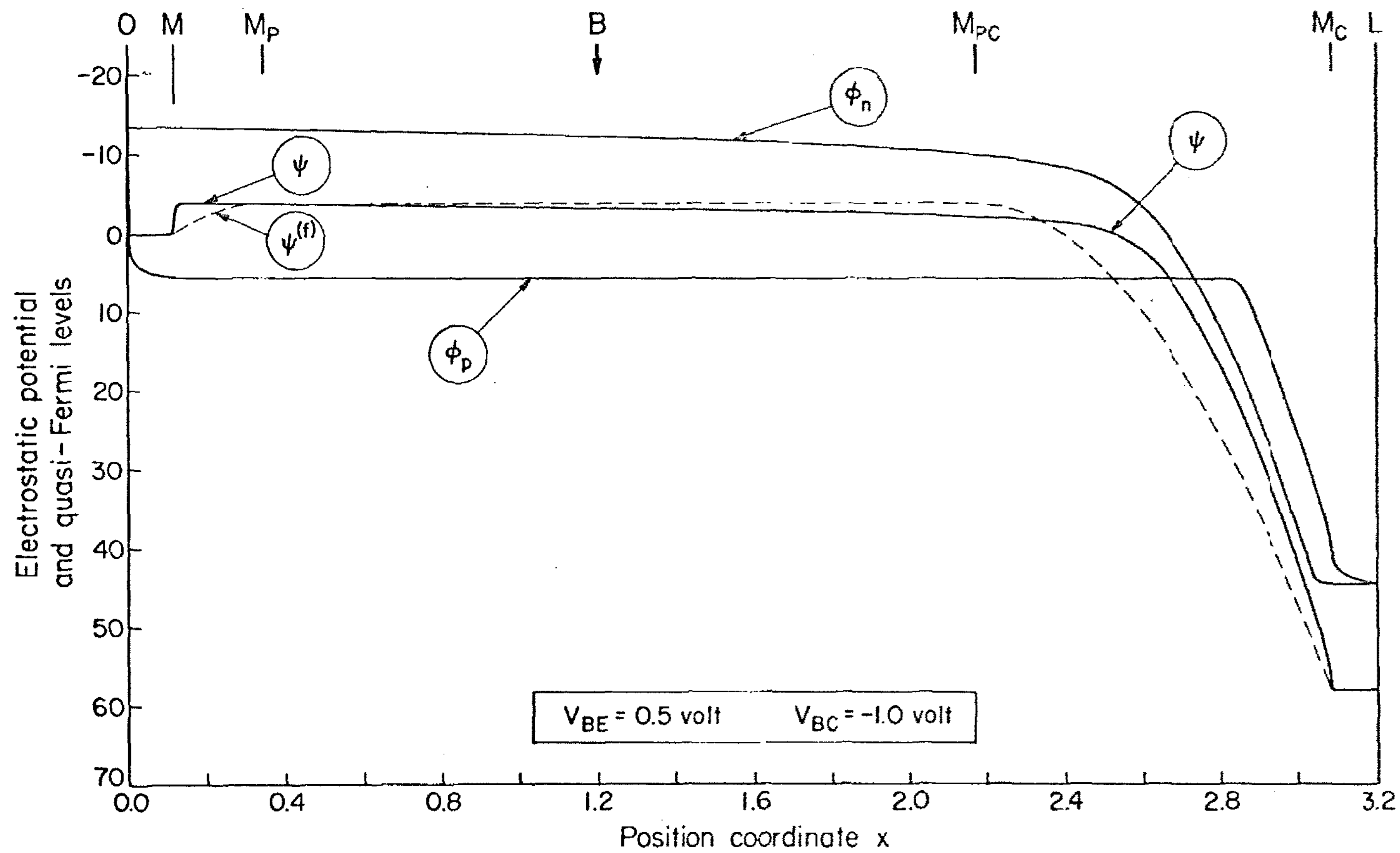

Fig. 6.12a. Device as in Fig. 6.9a. Electrostatic potential and quasi-Fermi levels as functions of position. Base-to-emitter voltage V_{BE} = 0.5 volt, base-to-collector voltage V_{BC} = -1 volt.

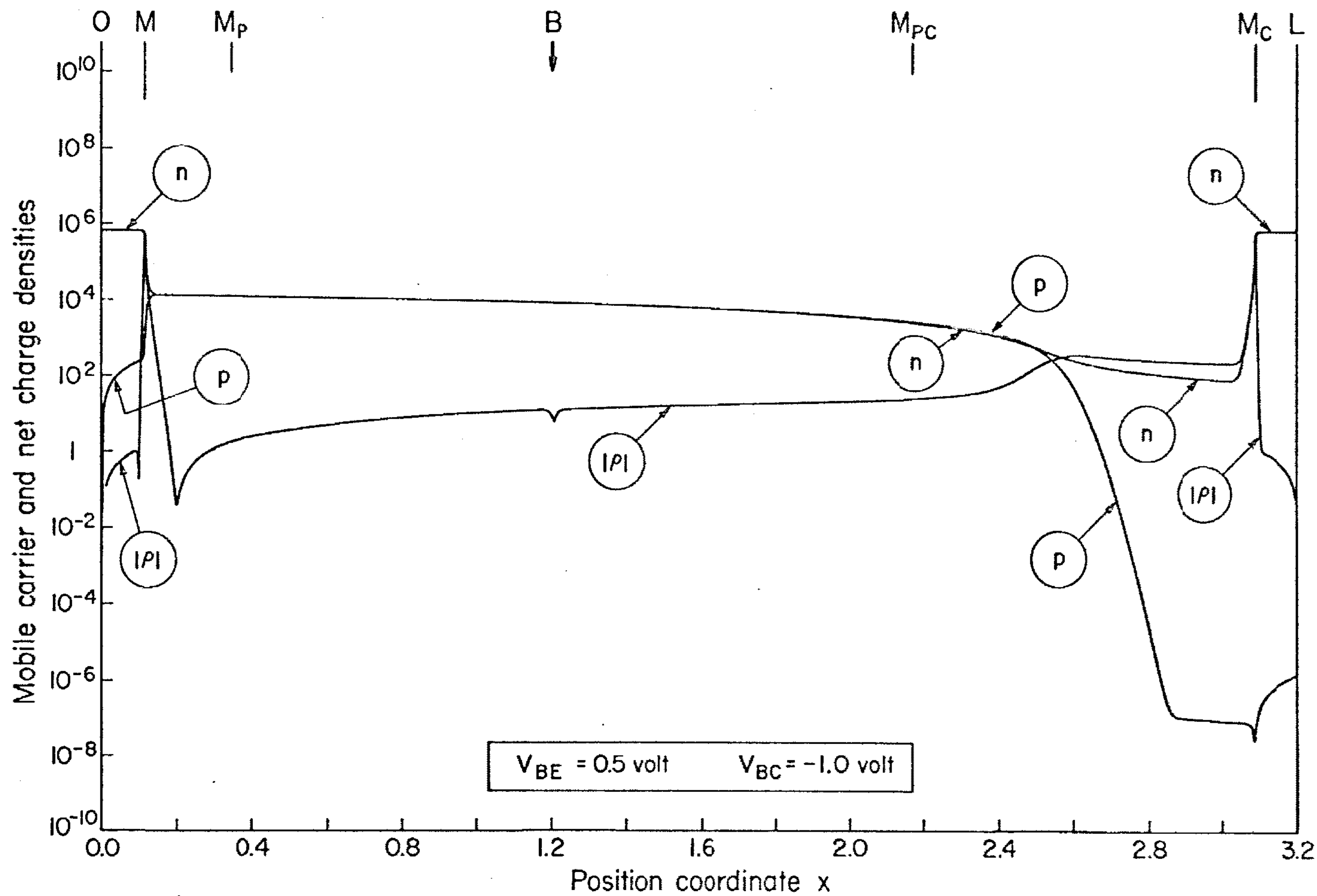

Fig. 6.12b. Device as in Fig. 6.9a. Mobile carrier and net charge densities as functions of position. Base-to-emitter voltage V_{BE} = 0.5 volt, base-to-collector voltage V_{BC} = -1 volt.

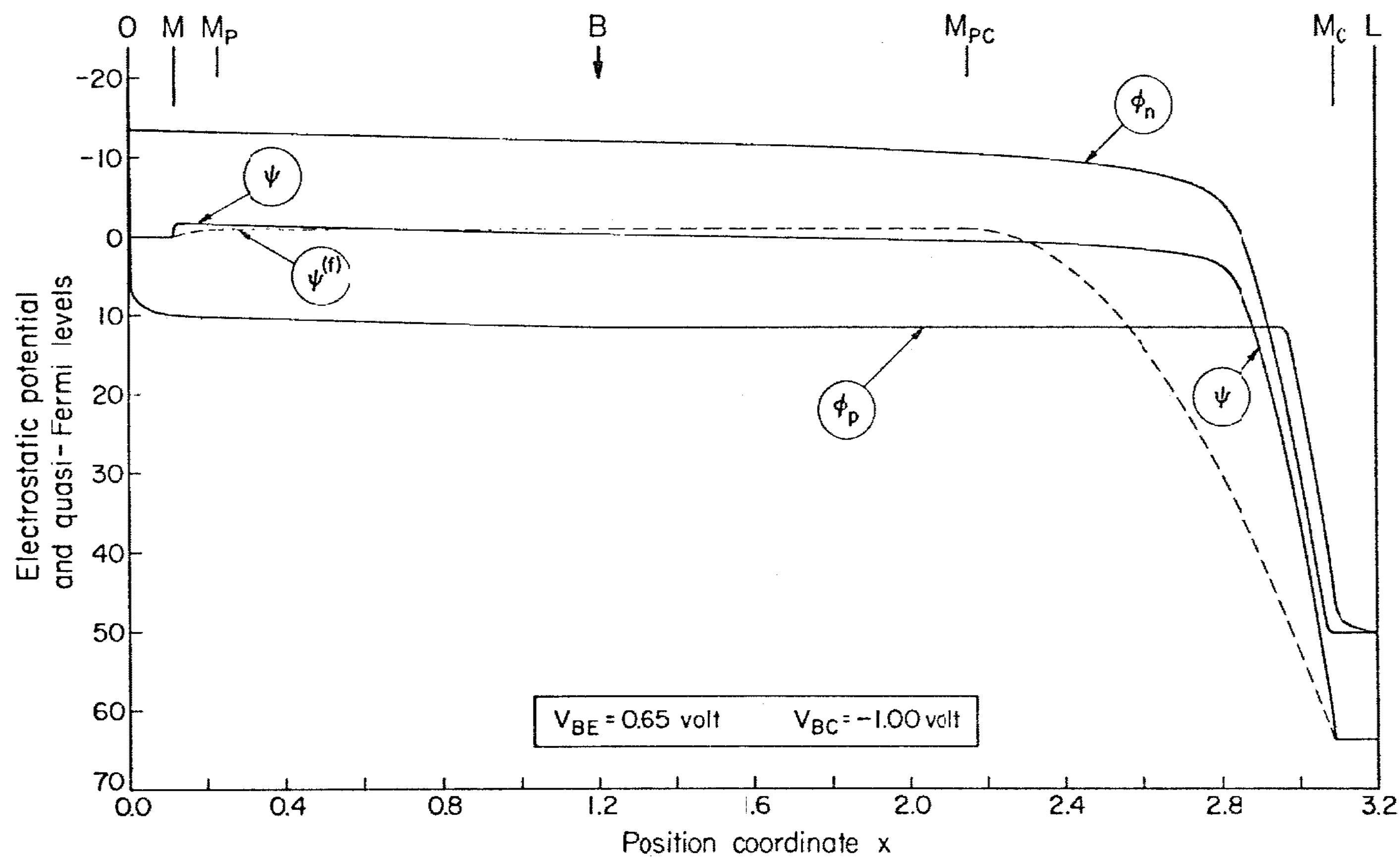

Fig. 6.13a. Device as in Fig. 6.9a. Electrostatic potential and quasi-Fermi levels as functions of position. Base-to-emitter voltage V_{BE} = 0.65 volt, base-to-collector voltage V_{BC} = - 1 volt.

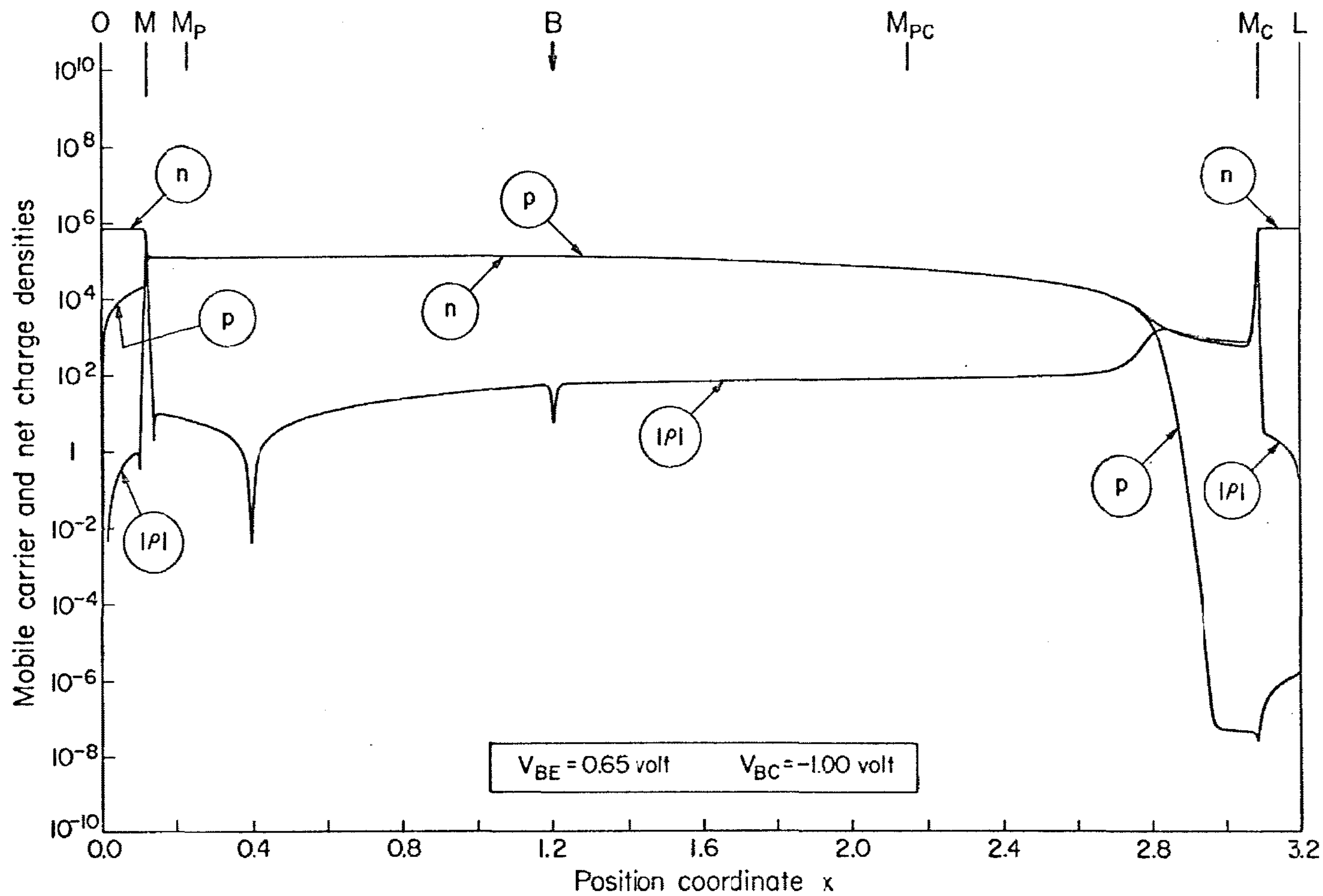

Fig. 6.13b. Device as in Fig. 6.9a. Mobile carrier and net charge densities as functions of position. Base-to-emitter voltage $V_{BE} = 0.65$ volt, base-to-collector voltage $V_{BC} = -1$ volt.

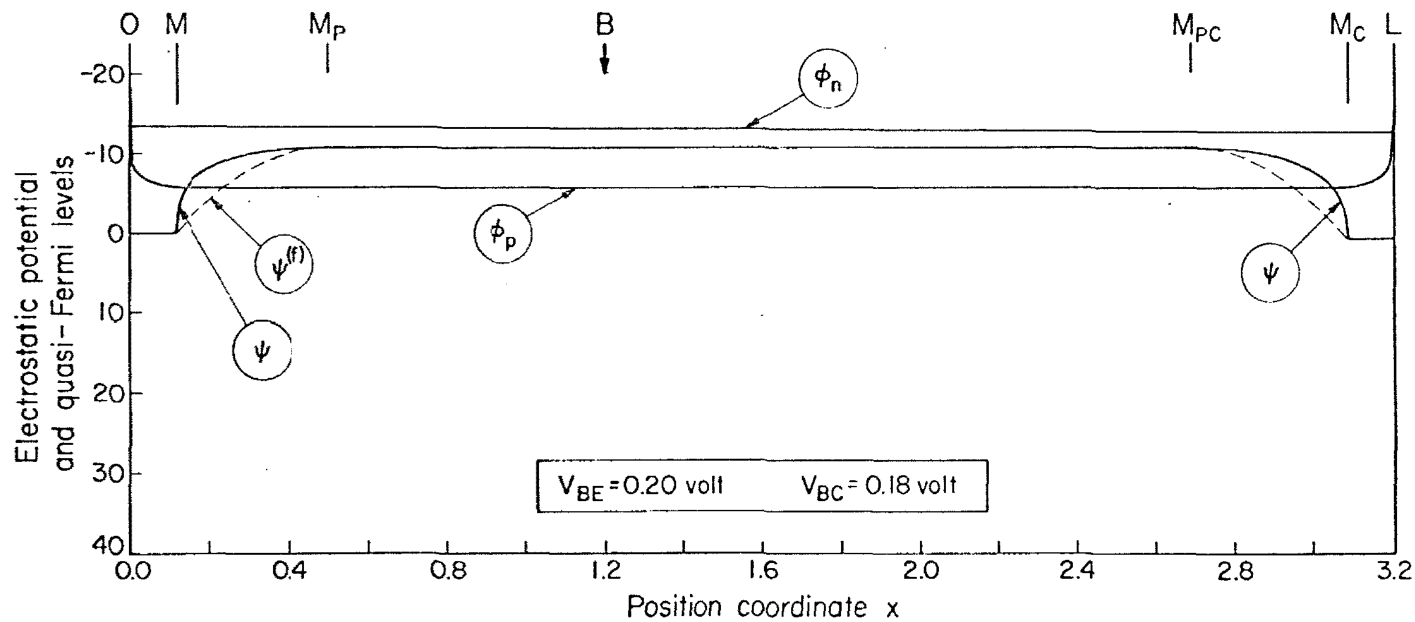

Fig. 6.14a.

Device as in Fig. 6.9a. Electrostatic potential and quasi-Fermi levels as functions of position. Base-to-emitter voltage V_{BE} = 0.2 volt, base-to-collector voltage V_{BC} = 0.18 volt.

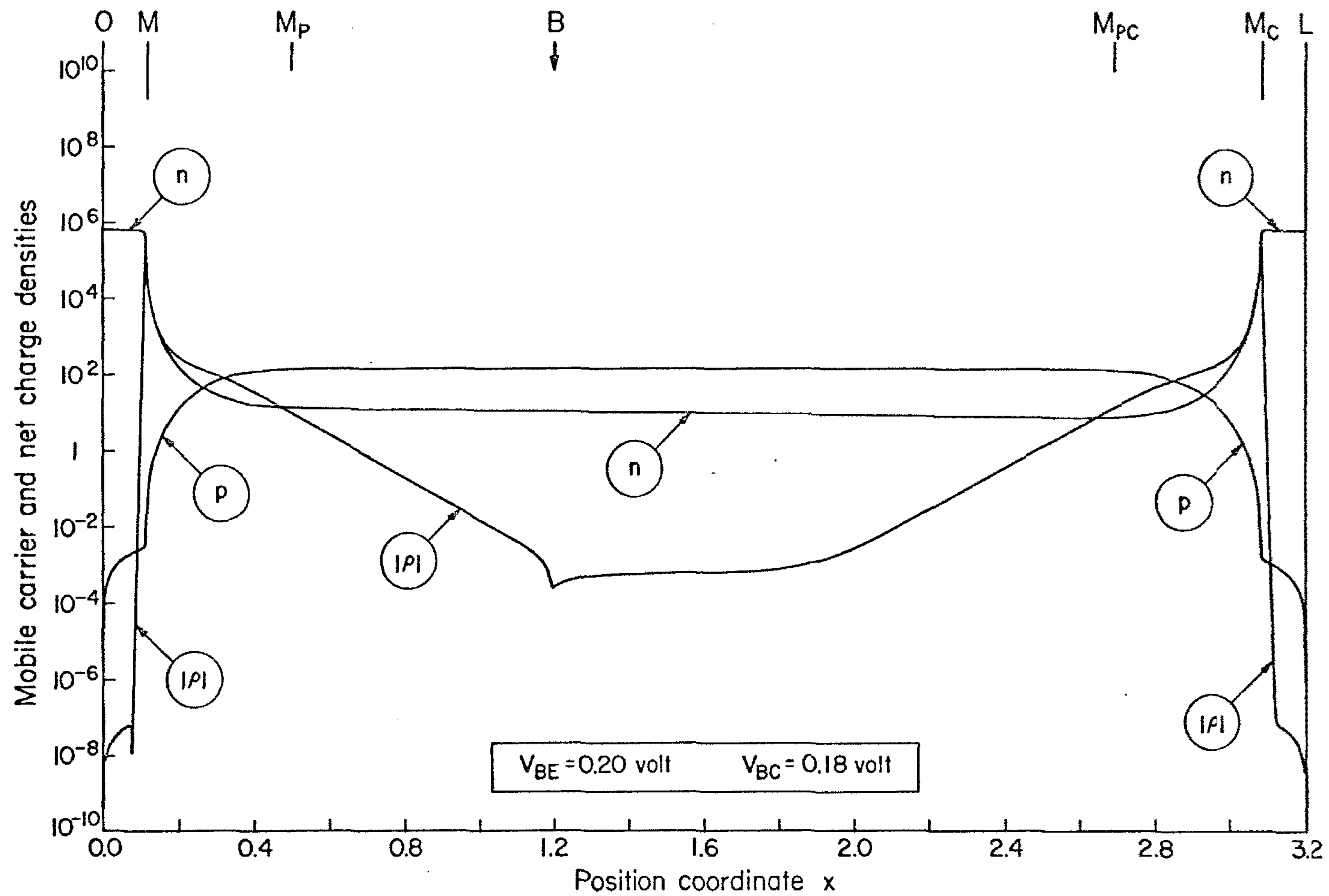

Fig. 6.14b. Device as in Fig. 6.9a. Mobile carrier and net charge densities as functions of position. Base-to-emitter voltage $V_{BE} = 0.2$ volt, base-to-collector voltage $V_{BC} = 0.18$ volt.

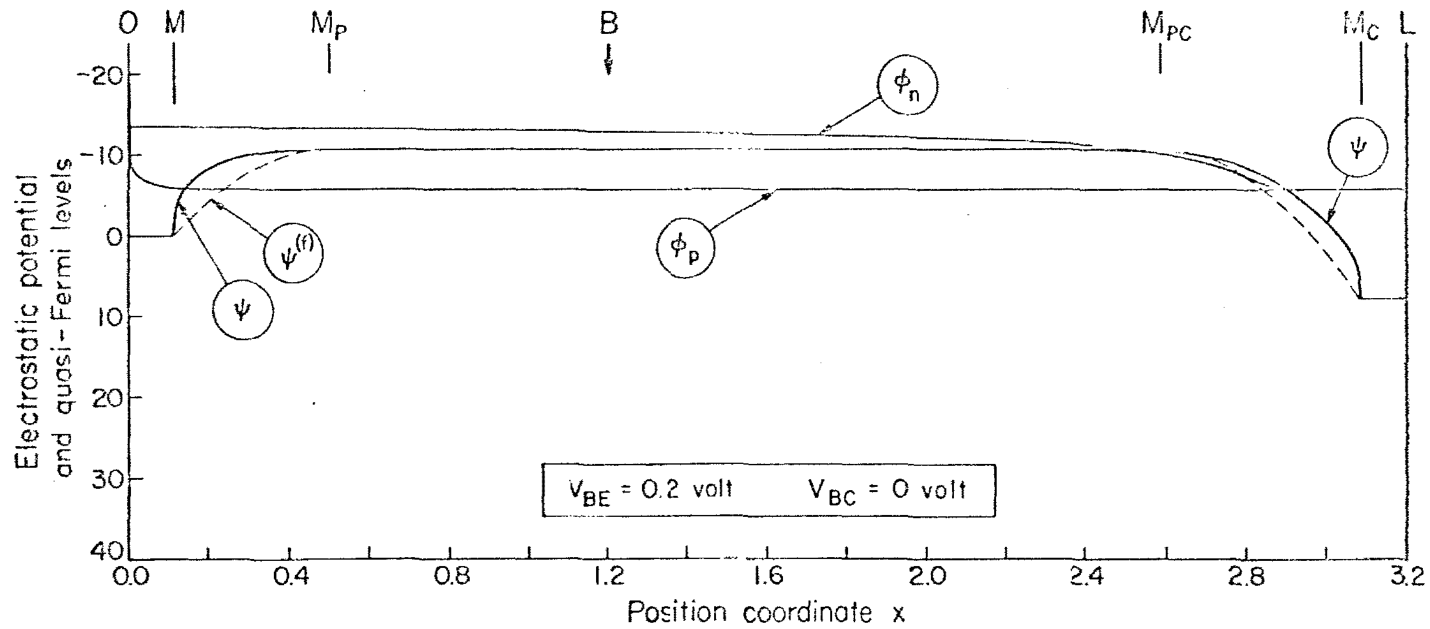

Fig. 6.15a. Device as in Fig. 6.9a. Electrostatic potential and quasi-Fermi levels as functions of position. Base-to-emitter voltage V_{BE} = 0.2 volt, base-to-collector voltage V_{BC} = 0 volt.

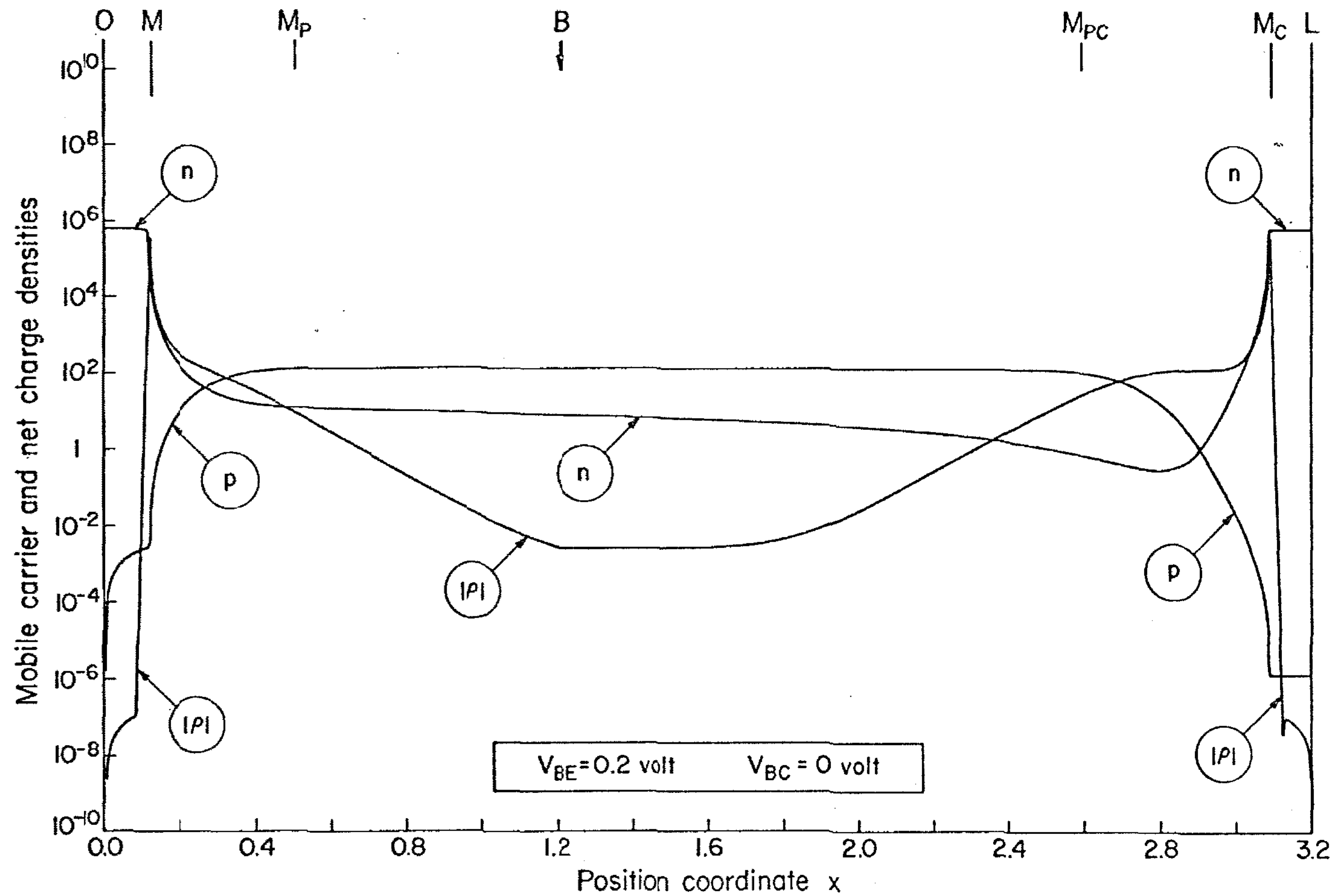

Fig. 6.15b. Device as in Fig. 6.9a. Mobile carrier and net charge densities as functions of position. Base-to-emitter voltage V_{BE} = 0.2 volt, base-to-collector voltage V_{BC} = 0 volt.

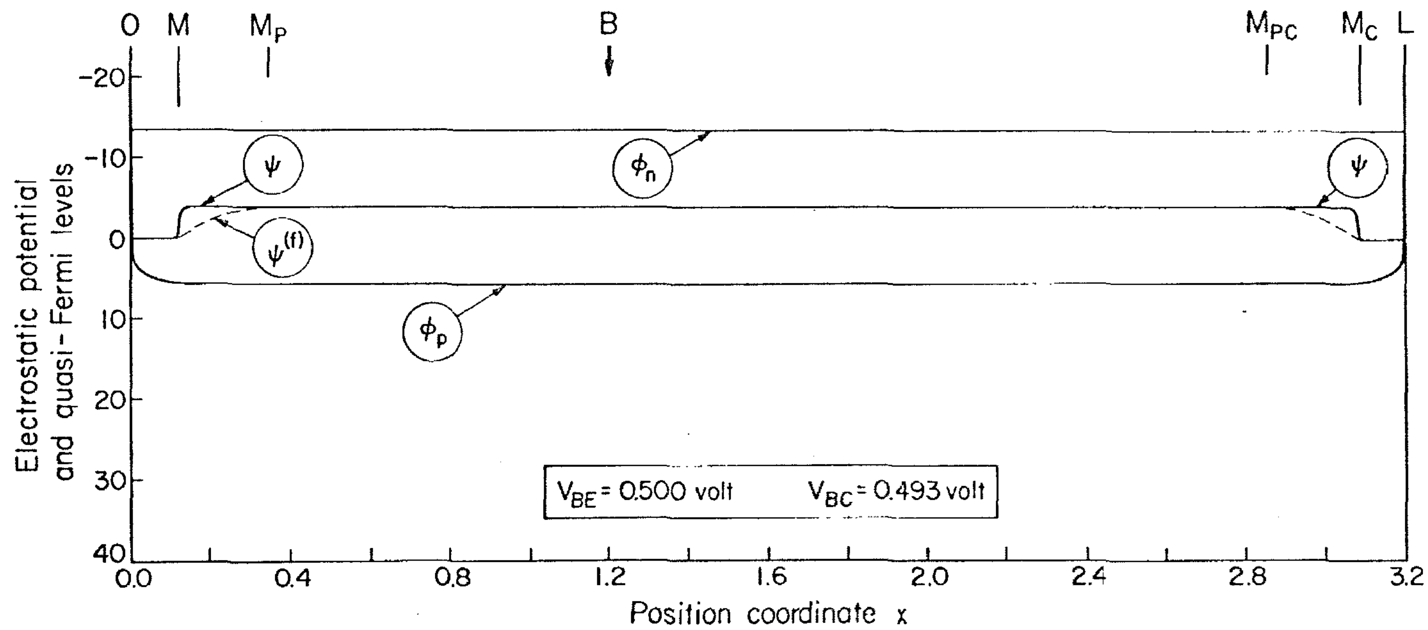

Fig. 6.16a. Device as in Fig. 6.9a. Electrostatic potential and quasi-Fermi levels as functions of position. Base-to-emitter voltage V_{BE} = 0.5 volt, base-to-collector V_{BC} = 0.493 volt.

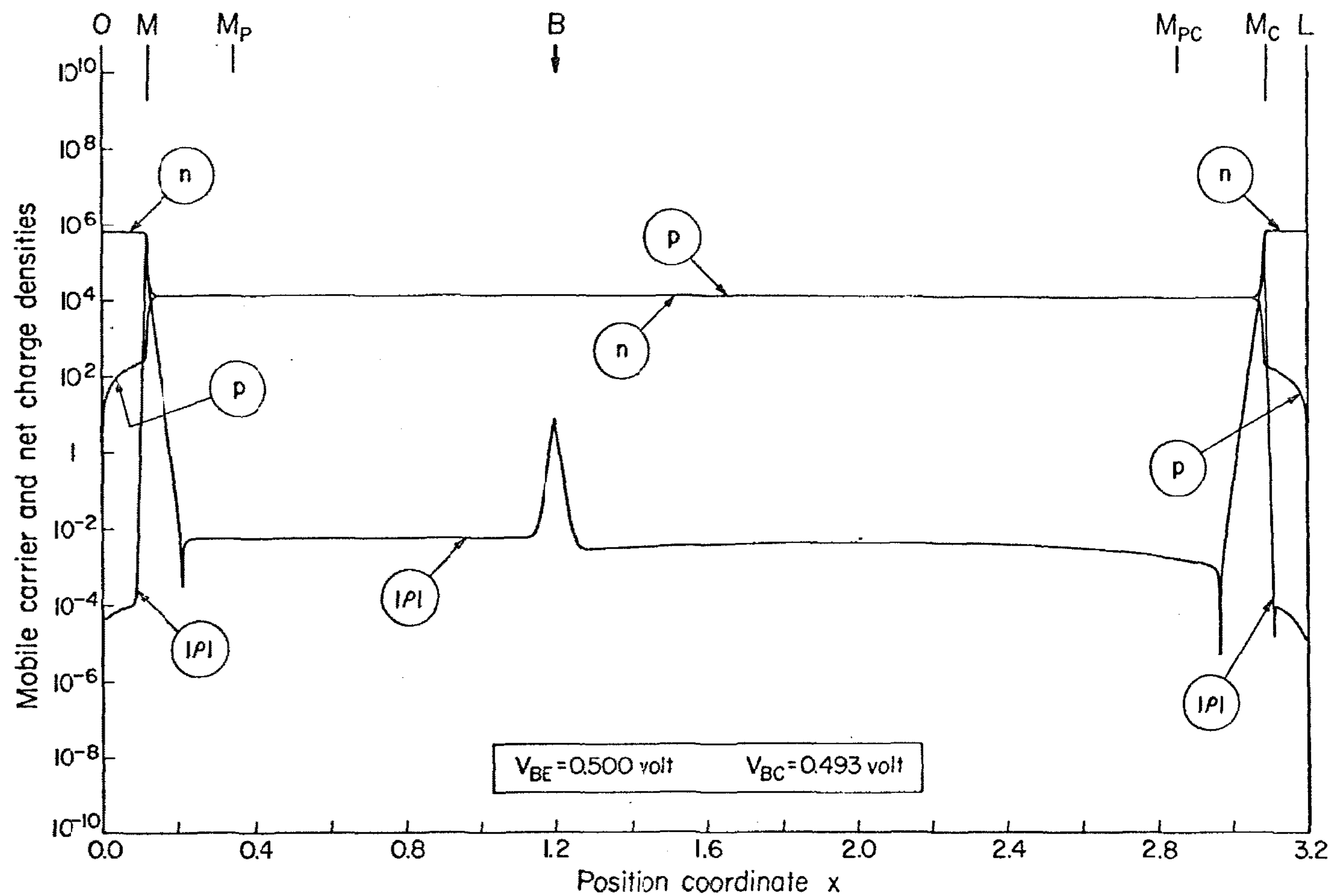

Fig. 6.16b. Device as in Fig. 6.9a. Mobile carrier and net charge densities as functions of position. Base-to-emitter voltage V_{BE} = 0.5 volt, base-to-collector voltage V_{BC} = 0.493 volt.

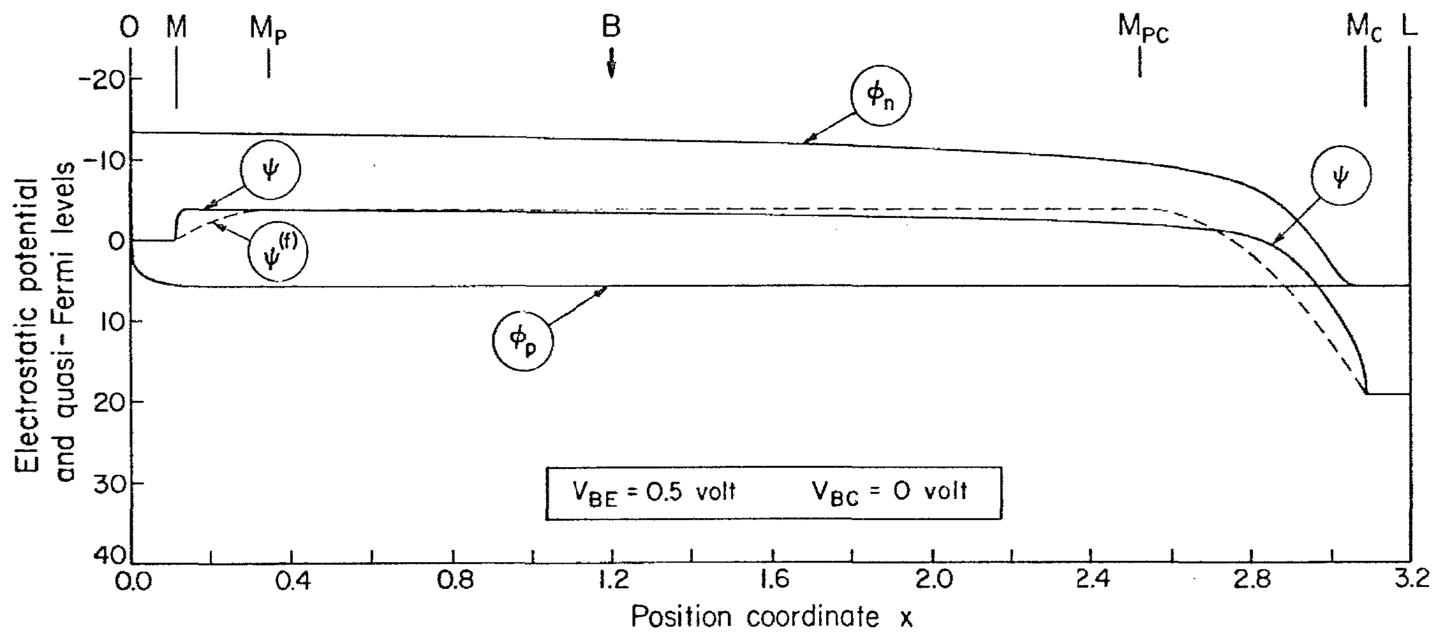

Fig. 6.17a. Device as in Fig. 6.9a. Electrostatic potential and quasi-Fermi levels as functions of position. Base-to-emitter voltage V_{BE} = 0.5 volt, base-to-collector voltage V_{BC} = 0 volt.

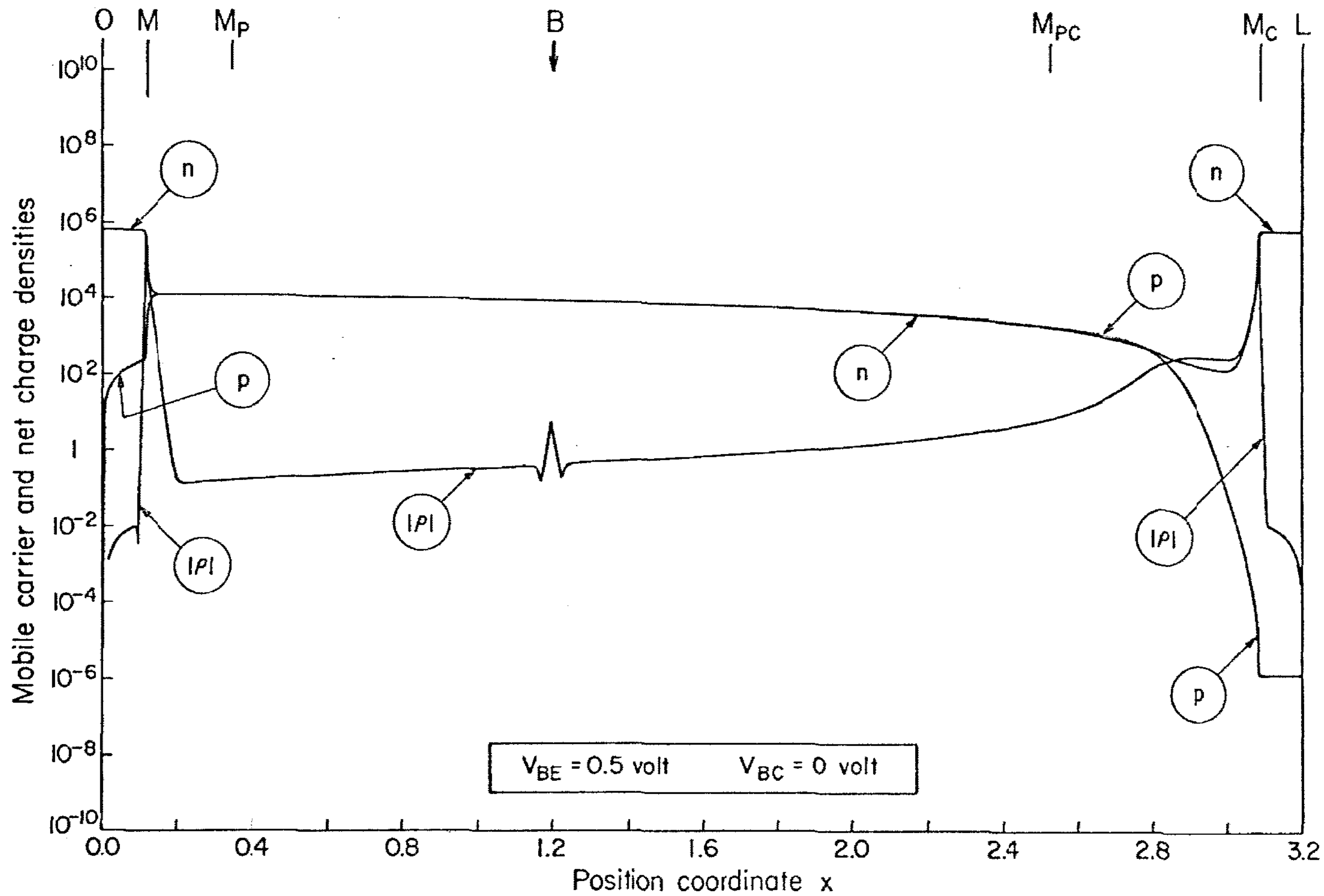

Fig. 6.17b. Device as in Fig. 6.9a. Mobile carrier and net charge densities as functions of position. Base-to-emitter voltage V_{BE} = 0.5 volt, base-to-collector voltage V_{BC} = 0 volt.

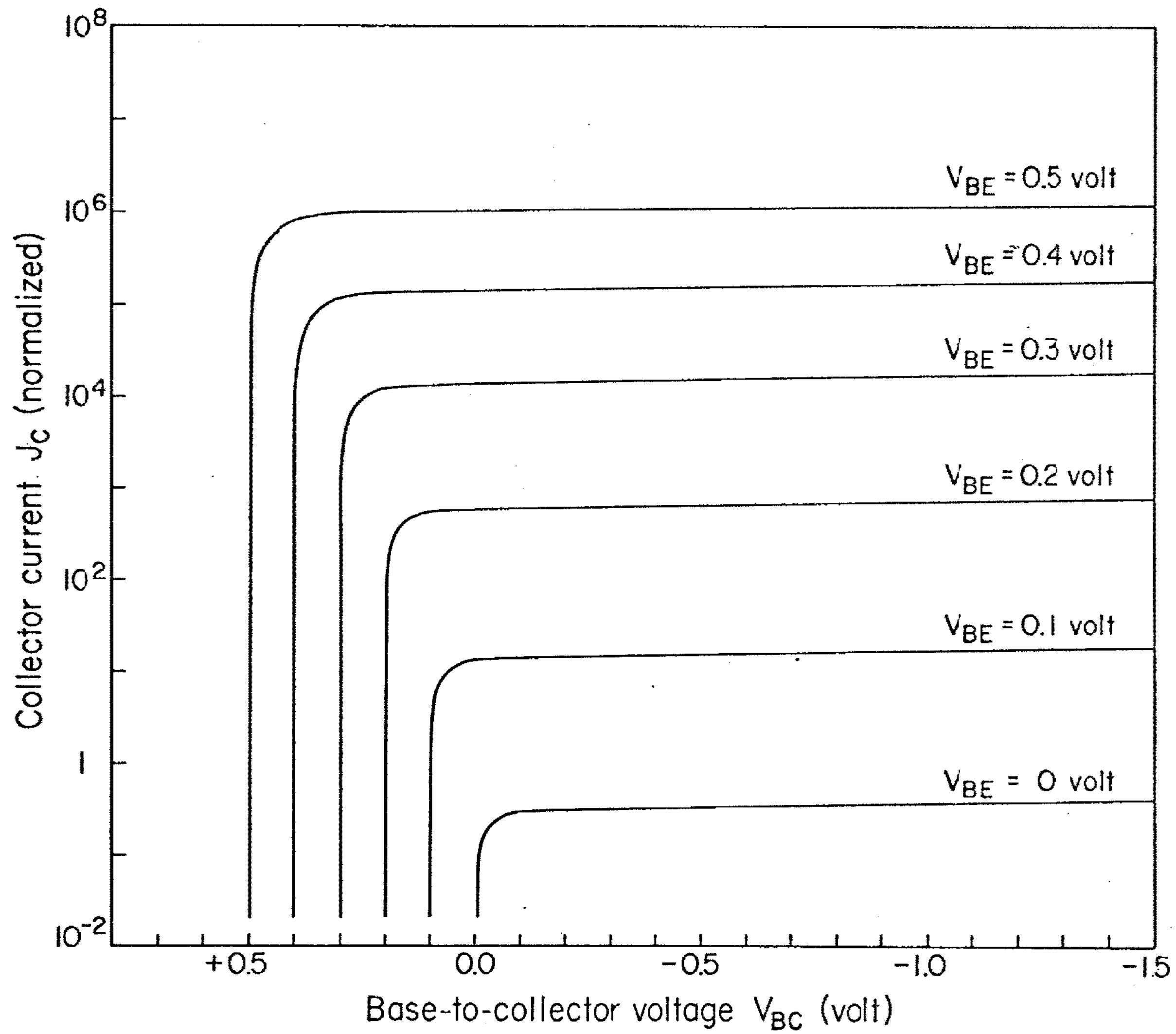

Fig. 6.18. Device as in Fig. 6.9a. Collector current as a function of the base-to-collector voltage for various base-to-emitter voltages.

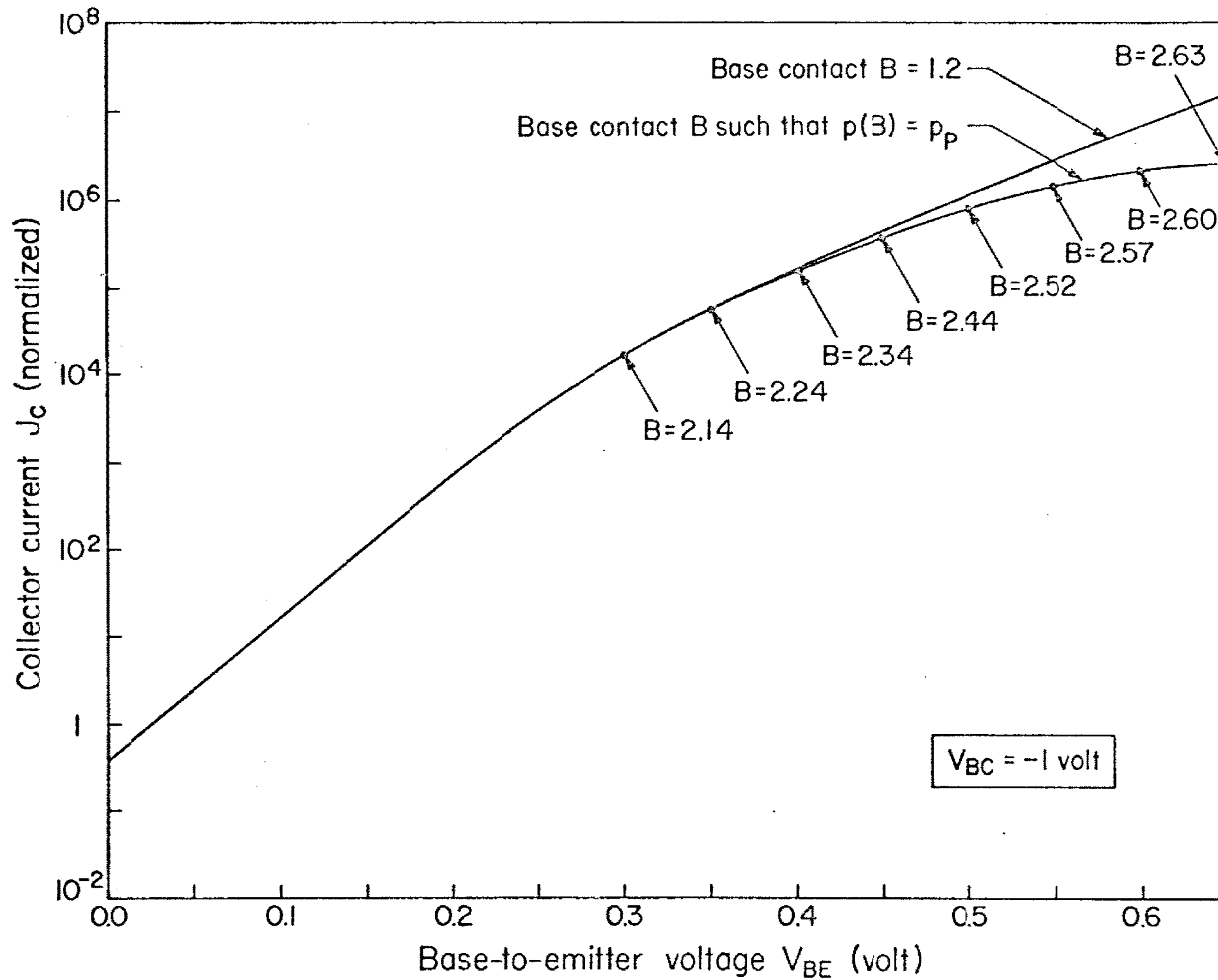

Fig. 6.19. Device of Fig. 6.9a (upper curve) compared to the same device with the modified boundary condition $p(B) = p_P$ on the external base contact (lower curve). Collector current as a function of base-to-emitter voltage, for a fixed base-to-collector reverse bias (V_{BC} = - 1 volt).

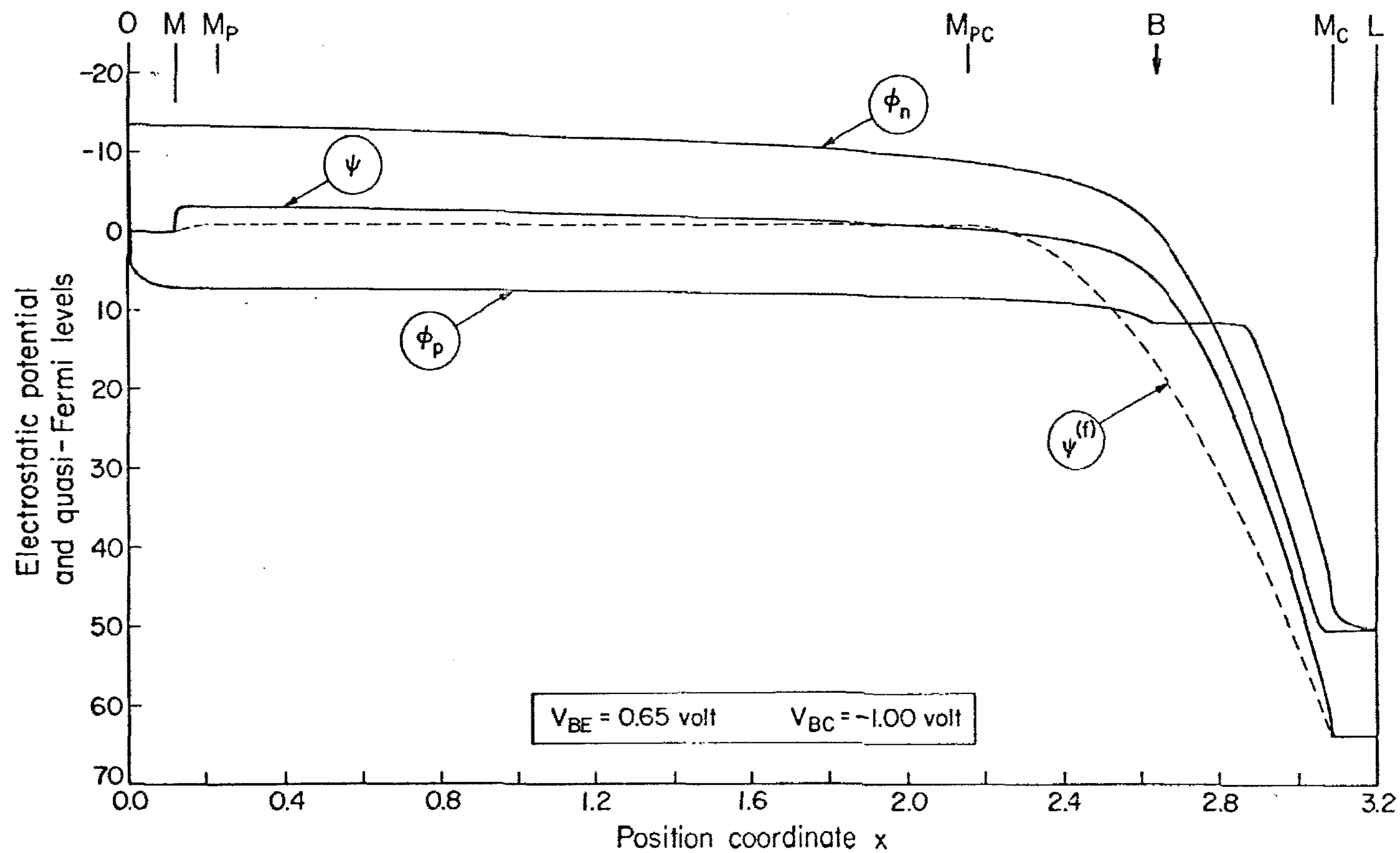

Fig. 6.20a. Device of Fig. 6.9a with the modified boundary condition $p(B) \simeq p_P$ on the external base contact. Electrostatic potential and quasi-Fermi levels as functions of position. Base-to-emitter voltage $V_{BE} = 0.65$ volt, base-to-collector voltage $V_{BC} = -1$ volt.

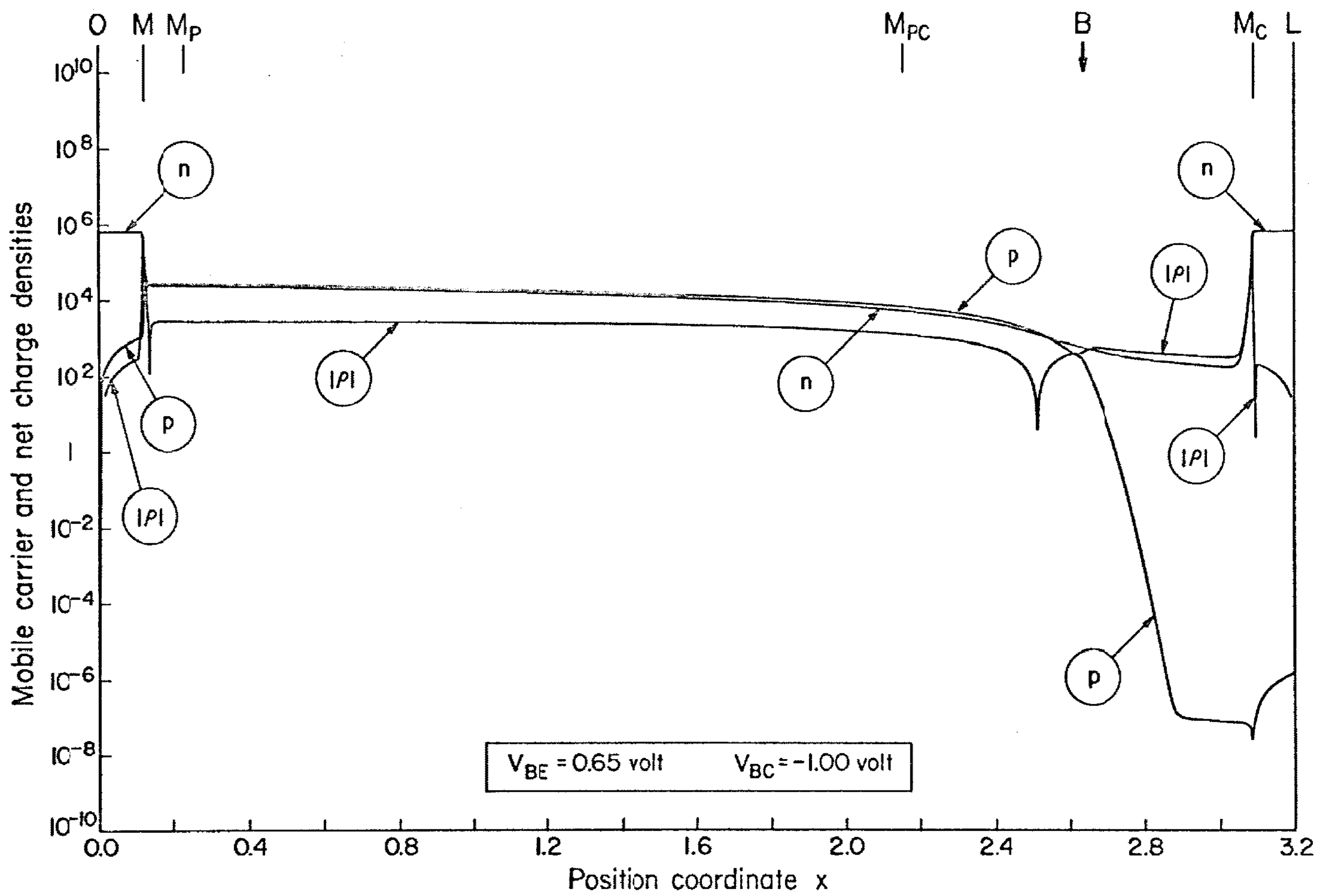

Fig. 6.20b. Device of Fig. 6.20a. Mobile carrier and net charge densities as functions of position. Base-to-emitter voltage V_{BE} = 0.65 volt, base-to-collector voltage V_{BC} = -1 volt.

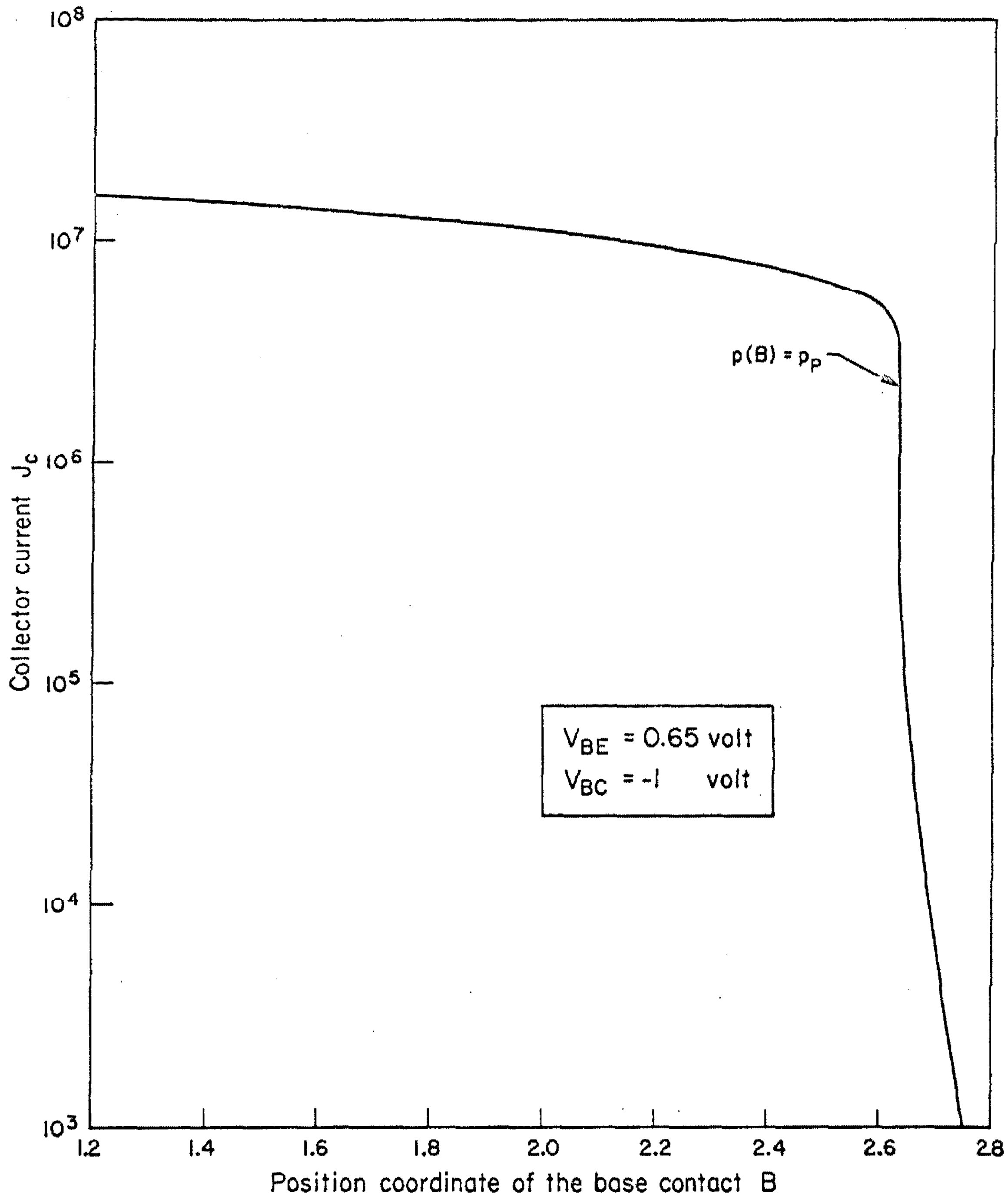

Fig. 6.21. Device of Fig. 6.9a, with exception of the position of the base contact taken as a variable. Collector current as a function of the position of the base contact B. Base-to-emitter voltage $V_{BE} = 0.65$ volt, base to collector voltage $V_{BC} = -1$ volt.

boundary conditions on the external base contact are illustrated in Figs. 6.19 to 6.21. The sign convention and the symbols adopted for the external currents and the applied voltages are depicted in Fig. 4.2.

As a consequence of the identical structure parameters of the emitter and collector regions, the thermal equilibrium case of Fig. 6.9 displays symmetric distributions with respect to the base, in spite of the asymmetric position of the external base contact. In consideration of the specified boundary conditions at the base contact (Section 4.1) it is apparent that such asymmetry becomes insignificant under equilibrium conditions, i.e. overall constancy and coincidence of the quasi-Fermi levels.

Figures 6.10 to 6.13 illustrate the internal distributions for a fixed base-to-collector reverse bias (V_{BC} = -1 volt) and increasing base-to-emitter forward bias from thermal equilibrium (V_{BE} = 0) to low injection (V_{BE} = 0.2 volt), high injection (V_{BE} = 0.5 volt) and very high injection (V_{BE} = 0.65 volt) conditions. Most features already discussed for the diode case (Section 6.2) are recognized here. The inadequacy of the assumption of fully depleted and neutral regions with abrupt boundaries, the severe discrepancy between "exact" and first-order minority carrier density at the edge of the neutral region in the base at the collector side in the presence of collected current (already analyzed by Middlebrook [5]), the discrepancy between "exact" and first-order depleted region widths and electrostatic potential distribution in the transition region of the emitter junction at high injection levels, are particularly evident. In addition, for increasing injection level of the emitter junction, the first-order theory prediction of the

properties of the collector junction worsens considerably: this is also apparent from the increasing discrepancy between the "exact" and first-order potential distribution in the transition region of the reverse-biased collector junction. Responsible for this effect is a high injection of minority carriers (electrons) into the base from the emitter, together with the narrowness of the base region: the "depleted" region of the base-collector junction, although reverse-biased, is prevented from being significantly depleted of mobile carriers and becomes considerably narrower than predicted by the first-order theory applied to an isolated P-N junction under the same bias conditions.* As a consequence, the transition region capacitance of the base-collector junction may vary significantly from the first-order theory prediction.

For the same fixed position of the base contact (B = 1.2), Figs. 6.14, 6.15, 6.11 and Figs. 6.16, 6.17, 6.12 display the internal distributions as functions of position for fixed base-to-emitter biases, a low-level injection (V_{BE} = 0.2 volt) and a high-level injection case (V_{BE} = 0.5 volt) respectively, and various base-to-collector biases, from a forward-bias condition in the "saturation" region (V_{BC} = 0.18 volt and V_{BC} = 0.493 volt respectively), to thermal equilibrium (V_{BC} = 0) and to a reverse-bias condition (V_{BC} = -1 volt). It is apparent, from the saturation conditions of Figs. 6.14 and 6.16, that both forward-biased junctions inject minority carriers (electrons) into

---

* This effect, referred to as "base push-out", is analytically investigated by Kirk [23].

the base such that the quasi-Fermi levels become nearly constant (but distinct) throughout the base. According to the relation

$$J = J_n + J_p = n \frac{d\varphi_n}{dx} + p \frac{d\varphi_p}{dx}$$

the total emitter and collector currents then vary considerably for a small variation of bias conditions, yielding the typical characteristic of the saturation region.

The above feature may be recognized in Fig. 6.18 which displays the total collector current density J_c (normalized) versus base-to-collector voltage V_{BC} (unnormalized) for various base-to-emitter voltages V_{BE} (unnormalized). Since generation-recombination effects have been neglected $[U(x) = 0]$, the collector current is essentially zero (not exactly for the asymmetric position of the base contact) if both junctions are equally forward-biased, and increases steeply for a small decrease of the base to collector bias. For a variation of the collector bias of a few V_t, the collector current reaches the constant value typical of the "linear" region of operation, rather insensitive to a further increase of collector reverse bias. The slight increase of collector current, for an increasing reverse bias on the collector junction, is essentially a consequence of the decreasing width of the quasi-neutral base region.

The effect of a modified boundary condition on the external base contact is shown in Fig. 6.19. Such a modified boundary condition on the mathematical base contact is determined by the simultaneous enforcement of two requirements:

(1) the requirement (4.1) on the majority carrier (hole) quasi-Fermi level at the position B of the base contact

$$\varphi_p(B) - \varphi_p(0) = V_{BE}$$

(2) thermal equilibrium conductivity of the neutral P-material at the point B for any bias condition.

The condition (1) is the original boundary condition on the external base contact, whereas the condition (2) represents an attempt to simulate in the one-dimensional model a base contact of the ohmic type. Since the position of the contact B affects (considerably at high injection, see Figs. 6.20 and 6.21) the internal distributions and terminal properties of the device, a method based on successive approximations requiring several "exact" solutions for various values of B is employed to satisfy the above condition (2). The position of B in the one-dimensional model becomes now a <u>dependent</u> parameter, implicitly determined by the introduction of the additional boundary condition (2) on the base contact. The total collector current density is displayed in Fig. 6.19 as a function of the base to emitter voltage for a fixed base to collector bias (V_{BC} = -1 volt) for both cases of fixed position of the base contact (B = 1.2) and modified boundary conditions with equilibrium conductivity at B. The considerable discrepancy between the two cases for high injection conditions is to be attributed to the inclusion within the emitter-base junction of a low-conductivity region, for the case of modified boundary conditions. For high-injection conditions, the conductivity of the quasi-neutral base region

at the left side of the fixed external base contact $(B = 1.2)$ is highly modulated, whereas if the position B is shifted sufficiently toward the collector junction to satisfy the modified boundary conditions, the region at the left of the point B features a low (close to thermal equilibrium) conductivity and is responsible for a significant decrease in both emitter and collector currents for specified bias conditions. The internal distributions for a very high injection case ($V_{BE} = 0.65$ volt, $V_{BC} = -1$ volt), with the modified boundary conditions at the external base contact, are shown in Figs. 6.20. In addition, for the same bias conditions, the total collector current density is shown in Fig. 6.21 as a function of the position B of the base contact, from $B = 1.2$ to slightly beyond the value B' ($B' \cong 2.633$) specified by the modified boundary conditions $p(B') \cong p_P$. The abruptness of the collector current about the point B' is indicative of the sensitivity of the terminal characteristics upon the choice of the boundary condition on the external base contact.

The analysis of the results obtained, rather than suggesting the use of modified boundary conditions at the position of the external base contact, merely exposes the inadequacy of the one-dimensional model in characterizing the properties of a three-contact device, typically a multi-dimensional problem.

6.4. Conclusion.

As an example of one-dimensional numerical solutions, results for idealized models of a two-contact (N-P diode) and a three-contact device (N-P-N transistor) have been reported and briefly discussed in this

Chapter. The electrostatic potential, quasi-Fermi levels, mobile carrier and net electric charge densities as functions of position and terminal properties have been illustrated, and the effect of modified boundary conditions has been investigated. "Exact" and first-order theory distributions have been quantitatively compared and discrepancies exposed, to achieve a thorough quantitative evaluation of the several assumptions and approximations conventionally introduced in analytical and numerical solutions of the problem. Although a one-dimensional model may closely characterize the properties of certain realistic structures of two-contact devices, the inadequacy of one-dimensional solutions of three-contact devices is confirmed by the analysis of the results obtained for the N-P-N transistor.

Calculations were performed on an IBM 7094-7040 shared file system. Output data were recorded on magnetic tape and directly displayed in graphical form by a Calcom plotter, connected to the IBM 7040. For the N-P diode, computation time for the achievement of one set of solutions (with five exact significant digits), including one point of the current-voltage characteristic, for one value of applied voltage, amounted to approximately 30 seconds for reverse bias and for low-level injection, and to 55 seconds for high injection, for a trial potential function given by the first-order theory. Two successive solutions were needed for the computation of the total incremental capacitance at a specified voltage. Higher computation times (especially at high injection conditions on the emitter junction and high reverse bias on the collector junction) were required for the N-P-N transistor to achieve results with comparable accuracy.

PART II

TIME-DEPENDENT ANALYSIS

CHAPTER VII

ANALYTICAL FORMULATION OF THE CURRENT-DRIVEN TRANSIENT PROBLEM FOR A TWO-CONTACT DEVICE.

In the previous chapters a method of solution and results for the one-dimensional two-carrier transport equations in steady-state have been presented. This and the following chapters are concerned with the analysis of the problem in transient conditions. This becomes essentially a two-dimensional problem, since quantities are functions of both position and time, and therefore it is of considerably higher degree of complexity.

7.1. Generalities.

Time-dependent solutions are available in the literature, at the present time, only for a set of approximate equations based on highly idealized models and limited to very special cases. Kennedy [24] analyzes the effect of a fictitious uniform electric field in a simplified form of the diffusion equation for minority carriers in a P-N junction under abrupt switching from a forward to a reverse bias condition; Kano and Reich [14] present transient solutions for a P-N junction driven by an external excitation of forward current. Both investigations are based on conventional assumptions and approximations, such as the abrupt separation of the interior of the device into fully depleted and quasi-neutral regions, highly asymmetric abrupt doping profile, linear recombination-generation law, and Boltzmann relation between the barrier voltage and the internal boundary value for the injected minority carrier density. In addition, solutions are only sought in the

quasi-neutral region of the low-conductivity side of the device.

It is in the scope of this and following chapters to present a numerical method of solution of the one-dimensional two-carrier transport equations under transient conditions, and to illustrate results for a particular structure. The method is of a very general character: none of the conventional assumptions and restrictions are introduced and freedom is available in the choice of the doping profile, recombination-generation law, mobility dependencies, injection level, and boundary conditions applied solely at the external contacts. For a specified arbitrary input signal of either current or voltage as a function of time, the solution yields terminal properties and all the quantities of interest in the interior of the device (such as carrier densities, electric field, electrostatic potential, particle and displacement currents) as functions of both position and time.

The physical model and corresponding basic equations, boundary conditions for a two contact device, and initial conditions are presented in this Chapter. The fundamental set of equations is rearranged to a more convenient form suitable for a numerical iterative scheme of solution of a very general character, for the case of an external excitation of total current as a function of time (current-driven transient). The general lines of the method are also illustrated.

The mathematical formulation of the problem is presented in the following Section.

7.2. Physical and mathematical model.

7.2.1. Normalized fundamental equations.

Under the assumptions stated in Subsection 1.1.1, the set of equations (1.1) to (1.6) describe mathematically the behavior of bipolar semiconductor junction devices. This fundamental set includes Maxwell's equation stating the solenoidal character of the total current expressed in terms of the electron, hole, and displacement contributions, the electron and hole current flow equations in terms of the respective drift and diffusion components, Poisson's equation and the continuity equations for electrons and holes. This basic system of equations represents the mathematical model and is now applied to the one-dimensional two-contact N-P structure of Fig. 1.1, to analyze time-dependent phenomena. With the aid of the normalization factors of Table 1.1, Eqs.(1.1) to (1.6), specialized for the one-dimensional case, may be rewritten in the following dimensionless form:

$$J(t) = J_n(x,t) + J_p(x,t) - \frac{\partial E(x,t)}{\partial t} \tag{7.1}$$

$$\frac{\partial J(t)}{\partial x} = 0 \tag{7.1a}$$

$$J_n(x,t) = -\frac{1}{\gamma_n(x,t)}\left[n(x,t)\,E(x,t) + \frac{\partial n(x,t)}{\partial x}\right] \tag{7.2}$$

$$J_p(x,t) = \frac{1}{\gamma_p(x,t)}\left[-\,p(x,t)\,E(x,t) + \frac{\partial p(x,t)}{\partial x}\right] \tag{7.3}$$

$$\frac{\partial E(x,t)}{\partial x} = p(x,t) - n(x,t) + N(x) \tag{7.4}$$

$$\frac{\partial n(x,t)}{\partial t} = - U(x,t) - \frac{\partial J_n(x,t)}{\partial x} \qquad (7.5)$$

$$\frac{\partial p(x,t)}{\partial t} = - U(x,t) + \frac{\partial J_p(x,t)}{\partial x} \qquad (7.6)$$

As already observed in Section 1.1.1, only six of the above equations are independent, since any one of Eqs.(7.1a), (7.4), (7.5), and (7.6) may be derived from the remaining three (and the knowledge of the doping profile $N(x)$ if Eq.(7.4) is omitted). The recombination-generation term $U(x,t)$ and the mobilities $1/\gamma_n(x,t)$, $1/\gamma_p(x,t)$ may be specified in the most general form in terms of the remaining variables, and complete freedom is available in the choice of the doping profile $N(x)$. These quantities are therefore left unspecified, since their exact form is unessential for the present purposes.

7.2.2. Boundary and initial conditions.

For a two-contact device of the type shown in Fig. 1.1, four boundary conditions on the mobile carrier densities may be specified. These may be characterized by the same generality of relations (1.28), which are here rewritten as:

$$\left.\begin{aligned} n(0,t) &= g_{n0}[J_n(0,t),\ J_p(0,t)] \\ p(0,t) &= g_{p0}[J_n(0,t),\ J_p(0,t)] \\ n(L,t) &= g_{nL}[J_n(L,t),\ J_p(L,t)] \\ p(L,t) &= g_{pL}[J_n(L,t),\ J_p(L,t)] \end{aligned}\right\} \qquad (7.7)$$

where, according to Eqs.(7.2), (7.3),

$$\left.\begin{aligned}
J_n(0,t) &= -\frac{1}{\gamma_n(0,t)}\left[\; n(0,t)\,E(0,t) + \left.\frac{\partial n(x,t)}{\partial x}\right|_{x=0}\right] \\
J_p(0,t) &= \frac{1}{\gamma_p(0,t)}\left[-p(0,t)\,E(0,t) + \left.\frac{\partial p(x,t)}{\partial x}\right|_{x=0}\right] \\
J_n(L,t) &= -\frac{1}{\gamma_n(L,t)}\left[\; n(L,t)\,E(L,t) + \left.\frac{\partial n(x,t)}{\partial x}\right|_{x=L}\right] \\
J_p(L,t) &= \frac{1}{\gamma_p(L,t)}\left[-p(L,t)\,E(L,t) + \left.\frac{\partial p(x,t)}{\partial x}\right|_{x=L}\right]
\end{aligned}\right\} \quad (7.8)$$

Relations (7.7) need not be specified, and may be assigned with the generality desired. A dependent boundary condition on the slope of the electric field is given by Poisson's equation (7.4):

$$\left.\begin{aligned}
\left.\frac{\partial E(x,t)}{\partial x}\right|_{x=0} &= p(0,t) - n(0,t) + N(0) \\
\left.\frac{\partial E(x,t)}{\partial x}\right|_{x=L} &= p(L,t) - n(L,t) + N(L)
\end{aligned}\right\} \quad (7.9)$$

The electric field and the mobile carrier density distributions throughout the interior of the device at the initial time $t = 0$:

$$\left.\begin{aligned}
&E(x,t) \\
&n(x,t) \\
&p(x,t)
\end{aligned}\right\} \text{ for } \; 0 \le x \le L \;, \quad \text{at} \quad t = 0 \quad (7.10)$$

may be specified as the independent initial conditions, which explicitly determine, with the aid of Eqs.(7.1) to (7.6), all the quantities of interest at the initial time. If the evolution of a time-dependent solution starts at a steady-state condition, the initial conditions

are available from the steady-state solutions obtained with the method described in the previous chapters.*

If the total current $J(t)$ through the device is specified at any instant of time $t > 0$, the fundamental equations (7.1) to (7.6) with the boundary conditions (7.7) and the initial conditions (7.10) represent the complete mathematical formulation of the problem. Solutions for all the relevant quantities as functions of both position x and time t are sought. As an aside, the electrostatic potential $\psi(x,t)$ and the terminal voltage $V_A(t)$ may be computed by the subsidiary relations:

$$\psi(x,t) = -\int_0^x E(x',t)\,dx' + \psi(0,t) \tag{7.11}$$

$$V_A(t) = -\int_0^L E(x,t)\,dx + V_d \tag{7.12}$$

where $\psi(0,t)$ may be taken as the reference value for the electrostatic potentials, and V_d is the diffusion potential defined by

$$V_d \triangleq \left[\int_0^L E(x)\,dx\right]_{\substack{\text{thermal}\\\text{equilibrium}}} \tag{7.13}$$

If external contacts of the ohmic type are specified, the boundary conditions (7.7) assume the simple form:

---

* An alternative method of solution, "compatible" with the formulation employed for the time-dependent solution, is presented in Section 9.3.

$$\left.\begin{aligned} n(0,t) &= n_N \\ p(0,t) &= p_N \\ n(L,t) &= n_P \\ p(L,t) &= p_P \end{aligned}\right\} \qquad (7.14)$$

where n_N, p_N, n_P, and p_P are the equilibrium carrier densities at the external contacts given by relations (1.32). The dependent boundary conditions (7.9) become then:

$$\left.\frac{\partial E(x,t)}{\partial x}\right|_{\substack{x=0 \\ x=L}} = 0 \qquad (7.15)$$

and are a consequence of the charge neutrality condition of the ohmic contacts.

7.3. Derivation of the reduced set of equations.

The fundamental equations (7.1) to (7.6) may be conveniently rearranged to a form more appropriate for numerical methods. If the expressions (7.2) and (7.3) for the electron and hole current densities are inserted in Maxwell's Eq.(7.1), the displacement term may be explicitly written as:

$$\frac{\partial E(x,t)}{\partial t} = -\left[\frac{n(x,t)}{\gamma_n(x,t)} + \frac{p(x,t)}{\gamma_p(x,t)}\right]E(x,t) - \frac{1}{\gamma_n(x,t)}\frac{\partial n(x,t)}{\partial x} + \frac{1}{\gamma_p(x,t)} \cdot \frac{\partial p(x,t)}{\partial x} - J(t) \qquad (7.16)$$

Moreover, if the expressions (7.2) and (7.3) are inserted in Eqs.(7.5) and (7.6) respectively, one obtains:

$$\frac{\partial n(x,t)}{\partial t} = \frac{1}{\gamma_n(x,t)}\left[\frac{\partial^2 n(x,t)}{\partial x^2} + E(x,t)\,\frac{\partial n(x,t)}{\partial x} + n(x,t)\,\frac{\partial E(x,t)}{\partial x} + J_n(x,t)\,\frac{\partial \gamma_n(x,t)}{\partial x}\right] - U(x,t)$$

$$\frac{\partial p(x,t)}{\partial t} = \frac{1}{\gamma_p(x,t)}\left[\frac{\partial^2 p(x,t)}{\partial x^2} - E(x,t)\,\frac{\partial p(x,t)}{\partial x} - p(x,t)\,\frac{\partial E(x,t)}{\partial x} - J_p(x,t)\,\frac{\partial \gamma_p(x,t)}{\partial x}\right] - U(x,t)$$

and with the aid of Poisson's Eq.(7.4) and Eqs.(7.2), (7.3):

$$\frac{\partial n(x,t)}{\partial t} = \frac{1}{\gamma_n(x,t)}\left\{\frac{\partial^2 n(x,t)}{\partial x^2} + \left[E(x,t) - \frac{1}{\gamma_n(x,t)}\,\frac{\partial \gamma_n(x,t)}{\partial x}\right]\frac{\partial n(x,t)}{\partial x} + \left[p(x,t) - n(x,t) - \frac{E(x,t)}{\gamma_n(x,t)}\,\frac{\partial \gamma_n(x,t)}{\partial x} + N(x)\right]n(x,t)\right\} - U(x,t) \tag{7.17}$$

$$\frac{\partial p(x,t)}{\partial t} = \frac{1}{\gamma_p(x,t)}\left\{\frac{\partial^2 p(x,t)}{\partial x^2} - \left[E(x,t) + \frac{1}{\gamma_p(x,t)}\,\frac{\partial \gamma_p(x,t)}{\partial x}\right]\frac{\partial p(x,t)}{\partial x} - \left[p(x,t) - n(x,t) - \frac{E(x,t)}{\gamma_p(x,t)}\,\frac{\partial \gamma_p(x,t)}{\partial x} + N(x)\right]p(x,t)\right\} - U(x,t) \tag{7.18}$$

The reduced set of Eqs.(7.16), (7.17), and (7.18), with the boundary conditions (7.7), initial conditions (7.10), and the specified external excitation $J(t)$, represents a complete formulation of the problem equivalent to that described in Section 7.2.* In this new formulation

---

* The dependencies of the carrier mobilities $\gamma_n^{-1}(x,t)$, $\gamma_p^{-1}(x,t)$ upon the quantities of interest (such as electric field, impurity density, etc.) must, of course, also be specified.

the electric field E, the electron density n and the hole density p are chosen as the independent quantities and represent the unknowns of the reduced set of equations.

If generation-recombination processes are neglected $[U(x) = 0]$, and mobilities are considered constant, Eqs.(7.16) to (7.18) assume the simpler form:

$$\frac{\partial E(x,t)}{\partial t} = -\left[\frac{n(x,t)}{\gamma_n} + \frac{p(x,t)}{\gamma_p}\right] E(x,t) - \frac{1}{\gamma_n}\frac{\partial n(x,t)}{\partial x} + \frac{1}{\gamma_p}\frac{\partial p(x,t)}{\partial x} - J(t) \tag{7.19}$$

$$\frac{\partial n(x,t)}{\partial t} = \frac{1}{\gamma_n}\left\{\frac{\partial^2 n(x,t)}{\partial x^2} + E(x,t)\frac{\partial n(x,t)}{\partial x} + [p(x,t)-n(x,t)+N(x)]\; n(x,t)\right\} \tag{7.20}$$

$$\frac{\partial p(x,t)}{\partial t} = \frac{1}{\gamma_p}\left\{\frac{\partial^2 p(x,t)}{\partial x^2} - E(x,t)\frac{\partial p(x,t)}{\partial x} - [p(x,t)-n(x,t)+N(x)]\; p(x,t)\right\} \tag{7.21}$$

7.4. Iterative method of solution.

Equations (7.16) to (7.18), or alternatively Eqs.(7.19) to (7.21), represent a system of three non-linear partial differential equations in the three unknowns E, n, p, in two dimensions: time t and position x. In particular Eqs.(7.17) and (7.18), or Eqs.(7.20) and (7.21) are non linear partial differential equations of the "parabolic" type.* The first step toward a numerical solution of such a system of equations requires the discretization of the relevant quantities at a

---

* See Appendix F.

finite number of points in both time and space. Appropriate numerical techniques must then be devised to determine at each instant of time the spatial distributions of the unknowns (throughout the interior of the device), that satisfy the set of equations for assigned boundary conditions.*

Although the discretization problem for partial differential equations of the parabolic type requires particular consideration,** a numerical method of solution may be schematically sketched at this stage. The simpler case of fixed boundary conditions (for example corresponding to ohmic contacts), absence of generation-recombination and constant mobilities is considered first. The mathematical formulation of the problem is then given by Eqs.(7.19) to (7.21), boundary conditions (7.14), initial conditions (7.10) and the external excitation $J(t)$. It is apparent that the highly non-linear character of the equations requires an iterative procedure at each instant of time to reach the desired consistency. From the knowledge of the spatial distributions at the initial time $t = t_0$, it is desired to determine the unknowns at the next instant of time $t = t_1$. A guess for the electron and hole density spatial distributions at t_1 is made (for example those available at the previous instant of time t_0), and these are inserted in Eq.(7.19) to solve for a preliminary (approximate) electric field spatial distribution at t_1, which in turn may be inserted,

---

* The existence and uniqueness of the solutions is justified on the basis of physical requirements.

** This is the subject of Appendix F.

together with the guess for the hole density distribution, in Eq.(7.20) to determine an improved value for the electron density spatial distribution at t_1. These improved distributions may now be inserted in Eq.(7.19), and the iteration cycle at the instant of time t_1 may be repeated until overall consistency is achieved at t_1. The "exact" distributions at the instant t_1 are then taken as initial conditions and the procedure is repeated to determine the "exact" distributions at the instant t_2. The process terminates when the final state is reached, that is when both the external excitation $J(t)$ has reached the final value and the right hand sides of Eqs.(7.19) to (7.21) are zero. The scheme is summarized in Fig. 7.1.

Extension to the more general case of Eqs.(7.16) to (7.18), featuring space and time dependent mobilities $\gamma_n^{-1}(x,t)$, $\gamma_p^{-1}(x,t)$ and a non-zero recombination-generation term $U(x)$, is straightforward. A slightly more intricate scheme is required for the case of variable boundary conditions (7.7). A secondary iteration loop at each main cycle at each instant of time may be required to resolve the non-linearities of the combination of Eqs.(7.7) with Eqs.(7.8) to determine the boundary values of the mobile carrier densities before attempting the solution of Eqs.(7.17) and (7.18).

7.5. Conclusion.

The problem of the time-dependent analysis of phenomena governing the behavior of semiconductor junction devices has been formulated. Fundamental equations, boundary conditions, initial conditions, and external excitations have been presented for the physical model chosen. The fundamental set of equations has been rearranged to a more

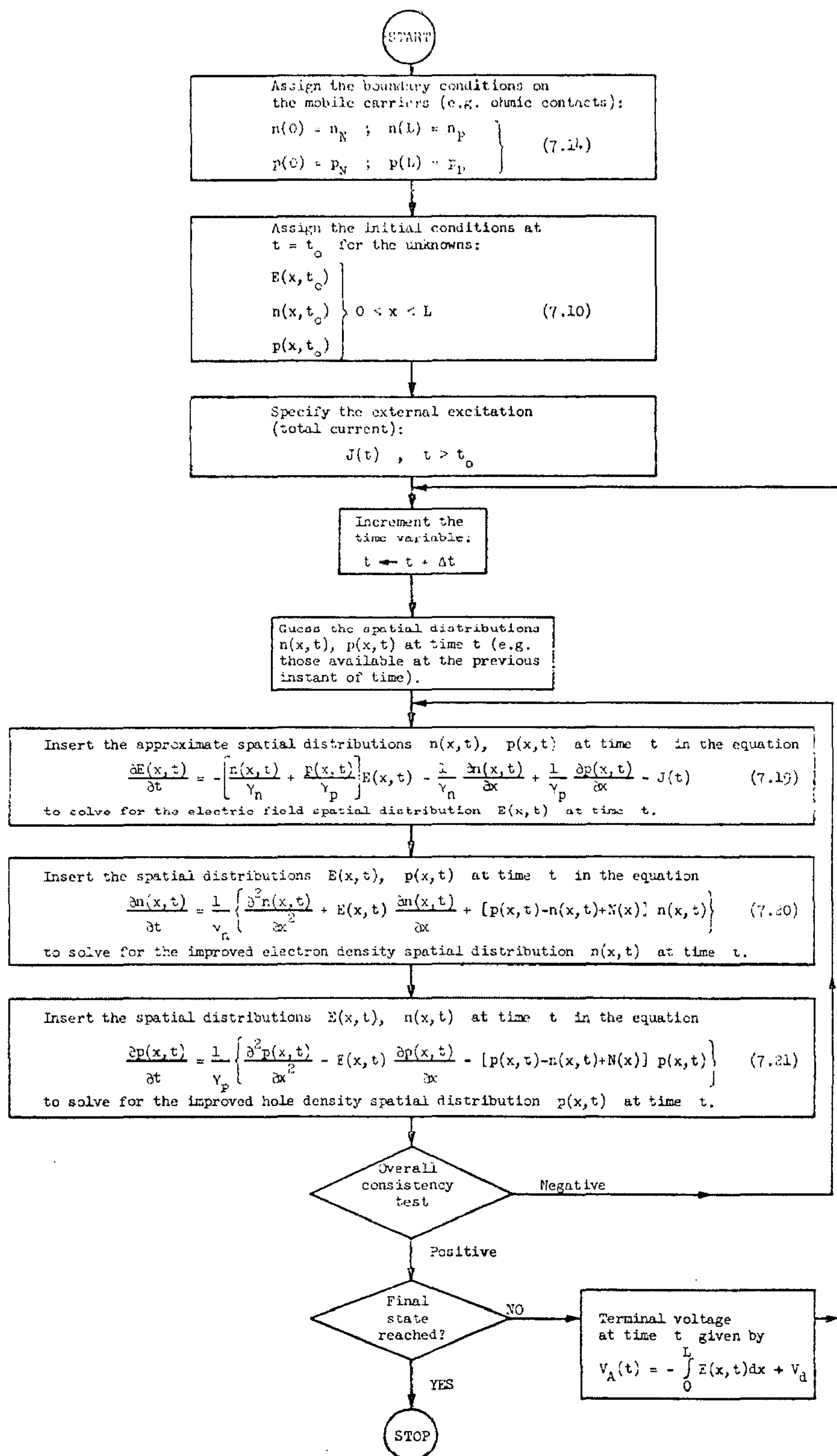

Fig. 7.1. Overall iterative procedure for the current-driven transient, for a special case.

convenient equivalent set of three non-linear partial differential equations and the general lines of an iterative numerical method of solution have been briefly outlined. The next step toward a detailed numerical solution requires the selection of a "sound" discretization scheme suitable for partial differential equations of the parabolic type. This problem will be considered in the next Chapter, on the basis of the theory of numerical analysis available for simpler cases, and summarized in Appendix F.

CHAPTER VIII

DISCRETIZATION OF THE ANALYTICAL FORMULATION FOR THE CURRENT-DRIVEN TRANSIENT

In this Chapter the problem of the selection of a numerically sound discretization scheme for the analytical formulation of the current-driven transient problem is analyzed. A particular type of discretization scheme is chosen, and details of two discretized formulations and of the iterative procedure of solution are presented. Criteria for the achievement of a non-uniform discretization mesh automatically adjusted by the computer during the entire evolution of the transient are stated. Inadequacies of the procedure arising under special conditions are exposed and will be the subject of a later chapter.

8.1. Selection of the discretization scheme.

In the previous Chapter the analytical formulation of the problem has been presented, centered on the solution of a system of three non-linear partial differential equations in the three unknowns $E(x,t)$, $n(x,t)$, $p(x,t)$, as functions of both position x and time t. Two of the equations have been recognized as non-linear partial differential equations of the parabolic type, the discretization of which requires particular attention.

In general, the continuous quantities appearing in the analytical formulation are discretized at a finite number of points in both position and time coordinates; the ensemble of these points constitutes a "grid" or "mesh" (two-dimensional in the present case). Finite

difference schemes are then employed to approximate the analytical differentiations and reduce the problem to the solution of a system of finite difference equations which represent the discretized formulation.

The exact solution of the original analytical formulation differs, in general, from the exact solution of the system of finite difference equations. The discrepancy between the two solutions is usually referred to as "discretization error". The problem of "convergence" deals with the conditions under which the discretization error becomes equal to zero in the limit of vanishing distance between adjacent position and time points. In addition the actual numerical solution, obtained as a result of computations on the basis of the discretized formulation, differs from the exact solution of the system of difference equations by an amount equal to the "numerical error". One reason for the presence of the numerical error arises from the limitation of the digital machines to accommodate only a finite number of significant digits: a "round off error" is then introduced at each elementary operation throughout the numerical solution. The problem of "stability" deals with the conditions under which the numerical error is small throughout the entire range of solution. The basic problem arising in the numerical solution of partial differential equations of the parabolic type is therefore the selection of a discretization scheme featuring both convergence and stability, together with a satisfactory degree of efficiency.

The currently available theory of numerical analysis furnishes several discretization schemes, the convergence and stability of which

are proven for the simpler cases. Whereas the theory is complete for the case of linear equations with constant coefficients, it is fragmentary for the case of linear equations with non-constant coefficients, and conditions of convergence and stability for the non-linear case are only available for a few special equations and discretization schemes.*
However, it seems appropriate to extrapolate from the conclusions available for the simpler cases, in the search for a discretization scheme with the desired features for the more complex situations, such as the non-linear system under consideration.

Convergence and stability requirements for certain types of discretization schemes are contingent upon restrictions on the mesh size. For example, for the linear cases with non-constant coefficients and for the semilinear Eq.(F-9) (of Appendix F), convergence and stability may be proven for the simplest "explicit" scheme with uniform mesh (see Appendix F) if the inequality (F-10) between the time step Δt and the spatial step Δx of the discretization mesh is satisfied. If extrapolation to the system of Eqs.(7.16) to (7.18) is made, the inequality (F-10) becomes:

$$\text{l.u.b.} \; \frac{2\,\Delta t}{\gamma(x,t)(\Delta x)^2} < 1 \tag{8.1}$$

where $\gamma(x,t)$ is either $\gamma_n(x,t)$ or $\gamma_p(x,t)$ whichever is smaller. The spatial step size will be selected with criteria similar to those

* A brief summary of the available information on the subject is gathered in Appendix F.

outlined in Subsection 2.3.1 and will lead to a step distribution of the type of Fig. 2.7, in which the order of magnitude of the smallest step is 10^{-5}. If the inequality (8.1) is extrapolated to a non-uniform mesh, and the order of magnitude of the minimum value of $\gamma(x,t)$ is taken as 10^{-2}, the restriction

$$\Delta t \lesssim 5 \times 10^{-9} \qquad (\text{or } \Delta t\big|_{\text{dimensioned}} \lesssim 5 \times 10^{-17} \text{ sec}) \tag{8.2}$$

on the time step size is necessary, to ensure convergence and stability. The condition (8.2) is highly undesirable because of the excessive number of points required for the time coordinate, with consequent unacceptable computation load.

Also in view of the convenience of adopting a highly non-uniform mesh, in both position and time directions, it is desirable to select a discretization scheme which features, at least in the simpler cases, unconditional convergence and stability without any constraint on the mesh size. It may be proven that a discretization scheme of the "implicit type" (see Appendix F) satisfies this requirement for the case of linear equations with constant coefficients. Preference will therefore be given to schemes of the implicit type; these will be generalized in the following Section and applied to the more complex case of the non-linear system under consideration.

A partial differential equation of the parabolic type, discretized with an implicit scheme, requires the simultaneous solution of a system of difference equations (one for each spatial point) at each instant of time, unnecessary for the discretization generated by explicit schemes.

The corresponding increase in computation time will be shown to represent a minor drawback, greatly compensated by the freedom available in the selection of the mesh size in both position and time coordinates.

8.2. Discretization by implicit schemes.

In the previous Section the choice of a scheme of the implicit type has been made for the discretization of the analytical formulation of Section 7.3. For a partial differential equation of the type:

$$\frac{\partial Y(x,t)}{\partial t} = F\left[\frac{\partial^2 Y(x,t)}{\partial x^2} \ , \quad \frac{\partial Y(x,t)}{\partial x} , \quad Y(x,t)\right] \tag{8.3}$$

a class of implicit discretization schemes may be summarized by the formula

$$\frac{{}_kY_i - {}_{k-1}Y_i}{{}_k\Delta t} = \theta \quad {}_kF_i + (1-\theta) \ {}_{k-1}F_i \tag{8.4}$$

$(i = 1, 2, 3, \cdots \ell \ ; k = 1, 2, 3, \cdots)$

where:

- θ is a parameter that determines the specific type of discretization scheme and may be chosen as $\frac{1}{2} \leq \theta \leq 1$,
- k is the index identifying the instant of time ${}_kt$ (time index; ${}_0t \triangleq$ initial time)
- i is the index identifying the spatial point x_i (spatial index; $x_1 \triangleq 0, x_\ell \triangleq L$)

${}_k\Delta t \triangleq {}_kt - {}_{k-1}t$ is the magnitude of the time step at the instant k,

$${}_kY_i \triangleq Y(x_i,\ {}_kt) \quad ,$$

$${}_kF_i \triangleq F\left[\left(\frac{\partial^2 Y(x,t)}{\partial x^2}\right)_{{}_kt,\,x_i} \ ,\ \left(\frac{\partial^2 Y(x,t)}{\partial x}\right)_{{}_kt,\,x_i} \ ,\ Y(x_i,\ {}_kt)\right] ,$$

and a two-point finite difference formula is chosen to approximate the time derivative of Eq.(8.3) (two-level finite difference scheme).

Two specific discretization schemes will be considered below, corresponding to Eq.(8.4) with $\theta = 1$ (referred to as "generalized pure implicit scheme") and to Eq.(8.4) with $\theta = \frac{1}{2}$ (referred to as "generalized Crank-Nicholson scheme"). Detailed difference equations will be derived, for the sake of conciseness, solely for the special case of Eqs.(7.19) to (7.21), characterized by absence of generation-recombination in the interior of the device, constant mobilities, and ohmic external contacts. Extension to the more general case is straightforward.

8.2.1. Generalized pure implicit discretization scheme.

The discretization scheme of the generalized pure implicit type, defined by Eq.(8.4) with $\theta = 1$, is schematically illustrated in Fig. 8.1. A typical non uniform two-dimensional mesh in the position and time coordinates is shown, with ℓ spatial points including the boundaries $i = 1$ and $i = \ell$, and $f + 1$ time points including the initial and final state $k = 0$, and $k = f$, respectively. The assigned boundary and initial conditions (of the open type) specify all the quantities at $i = 1$, $i = \ell$, and $k = 0$. The finite difference equation (8.4) ($\theta = 1$) represents a relationship between quantities at the

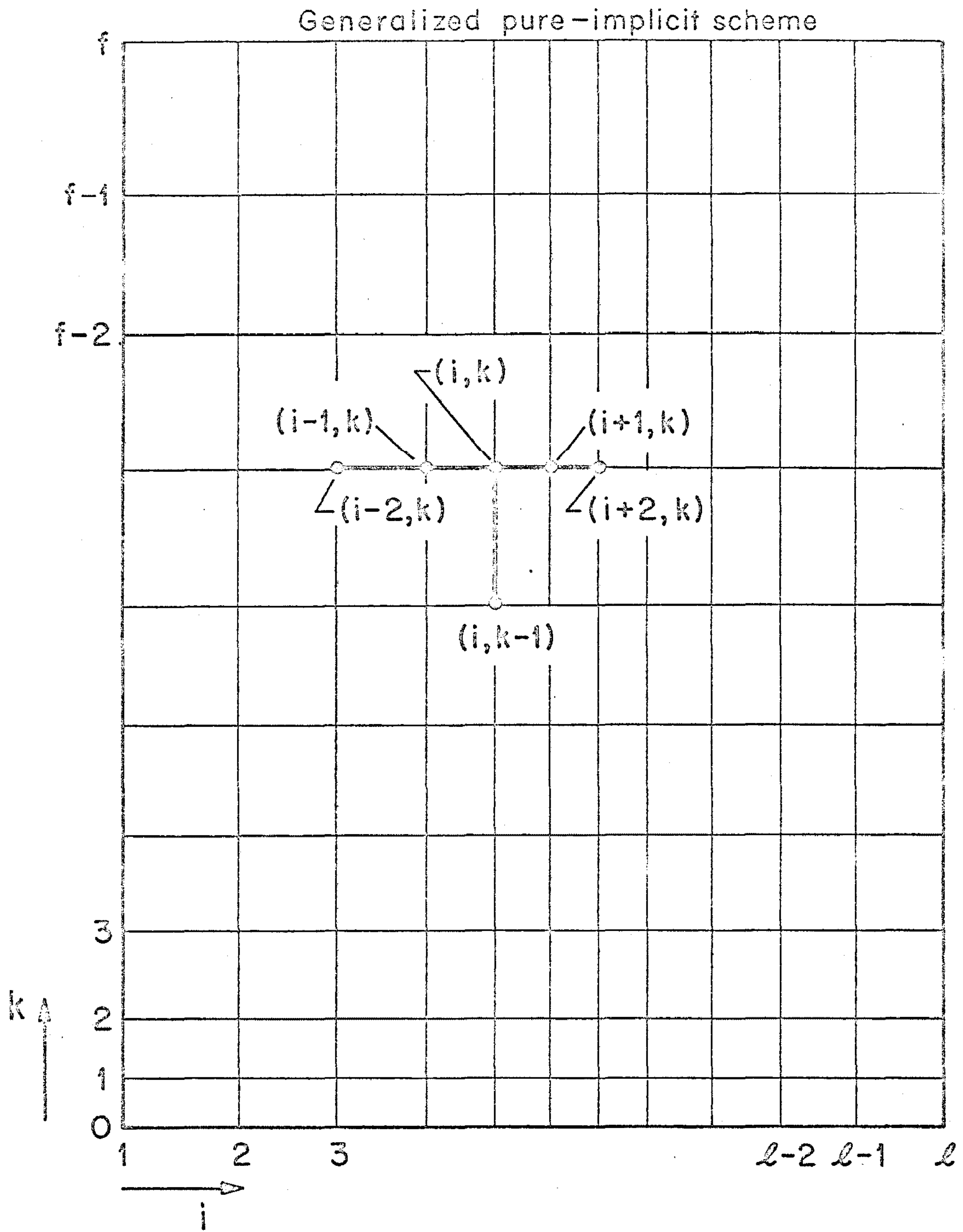

Fig. 8.1. Generalized pure implicit discretization scheme with a five-point formula for the numerical spatial differentiation (schematic).

point (i, k-1) and at a minimum of three adjacent points* i-1, i, i + 1 on the line k, the next instant of time. From the initial line k = 0 it is necessary to determine the quantities on the line k = 1, by solving the implicit system of simultaneous equations (8.4) with k = 0, i = 2, 3, 4, ⋯ ℓ-1, then proceed to the line k = 2, and so on.

For the case of interest, Eqs.(7.19) to (7.21), discretized on the basis of Eq.(8.4) with $\theta = 1$, generate the following system of difference equations:

$$\frac{{}_kE_i - {}_{k-1}E_i}{{}_k\Delta t} = -\left[\frac{{}_kn_i}{\gamma_n} + \frac{{}_kp_i}{\gamma_p}\right]{}_kE_i - \frac{1}{\gamma_n}\,{}_k\!\left(\frac{\partial n}{\partial x}\right)_i + \frac{1}{\gamma_p}\,{}_k\!\left(\frac{\partial p}{\partial x}\right)_i - {}_kJ \tag{8.5}$$

$$\frac{{}_kn_i - {}_{k-1}n_i}{{}_k\Delta t/\gamma_n} = {}_k\!\left(\frac{\partial^2 n}{\partial x^2}\right)_i + {}_kE_i\,{}_k\!\left(\frac{\partial n}{dx}\right)_i + \left[{}_kp_i - {}_kn_i + N_i\right]{}_kn_i \tag{8.6}$$

$$\frac{{}_kp_i - {}_{k-1}p_i}{{}_k\Delta t/\gamma_p} = {}_k\!\left(\frac{\partial^2 p}{\partial x^2}\right)_i - {}_kE_i\,{}_k\!\left(\frac{\partial p}{\partial x}\right)_i - \left[{}_kp_i - {}_kn_i + N_i\right]{}_kp_i \tag{8.7}$$

(k = 1, 2 ⋯ f ; i = 1, 2, 3, ⋯ ℓ)

Quantities at instants of time $t \le {}_{k-1}t$, at any spatial point $0 \le x_i \le L$, are supposed known, and solutions for the next instant of time ${}_kt$ are sought. According to the method briefly outlined in

---

* The number of such points on the line k depends upon the order of the finite difference formula employed for the numerical computation of the spatial derivatives in the right side of Eq.(8.4), and is usually 3, 5 or 7 (not higher for practical limitations).

Section 7.4, an iterative procedure is employed at each instant of time to determine the unknown quantities. A third index j ($j = 0, 1, 2 \cdots$) is introduced to identify the cycle of such an iterative procedure; quantities labeled with the superscript j are supposed available at the completion of the jth iteration. Since the iterative procedure is repeated at each instant ${}_kt$, the index j is set to zero each time consistency has been reached at one instant, the time index k is increased by unity, and the iteration restarts at the next instant. Quantities labeled with the superscript $j = 0$ are then the trial distributions required to initiate the iterative procedure at each instant of time.

It is convenient to introduce the corrections Δn and Δp for the electron and hole densities respectively, defined as the difference between densities corresponding to two successive iterations:

$$\left.\begin{aligned} {}_k\Delta n_i^{(j)} &\triangleq {}_kn_i^{(j)} - {}_kn_i^{(j-1)} \\ {}_k\Delta p_i^{(j)} &\triangleq {}_kp_i^{(j)} - {}_kp_i^{(j-1)} \end{aligned}\right\} \qquad (8.8)$$

($k = 0, 1, 2, \cdots f$; $i = 1, 2, 3, \cdots \ell$; $j = 0, 1, 2, \cdots$)

If convergence of the approximate spatial distributions towards the exact spatial distributions occurs during the iterative procedure at each instant of time, the following relations are readily verified with the aid of the definition (8.8):

$$\lim_{\substack{j\to\infty \\ 1\le i\le \ell \\ 0\le k\le f}} {}_k\Delta n_i^{(j)} = 0 \quad ; \quad \lim_{\substack{j\to\infty \\ 1\le i\le \ell \\ 0\le k\le f}} {}_k\Delta p_i^{(j)} = 0 \; . \tag{8.9}$$

In addition the time independent property of the boundary conditions (7.14) yields:

$$\left.\begin{aligned} {}_k\Delta n_{i=1}^{(j)} &= 0 \\ {}_k\Delta n_{i=\ell}^{(j)} &= 0 \\ {}_k\Delta p_{i=1}^{(j)} &= 0 \\ {}_k\Delta p_{i=\ell}^{(j)} &= 0 \end{aligned}\right\} \quad \begin{aligned} &\text{for} \quad 0 \le k \le f \\ &\text{and any} \quad j \end{aligned} \tag{8.10}$$

If the quantities labeled $k + 1$ in Eqs.(8.6) and (8.7) are identified with the superscript $j + 1$ (with exception of the term ${}_kp_i$ of Eq.(8.6), labeled j), and relations (8.8) are rewritten in the form

$${}_kn_i^{(j+1)} = {}_k\Delta n_i^{(j+1)} + {}_kn_i^{(j)} \tag{8.11}$$

$${}_kp_i^{(j+1)} = {}_k\Delta p_i^{(j+1)} + {}_kp_i^{(j)} \tag{8.12}$$

and inserted in Eqs.(8.6) and (8.7), one obtains:

$$
{}_k\left(\frac{\partial^2 \Delta n}{\partial x^2}\right)_i^{(j+1)} + {}_kE_i^{(j+1)}\; {}_k\left(\frac{\partial \Delta n}{\partial x}\right)_i^{(j+1)} + \left({}_kp^{(j)} - 2\,{}_kn_i^{(j)} + N_i - \frac{\gamma_n}{{}_k\Delta t}\right){}_k\Delta n_i^{(j+1)} -
$$

$$
-\left({}_k\Delta n_i^{(j+1)}\right)^2 = -\,{}_k\left(\frac{\partial^2 n}{\partial x^2}\right)_i^{(j)} - {}_kE_i^{(j+1)}\; {}_k\left(\frac{\partial n}{\partial x}\right)_i^{(j)} - \left({}_kp_i^{(j)} - {}_kn_i^{(j)} + N_i\right)\cdot
$$

$$
\cdot\,{}_kn_i^{(j)} + \frac{\gamma_n}{{}_k\Delta t}\left({}_kn_i^{(j)} - {}_{k-1}n_i\right) \triangleq {}_k(F_n)_i^{(j)}/(x_{i+1}-x_{i-1}) \tag{8.13}
$$

$$
{}_k\left(\frac{\partial^2 \Delta p}{\partial x^2}\right)_i^{(j+1)} - {}_kE_i^{(j+1)}\; {}_k\left(\frac{\partial \Delta p}{\partial x}\right)_i^{(j+1)} - \left(2\,{}_kp_i^{(j)} - {}_kn^{(j+1)} + N_i + \frac{\gamma_p}{{}_k\Delta t}\right)\cdot
$$

$$
\cdot\,{}_k\Delta p_i^{(j+1)} - \left({}_k\Delta p_i^{(j+1)}\right)^2 = -\,{}_k\left(\frac{\partial^2 p}{\partial x^2}\right)_i^{(j)} + {}_kE_i^{(j+1)}\; {}_k\left(\frac{\partial p}{\partial x}\right)_i^{(j)} + \left({}_kp_i^{(j)} - {}_kn^{(j+1)} + N_i\right)\cdot
$$

$$
\cdot\,{}_kp_i^{(j)} + \frac{\gamma_p}{{}_k\Delta t}\left({}_kp_i^{(j)} - {}_{k-1}p_i\right) \triangleq {}_k(F_p)_i^{(j)}/(x_{i+1}-x_{i-1}) \tag{8.14}
$$

where F_n and F_p are defined, for conciseness, as the right side of Eqs.(8.13) and (8.14) respectively, weighted by the factor $(x_{i+1}-x_{i-1})$.

On the other hand the electric field at the instant $k + 1$ may be explicitly recovered from Eq.(8.5) rewritten as:

$$ {}_kE_i^{(j+1)} = \frac{\dfrac{{}_{k-1}E_i}{{}_k\Delta t} - \dfrac{1}{\gamma_n}\,{}_k\!\left(\dfrac{\partial n}{\partial x}\right)_i^{(j)} + \dfrac{1}{\gamma_p}\,{}_k\!\left(\dfrac{\partial p}{\partial x}\right)_i^{(j)} - {}_kJ}{\dfrac{{}_kn_i^{(j)}}{\gamma_n} + \dfrac{{}_kp_i^{(j)}}{\gamma_p} + \dfrac{1}{{}_k\Delta t}} \triangleq {}_k(F_E)_i^{(j)} \tag{8.15} $$

where F_E is defined as the right side of Eq.(8.15). If the second-order terms $(\Delta n)^2$, $(\Delta p)^2$ are neglected, and the three-point formulae B-11 and B-12 (of Appendix B) are used for the numerical computation of the first and second derivatives of Δn and Δp in Eqs.(8.13) and (8.14), these assume the final form:

$$ {}_k(A_n)_i^{(j)}\;{}_k\Delta n_{i-1}^{(j+1)} + {}_k(B_n)_i^{(j)}\;{}_k\Delta n_i^{(j+1)} + {}_k(C_n)_i^{(j)}\;{}_k\Delta n_{i+1}^{(j+1)} = {}_k(F_n)_i^{(j)} \tag{8.16} $$

$$ {}_k(A_p)_i^{(j)}\;{}_k\Delta p_{i-1}^{(j+1)} + {}_k(B_p)_i^{(j)}\;{}_k\Delta p_i^{(j+1)} + {}_k(C_p)_i^{(j)}\;{}_k\Delta p_{i+1}^{(j+1)} = {}_k(F_p)_i^{(j)} \tag{8.17} $$

where

$$ \begin{cases} {}_k(C_n)_i^{j} \triangleq \dfrac{2}{S_i} + \dfrac{{}_kE_i^{(j+1)}}{\alpha_i} \\[2ex] {}_k(B_n)_i^{(j)} \triangleq \left[\left({}_kp_i^{(j)} - 2\,{}_kn_i^{(j)} + N_i - \dfrac{\gamma_n}{{}_k\Delta t}\right) S_{i-1} + {}_kE_i^{(j+1)} - {}_k(C_n)_i^{(j)}\right](\alpha_i+1) \\[2ex] {}_k(A_n)_i^{(j)} \triangleq \left(\dfrac{2}{S_i} - {}_kE_i^{(j+1)}\right)\alpha_i \end{cases} \tag{8.18} $$

$$\begin{cases} {}_k(C_p)_i^{(j)} \triangleq \dfrac{2}{S_i} - \dfrac{{}_kE_i^{(j+1)}}{\alpha_i} \\ {}_k(B_p)_i^{(j)} \triangleq -\left[\left(2\ {}_kp_i^{(j)} - {}_kn_i^{(j+1)} + N_i + \dfrac{\gamma_p}{{}_k\Delta t}\right)S_{i-1} + {}_kE_i^{(j+1)} + {}_k(C_p)_i^{(j)}\right]\cdot \\ \qquad\qquad \cdot(\alpha_i + 1) \\ {}_k(A_p)_i^{(j)} \triangleq \left(\dfrac{2}{S_i} + {}_kE_i^{(j+1)}\right)\alpha_i \end{cases} \tag{8.19}$$

$$S_i \triangleq x_{i+1} - x_i \quad , \quad \alpha_i \triangleq S_i/S_{i-1}$$

$$(i = 2, 3, 4, \cdots \ell-1 \ , \ k = 1, 2, 3, \cdots f \ , \ j = 0, 1, 2, \cdots)$$

The numerical spatial derivatives of the electron and hole densities of the expressions F_n and F_p may be computed with the aid of the formulation of Appendix B.

Equations (8.16) and (8.17), with the use of the boundary conditions (8.10), may also be rewritten in vector notations as:

$${}_k(T_n)^{(j)}\ {}_k\Delta n^{(j)} = {}_k(F_n)^{(j)} \tag{8.20}$$

$${}_k(T_p)^{(j)}\ {}_k\Delta p^{(j)} = {}_k(F_p)^{(j)} \tag{8.21}$$

where T_n and T_p are the tridiagonal matrices:

$$T_n \triangleq \begin{bmatrix} (B_n)_2 & (C_n)_2 & & & & & \\ (A_n)_3 & (B_n)_3 & (C_n)_3 & & & & \\ & \cdots & & & & & \\ & & (A_n)_i & (B_n)_i & (C_n)_i & & \\ & & & \cdots & & & \\ & & & & (A_n)_{\ell-2} & (B_n)_{\ell-2} & (C_n)_{\ell-2} \\ & & & & & (A_n)_{\ell-1} & (B_n)_{\ell-1} \end{bmatrix} \tag{8.22}$$

$$T_p \triangleq \begin{bmatrix} (B_p)_2 & (C_p)_2 & & & & & \\ (A_p)_3 & (B_p)_3 & (C_p)_3 & & & & \\ & \cdots & & & & & \\ & & (A_p)_i & (B_p)_i & (C_p)_i & & \\ & & & \cdots & & & \\ & & & & (A_p)_{\ell-2} & (B_p)_{\ell-2} & (C_p)_{\ell-2} \\ & & & & & (A_p)_{\ell-1} & (B_p)_{\ell-1} \end{bmatrix} \tag{8.23}$$

and Δn, Δp and F_n, F_p are the vectors:

$$\Delta n \triangleq \begin{bmatrix} \Delta n_2 \\ \Delta n_3 \\ \cdots \\ \Delta n_i \\ \cdots \\ \Delta n_{\ell-2} \\ \Delta n_{\ell-1} \end{bmatrix} , \quad \Delta p \triangleq \begin{bmatrix} \Delta p_2 \\ \Delta p_3 \\ \cdots \\ \Delta p_i \\ \cdots \\ \Delta p_{\ell-2} \\ \Delta p_{\ell-1} \end{bmatrix} \qquad (8.24)$$

$$F_n \triangleq \begin{bmatrix} (F_n)_2 \\ (F_n)_3 \\ \cdots \\ (F_n)_i \\ \cdots \\ (F_n)_{\ell-2} \\ (F_n)_{\ell-1} \end{bmatrix} , \quad F_p \triangleq \begin{bmatrix} (F_p)_2 \\ (F_p)_3 \\ \cdots \\ (F_p)_i \\ \cdots \\ (F_p)_{\ell-2} \\ (F_p)_{\ell-1} \end{bmatrix} \qquad (8.25)$$

The interpretation of the above formulation and the detailed iterative procedure is illustrated in Section 8.3.

8.2.2. Generalized Crank-Nicholson discretization scheme.

The discretization scheme of the generalized Crank-Nicholson type, defined by Eq.(8.4) with $\theta = 1/2$, is schematically illustrated in Fig. 8.2. The same boundary and initial conditions (8.10) and (7.10) of the open type again specify the quantities at the boundaries $i = 1$, $i = \ell$ and at the initial state $k = 0$. The finite difference equation

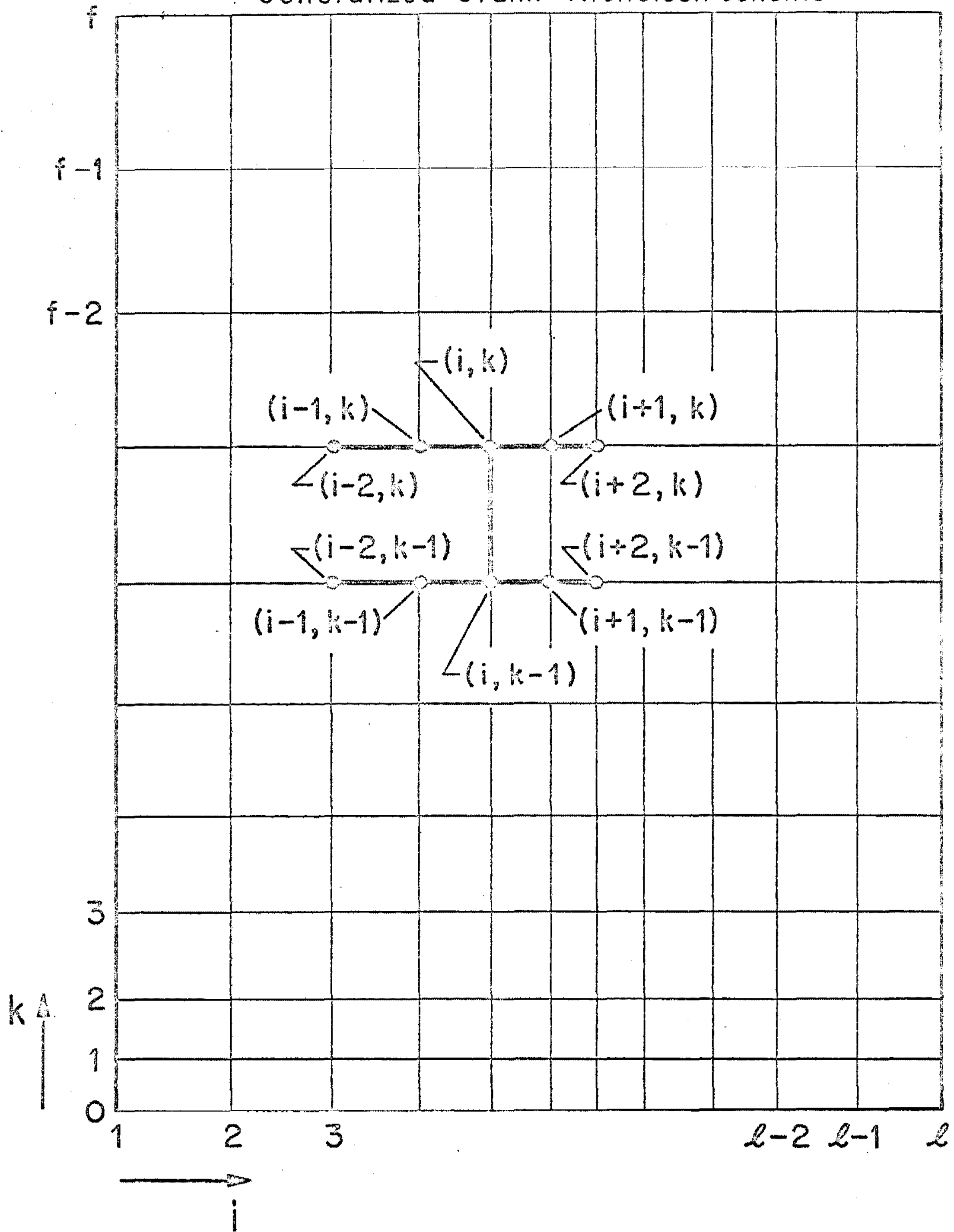

Fig. 8.2. Generalized Crank-Nicholson discretization scheme with a five-point formula for the numerical spatial differentiation (schematic).

(8.4) $(\theta = \frac{1}{2})$ represents a relationship between the quantities at a minimum of three adjacent points* $i - 1$, i, $i + 1$ on the line $k - 1$ and the quantities at the same number of adjacent points $i - 1$, i, $i + 1$ on the line k, the next instant of time. From the initial conditions at $k = 0$, the solution proceeds toward increasing k and determines the quantities on each k-line for $1 \le i \le \ell$.

Equations (7.19) to (7.21), discretized on the basis of Eq.(8.4) with $\theta = \frac{1}{2}$, generate a system of difference equations of the type of Eqs.(8.5) to (8.7); the right side of these equations assumes a more complex form since it averages the relevant expressions between the instant $k - 1$ and k. The same iterative procedure outlined in Section 7.4 is introduced, and the finite difference equations are expressed in terms of the corrections (8.8) to obtain, on the same path followed for the generalized pure inplicit scheme, the final discretized formulation described below.

If the following quantities are defined as

$$ {}_k(F_E')_i^{(j)} \triangleq \frac{\frac{1}{\gamma_n}\,{}_k\!\left(\frac{\partial n}{\partial x}\right)_i^{(j)} - \frac{1}{\gamma_p}\,{}_k\!\left(\frac{\partial p}{\partial x}\right)_i^{(j)} + \left(\frac{2}{{}_k\Delta t} + \frac{{}_{k-1}n_i}{\gamma_n} - \frac{{}_{k-1}p_i}{\gamma_p}\right){}_{k-1}E_i - \frac{1}{\gamma_n}\,{}_{k-1}\!\left(\frac{\partial n}{\partial x}\right)_i + \frac{1}{\gamma_p}\,{}_{k-1}\!\left(\frac{\partial p}{\partial x}\right)_i - {}_{k-1}J - {}_kJ}{\frac{2}{{}_k\Delta t} + \frac{{}_kn_i^{(j)}}{\gamma_n} + \frac{{}_kp_i^{(j)}}{\gamma_p}} \qquad (8.26) $$

---

* The footnote of the previous Subsection applies here to both k-l and k-lines.

$$
{}_k(F'_n)_i^{(j)} \triangleq -(S_i+S_{i-1})\left[{}_k\left(\frac{\partial^2 n}{\partial x^2}\right)_i^{(j)} + {}_kE_i^{(j+1)}\ {}_k\left(\frac{\partial n}{\partial x}\right)_i^{(j)} + {}_kn_i^{(j)}\ {}_k\rho_i^{(j)} - \right.
$$

$$
\left. - 2\frac{\gamma_n}{{}_k\Delta t}\ {}_k^D n_i^{(j)} + {}_{k-1}\left(\frac{\partial^2 n}{\partial x^2}\right)_i + {}_{k-1}E_i\ {}_{k-1}\left(\frac{\partial n}{\partial x}\right)_i + {}_{k-1}n_i\ {}_{k-1}\rho_i\right] \qquad (8.27)
$$

$$
{}_k(F'_p)_i^{(j)} \triangleq -(S_i+S_{i-1})\left[{}_k\left(\frac{\partial^2 p}{\partial x^2}\right)_i^{(j)} - {}_kE_i^{(j+1)}\ {}_k\left(\frac{\partial p}{\partial x}\right)_i^{(j)} - {}_kp_i^{(j)}\ {}_k\rho_i^{(j+\frac{1}{2})} - \right.
$$

$$
\left. - 2\frac{\gamma_p}{{}_k\Delta t}\ {}_k^D p_i^{(j)} + {}_{k-1}\left(\frac{\partial^2 p}{\partial x^2}\right)_i - {}_{k-1}E\ {}_{k-1}\left(\frac{\partial p}{\partial x}\right)_i + {}_{k-1}p_i\ {}_{k-1}\rho_i\right] \qquad (8.28)
$$

with

$$
\left.
\begin{aligned}
{}_k^D n_i^{(j)} &\triangleq {}_kn_i^{(j)} - {}_{k-1}n_i \\
{}_k^D p_i^{(j)} &\triangleq {}_kp_i^{(j)} - {}_{k-1}p_i
\end{aligned}
\right\} \qquad (8.29)
$$

$$
\left.
\begin{aligned}
{}_k\rho_i^{(j)} &\triangleq {}_kp_i^{(j)} - {}_kn_i^{(j)} + N_i \\
{}_k\rho_i^{(j+\frac{1}{2})} &\triangleq {}_kp_i^{(j)} - {}_kn_i^{(j+1)} + N_i
\end{aligned}
\right\} \qquad (8.30)
$$

and

$$
{}_k(B'_n)_i^{(j)} \triangleq \left[\left({}_k\rho_i^{(j)} - {}_kn_i^{(j)} - \frac{2\gamma_n}{{}_k\Delta t}\right) S_{i-1} + {}_kE_i^{(j)} - {}_k(C_n)_i^{(j)}\right](\alpha_i+1) \quad (8.31)
$$

$$ {}_k(B'_p)_i^{(j)} \triangleq -\left[\left({}_k\rho_i^{(j+\frac{1}{2})} + {}_kp_i^{(j)} + \frac{2\gamma_p}{{}_k\Delta t}\right)S_{i-1} + {}_kE_i^{(j)} + {}_k(C_p)_i^{(j)}\right](\alpha_i+1) \tag{8.32} $$

the system of finite difference equations may be written as:

$$ {}_kE_i^{(j+1)} = {}_k(F'_E)_i^{(j)} \tag{8.33} $$

$$ {}_k(A_n)_i^{(j)}\ {}_k\Delta n_{i-1}^{(j+1)} + {}_k(B'_n)_i^{(j)}\ {}_k\Delta n_i^{(j+1)} + {}_k(C_n)_i^{(j)}\ {}_k\Delta n_{i+1}^{(j+1)} = {}_k(F'_n)_i^{(j)} \tag{8.34} $$

$$ {}_k(A_p)_i^{(j)}\ {}_k\Delta p_{i-1}^{(j+1)} + {}_k(B'_p)_i^{(j)}\ {}_k\Delta p_i^{(j+1)} + {}_k(C_n)_i^{(j)}\ {}_k\Delta p_{i+1}^{(j+1)} = {}_k(F'_p)_i^{(j)} \tag{8.35} $$

where A_n, C_n, A_p and C_p are defined by relations (8.18), (8.19).

Equations (8.33) to (8.35), with the boundary and initial conditions (8.10) and (7.10), may of course be written in the matrix notation corresponding to Eqs.(8.20) to (8.25).

8.3. Detailed iterative procedure of solution.

The formulation generated by two discretization schemes of the implicit type has been presented in the previous Section for a special case characterized by absence of generation-recombination in the interior of the device, external contacts of the ohmic type, and constant mobilities. For such a simplified case the iterative procedure of solution, briefly outlined in Section 7.4, is here discussed in detail.

The generalized pure implicit discretization scheme is considered first. Reference is made to Fig. 8.3. The structural parameters, including the carrier mobilities, doping profile and boundary conditions, are specified. The initial spatial distributions of the electric field and of the mobile carrier densities at the instant $k = 0$ are assigned, for example as steady-state distributions obtained with the method described in Part I. An external excitation of total current as a function of time is specified, to drive the evolution of the transient. The spatial distributions of E, n, and p, the unknowns of the problem, are sought at the first instant of time $k = 1$, and will be obtained with the use of an iterative successive approximation scheme. The iteration index j is set to zero and the spatial distributions of the mobile carrier densities available at the previous instant $(k=0)$ are taken as trial functions to start the iterations at the instant $k = 1$. Equations (8.15) yield then explicitly a spatial distribution for the electric field, which may be inserted in the implicit system of Eqs.(8.16) to solve for the corrections ${}_k\Delta n_i^{(j+1)}$ $(i = 2, 3, 4, \cdots \ell-1)$ for the electron density. Equations (8.11) yield then an improved electron density distribution, which, together with the electric field distribution last obtained from Eqs.(8.15), is inserted in the implicit system of Eqs.(8.17) to solve for the corrections ${}_k\Delta p_i^{(j+1)}$, so that Eqs.(8.12) yield an improved hole distribution. As an aside, the terminal voltage may be obtained by integration of the electric field. A negative outcome of the test on the overall consistency at the considered instant of time $(k=1)$ increases the iteration index by unity and restarts the cycle with the insertion of the improved mobile carrier

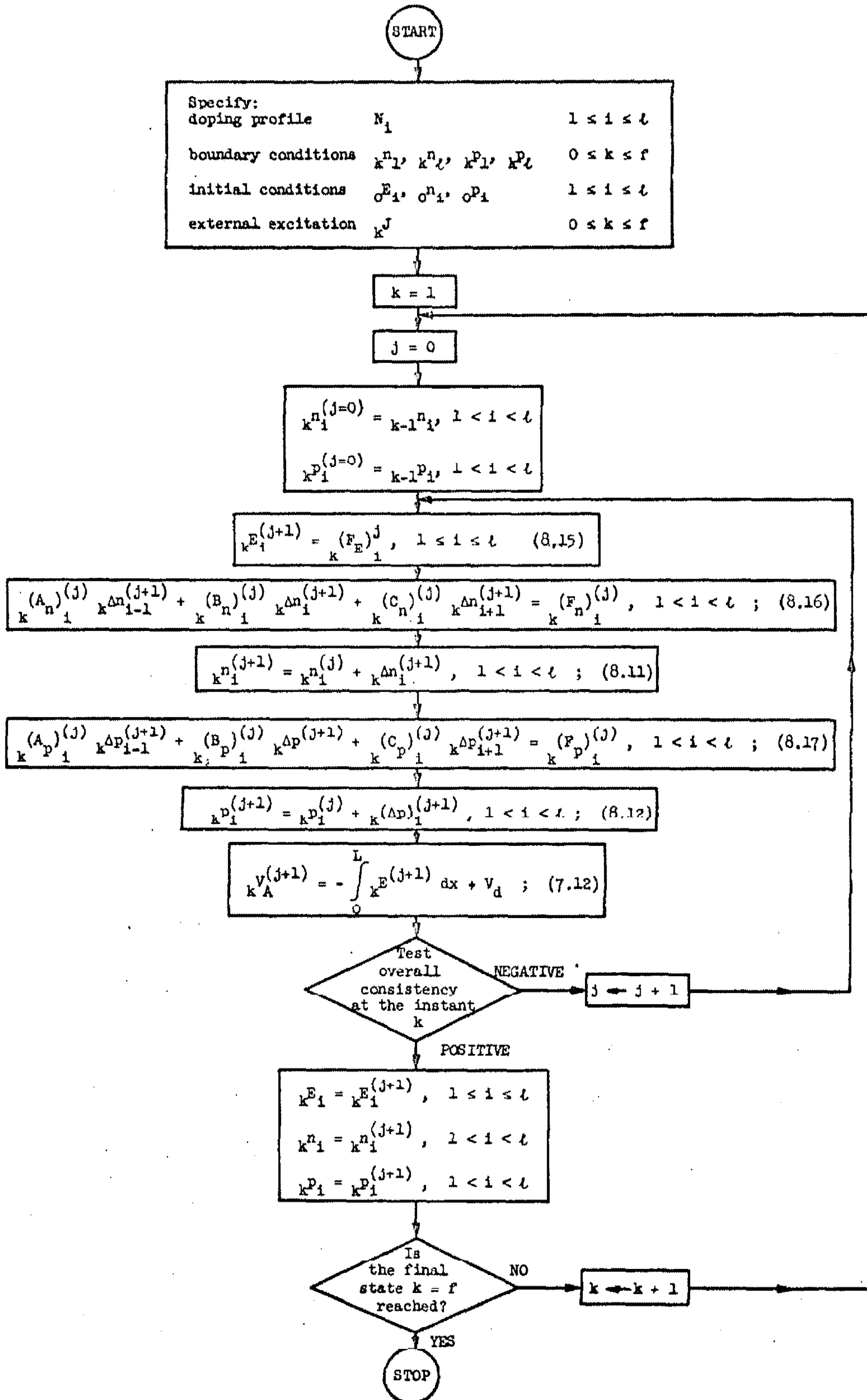

Fig. 8.3. Detailed iterative procedure for the generalized pure implicit scheme, for the current-driven transient case.

distributions in Eqs.(8.15), solved for an improved electric field distribution at the same instant of time (k=1). A positive outcome of the consistency test accepts the quantities obtained by the last iteration as the "exact" solutions at the instant of time considered (k=1). Unless the final state (k=f) is reached, the time index is increased by unity, the iteration index j is set to zero and solutions at the next instant of time (k=2) are sought. The iteration is restarted by taking as trial functions the mobile carrier distributions available from the previous instant (k=1), and inserted in Eqs.(8.15). The same iterative procedure is repeated to achieve "exact" solutions at the instant k = 2 and at the subsequent instants of time until the final state k = f is reached.

The spatial differentiations present in the right side of Eqs. (8.15) and Eqs.(8.16), (8.17) (explicitly shown in the right side of Eqs.(8.13), (8.14)), and the integration of Eq.(7.12) may be conveniently computed with the formulation of Appendix B, suitable for a non-uniform spatial step distribution. The numerical solutions of the tridiagonal systems of Eqs.(8.16) and of Eqs.(8.17) may be obtained with the same techniques successfully employed in Subsection 2.3.3 for the solution of the tridiagonal system (Eq.(2.38)) generated by the discretization of Poisson's equation in the steady-state analysis described in Part I. Identical considerations of Subsection 2.3.3 on the conservation of the same tridiagonal matrices (8.22) and (8.23) are here applicable if higher order interpolating schemes are employed for the numerical computation of the spatial derivatives in the right side of Eqs.(8.16) and (8.17). This property is a direct consequence of the

assumed convergence of the iterative procedure (relations (8.9)), and, in consideration of the large number of repetitive solutions of Eqs. (8.16) and (8.17) required during an entire evolution of a transient, it represents a decisive feature for the success of the method.

The overall consistency, between the unknowns E, n, p and the system of equations determining them, may be tested at any iteration cycle for each instant of time by considering the magnitude of the corrections Δn, Δp and of the difference of electric field distributions obtained by two successive iterations. If the magnitudes of these quantities are smaller than a specified value (the iteration error at each instant of time), achievement of overall consistency at that instant is assumed. The final state $k = f$ is reached when the external excitation has reached the final state $J = {}_fJ$ and the unknowns E, n, p are unchanged for an increase of time.

If the generalized Crank-Nicholson discretization scheme is used, Eqs.(8.34) and (8.35) substitute for Eqs.(8.16) and (8.17) respectively. Equations (8.33) may be used in place of Eqs.(8.15) only for cases in which the second time derivative of the specified total current within a time step (extremes included) is continuous and sufficiently small. This limitation arises from the presence in the expressions (8.26) of the average of total current values taken at consecutive instants of time. This average "effective" current as a function of time may become considerably different from the actual specified external excitation and thus generate highly inaccurate results, if the above restriction is not introduced. The same procedure described for the generalized pure implicit scheme and illustrated in Fig. 8.3 may be used for the

generalized Crank-Nicholson scheme, and applied to Eqs.(8.15) (or to Eqs.(8.33) with the above restriction) and to Eqs.(8.34), (8.35).

Although the computation load required by the formulation generated by the Crank-Nicholson scheme, as opposed to the pure implicit scheme, is slightly heavier, a considerably smaller truncation error in the time domain (approximately one order of magnitude; see Appendix F) may be achieved. On the other hand it may be expected, as an extrapolation of the simpler linear cases, that the generalized Crank-Nicholson scheme is more likely to become numerically unstable under conditions in which the generalized pure implicit scheme features numerical stability. This was indeed verified experimentally: for all the cases tested on the computer the latter discretization scheme consistently generated stable solutions, whereas numerical instability was observed in some instances if the former discretization scheme was employed. It may be concluded that, if more accurate solutions are sought with use of the Crank-Nicholson discretization scheme, particular care must be exerted in testing numerical stability during the evolution of a transient, and it should not cause surprise if in some cases the scheme fails.

A prime requirement for the success of the described method is the convergence of the iterative procedure to reach at each instant of time overall consistent solutions from a set of approximate trial distributions. In all the cases tested on the computer, for various structures and external excitations, convergence was always observed. In addition an excellent rate of convergence was experienced in situations in which significant variations (in time) of the total current occur, so that

the electric field (given by Eqs.(8.15)) becomes the quantity "driving" the variations of the mobile carrier distributions (Eqs.(8.16), (8.17) or (8.34), (8.35)) and is essentially responsible for the evolution of the transient. A slower convergence rate* was observed under conditions, opposite to those just described, in which the total current is maintained constant over a significant length of time and variations of mobile carrier densities (mostly diffusion processes) become the principal effect, now driving the variations of the electric field. The rate of convergence for such cases was found well within practical limitations, with the exception of conditions arising toward the termination of a transient solution, when the quantities approach the final steady-state distributions (usually within a few per cent of the overall excursion of the total current). Several artifices have been attempted, without success, to improve the convergence rate. Although this inadequacy of the iterative scheme may be considered unimportant for the sole purpose of achieving time-dependent solutions,** the method described for the current-driven transient may not be used for achieving "exact" steady-state solutions of sufficient accuracy from an initial guess of approximate trial distributions. The importance of starting a time-dependent solution with "exact" initial distributions obtained with the same formulation subsequently used for the transient solution will

---

* The convergence rate is also dependent upon the size of the discretization mesh, particularly upon the size of the time step. A reasonable number of points on the time coordinate (e.g. 100 - 200) is assumed.

** The spatial distributions for the final state may be determined easily by a steady-state solution, for instance of the type described in Part I.

be discussed in Chapter IX, and an efficient numerical procedure for achieving this will be presented.

The extension of the described iterative procedure to the more general case, characterized by arbitrary generation-recombination term U(x) and mobility dependencies, is straightforward. Equations (7.16), (7.17), and (7.18) apply in this case and may be discretized with the same schemes used in Section 8.2 for the simpler case. If generalized boundary conditions of the type of Eqs.(7.7) are also specified, a secondary iteration loop may be required to resolve additional non-linearities introduced in the relationships between the particle currents and the mobile carrier densities at the boundaries. In addition, at each cycle of the iterative procedure at each instant of time, the mobile carrier distributions must be modified to incorporate the time-dependent boundary conditions.

It is apparent from the method and the formulations described that complete freedom is available in the selection of both spatial and time step distributions, which may be conveniently chosen, and automatically adjusted by the computer during the entire evolution of the transient according to specified criteria. These are discussed in the following Section.

8.4. Automatically adjustable non-uniform discretization mesh.

It is desired to achieve an automatic adjustment of both spatial and time step sizes subject to the requirement of maintaining constant errors, throughout the space and time domains, of certain numerical operations. Apart from the integrations of Eq.(7.12), not an essential operation of the procedure, only numerical differentiations are present

in the described formulation. The total error introduced by such operations may be regarded as a sum of truncation and round-off errors. For a decrease in step size and an increase in the order of the interpolating scheme used, the former type of error decreases whereas the latter increases. In addition round-off errors increase with the order of the derivative desired. For the case under consideration, round-off errors may be usually considered negligible if double precision arithmetic (16 significant digits) is employed. This is a consequence of practical restrictions on both the order of the numerical scheme and the minimum step size that may be used (related to the maximum number of points, limited by both memory size and computation time) together with the considerable magnitude of truncation errors in the position domain in certain regions of the device (mostly transition regions). The efforts will be then toward achieving uniform distributions of the truncation errors in both domains.

The search for the "optimum" non-uniform spatial step distributions may be conducted with the same procedure used in Subsection 2.3.1 for the steady-state solution. The numerical schemes employed for the differentiations of the mobile carrier densities present in the expressions (8.13) and (8.14) are now considered, in place of relations (2.21), (2.22), and the corresponding stages of approximation, described in Subsection 2.3.1, may be used. The spatial step selection may be performed only once to satisfy the requirements of the initial distributions and then considered satisfactory for the entire evolution of the transient, or it may be repeated once at each instant of time or at each cycle of the iterative procedure at each instant of time. The

decision, usually not critical, is in general the result of a compromise between the accuracy desired and the computation time allowed.

On the other hand, the computation load of a search for the optimum step size in the time domain, based upon a trial-and-error procedure requiring successive "exact" solutions at each instant of time for various time step sizes,* well exceeds any practical limit. As a substitute, the following simple scheme, based on the extrapolation of the information available at one instant of time, may be used to adjust the size of the time step for the subsequent instant.

The Taylor expansion about a point $t = {}_k t$ of a continuous function $f(t)$ with continuous derivatives is considered:

$$f(t) = f({}_k t) + (t - {}_k t) \left.\frac{df}{dt}\right|_{t={}_k t} + \frac{1}{2!} (t - {}_k t)^2 \left.\frac{d^2 f}{dt^2}\right|_{t={}_k t} + \cdots \tag{8.36}$$

If a two-point formula is used to approximate the first derivative at the point $t = {}_k t$, such as

$$\left.\frac{df}{dt}\right|_{t={}_k t} \simeq \frac{{}_{k+1}\Delta f}{{}_{k+1}\Delta t} \tag{8.37}$$

where

$${}_{k+1}\Delta f \triangleq f({}_{k+1} t) - f({}_k t)$$

$${}_{k+1}\Delta t \triangleq {}_{k+1} t - {}_k t$$

---

* Such as a predictor-corrector method conventionally adopted for the numerical solution of ordinary differential equations.

and is inserted in the expansion (8.36) evaluated at the point $t = {}_{k+1}t$, one obtains:

$$f({}_{k+1}t) \cong f({}_{k}t) + {}_{k+1}\Delta f + \frac{1}{2}\,({}_{k+1}\Delta t)^2 \left.\frac{d^2 f}{dt^2}\right|_{t={}_k t} + \cdots \tag{8.38}$$

If higher order contributions of Eq.(8.38) are neglected, the term

$${}_{k}\epsilon = \frac{1}{2}\,{}_{k+1}\Delta t\;{}_{k}f''$$

where

$${}_{k}f'' \triangleq \left.\frac{d^2 f}{dt^2}\right|_{t={}_k t}$$

represents the error introduced in the approximation (8.37). The relative error is then defined as the ratio ${}_{k}\epsilon / \frac{{}_{k+1}\Delta f}{{}_{k+1}\Delta t}$. The above may be repeated for a sequence of adjacent points ${}_{k}t$ $(k = 1, 2, 3 \cdots)$, and the requirement of maintaining a constant magnitude of the relative error at each point may be specified. In this case the following relation must hold:

$$\left|\frac{({}_{k}\Delta t)^2\;{}_{k-1}f''}{{}_{k}\Delta f}\right| = \left|\frac{({}_{k+1}\Delta t)^2\;{}_{k}f''}{{}_{k+1}\Delta f}\right|$$

or

$${}_{k+1}\Delta t = \sqrt{\frac{{}_{k-1}f''\;{}_{k+1}\Delta f}{{}_{k}f''\;{}_{k}\Delta f}}\;{}_{k}\Delta t, \quad k = 1, 2, 3 \cdots \tag{8.39}$$

which represents a relationship between consecutive steps in terms of local increments and curvatures of the function $f(t)$.

In the case of interest, the magnitude of the time step ${}_{k+1}\Delta t$ at the next instant of time may be approximately predicted with the knowledge of quantities only available for times $t \le {}_k t$ if the expression (8.39) is modified to the following form

$$ {}_{k+1}\Delta t = \sqrt{\frac{{}_{k-2}f'' \; {}_k\Delta f}{{}_{k-1}f'' \; {}_{k-1}\Delta f}} \; {}_k\Delta t \quad , \quad k = 3,\ 4,\ 5 \cdots \qquad (8.40) $$

which merely adopts as the ratio between consecutive steps, at one instant of time, that corresponding to the previous instant. For the present purposes the terminal voltage $V_A(t)$, available at each instant of time from Eq.(7.12), may be conveniently chosen as the function $f(t)$ in relation (8.40), since it reflects the overall behavior of the device under the specified excitation. The second time derivatives required by the expression (8.40) may be computed with a three point formula (e.g. B-12 of Appendix B) suitable for unevenly spaced points. It is then apparent that the sizes of the initial three time steps $({}_k\Delta t,\ \ k = 1,\ 2,\ 3)$ must be independently specified, and that the size of the fourth (and following ones) may be predicted by relation (8.40). Instants of time for which the argument of the square root of Eq.(8.40) exceeds in magnitude the permissible range become singular points. These are likely to occur during the evolution of a transient solution and are easily taken care of by specifying upper and lower bounds for the ratio of consecutive steps and for the magnitude of the step size. These, as well as the initial steps, must be chosen with regard to the total number of instants of times that may be allowed and to the rate of convergence of the iterative procedure, very much

dependent upon the step size. In addition, at any instant of time, the prediction process may be discontinued, and an arbitrary magnitude of time step may be specified, until the process is reenforced.

Although a time step adjustment of the described type is not very accurate, it appears satisfactory from any practical point of view, also in consideration of the insignificant computation load required and by the observation that the selection of the time step is by no means critical.

8.5. Conclusion.

The discretization problem of the current-driven transient algorithm has been analyzed. Extrapolation from the simpler cases, treated by the theory of numerical analysis, leads to the choice of a discretization scheme of the implicit type, if restrictions on the discretization mesh are not desired. The discretized formulation for two implicit schemes, the generalized pure implicit and the generalized Crank-Nicholson schemes, have been presented for a special case and the details of the iterative procedure of solution have been outlined. Extension to the more general case has been shown to be straightforward. A brief discussion on the criteria responsible for the automatically adjustable step selection, in both space and time domains, has been given, together with a simple scheme for an approximate time step prediction, suitable for the problem under consideration. As a consequence of the worsening of the convergence rate of the iterative procedure at each instant of time for conditions approaching the final state during the evolution of a transient, accurate steady-state solutions may not be obtained, within practical limits of the currently

available machines, with the described formulation. Although this inadequacy may be considered unimportant for a transient solution, it is highly desirable to generate initial steady-state distributions with the same discretized formulation used for the achievement of time-dependent solutions. A successful approach to this problem is presented in the following Chapter, together with a method of solution of the voltage-driven transient.

CHAPTER IX

VOLTAGE-DRIVEN TRANSIENT

In this Chapter the time-dependent analysis of the bipolar semiconductor transport equations is completed with a solution for the voltage-driven transient problem and an alternative procedure suitable for steady-state calculations. A valuable feature of either method is the capability to generate solutions "compatible" with the formulation employed for the current-driven transient previously described. The iterative procedure adopted for the analysis of the response of the isolated semiconductor device, driven by an ideal time-dependent generator, is also extended to incorporate the interaction of the device with a general network of passive circuit elements and time-dependent current and voltage sources.

9.1. Generalities.

In the previous two Chapters, the analytical formulation, discretization schemes, and an iterative procedure of solution have been described for the current-driven transient for a two-contact device. The voltage-driven transient (the applied voltage as a function of time is specified as the external excitation and the total current is sought) may be considered equally important and of great interest, and is here considered to complete the general time-dependent analysis of the problem. Priority has been given initially to the former type of analysis, in view of the explicit appearance in one of the fundamental equations (Eq.(7.1)) of the total current, which may be easily incorporated in a reduced set of equations (Eqs.(7.16) to (7.18)) to drive at

each spatial point the internal distributions. A variation of the total current at one instant of time generates an immediate response of the driven quantities simultaneously throughout the entire length of the device, at each iterative cycle at that instant of time. This situation contributes to maintaining the rate of convergence of the iterative procedure at each instant of time within practical limits.

If the applied voltage as a function of time is to be incorporated instead, Eq.(7.16), expressing the time variation of the electric field in terms of the total current, must be substituted by Poisson's Eq.(7.4) written in terms of the electrostatic potential $\psi(x,t)$. The applied voltage appears then explicitly as a boundary condition for ψ in the solution of the second-order differential equation (7.4). The reduced set, equivalent to the fundamental set of Eqs.(7.1) to (7.6), includes now Eqs.(7.4), (7.17) and (7.18), written in terms of the new unknowns ψ, n and p. Equations (7.17) and (7.18) are still treated as described for the current-driven case, whereas the new equation of the set (Eq.(7.4)) may be discretized and solved with the same procedure adopted in Subsection 2.3.3, based on the solution of a tridiagonal matrix equation. An iterative procedure of the same type described in Section 8.3 may now be employed to reach the desired consistency between ψ, n, p and Eqs.(7.4), (7.17), (7.18) at each instant of time.

A considerably slower rate of convergence of the iterative procedure is to be expected in this case, since the error (arising from the variation of the boundary value on the electrostatic potential) is localized, at the beginning of the iterative scheme at each instant of time, near one external contact and must propagate throughout the whole

interior before the solution is allowed to proceed to the following instant of time. This may require a large number of iterative cycles for each time point. If compared to the current-driven transient case, the above formulation also requires a heavier computation load, which includes the additional solution of a triple-diagonal matrix and the computation of the first and second spatial derivatives of the electrostatic potential ψ. In addition, solutions generated by such an algorithm are not "compatible" with the formulation adopted for the current-driven transient, in the sense that the different discretization errors of the two formulations are responsible for slightly different steady-state solutions under otherwise identical conditions. This inconsistency may be responsible in some cases for undesirable effects (see Section 9.3).

Also in consideration of the above, an alternative method of solution for the voltage-driven transient is preferred. This is based on the combined use of the formulation adopted for the current-driven transient together with an interpolating scheme on the current-voltage characteristic at each instant of time. A similar concept was already used in Chapter III for the solution of the steady-state problem for a specified total current. The following Section illustrates the details of the method.

9.2. Voltage-driven transient: outline of the method.

The mathematical formulation of the problem is described by the fundamental set of Eqs.(7.1) to (7.6), with the boundary conditions (7.7) and initial conditions (7.10). The applied voltage $V_A(t)$ at the external contacts is specified as a function of time and the total

current $J(t)$ and the unknown distributions $E(x,t)$, $n(x,t)$ and $p(x,t)$ are sought. A method for the solution of the reverse problem of specifying the total current $J(t)$ and determining the terminal voltage V_A at each instant of time has been described in the previous Chapter and will be used as an integral part of the solution of voltage-driven transient described below.

"Exact" solutions for the total current and the internal distributions are supposed known for times $t \le {}_{k-1}t$, and quantities at the following instant of time ${}_k t$ are sought. If the total current ${}_k J$ were known, the iterative method described for the current-driven transient could be applied to obtain the unknown distributions at the instant k. The problem consists then in searching for the particular value of current ${}_k J$ that yields the specified terminal voltage ${}_k V_A$ at the instant k. This is achieved in two stages with the aid of the same algorithm employed for the current-driven transient at a specific instant of time. A "prediction" stage initially furnishes two estimates of the total current ${}_k^{(1)}J$ and ${}_k^{(2)}J$ close to the "exact" value ${}_k J$ which is to be determined. These estimates may be achieved easily with two different extrapolations from the quantities supposed available for times $t \le {}_{k-1}t$. A linear (two-point) and a parabolic (three-point) extrapolation on the current response as a function of time furnishes, in general, two different estimates* for the current ${}_k J$. Two independent applications of the current-driven transient algorithm yield for the

---

* The two values are coincident if the quantities ${}_{k-3}J$, ${}_{k-2}J$, ${}_{k-1}J$ lie on a straight line. In this situation a second estimate may be furnished by higher order extrapolation formulae or by an arbitrary value close to the first estimate. The nearness of such estimates to the "exact" value is by no means critical.

two currents ${}_k^{(1)}J$, ${}_k^{(2)}J$ the corresponding values of terminal voltages ${}_k^{(1)}V_A$, ${}_k^{(2)}V_A$, which, in general, differ from the specified terminal voltage ${}_kV_A$ (if this is not the case, solutions at the instant ${}_kt$ are found). A second stage, based on an interpolating procedure on the curve ${}_k^{(h)}J$ as a function of ${}_k^{(h)}V_A$ $(h = 1, 2, 3 \cdots)$ at the same instant of time k, may now be started to obtain an improved estimate of the total current that generates a terminal voltage within an assigned tolerance about the specified value. Two points, ${}_k^{(1)}J$, ${}_k^{(1)}V_A$ and ${}_k^{(2)}J$, ${}_k^{(2)}V_A$, are already available on the current-voltage graph "frozen" at the instant k, so that a linear interpolation yields a third estimate ${}_k^{(3)}J$ corresponding to the specified terminal voltage ${}_kV_A$. A third application of the current-driven transient algorithm at the instant k for the current ${}_k^{(3)}J$ furnishes a third point ${}_k^{(3)}J$, ${}_k^{(3)}V_A$ on the current-voltage graph, so that a parabolic interpolation may be used to further improve, if necessary, the estimate of the total current. The procedure continues with higher order interpolating schemes until the value ${}_k^{(h)}J$, that generates a terminal voltage ${}_k^{(h)}V_A$ sufficiently close to the specified ${}_kV_A$, is determined. Solutions at the instant of time k are then available and the overall procedure may be restarted at the following instant $k + 1$ with the prediction stage. Prediction stage, interpolation stage, and overall procedure at the instant k are schematically illustrated in Figs. 9.1, 9.2 and 9.3, respectively. For a few initial time points $(k = 1,2)$ the prediction stage may not be performed as described; an arbitrary estimation procedure may be employed equally well, if the time step is initially

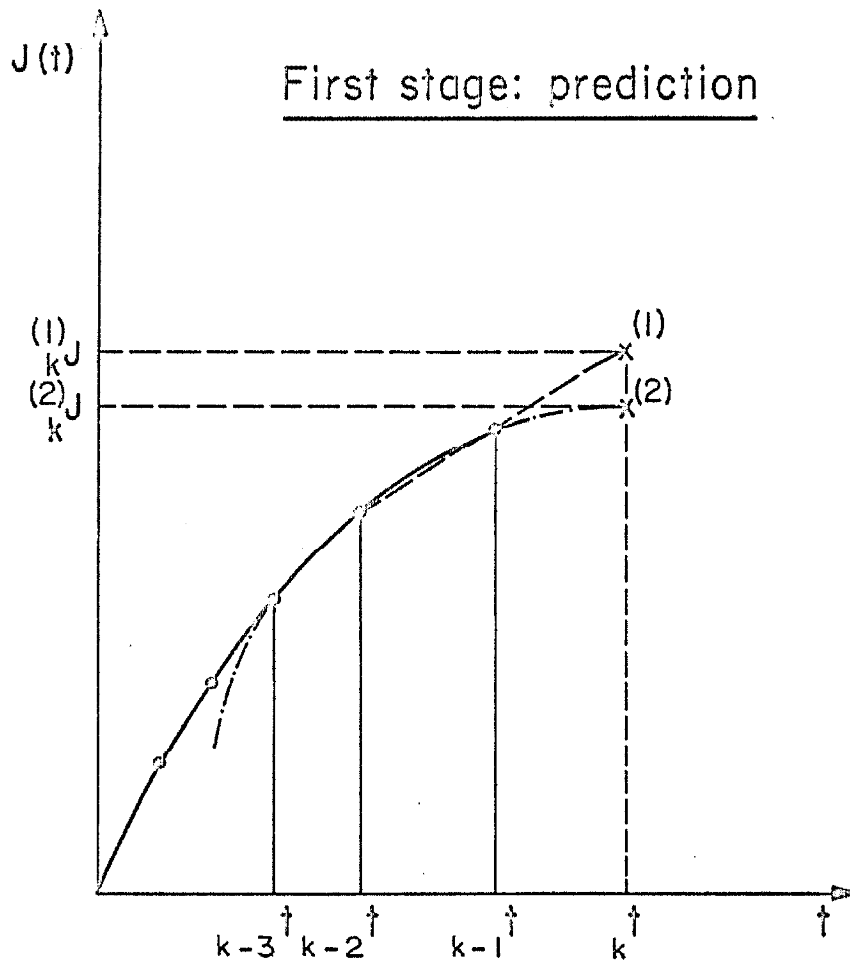

Fig. 9.1. Estimation of two values of current at the instant $_k t$ from the response known for $t \leqslant {}_{k-1}t$, during the prediction stage of the voltage-driven transient.

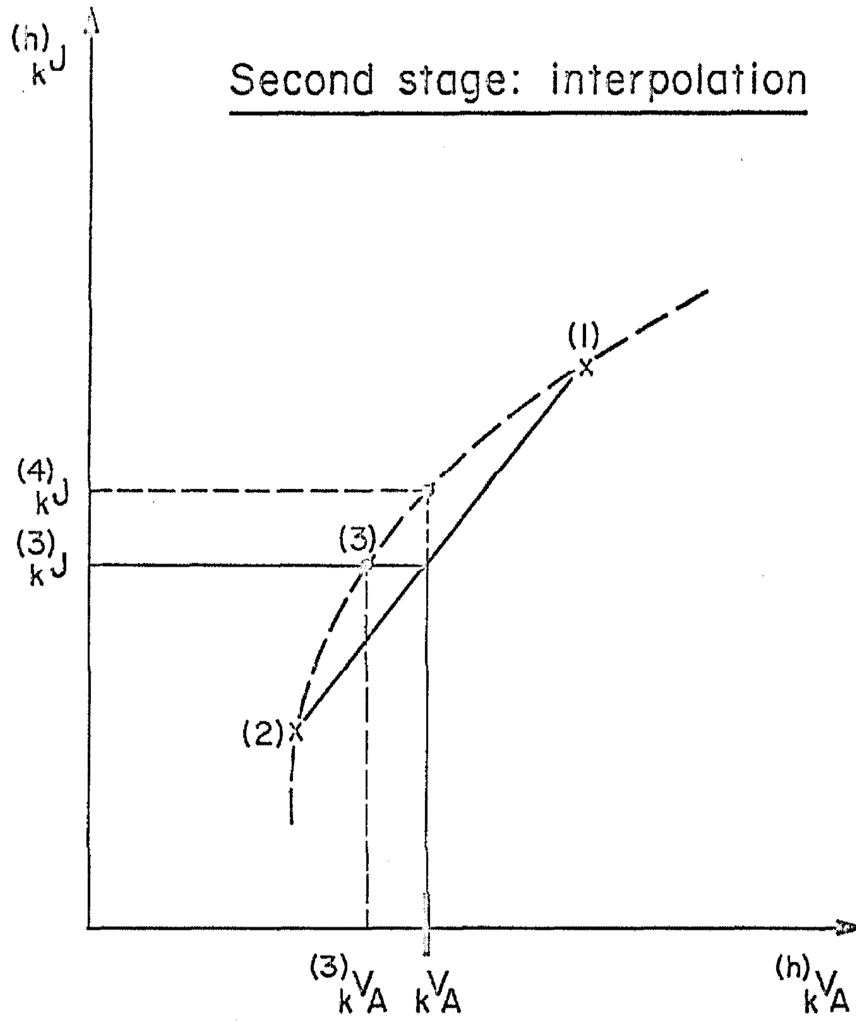

Fig. 9.2. Interpolation on the current-voltage characteristic at the instant $_kt$ to determine improved values for the total current during the second stage of the voltage-driven transient.

First phase: prediction on the $J = J(t)$ characteristic

${}_k^{(1)}J$

Current-driven transient

${}_k^{(1)}V_A$

${}_k^{(1)}V_A \simeq {}_kV_A$?

YES

Proceed to the next instant $k + 1$

${}_k^{(2)}J$

Current-driven transient

${}_k^{(2)}V_A$

${}_k^{(2)}V_A \simeq {}_kV_A$?

YES

Proceed to the next instant $k + 1$

Interpolation on the ${}_k^{(h)}J$, ${}_k^{(h)}V_A$ graph $(h = 1, 2)$

${}_k^{(3)}J$

Current-driven transient

${}_k^{(1)}V_A$

${}_k^{(3)}V_A$

${}_k^{(2)}V_A$

${}_k^{(3)}V_A \simeq {}_kV_A$?

YES

Proceed to the next instant $k + 1$

Interpolation on the ${}_k^{(h)}J$, ${}_k^{(h)}V_A$ graph $(h = 1, 2, 3)$

${}_k^{(4)}J$

Current-driven transient

${}_k^{(4)}V_A$

${}_k^{(4)}V_A \simeq {}_kV_A$?

YES

Proceed to the next instant $k + 1$

Fig. 9.3. Overall procedure for the voltage-driven transient at the instant of time k. (Schematic)

kept small enough in order to obtain a closely linear current-voltage characteristic in the interpolation stage.*

The efficiency of the method relies mainly on two features of the scheme. First, the prediction stage yields in general "good" estimates of the total current so that the current-voltage characteristic ${}_k^{(h)}J$, ${}_k^{(h)}V_A$ $(h = 1, 2, 3 \cdots)$ is closely linear and usually three applications of the current driven transient algorithm are sufficient at each instant of time to satisfy even a tight tolerance about the specified voltage ${}_kV_A$. In addition, an external voltage excitation of the general type generates a variable current as a function of time; this represents, as mentioned in Section 8.3, the condition in which the current driven transient algorithm features a fast rate of convergence. This characteristic is maintained, as expected and observed, throughout the entire evolution of the transient, so that the final steady-state distributions may be reached easily within practical computation times (a few minutes on the IBM 7094/7090 system), a feature unfortunately not occurring in the current-driven transient scheme described in the previous Chapter.

Results for a special structure under various external excitations of current and voltage have been obtained and will be illustrated in a later chapter. The corresponding computer program for both the current-driven and voltage-driven transient is reported in Appendix G.

---

* Such a linearity is a direct consequence of the relation between the total current and the electric field (Eq.(8.15) or (8.33)), essentially linear if the mobile carrier densities remain unchanged, which is indeed the case for small enough Δt and fast enough variation of the current. This is equivalent to considering the total current as essentially due the displacement current (Eq.(7.1)).

9.3. A "compatible" steady-state solution.

The set of initial distributions (7.7) for the unknowns of the problem is required to initiate a time-dependent solution. For the case in which the initial state is a steady-state one, the initial distributions were assumed available from the procedure illustrated in Part I. However, the analytical and discretized formulations there described are not "compatible" with the formulations adopted for the time-dependent solution, in the sense that the steady-state distributions feature truncation errors different from those introduced by the algorithm that generates transient solutions. Obviously, if a transient solution is initiated from a steady-state condition in absence of an external excitation, the internal distributions and the terminal properties should remain unchanged. Instead, as a consequence of the above incompatibility, a "drift" of the original steady-state distributions is observed throughout the execution of such a fictitious "transient" solution. This drift continues until compatibility between the spatial distributions and the new discretized formulation is achieved. Although the magnitude of the total shift of the quantities is relatively small (of the order of the truncation error), it may be significant for time-dependent solutions specifying small external excitations. Moreover, if a discretization scheme which may easily generate unstable solutions is used (such as the Crank-Nicholson scheme of Subsection 8.2.2), the initial incompatibility is often responsible for oscillations (the first symptom of an unstable solution) in the internal distributions and in the terminal response, such that the "exact" solution is completely obscured.

As a general rule, if solely initial conditions incompatible with the time-dependent formulation are available, a preliminary computation phase in absence of external excitations is required, before initiating the actual transient solution, to achieve overall compatibility. This preliminary phase of "adjustment" of the initial steady-state conditions is of course unnecessary if the same formulation is capable of generating both steady-state and transient solutions, therefore assuring full compatibility. This is a very desirable situation, also in consideration of the consequent conciseness and the simplicity of the overall algorithm.

It has been already mentioned in Section 8.3 that the current-driven transient scheme is unsuitable for generating steady-state solutions, whereas the procedure described in the previous Section for the voltage-driven transient is well capable of reaching the final steady-state of a time dependent solution within practical computation times. The same voltage-driven scheme may be used to generate steady-state solutions from a set of trial distributions for the unknowns. These distributions are treated as initial conditions of a fictitious "transient solution", in which the constant terminal voltage desired is specified as the external excitation and the time coordinate becomes a meaningless quantity. The time step, which appears in the discretized formulation, may be chosen large enough to cause a negligible contribution of the time-dependent terms, or may be usefully adjusted as a "convergence parameter" to shorten the convergence path toward the "exact" solution. In addition, the number of (j) iterations for each application of the current-driven transient algorithm (Fig. 9.3), the

tolerance about the specified terminal voltage ${}_kV_A = V_A$ (any k) at each instant of "time", and the number of "time" points, may be also all adjusted properly and treated as convergence parameters. The choice of the trial distributions $E(x)$, $n(x)$, and $p(x)$ is slightly critical, in the sense that if the inconsistency between the trial functions and any "exact" solution of the equations (for any terminal voltage) is too large, the iterative scheme may not be capable of resolving such discrepancies. Trial distributions available from the first-order theory, although considerably inaccurate (Section 6.2), usually generate satisfactory convergence patterns if an appropriate selection of the convergence parameters is made. Although the rate of convergence becomes considerably slower as the injection level increases, just as observed for the steady-state method of Part I, solutions may be still achieved within practical limits at high injection levels.

As an alternative, the fictitious "transient" solution generating compatible steady-state solutions may be started from "exact" steady-state distributions available for a terminal voltage (for instance for the thermal equilibrium case) different from the one desired. Rather than following the natural transient evolution toward the final state, an artificial convergence path may again be followed by a proper selection of the time step size, the number of (j) iterations, the tolerance about ${}_kV_A$ and the number of time points. The overall number of operations to reach the desired steady-state distributions may be then considerably reduced.

Although the method described in Part I is capable of generating

steady-state solutions in a shorter computation time* if compared to either of the above procedures, these feature the same formulation employed for the time-dependent algorithm and therefore generate compatible steady-state distributions that may be directly used as initial conditions for a transient analysis. Preference may then be given to the former method if solely steady-state solutions are desired, and to the latter if such distributions must serve as initial conditions for a time-dependent solution as well.

9.4. Time-dependent solutions for the combination of an active device with a network of passive circuit elements.

In this and the previous chapters, methods of solution of the fundamental equations describing the behavior of a two-contact semiconductor device under both steady-state and transient conditions have been described. The transient response of the device was supposed driven by an ideal time-dependent source of either voltage or current. A more realistic condition requires the incorporation in the external circuit of one or more passive circuit elements to represent circuital parasitic effects or actual passive components inserted in the circuit. More generally, the interaction of a semiconductor device with a network of ideal time-dependent current or voltage sources and passive elements is of great interest. This problem may be easily solved with a slight extension of the methods described for the transient analysis of the isolated semiconductor device.

---

* Usually from two to five times shorter, under similar conditions.

A general two-port network, composed of ideal current and/or voltage sources and passive circuit elements, is connected to the terminals of a two-contact semiconductor device, as shown in Fig. 9.4. Both the normalized total current density $J(t)$ of the device and the normalized terminal voltage $V_A(t)$ are quantities dependent upon the properties of both the semiconductor device and the network. At a particular instant of time k, the two unknowns ${}_kJ$ and ${}_kV_A$ are determined by the system

$$\begin{cases} {}_kV_A = f_S({}_kJ) & \text{(constant } k) \quad (9.1) \\ {}_kJ \cdot A = f_N({}_kV_A) & \text{(constant } k) \quad (9.2) \end{cases}$$

where A is the cross-sectional area of the device, and Eqs.(9.1) and (9.2) are essentially the discretized current-voltage relationships, at the instant k, of the device and of the network respectively. Equation (9.1) is a concise form of the system of equations determining the transient response of the isolated device at the instant k (e.g. Eqs.(8.15), (8.16), (8.17) and (7.12)), solved with the iterative procedure of Fig. 8.1. Equation (9.2) may be inserted within the iterative scheme, at the instant k and iteration j, in the form

$${}_kJ^{(j+1)} = \frac{1}{A} f_N [{}_kV_A^{(j)}] \qquad (9.3)$$

as the first equation of the set, to determine an improved value of total current density from the network response to the terminal voltage, available at the previous iteration. Actually, for a given k and j,

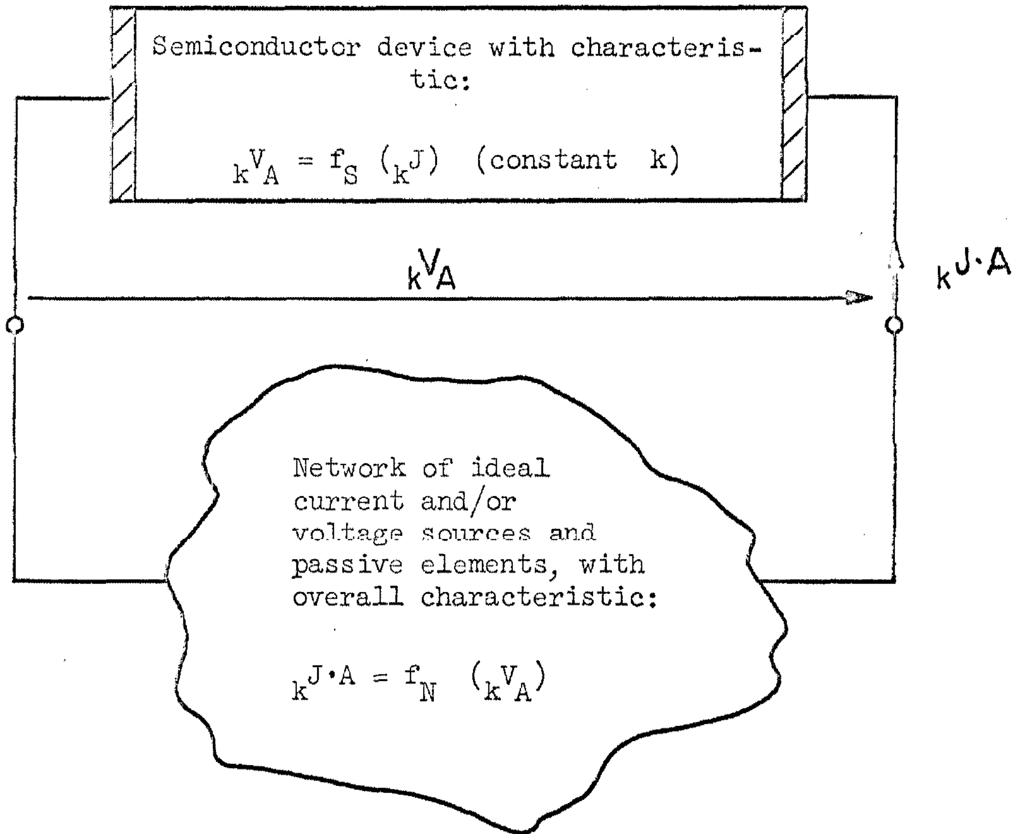

Fig. 9.4. The combination of a semiconductor device with a network of ideal time dependent generators and passive elements, with their overall characteristics at a given instant of time $_kt$.

Eq.(9.3) also represents a system of equations (for instance the mesh or nodal equations) describing the network properties. The time required for the solution of this system is usually insignificant (for a reasonable number of network elements) if compared to the computation time required by the system (9.1). The only undesirable effect of the incorporation of Eq.(9.3) within the original iterative procedure may result in a slower convergence rate to achieve overall consistency at each instant of time.

Alternatively, Eq.(9.2) may be combined, at a given instant k, with the current-voltage characteristic of the device (Eq.(9.1)), originally obtained during the interpolation phase of the voltage-driven transient (Fig. 9.2), to solve for the intersection ${}_kJ$, ${}_kV_A$ of the two curves.

For the simpler case in which only a resistor R in series with a time-dependent voltage source $V_S(t)$ (unnormalized) is present in the external circuit, the system (9.3) reduces to the single equation:

$$ {}_kJ^{(j+1)} = \frac{{}_kV_S - V_t \cdot {}_kV_A^{(j)}}{R\, A\, J_o} \qquad (9.4) $$

where

$$ J_o = - \frac{e\, D_o\, n_I}{L_D} $$

is the normalization factor for the current density (Table 1.1). As an example of numerical computation for this special case, results have been obtained for the combination of an N-P diode and an external

resistor under switching conditions from a forward to a reverse bias condition. These are reported and discussed in a later chapter.

9.5. Conclusion.

An iterative method of solution of the fundamental bipolar transport equations describing the behavior of semiconductor junction devices under a time-dependent excitation of terminal voltage has been presented in this Chapter. A valuable feature of the method, not available for the current-driven transient previously described, consists in its capability of reaching the final steady-state distributions without significant worsening of the convergence rate of the iterative procedure. The concept of "incompatibility" between solutions obtained with different formulations has been discussed and a method for achieving steady-state distributions, compatible with the time-dependent formulation and therefore suitable to serve as initial conditions for a transient solution, has been illustrated. This steady-state procedure, and the current-driven transient and voltage-driven transient methods, represent a self-sufficient algorithm to obtain compatible solutions for an external excitation of the most general form. The extension of the algorithm to incorporate a network of ideal current and voltage sources and passive circuit elements has also been illustrated.

The computation time usually required for the achievement of time-dependent solutions with sufficient accuracy amounts to a few minutes (five to twenty) on the IBM 7094/7040 system. A discussion on the accuracy of the time-dependent results is presented in the following Chapter.

CHAPTER X

ON THE ACCURACY OF THE TRANSIENT SOLUTIONS

In this Chapter the various sources of errors, arising in the time-dependent solutions of the type described in the previous chapters, are exposed and techniques suitable to estimate and control the accuracy of the final results are discussed. The influence on the discretization error of the order of the finite difference scheme, of the time step size and of the abruptness of the external excitation is considered. Among the various contributions to the numerical error of a stable discretization scheme, the iteration error is recognized as often being the dominant source of inaccuracy and therefore it is analyzed in detail.

10.1. Generalities.

In Chapter V a discussion on the various sources of errors present in the steady-state solution of Part I has been described. The overall accuracy of the final results has been evaluated with the aid of a set of testing relations, suitable to expose errors of different nature. A time-dependent solution of the type described in the previous chapters may be considered as a sequence of "pseudo-steady-state" solutions (one at each instant of time), whose function is to achieve consistency between the spatial distributions of the unknowns and the set of equations, starting from a set of trial distributions at each instant of time. The basic considerations of Chapter V, regarding the spatial domain, are therefore still valid for the iterative scheme searching consistency at a given time, provided that such an iterative scheme is considered isolated from the others. These considerations are now

applied to the new formulation, which includes the time-dependent terms. In addition, the interaction between the errors introduced by iterative schemes at different instants of time may become a dominant factor for the overall accuracy and deserves particular attention. This problem has already been considered in Chapter VIII in the process of selecting a sound discretization scheme for the numerical solution of partial differential equations of the parabolic type. The discretization error in the time domain and the growth of the numerical error for increasing time are responsible for this interaction and determine the conditions of convergence and stability respectively of the evolution of the transient.

In addition to the analysis of Chapter V, concerning inaccuracies within the spatial domain, the principal sources of error arising in the time-dependent solution, together with techniques suitable to evaluate and control the influence of such errors on the final results, are briefly discussed in the following sections.

10.2. Discretization error in the time domain.

In the formulation adopted for either the current-driven or the voltage-driven transient the left sides of Eqs.(7.16) to (7.18), expressing the variation with respect to time of the three unknowns of the problem, are the only terms in which the time coordinate appears explicitly. When such analytical derivatives are approximated by a discretized formulation, the discretization error is introduced. This approximation is often achieved by truncating a Taylor expansion at a convenient point (e.g. Eq.(8.36)) to obtain simple finite difference expressions. This truncation error depends upon the values of the

higher derivatives, on the size of the time step, and on the order of the finite difference scheme. The magnitude of the higher time derivatives of the function to be numerically differentiated is very much related to the abruptness of the time variation of the unknowns, directly dependent upon the time variation of the external excitation, for a given time step. For a decreasing time step, the dependence of the electric field upon an abrupt variation of external excitation is more emphasized, if compared to the dependence of the mobile carrier densities. This feature may be easily verified from the set of discretized equations (Eqs.(8.15) to (8.17)) and is a consequence of the physical properties of the mobile carrier densities (and therefore the particle currents) requiring a finite time for a significant variation, whereas the electric field (and therefore the displacement current) may respond immediately to any external excitation (see also Section 11.1).

If excitations with continuous and finite time derivatives are specified, the truncation errors introduced by the numerical time differentiations of the electric field and mobile carrier densities may be contained within limits with an appropriate choice of the time step at each instant of time. A simple application of this concept has been illustrated in Section 8.4 for the selection of a non-uniform time step distribution, subject to the criterion of maintaining a constant truncation error of the time differentiation of the spatial integral of the electric field throughout the entire evolution of the transient. In addition, higher order (multilevel) finite difference schemes, approximating time derivatives, may be employed to reduce truncation errors. These schemes are an integral part of the overall discretization scheme,

and therefore must be individually analyzed to investigate convergence and stability conditions. An example of a three-level scheme, featuring unconditional stability, is given in Subsection F-3.1.1 (Appendix F) for a very simple case. This, as well as higher level discretization schemes, may be generalized for the non-linear case under consideration, and numerical calculations experimented, although the stability of the solutions may not be guaranteed. An additional complication arises in the initial phase of a time-dependent solution, where higher level schemes may not be used and a different discretization based on lower level schemes (two-level initially) must be employed.

If ideal excitations such as ramp, step and delta functions, are specified instead, an overall control of the truncation error is not possible, since higher order time derivatives are either infinite or discontinuous. Both step functions and delta functions are represented in the discretized context as ramps, or combinations thereof, since only non-zero step sizes may be used. In addition, both the minimum step size and maximum amplitude of any excitation must satisfy the usual limitation on the permissible range of the particular machine. Although this idealized abrupt type of excitations may be considered only of academic interest, it has been consistently used in a series of preliminary test calculations (reported in the following Chapter) to focus the attention on the worst case represented by abrupt variations. For constant slopes of a sequence of specified ramps, calculations have been repeated for different time step sizes and for various discretization schemes, featuring truncation errors of different orders of magnitude in the time domain. As a result, the overall transient response

has been observed to be little sensitive to the variation of the time step size (within limits) and the adoption of more accurate schemes, with exception of the time points adjacent to the discontinuities of the time derivatives of the specified excitations. The considerable error introduced at these singular instants may be restricted to very short time intervals with the use of a time step compression technique of the same type used for the spatial step in the vicinity of the metallurgical junction of an abrupt doping profile (Subsection 5.2.1). A valuable feature consistently observed is that the error introduced in the neighborhood of the singular points does not affect significantly the response at later times.

It may be concluded that the discretization error of solutions obtained with the procedure and the formulation described may be considered sufficiently small for any practical purpose, even for the worst case considered above.

10.3. Numerical error and its growth in the time domain.

The numerical error is defined as the difference between the exact solution of the discretized formulation and the numerical solution actually achieved. The growth of the numerical error throughout the entire evolution of a time-dependent solution, governed by partial differential equations of the parabolic type, is ruled by the conditions of stability. These furnish, for the simpler cases, bounds for the amplification (for increasing time) of the numerical error introduced at one stage of the solution, for a given discretization scheme. For the more complex cases, such as the non-linear system under consideration, stability conditions may not be proven and must be experimented with

actual numerical calculations. Unstable conditions are easily recognized by unexpected oscillatory pattern, with increasing amplitude, of the solution evolving in the time domain.

The numerical error, in the form of round-off error, is always present in a numerical solution dealing with quantities represented by a finite number of digits. Small differences between nearly equal numbers also contribute to the numerical error and are present, in the discretized formulation adopted for the transient solutions, in the expressions for the net charge density (the right side of Poisson's equation, Eq.(7.4)) implicitly incorporated in the equations yielding the improved mobile carrier densities (e.g. Eqs.(8.13) and (8.14)). These sources of errors are usually not responsible for significant inaccuracies in the final results, since other contributions to the numerical error are dominant. These are briefly discussed in the following subsections.

10.3.1. Iteration error.

An iterative procedure at each instant of time has been described in Section 8.3 (Fig. 8.1 for a special case) to resolve the non-linearities of the problem by achieving consistency between the spatial distributions of the unknowns and the system of discretized equations. When the estimated discrepancy between the "exact" distributions and those achieved at the completion of an iterative cycle, at a given instant of time, is less than a specified amount, the procedure restarts at the following instant. Such discrepancy represents the iteration error at a given time.

The estimation may be obtained by an appropriate extrapolation of the corrections for the distributions available from the previous cycles

at the same instant, and is more accurate the faster the rate of convergence of the iterative procedure. A constant fraction of the maximum excursion (over all spatial points) of each unknown, at each instant of time, may be conveniently specified as the iteration error. It is often sufficient to limit the evaluation of the overall consistency, at each instant of time, to the terminal response, which (with the exception of singular points) reflects sufficiently well the behavior of the internal distributions.

An alternative and more accurate evaluation of the consistency at a given time may be performed with the aid of a set of testing relations, derived from the fundamental set (7.1) to (7.6), with the criteria stated in Section 5.4. This technique is not very suitable, from a practical point of view, to test the consistency at each iterative cycle, but may be occasionally used to refine the accuracy of the solutions at a particular instant of time, for which the spatial distributions of dependent quantities (such as the particle currents and net charge densities) are also desired.

The rate of convergence of the iterative procedure at each instant of time is considerably influenced by the rate of change of the external excitation. The most favorable condition arises when variations of the total current occur, particularly in the presence of a significant displacement current, so that the overall system of equations is essentially driven by the time variations of the electric field, rather than by the diffusion processes of the mobile carrier densities. This feature has already been mentioned in Section 8.3 and usefully exploited in Section 9.2 for the solution of the voltage-driven transient. A

dominant factor, governing the rate of convergence at a given instant of time, is the magnitude of the time step at that instant: larger time steps are always responsible for slower convergence rates. The time step size, directly related to the discretization error in the time domain, becomes a determinant parameter very much affecting also the magnitude of the iteration error if an upper bound for the computation time, or in equivalent terms for the total number of iterations during the entire solution, is specified. In such conditions the iteration error may dominate over the discretization error, so that it may be advantageous to select the time step size on the basis of the requirements dictated by a minimization of the iteration error. The total number of spatial points also affects the convergence rate of the iterative procedure. This phenomenon is related to the propagation of the inconsistencies of the approximate distributions throughout the length of the device during the execution of an iterative cycle at a given time. A smaller number of spatial points within certain limits usually increases the convergence rate. The same criterion used above for the selection of the time step size applies here if a maximum computation time is specified and the iteration error is dominant: a larger discretization error in the spatial domain is tolerated to decrease the number of spatial points, increase the convergence rate and consequently reduce the iteration error. The abruptness of the doping profile may be indirectly responsible for a larger iteration error in the vicinity of the metallurgical interface. This is a consequence of the larger discretization error (in the spatial domain), occurring near the interface if the spatial step there required to

maintain the overall constancy of the truncation error (Section 5.3) is smaller than the specified lower bound of the step. This is certainly the case for an ideal step distribution for the impurity density, which has been therefore chosen, as the worst case from a numerical standpoint, to characterize the structure analyzed under transient conditions in the following Chapter.

The accumulation, throughout the evolution of the transient solution, of the iteration error introduced at each instant of time is of great interest. If a constant fraction of the excursion of the unknowns within a time step is specified as the iteration error, a transient solution featuring a monotonic pattern is affected by the same relative error at any instant of time if the single iteration errors are simply accumulative. A considerably more favorable situation has been actually observed in the cases tested: the iteration error at a given time is partially compensated by a larger excursion of the unknowns at the following instant of time, so that the resulting error is less than the sum of the iteration errors introduced at the previous instants. This is a consequence of the deviation from the "exact" condition of dynamic equilibrium at a given time caused by the iteration error, and may be regarded as an automatic corrective feature inherent in the formulation adopted for the solution.

10.3.2. Inaccuracy of the initial conditions.

If a time-dependent solution is initiated from a steady-state condition, initial spatial distributions of the unknowns, available from a steady-state solution, must be furnished. The inaccuracy of these steady-state distributions represents a contribution to the

numerical error of the transient solution. As such, it may generate unstable solutions, if certain types of discretization schemes are adopted, and therefore must be contained to sufficiently small values. This problem has been already encountered in Section 9.3, where the importance of compatible initial steady-state distributions has been discussed and a method to achieve steady-state solutions compatible with the discretized formulation employed for the transient analysis has been described.

10.3.3. Tolerance on the specified excitation in the voltage-driven transient.

In the method of solution of the voltage-driven transient described in Section 9.2 (Figs. 9.1, 9.2, 9.3) a sequence of interpolations on the current-voltage characteristic at a given time is used to determine the value of total current that yields, within an assigned tolerance, the specified terminal voltage at that time. Such a tolerance may be regarded as the upper bound of an additional contribution to the numerical error at each instant of time, a necessary consequence of the procedure adopted. The combination of an accurate prediction phase, preceding the interpolation phase, together with the closely linear shape of the current-voltage characteristic within the range of interest at a given time, permits the achievement of excellent tolerances with just a few (three to four) interpolation cycles. This type of inaccuracy may therefore be considered of secondary importance, if compared to the other contributions to the numerical error.

10.4. Conclusion.

As an extension of the discussion of Chapter V concerning the error in the spatial domain, discretization and numerical errors in the time domain have been considered in this Chapter. Attention has been given to the growth of the numerical error throughout the entire evolution of a time-dependent solution, to achieve numerically stable solutions of sufficient accuracy. Empirical techniques suitable to estimate the overall accuracy of the results have been discussed, as a substitute for an exact error analysis prevented by the complexity of the analytical formulation of the problem and by the presence of several sources of errors of different nature. The majority of these errors may be controlled by parameters such as the order of the finite difference scheme, the spatial and time step size, the total number of spatial and time points, the number of cycles of the iterative procedure at each instant of time, and the tolerance on the specified excitation in a voltage-driven transient. The maximum efficiency of the method, that is, the best accuracy of the final results for a given computation time, is achieved by optimizing the selection of the above parameters toward an overall equalization of the various contributions to the discretization and numerical errors.

CHAPTER XI

RESULTS

As an example of numerical calculations, time-dependent solutions for a special structure of a two-contact device under typical excitations are presented. The transient behaviour of a short highly asymmetric abrupt N^+ - P diode, driven by steps and spikes of external current and terminal voltage, is analyzed. In addition, results for the interaction of a slightly longer structure of the same device with an external resistor, under switching from a forward to a reverse bias condition, are also reported and discussed. "Exact" and conventional approximate analytical results are compared and discrepancies are exposed. Furthermore, solutions obtained for various types of discretization schemes and time step sizes are compared, and the overall accuracy estimated.

11.1. Generalities.

In the previous chapters an algorithm suitable for solving the one-dimensional basic two-carrier transport equations under time-dependent excitations of current and voltage has been described. Although the method allows for arbitrary doping profile, generation-recombination law, mobility dependencies, boundary conditions and external excitations, results for a special case are presented. The same model adopted in Section 6.2 for a short structure, characterized by a highly asymmetric N^+ - P diode with abrupt doping profile, absence of recombination in the interior, ohmic external contacts and constant mobilities, is analyzed under idealized input signals (steps and spikes) of current

and voltage. In addition to the motivations of Section 6.1, this choice facilitates the interpretation of the phenomena responsible for the behavior of the device under transient conditions by a more distinct separation of effects of different nature.

The abrupt time-dependent excitations are approximated in the discretized context by a sequence of ramps (Section 10.2) of finite slope. Although this approximation does not introduce in most cases a significant alteration of the transient response to the ideal excitation, it may occasionally become the determinant factor characterizing the response in the vicinity of the quasi-abrupt variations. In such cases, in the examples analyzed in the following sections, the parameters identifying the discretized excitations actually used will be given and their influence discussed.

Solutions have been obtained within five to twenty minutes of computation time on an IBM 7094/7040 shared file system. The accuracy of the final results has been usually contained within a relative error of 0.02, considered satisfactory from any practical point of view. This is not to be regarded as a limitation of the algorithm: a considerably higher degree of accuracy may be easily achieved with a corresponding increase of computation time.

Two basic phenomena will be of interest in the following analysis: the variation of the electric field in the time domain without variation of carrier densities, and the motion of carriers in the presence of a time-invariant electric field. The former effect may be described mathematically by the combination of Eqs.(7.1), (7.2) and (7.3), which, specialized for the present case, may be written as:

$$\frac{\partial E(x,t)}{\partial t} + \sigma(x)\, E(x,t) = - J(t) + D(x)$$

where

$$D(x) = \frac{1}{\gamma_p}\frac{dp(x)}{dx} - \frac{1}{\gamma_n}\frac{dn(x)}{dx}$$

and $\sigma(x)$ is the conductivity of the material. Both $D(x)$ and $\sigma(x)$ are time invariant by assumption. If a positive step of current of amplitude J_S is imposed at $t = 0$ as external excitation, the solution of the above equation becomes:

$$E(x,t) - E(x,t{=}0^-) = - \frac{J_S}{\sigma(x)}\left[1 - e^{-\sigma(x)t}\right]$$

where

$$E(x,t{=}0^-) = \frac{1}{\sigma(x)}\left[- J(t{=}0^-) + D(x)\right]$$

is the initial steady-state electric field distribution. The time constant τ_r of the exponential time variation of the electric field is then:

$$\tau_r(x) = \frac{1}{\sigma(x)} \qquad \text{(normalized quantities)}$$

$$\tau_r(x) = \frac{\varepsilon}{\sigma(x)} \qquad \text{(unnormalized quantities)} \qquad (11.1)$$

and is referred to as the "dielectric relaxation constant". In a

homogeneous material τ_r is independent of position.

The time variation of the minority carriers in a certain region of width w of semiconductor material, in the presence of a time-invariant field, may be associated with the concept of steady-state transit time τ_t of minority carriers in that region. This quantity is conventionally defined as:

$$\tau_t = \frac{Q_m}{J_m} \tag{11.2}$$

where Q_m and J_m are the charge density and the current density respectively of minority carriers in the region considered. If the first-order theory parameters are used (Appendix A), two simple expressions of the transit time in the low-injection and high-injection limits may be determined. If electrons in a quasi-neutral P-region are considered, the definition (11.2) becomes:

$$\tau_t = \frac{\gamma_n w_P^2}{2} \qquad \text{(low injection)} \tag{11.2a}$$

$$\tau_t = \frac{\gamma_n w_P^2}{4} \qquad \text{(high injection)} \tag{11.2b}$$

Although the transit-time (11.2) is defined as a steady-state quantity, it may serve as the first-order estimation of a "time-constant" in a time-dependent phenomenon, involving solely motion of carriers. For instance, the conventional solution of the simple diffusion equation

$$\frac{\partial n(x,t)}{\partial t} = \frac{1}{\gamma_n} \frac{\partial^2 n(x,t)}{\partial x^2} \quad ,$$

driven by abrupt time variations of the boundary conditions, evolves usually within a period of time approximately equal to a few multiples of the low-injection transit time (11.2a).

The assumed absence of interaction between relaxation and transit-time effects is motivated by the considerably different magnitude of the respective time constants often arising in practical situations. Order-of-magnitude estimations, on the basis of the above considerations, will be therefore used in the following examples where applicable.

11.2. The N-P diode driven by ideal current and voltage sources.

A short N-P structure (Fig. 1.1) is analyzed under transient conditions for various types of excitations of external current and terminal voltage as functions of time. An idealized model characterized by absence of generation-recombination in the interior of the device, abrupt asymmetric impurity distribution, constant mobilities and ohmic contacts is assumed. The discretized formulations employed have been described in Section 8.2 and the iterative method of solution in Section 8.3 for the current-driven transient and in Section 9.2 for the voltage-driven transient.

The physical parameters characterizing the structure are listed in Table 11.1. Dependent parameters of interest are:

conductivities of the material in thermal equilibrium:
- N-side, $\sigma_N = 3.720 \times 10^6$ [or 575.8 $(\Omega\ cm)^{-1}$]
- P-side, $\sigma_P = 1.760 \times 10^3$ [or 0.2726 $(\Omega\ cm)^{-1}$]

dielectric relaxation constants of the material in thermal equilibrium:
- N-side, $\tau_{rN} = 2.688 \times 10^{-7}$ (or 2.460×10^{-15} sec)
- P-side, $\tau_{rP} = 5.678 \times 10^{-4}$ (or 5.197×10^{-12} sec)

Material:	germanium (relative permittivity $\varepsilon_r = 16$)
Temperature:	$300^\circ K$
Doping:	N-side, $N(x) = N_D = 4 \times 10^4$ (or 10^{18} cm^{-3})
	P-side, $-N(x) = N_A = 40$ (or 10^{15} cm^{-3})
Length:	N-side, M-O = 0.22 (or 0.2105×10^{-4} cm)
	P-side, L-M = 1.78 (or 1.703×10^{-4} cm)
	total, L-O = 2.00 (or 1.913×10^{-4} cm)
Carrier mobilities:	electron, $\gamma_n^{-1} = 93$ (or $\simeq$ 3600 cm^2/volt-sec)
	hole, $\gamma_p^{-1} = 44$ (or $\simeq$ 1700 cm^2/volt-sec)

Table. 11.1. Physical parameters characterizing the N-P structure of Fig. 1.1, analyzed under transient conditions.

first-order theory width of the quasi-neutral region in the P-side, in thermal equilibrium:

$$w_P = L - M_P = 0.9363 \quad (\text{or } 0.8957 \times 10^{-4} \text{ cm})$$

first-order theory low-injection transit time of electrons in the quasi-neutral P-region, in thermal equilibrium:

$$\tau_t = \frac{\gamma_n w_P^2}{2} = 5.150 \times 10^{-3} \text{ (or } 47.13 \times 10^{-12} \text{ sec)}$$

In addition, the "exact" total incremental capacitance (per unit area) of the device in thermal equilibrium, obtained with the method outlined in Section 3.2 is:

$$C = 1.668 \text{ (or } 24.70 \times 10^{-9} \text{ farad/cm}^2\text{)}$$

Results are displayed graphically in dimensionless form (according to the normalization factors of Table 1.1). A dashed vertical line at $x = M$, in the illustrations showing internal distributions, indicates the position of the metallurgical interface.

11.2.1. Excitation: a low current step.

An ideal current step in the forward direction is applied to the device initially in thermal equilibrium. This excitation is quantitatively determined by:

$$J(t) = 0 \qquad\qquad t \le 0$$

$$J(t) = J_F = 100 \qquad t > 0$$

and is recognized as generating a low-injection condition in the low-conductivity (P) side in the final state.*

The response of the device is illustrated in Figs. 11.1 to 11.6. The terminal voltage as a function of time is shown in Fig. 11.1; electron, hole, and displacement currents as functions of position are displayed at various instants of time in Fig. 11.2 (for short times) and 11.3 (for long times); time increments of the electric field and of the electrostatic potentials as functions of position are displayed in Fig. 11.4; and mobile carrier densities as functions of position in Figs. 11.5 (semilogarithmic scales) and 11.6 (linear scales).

The initial part $(t < 2 \times 10^{-3})$ of the terminal voltage response as a function of time (Fig. 11.1) represents the build-up of the ohmic voltage drop in the quasi-neutral region of the P-side. This phenomenon is ruled by the dielectric relaxation properties of the low-conductivity (P) side, and occurs within a period approximately equal to four times the dielectric relaxation constant τ_{rP}, as a consequence of the exponential nature with time constant τ_{rP} $(= 5.678 \times 10^{-4})$ of the phenomenon. If the first-order theory estimation of the ohmic drop

$$\Delta V\Big|_{ohmic} = \frac{J\, w_P}{\sigma_P} = \frac{100 \times 0.936}{1.76 \times 10^{-3}} \cong 0.053 \text{ (or } 1.37 \times 10^{-3} \text{ volt)} \qquad (11.3)$$

---

* The corresponding terminal voltage V_A amounts approximately to 4.06 (or 0.105 volt) and the first-order theory injection parameter χ (A-43, of Appendix A) to 0.035.

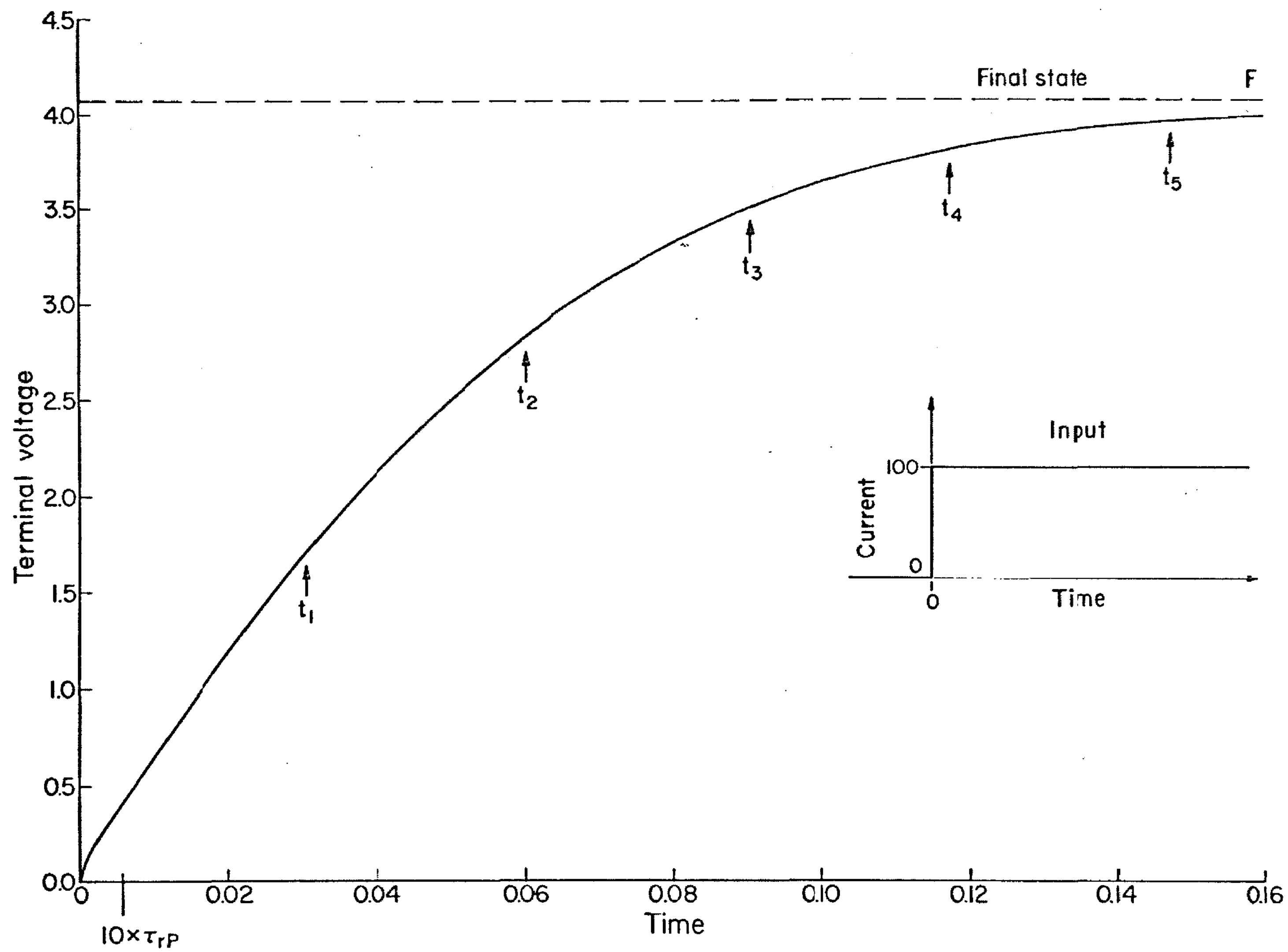

Fig. 11.1. Structure of Fig. 1.1; parameters of Table 11.1; boundary conditions (1.32). Terminal voltage as a function of time for an external excitation of a low current step.

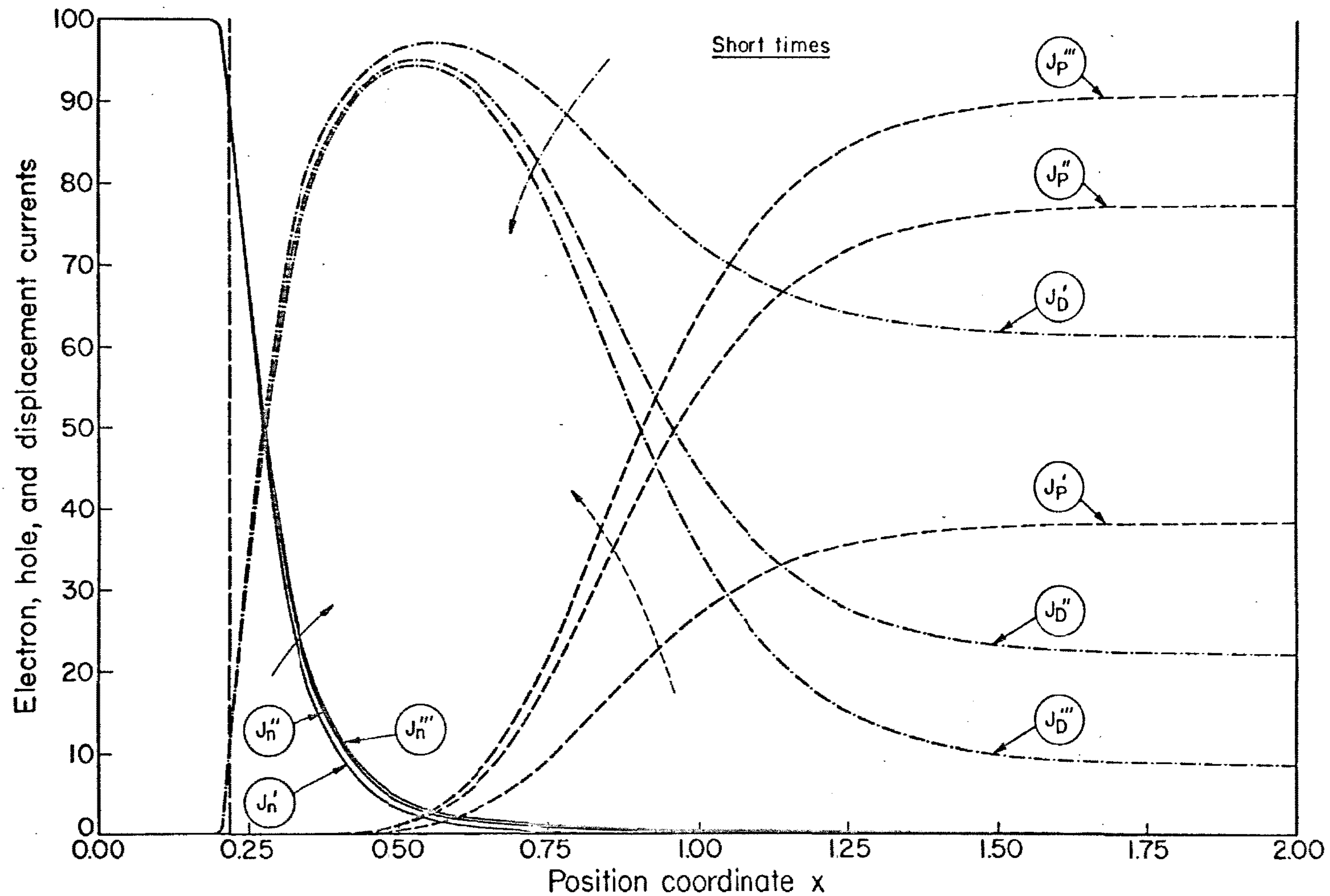

Fig. 11.2. Device as in Fig. 11.1. Electron, hole, and displacement currents as functions of position at various instants of time during the initial dielectric relaxation phase for an external excitation of a low current step ($t' = 3\times10^{-4}$, $t'' = 9.4\times10^{-4}$, $t''' = 1.57\times10^{-3}$).

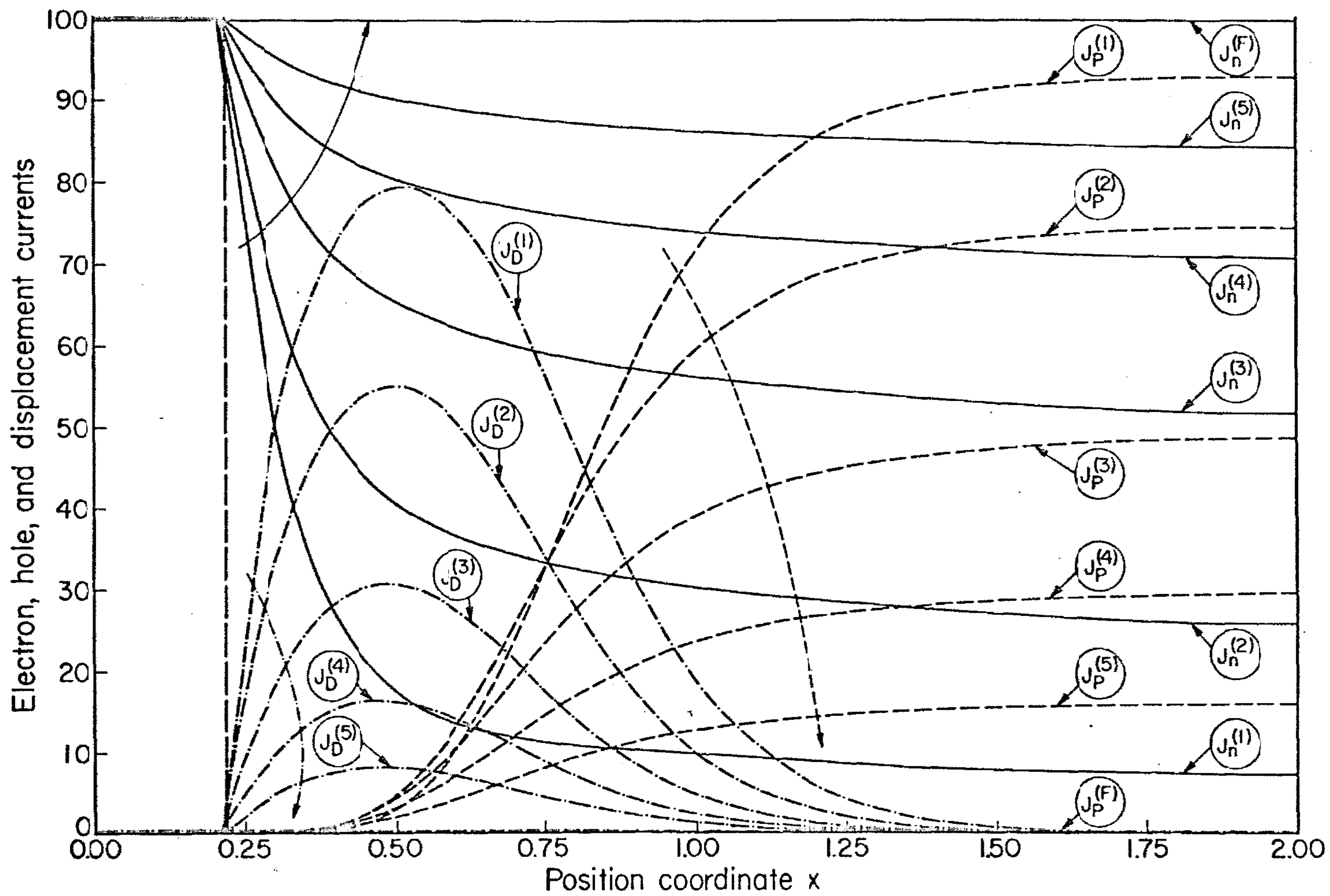

Fig. 11.3. Device as in Fig. 11.1. Electron, hole, and displacement currents as functions of position at various instants of time for an external excitation of a low current step (t_1 = 0.030, t_2 = 0.060, t_3 = 0.090, t_4 = 0.117, t_5 = 0.147).

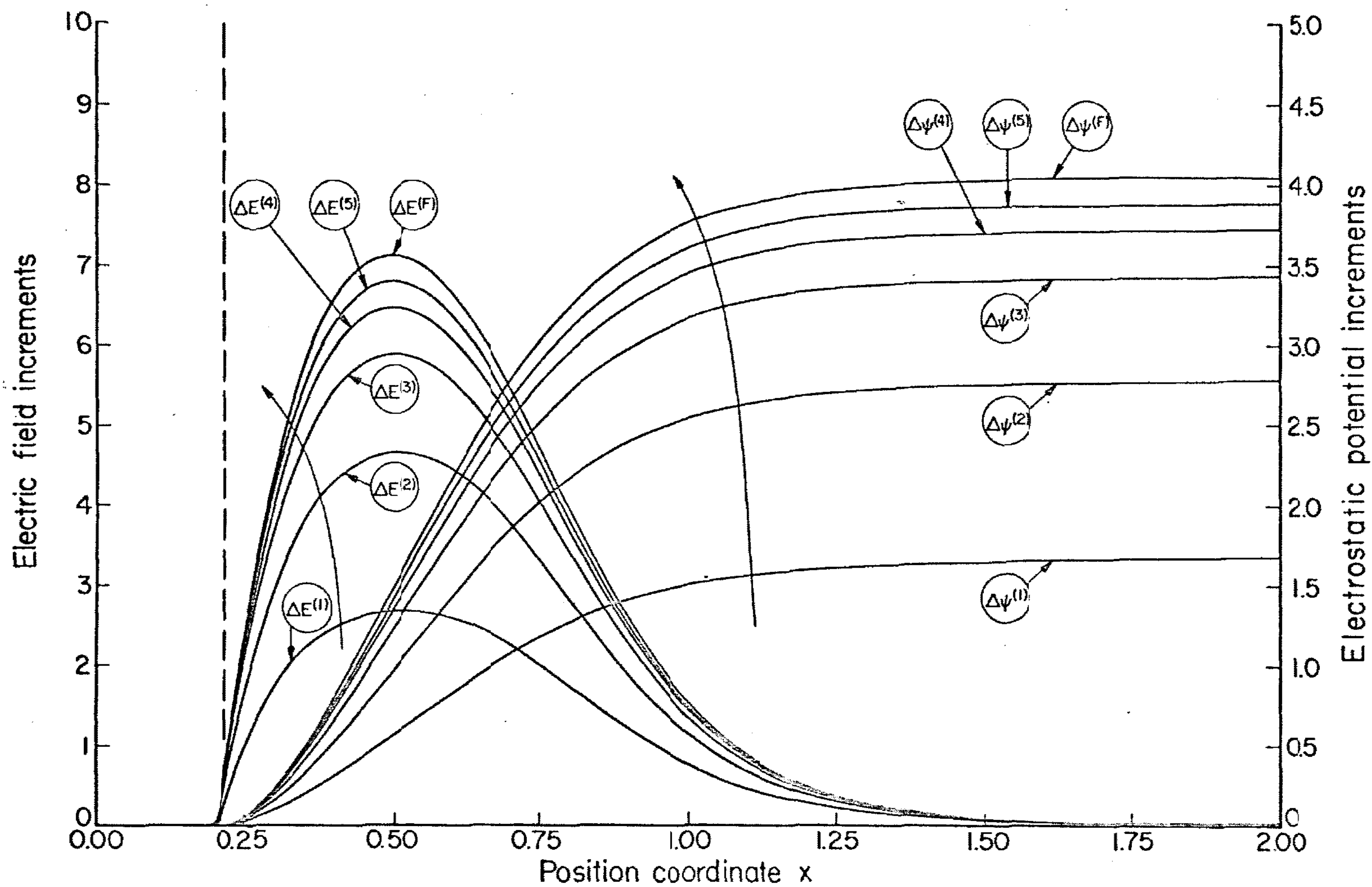

Fig. 11.4. Device as in Fig. 11.1. Time increments of the electric field and electrostatic potential as functions of position at various instants of time (as in Fig. 11.3, and $t_F = \infty$) for an external excitation of a low current step.

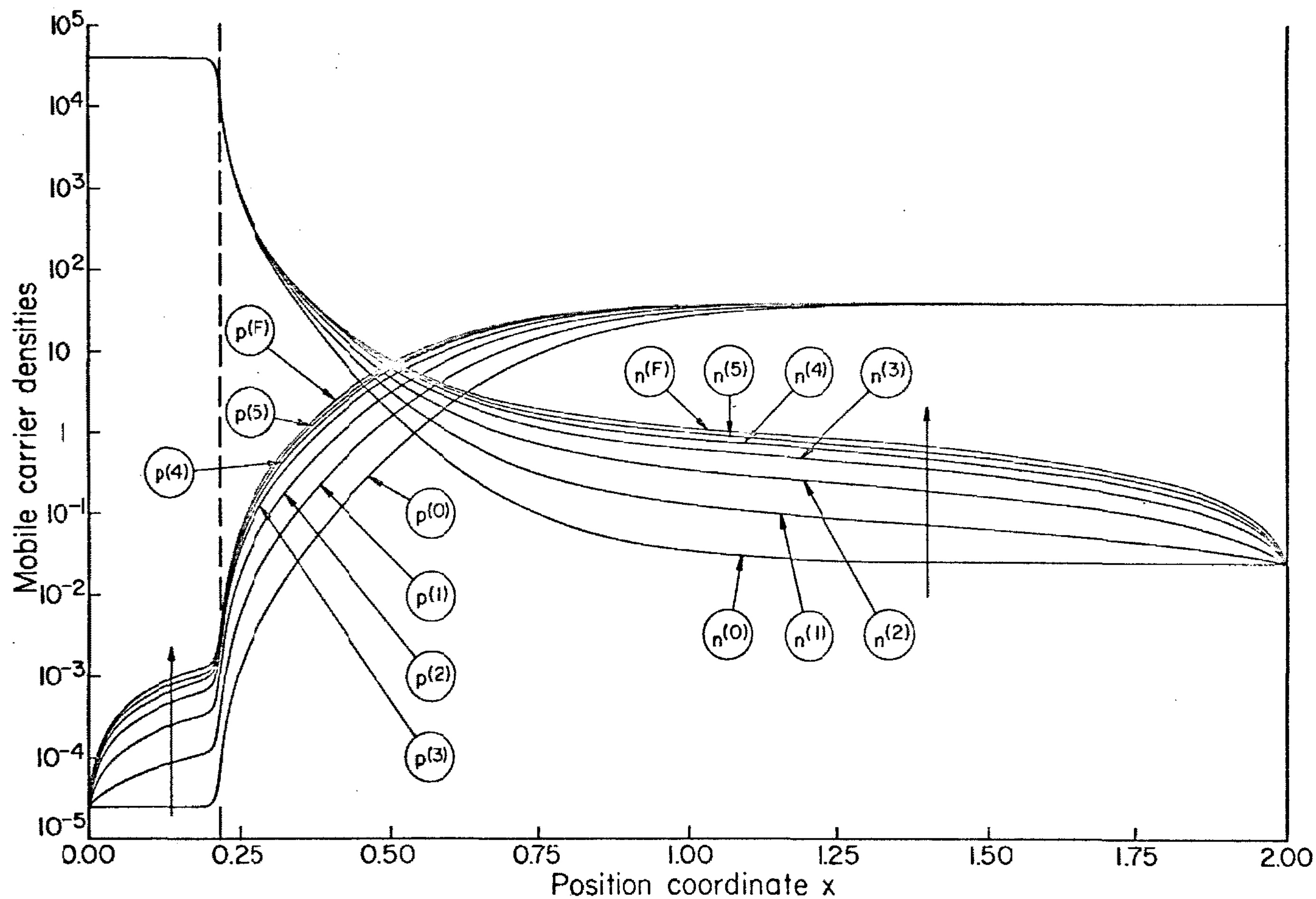

Fig. 11.5. Device as in Fig. 11.1. Mobile carrier densities as functions of position at various instants of time (as in Fig. 11.3, and $t_0 = 0$, $t_F = \infty$) for an external excitation of a low current step.

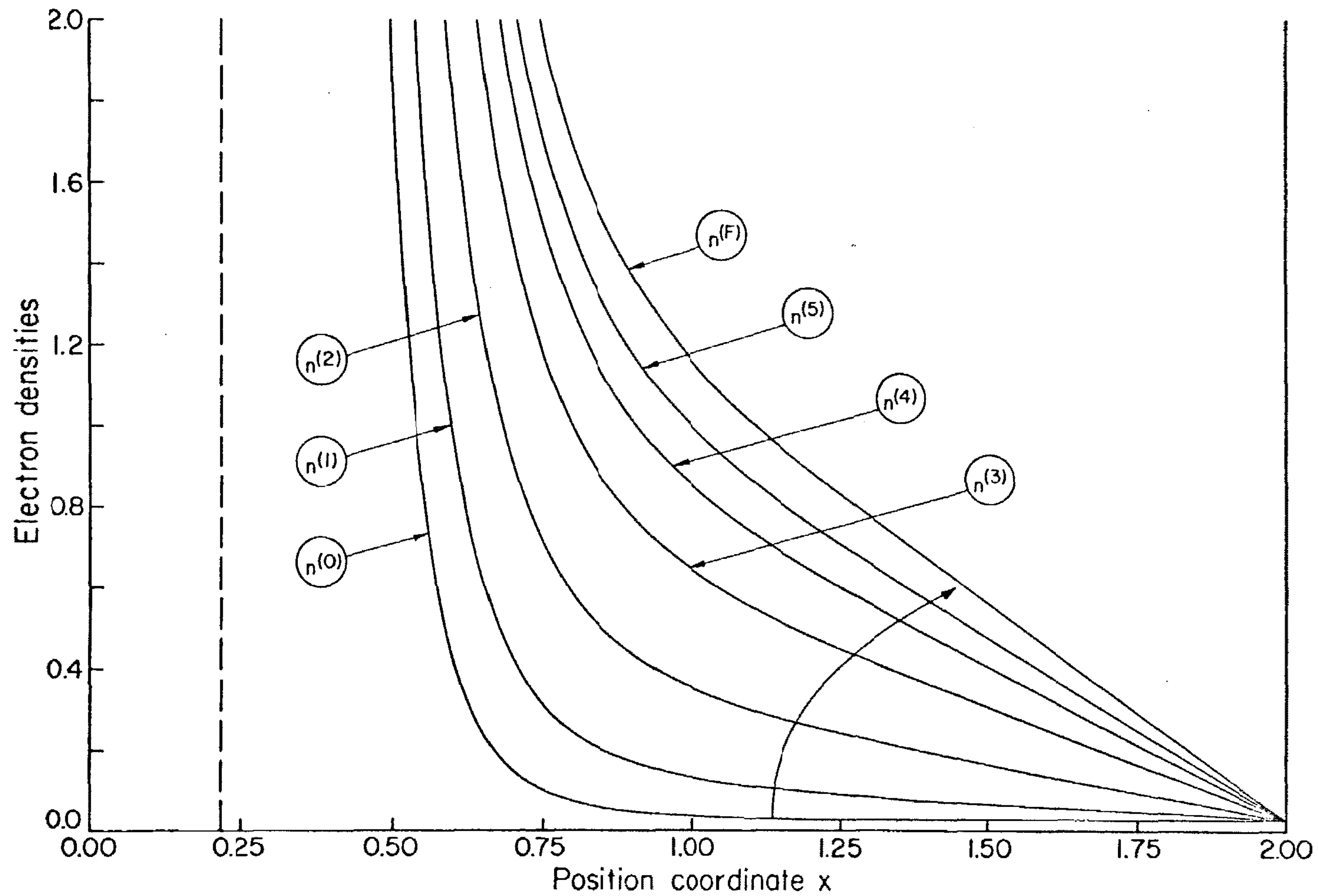

Fig. 11.6. Device as in Fig. 11.1. Electron density as a function of position at various instants of time (as in Fig. 11.5) for an external excitation of a low current step.

is compared to the "exact" one, an excellent agreement is observed. Such initial ohmic drop increases only slightly throughout the entire evolution of the transient as a result of an increase of $w_p (\simeq 14\%)$ and of the conductivity $\sigma_p (\simeq 3\%)$. When the relaxation effects have disappeared, the charge of the transition region capacitance* with the displacement current becomes the dominant phenomenon. The diffusion capacitance, a negligible contribution to the total capacitance at the low injection levels considered, has an insignificant influence on the transient response. The transition region capacitance is essentially charged with the constant current J_F during an initial period $(t < 0.02)$, in which the displacement current dominates over the convection components in the transition region. A simple first-order calculation yields

$$\frac{V_A(t)}{t} = \frac{J_F}{C} = \frac{100}{1.668} \cong 60 \qquad (11.4)$$

and

$$T = \frac{V_A(t_F)\ C}{J_F} = \frac{4.06 \times 1.668}{100} = 6.77 \times 10^{-2} \qquad (11.5)$$

as the slope of the terminal response in the linear region and as the time constant of the phenomenon respectively (t_F is the time at which the final steady-state is reached). These first-order results are again in good agreement with the "exact" ones of Fig. 11.1. At later

---

* "Incremental" capacitances are consistently assumed.

times, as the electron current becomes the dominant component, the displacement current charging the transition region capacitance gradually decreases to its steady-state zero value and the terminal voltage approaches its final state. Transit time effects are negligible during the entire evolution of the transient since the time constant(11.5)is considerably larger than the transit time $\tau_t (\cong 5.2 \times 10^{-3})$ of electrons in the quasi-neutral P-region. As a consequence, the conventional first-order analytical solutions of the diffusion equation of minority carriers into the quasi-neutral region of the low conductivity side, with omission of the electric field (see for example Ko [25]), are not applicable in the present situation.

A thorough understanding of the internal behaviour of the device is easily achieved with the analysis of the spatial distributions of Figs. 11.2 to 11.6. The electron current J_n, the hole current J_p, and the displacement current J_D $(= - \frac{\partial E}{\partial t})$ are displayed in Fig. 11.2 as functions of position for three instants of time $(t' = 3 \times 10^{-4}$, $t'' = 9.4 \times 10^{-4}$, $t''' = 1.57 \times 10^{-3})$ within the dielectric relaxation range. According to the sign convention consistently used, normalized currents are positive if flowing in the negative x direction. The three current components must, of course, add to the total current J_F at each position $0 \le x \le L$ and time $t > 0$. Immediately after the application of the step of current, at $t = 0^+$, the displacement current accounts for the total current throughout the interior of the device:

$$J_D(x, t=0^+) = J_F \quad , \quad 0 \le x \le L \quad ,$$

whereas the particle currents $J_n(x,t=0^+)$, $J_p(x,t=0^+)$ remain unchanged from the initial zero value. At the instant t', far greater than τ_{rN} but smaller than τ_{rP}, dielectric relaxation phenomena have already disappeared in the quasi-neutral region of the N-side so that the majority (electron) current essentially accounts for the total current and remains unchanged as the time increases to t'''. The transition region is dominated by the flow of displacement current which features only small variations within the time range considered. The absence of particle currents is a consequence of the little increment of the electric field and the mobile carrier densities from the initial equilibrium condition, despite a relatively large time derivative of the electric field. The increment of the field in the transition region is related to the build-up of junction voltage, in turn related to the charge of the transition-region capacitance, a phenomenon occurring with the considerably larger time constant (11.5). The dielectric relaxation phenomenon is well apparent in the quasi-neutral P-region, which illustrates the gradual changeover from a condition of displacement current flow to hole current flow, with absence of electron current flow. This is the typical feature of the build-up of the ohmic drop in a semiconductor material with finite nonzero dielectric relaxation constant, after the application of a step of total current.

The interplay of the three current components as functions of position may be followed in Fig. 11.3 at five subsequent instants of time ($t_1 = 0.030$, $t_2 = 0.060$, $t_3 = 0.090$, $t_4 = 0.117$, $t_5 = 0.147$) after the completion of the relaxation phenomena and during the charge of the transition-region capacitance (see also Fig. 11.1). The final

state of the currents is also displayed. The displacement current in the quasi-neutral P-region has essentially disappeared and the electron current is increasing, as t increases, as a result of the diffusion of electrons into the P-side, and the hole-current is decreasing accordingly. A similar situation, although on a minor scale, occurs in the quasi-neutral N-region, in which the hole current increases as a result of the diffusion of holes in the N-side, with a consequent decrease of electron current. This effect is hardly noticeable in Fig. 11.3 for the high conductivity characterizing the N-side. As the electron current also increases in the transition region, approaching the final state, the displacement current decreases in completing the charge of the transition-region capacitance.

The time dependence of the displacement current is directly related to the increments of electric field

$$E(x,t=0) - E(x,t)$$

and to their spatial integrals

$$\psi(x,t) - \psi(x,t=0)$$

displayed in Fig. 11.4 as functions of position x for the same instants of time t_1 to t_5, and for the final state. The increments of the electrostatic potential at $x = L$ of course coincide with the terminal voltage response:

$$V_A(t) = \psi(L,t)-\psi(L,t=0)$$

The mobile carrier densities are shown in Fig. 11.5 as functions of position for the instants $t = 0$, t_1 to t_5, and for the final state. The linear expansions of the electron density spatial distributions of Fig. 11.6, injected into the quasi-neutral P-region, are nearly linear and relatively close to the corresponding steady-state distributions,* evaluated for the same terminal voltage $V_A(t)$ at each instant of time. This is a consequence of the narrowness of the quasi-neutral P-region, responsible for the small transit time τ_t ($\cong 5.2 \times 10^{-3}$).

11.2.2. Excitation: a high current step.

The high forward current step defined by

$$J(t) = 0 \qquad t \le 0$$
$$J(t) = J_F = 5 \times 10^4 \qquad t > 0$$

is applied to the device initially in thermal equilibrium. The final state is in the high-injection region and corresponds to a terminal voltage $V_A(t_F) \cong 12.7$ (or $\cong 0.328$ volt) and to a first-order theory injection parameter $\chi = 13$.

The response of the device is illustrated in Figs. 11.7 to 11.12. The terminal voltage as a function of time is shown in Fig. 11.7, the

---

* The injected electron density at the edge of the transition region is slightly displaced from the first-order theory prediction of the Boltzmann relation (A-45) (of Appendix A) in terms of the "exact" voltage drop on the junction.

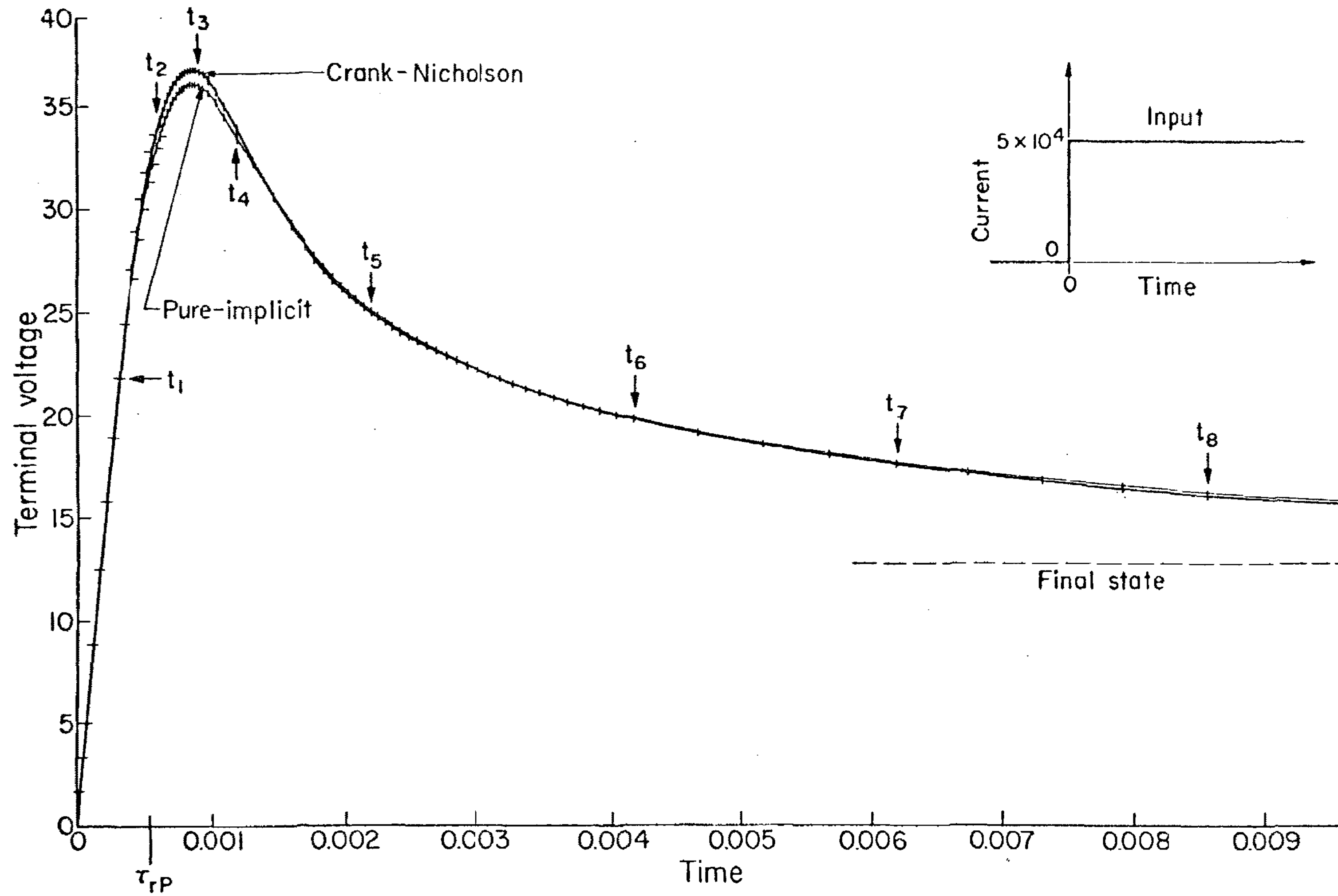

Fig. 11.7. Device as in Fig. 11.1. Terminal voltage as a function of time for an external excitation of a high current step.

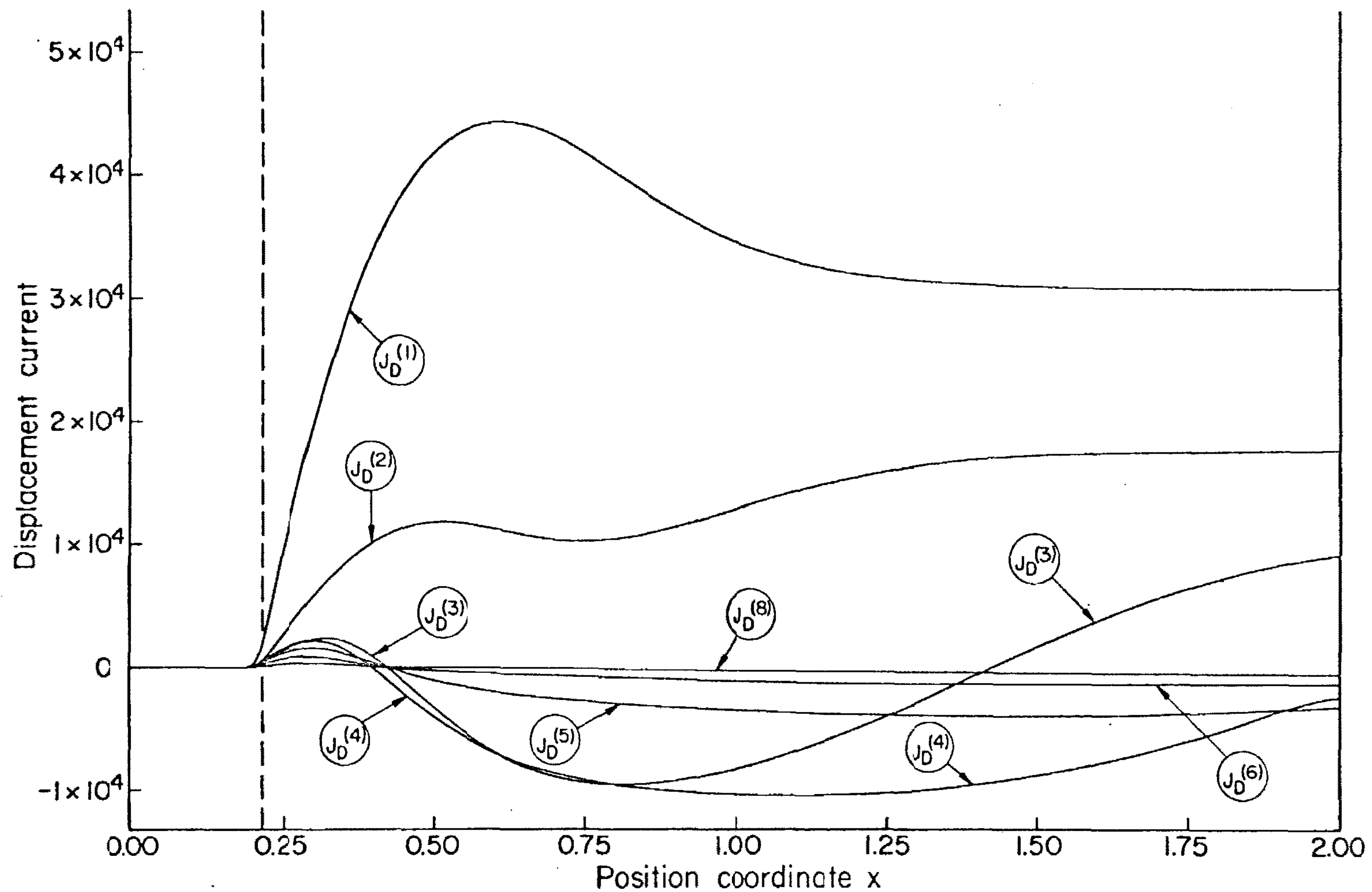

Fig. 11.8. Device as in Fig. 11.1. Displacement current as a function of position at various instants of time for an external excitation of a high current step ($t_1 = 0.31\times10^{-3}$, $t_2 = 0.61\times10^{-3}$, $t_3 = 0.90\times10^{-3}$, $t_4 = 1.19\times10^{-3}$, $t_5 = 2.20\times10^{-3}$, $t_6 = 4.17\times10^{-3}$, $t_7 = 6.19\times10^{-3}$, $t_8 = 8.57\times10^{-3}$).

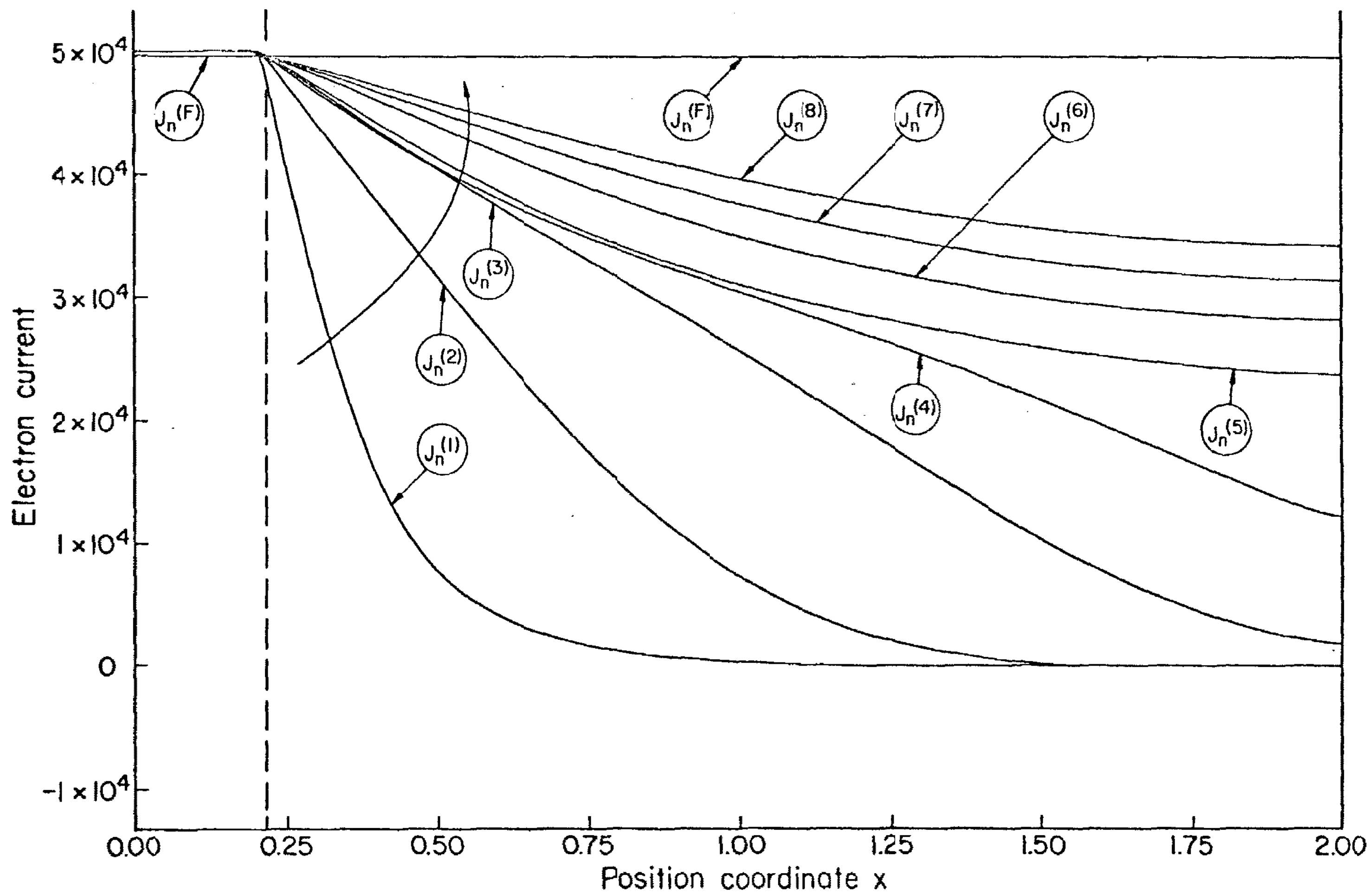

Fig. 11.9. Device as in Fig. 11.1. Electron current as a function of position at various instants of time (as in Fig. 11.8, and $t_F = \infty$) for an external excitation of a high current step.

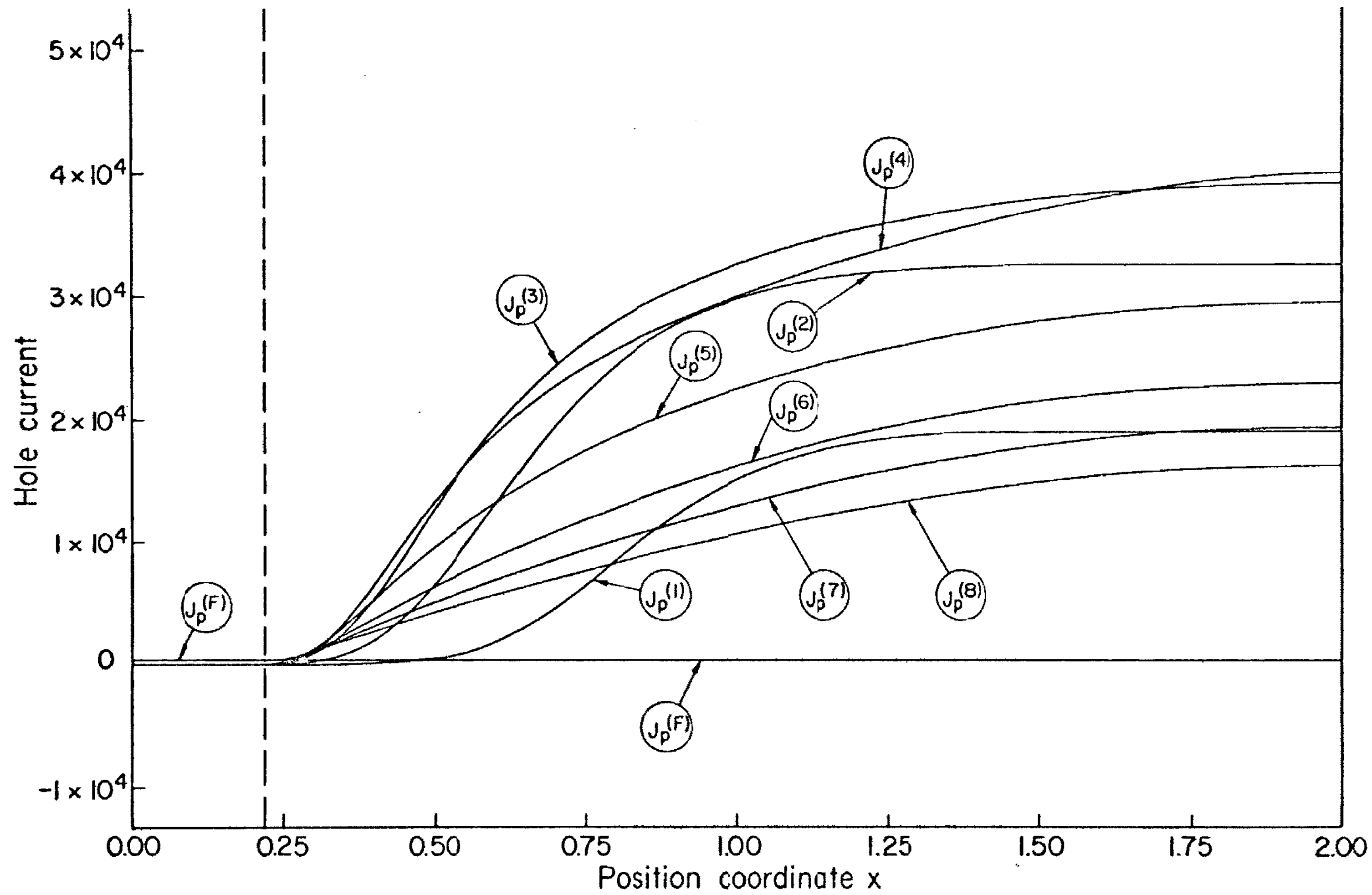

Fig. 11.10. Device as in Fig. 11.1. Hole current as a function of position at various instants of time (as in Fig. 11.9) for an external excitation of a high current step.

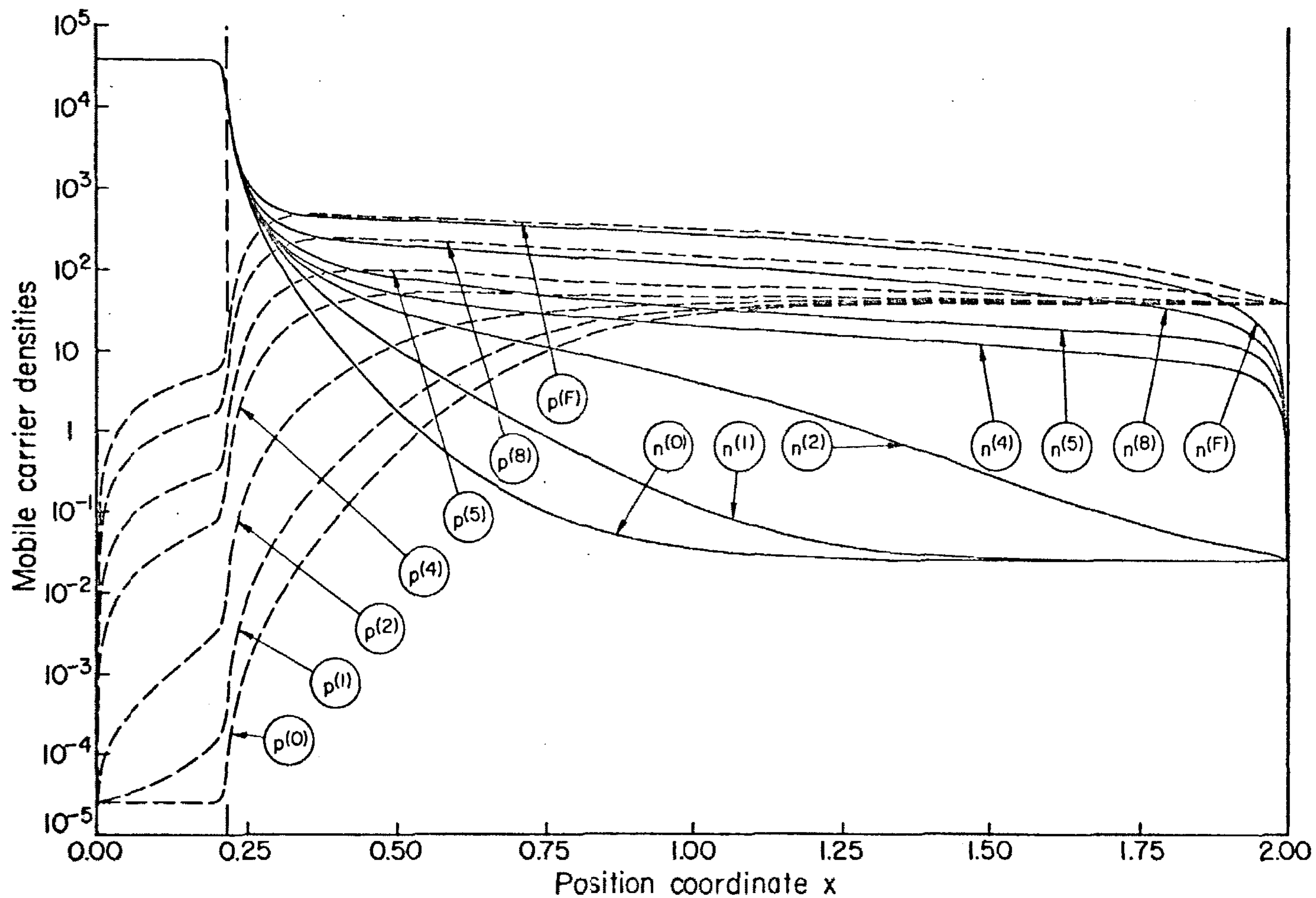

Fig. 11.11. Device as in Fig. 11.1. Mobile carrier densities as functions of position at various instants of time (as in Fig. 11.8, and $t_0 = 0$, $t_F = \infty$) for an external excitation of a high current step.

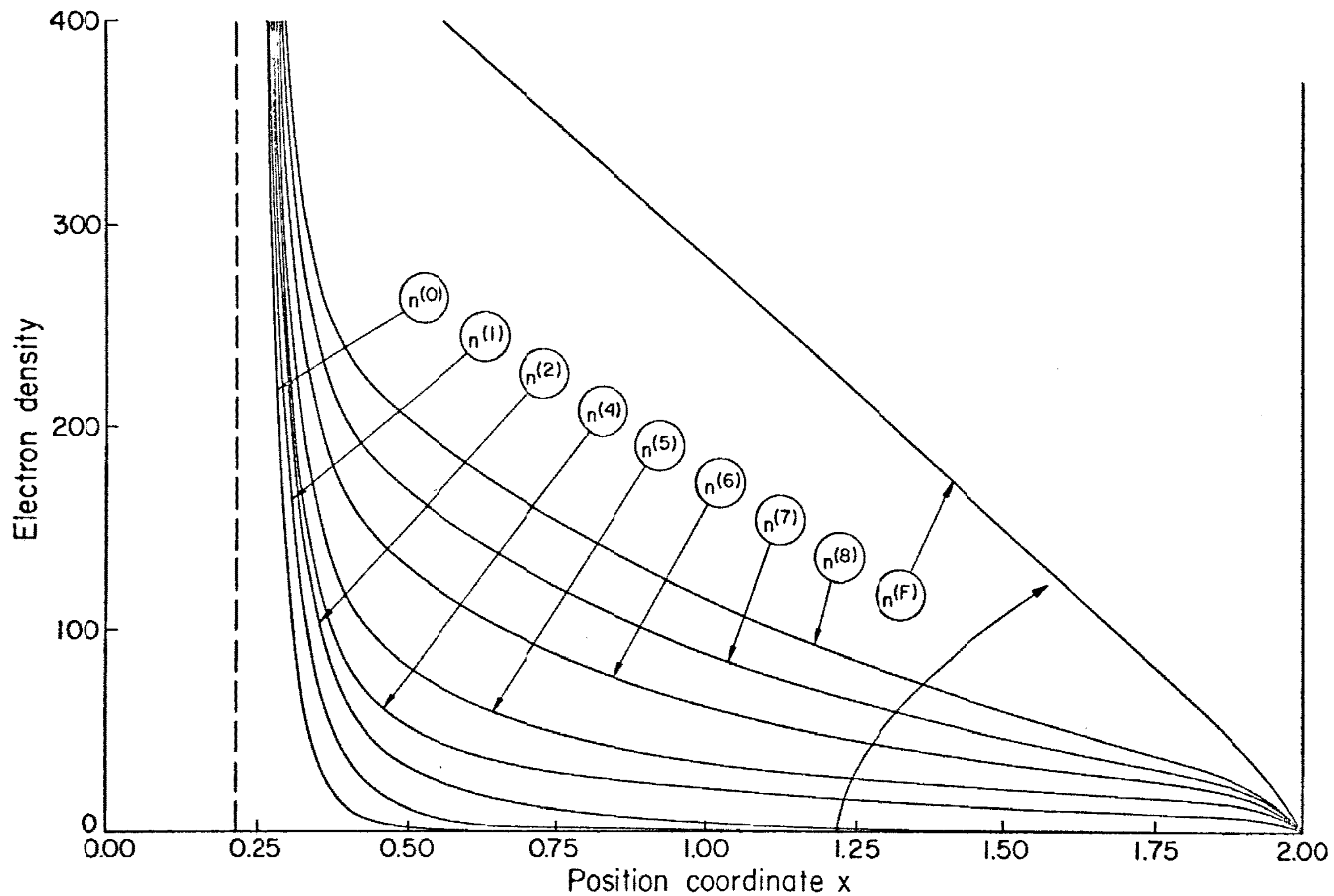

Fig. 11.12. Device as in Fig. 11.1. Electron density as a function of position at various instants of time (as in Fig. 11.11) for an external excitation of a high current step.

displacement, electron, and hole currents as functions of position are displayed at various instants of time in Figs. 11.8, 11.9, and 11.10 respectively, and the mobile carrier densities as functions of position in Figs. 11.11 (semilogarithmic scales) and 11.12 (linear scales).

The initial part $(t < \tau_{rP})$ of the terminal voltage time response (Fig. 11.7) is the result of the combination of two basic effects: the build-up of the ohmic voltage drop in the quasi-neutral P-region and the charge of the transition region capacitance. The first-order estimation of the ohmic voltage drop, in terms of the thermal equilibrium parameters w_P and σ_P, yields:

$$\Delta V\Big|_{\text{ohmic}} = \frac{J\, w_P}{\sigma_P} = 26.5 \quad \text{(or 0.685 volt)} \tag{11.6}$$

and an initial slope

$$\frac{V_A(t)}{t}\Bigg|_{\substack{\text{ohmic,}\\ \text{initial}}} = \frac{\Delta V\big|_{\text{ohmic}}}{\tau_{rP}} = \frac{26.5}{5.678\text{x}10^{-4}} \simeq 4.7 \times 10^4 \tag{11.7}$$

Furthermore the charge of the transition region capacitance C occurs with an estimated initial slope

$$\frac{V_A(t)}{t}\Bigg|_{\substack{\text{charge,}\\ \text{initial}}} = \frac{J_F}{C} = \frac{5 \times 10^4}{1.668} \simeq 3 \times 10^4 \tag{11.8}$$

The combination of the two effects yields a total slope of the initial part of the terminal voltage response:

$$\frac{V_A(t)}{t}\Bigg|_{\substack{\text{total,}\\ \text{initial}}} = \frac{V_A(t)}{t}\Bigg|_{\substack{\text{ohmic,}\\ \text{initial}}} + \frac{V_A(t)}{t}\Bigg|_{\substack{\text{charge,}\\ \text{initial}}} = 7.7 \times 10^4 \tag{11.9}$$

The "exact" response (Fig. 11.7) is well in agreement with the estimation(11.9). It may be noted that, for increasing times, both w_p and C increase, so that the above estimation, in terms of thermal equilibrium parameters, is only valid for short times. At later times $(t > 8 \times 10^{-4})$ conductivity modulation effects, essentially absent in the initial part of the response, are dominant so that the terminal voltage decays to its final steady-state value with a time constant essentially equal to the transit time of electrons in the quasi-neutral P-region. This transit time differs from the low-injection value(11.2)since the motion of minority carriers (electrons) is ruled by both drift and diffusion phenomena, as a result of the conductivity modulation, and since the quasi-neutral P-region is significantly wider at high injection levels.

The two curves of Fig. 11.7 refer to solutions obtained in identical conditions with two different discretization schemes: the generalized pure implicit (Subsection 8.2.1) and the generalized Crank-Nicholson scheme (Subsection 8.2.2). The two schemes feature truncation errors in the time domain differing essentially by one order of magnitude (Appendix F). The comparison between the two results may serve as an estimation of the overall influence of the truncation error, for the time step size employed. The unevenly spaced time points actually used for this calculation are indicated by vertical segments on the curves, and have been automatically selected by the procedure described in Section 8.4. The little discrepancy $(< 1.5\%)$ between the two curves, despite the relatively large size of the time steps, is an indication of the sufficient accuracy of the discretization schemes. Additional calculations have been performed with considerably larger time steps, for a

given discretization scheme, to test the influence of the time step size on the truncation error in the time domain. The insignificant variations of the respective responses are once more indicative of the insensitivity of the results achieved upon the discretization error.

The three current components are separately displayed in Figs. 11.8 to 11.10 as functions of position for various instants of time ($t_1 = 0.31 \times 10^{-3}$, $t_2 = 0.61 \times 10^{-3}$, $t_3 = 0.90 \times 10^{-3}$, $t_4 = 1.19 \times 10^{-3}$, $t_5 = 2.20 \times 10^{-3}$, $t_6 = 4.17 \times 10^{-3}$, $t_7 = 6.19 \times 10^{-3}$, $t_8 = 8.57 \times 10^{3}$, $t_F = \infty$). The same situation discussed in the previous example for the low current step is here present in the high conductivity (N) side and in the transition region, aside from quantitative discrepancies such as a more significant decrease of the transition region width for increasing time. In the quasi-neutral P-region, though, the displacement current features a basically different pattern. The initial decrease of the (positive) displacement current, which corresponds to the build-up of the ohmic potential drop in the P-side, is followed by an inversion of sign and subsequent decrease in magnitude toward its steady-state zero value. The reversal of the direction of the displacement current flow is a consequence of the decrease of voltage drop in a region whose conductivity is becoming modulated. The modulation initiates in the quasi-neutral P-region at the edge of the transition region and evolves gradually towards the external contact L. This evolution is particularly evident in the spatial distribution of the displacement current at the instant t_3 (Fig. 11.8) which shows how the voltage drop is already decreasing (for increasing time) in the increasingly modulated

region close to the transition region, and is still increasing in the region close to the external contact.

The conductivity modulation is well apparent in the spatial distribution of the mobile carrier densities of Fig. 11.11. The discrepancy between the injected minority carrier density in the P-region at the instants t_8 and t_F, exposed in the linear expansion of Fig. 11.12, and the absence of displacement current for $t_8 \le t \le t_F$ indicates that the terminal part of the transient response is essentially determined by the motion of mobile carriers.

11.2.3. Excitation: a spike of current.

The forward current spike defined by:

$$J(t) = 0 \qquad t \le 0$$

$$J(t) = 5 \times 10^4 \; t/t_1 \qquad 0 < t \le t_1 = 4 \times 10^{-5}$$

$$J(t) = 0 \qquad t > t_1$$

is applied to the device initially in thermal equilibrium. This is, of course, also the final state of the device.

The response of the device is illustrated in Figs. 11.13 to 11.15. The terminal voltage as a function of time is shown in Fig. 11.13, the electric field and the increments of mobile carrier densities $[n(x,t) - n(x,t{=}0),\ p(x,t) - p(x,t{=}0)]$ as functions of position are displayed at various instants of time ($t_1 = 4 \times 10^{-5}$, $t_2 = 3 \times 10^{-4}$, $t_3 = 1.4 \times 10^{-3}$, $t_4 = 5.4 \times 10^{-2}$, $t_5 = 0.405$, $t_6 = 1.205$) in Figs. 11.14 and 11.15 respectively. Three distinct phases characterize the evolution of the overall transient response.

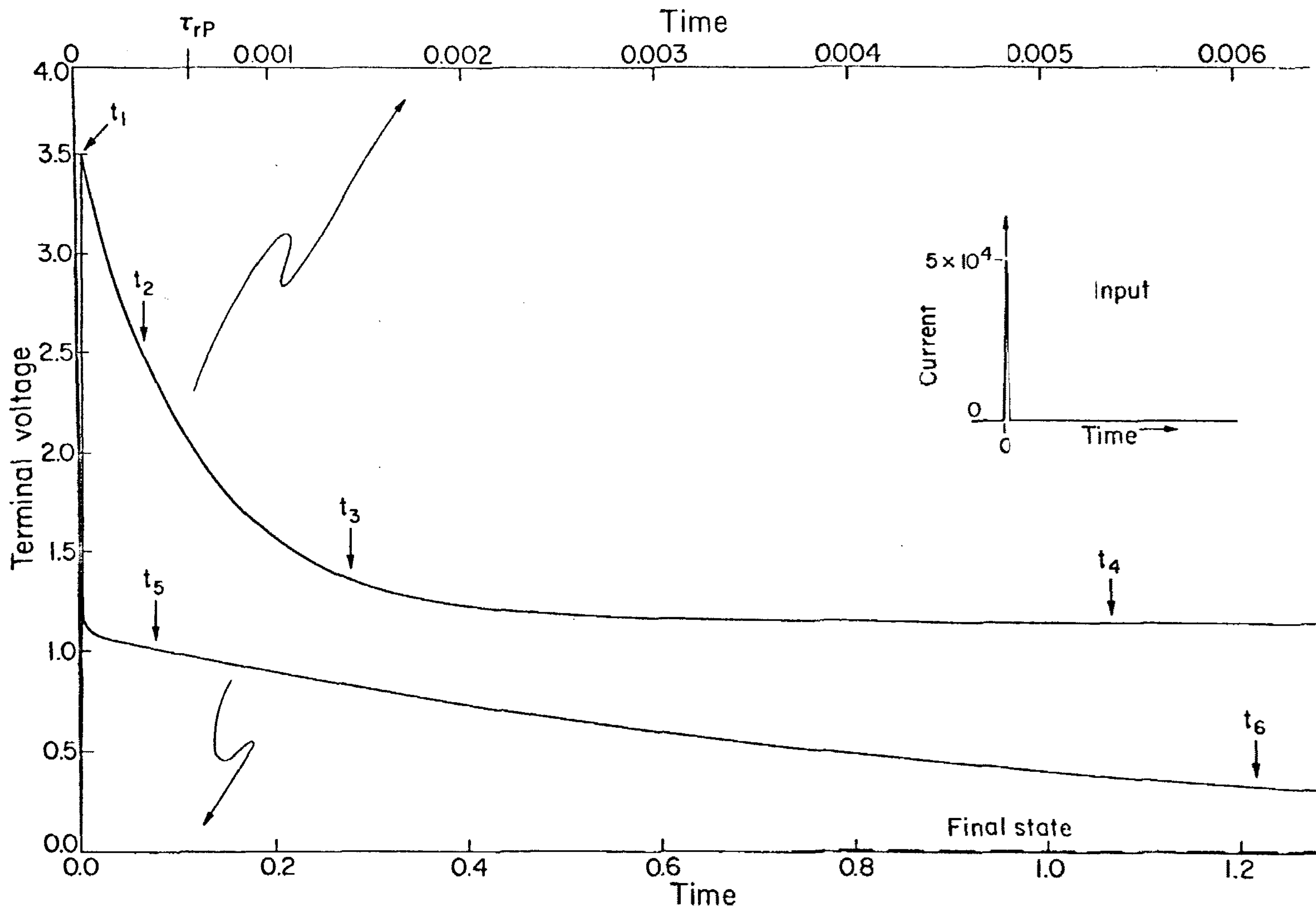

Fig. 11.13. Device as in Fig. 11.1. Terminal voltage as a function of time for an external excitation of a current spike.

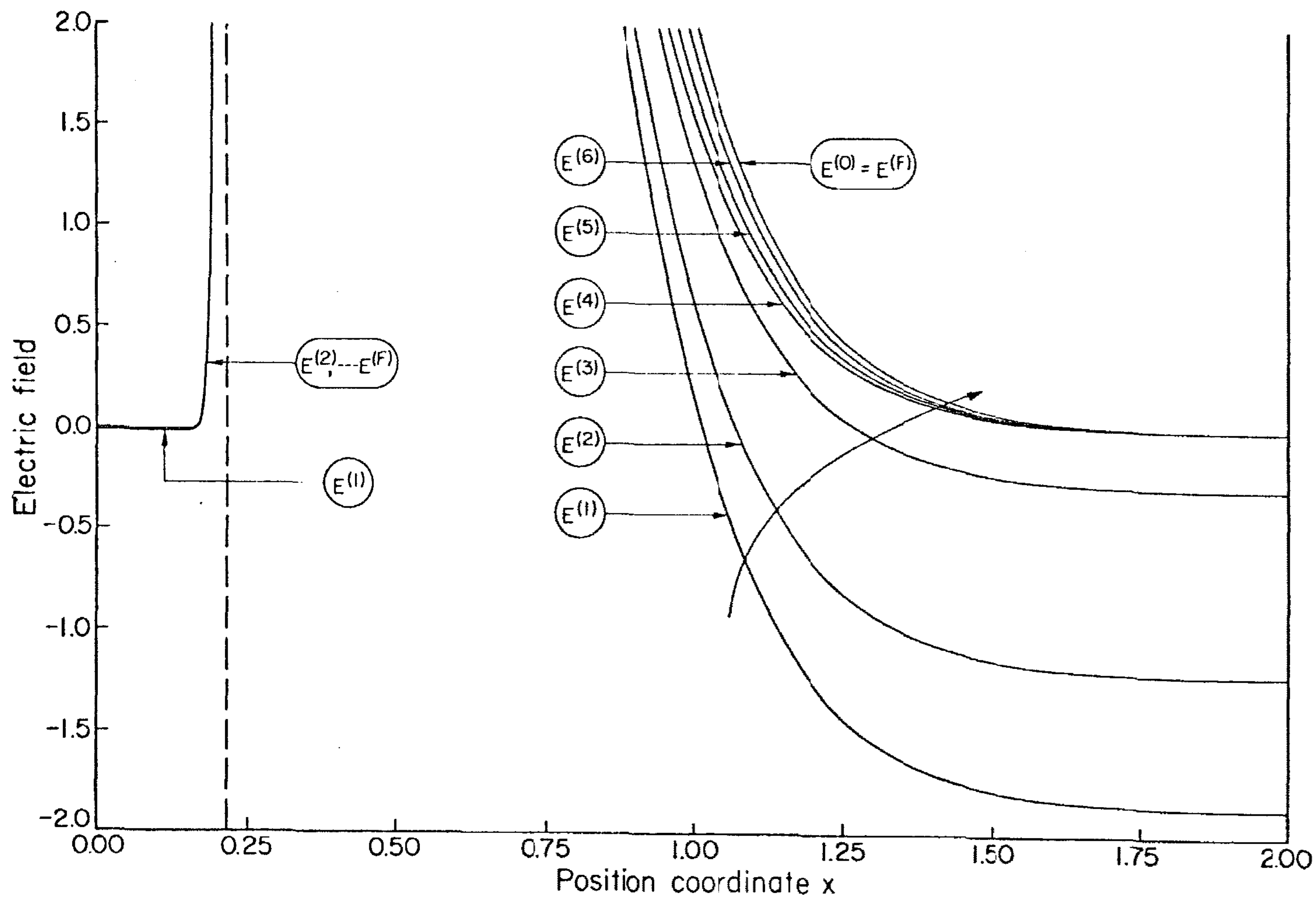

Fig. 11.14. Device as in Fig. 11.1. Electric field as a function of position at various instants of time for an external excitation of a current spike ($t_0 = 0$, $t_1 = 4\text{x}10^{-5}$, $t_2 = 3\text{x}10^{-4}$, $t_3 = 1.4\text{x}10^{-3}$, $t_4 = 5.4\text{x}10^{-2}$, $t_5 = 0.405$, $t_6 = 1.205$, $t_F = \infty$).

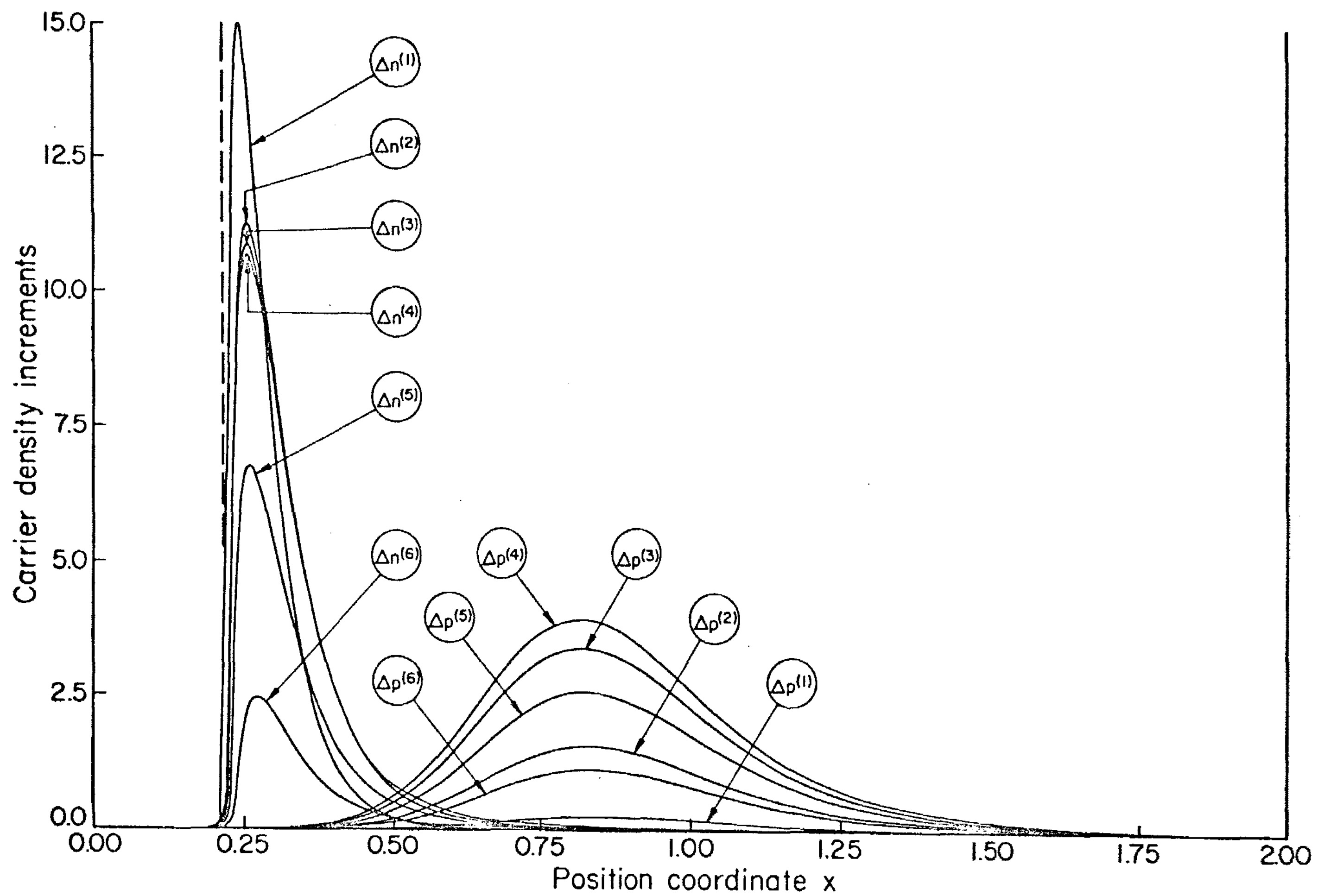

Fig. 11.15. Device as in Fig. 11.1. Time increments of mobile carrier densities as functions of position at various instants of time (as in Fig. 11.14) for an external excitation of a current spike.

Phase I. The initial part $(t \le t_1)$ of the terminal voltage response is due to the combined effects of the ohmic voltage drop in the quasi-neutral P-region and of the charge of the transition region capacitance. An identical situation was discussed in the previous example (Subsection 11.2.2), where the phenomena evolved until completion. In the present case, instead, they are aborted for $t > t_1$. The first-order estimation of the initial slope of the terminal voltage response is given by the relation (11.9), so that the value of the terminal voltage at $t = t_1$ may be estimated as:

$$V_A(t = t_1) = \left.\frac{V_A(t)}{t}\right|_{\text{initial}} \times t_1 = 7.7 \times 10^4 \times 4 \times 10^{-5} = 3.08$$

which is sufficiently in agreement with the "exact" value of Fig. 11.13. During this initial phase the electric field changes significantly both in the transition region and in the quasi-neutral P-region (Fig. 11.14). A considerable increment of electric charge density (due to electrons, Fig. 11.15) is built up in the transition region at the edge of the N-side, balanced by an essentially equivalent dielectric charge on the surface $x = L$ in the amount $-E(x=L) \cong 1.93$ (Fig. 11.14, and Eq. (7.4)), apart from the small contribution of the increment of hole density at $t = t_1$.

Phase II. The dominant phenomenon of this second phase $(t_1 < t < 4\tau_{rP} \cong 2.3 \times 10^{-3})$ is the relaxation of the ohmic voltage drop in the quasi-neutral P-region to its thermal equilibrium zero value (Fig. 11.14), with time constant τ_{rP}. As a consequence, the terminal voltage decays to a value V_C essentially equal to the initial voltage

drop on the transition region capacitance estimated on the basis of the slope (11.8) as:

$$V_C = \left.\frac{V_A(t)}{t}\right|_{\substack{\text{charge,}\\ \text{initial}}} \times t_1 = 3 \times 10^4 \times 4 \times 10^{-5} = 1.2 \qquad (11.10)$$

in agreement with the "exact" response (Fig. 11.13). Simultaneously, the increment of hole density increases (Fig. 11.15), as a result of a drift of holes governed by the electric field converging, on both sides, toward the interface between the transition region and the quasi-neutral P-region. Furthermore, the peak of the electron density increment decreases, even though the overall electron charge remains constant, and becomes balanced by an equal amount of charge due to the hole increment, as the sheet of charge at $x = L$ disappears.

Phase III. The transition region capacitance, initially charged to V_C (relation (11.10)), is discharged essentially through the incremental resistance of the diode. This is the only phenomenon responsible for the terminal voltage decay from V_C to the final steady-state zero value, since the only variations of the field occur in the transition region (Fig. 11.14). A first-order estimation of the terminal voltage response during this phase may be attempted by analyzing the discharge of a lumped constant capacitor C (equal in value to the transition region capacitance), initially charged at V_C, through a variable resistor whose characteristic is determined by the steady-state current-voltage relationship of the diode ((A-51), of Appendix A) for low injection levels. If J_{Sat} is the saturation current (A-53), the terminal voltage obeys then the equation:

$$\frac{dV_A(t)}{dt} = -\frac{J_{Sat}}{C}\left[e^{V_A(t)} - 1\right] \qquad (11.11)$$

with solution

$$V_A(t) = V_C + \frac{J_{Sat}}{C} t + \ln\left[\frac{e^{V_A(t)} - 1}{e^{V_C} - 1}\right]. \qquad (11.12)$$

The estimation (11.11) yields at $V_A(t) = 1$ a slope

$$\frac{dV_A(t)}{dt} = -\frac{n_P}{\gamma_n w_P C}(e-1) \simeq -\frac{93}{40 \times 0.94 \times 1.67}(1.7) \simeq 2.5$$

which differs essentially by a factor of 2 from the "exact" value of Fig. 11.13. This discrepancy, not at all surprising, is to be attributed to the insufficiency of the model, on which the estimation is based, and to the inaccuracy of the steady-state first-order parameters used.

11.2.4. Excitation: a low voltage-step.

A step of voltage in the forward direction is applied to the device initially in thermal equilibrium. In the discretized context the ideal step is approximated by a ramp, whose slope is a determinant parameter very much affecting the initial response of the device. The applied voltage ramp is defined by:

$$\left.\begin{array}{ll} V_A(t) = 0 & t \le 0 \\ V_A(t) = 3.86\,\frac{t}{t_1} & 0 \le t \le t_1 = 2 \times 10^{-5} \\ V_A(t) = V_{AF} = 3.86 \text{ (or 0.1 volt)} & t \ge t_1 \end{array}\right\} \qquad (11.13)$$

The instant t_1 is taken as the first time point in the actual generation of the solution. The final state is a low-injection steady-state condition, characterized by a total current $J_F \cong 84$ and a first-order injection parameter $\chi \cong 0.029$.

The response of the device is illustrated in Figs. 11.16 to 11.22. The total current as a function of time is shown in Fig. 11.16 (in two different time scales), the ratios between the three current components and the total current as functions of position are separately displayed in Figs. 11.17, 11.18, and 11.19 respectively, the electrostatic potential and the mobile carrier densities as functions of position in Figs. 11.20, 11.21 and 11.22. The spatial distributions are shown at various instants of time ($t_1 = 2 \times 10^{-5}$, $t_2 = 5 \times 10^{-4}$, $t_3 = 1.9 \times 10^{-3}$, $t_4 = 3.9 \times 10^{-3}$, $t_5 = 7.9 \times 10^{-3}$, $t_6 = 1.6 \times 10^{-2}$, $t_7 = 3.6 \times 10^{-2} \cong t_F$).

Whereas an ideal step of voltage would be responsible for an infinite total current (essentially displacement current) at $t = 0^+$, the ramp of voltage (11.13) generates a finite current at any instant of time. The initial part $(t \le t_1)$ of the current response (Fig. 11.16) is ruled, just as in the previous examples, by the build-up of the ohmic voltage drop in the quasi-neutral P-region and by the charge of the transition region capacitance. Since the time constants of these two phenomena are considerably larger than t_1, the linear approximation on the initial terminal voltage response of Subsections 11.2.1 to 11.2.3 may also be used here to estimate the current at the instant t_1. The ohmic voltage drop may be attributed to a fraction α of the slope of the voltage ramp (11.13), and the charge of the transition region

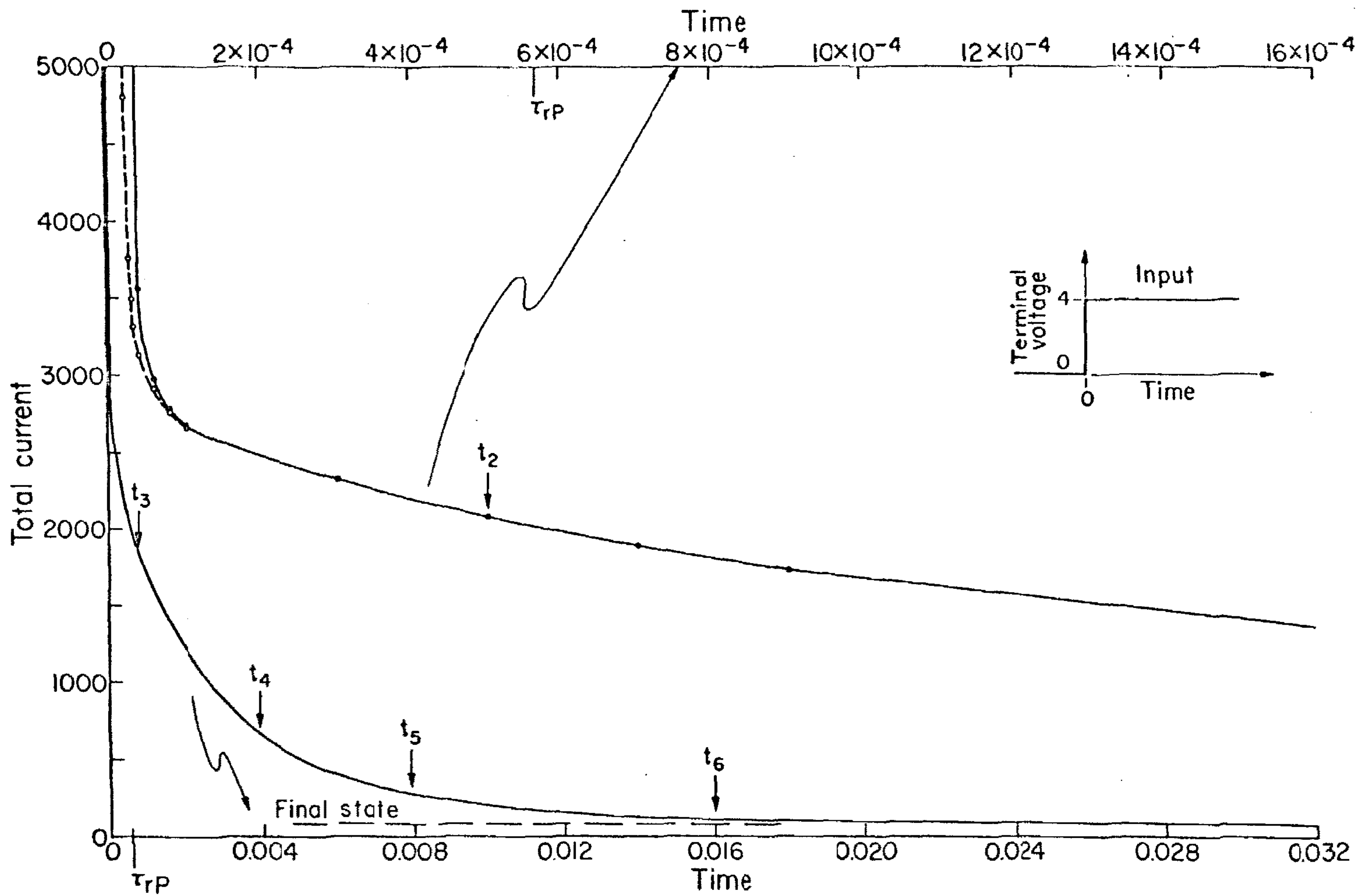

Fig. 11.16. Device as in Fig. 11.1. Total current as a function of time for an external excitation of a low terminal voltage step.

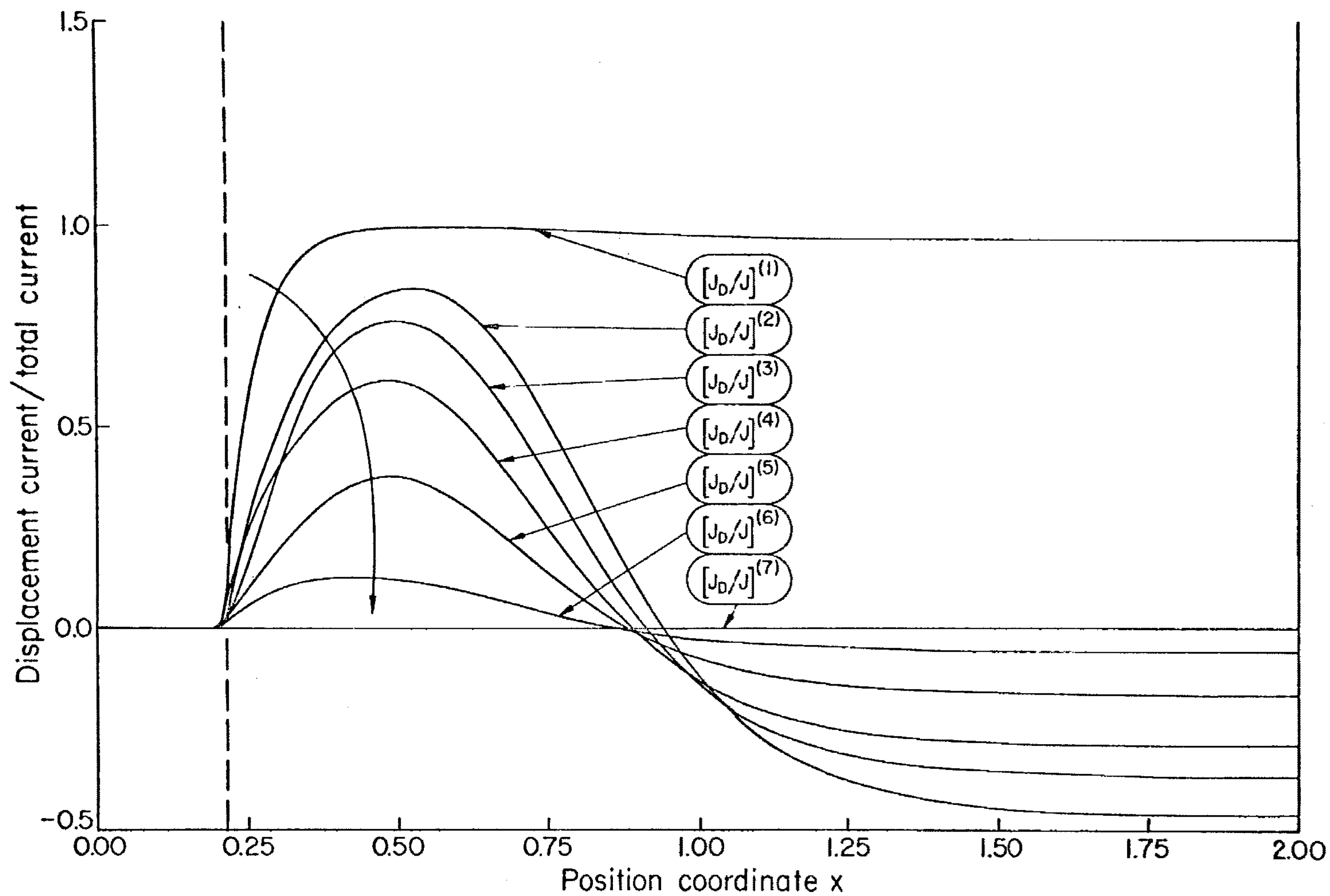

Fig. 11.17. Device as in Fig. 11.1. Ratio between the displacement current and the total current as a function of position at various instants of time for an external excitation of of a low terminal voltage step ($t_1 = 2\times10^{-5}$, $t_2 = 5\times10^{-4}$, $t_3 = 1.9\times10^{-3}$, $t_4 = 3.9\times10^{-3}$, $t_5 = 7.9\times10^{-3}$, $t_6 = 1.6\times10^{-2}$, $t_7 = 3.6\times10^{-2}$).

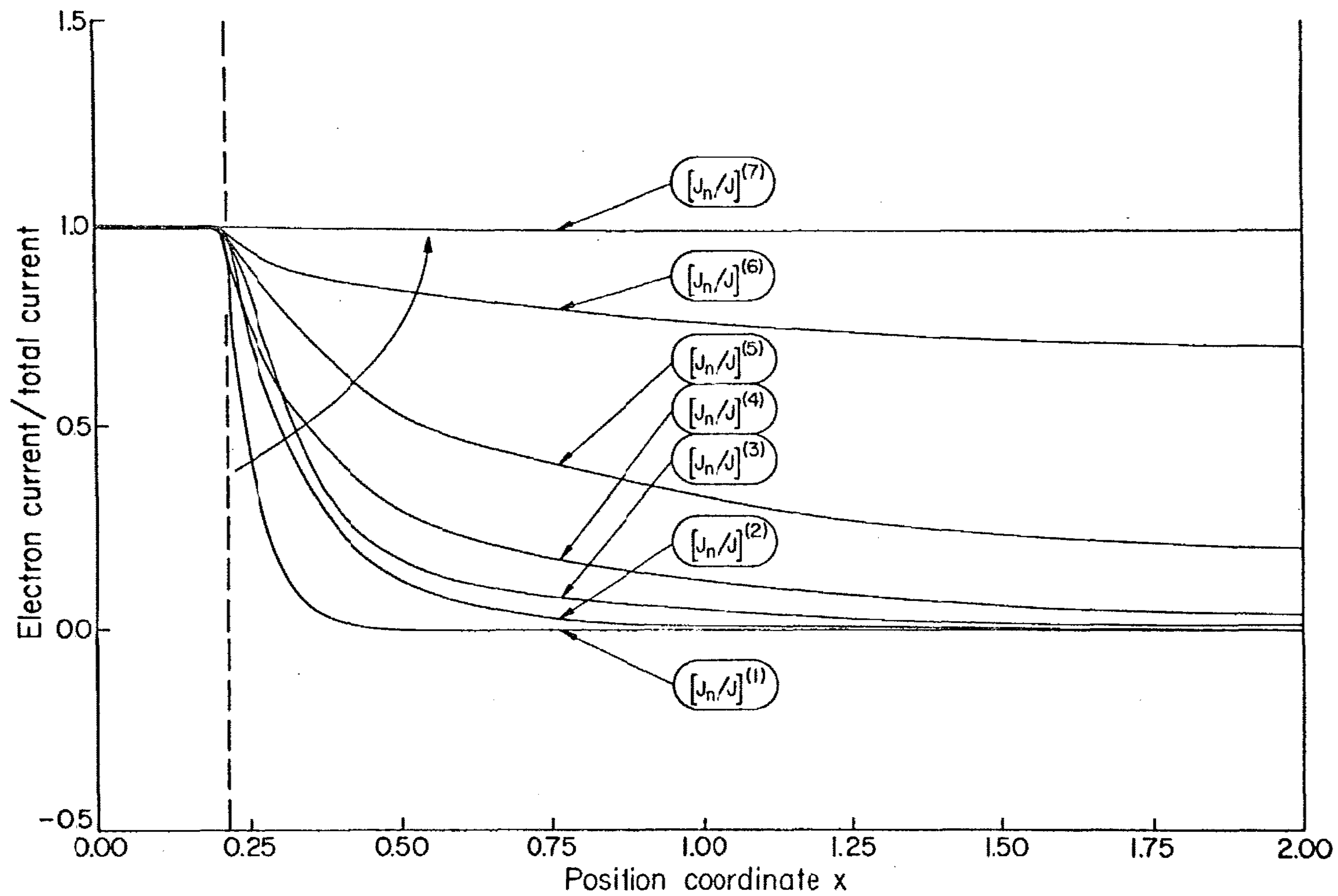

Fig. 11.18. Device as in Fig. 11.1. Ratio between the electron current and the total current as a function of position at various instants of time (as in Fig. 11.17) for an external excitation of a low terminal voltage step.

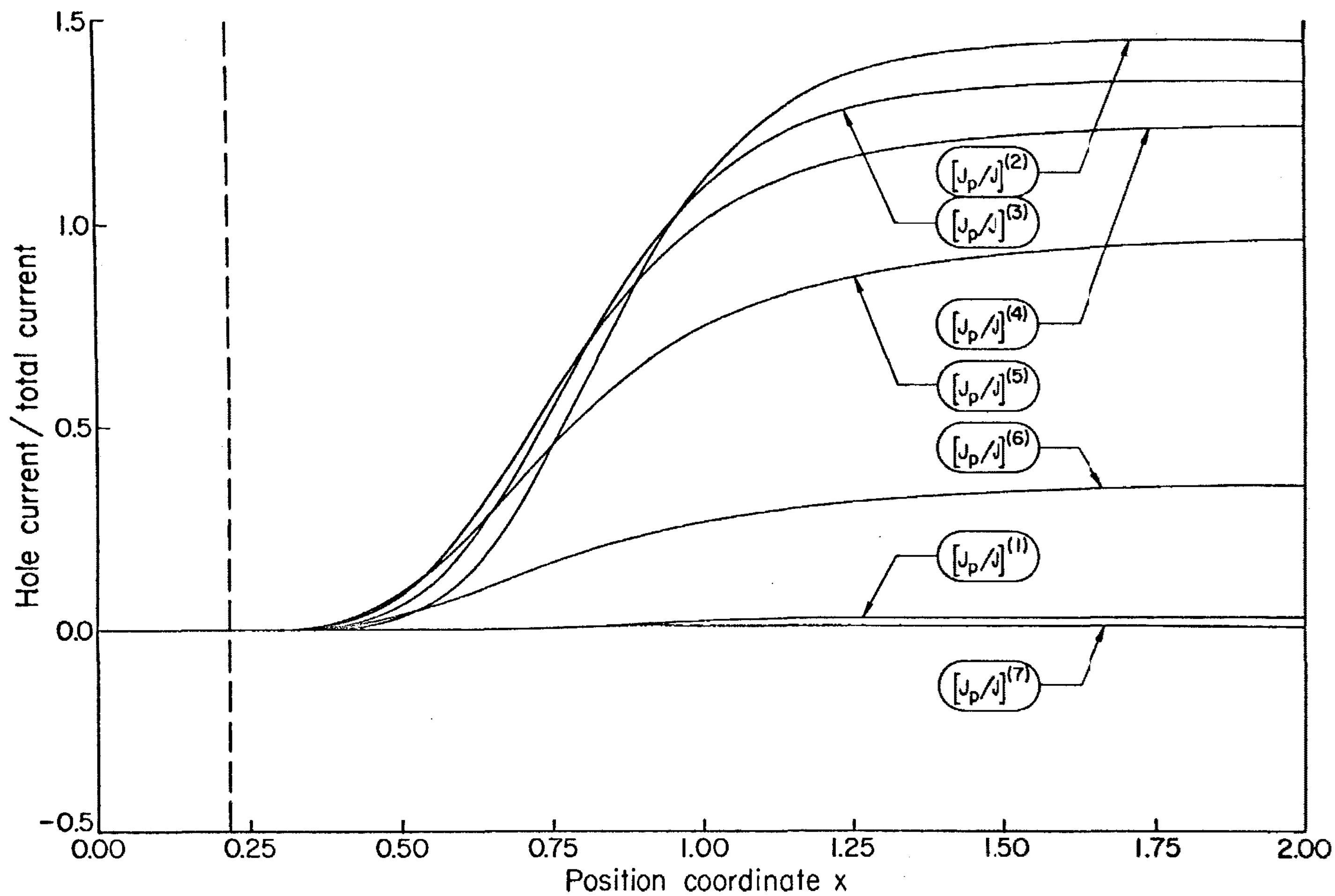

Fig. 11.19. Device as in Fig. 11.1. Ratio between the hole current and the total current as a function of position at various instants of time (as in Fig. 11.17) for an external excitation of a low terminal voltage step.

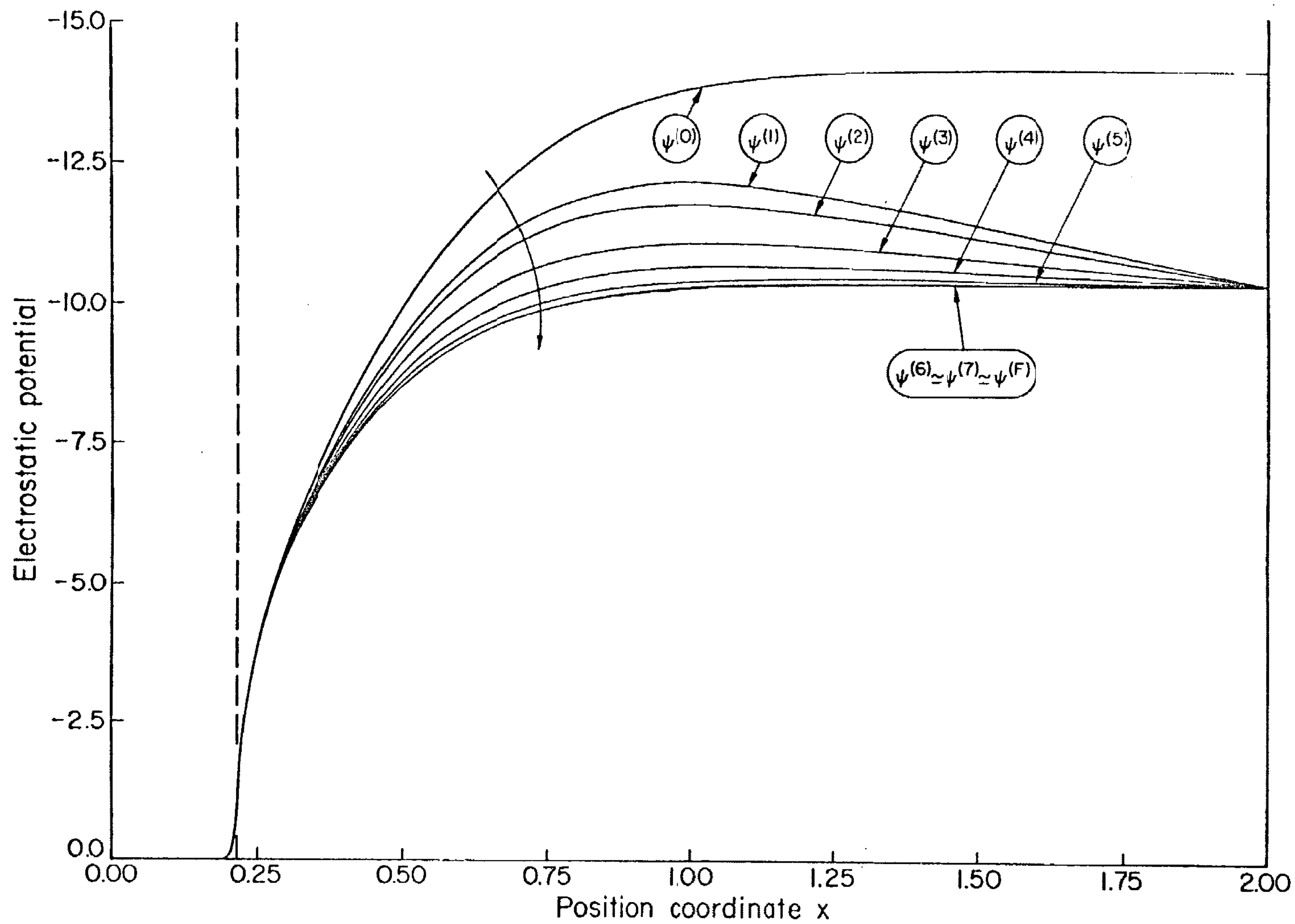

Fig. 11.20. Device as in Fig. 11.1. Electrostatic potential as a function of position at various instants of time (as in Fig. 11.17 and $t_0 = 0$, $t_F = \infty$) for an external excitation of a low terminal voltage step.

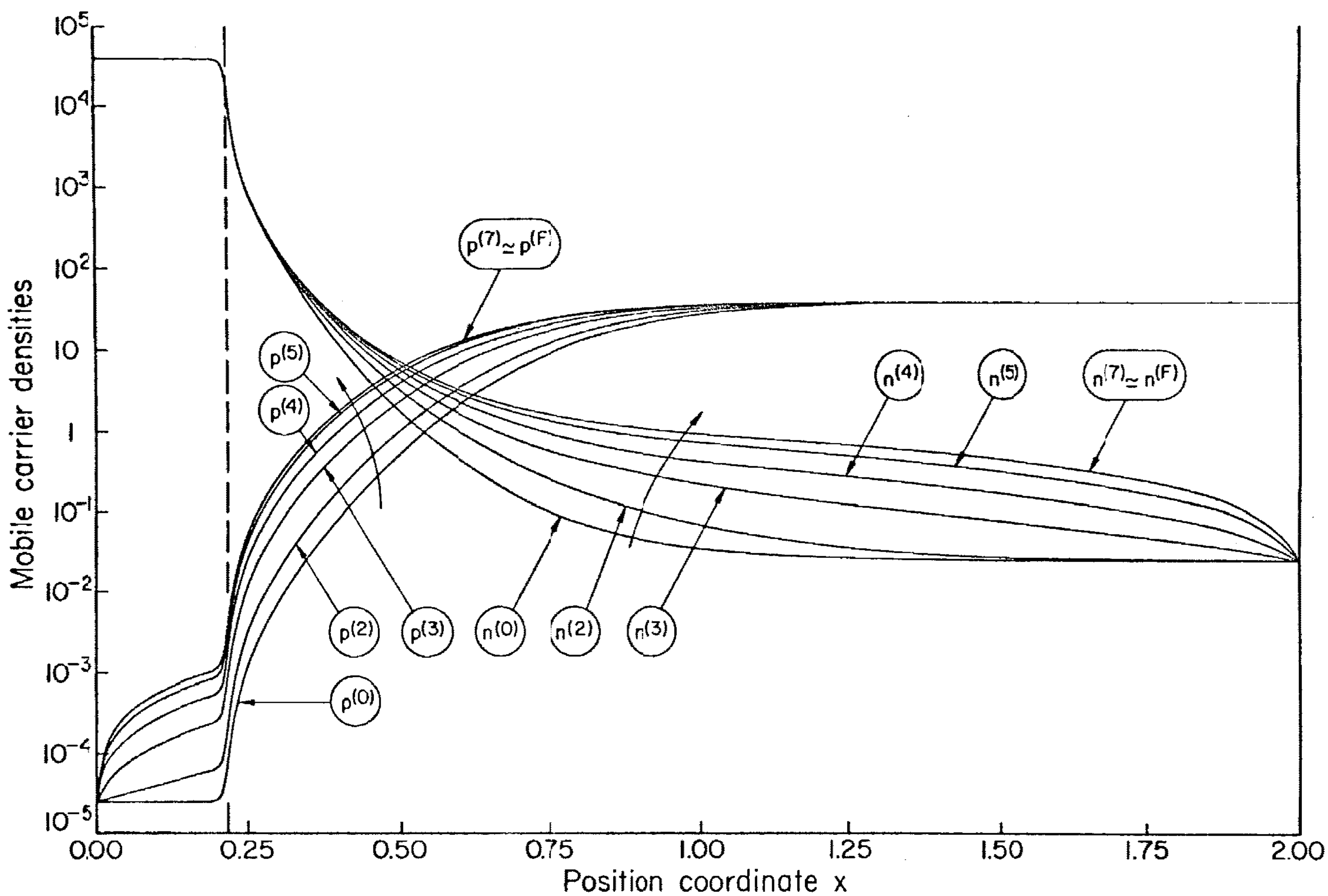

Fig. 11.21. Device as in Fig. 11.1. Mobile carrier densities as functions of position at various instants of time (as in Fig. 11.20) for an external excitation of a low terminal voltage step.

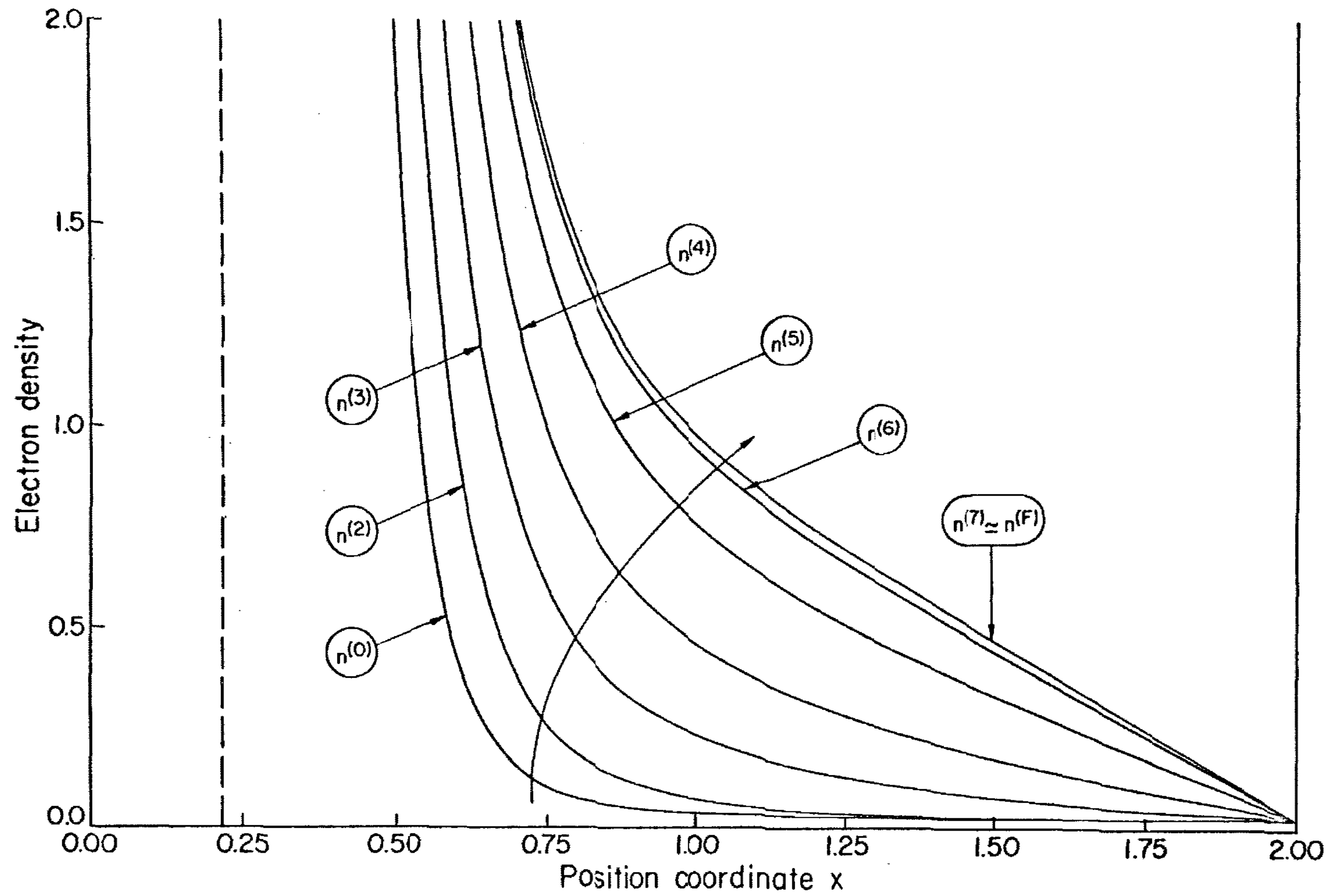

Fig. 11.22. Device as in Fig. 11.1. Electron density as a function of position at various instants of time (as in Fig. 11.20) for an external excitation of a low terminal voltage step.

capacitance to the remaining fraction $1 - \alpha$. If the expressions (11.6) to (11.9) are used with the first-order thermal equilibrium parameters, the estimated value of the current a the instant t_1 is given by:

$$\left.\begin{aligned} J(t_1) &= \alpha \frac{V_{AF}}{t_1} \frac{\sigma_P \tau_{rP}}{w_P} \\ J(t_1) &= (1-\alpha) \frac{V_{AF}}{t_1} C \end{aligned}\right\} \qquad (11.14)$$

or

$$J(t_1) = \frac{V_{AF}}{t_1}\left[\frac{w_P}{\sigma_P \tau_{rP}} + \frac{1}{C}\right]^{-1} \simeq 1.25 \times 10^5$$

which is sufficiently in agreement with the exact value 1.13×10^5 (not shown in Fig. 11.16). Except in the N-side, the displacement current accounts essentially for the total current at the instant t_1 (since $\tau_{rN} << t_1 << \tau_{rP}$). This is related to the relatively abrupt initial change of the spatial distribution of the electrostatic potential well apparent in Fig. 11.20, with consequent increase of the magnitude of the (negative) electric field in the quasi-neutral P region.

At later times $(t > t_1)$ the response of the device is governed by three phenomena: the relaxation of most of the ohmic voltage drop in the quasi-neutral P-region, the completion of the charge of the transition region capacitance, and the diffusion of the minority carriers (electrons) in the quasi-neutral P-region. Whereas the time constants of the first two effects are dependent upon the current, and therefore are time dependent, the time constant of the third effect may be taken

as the steady-state transit time τ_t, current independent and therefore essentially constant. The relaxation of the ohmic drop generates an inversion of the displacement current in the quasi-neutral P region (Fig. 11.17), related to the decrease of the magnitude of the (negative) electric field (Fig. 11.20). This current is balanced by an essentially equal and opposite hole current in that region until the electron current fraction is permitted to increase significantly at later times $(t > \tau_t)$ and become the dominant component. In the transition region the decreasing displacement current fraction, balanced by an increasing electron current contribution, completes the charge of the transition region capacitance.

The overall transient response essentially reaches the final state within $5\,\tau_t \cong 0.026$, since transit time effects become dominant at later times. The influence of these effects may be recognized in the spatial distributions of the injected minority carriers (electrons) in the quasi-neutral P-region (Fig. 11.22): these feature a significant curvature in the vicinity of the transition region, as opposed to the closely linear quasi-steady-state distributions.

In order to test the influence of the discretization error in the time domain due to abrupt variations of the external excitation in the critical part of the response $(t < 4\,\tau_{rP})$, calculations have been repeated for smaller time step sizes in both the initial phase $(t \leq t_1)$ and in the following relaxation period. Of course, the original excitation has been maintained in the original form (11.13). As a result, transient responses have been observed to be very much sensitive in the critical period to the step size, as expected. However, the current

at the instant t_1 is not affected significantly (within a few percent) by the time step size, even for the extreme case (discussed above) in which t_1 is taken as the first internal time point of the discretization mesh. Furthermore, for $t > t_1$, various current responses, obtained for different time step sizes, converge after a short time to a unique curve, rather insensitive (within limits) to a variation of the mesh size. This is indicated in Fig. 11.16 by the dashed curve converging to the solid curve (the original response) at $t = 4\ \tau_{rP}$. The actual time points employed for the calculation are indicated by dots on the two curves. It may be concluded that, although the transient response is highly dependent upon the time-step size within critical time intervals featuring abrupt excitations, accurate solutions are generated for later times even by coarse discretization schemes. This valuable feature may be usefully exploited to decrease the computation load, if the achievement of a high degree of accuracy in the vicinity of abrupt excitations is not of interest.

11.3. The interaction of the N-P diode and an external resistor under switching conditions.

A slightly longer N-P structure (Fig. 11.23) is analyzed under switching conditions from a forward bias [initial external current $I(t=0) = 2$ ma] to a reverse bias condition driven by a constant voltage source $V_B(\ = 3$ volt) through a resistor $R(= 150\ \Omega)$. The same idealized model of Section 11.2, characterized by absence of generation-recombination in the interior, abrupt asymmetric impurity distribution, constant mobilities and ohmic contacts, is assumed. The method of solution employed has been illustrated in Section 9.4.

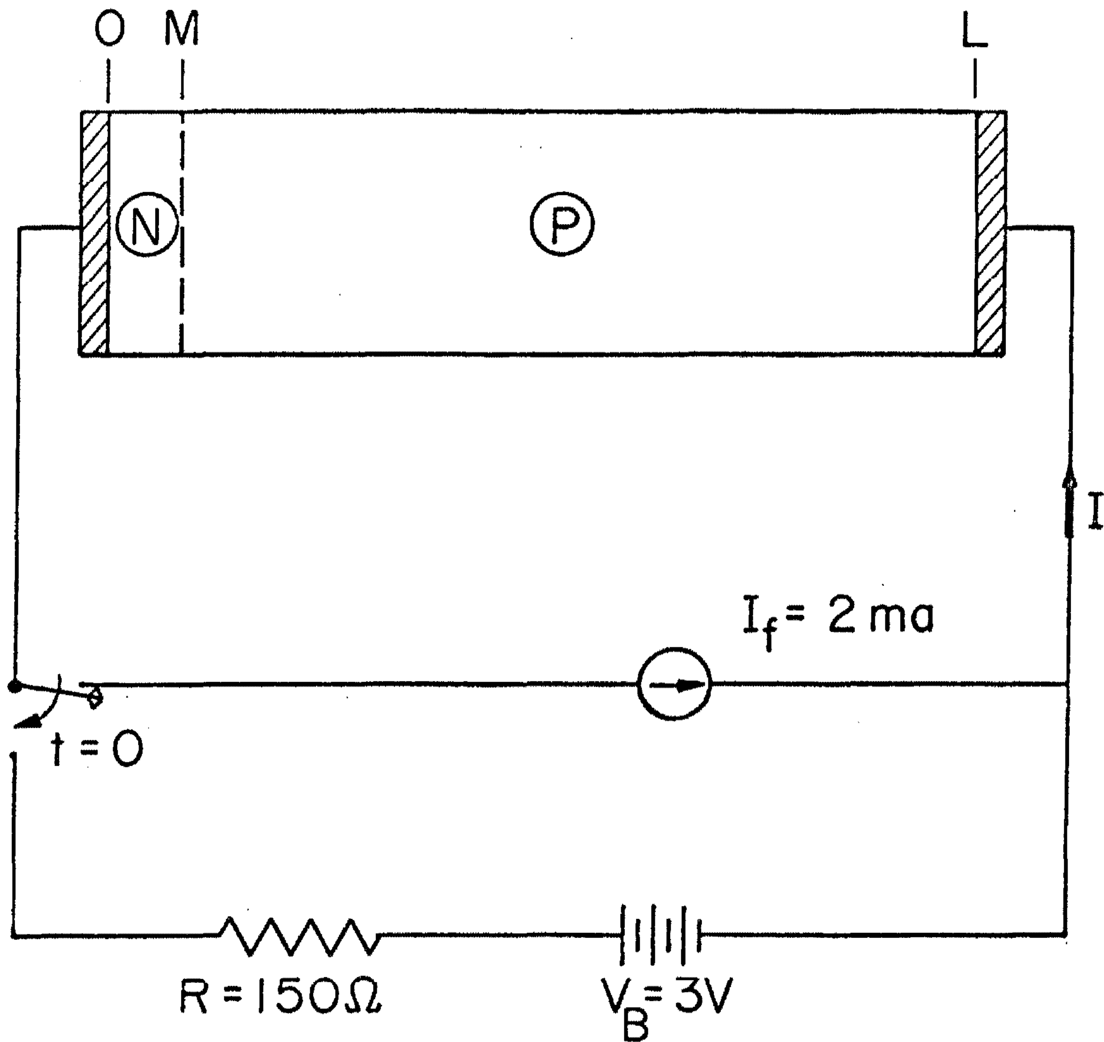

Fig. 11.23. Parameters of Table 11.1 with modified lengths as in Section 11.3; boundary conditions (1.32). Circuit topology for the analysis of the interaction of an N-P diode and an external resistor under switching from a forward to a reverse bias condition.

The structure is characterized by the physical parameters listed in Table 11.1 and in Section 11.2, with exception of the following:

$$\text{length:} \begin{cases} \text{N-side,} & M-O = 0.22 \quad (\text{or } 0.2105 \times 10^{-4} \text{ cm}) \\ \text{P-side,} & L-M = 29.78 \quad (\text{or } 28.49 \times 10^{-4} \text{ cm}) \\ \text{total,} & L-O = 30.00 \quad (\text{or } 28.70 \times 10^{-4} \text{ cm}) \end{cases}$$

cross-sectional area of the device:

$$A = 2.8954 \times 10^{4} \qquad (\text{or } 2.65 \times 10^{-4} \text{ cm}^2)$$

first-order theory width of the quasi-neutral P region:

$$\begin{cases} \text{initial state,} & w_P\big|_{in} = L - M_P\big|_{in} = 29.2 \quad (\text{or } 27.9 \times 10^{-4} \text{ cm}) \\ \text{final state,} & w_P\big|_{fin} = L - M_P\big|_{fin} = 27.2 \quad (\text{or } 26.0 \times 10^{-4} \text{ cm}) \end{cases}$$

first-order theory low-injection transit time of electrons in the quasi-neutral P-region, corresponding to an average $w_P\big|_{av} \cong 28.2$:

$$\tau_t\big|_{av} = \frac{\gamma_n\left(w_P\big|_{av}\right)^2}{2} \cong 4.3 \quad (\text{or } 39.4 \times 10^{-9} \text{ sec})$$

$$\text{initial state:} \begin{cases} \text{external current,} & I(t=0) = 2 \text{ ma} \\ \text{terminal voltage,} & V_A(t=0) = 0.2115 \text{ volt} \\ \text{injection parameter,} & \chi(t=0) \cong 0.95 \end{cases} \qquad (11.15)$$

$$\text{final state:} \begin{cases} \text{external current,} & I(t=t_F) = 1\ \mu a \\ \text{terminal voltage,} & V_A(t=t_F) \cong -3\ \text{volt} \end{cases} \qquad (11.16)$$

Furthermore, the relation

$$I(t) = -\frac{V_B + V_A(t)}{R} \qquad (11.17)$$

is valid at any time $t > 0$.

A structure featuring a considerably longer P-side, as opposed to that analyzed in the previous Section, has been selected, in order to expose the various phenomena occuring in the present case. For convenience, quantities referring to the external circuit (time, current, voltage, resistance) are consistently given in unnormalized form throughout this Section.

The response of the device is illustrated in Figs. 11.24 to 11.28. The terminal voltage of the diode and the external current as functions of time are shown in Figs. 11.24 and 11.25 with different time scales, the electric field and the injected minority carriers in the P-side as functions of position in Figs. 11.26, 11.27 and in Fig. 11.28 respectively at various instants of time. The transient response may be separated into three distinct phases: the build-up of the ohmic voltage drop in the quasi-neutral P-region, the limitation of the reverse current to a constant value essentially determined by the external circuit parameters, and the decay of the reverse current toward the final steady-state value.

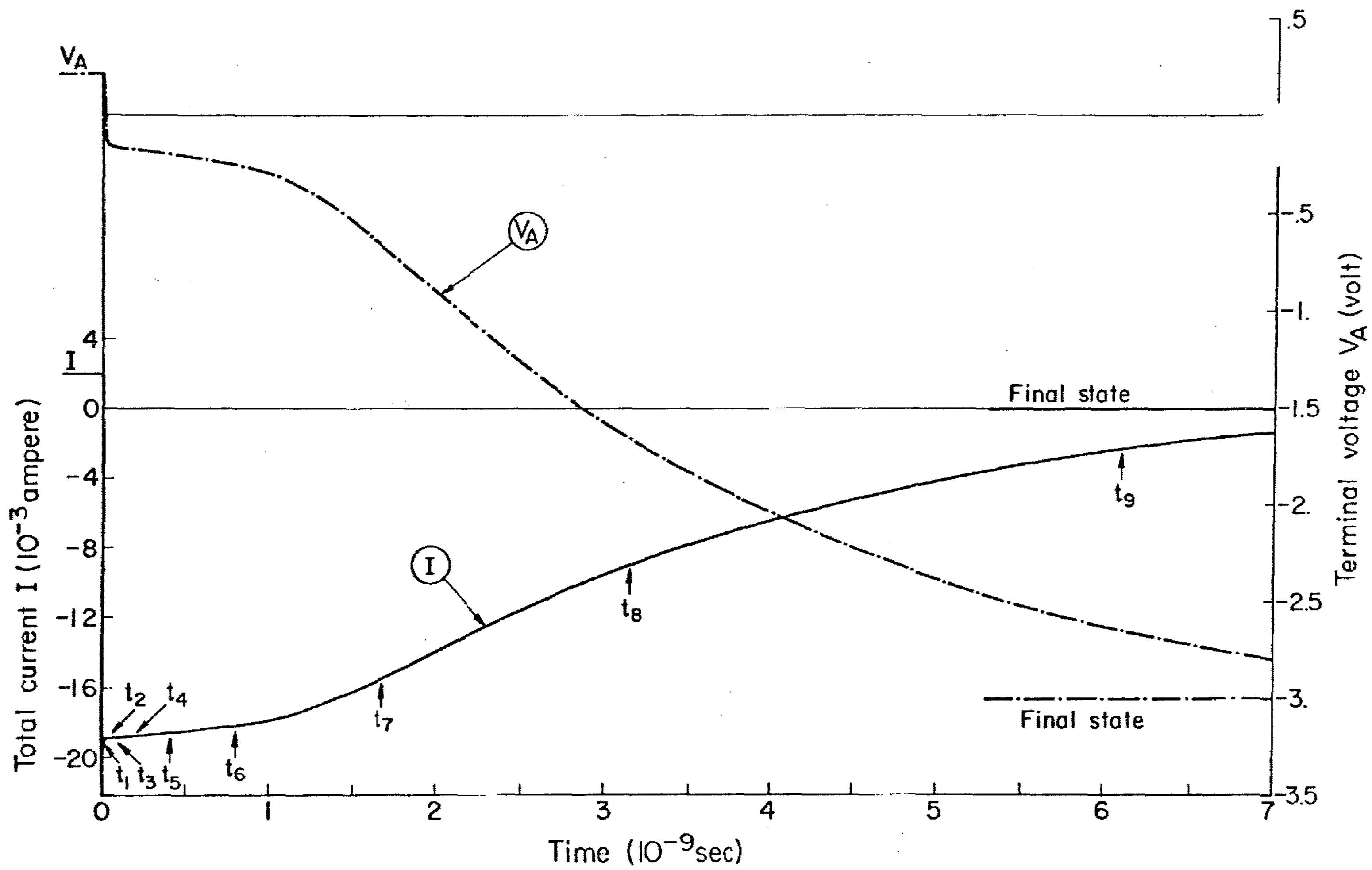

Fig. 11.24. Device as in Fig. 11.23. Voltage at the terminals of the diode and external current as functions of time during switching from a forward to a reverse bias condition.

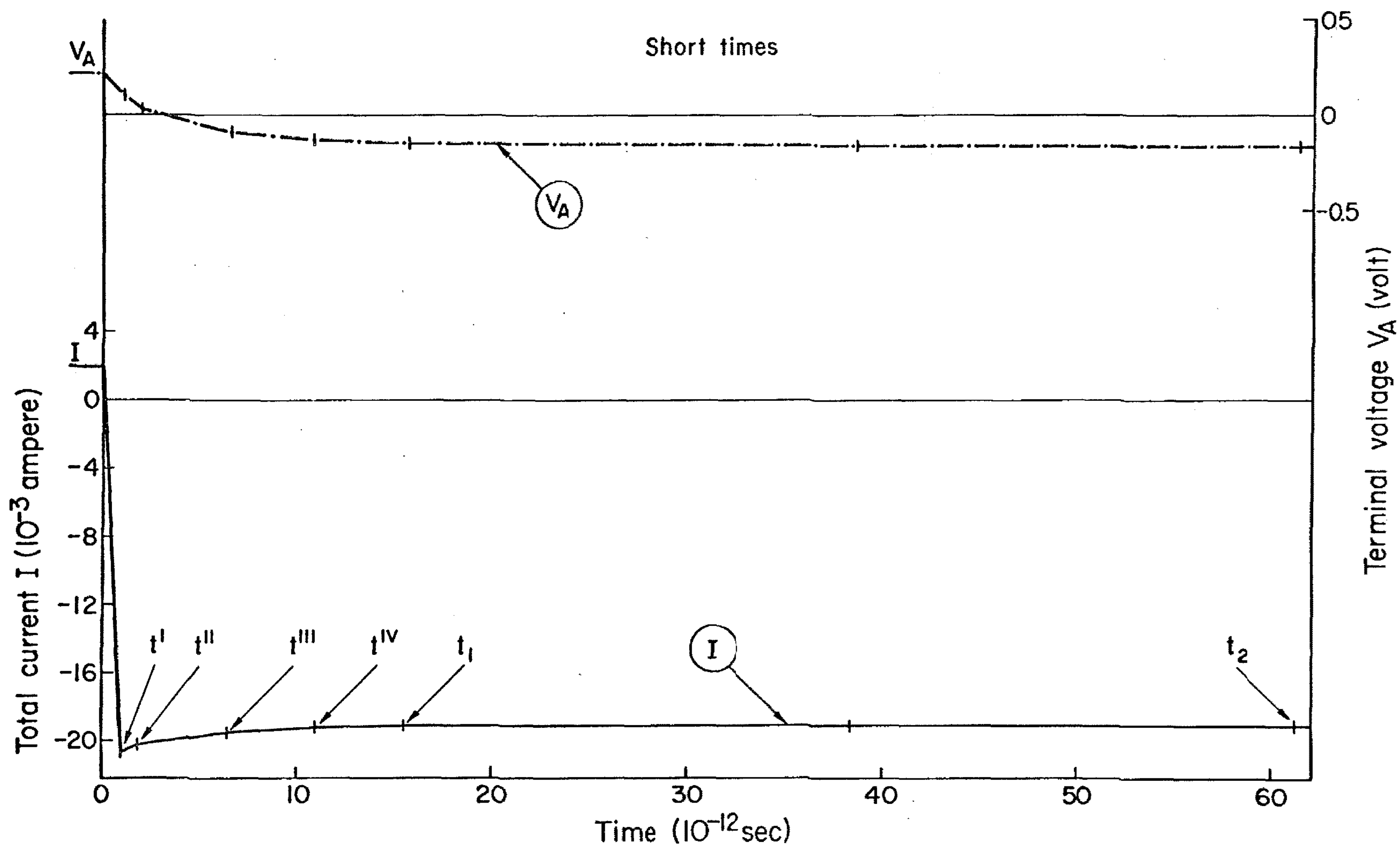

Fig. 11.25. Device as in Fig. 11.23. Voltage at the terminals of the diode and external current as functions of time during switching from a forward to a reverse bias condition. The time scale expansion shows the evolution of the dielectric relaxation phase (Phase I).

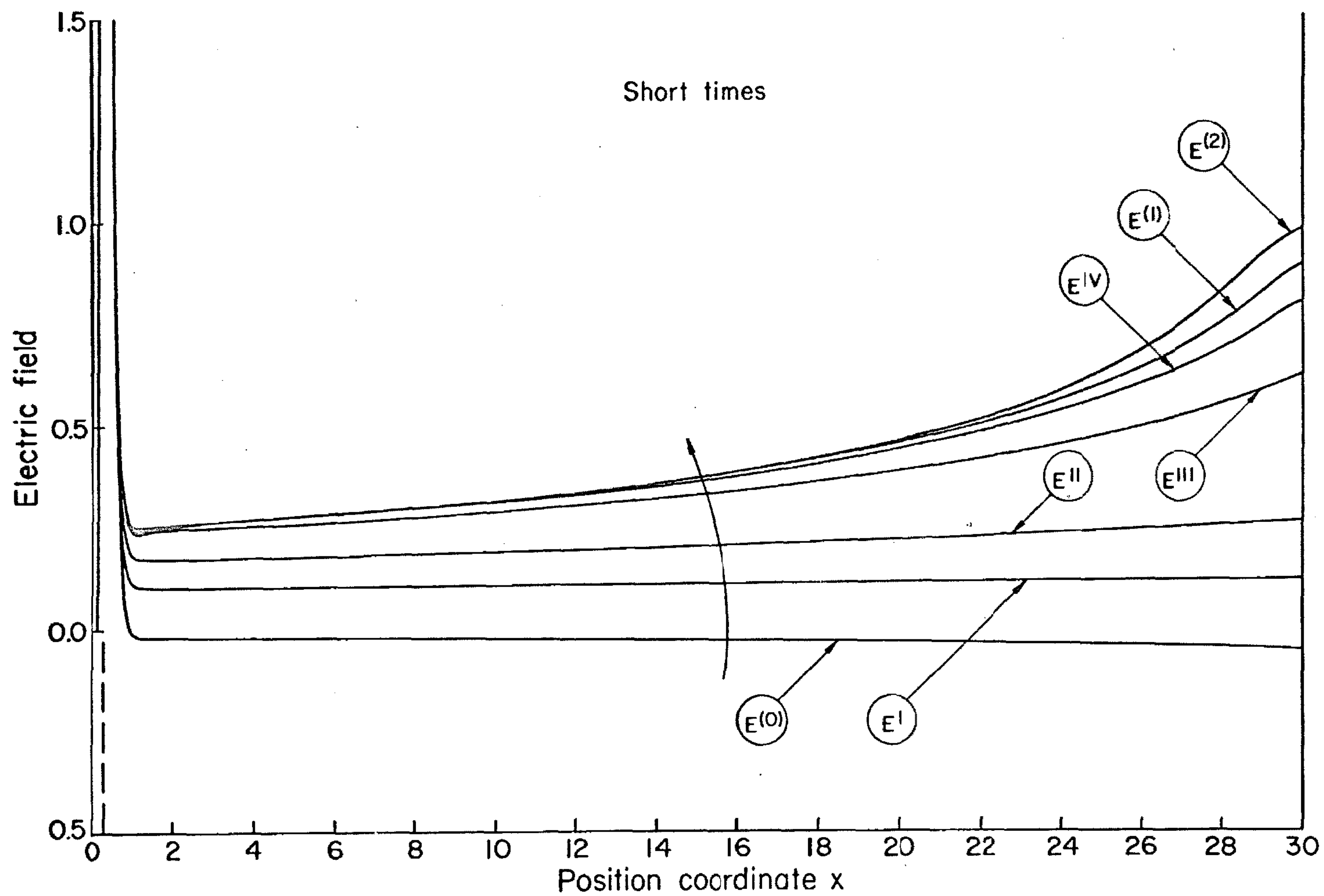

Fig. 11.26. Device as in Fig. 11.23. Electric field as a function of position at various instants of time during the initial dielectric relaxation phase (Phase I) of the transient evolution from a forward to a reverse bias condition ($t_0 = 0$, $t^{I} = 0.92$, $t^{II} = 1.83$, $t^{III} = 5.7$, $t^{IV} = 11.0$, $t_1 = 15.5$, $t_2 = 61.4$ in picoseconds).

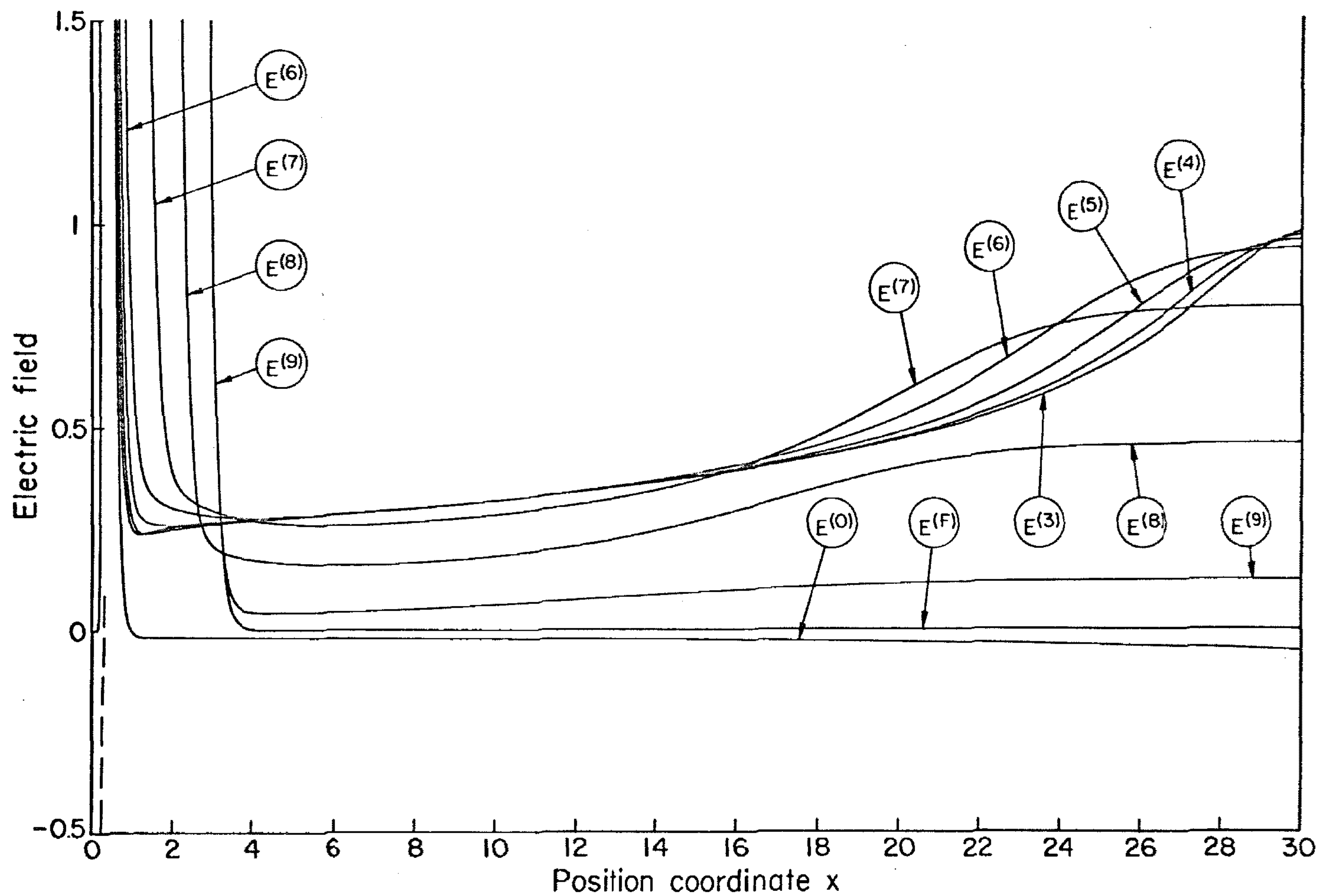

Fig. 11.27. Device as in Fig. 11.23. Electric field as a function of position at various instants of time during switching from a forward to a reverse bias condition (Phase II and Phase III; $t_0 = 0$, $t_3 = 0.107$, $t_4 = 0.199$, $t_5 = 0.405$, $t_6 = 0.794$, $t_7 = 1.65$, $t_8 = 3.12$, $t_9 = 6.05$, $t_F = \infty$ in nanoseconds).

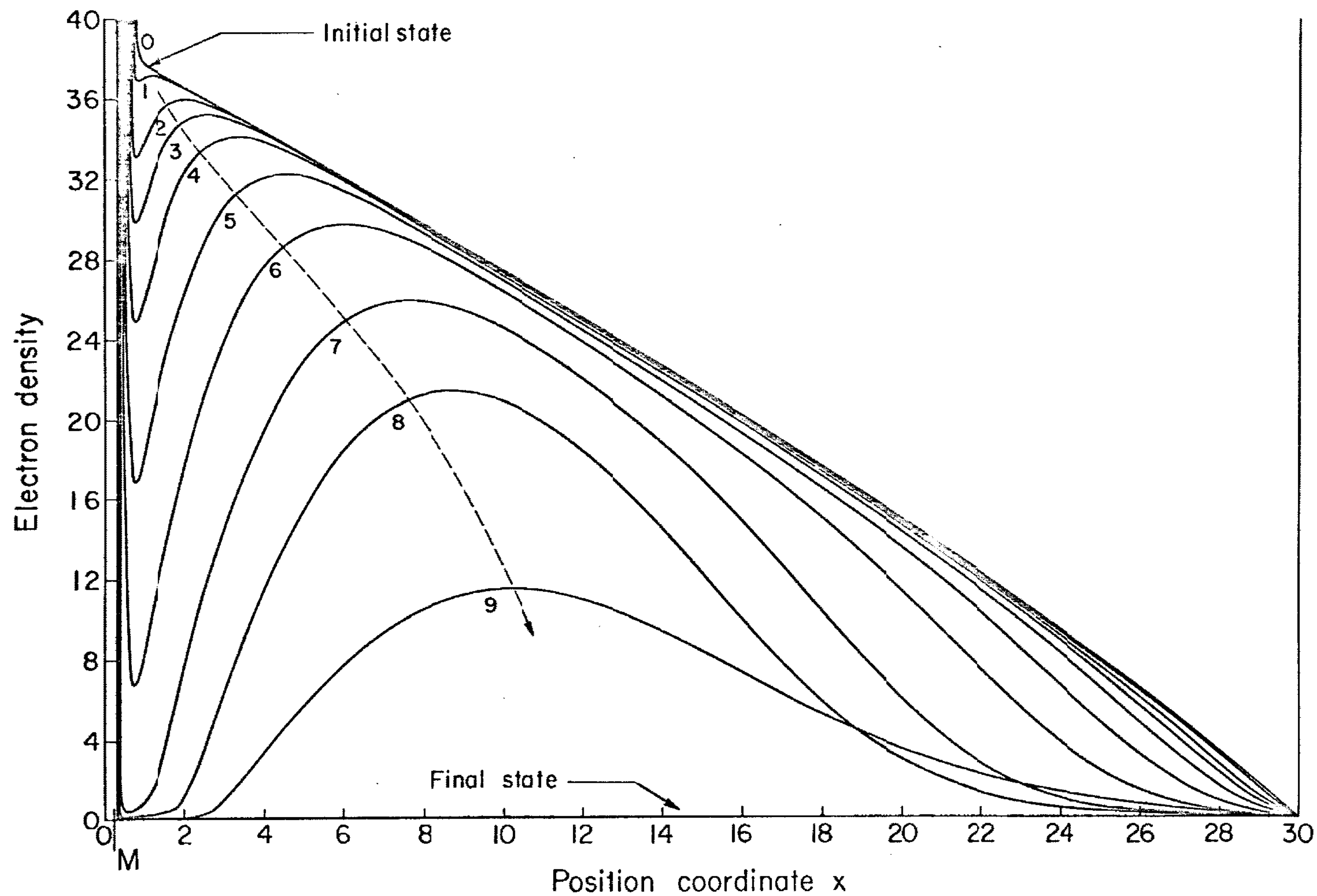

Fig. 11.28. Device as in Fig. 11.23. Electron density as a function of position at various instants of time (as in Fig. 11.27, and $t_1 = 15.5$, $t_2 = 61.4$ in picoseconds).

<u>Phase I. Build-up of the ohmic voltage drop in the quasi-neutral P-region.</u> At the instant $t = 0^+$, a current

$$I(t=0^+) = -\frac{V_B + V_A(t=0)}{R} \cong 21.4 \text{ ma}$$

is forced through the device, since its terminal voltage V_A remains unchanged from $t = 0$ to $t = 0^+$. Subsequently the establishment of the ohmic voltage drop in the quasi-neutral P-region becomes the dominant effect and occurs with the time constant:

$$\tau_{rP} = \frac{\varepsilon}{\sigma_P\Big|_{\substack{\text{initial}\\ \text{average}}}} \cong 3.8 \times 10^{-4} \quad (\text{or} \cong 3.5 \times 10^{-12} \text{ sec}) \tag{11.18}$$

where an average conductivity of the quasi-neutral P-region in the initial state has been employed, evaluated on the basis of the assumptions of the charge neutrality and linear mobile carrier distributions as

$$\sigma_P\Big|_{\substack{\text{initial}\\ \text{average}}} = \left(\frac{n}{\gamma_n} + \frac{p}{\gamma_p}\right)_{\substack{\text{initial}\\ \text{average}\\ M_P \le x \le L}} \cong 93 \times 19 + 44 \times 57 \cong 4.27 \times 10^3$$

$$(\text{or} \quad 0.66 \ \Omega^{-1} \text{ cm}^{-1})$$

The ohmic voltage drop may be estimated as:

$$\Delta V\Big|_{\text{ohmic}} = \frac{[I(t_1)-I(0)]w_P\Big|_{\text{in}}}{A\ \sigma_P\Big|_{\substack{\text{initial}\\ \text{average}}}} = -\frac{(19 + 2) \times 10^{-3} \times 27.9 \times 10^{-4}}{2.65 \times 10^{-4} \times 0.66}$$

$$\cong -0.34 \text{ volt} \tag{11.19}$$

where $t_1 = 15.5$ picosec., and $I(t_1)$ is the external current flowing once the ohmic voltage drop is established.* The estimation (11.19) agrees well with the "exact" value of Fig. 11.24.

The evolution of the response during this first phase may be conveniently followed in the time expansion of Fig. 11.25 and in the spatial distributions of the electric field of Fig. 11.26 at various instants of time ($t_0=0$, $t^I = 0.92$, $t^{II} = 1.83$, $t^{III} = 5.7$, $t^{IV} = 11.0$, $t_1 = 15.5$, $t_2 = 61.4$, in picoseconds). The external (negative) current decreases slightly in magnitude from the value at $t = t^I$ (taken as the first time point for the generation of the solution), according to the relation (11.17) as the terminal voltage V_A of the diode decreases by the amount of (11.19), with the time constant (11.18). The electric field (Fig. 11.26), initially in the steady-state condition $E(x,t=t_0)$, gradually assumes the new spatial distribution $E(x,t=t_2)$, consistent with the dynamic equilibrium condition governed by the reverse current I. At the instant t_2 the ohmic voltage drop in the quasi-neutral P-region has been essentially established. Simultaneously, in the same region, a changeover from displacement current to particle current takes place; the motion of carriers initiates toward the end of this phase ($t \cong t_1$), and the second phase begins.

Phase II. Constant reverse current phase. A partial depletion of the injected minority carriers in the quasi-neutral P-region represents the

* Of course, the numerical value for $I(t_1)$ must be determined by the solution of the system of simultaneous Eqs.(11.17) and (11.19).

dominant phenomenon of this phase. The evolution of the response may be followed in Fig. 11.27, which illustrates the spatial distributions of the electric field at various instants of time (t_3 =0.107, t_4 =0.199, t_5 =0.405, t_6 =0.794, t_7 = 1.65, t_8 = 3.12, t_9 = 6.05, $t_F = \infty$, in nanoseconds) and in Fig. 11.28, which displays the minority carrier densities as functions of position at the instants t_0 and t_1 to t_9.

The changeover from displacement to electron current (due essentially to diffusion) at the transition region edge M_P of the quasi-neutral P-region, during the first phase, is apparent in Fig. 11.28, which shows the adjustment of the spatial slope of the electron density at M_P to the new high reverse current at $t = t_2$ from the initial forward value. The small electric field in the quasi-neutral P-region, particularly in the vicinity of M_P (Fig. 11.27), ensures that the electron drift current is a minor contribution to the total current, which is therefore essentially proportional to the spatial slope of the electron density at M_P. The electron flow from the quasi-neutral P-region to the N-side occurs then with a nearly constant rate, essentially determined by the external voltage source V_B and the resistor R. Therefore the electron density at M_P decreases with a nearly constant slope generating the typical distributions of Fig. 11.28, until the depletion of carriers at the edge of the transition region is completed ($t \cong 1.2 \times 10^{-9}$ sec). The (negative) external current, essentially constant during this phase, is then forced to decrease in magnitude and the third phase begins.

Although the electron flow in the quasi-neutral P-region is mostly ruled by diffusion in this second phase, the effect of a small drift

component is apparent in the distributions of Fig. 11.28, which shows how the electrons are "pushed" from the external contact of the P-side toward the transition region by the (positive) electric field.

Phase III. Decaying reverse current phase. The dominant phenomenon of this phase is the termination of the depletion process of the excess electron charge remaining in the quasi-neutral P-region at the completion of the second phase. The diode becomes a high impedance device, forcing the reverse current to decrease to its steady-state value and the terminal voltage V_A to approach the voltage source V_B according to relation (11.17). Simultaneously the electric field distribution (Fig. 11.27), essentially unchanged during the second phase, relaxes toward its final steady-state distribution both in the transition region, whose width gradually increases, and in the quasi-neutral P-region. The former effect is related to the discharge of the transition region capacitance, whereas the latter allows a noticeable diffusion of the electrons also toward the external contact in the quasi-neutral P-region ($t = t_9$, Fig. 11.28). The spatial distributions of the electric field (Fig. 11.27), featuring zero slope in part of the quasi-neutral P-region in the vicinity of the external contact, are indicative of the achieved electric charge neutrality condition in that region during this third phase.

The prediction of the duration of the various phases, characterizing the transient response discussed above, is of great practical interest. An estimation of the time constant of the dielectric relaxation process of Phase I has already been given and a good agreement with

the "exact" value has been observed. Both Phase II and Phase III are conventionally analyzed on the basis of a highly simplified form of the diffusion equation for minority carriers in the quasi-neutral region of the low conductivity side, with the aid of the usual first order assumptions (for instance, Steele [26] and Byczkowski [27]). These first-order results are gathered by Grove [28], with explicit asymptotic expressions for the model under consideration (short structure in absence of recombination in the interior).

The duration of the constant-current phase (II) is predicted as:

$$\Delta t\Big|_{\text{phase II}} = \left(\frac{\pi}{4}\right) \frac{\gamma_p \left(w_P\big|_{in}\right)^2}{[1 + I(t_2)/I(t_0)]} \cong 0.6 \times 10^{-9} \text{ sec} \tag{11.20}$$

where $I(t_0)$ and $I(t_2)$ are the forward and reverse currents respectively, and $w_P\big|_{in}$ is the width of the quasi-neutral P-region, essentially unchanged during Phase II. The time required by the decaying current to reach 10% of the constant value of Phase II is defined as the duration of Phase III and is predicted as

$$\Delta t\Big|_{\text{phase III}} = \frac{2}{\pi}\left[\frac{1}{[1 + 0.1\ I(t_2)/I(t_0)]^2} - \frac{1}{[I + I(t_2)/(t_0)]^2}\right] \cdot \tau_t\Big|_{av} \cong 6.3 \times 10^{-9} \text{ sec} \tag{11.21}$$

The total switching time, essentially determined by Phase II and III, is then:

$$\Delta t\Big|_{\text{total}} \cong \Delta t\Big|_{\text{Phase II}} + \Delta t\Big|_{\text{Phase III}} \cong 6.9 \times 10^{-9} \text{ sec} \tag{11.22}$$

The prediction (11.20) differs considerably from the "exact" value ($\simeq 1.1 \times 10^{-9}$ sec) of Fig. 11.24. The discrepancy is to be attributed partially to the influence of the electric field which tends to accumulate electrons at the edge of the transition region in the quasi-neutral P-region, and deplete the region close to the external contact during the Phase II. This effect, not accounted for by the first-order analysis, is apparent in the distributions of Fig. 11.28 and is responsible for a longer duration of Phase II, as compared to the first-order estimation (11.20) ($\simeq 0.6 \times 10^{-9}$ sec)*. On the contrary, as a consequence of the above, the smaller excess of minority carriers, left in the quasi-neutral P-region at the completion of Phase II, is responsible for a shorter duration of Phase III ($\simeq 5.5 \times 10^{-9}$ sec, Fig. 11.28), as opposed to the first-order estimation (11.21) ($\simeq 6.3 \times 10^{-9}$ sec). It may be recalled that the electric field in the quasi-neutral P-region is essentially absent during Phase III, so that the first-order diffusion equation becomes considerably more accurate. As the result of the compensation of the discrepancies of the first-order estimations of the durations of Phase II and III, the total "exact" switching time ($\simeq 6.6 \times 10^{-9}$ sec) agrees sufficiently well with the prediction (11.22) ($\simeq 6.9 \times 10^{-9}$ sec).

---

* A qualitative agreement between the "exact" results and Kennedy's [24] "second-order" solutions of the diffusion equation of minority carriers in the quasi-neutral region in the low conductivity side, in presence of a uniform field, may be recognized.

11.4. Conclusion.

Numerical results for a special structure of an isolated $N^+ - P$ diode driven by typical time-dependent excitations of ideal current and voltage sources have been presented. In addition, the transient response of the combination of the $N^+ - P$ diode and an external resistor has been analyzed under switching from a forward to a reverse bias condition. Accuracy tests have been performed by comparing solutions obtained for various discretization schemes and step sizes.

The "exact" results, displayed in graphical form as functions of position and time, allow a thorough understanding of the contribution of each quantity to the overall behaviour of the device. The first-order estimations, consistently attempted as an integral part of the interpretation of the computed solutions, are usually in good agreement with the "exact" results, provided that only one isolated phenomenon is responsible for the generation of a portion of the transient response. On the other hand, only order-of-magnitude estimations are available if a simultaneous interaction of basic effects contributes to the characterization of the time-dependent behavior of the device.

CHAPTER XII

CONCLUSIONS

Numerical methods of solution of the one-dimensional basic two-carrier transport equations describing the behaviour of semiconductor junction devices under both steady-state and transient conditions have been presented in this work. The methods described are of a very general character: none of the conventional assumptions and restrictions are introduced, and freedom is available in the choice of the doping profile, generation-recombination law, mobility dependencies, injection level, and boundary conditions applied solely at the external contacts. For a specified arbitrary excitation of either current or voltage (as a function of time for a transient analysis) the solution yields the terminal properties and all the quantities of interest throughout the entire device as functions of position (and time).

The physical and mathematical model, which includes the conventional simplified form of the Boltzmann transport equation in terms of drift and diffusion processes, is described in Chapter I. Considerable attention is focused on the numerical analysis of the problem in order to achieve a numerical algorithm sufficiently sound and efficient to cope with the several basic difficulties of the problem. Some of the basic difficulties are already recognized in Chapter II, in which a steady-state iterative scheme, already available in the literature and presented in a slightly different form in Chapter I, is numerically analyzed. The inadequacies of the original analytical formulation are overcome by an improved algorithm, which, together with the aid of appropriate numerical techniques, is capable of generating very accurate

steady-state solutions under the above general conditions.

Additional difficulties of fundamental nature arise in the time-dependent analysis of the problem, whose formulation, described in Chapter VII, calls for the discretization of a system of non-linear partial differential equations of the parabolic type. This problem is approached in Chapter VIII, on the basis of extrapolations from the results available in the theory of numerical analysis for the simpler cases. Preference is given to discretization schemes of the implicit type, featuring unconditional stability without restrictions on the discretization mesh adopted. It is in fact very convenient to employ an automatically adjustable non-uniform mesh, in both the position and time coordinates, consistent with the criterion of maintaining constant truncation errors throughout the entire evolution of a transient solution, without endangering numerical stability.

The importance of achieving numerical compatibility between steady-state and transient solutions is emphasized in Chapter IX, in which an algorithm for the solution of the voltage-driven transient, compatible with the current-driven transient of Chapter VIII, is described. The procedure employed for the voltage-driven transient is also capable of generating compatible steady-state distributions, therefore very suitable to serve as initial conditions for a time-dependent solution.

As an example of numerical calculations, results for special structures under steady-state and transient conditions are reported in Chapters VI and XI, respectively. The analysis of solutions for idealized models and excitations allows a thorough evaluation of the conventional first-order theory, based on several drastic assumptions

and approximations, and a comprehensive test of the accuracy of the results for the numerically worst case. For the steady-state case, the "exact" and first-order terminal properties are sufficiently in agreement only for reverse bias conditions and low to moderate injection levels, despite of the discrepancies of the internal distributions. Although this insufficiency of the first-order theory is well known qualitatively, the "exact" analysis permits a valuable quantitative comparison, for any type of structure and bias condition. On the other hand, the conventional time-dependent solutions are available in closed form only for very particular situations, and require the usual drastic assumptions of the first-order theory. More generally, only order-of-magnitude estimations may be used to achieve qualitative predictions of the overall transient response, even for the simplest structures and external excitations. This difficulty is a consequence of the interaction of several effects of basic nature, which require the simultaneous solution of the system of fundamental equations throughout the entire device.

The principal sources of errors, and techniques suitable to control their influence on the overall accuracy, are discussed in Chapters V and X for the steady-state and transient cases, respectively. The accuracy of the final steady-state results is evaluated on the basis of consistency tests between the achieved solutions and a set of dependent relations suitable to expose discretization and numerical errors. Partial results at the completion of the iterative scheme at each instant of time in a transient solution, may also be evaluated with the aid of a set of time-dependent testing relations. The overall accuracy of the

transient results is estimated by comparison of solutions obtained for different discretization schemes and mesh sizes.

The FORTRAN programs for the steady-state method of Part I and for the transient solutions (current or voltage driven) of Part II are reported in detail in the Appendices for a special case. Whereas the usage of the former is rather straightforward, the latter requires usually more attention in order to achieve a uniform contribution of the various sources of errors, and therefore the minimization of the computation time for a desired overall accuracy. This may be attained by an appropriate choice of the discretization scheme, discretization mesh size, total number of spatial and time points, iteration error and terminal voltage tolerance (in a voltage-driven transient). The magnitude of these parameters may vary widely, and is highly dependent upon the abruptness of the doping profile and of the external excitation. Experience may serve as a useful guide for the optimization of the selection of the determinant parameters. This situation is a direct consequence of the degree of complexity of the transient solution, one order of magnitude higher than that of the steady-state analysis.

The numerical solutions of the steady-state and transient problems, for the simple physical model considered, are intended to expose the several difficulties of fundamental nature present in the numerical analysis. The overcoming of these difficulties opens the path to the inclusion of additional effects and to the extension to more complex situations. As an example of straightforward applications of the steady-state procedure in slightly more intricate schemes, the computation of the total incremental capacitance for a two-contact device and

a solution for the reverse steady-state problem are presented in Chapter III. The extension of the steady-state formulation to a three-contact device is described in Chapter IV, although the inadequacy of the one-dimensional model prevents achievement of sufficiently realistic results. The time-dependent algorithm is extended in Chapter IX to incorporate a network of ideal generators and passive circuit elements, and a numerical example is reported in Chapter XI.

The powerful tool developed in the present work opens the door to a wide variety of investigations of both practical and theoretical interest. Some are listed below.

(1) Application of the numerical methods to diffusion-controlled structures with multiple junctions, more complex geometries, and ultimately to ensembles of passive and active circuit elements.

(a) Inclusion of recombination and trapping mechanisms of various degrees of complexity in junction transistors.

(b) Use of the numerical solutions to suggest and to validate more comprehensive and improved analytical results.

(c) Use of the numerical transient solutions to investigate the switching properties of junction diodes and transistors, particularly diode reverse recovery and transistor storage time.

(d) Determination of impurity doping profiles to optimize specific device performance parameters.

(e) Device modeling, as a basis for computer-aided circuit design and analysis.

(2) Extension of the numerical methods to include zener and avalanche multiplication mechanisms. Junction breakdown effects can then be

studied, and thermal effects could be incorporated so that possibility of thermal runaway can be investigated, and the complete terminal properties under transient as well as steady-state conditions can be determined.

(3) Study of radiation effects in semiconductor devices. The program for transient solutions is directly applicable to these investigations, for both cases of transitory and permanent radiation effects.

(4) Application of the numerical methods to space-charge-limited structures, both single and double injection types.

(5) Extension of the numerical methods to multi-dimensional geometries. Two-dimensional solutions may become necessary if meaningful results for realistic models of commonly used structures (such as planar devices, field-effect transistors, integrated structures, etc.) are desired.

APPENDIX A

SOME RESULTS OF THE CONVENTIONAL FIRST-ORDER THEORY FOR THE N-P JUNCTION IN STEADY STATE

It is of interest to report, with a brief derivation, some approximate results of the conventional theory (referred to here as the "first-order" theory) for the P-N junction in steady-state in a simple formulation.

A-1. Mathematical model.

The N-P structure that will be considered, with definition of its parameters, is shown in Fig. A-1.

The simplified model is based on the following assumptions (in addition to those listed in Subsection 1.1.1 for the "exact" approach):

(e) step distribution for the doping profile

(f) highly asymmetric junction with $\sigma_N \gg \sigma_P$ (σ_N and σ_P being the conductivities of the N and P side respectively)

(g) separation of the interior of the device into fully depleted and charge-neutral regions

(h) absence of recombination-generation in the interior $[U(x) = 0]$

(i) constant mobilities

(j) ohmic external contacts

Restriction to a specific injection level range is not introduced.

According to Fig. A-1, M_N, w_N, and x_N (M_P, w_P and x_P) are defined as the interface between the neutral and depleted regions, the neutral region length, and the depleted region length respectively in the N-material (P-material).

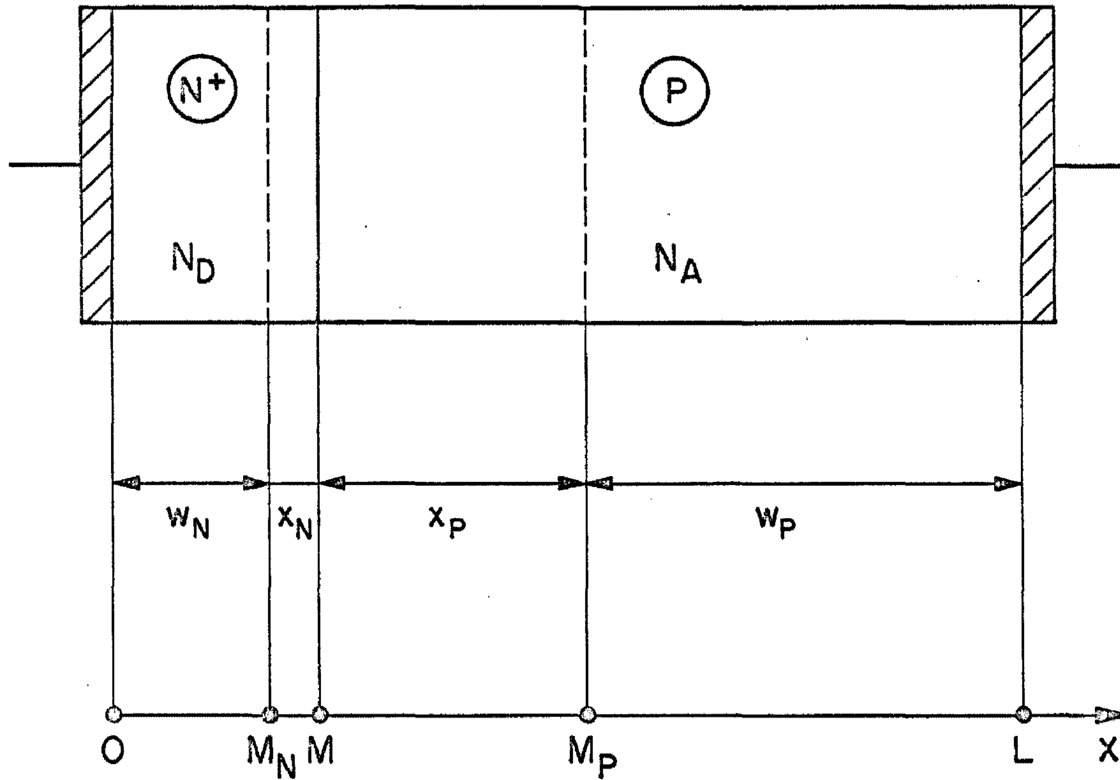

Fig. A-1. One-dimensional abrupt asymmetric N^+-P diode model with definition of the conventional first-order theory parameters.

The normalized fundamental Eqs.(1.16) to (1.21), specialized for the simpler model, become:

$$J = J_n(x) + J_p(x) \tag{A-1}$$

$$\frac{dJ}{dx} = 0 \tag{A-1a}$$

$$J_n = \frac{1}{\gamma_n}\left[n(x)\,\frac{d\psi(x)}{dx} - \frac{dn(x)}{dx}\right] \tag{A-2}$$

$$J_p = \frac{1}{\gamma_p}\left[p(x)\,\frac{d\psi(x)}{dx} + \frac{dp(x)}{dx}\right] \tag{A-3}$$

$$\frac{d^2\psi(x)}{dx^2} = n(x) - p(x) - N_D + N_A \tag{A-4}$$

$$\frac{dJ_n}{dx} = \frac{dJ_p}{dx} = 0 \tag{A-5}$$

with the subsidiary relations:

$$E(x) = -\frac{d\psi}{dx} \quad ; \quad \begin{cases} N_A = 0 \quad \text{for} \quad 0 \le x \le M \quad \text{(N-region)} \\ N_D = 0 \quad \text{for} \quad M < x \le L \quad \text{(P-region)} \end{cases}$$

$$\varphi_n(x) = \psi(x) - \ln n(x) \tag{A-6a}$$

$$\varphi_p(x) = \psi(x) + \ln p(x) \tag{A-6b}$$

Assumption (f) leads to the inequality

$$|J_n| \gg |J_p| \quad , \quad (\text{or} \quad J \simeq J_n) \tag{A-7}$$

whereas assumption (h) is responsible for the solenoidal character of each of the two current densities J_n, J_p. Assumption (j) furnishes the boundary conditions on the mobile carriers of the external contacts as the equilibrium values:

$$n(0) = n_N = \sqrt{\left(\frac{N_D}{2}\right)^2 + 1} + \frac{N_D}{2}$$

$$p(0) = p_N = 1/n_N$$

$$p(L) = p_P = \sqrt{\left(\frac{N_A}{2}\right)^2 + 1} + \frac{N_A}{2}$$

$$n(L) = n_P = 1/p_P$$

whereas the boundary conditions on the electrostatic potential are taken as:

$$\psi(0) = \text{potential reference}$$

$$\psi(L) = \psi(0) + V_A - V_d \tag{A-8}$$

The quantities of interest will be obtained separately in each region and boundary conditions at the internal interfaces will be determined by matching the corresponding distributions.

A-2. Neutral region in the low-conductivity (P) side ($M_P \le x \le L$).

Charge neutrality implies:

$$p(x) - n(x) = p_P - n_P \qquad \text{(A-9)}$$

The combination of inequality (A-7) with Eqs.(A-2) and (A-3) yields:

$$\frac{d\psi(x)}{dx}\,[n(x) - n_P + p_P] = -\frac{dn(x)}{dx} \qquad \text{(A-10)}$$

or:

$$n(x) - n_P + p_P = p_P\, e^{\psi(L)-\psi(x)} \qquad \text{(A-11)}$$

From Eqs.(A-2), (A-10) one obtains:

$$\gamma_n J_n = -\left[1 + \frac{n(x)}{n(x)-n_P+p_P}\right]\frac{dn(x)}{dx}$$

or

$$\gamma_n J_n(L-x) = 2[n(x)-n_P] - (p_P-n_P)\,\ln\left[\frac{n(x)-n_P+p_P}{p_P}\right] \qquad \text{(A-12)}$$

which shows the dependence of $n(x)$ upon x. Specialized at $x = M_P$, Eq.(A-12) becomes:

$$\gamma_n J_n(L-M_P) = 2[n(M_P)-n_P] - (p_P-n_P)\,\ln\left[\frac{n(M_P)-n_P+p_P}{p_P}\right] \qquad \text{(A-13)}$$

If $n(x) \gg p_P$, or $n(x) \ll p_P$, Eq.(A-12) can be linearized to yield, with the aid of Eq.(A-13), an explicit relationship between $n(x)$ and x:

$$n(x) - n_P = [n(M_P)-n_P] \frac{L-x}{L-M_P} \quad \text{(A-14)}$$

Otherwise, integration of Eq.(A-10) yields:

$$\psi(x) - \psi(L) = - \ln\left[\frac{n(x)-n_P+p_P}{p_P}\right] \quad \text{(A-15)}$$

which combined with Eq.(A-12) gives the dependence of ψ upon x. In the linear approximation of Eq.(A-14), the relationship can be obtained in closed form:

$$\psi(x) - \psi(L) = - \ln\left\{\left[\frac{n(M_P)-n_P}{p_P}\right] \frac{L-x}{L-M_P} + 1\right\} \quad \text{(A-16)}$$

Equation (A-6) can be rearranged as

$$\psi(x) - \varphi_n(x) = \ln n(x) = \ln \frac{n(x)}{n_P} + \ln n_P = \ln \frac{n(x)}{n_P} + [\psi(L)-\varphi_n(L)] \quad \text{(A-17)}$$

which, with the aid of Eq.(A-9), becomes:

$$\varphi_n(x) - \varphi_n(L) = \psi(x) - \psi(L) - \ln \frac{n(x)}{n_P} = - \ln \{n(x)[n(x)-n_P+p_P]\} \quad \text{(A-18)}$$

Equation (A-18), combined with Eq.(A-12), gives the dependence of φ_n upon x.

A-3. Neutral region in the high-conductivity (N) side ($0 \le x \le M_N$).

An electric field of significant amount (for the flow of minority carriers) cannot be sustained in the neutral high conductivity (N) side, so that in Eq.(A-3) the hole current may well be approximated, in this region, solely by its diffusion component:

$$J_p = \frac{1}{\gamma_p} \frac{dp(x)}{dx}$$

This leads to a linear hole density distribution:

$$p(x) = \left[\frac{p(M_N)-p_N}{M_N - 0}\right](x-0) + p_N \qquad \text{(A-19)}$$

Moreover, in virtue of assumption (f), the following approximations are made in this region:*

$$n(x) = n_N \qquad \text{(A-20)}$$

$$\psi(x) = \psi(0) = 0 \qquad \text{(A-21)}$$

from which:

$$\varphi_n(x) = \varphi_n(0) \qquad \text{(A-22)}$$

---

* The goodness of these approximations worsens with the increase in forward bias. This pattern is consistent with the behavior of the remaining assumptions, which all become poor at very high injection levels.

Equation (A-6b) yields then:

$$p(x) = \exp\left[\varphi_p(x)\right]$$

$$p(0) = \exp\left[\varphi_p(0)\right] = p_N$$

or

$$\varphi_p(x) - \varphi_p(0) = \ln \frac{p(x)}{p_N} \tag{A-23}$$

and with the aid of Eq.(A-19):

$$\varphi_p(x) = \varphi_p(0) + \ln\left\{\left[\frac{p(M_N)}{p_N} - 1\right]\frac{x-0}{M_N-0} + 1\right\} \tag{A-24}$$

which gives the dependence of φ_p upon x in this region.

A-4. Transition region $(M_N \leq x \leq M_P)$.

In virtue of assumption (g), mobile carrier concentrations are neglected with respect to the fixed impurity concentrations. A very strong electric field together with a high gradient of carrier density is to be expected; an estimation of the orders of magnitude and sign of the drift and diffusion current components leads to the conventional approximation

$$J_n \cong 0 \quad , \quad J_p \cong 0 \tag{A-25}$$

when such net currents are compared to their respective components of Eqs.(A-2) and (A-3).

The condition $J_n = 0$, applied to Eq.(A-2), yields:

$$n(x) \propto e^{\psi(x)} \tag{A-26}$$

which can be specialized at the boundaries of the transition region in the forms:

$$n_N = n_P \, e^{V_d} \tag{A-27}$$

$$n(M_P) = n_N \, e^{\psi(M_P) - \psi(0)} \tag{A-28}$$

or

$$n(M_P) = n_P \, e^{\psi(M_P) - \psi(0) + V_d} \tag{A-29}$$

and

$$n(x) = n(M_P) \, e^{\psi(x) - \psi(M_P)} \tag{A-30}$$

where use of the relations

$$\psi(M_N) = \psi(0)$$

$$n(M_N) = n(0)$$

has been made.

Similarly, if the condition $J_p = 0$ is applied to Eq.(A-3), one obtains:

$$p(x) \propto e^{-\psi(x)} \tag{A-31}$$

or

$$p_P = p_N\, e^{V_D} \tag{A-32}$$

$$p(M_N) = p(M_P)\, e^{\psi(M_P)-\psi(0)} \tag{A-33}$$

The combination of Eqs.(A-27), (A-28), (A-32), (A-33) and the neutrality condition at $x = M_P$

$$p(M_P) = p_P + n(M_P) - n_P$$

yields:

$$p(M_N) = p_N \exp[\psi(M_P)-\psi(0)+V_d] \cdot \left[1 + n_N^2 \exp[\psi(M_P)-\psi(0)-V_d] - n_P^2\right] \tag{A-34}$$

and

$$p(x) = p(M_N)\, e^{\psi(0)-\psi(x)} \tag{A-35}$$

Otherwise Poisson's equation (A-4) may be readily integrated if the mobile carriers are neglected:

for $\quad M_N \le x \le M \begin{cases} \dfrac{d^2\psi(x)}{dx^2} = -N_D \\ \psi(x) = -\dfrac{N_D}{2}(x-M_N)^2 + \psi(M_N) \end{cases}$ (A-36)

for $\quad M \le x \le M_p \begin{cases} \dfrac{d^2\psi(x)}{dx^2} = N_A \\ \psi(x) = \dfrac{N_A}{2}(x-M_P)^2 + \psi(M_P) \end{cases}$ (A-37)

where the conditions $\left.\dfrac{d\psi(x)}{dx}\right|_{\substack{x=M_N \\ x=M_P}} = 0$ have been used.

If the condition of continuity of $\psi(x)$ at $x = M$

$$-\frac{N_D}{2}(M-M_N)^2 + \psi(M_N) = \frac{N_A}{2}(M-M_P)^2 + \psi(M_P)$$

and overall charge neutrality

$$N_D(M-M_N) = N_A(M_P-M)$$

are imposed, the width of the depleted region in the N-side and in the P-side may be determined:

$$x_N \triangleq M-M_N = \left[2[\psi(0)-\psi(M_P)]/(1 + N_D/N_A)\right]^{1/2} \qquad \text{(A-38)}$$

$$x_P \triangleq M_P-M = \left[2[\psi(0)-\psi(M_P)]/(1 + N_A/N_D)\right]^{1/2} \qquad \text{(A-39)}$$

A-5. Internal boundary values.

The above results have been expressed in terms of the boundary values $\psi(M_P)$, $n(M_P)$ at the interface between the depleted and neutral P-region. These quantities may be determined by matching the electron density distribution at $x = M_P$.

The combination of Eq.(A-11), specialized at $x = M_P$, Eqs.(A-29) and (A-8) yields:

$$n(M_P)[n(M_P)-n_P+p_P] = e^{V_A} \tag{A-40}$$

or

$$n(M_P) = \frac{e^{V_A}}{\sqrt{\left(\frac{p_P+n_P}{2}\right)^2 + e^{V_A} - 1} + \frac{p_P-n_P}{2}} \tag{A-41}$$

which relates the value of injected electron density, at the edge of the neutral P-region, with the applied voltage V_A.

If relation (A-41) is inserted in relation (A-29), the boundary value of the potential at $x = M_P$ may be explicitly determined:

$$\psi(M_P) = V_A - \ln\left\{\left[\sqrt{\left(\frac{p_P+n_P}{2}\right)^2 + e^{V_A} - 1} + \frac{p_P-n_P}{2}\right]/p_P\right\} + \psi(0)-V_d \tag{A-42}$$

Expression (A-41) may also be inserted in Eq.(A-13) to obtain the relation between the dominant current J_n (essentially the total current J) and the applied voltage V_A.

A qualitative illustration of the distributions of interest, as

given by the above first-order formulation, is shown in Fig. A-2 for three different bias conditions.

A-6. Two special cases: low-level and high-level injection.

The quantity

$$\chi \triangleq \frac{n(M_P)}{p_P} \tag{A-43}$$

is defined as the injection parameter, and may be conveniently chosen to separate two different ranges of operation of the device, determined by:

$$\left.\begin{array}{ll} \chi \ll 1 & \text{low-level injection range} \\ \chi \gg 1 & \text{high-level injection range} \end{array}\right\} \tag{A-44}$$

The injection parameter is closely related to the applied voltage for a given device structure; Eq.(A-40), combined with the definition (A-43), yields:

$$e^{V_A} = \chi\left[\frac{p_P}{n_P}(\chi+1) - 1\right]$$

The inequalities (A-44) become then:

$$e^{V_A} \ll \left(2\,\frac{p_P}{n_P} - 1\right) \quad \text{low-level injection}$$

$$e^{V_A} \gg \left(2\,\frac{p_P}{n_P} - 1\right) \quad \text{high-level injection}$$

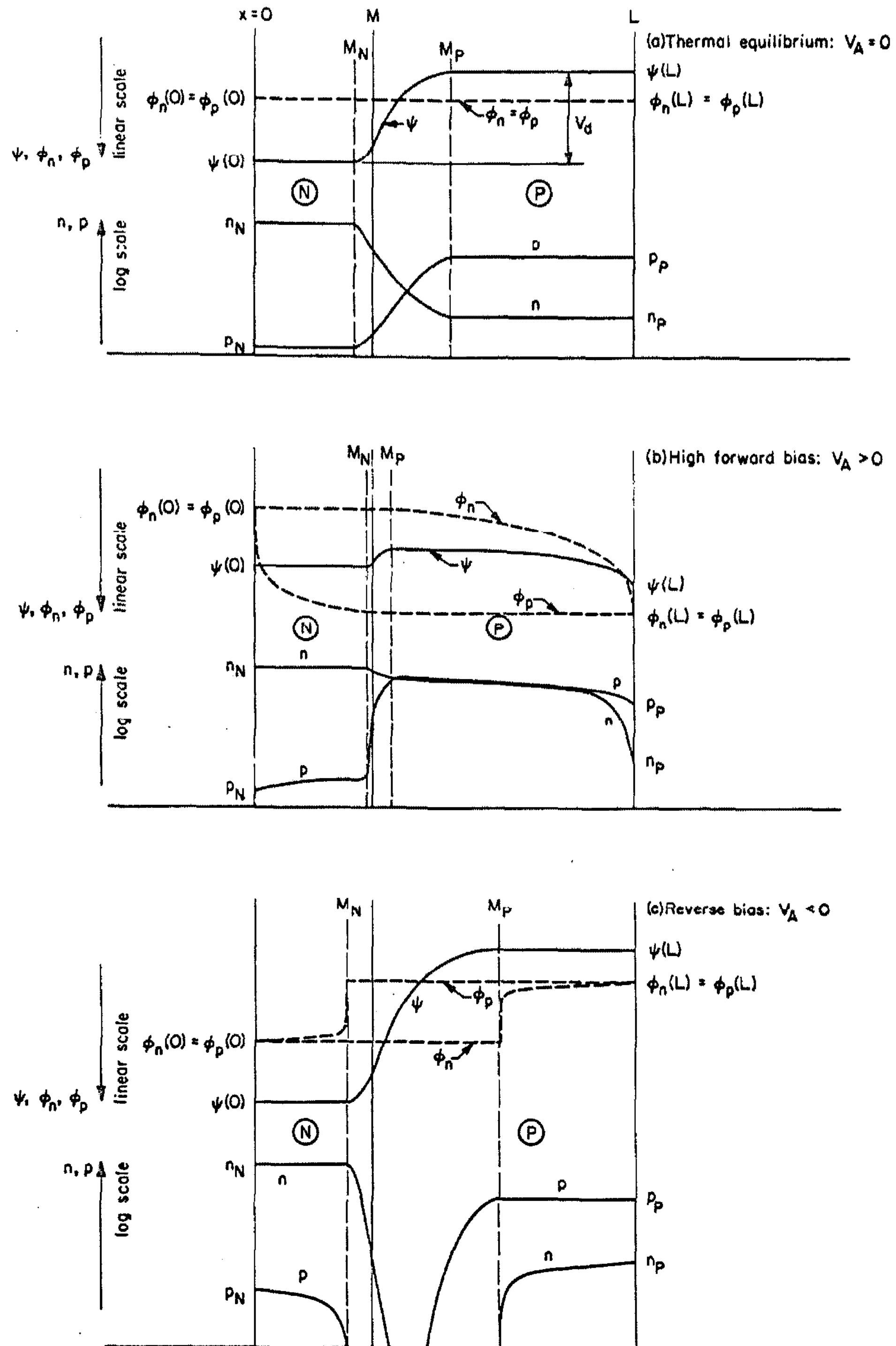

Fig. A-2. First-order spatial distributions for different bias conditions: (a) thermal equilibrium, (b) high forward bias, (c) reverse bias. (Schematic)

With the additional assumption

$$p_P \gg n_P$$

the results of the previous sections may be specialized for the two injection ranges and reduced to a simpler and more familiar approximate form. For instance, Eq.(A-41) becomes:

$$n(M_P) = n_P\, e^{V_A} \qquad \text{low-level} \qquad \text{(A-45)}$$

$$n(M_P) = e^{V_A/2} \qquad \text{high-level} \qquad \text{(A-46)}$$

which inserted in Eq.(A-29), yield :

$$\psi(M_P) = \psi(L) \qquad \text{low level} \qquad \text{(A-47)}$$

$$\psi(M_P) = \psi(0) - V_d + V_A/2 + \ln p_P \qquad \text{high level} \qquad \text{(A-48)}$$

If V_j is defined as the fraction of the applied voltage that modifies the potential drop on the barrier, that is

$$V_j \triangleq \psi(M_P) - \psi(0) + V_d = \psi(M_P) + V_A - \psi(L) \quad ,$$

relations (A-47), (A-48) may be written as

$$V_j = V_A \qquad \text{low-level} \tag{A-49}$$

$$V_j = \frac{V_A}{2} + \ln p_P \qquad \text{high-level} \tag{A-50}$$

If relations (A-45), (A-46) are inserted in the linear approximations of Eq.(A-13), the relationships between current and applied voltage are easily recovered:

$$J \simeq J_n = J_{Sat}\left(e^{V_A} - 1\right) \qquad \text{low-level} \tag{A-51}$$

$$J \simeq J_n = 2\, p_P\, J_{Sat}\, e^{V_A/2} \qquad \text{high-level} \tag{A-52}$$

where

$$J_{Sat} \triangleq \frac{n_P}{\gamma_n (L - M_P)} \tag{A-53}$$

is the saturation current.

A-7. Transition region and diffusion incremental capacitances.

(a) The incremental transition region capacitance* C_t is conventionally computed as the variation of the net electric charge density Q_t in the depleted region (on one side of the metallurgical interface) with respect to the applied voltage:

---

* Capacitances are intended per unit cross-sectional area.

$$C_t = \frac{dQ_t}{dV_A} = - N_A \frac{dx_P}{dV_A}$$

This is the dominant incremental capacitance of the device under reverse-bias and low forward-bias conditions. In this case

$$\psi(M_P) \cong \psi(L)$$

so that the expression (A-39), with the aid of relation (A-8), may be readily differentiated, to obtain Schottky's formula:

$$C_t = \left[\frac{N_A}{2\left(V_d - V_A\right)\left(1 + \frac{N_A}{N_D}\right)} \right]^{1/2} \qquad \text{(A-54)}$$

which shows the linear dependence of $(C_t)^{-2}$ on the applied voltage V_A.

(b) The incremental diffusion capacitance is conventionally evaluated as the variation of the electric charge, in the neutral region of the low conductivity (P) side, due to one type of mobile carriers (either one for the assumed neutrality condition), with respect to the applied voltage. This capacitance is therefore the dominant one under moderate and high forward-bias conditions.

If Q_P is the electric charge due to holes in the neutral P-region, and Q_{Po} is the same at thermal equilibrium, then:

$$Q_{Po} = e\, p_P w_P$$

$$Q_P - Q_{Po} \cong \frac{Q_{Po}}{2p_P} \left[n(M_P) - n_P \right]$$

If Eq.(A-40) is differentiated to obtain

$$\frac{d[n(M_P)]}{dV_A} = \frac{n(M_P)[n(M_P)-n_P+p_P]}{2n(M_P)-n_P+p_P}$$

the incremental diffusion capacitance C_d may be easily determined:

$$C_d = \frac{dQ_P}{dV_A} = \frac{dQ_P}{d[n(M_P)]} \quad \frac{d[n(M_P)]}{dV_A} = \frac{w_P n(M_P)[n(M_P)-n_P+p_P]}{[2n(M_P)-n_P+p_P]\cdot 2} \qquad \text{(A-55)}$$

APPENDIX B

NUMERICAL INTEGRATION AND DIFFERENTIATION

It is of interest to report, as a convenient reference, a few of the simplest schemes suitable for the numerical evaluation of derivatives of the first and second order and integrals of a given function. Such a function is assumed available in discretized form, at a finite number of points unevenly spaced, for which a method based on local interpolation with a polynomial and subsequent manipulation of the same is appropriate.

The following notation is used:

x_i = value of the abscissa x at point i, $i = 1, 2, 3, \cdots \ell$

$S_i \triangleq x_{i+1} - x_i$ step magnitude at point i

$\alpha_i \triangleq S_i / S_{i-1}$ ratio of consecutive steps at point i

Y_i = one dimensional array representing the continuous function $y(x)$ given in discretized form at the ℓ points.

B-1. Integration.

The numerical computation of the integral of the function $y(x)$, defined in the interval x_1, x_ℓ, is desired, limits of integration being one extreme of the interval (either x_1 or x_ℓ) and each point x_i $(i = 1, 2, \cdots \ell)$.

B-1.1. Two-point formula (trapezoidal rule).

Linear interpolation is used to approximate the integrand $y(x)$ in each elementary interval x_i, x_{i+1}:

$$\int_{x_i}^{x_{i+1}} y(x)dx \cong (Y_i+Y_{i+1})\ S_i/2 \qquad \text{(B-1)}$$

B-1.2. Three-point formula (parabolic interpolation).

The integrand $y(x)$ is approximated by a second-order polynomial passing through three consecutive points

$$(Y_{i-1},\ x_{i-1})\ ,\ (Y_i,\ x_i)\ ,\ (Y_{i+1},\ x_{i+1})$$

If the origin of the abscissae is shifted for convenience to the point x_i, the condition of passage of the parabola $A + Bx + Cx^2$ through the points

$$(Y_{i-1},\ -S_{i-1})\ ,\ (Y_i,\ 0)\ ,\ (Y_{i+1},\ S_i)$$

becomes:

$$\begin{bmatrix} 1 & -S_{i-1} & S_{i-1}^2 \\ 1 & 0 & 0 \\ 1 & S_i & S_i^2 \end{bmatrix} \begin{bmatrix} A \\ B \\ C \end{bmatrix} = \begin{bmatrix} Y_{i-1} \\ Y_i \\ Y_{i+1} \end{bmatrix}$$

from which:

$$\left.\begin{aligned} A &= Y_i \\ B &= \frac{S_i^2 Y_{i-1} + (S_{i-1}^2 - S_i^2)\; Y_i - S_{i-1}^2\; Y_{i+1}}{-\; S_i S_{i-1}(S_i + S_{i+1})} \\ C &= \frac{-S_i Y_{i-1} + (S_i + S_{i-1})\; Y_i - S_{i-1}\; Y_{i+1}}{-\; S_i S_{i-1}(S_i + S_{i+1})} \end{aligned}\right\} \qquad \text{(B-2)}$$

Moreover

$$\int_{x_a}^{x_b} (A + Bx + Cx^2)dx = \left(Ax + \frac{B}{2}\,x^2 + \frac{C}{3}\,x^3\right)\Bigg|_{x_a}^{x_b}$$

so that:

$$\int_{x_{i-1}}^{x_{i+1}} y(x)\;dx \simeq \frac{S_i S_{i-1}}{6}\left[(2-\alpha_i)Y_{i-1} + (\alpha_i + 2 + 1/\alpha_i)Y_i + (2 - 1/\alpha_i)Y_{i+1}\right] \qquad \text{(B-3)}$$

which reduces to Simpson's formula if the step is uniform ($S_i = S_{i-1}$, i.e. $\alpha_i = 1$). In each of the two elementary intervals the integral becomes:

$$\int_{x_{i-1}}^{x_i} y(x)dx \simeq \frac{S_{i-1}}{6}\left[\left(3 - \frac{1}{\alpha_i + 1}\right) Y_{i-1} + \left(3 + \frac{1}{\alpha_i}\right) Y_i - \frac{1}{\alpha_i(\alpha_i + 1)}\; Y_{i+1}\right] \qquad \text{(B-4)}$$

$$\int_{x_i}^{x_{i+1}} y(x)dx \simeq \frac{S_i}{6}\left[-\frac{\alpha_i^2}{\alpha_i + 1}\; Y_{i-1} + (\alpha_i + 3)Y_i + \left(3 - \frac{\alpha_i}{\alpha_i + 1}\right)Y_{i+1}\right] \qquad \text{(B-5)}$$

B-1.3. Four-point formula (cubic interpolation).

The integrand $y(x)$ is approximated by a third order polynomial, passing through four consecutive points

$$(Y_{i-1}, x_{i-1}),\ (Y_i, x_i),\ (Y_{i+1}, x_{i+1}),\ (Y_{i+2}, x_{i+2}) \quad .$$

If the origin of the abscissae is shifted to the point x_i, the condition of passage of the cubic $A + Bx + Cx^2 + Dx^3$ through the points

$$(Y_{i-1}, z_{-1}),\ (Y_i, 0),\ (Y_{i+1}, z_1),\ (Y_{i+2}, z_2)$$

where

$$z_{j-i} = x_j - x_i \quad , \qquad j = i-1,\ i,\ i+1,\ i+2$$

becomes:

$$\begin{bmatrix} 1 & 0 & 0 & 0 \\ 1 & z_{-1} & z_{-1}^2 & z_{-1}^3 \\ 1 & z_1 & z_1^2 & z_1^3 \\ 1 & z_2 & z_2^2 & z_2^3 \end{bmatrix} \begin{bmatrix} A \\ B \\ C \\ D \end{bmatrix} = \begin{bmatrix} Y_i \\ Y_{i-1} \\ Y_{i+1} \\ Y_{i+2} \end{bmatrix}$$

or

$$\begin{bmatrix} 1 & z_{-1} & z_{-1}^2 \\ 1 & z_1 & z_1^2 \\ 1 & z_2 & z_2^2 \end{bmatrix} \begin{bmatrix} B \\ C \\ D \end{bmatrix} = \begin{bmatrix} \dfrac{Y_{i-1}-Y_i}{z_{-1}} \\ \dfrac{Y_{i+1}-Y_i}{z_1} \\ \dfrac{Y_{i+2}-Y_i}{z_2} \end{bmatrix} \quad ; \quad A = Y_i$$

Finally: $A = Y_i$

$$B = \frac{\begin{vmatrix} (Y_{i-1}-Y_i)/z_{-1} & z_{-1} & z_{-1}^2 \\ (Y_{i+1}-Y_i)/z_1 & z_1 & z_1^2 \\ (Y_{i+2}-Y_i)/z_2 & z_2 & z_2^2 \end{vmatrix}}{V}$$

$$C = \frac{\begin{vmatrix} 1 & (Y_{i-1}-Y_i)/z_{-1} & z_{-1}^2 \\ 1 & (Y_{i+1}-Y_i)/z_1 & z_1^2 \\ 1 & (Y_{i+2}-Y_i)/z_2 & z_2^2 \end{vmatrix}}{V}$$

$$D = \frac{\begin{vmatrix} 1 & z_{-1} & (Y_{i-1}-Y_i)/z_{-1} \\ 1 & z_1 & (Y_{i+1}-Y_i)/z_1 \\ 1 & z_2 & (Y_{i+2}-Y_i)/z_2 \end{vmatrix}}{V}$$

where V is the Vandermondian determinant

$$V = \begin{vmatrix} 1 & z_{-1} & z_{-1}^2 \\ 1 & z_1 & z_1^2 \\ 1 & z_2 & z_2^2 \end{vmatrix} = (z_1 - z_{-1})(z_2 - z_{-1})(z_2 - z_1)$$

Moreover

$$\int_{x_a}^{x_b} (A + Bx + Cx^2 + Dx^3)dx = \left(Ax + \frac{B}{2} x^2 + \frac{C}{3} x^3 + \frac{D}{4} x^4 \right) \Bigg|_{x_a}^{x_b} = Q(x_b) - Q(x_a)$$

where*

$$Q(x) = x\left\{ x\left[x\left(\frac{D}{4} x + \frac{C}{3} \right) + \frac{B}{2} \right] + A \right\}$$

so that

$$\int_{x_i}^{x_{i+1}} y(x)dx \cong Q(x)\Big|_{x=S_i} \qquad \text{(B-6)}$$

$$\int_{x_{i-1}}^{x_i} y(x)dx \cong -Q(x)\Big|_{x=-S_{i-1}} \qquad \text{(B-7)}$$

$$\int_{x_{i+1}}^{x_{i+2}} y(x)dx \cong Q(x)\Big|_{x=S_i} - Q(x)\Big|_{x=S_i+S_{i+1}} \qquad \text{(B-8)}$$

The highest accuracy is of course achieved with the use at each point of relation (B-6) only, at the expense of computing a new interpolating

---

* Such factorization represents the most efficient algorithm for computing the value of a polynomial at one point.

polynomial at each point in the interior of the interval of integration. Exception must be made for the points adjacent to the extremes (and in the interior for points of discontinuity of a derivative of $y(x)$) for which formulae (B-7), (B-8) are suitable.

In view of the rapid increase in the load of operations involved, higher order interpolation formulae are not considered practical in the present case, and are not reported.

B-2. Differentiation.

The first and second derivatives of the function $y(x)$ are desired at each point x_i, with exclusion of the extremes for the second derivative, assumed small at such points.

B-2.1. Two-point formula.

Only the first derivative may be computed in this case with the aid of a linear interpolation to approximate the function $y(x)$ in each elementary interval:

$$y'(x)\Big|_{x=x_i} \cong \frac{Y_{i+1}-Y_i}{S_i} \qquad i = 1, 2, \cdots \ell-1 \tag{B-9}$$

or alternatively

$$y'(x)\Big|_{x=x_i} \cong \frac{Y_i-Y_{i-1}}{S_{i-1}} \qquad i = 2, 3, \cdots \ell \tag{B-10}$$

B-2.2. Three-point formulae.

The same second order interpolating polynomial of Section B-1.2 to approximate the function $y(x)$ is employed, with coefficients

A, B, C given by relations (B-2).

The first and second derivatives at the point x_i are then:

$$y'(x)\Big|_{x=x_i} \cong B = \left[Y_{i+1} + (\alpha_i^2-1)Y_i - \alpha_i^2 Y_{i-1}\right] / \left[\alpha_i(S_i+S_{i-1})\right]; \quad i=2,3,\cdots \ell-1 \tag{B-11}$$

$$y''(x)\Big|_{x=x_i} \cong 2\,C = 2\left[Y_{i+1} - (\alpha_i+1)Y_i + \alpha_i Y_{i-1}\right] / \left[S_i(S_i+S_{i-1})\right]; \quad i=2,3,\cdots \ell-1 \tag{B-12}$$

The first derivative at the extremes may be computed with the lower-order formulae of Section B-2.1.

B-2.3. Five-point formulae.

The function $y(x)$ is approximated by a fourth-order polynomial passing through the points

$$(Y_{i-2},x_{i-2}),\ (Y_{i-1},x_{i-1}),\ (Y_i,x_i),\ (Y_{i+1},x_{i+1}),\ (Y_{i+2},x_{i+2})$$

If the origin of the abscissae is shifted to the point x_i, the condition of passage of the polynomial $A + Bx + Cx^2 + Dx^3 + Ex^4$ through the points

$$\left.\begin{array}{l}(Y_j, z_{j-i}) \\ \text{where} \quad z_{j-i} = x_j - x_i\end{array}\right\} \quad j=i-2,\ i-1,\ \cdots\ i+2$$

becomes

$$\begin{bmatrix} 1 & z_{-2} & z_{-2}^2 & z_{-2}^3 & z_{-2}^4 \\ 1 & z_{-1} & z_{-1}^2 & z_{-1}^3 & z_{-1}^4 \\ 1 & 0 & 0 & 0 & 0 \\ 1 & z_1 & z_1^2 & z_1^3 & z_1^4 \\ 1 & z_2 & z_2^2 & z_2^3 & z_2^4 \end{bmatrix} \begin{bmatrix} A \\ B \\ C \\ D \\ E \end{bmatrix} = \begin{bmatrix} Y_{i-2} \\ Y_{i-1} \\ Y_i \\ Y_{i+1} \\ Y_{i+2} \end{bmatrix}$$

or

$$\begin{bmatrix} 1 & z_{-2} & z_{-2}^2 & z_{-2}^3 \\ 1 & z_{-1} & z_{-1}^2 & z_{-1}^3 \\ 1 & z_1 & z_1^2 & z_1^3 \\ 1 & z_2 & z_2^2 & z_2^3 \end{bmatrix} \begin{bmatrix} B \\ C \\ D \\ E \end{bmatrix} = \begin{bmatrix} (Y_{i-2}-Y_i)/z_{-2} \\ (Y_{i-1}-Y_i)/z_{-1} \\ (Y_{i+1}-Y_i)/z_1 \\ (Y_{i+2}-Y_i)/z_2 \end{bmatrix}; \quad A = Y_i$$

so that:

$$y'(x)\Big|_{x=x_i} \simeq B = \frac{\begin{vmatrix} (Y_{i-2}-Y_i)/z_{-2} & z_{-2} & z_{-2}^2 & z_{-2}^3 \\ (Y_{i-1}-Y_i)/z_{-1} & z_{-1} & z_{-1}^2 & z_{-1}^3 \\ (Y_{i+1}-Y_i)/z_1 & z_1 & z_1^2 & z_1^3 \\ (Y_{i+2}-Y_i)/z_2 & z_2 & z_2^2 & z_2^3 \end{vmatrix}}{W} \qquad \text{(B-13)}$$

$$y''(x)\Big|_{x=x_i} \cong 2\,C = \frac{2\begin{vmatrix} 1 & (Y_{i-2}-Y_i)/z_{-2} & z_{-2}^2 & z_{-2}^3 \\ 1 & (Y_{i-1}-Y_i)/z_{-1} & z_{-1}^2 & z_{-1}^3 \\ 1 & (Y_{i+1}-Y_i)/z_1 & z_1^2 & z_1^3 \\ 1 & (Y_{i+2}-Y_i)/z_2 & z_2^2 & z_2^3 \end{vmatrix}}{W} \tag{B-14}$$

where W is the Vandermondian determinant

$$W = \begin{vmatrix} 1 & z_{-2} & z_{-2}^2 & z_{-2}^3 \\ 1 & z_{-1} & z_{-1}^2 & z_{-1}^3 \\ 1 & z_1 & z_1^2 & z_1^3 \\ 1 & z_2 & z_2^2 & z_2^3 \end{vmatrix} = (z_{-1}-z_{-2})\cdot(z_1-z_{-2})\cdot(z_2-z_{-2})\cdot \cdot(z_1-z_{-1})\cdot(z_2-z_{-1})\cdot \cdot(z_2-z_1)$$

The above relations allow the computation of the derivatives at the points

$$i = 3,\ 4\ \cdots,\ \ell-2\ ,$$

whereas the lower order formulae of Sections B-2.1, B-2.2 may be employed for the points close to the extremes.

APPENDIX C

COMPUTER PROGRAM FOR THE DIRECT STEADY-STATE PROBLEM.

In this Appendix the computer program (in FORTRAN IV, version 4) for the steady-state basic direct problem is reported. The method of solution and the mathematical formulation are described in Chapters I and II, and the illustration of the various alternatives chosen is shown in Fig. 2.2.

The program consists of a main program (deck 'PND'), a first set of subprograms (decks 'S01' to 'S15') each performing logically different operations of the algorithm, and a second set of subprograms ('SP1' to 'SP4' or 'SP5') driving various types of peripheral equipment to display and record the results. This modular organization of the program allows the most efficient core memory usage for the selection of several options, without modification of the program, by simple interchange of the relevant decks. It also facilitates considerably partial alterations of the program to incorporate new features.

Double precision arithmetic has been mostly used. The size of the vectors and matrices has been chosen according to the memory size of the machine available (32,000 locations).

The following remarks, in addition to the comments incorporated within the program, may contribute to clarification of the various algorithms selected.

Main program.

Deck 'PND'. The main program drives the subprograms actually performing the required calculations.

Subroutine 'STRUCT'.

Deck 'S01'. Furnishes the structure parameters of the device determined by two DATA cards. An option available in the solution allows the selection of the structure in the following "standard" configuration. If a fictitious abrupt doping profile is specified by a first DATA card, the structural points M and L are then furnished according to the following relations (Fig. A-1):

$$M_N = \begin{cases} x_P/4 & \text{if } x_N \le x_P/4 \\ x_N & \text{if } x_N > x_P/4 \end{cases}$$

$$M = M_N + x_N$$

$$L = M + 2\, x_P$$

where x_N (x_P) is the depleted region width [(A-38), (A-39)] in the N (P) material in thermal equilibrium corresponding to the fictitious doping profile assigned. This profile may or may not coincide with the actual doping profile used for the device of interest, and defined by a second DATA card. The first-order parameters x_N and x_P are computed by the subroutine 'FSTORD'.

Subroutine 'FSTORD'.

Deck 'S02'. Computes several first-order parameters for an abrupt asymmetric junction, on the basis of Eqs.(A-41), (A-42), (A-38), (A-39), (A-13), (A-55), (A-54) (Appendix A).

Subroutine 'STPSEL'.

Deck 'S03'. Performs the interpolation scheme of Subsection 2.3.1 (Fig. 2.3), concerning the selection of the step distribution throughout the device for a specified total number of points.

Subroutine 'XSTEP2'.

Deck 'S04'. Computes the step distribution and the total number of points for a given accuracy ε_S on the basis of the algorithm of Subsection 2.3.1b (Fig. 2.6).

Subroutine 'SLAGR'.

Deck 'S05'. Performs a Lagrangian interpolation on two one-dimensional arrays unevenly spaced.

Subroutine 'STPADJ'.

Deck 'S06'. Performs a minor adjustment on a preliminary non-uniform step distribution in a certain region (N or P), in order to improve the accuracy of the relation

$$\sum \text{all steps in region} = \text{length of region} \qquad \text{(C-1)}$$

without altering the ratio of consecutive steps. The preliminary step distribution which enters this subroutine satisfies the relation (C-1) within one half of the largest step in that region.

Subroutine 'DOPING'.

Deck 'S07'. Furnishes an abrupt impurity distribution, uniform in both N and P regions (Fig. 1.1).

Subroutine 'PSITRL'.

Deck 'S08'. Furnishes the trial potential function given by relations (A-21), (A-36), (A-37), and (A-16) (Appendix A).

Subroutine 'MOBCAR'.

Deck 'S09'. Computes the mobile carrier distributions throughout the device for a given electrostatic potential according to Eqs.(2.3), (2.4) for forward bias, and (2.13), (2.16) for reverse bias conditions (summarized in Table 2.2). Electron and hole currents are computed with the aid of Eqs.(1.41) and (1.42).

Subroutine 'INTEGR'.

Computes the integral of a function given in discretized form throughout the device, limits of integration being one boundary and each of the internal points. Two versions of this routine are available. Only one must be inserted in the actual program.

Deck 'S10A'. A two-point formula (trapezoidal rule) is used, according to relation (B-1) (Appendix B).

Deck 'S10B'. A four-point formula (cubic interpolation) is used according to relation (B-6).

Double precision function 'DET'.

Deck 'S11'. Computes the determinant of a matrix.

Subroutine 'INTGSF'.

Deck 'S12'. Computes the integrals (2.11a) and (2.15a) with the insertion of the scale factors (2.11) and (2.15) whenever needed. Trapezoidal rule is used.

Subroutine 'POISSN'.

Deck 'S13'. Solves Poisson's equation (1.45) with a finite difference scheme and solution of a triple-diagonal matrix equation.

Subroutine 'CURV'.

Computes the curvature of a function, given in discretized form, at each internal point throughout the interior of the device. Two versions are available. Only one must be inserted in the actual program.

Deck 'S14A'. A three-point formula (parabolic interpolation) is used, according to relation (B-12) (Appendix B).

Deck 'S14B'. A five-point formula (fourth-order polynomial) is used, according to the formulation of Subsection B-2.3. The relevant matrices are slightly rearranged in this routine in order to achieve a higher efficiency.

Subroutine 'TRIDU1'.

Deck 'S15'. Solves a triple-diagonal system of the form (2.44) with a direct method, according to the algorithm (2.45).

Subroutine 'PRINT'.

Deck 'SP1'. Writes on the printout sheet the results of interest.

Subroutine 'PUNCH'.

Records on punched cards the results of interest. Two versions are available. Only one must be inserted in the actual program.

Deck 'SP2'. Recording on cards is actually performed.

Deck 'SP2D'. Recording on cards is not performed.

Subroutine 'PLOT'.

Displays in graphical form the results of interest. The actual routine is not reported since it is highly dependent upon the plotting equipment available and therefore not of general interest. If graphical recording is not desired the following deck must be inserted in the actual program.

Deck 'SP3D'. Graphical recording is not performed.

Subroutine 'TAPE'.

Records on magnetic tape results of interest. Two versions are available. Only one must be inserted in the actual program.

Deck 'SP4'. Recording on tape is made available during the execution of the program.

Deck 'SP4D'. Recording on tape is not performed.

Deck 'SP5'. This subprogram (written in Assembler language IBMAP) defines the file for one magnetic save tape needed by the deck 'SP4'. If the deck 'SP4D' is used instead (i.e. recording on magnetic tape is not desired) the deck 'SP5' may be omitted.

```
$IBFTC PND     DECK
C***********************************************************************
C*                 M A I N     P R O G R A M       (DIRECT PROBLEM)    *
C***********************************************************************
C*                                                                     *
C***********************************************************************
C*                THIS PROGRAM SOLVES THE BASIC TWO-CARRIER TRANSPORT EQUA- *
C*   TIONS, GOVERNING THE BEHAVIOR OF SEMICONDUCTOR DEVICES, APPLIED TO AN N-P *
C*   JUNCTION UNDER THE FOLLOWING ASSMUMPTIONS                          *
C*   (A)  NON DEGENERATE CONDITIONS                                     *
C*   (B)  CONSTANT TEMPERATURE                                          *
C*   (C)  TIME INDEPENDENT IMPURITY DISTRIBUTION                        *
C*   (D)  FULL IONIZATION OF THE IMPURITIES                             *
C*   (E)  ONE-DIMENSIONAL STRUCTURE                                     *
C*   (F)  STEADY-STATE CONDITIONS ONLY                                  *
C*   (G)  OHMIC CONTACTS                                                *
C*   (H)  ABSENCE OF GENERATION-RECOMBINATION IN THE INTERIOR           *
C*   (I)  CONSTANT MOBILITIES                                           *
C*   (J)  DIRECT PROBLEM.     GIVEN   AN APPLIED VOLTAGE, THE TOTAL CURRENT *
C*        THROUGH THE DEVICE IS OBTAINED (TOGETHER WITH ALL THE PARAMETERS *
C*        AND DISTRIBUTIONS OF INTEREST).                               *
C*   NO APPROXIMATIONS IN THE SET OF EQUATIONS HAVE BEEN INTRODUCED.    *
C*   THE  N-REGION IS ASSUMED LOCATED ON THE LEFT SIDE OF THE METALLURGICAL *
C*   INTERFACE  M.                                                      *
C*                                                                     *
C*                THIS PROGRAM USES AN ITERATIVE SCHEME BASED ON THE COMPU- *
C*   TATION OF THE MOBILE CARRIERS FROM A POTENTIAL DISTRIBUTION THROUGH DIR- *
C*   ECT INTEGRATION FOLLOWED BY CORRECTION OF THE POTENTIAL DISTRIBUTION *
C*   THROUGH THE SOLUTION OF POISSON'S EQUATION.  A TRIAL POTENTIAL DISTRIBU- *
C*   TION IS REQUIRED TO START THE ITERATIONS.                          *
C*   THE WHOLE PROGRAM IS BUILT IN A HIGHLY MODULAR FASHION, FEATURING A MAIN *
C*   PROGRAM CALLING SEVERAL SUBPROGRAMS, IN FAVOR OF  A GREATER FLEXIBILITY *
C*   AND SIMPLICITY OF LOGIC ORGANIZATION.                              *
C*   SUBPROGRAMS EXPLICITLY CALLED BY THIS MAIN PROGRAM ARE             *
C*                SUBROUTINE  'STRUCT'  (DEFINES THE STRUCTURE PARAMETERS) *
C*                SUBROUTINE  'FSTORD'  (COMPUTES FIRST-ORDER THEORY PARAME- *
C*                                       TERS)                          *
C*                SUBROUTINE  'STPSEL'  (SELECTS THE STEP DISTRIBUTION) *
C*                SUBROUTINE  'DOPING'  (FURNISHES THE IMPURITY DISTRIBUTION) *
C*                SUBROUTINE  'PSITRL'  (FURNISHES THE TRIAL POTENTIAL FUNC- *
C*                                       TION)                          *
C*                SUBROUTINE  'MOBCAR'  (YIELDS THE MOBILE CARRIER CONCEN- *
C*                                       TRATIONS FOR A GIVEN POTENTIAL ) *
C*                SUBROUTINE  'POISSN'  (FURNISHES AN IMPROVED POTENTIAL DI- *
C*                                       STRIBUTION BY SOLVING POISSON'S *
C*                                       EQUATION FOR GIVEN MOBILE CARRIERS) *
C*                SUBROUTINE  'PRINT'   (WRITES OUTPUT DATA ON PRINTOUT *
C*                                       SHEET)                         *
C*                SUBROUTINE  'PUNCH'   (PUNCHES ON OUTPUT CARDS RELEVANT *
C*                                       QUANTITIES)                    *
C*                SUBROUTINE  'PLOT'    (EXECUTES PLOTS OF RELEVANT QUANTI- *
C*                                       TIES)                          *
C*                SUBROUTINE  'TAPE'    (RECORDS ON MAGNETIC TAPE RELEVANT *
C*                                       QUANTITIES)                    *
C*   OTHER SUBPROGRAMS MAY BE CALLED BY THE ABOVE SUBROUTINES.          *
C*   DOUBLE PRECISION ARITHMETIC IS USED.                               *
C*                                                                     *
C*                                                                     *
C*                INPUT PARAMETERS ARE                                  *
C*                                                                     *
C*   DATA CARD    1. PARAMETERS CONCERNING THE STRUCTURE ARE READ IN THE SUB- *
C*                   ROUTINE  'STRUCT'  (SEE SUBROUTINE  'STRUCT'  )    *
C*   DATA CARD    2. PARAMETERS CONCERNING THE MATERIAL PROPERTIES ARE READ  IN *
C*                   THE SUBROUTINE  'STRUCT'  (SEE SUBROUTINE  'STRUCT'  ) *
C*                                                                     *
C*   DATA CARD    3. PARAMETERS CONCERNING THE ACTUAL APPLIED VOLTAGE ARE READ *
C*                   IN THIS MAIN PROGRAM AS FOLLOWS                    *
C*   VAA   = APPLIED VOLTAGE,GIVEN IN   NORMALIZED FORM IF THE (BELOW) INPUT *
C*           PARAMETER  IVAA  IS EQUAL TO  ONE,IN UNNORMALIZED FORM OTHERWISE. *
C*   FXP   = (OPTIONAL) MULTIPLICATIVE CORRECTION FACTOR TO THE FIRST-ORDER *
C*           WIDTH OF THE DEPLETED REGION IN THE LOW-CONDUCTIVITY SIDE (IF OMIT- *
C*           TED, NO CORRECTION IS PERFORMED)                           *
C*   ITMAX= MAXIMUM NUMBER OF POISSON'S ITERATIONS                      *
C*   ERRPS= MAXIMUM ERROR ALLOWED ON THE FINAL POTENTIAL FUNCTION.   THE NUM- *
C*           BER OF POISSON'S ITERATIONS IS DETERMINED EITHER BY  ITMAX  OR BY *
C*           ERRPS, WHICHEVER APPLIES FIRST                             *
C*   PSIMPR=(REQUIRED AT EXTREMELY HIGH INJECTION LEVELS, OPTIONAL OTHERWISE) *
C*           PARAMETER THAT DETERMINES THE VALUE OF THE FIRST-ORDER TRIAL ELEC- *
C*           TROSTATIC POTENTIAL AT THE INTERFACE BETWEEN THE DEPLETED AND NEU- *
C*           TRAL REGION IN THE LOW-CONDUCTIVITY SIDE.(IF OMITTED, NO CORRECTION *
C*           IS PERFORMED)                                              *
C*   IWR   = PARAMETER THAT CONTROLS THE PRINTOUT IN THE SUBROUTINE  'PRINT' *
C*           (SEE SUBROUTINE  'PRINT' )                                 *
C*   INTAPE=PARAMETER THAT CONTROLS THE PROCEDURE OF RECORDING DATA ON MAGNE- *
C*           TIC TAPE  (SEE SUBROUTINE  'TAPE'  )                       *
C*   IVAA = (INTEGER) PARAMETER THAT CONTROLS    THE    INPUT OF THE APPLIED *
C*           VOLTAGE   VAA  (SEE ABOVE)                                 *
C*   ISTOP= PARAMETER THAT CONTROLS THE REPETITION OF THE SOLUTION FOR SEVERAL *
C*           APPLIED VOLTAGES AS FOLLOWS                                *
C*                   ISTOP = 0   THE STRUCTURE AND MATERIAL PARAMETERS ARE NOT *
C*                               CHANGED FOR THE FOLLOWING APPLIED VOLTAGE *
C*                               (NEW STRUCTURE AND MATERIAL DATA CARDS  1. AND *
C*                               2.  MUST NOT BE INSERTED FOR THE FOLLOWING AP- *
C*                               PLIED VOLTAGE)                         *
C*                   ISTOP = 1   LAST APPLIED VOLTAGE OF THE SET        *
C*                   ISTOP = 2   THE STRUCTURE AND MATERIAL PARAMETERS ARE CHAN- *
C*                               GED FOR THE FOLLOWING APPLIED VOLTAGE (NEW *
C*                               STRUCTURE AND MATERIAL DATA CARDS  1.  AND  2. *
C*                               MUST BE INSERTED FOR THE FOLLOWING APPLIED VOL- *
C*                               TAGE)                                  *
C*                                                                     *
C*   DATA CARD    4. PARAMETERS CONCERNING THE AUTOMATIC STEP SELECTION PROCE- *
C*                   DURE, INCLUDING THE TOTAL NUMBER OF POINTS DESIRED, ARE *
C*                   READ IN THE SUBROUTINE  'STPSEL'  (SEE SUBROUTINE 'STPSEL'). *
C*                   ONE DATA CARD FOR EACH APPLIED VOLTAGE MUST BE FURNISHED *
C*                   IN THE APPROPRIATE ORDER.                          *
C*                                                                     *
C*                                                                     *
C*                   OUTPUT PARAMETERS ARE                              *
C*                                                                     *
C*   PSI   = ONE-DIMENSIONAL ARRAY, EXACT POTENTIAL DISTRIBUTION        *
C*   N     = ONE-DIMENSIONAL ARRAY, EXACT ELECTRON DISTRIBUTION         *
C*   P     = ONE-DIMENSIONAL ARRAY, EXACT HOLE DISTRIBUTION             *
C*   X     = ONE-DIMENSIONAL ARRAY, ABSCISSA OF EACH POINT THROUGHOUT THE JUNC- *
C*           TION                                                       *
C*   STEP  = ONE-DIMENSIONAL ARRAY, NON UNIFORM STEP MAGNITUDE AT EACH POINT *
C*   JN    = ELECTRON CURRENT                                           *
C*   JP    = HOLE CURRENT                                               *
C*   J     = TOTAL CURRENT                                              *
C*                                                                     *
C*                   ALLOWANCE FOR  SEVEN DOUBLE PRECISION ARRAYS  (STEP,PSI, *
C*   N,P,DELTA  +  TWO WORKING ARRAYS IN THE LABELED  COMMON  /WORK/ ) AND *
```

```
C*  ONE SINGLE PRECISION ARRAY  (NIM), ALL OF DIMENSION  1000, HAS BEEN MADE.  *
C*******************************************************************************
      DOUBLE PRECISION STEP(1000),PSI(1000),VA
     $,N(1000),P(1000),DELTA(1000),DUMMY(2000)
     $,          ND,NA,NN,PP,NP,PN,VD,M,L
      REAL NIM(1000),JN,JP
      COMMON /STRC/ ND,NA,NN,PP,NP,PN,VD,M,L,IM,IL,VT,GAMN,GAMP
     $        /MCAR/ N,P,JN,JP
     $        /XST / STEP
     $        /WORK/ DUMMY
     $        /TRDG/ DELTA
     $        /PSNM/ PSI,NIM
10    FORMAT (2E10.0,10X,I10,2E10.0,4I5)
15    FORMAT (1H1, 54H THE APPLIED VOLTAGE AND RELATED INPUT PARAMETERS
     $ARE  ///////////10H VAA     = ,F9.5// 10H FXP     = ,F9.5//
     $                         10H ERRPS  = ,E13.5//10H ITMAX  = ,I3//////)

C*****************STRUCTURE AND MATERIAL PROPERTIES DEFINITIONS***************
100   CALL STRUCT

C*****************READING OF THE APPLIED VOLTAGE AND CONTROL PARAMETERS FROM  *
C*  DATA CARD  3,***************************************************************
120   READ (5,10) VAA,FXP,        ITMAX,ERRPS, PSIMPR, IWR,INTAPE,IVAA
     $,ISTOP
      VA=VAA /VT
      IF (IVAA.NE.1) GO TO 130
      VA=VAA
      VAA=VA*VT
130   CONTINUE
      WRITE (6,15)VAA,FXP,        ERRPS,ITMAX
      IF (IWR1.EQ.0) IWR1=10

C*****************DETERMINATION OF FIRST-ORDER THEORY PARAMETERS (DEPLETED    *
C*  REGION LENGTHS ONLY) TO BE USED IN THE STEP SELECTION PROCEDURE************
      KW=1
      CALL FSTORD (VA ,FXP,KW,PSIMPR)
      IF (KW.LT.0) GO TO 9999

C*****************AUTOMATIC SELECTION OF THE STEP*****************************
      CALL STPSEL (JRET,1,1)
      IF (JRET.EQ.1) GO TO 9999

C*****************DEFINITION OF THE IMPURITY DISTRIBUTION*********************
      CALL DOPING (NIM)

C*****************DETERMINATION OF FIRST-ORDER PARAMETERS*********************
      KW=2
      CALL FSTORD (VA ,FXP,KW,PSIMPR)

C*****************CHOICE OF THE TRIAL POTENTIAL DISTRIBUTION*******************
      CALL PSITRL (PSI,VA)
      DELTAM=1.E20
      ITER=0

C*****************DETERMINATION OF THE MOBILE CARRIER DISTRIBUTIONS FROM THE  *
C*  POTENTIAL DISTRIBUTION******************************************************
170   CALL MOBCAR (PSI,VA)
      IF (ITER.EQ.ITMAX.OR. DELTAM.LE.ERRPS ) GO TO 300

C*****************IMPROVEMENT OF THE POTENTIAL DISTRIBUTION THROUGH THE SOLU- *
C*  TION OF POISSON'S EQUATION**************************************************
      CALL POISSN (DELTAM,IL)
      ITER=ITER+1
      GO TO 170
300   CONTINUE

C*****************DISPLAYING AND RECORDING RESULTS****************************
      CALL PRINT (IWR,ITER,VA,DELTAM,ERRPS)
      CALL PUNCH (VA,DELTAM,FXP,ITER)
      CALL PLOT (VA,IL)
      CALL TAPE (VA,DELTAM,ITER,IDTP,INTAPE)
9999  IF (ISTOP.EQ.2) GO TO 100
      IF (ISTOP.EQ.0) GO TO 120
      CALL TAPE (VA,DELTAM,ITER,  0,  4)
      STOP
      END


$IBFTC S01     DECK
      SUBROUTINE STRUCT
C*******************************************************************************
C*                THE SUBROUTINE  'STRUCT'  FURNISHES THE STRUCTURE PARAME-   *
C*  TERS  INCLUDING THE THERMAL EQUILIBRIUM CONCENTRATIONS FOR THE MOBILE     *
C*  CARRIERS.                                                                 *
C*                                                                            *
C*                THIS ROUTINE READS FROM THE FIRST DATA CARD PARAMETERS RELA-*
C*  TED TO THE STRUCTURE AND FROM THE SECOND DATA CARD PARAMETERS CONCERNING  *
C*  THE PROPERTIES OF THE MATERIALS.   VARIOUS ALTERNATIVES ARE PROVIDED, AS  *
C*  INDICATED BELOW.                                                          *
C*  SUBPROGRAM NEEDED                                                         *
C*                           SUBROUTINE  'FSTORD'                             *
C*                                                                            *
C*                                                                            *
C*                INPUT PARAMETERS ARE                                        *
C*        FIRST DATA CARD.   EITHER                                           *
C*  MA    = ABSCISSA OF THE METALLURGICAL INTERFACE                           *
C*  LA    = ABSISSA OF THE EXTERNAL CONTACT ON THE RIGHT SIDE (ALSO LENGTH OF *
C*          THE WHOLE STRUCTURE)                                              *
C*  IF THE PARAMETERS  MA, LA  ARE GIVEN IN UNNORMALIZED FORM, THE QUANTITY   *
C*  MA  MUST BE POSITIVE, IF GIVEN IN NORMALIZED FORM THE QUANTITY  MA  MUST  *
C*  BE NEGATIVE.                                                              *
C*                                                                            *
C*        OR                                                                  *
C*  CNST = FICTITIOUS CONDUCTIVITY OF THE  N-REGION                           *
C*  CPST = FICTITIOUS CONDUCTIVITY OF THE  P-REGION                           *
C*  VSTA = FICTITIOUS APPLIED VOLTAGE (UNNORMALIZED)                          *
C*  THE SET  CNST,CPST, VSTA  DETERMINES THE POINTS M  AND  L  IN A STANDARD  *
C*  CONFIGURATION  (SEE SUBROUTINE DESCRIPTION).                              *
C*                                                                            *
C*        OR                                                                  *
C*  NDST = FICTITIOUS DONOR CONCENTRATION IN THE N-REGION                     *
C*  NAST = FICTITIOUS ACCEPTOR  CONCENTRATION IN THE P-REGION                 *
C*  VSTA = FICTITIOUS APPLIED VOLTAGE  (UNNORMALIZED)                         *
C*  IF PARAMETERS  NDST, NAST  ARE GIVEN IN UNNORMALIZED FORM THE QUANTITY    *
C*  NDST MUST BE POSITIVE, IF GIVEN IN NORMALIZED FORM THE QUANTITY  NDST     *
C*  MUST BE NEGATIVE.                                                         *
C*  THE SET  NDIS,NASI, VAST DETERMINES THE POINTS  M  AND  L  IN A STANDARD  *
C*  CONFIGURATION (SEE SUBROUTINE DESCRIPTION).                               *
C*                                                                            *
C*        SECOND DATA CARD.      EITHER                                       *
C*  CONDN= ACTUAL CONDUCTIVITY OF THE  N  MATERIAL IN THERMAL EQUILIBRIUM     *
```

```
C*          (UNNORMALIZED)                                                 *
C*  CONDP= ACTUAL CONDUCTIVITY OF THE  P  MATERIAL IN THERMAL EQUILIBRIUM  *
C*          (UNNORMALIZED)                                                 *
C*       OR                                                                *
C*  NDA  = ACTUAL DONOR CONCENTRATION IN THE N MATERIAL  IN THERMAL EQUILI- *
C*          BRIUM  (AT THE EXTERNAL CONTACT)                               *
C*  NAA  = ACTUAL ACCEPTOR CONCENTRATION IN THE P MATERIAL IN THERMAL EQUILI- *
C*          BRIUM  (AT THE EXTERNAL CONTACT)                               *
C*  IF THE PARAMETERS  NDA,NAA   ARE GIVEN IN UNNORMALIZED FORM THE QUANTITY *
C*  NDA  MUST BE POSITIVE. IF GIVEN IN NORMALIZED FORM THE QUANTITY  NDA   *
C*  MUST BE NEGATIVE.                                                      *
C*                                                                         *
C*                    OUTPUT PARAMETERS ARE                                *
C*  M     = ABSCISSA OF THE LAST POINT OF THE  N REGION AT THE METALLURGICAL *
C*          INTERFACE                                                      *
C*  L     = ABSCISSA OF THE EXTERNAL CONTACT ON THE RIGHT SIDE (ALSO LENGTH OF *
C*          THE WHOLE STRUCTURE)                                           *
C*  ND    = DONOR CONCENTRATION IN THE N MATERIAL (AT THE EXTERNAL CONTACT) *
C*  NA    = ACCEPTOR CONCENTRATION IN THE P MATERIAL (AT THE EXTERNAL CONTACT) *
C*  NN    = BOUNDARY VALUE FOR THE ELECTRON CONCENTRATION IN THE N-REGION  *
C*          (AT THE EXTERNAL CONTACT)                                      *
C*  NP    = BOUNDARY VALUE FOR THE ELECTRON CONCENTRATION IN THE P-REGION  *
C*          (AT THE EXTERNAL CONTACT)                                      *
C*  PP    = BOUNDARY VALUE FOR THE    HOLE  CONCENTRATION IN THE P-REGION  *
C*          (AT THE EXTERNAL CONTACT)                                      *
C*  PN    = BOUNDARY VALUE FOR THE    HOLE  CONCENTRATION IN THE N-REGION  *
C*          (AT THE EXTERNAL CONTACT)                                      *
C*  VD    = DIFFUSION POTENTIAL  (BARRIER POTENTIAL)                       *
C*  VT    = THERMAL VOLTAGE                                                *
C*  GAMN = RECIPROCAL OF THE NORMALIZED DIFFUSION CONSTANT FOR ELECTRONS   *
C*  GAMP = RECIPROCAL OF THE NORMALIZED DIFFUSION CONSTANT FOR HOLES       *
C**************************************************************************
      DOUBLE PRECISION
     $               ND,NA,NN,PP,NP,PN,VD,M,L
      REAL             MN,MP,INJPAR,NAST,NDST,NDA,NAA,NINT,MOBN,MOBP,LD
     $,MA,LA ,JNFSOR
      COMMON /STRC/ ND,NA,NN,PP,NP,PN,VD,M,L,IM,IL,VT,GAMN,GAMP
     $        /FSO / XN,XP,MN,MP,INJPAR,PSIMP,JNFSOR
10    FORMAT (7E10.0)
15    FORMAT (1H1,62HTHE STRUCTURE IS DETERMINED BY THE FOLLOWING INPUT
     $PARAMETERS  ///
     $ 7H CNST =,E15.8//7H CPST =,E15.8//7H NDST =,E15.8//7H NAST =,E15.
     $8//7H VSTA =,E15.8//////////////////////)
20    FORMAT (1H1,29HTHE STRUCTURE PARAMETERS ARE  ////10X,12H(NORMALIZE
     $D) ,32X,14H(UNNORMALIZED) ,23X,25H(NORMALIZATION CONSTANTS)///
     $7H M     =,D23.16,
     $20X,7H MA    =,E15.8,20X,7H LD    =,E15.8//
     $7H L     =,D23.16,20X, 7H LA    =,E15.8////50X,7H CONDN=,E15.8//
     $50X,7H CONDP=,E15.8////7H ND    =,D23.16,20X,7H NDA   =,E15.8,20X,
     $ 7H NINT =,E15.8//7H NA    =,D23.16,20X,7H NAA   =,E15.8//7H NN    =,
     $D23.16//7H PP    =,D23.16//7H NP    =,D23.16//7H PN    =,D23.16////
     $ 7H VD    =,D23.16,20X, 7H VDA   =,E15.8,20X, 7H VT    =,E15.8/)
30    FORMAT (4E10.0)

C******************SET CONSTANTS*******************************************
      VT=.025875
      ELCH=1.60206E-19
      NINT=2.5E13
      PERM=8.85434E-14*16.
      MOBN=93./VT
      MOBP=44./VT
      GAMN=1./93.
      GAMP=1./44.
      Z=NINT*ELCH
      LD= SQRT(PERM*VT/Z)
      ISTR=0

C******************READ FROM A DATA CARD PARAMETERS PERTINENT TO THE DETERMI-  *
C*  NATION OF THE STRUCTURE POINTS  M   AND  L   ONLY*****************************
      READ (5,10) MA,LA,CNST,CPST,NDST,NAST,VSTA
      M=MA/LD
      L=LA/LD
      IF (MA.GE.0.) GO TO 33
      L=ABS(LA)
      M=ABS(MA)
33    IF (M.NE.0.) GO TO 80
      WRITE (6,15) CNST,CPST,NDST,NAST,VSTA
      CONDN=CNST
      CONDP=CPST
      NDA=NDST
      NAA=NAST
40    IF(NDA.EQ.0.) GO TO 50
      ND=NDA/NINT
      NA=NAA/NINT
      IF (NDA.GT.0.) GO TO 43
      ND=ABS(NDA)
      NA=ABS(NAA)
43    NN=DSQRT(ND*ND/4.D0+1.D0)-ND/2.D0
      PP=DSQRT(NA*NA/4.D0+1.D0)-NA/2.D0
      NP=1.D0/PP
      PN=1.D0/NN
      CONDN=Z*(MOBN*NN+MOBP*PN)
      CONDP=Z*(MOBN*NP+MOBP*PP)
      GO TO 70
50    Y=MOBN*MOBP
      ND=(CONDN*(MOBP-MOBN)+(MOBN+MOBP)*  SQRT(CONDN**2+4.*Y*Z*Z))/
     $(2.*Y*Z)
      NA=(CONDP*(MOBN-MOBP)+(MOBN+MOBP)*  SQRT(CONDP**2+4.*Y*Z*Z))/
     $(2.*Y*Z)
      NN=DSQRT(ND*ND/4.D0+1.D0)-ND/2.D0
      PP=DSQRT(NA*NA/4.D0+1.D0)-NA/2.D0
      PN=1.D0/NN
      NP=1.D0/PP
70    CONTINUE
      VD=DLOG(NN*PP)
      IF (ISTR.EQ.0) GO TO 75
      MA=M*LD
      LA=L*LD
      NDA=ND*NINT
      NAA=NA*NINT
      VDA=VD*VT
      WRITE (6,20) M,MA,LD,L,LA,CONDN,CONDP,ND,NDA,NINT,
     $ NA,NAA,NN,PP,NP,PN,VD,VDA,VT
      RETURN
75    KW=0
      VST=VSTA/VT
      CALL FSTORD (VST,1.,KW,0.)
      MN=XP/4.
      IF (XN.GT.MN) MN=XN
      M=MN+XN
      L=M+2.*XP
80    ISTR=1
```

```
C******************READ FROM A DATA CARD PARAMETERS PERTINENT TO THE ACTUAL      *
C*   PROPERTY OF THE MATERIAL ONLY**********************************************
      READ (5,30) CONDN,CONDP,NDA,NAA
      GO TO 40
      END


$IBFTC S02      DECK
      SUBROUTINE FSTORD (VA ,FXP,KW,PSIMPR)
C*******************************************************************************
C*                    THE SUBROUTINE 'FSTORD'  COMPUTES SEVERAL FIRST-ORDER     *
C*   THEORY PARAMETERS FOR AN ABRUPT ASYMMETRIC JUNCTION.                       *
C*                                                                              *
C*                    INPUT PARAMETERS ARE                                      *
C*   VA    = APPLIED VOLTAGE (NORMALIZED, DOUBLE PRECISION)                     *
C*   FXP   = (OPTIONAL) MULTIPLICATIVE CORRECTION FACTOR TO THE FIRST-ORDER     *
C*           WIDTH OF THE DEPLETED REGION IN THE LOW-CONDUCTIVITY SIDE (IF OMIT- *
C*           TED, NO CORRECTION IS PERFORMED)                                   *
C*   KW    = 0,1,2  OR 3  DEPENDING UPON THE VARIOUS FIRST ORDER THEORY PARAME- *
C*           TERS DESIRED                                                       *
C*   PSIMPR=(REQUIRED AT EXTREMELY HIGH INJECTION LEVELS, OPTIONAL OTHERWISE:   *
C*           PARAMETER THAT DETERMINES THE VALUE OF THE FIRST-ORDER TRIAL ELEC- *
C*           TROSTATIC POTENTIAL AT THE INTERFACE BETWEEN THE DEPLETED AND NEU- *
C*           TRAL REGION IN THE LOW-CONDUCTIVITY SIDE.(IF OMITTED, NO CORRECTION *
C*           IS PERFORMED).                                                     *
C*   STRUCTURE PARAMETERS(INCLUDED IN THE LABELED  COMMON  /STRC/ )             *
C*                                                                              *
C*                    OUTPUT PARAMETERS ARE                                     *
C*   XN    = WIDTH OF THE DEPLETED  N- REGION                                   *
C*   XP    = WIDTH OF THE DEPLETED  P- REGION                                   *
C*   MN    = ABSCISSA OF THE INTERFACE BETWEEN  THE  NEUTRAL AND DEPLETED       *
C*           N-REGION                                                           *
C*   MP    = ABSCISSA OF THE INTERFACE BETWEEN  THE  NEUTRAL AND DEPLETED       *
C*           P-REGION                                                           *
C*   KW    = A NEGATIVE NUMBER  IF THE SPECIFIED APPLIED VOLTAGE EXCEEDS THE    *
C*           MAXIMUM ALLOWED BY THE FIRST-ORDER THEORY  TRIAL FUNCTION          *
C*   INJPAR = INJECTION PARAMETER                                               *
C*   PSIMP  = VALUE OF THE POTENTIAL AT THE POINT   MP  (ORIGIN OF THE POTEN-   *
C*              TIAL IS THE EXTERNAL CONTACT OF THE  N-REGION)                  *
C*                                                                              *
C*                    OTHER FIRST-ORDER THEORY PARAMETERS COMPUTED AND WRITTEN  *
C*   ON  PRINTOUT SHEET                                                         *
C*   JNFSOR = FIRST-ORDER ELECTRON  (DOMINANT)  CURRENT                         *
C*  .CAPDF  = DIFFUSION CAPACITANCE                                             *
C*   CAPDFR = DIFFUSION CAPACITANCE TO THE  -2  POWER                           *
C*   CAPSK  = SCHOTTKY CAPACITANCE                                              *
C*   CAPSKR = SCHOTTKY CAPACITANCE TO THE  -2  POWER                            *
C*******************************************************************************
      DOUBLE PRECISION FPSO,PPK,VA
     $,            ND,NA,NN,PP,NP,PN,VD,M,L
      REAL MN,MP,INJPAR,NMP,JNFSOR
      COMMON /STRC/ ND,NA,NN,PP,NP,PN,VD,M,L,IM,IL,VT,GAMN,GAMP
     $       /FSO / XN,XP,MN,MP,INJPAR,PSIMP,JNFSOR
10    FORMAT (1H1,53H THE FIRST-ORDER THEORY (NORMALIZED) PARAMETERS ARE
     $      ///////
     $ 9H MN      =, E15.8//9H MP      =, E15.8//9H XN      =,E15.8//
     $ 9H XP      =,E15.8//9H INJPAR =,E15.8//9H JNFSOR =, E15.8////
     $9H CAPDF  =,E15.8, 30X,9H CAPDFR =, E15.8//9H CAPSK  =,E15.8,30X,
     $9H CAPSKR =, E15.8 ////////)
      IF (KW.EQ.2) GO TO 50
      INJPAR=0.
      IF (VA.GT.(-85.))INJPAR= NP* DEXP(VA)/(DSQRT(( PP+NP)**2/4.D0+
     $(DEXP(VA)-1.))+(PP-NP)/2.D0)
      IF (FXP.EQ.0.) FXP=1.
      PSIMP=VA-VD
      IF (INJPAR.GT.1.E-4) PSIMP= -VD+DLOG(PP*PP*INJPAR)
      IF (PSIMPR.NE.0.) PSIMP=PSIMPR
      IF (PSIMP.GT.0.) GO TO 99
      XN= DSQRT(2./ND*(-PSIMP)/(1.+ND/NA))
      XP=DSQRT(2./NA*(-PSIMP)/(1.+NA/ND))*FXP
      IF (KW.EQ.0) RETURN
50    MN=M-XN
      MP=M+XP
      IF (KW.EQ.1) RETURN
      NMP=PP*INJPAR
      JNFSOR=(2.D0*(NMP-NP) -(PP-NP)*DLOG((NMP-NP+PP)/PP))/((L-MP)*GAMN)
      IF (KW.EQ.3) RETURN
      CAPDF=PP*(L-MP)/2.*INJPAR*(1.+INJPAR-NP)/(1.-NP+2.*INJPAR)
      IF (INJPAR.NE.0.) CAPDFR=1./CAPDF**2
      CAPSK=DSQRT (PP/(2.*(-PSIMP)*(1.+PP/NN)))
      CAPSKR=1./CAPSK**2
      WRITE (6,10) MN,MP,XN,XP,INJPAR,JNFSOR,CAPDF,CAPDFR,CAPSK,CAPSKR
      RETURN
99    WRITE (6,100) PSIMP
100   FORMAT (1H1,41H ERROR IN THE SPECIFIED APPLIED VOLTAGE   /85H THE
     $TEST ON ITS MAXIMUM ALLOWED VALUE IN SUBROUTINE FSTORD FAILS YIELD
     $ING  PSIMP = ,E16.8//)
      KW=-99
      RETURN
      END


$IBFTC S03      DECK
      SUBROUTINE STPSEL (JRET,IREAD,IPRINT)
C*******************************************************************************
C*                    THE SUBROUTINE  'STPSEL'  PERFORMS THE SELECTION OF THE   *
C*   STEP DISTRIBUTION THROUGHOUT THE DEVICE FOR A SPECIFIED TOTAL NUMBER OF    *
C*   POINTS.  THE SELECTED STEP DISTRIBUTION WILL BE CONSISTENT WITH THE REQUI- *
C*   REMENT OF CONSTANT ERROR AT EACH STEP OF THE INTEGRATION OF THE FUNCTIONS  *
C*   EXP(PSI)  OR  EXP(-PSI)  THROUGHOUT THE JUNCTION.                          *
C*                                                                              *
C*                    THIS ROUTINE USES AN INTERPOLATION SCHEME ON THE FUNCTION *
C*   'ERROR VERSUS NUMBER OF POINTS'  TOGETHER WITH THE SUBROUTINE  'XSTEP2'    *
C*   WHICH YIELDS THE STEP DISTRIBUTION AND THE TOTAL NUMBER OF POINTS FOR A    *
C*   SPECIFIED ERROR.                                                           *
C*   SUBPROGRAMS NEEDED ARE                                                     *
C*                                  SUBROUTINE  'XSTEP2'                        *
C*                                  SUBROUTINE  'SLAGR'                         *
C*                                  SUBROUTINE  'STPADJ'                        *
C*                                                                              *
C*                    INPUT PARAMETERS ARE                                      *
C*   IPRINT=PARAMETER THAT CONTROLS THE PRINTOUT OF THE INFORMATION REGARDING   *
C*          THE STEP SELECTION AS FOLLOWS                                       *
C*                    IPRINT = 1    PRINTOUT TAKES PLACE                        *
C*                    IPRINT = 0    PRINTOUT DOES NOT TAKE PLACE                *
C*   IREAD= PARAMETER THAT CONTROLS THE INPUT OF THE PARAMETERS LISTED BELOW    *
C*          AS FOLLOWS                                                          *
C*                    IREAD = 1     THE DATA ARE READ FROM THE DATA CARD        *
C*                    IREAD = 0     THE DATA ENTER THROUGH COMMON STATEMENTS    *
```

```
C*  ERRL = SUGGESTED ERROR TO START THE INTERPOLATION SCHEME                  *
C*         IF OMITTED, A STANDARD VALUE IS CHOSEN BY THE ROUTINE              *
C*  RATMX = UPPER BOUND FOR THE RATIO OF CONSECUTIVE STEPS                    *
C*         IF OMITTED, A STANDARD VALUE IS CHOSEN BY THE ROUTINE              *
C*  RSMX = PARAMETER RELATED TO THE UPPER BOUND  SMX  FOR THE STEP THROUGH    *
C*         THE RELATION             SMX = L / RSMX                            *
C*         IF OMITTED, A STANDARD VALUE IS CHOSEN BY THE ROUTINE              *
C*  ILW  = TOTAL NUMBER OF POINTS SPECIFIED .                                 *
C*  ILRG = PRIMARY TOLERANCE RANGE  ON  ILW.  MUST BE GREATER THAN ZERO.      *
C*  ILRG2= SECONDARY TOLERANCE RANGE ON  ILW                                  *
C*  THE FOLLOWING RESTRICTION MUST BE OBSERVED                                *
C*                              (ILW-ILRG).LT.MDIM                            *
C*  WHERE  MDIM  IS THE  MAXIMUM NUMBER OF POINTS PERMITTED.                  *
C*  FAILURE   TO  DO SO CAUSES THE PRINTOUT OF AN ERROR MESSAGE AND RETURN TO *
C*  THE CALLING PROGRAM.                                                      *
C*                                                                            *
C*                   OUTPUT PARAMETERS ARE                                    *
C*  STEP = ONE-DIMENSIONAL ARRAY, NON-UNIFORM STEP MAGNITUDE AT EACH POINT    *
C*  IM   = LAST POINT OF THE  N  REGION AT THE METALLURGICAL INTERFACE        *
C*  IL   = TOTAL NUMBER OF POINTS                                             *
C*  JRET = INDEX OF PERFORMANCE OF THIS ROUTINE                               *
C*                   JRET = 0      THE STEP SELECTION HAS BEEN ACHIEVED       *
C*                   JRET = 1      THE STEP SELECTION HAS NOT BEEN ACHIEVED.  *
C*                                 PRINTOUT OF AN ERROR MESSAGE AND RETURN TO *
C*                                 THE CALLING PROGRAM TAKES PLACE.           *
C*  IF THE  N  AND  P  REGION WIDTHS ARE SMALLER THAN THEIR RESPECTIVE DEPLE- *
C*  TED REGION WIDTHS, THE STEP SELECTION MAY NOT BE ACHIEVED, THEREFORE THE  *
C*  PARAMETER  JRET  IS SET TO UNITY AND THE PRINTOUT OF AN ERROR MESSAGE     *
C*  AND RETURN TO THE CALLING PROGRAM TAKES PLACE.                            *
C*                                                                            *
C*                   THE ARRAY  STEP IS OF DIMENSION  1000  AND IN DOUBLE PRE- *
C*  CISION.                                                                   *
C******************************************************************************
      DOUBLE PRECISION STEP(1000)
     $,        ND,NA,NN,PP,NP,PN,VD,M,L
      REAL      PNT(10),ER(10),MN,MP,INJPAR,JNFSOR
      COMMON /STRC/ ND,NA,NN,PP,NP,PN,VD,M,L,IM,IL,VT,GAMN,GAMP
     $        /XST / STEP
     $        /SSTEP/   SMX,RATMX,MDIM
     $        /FSO /XN,XP,MN,MP,INJPAR,PSIMP,JNFSOR
     $        /STSEL/ERRL       ,RSMX,ILW,ILRG,ILRG2
7     FORMAT (3E10.0,3I10)
8     FORMAT   (1H1,49HTHE PARAMETERS CONCERNING THE STEP SELECTION ARE
     $ ///////////1X,9H RATMX = ,F6.3,10X,  7HERRST =, E13.6,10X, 5HSMX
     $=,F8.2,///12X,28HNUMBER OF XSTEP ITERATIONS =,I4///
     $12X,4HILN=,I5,10X,5HILRG=,I5,10X,3HIL=,I5////////
     $68H CHECK ON THE STRUCTURE POINTS  M  AND  L  AFTER THE STEP SELEC
     $TION          ,20X,
     $ 4H M =,D23.16 // 88X, 4H L = ,D23.16///////////////////////)
10    FORMAT (1H0, 23HERROR IN STPSEL      M = ,D17.10, 19H SMALLER THAN
     $XN = , E15.8//)
12    FORMAT (1H0, 23HERROR IN STPSEL   L-M = ,E15.8 , 19H SMALLER THAN
     $XP = , E15.8//)
      JRET=0
      MDIM=1000

C*****************OBTAIN PARAMETERS FROM DATA CARD, IF OMITTED SET STANDARD *
C*  VALUES, TEST CONSISTENCY****************************************************
      IF (IREAD.EQ.1) READ (5,7) ERRL,RATMX,RSMX,ILW,ILRG,ILRG2
      IF (M.GE.XN) GO TO 14
      WRITE (6,10) M,XN
      GO TO 800
14    XLM=L-M
      IF (XLM.GE.XP) GO TO 16
      WRITE (6,12) XLM,XP
      GO TO 800
16    PNG2= ILRG2
      MLGR=0
      FCT=2.
      IL=ILW
      PNW=ILW
      ILWMX=ILW+ILRG
      ILWMN=ILW-ILRG
      IF (ILWMN.GE.MDIM) GO TO 700
      IF (ILWMX.GT.MDIM) ILWMX=MDIM
      IF (RATMX.EQ.0.) RATMX=1.05
      IF (RSMX.EQ.0.) RSMX=200.
      IF (ERRL.EQ.0.) ERRL=1.E-4

C*****************EXECUTE INTERPOLATION SCHEME********************************
      DO 500 JM=1,20
      SMX=L/RSMX
17    IF (JM.EQ.1) INC=5
      KMDIM=1
      ERRST=ERRL
      CALL XSTEP2 (ERRST,IRET)
      IF (IRET.EQ.1) GO TO 195
      MI=JM
      IF (IL.GT.ILWMX) GO  TO 200
      IF (IL.LT.ILWMN) GO TO 100
55    CONTINUE
      CALL STPADJ (0.D0,M,1,IM)
      CALL STPADJ (M,L,IM,IL)
      M=0.
      IMP1=IM+1
      DO 60 I=2,IM
60    M=M+STEP(I-1)
      L=M
      DO 70 I=IMP1,IL
70    L=L+ STEP(I-1)
80    IF (IPRINT.EQ.1) WRITE (6,8) RATMX,ERRST,RSMX,MI,ILW,ILRG,IL,M,L
      RETURN
100   IF (INC.NE.1) GO TO 105
      FCT=FCT/3.
      MLGR=21
105   INC=0
      ERRL=ERRST/(1.+FCT)
      GO TO 300
195   KMDIM=2
200   IF (INC.NE.0) GO TO 205
      FCT=FCT/3.
      MLGR=21
205   INC=1
      ERRL=ERRST*(1.+FCT)
      IF (KMDIM.EQ.2) GO TO 17
300   MD=JM
      MM=JM
      IF (JM.LT.6) GO TO 305
      MD=5
      MM=1
      DO 302 LS=2,5
302   IF (ABS(PNT(LS)-PNW).GT.ABS( PNT(MM)-PNW))   MM=LS
```

```
305    ER(MM)=ALOG(ERRST)
       PNT(MM)=IL
       IF (JM.GT.MLGR) GO TO 500
       DO 310 KS=2,MD
       DO 310 KK=KS,MD
310    IF (ABS(PNT(KK)-PNT(KS-1)).LT..5) GO TO 550
       CALL SLAGR(PNT,ER,PNW,MD,ERRL)
       ERRL=EXP(ERRL)
500    CONTINUE

C*****************INTERPOLATION SCHEME TERMINATED WITHOUT HAVING REACHED THE  *
C*  PRIMARY TOLERANCE RANGE. TEST ON THE SECONDARY TOLERANCE RANGE IS PERFOR-  *
C*  MED***************************************************************************
550    LM=1
       DO 555 LS=2,5
555    IF (ABS(PNT(LS)-PNW).LT.ABS(PNT(LM)-PNW)) LM=LS
       IF (ABS(PNT(LM)-PNW).GT.RNG2) GO TO 580
       IL=PNT(LM)
       ERRST=EXP(ER(LM))
       GO TO 55

C*****************ERROR MESSAGES PRINTOUT FOR ABNORMAL CONDITIONS**************
580    WRITE (6,600)
600    FORMAT (1H0,23HERROR IN ILRG TOO SMALL  /)
       GO TO 800
700    WRITE (6,701)
701    FORMAT (1H0,20HERROR IN ILW GT MDIM   /)
800    JRET=1
       RETURN
       END


$IBFTC S04      DECK
       SUBROUTINE XSTEP2 (ERRST,IRET)
C******************************************************************************
C*                   THE SUBROUTINE  'XSTEP2'  COMPUTES THE STEP DISTRIBUTION.  *
C*  AND THE TOTAL NUMBER OF POINTS FOR A GIVEN ACCURACY DESIRED ON THE INTE-    *
C*  GRATION OF THE FUNCTIONS  EXP(PSI)  AND  EXP(-PSI)  THROUGHOUT THE DEVICE. *
C*                                                                              *
C*                   THIS ROUTINE OPERATES ON THE FIRST-ORDER TRIAL POTENTIAL   *
C*  FUNCTION ONLY AND IS BASED ON THE EXPLICIT ANALYTICAL RELATIONSHIP BET-     *
C*  WEEN THE STEP AT EACH POINT AND THE SPECIFIED ERROR.                        *
C*                                                                              *
C*                   INPUT PARAMETERS ARE                                       *
C*  ERRST = MAXIMUM ALLOWED ERROR ON THE INTEGRATIONS                           *
C*  SMX   = UPPER BOUND FOR THE STEP                                            *
C*  RATMX = UPPER BOUND FOR THE RATIO OF CONSECUTIVE STEPS                      *
C*  MDIM  = MAXIMUM NUMBER OF POINTS PERMITTED                                  *
C*  STRUCTURE PARAMETERS(INCLUDED IN THE LABELED  COMMON  /STRC/   WITH EXCEP- *
C*  TION OF THE PARAMETERS  IM  AND  IL).                                       *
C*  FIRST-ORDER THEORY PARAMETERS(INCLUDED IN THE LABELED  COMMON  /FSO/ ).     *
C*                                                                              *
C*                   OUTPUT PARAMETERS ARE                                      *
C*  STEP = ONE-DIMENSIONAL ARRAY, NON-UNIFORM STEP MAGNITUDE AT EACH POINT      *
C*  IM   = LAST POINT OF THE  N  REGION AT THE METALLURGICAL INTERFACE          *
C*  IL   = TOTAL NUMBER OF POINTS                                               *
C*  IRET = PARAMETER THAT DETERMINES THE EXIT OF THE ROUTINE                    *
C*         IRET = 1  IF  IL  IS GREATER THAN  MDIM                              *
C*         IRET = 0  IF  IL  IS NOT GREATER THAN  MDIM                          *
C*                                                                              *
C*                   ALL THE ARRAYS ARE OF DIMENSION  1000  AND IN DOUBLE PRE-
C*  CISION.                                                                     *
C*                                                                              *
C*                   ALLOWANCE FOR ONE  DOUBLE PRECISION ARRAY  (WORKING LOCA-  *
C*  TIONS)  FOR TEMPORARY STORAGE MUST BE MADE.  THIS IS AVAILABLE EXTERNALLY  *
C*  THROUGH THE LABELED  COMMON  /WORK/.                                        *
C******************************************************************************
       REAL MN,MP,INJPAR,JNFSOR
       DOUBLE PRECISION STEP(1000),TSTEP(1000),DUMMY(1000)
      $,X,XA    ,XB,SNTR,SPTR,SPNT
      $,      ND,NA,NN,PP,NP,PN,VD,M,L
       COMMON /STRC/ ND,NA,NN,PP,NP,PN,VD,M,L,IM,IL,VT,GAMN,GAMP
      $        /SSTEP/    SMX,RATMX,MDIM
      $        /WORK/TSTEP,DUMMY
      $        /FSO / XN,XP,MN,MP,INJPAR,PSIMP,JNFSOR
      $        /XST / STEP

C*****************ARITHMETIC FUNCTIONS DEFINITION FOR THE RELATIONSHIP BET-   *
C*  WEEN THE STEP AND THE SPECIFIED ERROR IN THE VARIOUS REGIONS***************
       SNTR(X)= DSQRT(ERR12/((ND*(X-MN))**2+ND))
       SPTR(X)= DSQRT(ERR12/((NA*(MP-X))**2+NA))
       SPNT(X)= ERRSR*(W-X)
       ERR12=ERRST*12.
       ERRSR= SQRT(6.*ERRST)
       W=1.E10
       IF (INJPAR.GT.NP) W= (L-MP)/(INJPAR-NP*NP)+L

C******************OBTAIN THE STEP DISTRIBUTION IN THE   N-REGION**************
       IRET=0
       IBR=1
       I=2
       X=M
       TSTEP(1)=SNTR(M)
       IF (TSTEP(1).GT.SMX) TSTEP(1)=SMX
       TSTEP(2)=TSTEP(1)
50     X=X-TSTEP(I)
       I=I+1
       IF (I.GT.MDIM) GO TO 400
       TSTEP(I)=SMX
55     IF (X.GT.MN) GO TO 65
       IF (X.GT.(TSTEP(I-1)/2.)) GO TO (70,50),IBR
       GO TO 75
65     TSTEP(I)=SNTR(X)
70     SMXI=TSTEP(I-1)*RATMX
       IF (TSTEP(I).GT.SMXI) TSTEP(I)=SMXI
       IF (TSTEP(I).LT.SMX) GO TO 50
       IBR=2
       TSTEP(I)=SMX
       GO TO 50
75     IM=I-1
       IM1=IM-1
       DO 80 IS=1,IM1
       IT=IM-IS+1
80     STEP(IS)=TSTEP(IT)

C******************OBTAIN THE STEP DISTRIBUTION IN THE  DEPLETED P-REGION*******
       I=IM
       X=M
       STEP(I)=STEP(I-1)
150    X=X+STEP(I)
       I=I+1
```

```
      IF (I.GT.MDIM) GO TO 400
      STEP(I)=SMX
      IF (X.LT.MP) STEP(I)=SPTR(X)
170   SMXI=STEP(I-1)*RATMX
      IF (STEP(I).GT.SMXI) STEP(I)=SMXI
      IF (STEP(I).LT.SMX) GO TO 150
175   IA=I-1

C*****************OBTAIN THE STEP DISTRIBUTION IN THE  NEUTRAL  P-REGION*******
      XA=X
      MDIMA=MDIM-IA
      IP=2
      X=L
      TSTEP(1)=SPNT(L)
      IF (TSTEP(1).GT.SMX) TSTEP(1)=SMX
      TSTEP(2)=TSTEP(1)
250   X=X-TSTEP(IP)
      IP=IP+1
      IF (IP.GT.MDIMA) GO TO 400
      IF (X.LT.XA) GO TO 500
      TSTEP(IP)=SPNT(X)
      SMXI=TSTEP(IP-1)*RATMX
      IF (TSTEP(IP).GT.SMXI) TSTEP(IP)=SMXI
      IF (TSTEP(IP).LT.SMX )GO TO 250
      SMXB=SMX
260   XB=X-SMXB/2.
      X=XA
300   IF (X.GT.XB) GO TO 310
      STEP(I)=SMXB
      X=X+STEP(I)
      I=I+1
      IF (I.GT.MDIM) GO TO 400
      GO TO 300
310   IP1=IP-1
      DO 320 II=2,IP1
      IS=I+II-2
      IT=IP1+2-II
      IF (IS.GE.MDIM) GO TO 400
320   STEP(IS)=TSTEP(IT)
      IL=IS+1
      WRITE (6,963)IL,ERRST
      RETURN
400   IRET=1
      I=MDIM+1
      WRITE (6,963) I,ERRST
963   FORMAT (1H0,I5,10X,E15.7)
      RETURN

C*****************MATCH THE STEP DISTRIBUTIONS BETWEEN  P-DEPLETED AND P-    *
C*  NEUTRAL REGIONS TO SATISFY THE REQUIREMENT DICTATED BY THE UPPER BOUND   *
C*  OF THE RATIO OF CONSECUTIVE STEPS.****************************************
500   SMXB=TSTEP(IP)
510   XA=XA-STEP(IA)
      IA=IA-1
      IF (STEP(IA).GT. SMXB    ) GO TO 510
      I=IA+1
      GO TO 260
      END
```

```
$IBFTC S05      DECK
      SUBROUTINE SLAGR (JT,VAIT,JTW,MM,DP)
C****************************************************************************
C*                 THE SUBROUTINE  'SLAGR' EXECUTES A LAGRANGIAN INTERPOLA-   *
C*  TION ON TWO ONE-DIMENSIONAL ARRAYS NOT UNIFORMLY SPACED.                  *
C*                                                                            *
C*                 THIS ROUTINE CONSTRUCTS THE PERTINENT MATRIX,TRIANGULARI-  *
C*  ZES IT WITH THE GAUSSIAN ELIMINATION PROCESS, SOLVES THE SYSTEM BY BACK-  *
C*  SUBSTITUTION TO OBTAIN THE COEFFICIENTS OF THE INTERPOLATING POLYNOMIAL,  *
C*  AND COMPUTES THE VALUE OF SUCH POLYNOMIAL AT THE DESIRED POINT.           *
C*  DOUBLE PRECISION ARITHMETIC IS USED.                                      *
C*                                                                            *
C*                 INPUT PARAMETERS ARE                                       *
C*  JT   = ONE-DIMENSIONAL ARRAY, ABSCISSA OF THE GIVEN POINTS (DIMENSION=10) *
C*  VAIT = ONE-DIMENSIONAL ARRAY, ORDINATE OF THE GIVEN POINTS (DIMENSION=10) *
C*  JTW  = ABSCISSA OF THE DESIRED POINT                                      *
C*  MM   = NUMBER OF POINTS GIVEN  (THE ORDER OF THE INTERPOLATING POLYNOMIAL *
C*         IS MM-1).    MAXIMUM  MM VALUE  =  10.                             *
C*                                                                            *
C*                 OUTPUT PARAMETERS ARE                                      *
C*  DP   = ORDINATE OF THE DESIRED POINT                                      *
C*                                                                            *
C*                 ALL THE INPUT AND OUTPUT QUANTITIES ARE IN SINGLE PRECISION *
C****************************************************************************
      REAL JT(10),VAIT(10),JTW
      DOUBLE PRECISION JTM(10,11),ZZ,SUM,CF(10)
1     FORMAT (1X,//1X,8D16.8)
      IF(MM.LE.10) GO TO 100
      WRITE (6,10) MM
10    FORMAT (49H ERROR IN SUBROUTINE 'SLAGR'.   THE PARAMETER MM=, I6,
     $ 30HEXCEEDS THE MAXIMUM PERMITTED   ///)

C*****************BUILD THE PERTINENT MATRIX*********************************
100   MIT=MM+1
200   DO 205 I=1,MM
      JTM(I,1)=1.
205   JTM(I,MIT)=VAIT(I)
      DO 210 I=1,MM
      DO 210 K=2,MM
210   JTM(I,K)=JTM(I,K-1)*JT(I)

C*****************TRIANGULARIZE THE MATRIX BY GAUSSIAN ELIMINATION************
      M1=MM-1
      DO 300 KK=1,M1
      IL=1+KK
      DO 300 IR=IL,MM
      ZZ=JTM(IR,KK)/JTM(KK,KK)
      DO 300 K=IL,MIT
300   JTM(IR,K)=JTM(IR,K)-ZZ*JTM(KK,K)

C*****************SOLVE THE MATRIX BY BACK-SUBSTITUTION***********************
      CF(MM)=JTM(MM,MIT)/JTM(MM,MM)
      DO 320 I=2,MM
      IR=MIT-I
      IRP1=IR+1
      SUM=0.
      DO 310 J=IRP1,MM
310   SUM=JTM(IR,J)*CF(J)+SUM
320   CF(IR)=(JTM(IR,MIT)-SUM)/JTM(IR,IR)
```

```
C*****************COMPUTE THE VALUE OF THE INTERPOLATING POLYNOMIAL AT THE*****
C*  DESIRED POINT***************************************************************
      DP=CF(MM)
      DO 350 I=2,MM
      IR=MIT-I
  350 DP= JTW*DP+CF(IR)
      RETURN
      END


$IBFTC S06     DECK
      SUBROUTINE STPADJ(XIN,XFIN,IST,IFINP1)
C******************************************************************************
C*                  THE SUBROUTINE  'STPADJ'  PERFORMS A MINOR ADJUSTMENT OF   *
C*  THE PRELIMINARY NON-UNIFORM STEP DISTRIBUTION IN A CERTAIN REGION IN ORDER *
C*  TO IMPROVE THE ACCURACY OF THE RELATION                                    *
C*                  SUM OF THE STEPS  =  LENGTH OF REGION              (1)     *
C*                                                                             *
C*                  THIS ADJUSTMENT IS ACHIEVED BY DETERMINING,WITH AN INTERPO- *
C*  LATING PROCEDURE, A MULTIPLICATIVE FACTOR FOR THE STEP SIZE SUCH THAT THE  *
C*  RELATION  (1)  IS SATISFIED WITHIN A CERTAIN TOLERANCE  (SPECIFIED AS      *
C*  TOLER  = SMX*1.E-5 ).  THIS TECHNIQUE MAINTAINS UNCHANGED THE RATIO OF     *
C*  CONSECUTIVE STEPS OF THE ORIGINAL STEP DISTRIBUTION.                       *
C*                                                                             *
C*                  SUBPROGRAM NEEDED                                          *
C*                            SUBROUTINE  'SLAGR'                              *
C*                                                                             *
C*                  INPUT PARAMETERS ARE                                       *
C*  XIN    = ABSCISSA OF THE LEFT BOUNDARY OF THE REGION (DOUBLE-PRECISION)    *
C*  XFIN   = ABSCISSA OF THE RIGHT BOUNDARY OF THE REGION (DOUBLE-PRECISION)   *
C*  ISTN   = INDEX IDENTIFYING THE STEP AT  XIN  (FIRST STEP)                  *
C*  IFINP1= INDEX IDENTIFYING THE STEP AT  XFIN                                *
C*  STEP   = ONE-DIMENSIONAL ARRAY, NON-UNIFORM STEP MAGNITUDE AT EACH POINT   *
C*           (TO BE ADJUSTED)                                                  *
C*                                                                             *
C*                  OUTPUT PARAMETERS ARE                                      *
C*  STEP   = ONE-DIMENSIONAL ARRAY, NON-UNIFORM STEP MAGNITUDE AT EACH POINT   *
C*           (ADJUSTED)                                                        *
C*                                                                             *
C*                  THE ARRAY  STEP  IS OF DIMENSION  1000  AND IN DOUBLE      *
C*  PRECISION.                                                                 *
C******************************************************************************
      DOUBLE PRECISION STEP(1000),X,XIN,XFIN
      DIMENSION DIFF(10),FC(10)
      COMMON   /XST/ STEP
     $         /SSTEP/   SMX,RATMX,MDIM
      FACT=1.E-3 +1.
      IFIN=IFINP1-1
      NRP=0
      TOLER=SMX*1.E-5
      NRPMX=5
   25 X=XIN
      DO 30 I=IST,IFIN
   30 X=X+FACT*STEP(I)
      NRP=NRP+1
      FC(NRP)=FACT -1.
      DIFF(NRP)=X-XFIN
      IF (NRP.GT.1)  GO TO 33
      FACT=FC(NRP)*10.+1.
      IF ((X-XFIN).GT.0.) FACT=FC(NRP)/100.+1.
      GO TO 25
   33 IF (DABS(X-XFIN).LT.TOLER.OR.NRP.GT.NRPMX) GO TO 35
      CALL SLAGR (DIFF,FC,0.,NRP,FCIMPR)
      FACT=FCIMPR+1.
      GO TO 25
   35 NRPMN=1
      DO 37 I=2,NRP
   37 IF (ABS(DIFF(NRP)).LT.ABS(DIFF(NRPMN))) NRPMN=NRP
      FACT=FC(NRPMN)+1.
      DO 40 I=IST,IFIN
   40 STEP(I)=FACT*STEP(I)
      RETURN
      END


$IBFTC S07     DECK
      SUBROUTINE DOPING (NIM)
C******************************************************************************
C*                  THE SUBROUTINE  'DOPING'  FURNISHES THE IMPURITY DISTRIBU- *
C*  TION THROUGHOUT THE  DEVICE.                                               *
C*                                                                             *
C*                  THIS ROUTINE YIELDS A STEP DOPING PROFILE WHICH CHARACTE-  *
C*  RIZES AN ABRUPT JUNCTION WITH THE N-REGION ON THE LEFT SIDE.               *
C*                                                                             *
C*                  INPUT PARAMETERS ARE                                       *
C*  IM    = LAST POINT OF THE   N-REGION AT THE METALLURGICAL INTERFACE        *
C*  IL    = TOTAL NUMBER OF POINTS                                             *
C*  ND    = DONOR CONCENTRATION IN THE  N- REGION (DOUBLE PRECISION)           *
C*  NA    = ACCEPTOR CONCENTRATION IN THE  P- REGION (DOUBLE PRECISION)        *
C*                                                                             *
C*                  OUTPUT PARAMETERS ARE                                      *
C*  NIM   = ONE-DIMENSIONAL ARRAY, IMPURITY DISTRIBUTION  (SINGLE PRECISION,   *
C*           DIMENSION  1000)                                                  *
C******************************************************************************
      DOUBLE PRECISION
     $              ND,NA,NN,PP,NP,PN,VD,M,L
      REAL NIM(1000)
      COMMON /STRC/ ND,NA,NN,PP,NP,PN,VD,N,L,IM,IL,VT,GAMN,GAMP
      DO 10 I=1,IM
   10 NIM(I)=ND
      IMP1=IM+1
      DO 20 I=IMP1,IL
   20 NIM(I)=-NA
      RETURN
      END


$IBFTC S08     DECK
      SUBROUTINE PSITRL (PSI,VA)
C******************************************************************************
C*                  THE SUBROUTINE  'PSITRL'  FURNISHES THE TRIAL POTENTIAL    *
C*  FUNCTION.                                                                  *
C*                                                                             *
C*                  THIS ROUTINE YIELDS THE FIRST-ORDER THEORY POTENTIAL DIS-  *
C*  TRIBUTION FOR AN ABRUPT JUNCTION,WITHOUT RESTRICTIONS ON THE INJECTION     *
C*  LEVEL IN THE LOW CONDUCTIVITY  (P)  REGION.                                *
C*                                                                             *
C*                  INPUT PARAMETERS ARE                                       *
```

```
C*  VA   = APPLIED VOLTAGE (NORMALIZED,DOUBLE PRECISION)                      *
C*  IL   = TOTAL NUMBER OF POINTS                                            *
C*  STEP = ONE-DIMENSIONAL ARRAY, NON-UNIFORM STEP MAGNITUDE AT EACH POINT   *
C*  STRUCTURE PARAMETERS(INCLUDED IN THE LABELED  COMMON  /STRC/ )           *
C*  FIRST-ORDER THEORY PARAMETERS(INCLUDED IN THE LABELED  COMMON  /FSO/  )  *
C*                                                                           *
C*                  OUTPUT PARAMETERS ARE                                    *
C*  PSI  = ONE-DIMENSIONAL ARRAY, TRIAL POTENTIAL FUNCTION                   *
C*                                                                           *
C*                  ALL THE ARRAYS ARE OF DIMENSION  1000  AND IN DOUBLE PRE- *
C*  CISION.                                                                  *
C****************************************************************************
      DOUBLE PRECISION STEP(1000),PSI(1000),X
     $,               ND,NA,NN,PP,NP,PN,VD,M,L,VAD
      REAL            MN,MP,INJPAR,JNFSOR
      COMMON /STRC/ ND,NA,NN,PP,NP,PN,VD,M,L,IM,IL,VT,GAMN,GAMP
     $        /FSO / XN,XP,MN,MP,INJPAR,PSIMP,JNFSOR
     $        /XST / STEP
      CST1= -PSIMP/(XP*(XN+XP))
      CST2= -PSIMP/(XN*(XN+XP))
      MN=M-XN
      MP=M+XP
      VAD=VA-VD
      CONST=(INJPAR-NP/PP)/(L-MP)
      IF (INJPAR.GT.1.E-4) CONST= (DEXP(VAD-PSIMP)-1.)/(L-MP)
      X=0.
      PSI(1)=0.
      DO 20 I=2,IL
      X=X+STEP(I-1)
      PSI(I)=0.
      IF (X.GT.MN.AND.X.LE.M)  PSI(I)=-CST2 *(X-MN)**2
      IF (X.GT.M.AND.X.LE.MP) PSI(I)= CST1 *(MP-X)**2+PSIMP
      IF (X.LE.MP) GO TO 20
      PSI(I)=VAD
      IF (INJPAR.GT.1.E-4) PSI(I)= -DLOG(CONST*(L-X)+1.)+VAD
20    CONTINUE
      RETURN
       END


$IBFTC S09     DECK
      SUBROUTINE MOBCAR (PSI,VA)
C****************************************************************************
C*                  THE SUBROUTINE  'MOBCAR'  COMPUTES THE ELECTRON AND HOLE *
C*  DISTRIBUTIONS THROUGHOUT  THE DEVICE, GIVEN THE POTENTIAL DISTRIBUTION   *
C*  PSI.                                                                     *
C*                                                                           *
C*                  THIS ROUTINE USES A PROCESS OF DIRECT INTEGRATION. SUBPRO- *
C*  GRAMS NEEDED ARE                                                         *
C*                            SUBROUTINE  'INTGSF'                           *
C*                            SUBROUTINE  'INTEGR'                           *
C*  DOUBLE PRECISION ARITHMETIC IS USED.                                     *
C*                                                                           *
C*                  INPUT PARAMETERS ARE                                     *
C*  PSI  = ONE-DIMENSIONAL ARRAY, POTENTIAL DISTRIBUTION                     *
C*  VA   = APPLIED VOLTAGE (NORMALIZED,DOUBLE PRECISION)                     *
C*  STRUCTURE PARAMETERS(INCLUDED IN THE LABELED  COMMON  /STRC/  )          *
C*                                                                           *
C*                  OUTPUT PARAMETERS ARE                                    *
C*  N    = ONE-DIMENSIONAL ARRAY, ELECTRON DISTRIBUTION                      *
C*  P    = ONE-DIMENSIONAL ARRAY, HOLE DISTRIBUTION                          *
C*  JN   = ELECTRON CURRENT                                                  *
C*  JP   = HOLE CURRENT                                                      *
C*                                                                           *
C*                  ALL THE ARRAYS ARE OF DIMENSION  1000  AND IN DOUBLE PRE- *
C*  CISION                                                                   *
C*                                                                           *
C*                  ALLOWANCE FOR TWO DOUBLE PRECISION ARRAYS (WORKING LOCA- *
C*  TIONS) FOR TEMPORARY STORAGE MUST BE MADE. THESE ARE AVAILABLE EXTERNALLY *
C*  THROUGH THE LABELED COMMON  /WORK/                                       *
C****************************************************************************
      REAL JN,JP
      DOUBLE PRECISION  VA,PSI(1000), N(1000),P(1000),EPSI(1000),
     $EMPSI(1000),FIP(1000),FP(1000),FIN(1000), FN(1000), CN,CP,THETA,
     $FPR(1000),FNR(1000),CCN,CCP,THETA1,PSIOL
     $,               ND,NA,NN,PP,NP,PN,VD,M,L
      COMMON /STRC/ ND,NA,NN,PP,NP,PN,VD,M,L,IM,IL,VT,GAMN,GAMP
     $        /MCAR/ N,P,JN,JP
     $        /WORK/ EPSI,FIP
      EQUIVALENCE (EPSI,EMPSI), (FIP,FIN,FPR,FNR),(FP,P),(FN,N)
      IF (VA.LT.0.) GO TO 300

C*****************FOR FORWARD BIAS  ONLY*************************************
      DO 110 I=1,IL
110   EPSI(I)=DEXP(PSI(I))
      THETA=NN*PP/EPSI(1)*EPSI(IL)
      CALL INTEGR(EPSI,FIP,IM,IL,-1)
      CALL INTEGR(EPSI,FP,IM,IL, 1)
      JP=(PP*EPSI(IL)-EPSI(1)*PN)/(FIP(1)*GAMP)
      CP=FIP(1)*NN/EPSI(1)
      DO 120 I=1,IL
120   P(I)=(FIP(I)+THETA*FP(I))/(CP*EPSI(I))
      DO 210 I=1,IL
210   EMPSI(I)=1.D0/EPSI(I)
      CALL INTEGR(EMPSI,FIN,IM,IL,-1)
      CALL INTEGR(EMPSI,FN,IM,IL,1)
      JN=(NN*EMPSI(1)-NP*EMPSI(IL))/(GAMN*FN(IL))
      CN=FN(IL)*PP/EMPSI(IL)
      DO 220 I=1,IL
220   N(I)=(FN(I)+THETA*FIN(I))/(CN*EMPSI(I))
      RETURN

C*****************FOR REVERSE BIAS  ONLY*************************************

C*                  COMPUTE THE ELECTRON DISTRIBUTION  N(I)                  *
300   PSIOL=PSI(1)-PSI(IL)
      THETA1=1.D0
      IF (PSIOL.LE.70.) THETA1=1.D0-NN*PP/DEXP(PSIOL)
      CALL INTGSF (PSI,EMPSI,FNR,IM,IL,1)
      CN=PP*FNR(IL)/EMPSI(IL)
      CCN=CN*NN
      DO 340 I=1,IL
      IF ((PSI(1)-PSI(I)).GT.70.) GO TO 335
      N(I)=(THETA1*FNR(I)+CCN)/(CN*EMPSI(I))
      GO TO 340
335   N(I)=FNR(I)/(CN*EMPSI(I))
340   CONTINUE
      JN= -EMPSI(IL)*NP/(GAMN*FNR(IL))
      IF (PSIOL.LE.70.) JN=JN+NN*EMPSI(1)/(GAMN*FNR(IL))

C*                  COMPUTE THE HOLE DISTRIBUTION   P(I)                     *
```

```
      CALL INTGSF (PSI,EPSI,FPR,IM,IL,-1)
      CP=NN*FPR(1)/EPSI(1)
      CCP=PP*CP
      DO 440 I=1,IL
      IF ((PSI(1)-PSI(IL)).GT.70.) GO TO 435
      P(I)=(THETA1*FPR(I)+CCP)/(CP*EPSI(I))
      GO TO 440
435   P(I)=FPR(I)/(CP*EPSI(I))
440   CONTINUE
      JP= -EPSI(1)*PN/(GAMP*FPR(1))
      IF (PSIOL.LE.70.) JP=JP+PP/(GAMP*FPR(1))
      RETURN
      END
```

```
$IBFTC S10A    DECK
      SUBROUTINE INTEGR(Y,Q,IM,IL,ID)
C*****************************************************************************
C*                   THE SUBROUTINE  'INTEGR'  COMPUTES THE INTEGRAL OF A FUNC-  *
C*  TION GIVEN IN DISCRETIZED FORM THROUGHOUT THE POINT INTERVAL  1 - IL  ,     *
C*  LIMITS OF INTEGRATION  BEING ONE BOUNDARY AND EACH OF THE IL  POINTS.       *
C*                                                                              *
C*                   THIS ROUTINE USES A LINEAR INTERPOLATION AT EACH POINT     *
C*  ( TRAPEZOIDAL RULE OR TWO POINT FORMULA ) .                                 *
C*  DOUBLE PRECISION ARITHMETIC IS USED.                                        *
C*                                                                              *
C*                   INPUT PARAMETERS ARE                                       *
C*  Y     = ONE-DIMENSIONAL ARRAY TO BE INTEGRATED                              *
C*  IM    = IRRELEVANT PARAMETER FOR THIS ROUTINE                               *
C*  IL    = TOTAL NUMBER OF POINTS                                              *
C*  ID    = INDICATES THE DIRECTION OF INTEGRATION AS FOLLOWS                   *
C*          ID GREATER THAN ZERO FOR FORWARD DIRECTION                          *
C*          ID LESS THAN ZERO FOR REVERSE DIRECTION                             *
C*  STEP = ONE-DIMENSIONAL ARRAY, NON-UNIFORM STEP MAGNITUDE AT EACH POINT      *
C*                                                                              *
C*                   OUTPUT PARAMETERS ARE                                      *
C*  Q = ONE-DIMENSIONAL ARRAY RESULT OF THE INTEGRATION AT EACH POINT           *
C*                                                                              *
C*                   ALL THE ARRAYS ARE OF DIMENSION  1000  AND IN DOUBLE PRE-  *
C*  CISION.                                                                     *
C*****************************************************************************
      COMMON /XST/ STEP
      DOUBLE PRECISION Y(1000),Q(1000),STEP(1000)
      IL1=IL-1
      IF (ID.LT.0) GO TO 15

C*****************INTEGRATION IN THE FORWARD DIRECTION ONLY******************
      Q(1)=0.
      DO 10 I=1,IL1
10    Q(I+1)=(Y(I+1)+Y(I))/2.D0*STEP(I)+Q(I)
      RETURN

C*****************INTEGRATION IN THE REVERSE DIRECTION ONLY******************
15    Q(IL)=0.
      DO 20 I=1,IL1
      IR=IL-I
20    Q(IR)= (Y(IR)+Y(IR+1))/2.D0*STEP(IR) +Q(IR+1)
      RETURN
      END
```

```
$IBFTC S10B    DECK
      SUBROUTINE  INTEGR(Y,Q,IM,IL,ID)
C*****************************************************************************
C*                   THE SUBROUTINE  'INTEGR'  COMPUTES THE INTEGRAL OF A FUNC-  *
C*  TION GIVEN IN DISCRETIZED FORM THROUGHOUT THE POINT INTERVAL  1 - IL  ,     *
C*  LIMITS OF INTEGRATION  BEING ONE BOUNDARY AND EACH OF THE IL  POINTS.       *
C*                                                                              *
C*                   THIS ROUTINE USES A CUBIC INTERPOLATION SCHEME AT EACH     *
C*  POINT (FOUR POINT FORMULA).                                                 *
C*  A DISCONTINUITY AT IM OF A DERIVATIVE OF THE FUNCTION IS ALLOWED.           *
C*                   SUBPROGRAM NEEDED                                          *
C*                                 DOUBLE PRECISION FUNCTION  'DET'             *
C*  DOUBLE PRECISION ARITHMETIC IS USED.                                        *
C*                                                                              *
C*                   INPUT PARAMETERS ARE                                       *
C*  Y     = ONE-DIMENSIONAL ARRAY TO BE INTEGRATED                              *
C*  IM    = POINT OF DISCONTINUITY OF A DERIVATIVE OF THE INTEGRAND             *
C*  IL    = TOTAL NUMBER OF POINTS                                              *
C*  ID    = INDICATES THE DIRECTION OF INTEGRATION AS FOLLOWS                   *
C*          ID GREATER THAN ZERO FOR FORWARD DIRECTION                          *
C*          ID LESS THAN ZERO FOR REVERSE DIRECTION                             *
C*  STEP = ONE-DIMENSIONAL ARRAY, NON-UNIFORM STEP MAGNITUDE AT EACH POINT      *
C*                                                                              *
C*                   OUTPUT PARAMETERS ARE                                      *
C*  Q = ONE-DIMENSIONAL ARRAY RESULT OF THE INTEGRATION AT EACH POINT           *
C*                                                                              *
C*                   ALL THE ARRAYS ARE OF DIMENSION  1000  AND IN DOUBLE PRE-  *
C*  CISION.                                                                     *
C*****************************************************************************
      LOGICAL BACK
      DOUBLE PRECISION  Y(1    ), Q(1    ), STEP(1    ), X(3), US(5,5),
     $UA(2,2), UB(2,2)
     $,Z,D,POL,ALFA,BETA,GAMMA,DELTA,W     ,QIN
      COMMON  /XST/ STEP
      POL(Z) = Z*( Z*( Z*( Z*ALFA/4.0D0 + BETA/3.0D0) + GAMMA/2.0D0) +
     $  DELTA)
      IMPL = IM + 1
      IL1 = IL - 1
      IL2 = IL - 2
      IM2 = IM - 2
      IM1 = IM - 1
      Q(1)=0.
      Q(IL)=0.
      BACK = .FALSE.
      IF (ID.LT.0)  BACK = .TRUE.
      DO 100 J=2,IL2
      I = J
      IF (BACK) I = IL - J
      IF (I.EQ.IM1.OR. I.EQ.IM  )  GO TO 100
      Z = STEP(I)
      X(1) = -STEP(I-1)
      X(2) = Z
      X(3) = STEP (I+1) + Z
      D = (X(2)-X(1)) * (X(3)-X(1)) * (X(3)-X(2))
      DO 30 IR=1,3
      IV = I-1+IR
      IF (IV.EQ.I)  IV = IV-1
      US(IR,1) = X(IR)
      US (IR,2) = (Y(IV) - Y(I))/ X(IR)
30    US (IR,3) = X(IR) * X(IR)
      DO 50 IR = 1,2
```

```
      DO 50 IC = 1,2
      ICP1 = IC + 1
      UA(IR,IC) = US(IR,IC) - US(3,IC)
50    UB(IR,IC) = US(IR,ICP1) - US(3,ICP1)
      ALFA = (UA(2,1) + UA(1,2) - UA(1,1) *UA(2,2)) / D
      BETA = (UB(2,1) + UB(1,2) - UB(1,1) * UB(2,2)) / D
      GAMMA = -DET (US,3) / D
      DELTA = Y(I)
      I1 = I-1
      IP1 = I+1
      IP2 = I + 2
      IF (.NOT.BACK)  GO TO 70

C*****************INTEGRATION IN THE REVERSE DIRECTION ONLY*******************
      IF (.NOT. (I.EQ.IM2 .OR. I.EQ.IL2)) GO TO 60
      W = Z + STEP(IP1)
      Q(IP1) = POL(W) - Q(IP2) - POL(Z)
60    Q(I) =  POL(Z) + Q(IP1)
      IF (.NOT.(I.EQ.2 .OR. I.EQ.IMP1)) GO TO 100
      W = -STEP(I1)
      Q(I1) = -POL(W) - Q(I)
      GO TO 100

C*****************INTEGRATION IN THE FORWARD DIRECTION ONLY*******************
70    IF (.NOT.(I.EQ.2 .OR. I.EQ.IMP1)) GO TO 80
      W = -STEP(I1)
      Q(I)  = -POL(W) - Q(I1)
80    Q(IP1) = POL(Z) - Q(I)
      IF (.NOT. (I.EQ.IM2 .OR. I.EQ.IL2)) GO TO 100
      W = Z + STEP(IP1)
      Q(IP2) = POL(W) + Q(I)
100   CONTINUE
      RETURN
       END


$IBFTC S11     DECK
      DOUBLE PRECISION  FUNCTION DET (Y,M)
C****************************************************************************
C*                  THE DOUBLE PRECISION FUNCTION  'DET'  COMPUTES THE DETER-  *
C*  MINANT OF A MATRIX.                                                       *
C*                                                                            *
C*                  THIS ROUTINE USES A SCHEME BASED ON TRIANGULARIZATION OF  *
C*  THE MATRIX BY GAUSSIAN ELIMINATION AND CROSS MULTIPLICATION OF THE DIA-   *
C*  GONAL.                                                                    *
C*  DOUBLE PRECISION ARITHMETIC IS USED.                                      *
C*                                                                            *
C*                  INPUT PARAMETERS ARE                                      *
C*  Y     = TWO-DIMENSIONAL ARRAY, MATRIX WHOSE DETERMINANT IS SOUGHT         *
C*  M     = SIZE OF THE MATRIX  Y , MAXIMUM SIZE = 5                          *
C*                                                                            *
C*                  OUTPUT PARAMETERS ARE                                     *
C*  DET   = VALUE OF THE DETERMINANT OF THE MATRIX  Y                         *
C****************************************************************************
      DOUBLE PRECISION Y(5 ,5 ) ,ZZ
      M1=M-1
      DET=Y(1,1)
      DO 25 MC=1,M1
      MCP1=MC+1
      DO 23 MR=MCP1,M
      ZZ=Y(MR,MC)/Y(MC,MC)
      DO 23 I=MCP1,M
23    Y(MR,I)=Y(MR,I)-ZZ*Y(MC,I)
25    DET=DET*Y(MCP1,MCP1)
      RETURN
      END


$IBFTC S12     DECK
      SUBROUTINE INTGSF (PSI,Y,Q,IM,IL,ID)
C****************************************************************************
C*                  THE SUBROUTINE  'INTGSF'  COMPUTES THE EXPONENTIAL OF A   *
C*  FUNCTION GIVEN IN DISCRETIZED FORM AND THE INTEGRAL OF SUCH AN EXPONEN-  *
C*  TIAL THROUGHOUT THE POINT INTERVAL   1 - IL .LIMITS OF INTEGRATION BEING  *
C*  ONE BOUNDARY AND EACH OF THE  IL  POINTS.                                 *
C*  SCALE FACTORS ARE INTRODUCED IN CASE THE INTEGRAND EXCEEDS THE MAXIMUM    *
C*  ALLOWED RANGE. BOTH THE EXPONENTIAL AND THE INTEGRAL WILL BE SCALED AC-   *
C*  CORDINGLY.                                                                *
C*                                                                            *
C*                  THIS ROUTINE USES A LINEAR INTERPOLATION SCHEME AT EACH   *
C*  POINT ( TRAPEZOIDAL RULE OR TWO POINT FORMULA ) .                         *
C*  DOUBLE PRECISION ARITHMETIC IS USED.                                      *
C*                                                                            *
C*                  INPUT PARAMETERS ARE                                      *
C*  PSI  = ONE-DIMENSIONAL ARRAY TO BE INTEGRATED                             *
C*  IM   = IRRELEVANT PARAMETER FOR THIS ROUTINE                              *
C*  IL   = TOTAL NUMBER OF POINTS                                             *
C*  ID   = INDICATES THE INTEGRAND AND THE DIRECTION OF INTEGRATION AS FOL-   *
C*         LOWS                                                               *
C*       ID GREATER THAN ZERO FOR FORWARD DIRECTION AND INTEGRAND DEXP(-PSI)  *
C*       ID LESS THAN ZERO FOR REVERSE DIRECTION AND INTEGRAND DEXP(PSI)      *
C*  STEP = ONE-DIMENSIONAL ARRAY, NON-UNIFORM STEP MAGNITUDE AT EACH POINT    *
C*                                                                            *
C*                  OUTPUT PARAMETERS ARE                                     *
C*  Y    = ONE-DIMENSIONAL ARRAY,INTEGRAND                                    *
C*  Q    = ONE-DIMENSIONAL ARRAY,RESULT OF THE INTEGRATION AT EACH POINT      *
C****************************************************************************
      COMMON /XST/ STEP
      DOUBLE PRECISION  PSI(1000),Y(1000),Q(1000),STEP(1000)
     $,SCLF,VO,QOLD,YOLD
      SCLF= DEXP(70.D0)
      IF (ID.LT.0) GO TO 100

C*****************INTEGRATION IN THE FORWARD DIRECTION AND FOR THE INTEGRAND  *
C*  DEXP(-PSI)  ONLY**********************************************************
      VO=PSI(1)
      Y(1)=1.D0
      Q(1)=0.
      DO 10 I=2,IL
      QOLD=Q(I-1)
      YOLD=Y(I-1)
      IF ((VO-PSI(I)).LE.70.) GO TO 8
      VO=VO-140.D0
      YOLD=DEXP(VO-PSI(I-1))
      QOLD=(Q(I-1)/SCLF)/SCLF
8     Y(I)= DEXP(VO-PSI(I))
10    Q(I)=(YOLD+Y(I))/2.D0*STEP(I-1)+QOLD
      RETURN

C*****************INTEGRATION IN THE REVERSE DIRECTION AND FOR THE INTEGRAND  *
```

```
C*   DEXP(PSI)  ONLY*************************************************************
100    VO=PSI(IL)
       Y(IL)=1.D0
       Q(IL)=0.
       DO 110 I=2,IL
       K=IL+1-I
       QOLD=Q(K+1)
       YOLD=Y(K+1)
       IF ((PSI(K)-VO).LE.70.) GO TO 108
       VO=VO+140.D0
       YOLD=DEXP(PSI(K+1)-VO)
       QOLD=(Q(K+1)/SCLF)/SCLF
108    Y(K)=DEXP(PSI(K)-VO)
110    Q(K)=(YOLD+Y(K))/2.D0*STEP(K)+QOLD
       RETURN
       END
```

```
$IBFTC S13     DECK
      SUBROUTINE POISSN (DELTAM,IL)
C******************************************************************************
C*                 THE SUBROUTINE  'POISSN'  SOLVES THE SECOND ORDER DIFFE-    *
C*  RENTIAL POISSON'S EQUATION, FOR GIVEN ELECTRON AND HOLE DISTRIBUTIONS.     *
C*                                                                             *
C*                 THIS ROUTINE  USES FINITE DIFFERENCES TO APPROXIMATE THE    *
C*  ANALYTICAL DERIVATIVES AND SOLVES A TRIPLE-DIAGONAL SYSTEM OF ALGEBRAIC    *
C*  LINEAR EQUATIONS.                                                          *
C*  SUBPROGRAMS NEEDED ARE                                                     *
C*                             SUBROUTINE    'CURV'                            *
C*                             SUBROUTINE    'TRIDU1'                          *
C*  DOUBLE PRECISION ARITHMETIC IS USED.                                       *
C*                                                                             *
C*                 INPUT PARAMETERS ARE                                        *
C*  PSI  = ONE-DIMENSIONAL ARRAY, UNCORRECTED POTENTIAL FROM PREVIOUS ITERATION*
C*  N    = ONE-DIMENSIONAL ARRAY, ELECTRON DISTRIBUTION FROM PREVIOUS ITERATION*
C*  P    = ONE-DIMENSIONAL ARRAY, HOLE DISTRIBUTION     FROM PREVIOUS ITERATION*
C*  NIM  = ONE-DIMENSIONAL ARRAY, IMPURITY DISTRIBUTION                        *
C*  IL   = TOTAL NUMBER OF POINTS                                              *
C*  STEP = ONE-DIMENSIONAL ARRAY, NON-UNIFORM STEP MAGNITUDE AT EACH POINT     *
C*                                                                             *
C*                 OUTPUT PARAMETERS ARE                                       *
C*  DELTA = ONE-DIMENSIONAL ARRAY, CORRECTION FOR THE POTENTIAL  PSI           *
C*  PSI   = ONE-DIMENSIONAL ARRAY, CORRECTED POTENTIAL                         *
C*  DELTAM = MAXIMUM ABSOLUTE VALUE OF THE CORRECTION  DELTA                   *
C*                                                                             *
C*                 ALL THE ARRAYS ARE OF DIMENSION  1000  AND IN DOUBLE PRE-   *
C*  CISION WITH EXCEPTION OF THE ARRAY  NIM                                    *
C*                                                                             *
C*                 ALLOWANCE FOR TWO DOUBLE PRECISION ARRAYS (WORKING LOCA-    *
C*  TIONS) FOR TEMPORARY STORAGE MUST BE MADE. THESE ARE AVAILABLE EXTERNALLY  *
C*  THRU THE LABELED  COMMON  /WORK/                                           *
C******************************************************************************
      REAL NIM(1000) ,JN,JP
      DOUBLE PRECISION PSI(1000),PSICV(1000),A(1000),B(1000),DELTA(1000)
     $ ,D(1000),ALFA,ETA ,STEP( 1000),N(1000),P(1000)
      COMMON /XST/ STEP
     $       /TRDG/ D
     $       /WORK/A,B
     $       /MCAR/ N,P,JN,JP
     $       /PSNM/ PSI,NIM
      EQUIVALENCE (PSICV,D,DELTA)
      IL1=IL-1
      CALL CURV (PSI,PSICV,IL)
      DO 50 I=2,IL1
      ALFA=STEP(I)/STEP(I-1)
      ETA=STEP(I)/2.D0*(STEP(I)+STEP(I-1))
      A(I)=ALFA
      B(I)=-ALFA-1.D0-ETA*(N(I)+P(I))
50    D(I)=(-PSICV(I)+N(I)-P(I)-NIM(I))*ETA
      CALL TRIDU1 (IL)
      DELTAM=0.
      DO 60 I=2,IL1
      PSI(I)=PSI(I)+DELTA(I)
      ABDEL=DABS(DELTA(I))
60    IF (DELTAM.LT.ABDEL) DELTAM=ABDEL
      RETURN
      END
```

```
$IBFTC S14A    DECK
      SUBROUTINE CURV (Y,YCURV,IL)
C******************************************************************************
C*                 THE SUBROUTINE  'CURV'  COMPUTES THE CURVATURE OF A FUNC-   *
C*  TION GIVEN IN DISCRETIZED FORM THROUGHOUT THE POINT INTERVAL  2 - (IL-1).  *
C*                                                                             *
C*                 THIS ROUTINE USES A PARABOLIC INTERPOLATION SCHEME AT EACH  *
C*  POINT (THREE-POINT FORMULA) SUITABLE FOR NON-UNIFORM STEPS. THE CURVATURE  *
C*  AT EACH POINT IS THAT    OF THE PARABOLA TRACED THROUGH THE POINT ITSELF   *
C*  AND THE TWO ADJACENT POINTS.                                               *
C*  DOUBLE PRECISION ARITHMETIC IS USED.                                       *
C*                                                                             *
C*                 INPUT PARAMETERS ARE                                        *
C*  Y    = ONE-DIMENSIONAL ARRAY WHOSE CURVATURE IS SOUGHT                     *
C*  IL   = TOTAL NUMBER OF POINTS                                              *
C*  STEP = ONE-DIMENSIONAL ARRAY, NON-UNIFORM STEP MAGNITUDE AT EACH POINT     *
C*                                                                             *
C*                 OUTPUT PARAMETERS ARE                                       *
C*  YCURV = ONE-DIMENSIONAL ARRAY, SECOND DERIVATIVE AT EACH POINT OF THE      *
C*          GIVEN ARRAY   Y                                                    *
C*                                                                             *
C*                 ALL THE ARRAYS ARE OF DIMENSION  1000  AND IN DOUBLE PRE-   *
C*  CISION.                                                                    *
C******************************************************************************
      DOUBLE PRECISION Y(1000),YCURV(1000),STEP(1000),ALFA
      COMMON /XST/ STEP
      IL1=IL-1
      DO 10 I=2,IL1
      ALFA=STEP(I)/STEP(I-1)
10    YCURV(I)=2.D0*( Y(I+1)-(ALFA+1.D0)*Y(I)+ALFA*Y(I-1))/( STEP(I)*
     $( STEP(I-1)+ STEP(I)))
      RETURN
      END
```

```
$IBFTC S14B    DECK
      SUBROUTINE CURV (Y,YCURV,IL)
C******************************************************************************
C*                 THE SUBROUTINE  'CURV'  COMPUTES THE CURVATURE OF A FUNC-   *
C*  TION GIVEN IN DISCRETIZED FORM THROUGHOUT THE POINT INTERVAL  2 - (IL-1).  *
```

```
C*                                                                         *
C*                  THIS ROUTINE USES A LAGRANGIAN INTERPOLATION SCHEME AT *
C*   EACH POINT (A FIVE POINT FORMULA) SUITABLE FOR NON-UNIFORM STEP.      *
C*   THE CURVATURE AT EACH POINT IS THAT    OF THE FOURTH ORDER POLYNOMIAL *
C*   TRACED TROUGH THE POINT ITSELF AND THE FOUR ADJACENT POINTS.          *
C*   DOUBLE PRECISION ARITHMETIC IS USED.                                  *
C*                                                                         *
C*                  INPUT PARAMETERS ARE                                   *
C*   Y    = ONE-DIMENSIONAL ARRAY WHOSE CURVATURE IS SOUGHT                *
C*   IL   = TOTAL NUMBER OF POINTS                                         *
C*   STEP = ONE-DIMENSIONAL ARRAY, NON-UNIFORM STEP MAGNITUDE AT EACH POINT *
C*                                                                         *
C*                  OUTPUT PARAMETERS ARE                                  *
C*   YCURV = ONE-DIMENSIONAL ARRAY, SECOND DERIVATIVE AT EACH POINT OF THE *
C*           GIVEN ARRAY  Y                                                *
C*                                                                         *
C*                  ALL THE ARRAYS ARE OF DIMENSION  1000  AND IN DOUBLE PRE- *
C*   CISION.                                                               *
C**************************************************************************
      DOUBLE PRECISION STEP(1000),YCURV(1000),Y(1000)
     $,WC,BC,W,ALFA,R(5,5),U(3,4)
      COMMON /XST/ STEP
      IL2=IL-2
      IL3=IL-3
      R(1,2)=-STEP(1)-STEP(2)
      R(1,3)=1.D0/R(1,2)
      R(2,2)=-STEP(2)
      R(2,3)=1.D0/R(2,2)
      R(5,2)=-STEP(2)-STEP(3)
      R(5,3)=1.D0/R(5,2)
      DO 50 K=4,5
      R(1,K)=R(1,K-1)*R(1,3)
      R(2,K)=R(2,K-1)*R(2,3)
50    R(5,K)=R(5,K-1)*R(5,3)
C**************************************************************************
      DO 300 I=3,IL2
      R(3,2)= STEP(I)
      R(4,2)=STEP(I)+STEP(I+1)
      R(3,3)=1.D0/R(3,2)
      R(4,3)=1.D0/R(4,2)
      R(3,4)=R(3,3)*R(3,3)
      R(4,4)=R(4,3)*R(4,3)
      R(3,5)=R(3,4)*R(3,3)
      R(4,5)=R(4,4)*R(4,3)
      R(1,1)=(Y(I-2)-Y(I))*R(1,5)
      R(2,1)=(Y(I-1)-Y(I))*R(2,5)
      R(3,1)=(Y(I+1)-Y(I))*R(3,5)
      R(4,1)=(Y(I+2)-Y(I))*R(4,5)
      DO 200 IR=1,3
      DO 200 IC=1,4
200   U(IR,IC)=R(IR,IC)-R(4,IC)
      WB=U(2,2)*U(3,3)-U(3,2)*U(2,3)
      WC=U(2,2)*U(3,4)-U(3,2)*U(2,4)
      BC=U(2,1)*U(3,2)-U(3,1)*U(2,2)
      W=U(1,2)* (U(2,3)*U(3,4)-U(3,3)*U(2,4))-  U(1,3)*WC +U(1,4)*WB
      YCURV(I)= -2.D0* (U(1,1)*WC -U(1,2)*(U(2,1)*U(3,4)-U(3,1)*U(2,4))+
     $ U(1,4)*BC)/W
      DO 250 K=2,5
      R(1,K) =R(5,K)
      R(2,K)=-R(3,K)
250   R(5,K)=-R(4,K)
      R(2,4)=-R(2,4)
      R(5,4)=-R(5,4)
300   CONTINUE
C**************************************************************************
      DO 400 I=2,IL,IL3
      ALFA=STEP(I)/STEP(I-1)
400   YCURV(I)= 2.D0*( Y(I+1)-(ALFA+1.D0)*Y(I)+ALFA*Y(I-1))/ (STEP(I)*
     $ (STEP(I-1)+STEP(I)))
      RETURN
      END


$IBFTC 515     DECK
      SUBROUTINE TRIDU1 (IL)
C**************************************************************************
C*                  THE SUBROUTINE  'TRIDU1'  SOLVES A TRIPLE-DIAGONAL SYSTEM  *
C*   OF THE FORM    T * DELTA  =  D  ,WHERE  T  IS A GIVEN TRIPLE-DIAGONAL    *
C*   MATRIX WITH UPPER DIAGONAL ENTRIES EQUAL TO UNITY,  DELTA  IS THE UNKNOWN *
C*   VECTOR,  D  IS THE KNOWN VECTOR.                                         *
C*                                                                            *
C*                  THIS ROUTINE USES A DIRECT METHOD BASED ESSENTIALLY ON    *
C*   GAUSSIAN ELIMINATION AND BACKSUBSTITUTION WHICH REDUCES IN THE CASE CON- *
C*   SIDERED TO A SET OF RECURSION RELATIONS.                                 *
C*   DOUBLE PRECISION ARITHMETIC IS USED.                                     *
C*                                                                            *
C*                  INPUT PARAMETERS ARE                                      *
C*   A      = ONE-DIMENSIONAL ARRAY, LOWER DIAGONAL OF THE TRIPLE-DIAGONAL MATRIX *
C*   B      = ONE-DIMENSIONAL ARRAY, DIAGONAL OF THE TRIPLE-DIAGONAL MATRIX    *
C*   D      = ONE-DIMENSIONAL ARRAY, KNOWN VECTOR                             *
C*   (IL-2) = NUMBER OF EQUATIONS (SIZE OF THE TRIPLE-DIAGONAL MATRIX )       *
C*                                                                            *
C*                  OUTPUT PARAMETERS ARE                                     *
C*   DELTA = ONE-DIMENSIONAL ARRAY, ORIGINALLY THE UNKNOWN VECTOR             *
C*                                                                            *
C*                  ALL THE ARRAYS ARE OF DIMENSION  1000  AND IN DOUBLE PRE- *
C*   CISION                                                                   *
C*                                                                            *
C*                  NO WORKING ARRAYS ARE NEEDED.  THIS IS ACHIEVED THROUGH   *
C*   USE OF EQUIVALENCE STATEMENTS.  DURING THE EXECUTION OF THIS ROUTINE THE *
C*   ARRAYS  B  AND  D  ARE ERASED.                                           *
C**************************************************************************
      DOUBLE PRECISION A(1000),B(1000),D(1000),DELTA(1000),G(1000)
     $,H(1000)
      COMMON /TRDG/ D
     $       /WORK/A,B
      EQUIVALENCE (D,DELTA,G),(H,B)
      IL1=IL-1
      IL2=IL-2
C*********    NOTE THAT H(2)=B(2) FROM EQUIVALENCE STATEMENT    ****************
      G(2)=D(2)/B(2)
      DO 20 I=3,IL1
      H(I)=B(I)-A(I)/H(I-1)
20    G(I)=(D(I)-A(I)*G(I-1))/H(I)
C*******    NOTE THAT DELTA(IL1)=G(IL1) FROM EQUIVALENCE STATEMENT     *********
      DO 30 I=2,IL2
      K=IL-I
30    DELTA(K)=G(K)-DELTA(K+1)/H(K)
      DELTA (1)=0.
      DELTA (IL)=0.
      RETURN
      END
```

```
$IBFTC SP1     DECK
      SUBROUTINE PRINT (IWR,ITER,VA,DELTAM,ERRPS)
C*************************************************************************
C*                   THE SUBROUTINE  'PRINT'  WRITES ON THE PRINTOUT SHEET THE   *
C*  RELEVANT PARAMETERS AND DISTRIBUTIONS  (PERTINENT TO ONE VALUE OF APPLIED  *
C*  VOLTAGE) , THAT REPRESENT THE SOLUTION OF THE PROBLEM.                    *
C*                                                                          *
C*                   THE DISTRIBUTIONS OF INTEREST ARE PRINTED OUT IN A NUMBER  *
C*  OF POINTS CONTROLLED BY THE PARAMETER   IWR  .   EVERY  (IWR)TH  POINT IS  *
C*  PRINTED OUT.    IF THE PARAMETER  IWR  IS OMITTED, A STANDARD VALUE (IWR=  *
C*  10) WILL BE CHOSEN BY THIS ROUTINE.                                       *
C*************************************************************************
      DOUBLE PRECISION STEP(1000),PSI(1000),N(1000),P(1000)
     $,              ND,NA,NN,PP,NP,PN,VD,M,L
     $,VA,DELTA(1000),DELTAT(1000),X(1000) ,PSITR(1000)
      REAL NIM(1000),JN,JP,J,JNORM,JNA,JPA,JA,NINT
      COMMON /STRC/ ND,NA,NN,PP,NP,PN,VD,M,L,IM,IL,VT,GAMN,GAMP
     $        /MCAR/ N,P,JN,JP
     $        /XST / STEP
     $        /TRDS/ DELTA
     $        /PSNM/ PSI,NIM
     $        /WORK/ X,DELTAT
      EQUIVALENCE (PSITR,DELTAT)
25    FORMAT (1H1,58H THE EXACT PARAMETERS AND DISTRIBUTIONS ARE THE FOL
     $LOWING        //////////////////25H APPLIED VOLTAGE   VAA = , F14.8,
     $7H  VOLTS ,41X, 4HVA =,D24.16, 14H  (NORMALIZED)  ////
     $          34H NUMBER OF POISSON'S ITERATIONS  =, I3, 22H TO ACHIEVE
     $ DELTAM = ,E12.5, 10X, 25HFOR A REQUESTED  ERRPS = ,E12.5//////
     $33H ELECTRON CURRENT DENSITY   JNA = ,E16.8,3X, 27HAMPERES / SQUAR
     $E CENTIMETER ,16X,4HJN = ,E16.8, 14H  (NORMALIZED) /
     $33H HOLE      CURRENT DENSITY   JPA = ,E16.8,3X, 27HAMPERES / SQUAR
     $E CENTIMETER ,16X,4HJP = ,E16.8, 14H  (NORMALIZED) /
     $33H TOTAL     CURRENT DENSITY   JA  = ,E16.8,3X, 27HAMPERES / SQUAR
     $E CENTIMETER ,16X,4HJ  = ,E16.8, 14H  (NORMALIZED) / )
100   FORMAT (1H1,      3X,1HI,10X,4HX(I), 19X,6HPSI(I), 12X,9HDELTAT(I),
     $ 8X,8HDELTA(I), 14X,4HN(I), 20X,4HP(I)///
     $ (I5,D23.16,D24.16,2D16.8,2D24.16))
      IF (IWR.EQ.0) IWR=10
      ELCH=1.60206E-19
      NINT=2.5E13
      PERM=8.85434E-14*16.
      JNORM=ELCH*NINT/SQRT (PERM/ELCH*VT/NINT)
      J=JN+JP
      JNA=JN*JNORM
      JPA=JP*JNORM
      JA =J *JNORM
      VAA=VA*VT
      WRITE (6,25) VAA,VA,ITER,DELTAM,ERRPS, JNA,JN,JPA,JP,JA,J
      CALL PSITRL (PSITR,VA)
      X(1)=0.
      DO 110 I=2,IL
110   X(I)=X(I-1)+STEP(I-1)
      DO 120 I=1,IL
120   DELTAT(I)=PSI(I)-PSITR (I)
      IWRM=IWR*50
      NPAGES=IL/IWRM
      IF(MOD(IL,IWRM).NE.0) NPAGES=NPAGES+1
      DO 200 K=1,NPAGES
      ILMD=IWRM*K
      IF (ILMD.GT.IL) ILMD=IL
      IIN=IWRM*(K-1) +1
200   WRITE (6,100) (I,X(I),PSI(I) ,DELTAT(I),DELTA(I),N(I),P(I),I=IIN,
     $ ILMD,IWR)
      RETURN
      END


$IBFTC SP2     DECK
      SUBROUTINE PUNCH (VA,DELTAM,EXP,ITER)
C*************************************************************************
C*                   THE SUBROUTINE  'PUNCH'  RECORDS ON PUNCHED CARDS THE RE-  *
C*  LEVANT EXACT PARAMETERS AND  DISTRIBUTIONS (PERTINENT TO ONE VALUE OF AP-  *
C*  PLIED VOLTAGE), THAT REPRESENT THE SOLUTION OF THE PROBLEM.               *
C*                                                                          *
C*                   THE NUMBER OF CARDS PUNCHED FOR EACH APPLIED VOLTAGE IS    *
C*                                 IL + 6                                   *
C*  WHERE            IL  = TOTAL NUMBER OF POINTS                             *
C*************************************************************************
      DOUBLE PRECISION STEP(1000),PSI(1000),N(1000),P(1000) ,VA
     $,              ND,NA,NN,PP,NP,PN,VD,M,L
      REAL NIM(1000),JN,JP,J,MN,MP,INJPAR,JNFSOR
      COMMON /STRC/ ND,NA,NN,PP,NP,PN,VD,M,L,IM,IL,VT,GAMN,GAMP
     $        /MCAR/ N,P,JN,JP
     $        /PSNM/ PSI,NIM
     $        /XST / STEP
     $        /FSO / XN,XP,MN,MP,INJPAR,PSIMP,JNFSOR
20    FORMAT (3D26.16/3D26.16/3D26.16/ D25.16,3I5,2E20.8/ 4E20.8/
     $4E20.8/ (4D20.13))
40    FORMAT (5E16.8)
      J=JN+JP
      PUNCH 20 , ND,NA,NN,PP,NP,PN,VD,VA,M,L,IM,IL,ITER,EXP,DELTAM,VT
     $,JN,JP,J,MN,MP,INJPAR,PSIMP
     $, (STEP(I),PSI(I),N(I),P(I),I=1,IL)
      PUNCH 40,  NIM
      RETURN
      END


$IBFTC SP2D    DECK
      SUBROUTINE PUNCH (DUMMY)
C*************************************************************************
C*                   THIS DECK  'SP2D' (DUMMY SUBROUTINE  'PUNCH' ) MAY BE IN-   *
C*  SERTED IN PLACE OF THE   DECK  'SP2'  (ACTUAL SUBROUTINE  'PUNCH'  )      *
C*  IN CASE RECORDING ON PUNCHED CARDS IS NOT REQUESTED.                      *
C*                                                                          *
C*                   THIS TECHNIQUE DECREASES THE AMOUNT OF CORE STORAGE REQUI-  *
C*  RED BY THE WHOLE PROGRAM.                                                 *
C*************************************************************************
      DIMENSION DUMMY (5)
      RETURN
      END


$IBFTC SP3D    DECK
      SUBROUTINE PLOT (DUMMY)
C*************************************************************************
C*                   THIS DECK  'SP3D'  (DUMMY SUBROUTINE  'PLOT'  )  MAY BE IN- *
C*  SERTED IN PLACE OF THE   DECK  'SP3'  (ACTUAL SUBROUTINE  'PLOT'  )       *
C*  IN CASE DISPLAY  OF THE DISTRIBUTIONS ON GRAPHS IS NOT REQUESTED.          *
```

```
C*                                                                          *
C*                THIS TECHNIQUE DECREASES THE AMOUNT OF CORE STORAGE REQUI- *
C*  RED BY THE WHOLE PROGRAM.                                               *
C****************************************************************************
      DIMENSION DUMMY (3)
      RETURN
      END


$IBFTC SP4      DECK
      SUBROUTINE TAPE (VA,DELTAM,ITER,IDTP,INTAPE)
C****************************************************************************
C*                THE SUBROUTINE  'TAPE'  RECORDS ON MAGNETIC TAPE PARAME-   *
C*  TERS AND DISTRIBUTIONS OF INTEREST (PERTINENT  TO ONE VALUE OF APPLIED   *
C*  VOLTAGE) , THAT  REPRESENT THE SOLUTION OF THE PROBLEM.                 *
C*  SUBPROGRAM NEEDED                                                       *
C*                FILE DEFINITION  DECK  'SP5' (IN ASSEMBLER LANGUAGE IBMAP) *
C*                                                                          *
C*  THE MAGNETIC TAPE IS DEFINED AS   'UNIT 25' .                           *
C*                                                                          *
C*                                                                          *
C*                THE PROCEDURE IS CONTROLLED BY THE PARAMETER  INTAPE (READ *
C*  FROM A DATA CARD, FOR EACH APPLIED VOLTAGE, IN THE CALLING PROGRAM)  IN *
C*  THE FOLLOWING FASHION                                                   *
C*                INTAPE = 0   RECORDING WILL NOT OCCUR. NO OPERATION WILL  *
C*                             BE PERFORMED ON THE TAPE.                    *
C*                                                                          *
C*        AT THE FIRST CALL OF THIS ROUTINE  INTAPE  MUST BE  EITHER 1  OR 2 *
C*                INTAPE = 1   RECORDING STARTS AT THE BEGINNING OF THE TAPE *
C*                INTAPE = 2   SEARCH FOR THE FLAG  IDTP=0 (LOCATED ON THE  *
C*                             TAPE AFTER THE LAST RELEVANT LOGICAL RECORD) *
C*                             IS PERFORMED. TO INITIATE THE RECORDING AFTER *
C*                             THE LAST RELEVANT LOGICAL RECORD ALREADY PRE- *
C*                             SENT ON THE TAPE.                            *
C*                                                                          *
C*        FOR OTHER THAN THE FIRST CALL OF THIS ROUTINE  INTAPE MUST BE  3  *
C*                INTAPE = 3   RECORDING OCCURS BY DIRECT ADDITION OF ONE LO- *
C*                             GICAL RECORD                                 *
C*                                                                          *
C*        THE EXECUTION OF THE MAIN PROGRAM TERMINATES WITH A LAST CALL OF  *
C*        THIS ROUTINE, FOR WHICH                                           *
C*                INTAPE = 4 (AUTOMATICALLY SET BY CALLING PROGRAM)         *
C*        TO SET THE FLAG  IDTP=0 AFTER THE LAST LOGICAL RECORD WRITTEN.    *
C*                                                                          *
C*                                                                          *
C*                IN CASE RECORDING OCCURS, A MESSAGE IS WRITTEN  ON THE    *
C*  PRINTOUT SHEET FOR EACH APPLIED VOLTAGE.                                *
C*                                                                          *
C*                THE NUMBER OF WORDS IN EACH LOGICAL RECORD IS  8*IL + 30 . *
C****************************************************************************
      DOUBLE PRECISION STEP(1000),PSI(1000),N(1000),P(1000),VA
     $,       ND,NA,NN,PP,NP,PN,VD,M,L
      REAL NIM(1000),JN,JP,J
      COMMON /STRC/ ND,NA,NN,PP,NP,PN,VD,M,L,IM,IL,VT,GAMN,GAMP
     $        /MCAR/ N,P,JN,JP
     $        /PSNM/ PSI,NIM
     $        /XST / STEP
    4 FORMAT (1H0, 34HMAGNETIC TAPE RECORDED WITH IDTP = ,I4//////)
    8 FORMAT (1H0, 42H ERROR ON MAGNETIC TAPE PARAMETER INTAPE = ,I6///)
      IF (INTAPE.LT.0.OR.INTAPE.GT.4) GO TO 100
      IF (INTAPE.EQ.0) GO TO 200
      GO TO (10,15,30,60),INTAPE
   10 IDTP=0
      GO TO 30
   15 IDTP=-1
   20 READ (25) IDDUM
      IDTP=IDTP+1
      IF (IDDUM.NE.0) GO TO 20
      BACKSPACE 25
   30 IDTP=IDTP+1
      J=JN+JP
      WRITE (25) IDTP,ND,NA,NN,PP,NP,PN,VD,VA,M,L,IM,IL,ITER,EXP,DELTAM
     $,VT,JN,JP,J
     $,  (STEP(I),PSI(I),N(I),P(I),I=1,IL)
      WRITE (6,4 ) IDTP
      RETURN
   60 WRITE (25) IDTP
      RETURN
  100 WRITE (6,8) INTAPE
  200 RETURN
      END


$IBFTC SP4D     DECK
      SUBROUTINE TAPE  (DUMMY)
C****************************************************************************
C*                THIS DECK  'SP4D'  (DUMMY SUBROUTINE  'TAPE'  )  MAY BE IN- *
C*  SERTED IN PLACE OF BOTH DECKS                                           *
C*                           DECK  'SP4'  (ACTUAL SUBROUTINE  'TAPE'  )     *
C*                           DECK  'SP5'  (FILE DEFINITION SUBPROGRAM,IBMAP) *
C*  IN CASE RECORDING ON MAGNETIC TAPE IS NOT REQUESTED.                    *
C*                                                                          *
C*                THIS TECHNIQUE DECREASES THE AMOUNT OF CORE STORAGE REQUI- *
C*  RED BY THE WHOLE PROGRAM.                                               *
C****************************************************************************
      DIMENSION DUMMY (6)
      RETURN
      END


$IBMAP SP5
*****************************************************************************
**                THIS SUBPROGRAM DEFINES THE FILE (AND RELEVANT PARAMETERS) *
**  FOR ONE MAGNETIC SAVE TAPE FOR DATA RECORDING PURPOSES.                  *
**                                                                           *
**                THE TAPE IS DEFINED AS   'UNIT 25'  ON CHANNEL  A(1)       *
**                'DATA'  = TITLE GIVEN TO THE TAPE                          *
**                'BIN'   = OPTION THAT SPECIFIES BINARY RECORDING           *
**                'INOUT' = OPTION THAT SPECIFIES BOTH READING AND WRITING   *
**                          ON THE TAPE                                      *
**                'BLK'   = OPTION THAT SPECIFIES THE LENGTH OF ONE RECORDING *
**                          BLOCK                                            *
*****************************************************************************
        ENTRY   .UN25.
.UN25.  PZE     UNIT25
UNIT25  FILE    DATA,A(1),BIN,INOUT,BLK=256,HOLD
        END
```

APPENDIX D

COMPUTER PROGRAM FOR THE CALCULATION OF THE TOTAL INCREMENTAL CAPACITANCE

In this Appendix the computer program (in Fortran IV, version 4) for the calculation of the total incremental capacitance is reported. The method and the mathematical formulation are described in Section 3.2. Two successive solutions of the direct problem for two slightly different applied voltages are required.

The program consists of a main program (deck 'PNC'), a first set of subprograms (decks 'S01' to 'S15' of Appendix C, and 'S16C'), and a second set of subprograms (decks 'SP1C', and 'SP2' to 'SP4' or 'SP5' of Appendix C), organized with the same criteria of Appendix C. A magnetic "scratch" tape is required for temporary storage.

Main program.

Deck 'PNC'. The main program drives the subprograms actually performing the required calculations.

Decks 'S01' to S15'. As in Appendix C.

Double precision function 'QSIMP'.

Deck 'S16C'. Computes in a certain region the integral of a function given in discretized form at unevenly spaced points. Parabolic interpolation (three-point formula) is used.

Subroutine 'PRINT'.

Deck 'SP1C'. Writes on the printout sheet the results of interest.

Decks 'SP2' to 'SP5'. As in Appendix C.

```
$IBFTC PNC     DECK
C*************************************************************************
C*             M A I N    P R O G R A M    (CAPACITANCE + DIRECT PROBLEM) *
C*************************************************************************
C*                                                                        *
C*************************************************************************
C*                THIS PROGRAM SOLVES THE BASIC TWO-CARRIER TRANSPORT EQUA-  *
C*   TIONS, GOVERNING THE BEHAVIOR OF SEMICONDUCTOR DEVICES, APPLIED TO AN N-P *
C*   JUNCTION UNDER THE FOLLOWING ASSUMPTIONS                             *
C*   (A)  NON DEGENERATE CONDITIONS                                       *
C*   (B)  CONSTANT TEMPERATURE                                            *
C*   (C)  TIME INDEPENDENT IMPURITY DISTRIBUTION                          *
C*   (D)  FULL IONIZATION OF THE IMPURITIES                               *
C*   (E)  ONE-DIMENSIONAL STRUCTURE                                       *
C*   (F)  STEADY-STATE CONDITIONS ONLY                                    *
C*   (G)  OHMIC CONTACTS                                                  *
C*   (H)  ABSENCE OF GENERATION-RECOMBINATION IN THE INTERIOR             *
C*   (I)  CONSTANT MOBILITIES                                             *
C*   (J)  DIRECT PROBLEM.   SPECIFIED AN APPLIED VOLTAGE, THE TOTAL CURRENT *
C*        THROUGH THE DEVICE IS OBTAINED (TOGETHER WITH ALL THE PARAMETERS *
C*        AND DISTRIBUTIONS OF INTEREST)                                  *
C*   NO APPROXIMATIONS IN THE SET OF EQUATIONS HAVE BEEN INTRODUCED.      *
C*   THE  N-REGION IS ASSUMED LOCATED ON THE LEFT SIDE OF THE METALLURGICAL *
C*   INTERFACE  M.                                                        *
C*                                                                        *
C*   IN ADDITION TO THE ABOVE THIS PROGRAM COMPUTES THE TOTAL INCREMENTAL CA- *
C*   PACITANCE OF THE  DEVICE  THROUGH DIRECT INTEGRATION OF THE INCREMENTS OF *
C*   ONE TYPE OF MOBILE CARRIERS GENERATED BY AN INCREMENT OF APPLIED VOLTAGE. *
C*                                                                        *
C*                THIS PROGRAM USES AN ITERATIVE SCHEME BASED ON THE COMPU- *
C*   TATION OF THE MOBILE CARRIERS FROM A POTENTIAL DISTRIBUTION THROUGH DIR- *
C*   ECT INTEGRATION FOLLOWED BY CORRECTION OF THE POTENTIAL DISTRIBUTION  *
C*   THROUGH THE SOLUTION OF POISSON'S EQUATION.  A TRIAL POTENTIAL DISTRIBU- *
C*   TION IS REQUIRED TO START THE ITERATIONS.                            *
C*   TWO SOLUTIONS  OF THE DIRECT PROBLEM ARE REQUIRED FOR ACHIEVING ONE VALUE *
C*   OF CAPACITANCE FOR A SPECIFIED APPLIED VOLTAGE.                      *
C*   THE WHOLE PROGRAM IS BUILT IN A HIGHLY MODULAR FASHION, FEATURING A MAIN *
C*   PROGRAM CALLING SEVERAL SUBPROGRAMS, IN FAVOR OF  A GREATER FLEXIBILITY *
C*   AND SIMPLICITY OF LOGIC ORGANIZATION.                                *
C*   SUBPROGRAMS EXPLICITLY CALLED BY THIS MAIN PROGRAM ARE               *
C*                SUBROUTINE  'STRUCT'  (DEFINES THE STRUCTURE PARAMETERS) *
C*                SUBROUTINE  'FSTORD'  (COMPUTES FIRST-ORDER THEORY PARAME- *
C*                                       TERS)                            *
C*                SUBROUTINE  'STPSEL'  (SELECTS THE STEP DISTRIBUTION)    *
C*                SUBROUTINE  'DOPING'  (FURNISHES THE IMPURITY DISTRIBUTION) *
C*                SUBROUTINE  'PSITRL'  (FURNISHES THE TRIAL POTENTIAL FUNC- *
C*                                       TION)                            *
C*                SUBROUTINE  'MOBCAR'  (YIELDS THE MOBILE CARRIER CONCEN- *
C*                                       TRATIONS FOR A GIVEN POTENTIAL )  *
C*                SUBROUTINE  'POISSN'  (FURNISHES AN IMPROVED POTENTIAL DI- *
C*                                       STRIBUTION BY SOLVING POISSON'S   *
C*                                       EQUATION FOR GIVEN MOBILE CARRIERS) *
C*                DOUBLE PRECISION FUNCTION  'QSIMP'  (COMPUTES THE INTEGRAL *
C*                                                   OF A FUNCTION BETWEEN *
C*                                                   THE LIMITS   1 , IL ) *
C*                SUBROUTINE  'PRINT'   (WRITES OUTPUT DATA ON PRINTOUT    *
C*                                       SHEET)                           *
C*                SUBROUTINE  'PUNCH'   (PUNCHES ON OUTPUT CARDS RELEVANT  *
C*                                       QUANTITIES)                      *
C*                SUBROUTINE  'PLOT'    (EXECUTES PLOTS OF RELEVANT QUANTI- *
C*                                       TIES)                            *
C*                SUBROUTINE  'TAPE'    (RECORDS ON MAGNETIC TAPE RELEVANT *
C*                                       QUANTITIES)                      *
C*   OTHER SUBPROGRAMS MAY BE CALLED BY THE ABOVE SUBROUTINES.            *
C*   DOUBLE PRECISION ARITHMETIC IS USED.                                 *
C*                                                                        *
C*                                                                        *
C*                INPUT PARAMETERS ARE                                    *
C*                                                                        *
C*   DATA CARD   1. PARAMETERS CONCERNING THE STRUCTURE ARE READ IN THE SUB- *
C*                  ROUTINE  'STRUCT'  (SEE SUBROUTINE  'STRUCT'  )       *
C*   DATA CARD   2. PARAMETERS CONCERNING THE MATERIAL PROPERTIES ARE READ  IN *
C*                  THE SUBROUTINE  'STRUCT'  (SEE SUBROUTINE  'STRUCT'  ) *
C*                                                                        *
C*   DATA CARD   3. PARAMETERS CONCERNING THE ACTUAL APPLIED VOLTAGE AND THE *
C*                  APPLIED VOLTAGE INCREMENT (FOR CAPACITANCE COMPUTATION) *
C*                  ARE READ IN THIS MAIN PROGRAM AS FOLLOWS              *
C*   VAA   = APPLIED VOLTAGE GIVEN IN   NORMALIZED FORM IF THE (BELOW) INPUT *
C*           PARAMETER  IVAA  IS EQUAL TO  ONE,IN UNNORMALIZED FORM OTHERWISE. *
C*   FXP   = (OPTIONAL) MULTIPLICATIVE CORRECTION FACTOR TO THE FIRST-ORDER *
C*           WIDTH OF THE DEPLETED REGION IN THE LOW-CONDUCTIVITY SIDE (IF OMIT- *
C*           TED, NO CORRECTION IS PERFORMED)                             *
C*   DELVAR=PARAMETER DETERMINING THE APPLIED VOLTAGE INCREMENT FOR CAPACITAN- *
C*           CE COMPUTATION ACCORDING TO THE RELATION                     *
C*                  VOLTAGE INCREMENT = DELVAR * POTENTIAL DROP ON THE BARRIER *
C*           IF     DELVAR = 0   COMPUTATION OF THE CAPACITANCE WILL NOT OCCUR. *
C*           ONLY THE SOLUTION OF THE DIRECT PROBLEM WILL THEN TAKE PLACE. *
C*   ITMAX= MAXIMUM NUMBER OF POISSON'S ITERATIONS                        *
C*   ERRPS= MAXIMUM ERROR ALLOWED ON THE FINAL POTENTIAL FUNCTION.   THE NUM- *
C*           BER OF POISSON'S ITERATIONS IS DETERMINED EITHER BY  ITMAX  OR BY *
C*           ERRPS, WHICHEVER APPLIES FIRST.                              *
C*   PSIMPR=(REQUIRED AT EXTREMELY HIGH INJECTION LEVELS, OPTIONAL OTHERWISE) *
C*           PARAMETER THAT DETERMINES THE VALUE OF THE FIRST-ORDER TRIAL ELEC- *
C*           TROSTATIC POTENTIAL AT THE INTERFACE BETWEEN THE DEPLETED AND NEU- *
C*           TRAL REGION IN THE LOW-CONDUCTIVITY SIDE.(IF OMITTED, NO CORRECTION *
C*           IS PERFORMED).                                               *
C*   IWR   = PARAMETER THAT CONTROLS THE PRINTOUT IN THE SUBROUTINE  'PRINT' *
C*           (SEE SUBROUTINE  'PRINT' )                                   *
C*   INTAPE=PARAMETER THAT CONTROLS THE PROCEDURE OF RECORDING DATA ON MAGNE- *
C*           TIC TAPE  (SEE SUBROUTINE  'TAPE'  )                         *
C*   IVAA = (INTEGER) PARAMETER THAT CONTROLS    THE    INPUT OF THE APPLIED *
C*           VOLTAGE   VAA  (SEE ABOVE).                                  *
C*   ISTOP= PARAMETER THAT CONTROLS THE REPETITION OF THE SOLUTION FOR SEVERAL *
C*           APPLIED VOLTAGES AS FOLLOWS                                  *
C*                  ISTOP = 0   THE STRUCTURE AND MATERIAL PARAMETERS ARE NOT *
C*                              CHANGED FOR THE FOLLOWING APPLIED VOLTAGE *
C*                              (NEW STRUCTURE AND MATERIAL DATA CARDS  1. AND *
C*                              2.  MUST NOT BE INSERTED FOR THE FOLLOWING AP- *
C*                              PLIED VOLTAGE)                            *
C*                  ISTOP = 1   LAST APPLIED VOLTAGE OF THE SET           *
C*                  ISTOP = 2   THE STRUCTURE AND MATERIAL PARAMETERS ARE CHAN- *
C*                              GED FOR THE FOLLOWING APPLIED VOLTAGE (NEW *
C*                              STRUCTURE AND MATERIAL DATA CARDS  1.  AND  2. *
C*                              MUST BE INSERTED FOR THE FOLLOWING APPLIED VOL- *
C*                              TAGE)                                     *
C*                                                                        *
C*   DATA CARD   4. PARAMETERS CONCERNING THE AUTOMATIC STEP SELECTION PROCE- *
C*                  DURE, INCLUDING THE TOTAL NUMBER OF POINTS DESIRED, ARE *
C*                  READ IN THE SUBROUTINE  'STPSEL'  (SEE SUBROUTINE 'STPSEL') *
C*                  ONE DATA CARD FOR EACH APPLIED VOLTAGE MUST BE FURNISHED *
C*                  IN THE APPROPRIATE ORDER.                             *
C*                                                                        *
```

```
C*                                                                          *
C*                 OUTPUT PARAMETERS ARE                                    *
C*                                                                          *
C*  PSI  = ONE-DIMENSIONAL ARRAY, EXACT POTENTIAL DISTRIBUTION              *
C*  N    = ONE-DIMENSIONAL ARRAY, EXACT ELECTRON DISTRIBUTION               *
C*  P    = ONE-DIMENSIONAL ARRAY, EXACT HOLE DISTRIBUTION                   *
C*  X    = ONE-DIMENSIONAL ARRAY, ABSCISSA OF EACH POINT THROUGHOUT THE JUNC- *
C*         TION                                                             *
C*  STEP = ONE-DIMENSIONAL ARRAY, NON UNIFORM STEP MAGNITUDE AT EACH POINT  *
C*  JN   = ELECTRON CURRENT                                                 *
C*  JP   = HOLE CURRENT                                                     *
C*  J    = TOTAL CURRENT                                                    *
C*  CAPN = TOTAL INCREMENTAL CAPACITANCE OBTAINED BY INTEGRATION OF ELECTRON *
C*         INCREMENTS                                                       *
C*  CAPP = TOTAL INCREMENTAL CAPACITANCE OBTAINED BY INTEGRATION OF   HOLE  *
C*         INCREMENTS                                                       *
C*                                                                          *
C*                 IN CASE COMPUTATION OF THE CAPACITANCE TAKES PLACE, TEMPO- *
C*  RARY STORAGE OF  4,000  WORDS ON ONE SCRATCH TAPE (ON UNIT  1 ) IS REQUI- *
C*  RED.                                                                    *
C*                                                                          *
C*                 ALLOWANCE FOR  SEVEN DOUBLE PRECISION ARRAYS  (STEP,PSI,  *
C*  N,P,DELTA  +  TWO WORKING ARRAYS IN THE LABELED  COMMON  /WORK/ ) AND    *
C*  ONE SINGLE PRECISION ARRAY  (NIM), ALL OF DIMENSION  1000, HAS BEEN MADE. *
C****************************************************************************
      DOUBLE PRECISION STEP(1000),PSI(1000),VA
     $,N(1000),P(1000),DELTA(1000)
     $,NINC(1000),PINC(1000), DELTAN(1000),DELTAP(1000)
     $,           ND,NA,NN,PP,NP,PN,VD,M,L,QSIMP
      REAL NIM(1000),JN,JP
      COMMON /STRC/ ND,NA,NN,PP,NP,PN,VD,M,L,IM,IL,VT,GAMN,GAMP
     $        /MCAR/ N,P,JN,JP
     $        /XST / STEP
     $        /WORK/ NINC,PINC
     $        /TRDG/ DELTA
     $        /PSNM/ PSI,NIM
     $        /CAP / CAPN,CAPP,DELC ,DELVAR,DELVA
      EQUIVALENCE (NINC,DELTAN),(PINC,DELTAP)
10    FORMAT (3E10.0,I10,2E10.0,4I5)
15    FORMAT (1H1, 54H THE APPLIED VOLTAGE AND RELATED INPUT PARAMETERS
     $ARE  //////////10H VAA     = ,F9.5// 10H FXP     = ,F9.5//
     $ 10H DELVAR = ,F9.5// 10H ERRPS  = ,E13.5//10H ITMAX  = ,I3//////)

C*****************STRUCTURE AND MATERIAL PROPERTIES DEFINITIONS***************
100   CALL STRUCT

C*****************READING OF THE APPLIED VOLTAGE,ITS INCREMENT, AND CONTROL  *
C*  PARAMETERS FROM  DATA CARD  3.*********************************************
120   READ (5,10) VAA,FXP,DELVAR,ITMAX,ERRPS, PSIMPR, IWR,INTAPE,IVAA
     $,ISTOP
      VA=VAA /VT
      IF (IVAA.NE.1) GO TO 130
      VA=VAA
      VAA=VA*VT
130   CONTINUE
      WRITE (6,15)VAA,FXP,DELVAR,ERRPS,ITMAX
      IF (IWR1.EQ.0) IWR1=10
      IBRCAP=0
      IF (DELVAR.NE.0.) REWIND 1

C****************************************************************************
```

```
C*                   BASIC PROGRAM FOR THE DIRECT PROBLEM                   *
C****************************************************************************
      KW=1
      CALL FSTORD (VA ,FXP,KW,PSIMPR)
      IF (KV.LT.0) GO TO 9999
      CALL STPSEL (JRET,1,1)
      IF (JRET.EQ.1) GO TO 9999
      CALL DOPING (NIM)
      KW=2
150   CALL FSTORD (VA ,FXP,KW,PSIMPR)
      CALL PSITRL (PSI,VA)
      DELTAM=1.E20
      ITER=0
170   CALL MOBCAR (PSI,VA)
      IF (ITER.EQ.ITMAX.OR. DELTAM.LE.ERRPS ) GO TO 300
      CALL POISSN (DELTAM,IL)
      ITER=ITER+1
      GO TO 170
300   CONTINUE
      IF (IBRCAP.EQ.1) GO TO 450

C*****************DISPLAYING AND RECORDING RESULTS***************************
      CALL PRINT (IWR,ITER,VA,DELTAM,ERRPS)
      CALL PUNCH (VA,DELTAM,FXP,ITER)
      CALL PLOT (VA,IL)
      CALL TAPE (VA,DELTAM,ITER,IDTP,INTAPE)
      IF (DELVAR.EQ.0.) GO TO 9999

C*****************DETERMINATION OF THE INCREMENTED APPLIED VOLTAGE************
      WRITE (1) N,P
      PSIMIN=PSI(1)
      DO 400 I=2,IL
400   IF (PSIMIN.GT.PSI(I)) PSIMIN=PSI(I)
      DELVA=DELVAR*ABS(PSIMIN)
      VA=VA-DELVA
      IBRCAP=1
      KW=3
      PINCL=PSI(IL)-PSI(IL-1)
      PINCO=PSI(2)-PSI(1)
      REWIND 1
      GO TO 150

C*****************COMPUTATION OF THE MOBILE CARRIER INCREMENTS AND THEIR IN-  *
C*  TEGRATION*****   CHECK WITH THE RESULT OF AN ALTERNATIVE FORMULATION (THE *
C*  DIFFERENTIATION OF THE DIFFERENCE OF THE ELECTRIC FIELD AT THE EXTERNAL  *
C*  CONTACTS WITH RESPECT TO THE APPLIED VOLTAGE )  IS ALSO PERFORMED.  ******
450   CONTINUE
      READ (1) NINC,PINC
      DELC= ((PINCL-(PSI(IL)-PSI(IL-1)))/  STEP(IL-1)-
     $      (PINCO-(PSI(2)-PSI(1)))/STEP(1)   ) /DELVA
      DO 480 I=1,IL
      DELTAN(I)=N(I)-NINC(I)
480   DELTAP(I)=P(I)-PINC(I)
      CALL TAPE (VA,DELTAM,ITER,IDTP,5)
      CAPN= QSIMP (DELTAN,IL)/DELVA
      CAPP= QSIMP (DELTAP,IL)/DELVA
      CALL PRINT (IWR, -1 ,VA,DELTAM,ERRPS)
C****************************************************************************
9999  IF (ISTOP.EQ.2) GO TO 100
      IF (ISTOP.EQ.0) GO TO 120
      CALL TAPE (VA,DELTAM,ITER,  0,  4)
```

```
      STOP
      END
```

```
***********************   DECKS   'S01'  TO  'S15'   ***********************
```

```
$IBFTC S16C    DECK
      DOUBLE PRECISION FUNCTION QSIMP  (Y,IL)
C****************************************************************************
C*                  THE DOUBLE PRECISION FUNCTION  'QSIMP'  COMPUTES THE INTE-  *
C*  GRAL OF A FUNCTION GIVEN IN DISCRETIZED FORM, LIMITS OF INTEGRATION BEING  *
C*  THE POINT BOUNDARIES   1 , IL .                                            *
C*                                                                             *
C*                  THIS ROUTINE USES A PARABOLIC INTERPOLATION AT EVERY OTHER *
C*  POINT, SUITABLE FOR NON-UNIFORM STEP SIZE.    SPECIALIZED FOR THE CASE OF  *
C*  UNIFORM STEP, THE SCHEME REDUCES TO SIMPSON'S RULE.                        *
C*  DOUBLE PRECISION ARITHMETIC IS USED.                                       *
C*                                                                             *
C*                  INPUT PARAMETERS ARE                                       *
C*  Y     = ONE-DIMENSIONAL ARRAY TO BE INTEGRATED                             *
C*  IL    = TOTAL NUMBER OF POINTS                                             *
C*  STEP  = ONE-DIMENSIONAL ARRAY, NON-UNIFORM STEP MAGNITUDE AT EACH POINT    *
C*                                                                             *
C*                  OUTPUT PARAMETER IS                                        *
C*  QSIMP = RESULT OF THE INTEGRATION                                          *
C*                                                                             *
C*                  ALL THE ARRAYS ARE OF DIMENSION  1000  AND IN DOUBLE PRE-  *
C*  CISION.                                                                    *
C****************************************************************************
      COMMON / XST/ STEP
      DOUBLE PRECISION STEP(1000),Y(1000),ALFA,C1,C3
      IL2=IL-2
      QSIMP=0.
      DO 10 I=1,IL2,2
      K=IL-I
      ALFA=STEP(K)/STEP(K-1)
      C1=2.D0-ALFA
      C3=2.D0-1.D0/ALFA
10    QSIMP= ( C1*Y(K-1)+(6.D0-C1-C3)*Y(K)+C3*Y(K+1))*(STEP(K)+STEP(K-1)
     $) / 6.D0 + QSIMP
      IF (K.EQ.3) QSIMP=(Y(2)+Y(1))*STEP(1) / 2.D0 + QSIMP
      RETURN
      END
```

```
$IBFTC SPIC    DECK
      SUBROUTINE PRINT (IWR,ITER,VA,DELTAM,ERRPS)
C****************************************************************************
C*                  THE SUBROUTINE  'PRINT'  WRITES ON THE PRINTOUT SHEET THE  *
C*  RELEVANT PARAMETERS AND DISTRIBUTIONS  (PERTINENT TO THE VALUE OF APPLIED  *
C*  VOLTAGE SPECIFIED ON THE DATA CARD), THAT REPRESENT THE SOLUTION OF THE    *
C*  PROBLEM.                                                                   *
C*  RESULTS CONCERNING TOTAL INCREMENTAL CAPACITANCE CALCULATIONS ARE ALSO     *
C*  INCLUDED.                                                                  *
C*                                                                             *
C*                  THE DISTRIBUTIONS OF INTEREST ARE PRINTED OUT IN A NUMBER  *
C*  OF POINTS CONTROLLED BY THE PARAMETER   IWR  .  EVERY  (IWR)TH  POINT IS   *
C*  PRINTED OUT.    IF THE PARAMETER  IWR  IS OMITTED, A STANDARD VALUE (IWR=  *
C*  10) WILL BE CHOSEN BY THIS ROUTINE.                                        *
C****************************************************************************
      DOUBLE PRECISION STEP(1000),PSI(1000),N(1000),P(1000)
     $,             ND,NA,NN,PP,NP,PN,VD,M,L
     $,VA,DELTA(1000),DELTAT(1000),X(1000) ,PSITR(1000)
      REAL NIM(1000),JN,JP,J,JNORM,JNA,JPA,JA,NINT
      COMMON /STRC/ ND,NA,NN,PP,NP,PN,VD,M,L,IM,IL,VT,GAMN,GAMP
     $        /MCAR/ N,P,JN,JP
     $        /XST / STEP
     $        /TRDG/ DELTA
     $        /PSNM/ PSI,NIM
     $        /WORK/ X,DELTAT
     $        /CAP / CAPN,CAPP,DELC ,DELVAR,DELVA
      EQUIVALENCE (PSITR,DELTAT)
25    FORMAT (1H1,58H THE EXACT PARAMETERS AND DISTRIBUTIONS ARE THE FOL
     $LOWING       ////////////////25H APPLIED VOLTAGE   VAA = , F14.8,
     $7H  VOLTS ,41X, 4HVA =,D24.16, 14H  (NORMALIZED)  ////
     $          34H NUMBER OF POISSON'S ITERATIONS  =, I3, 22H TO ACHIEVE
     $ DELTAM = ,E12.5, 10X, 25HFOR A REQUESTED  ERRPS = ,E12.5//////
     $33H ELECTRON CURRENT DENSITY   JNA = ,E16.8,3X, 27HAMPERES / SQUAR
     $E CENTIMETER ,15X,4HJN = ,E16.8, 14H  (NORMALIZED) /
     $33H HOLE     CURRENT DENSITY   JPA = ,E16.8,3X, 27HAMPERES / SQUAR
     $E CENTIMETER ,15X,4HJP = ,E16.8, 14H  (NORMALIZED) /
     $33H TOTAL    CURRENT DENSITY   JA  = ,E16.8,3X, 27HAMPERES / SQUAR
     $E CENTIMETER ,15X,4HJ  = ,E16.8, 14H  (NORMALIZED) / )
30    FORMAT (1H1,53HEXACT CAPACITANCE CALCULATION RESULTS FOR   DELVAR
     $= , E15.8, 20X, 8HDELVA = ,E15.8////////////
     $ 9H CAPN  = ,E15.8, 20X,9H CAPP  = ,E15.8/
     $ 9H CAPNR = ,E15.8, 20X,9H CAPPR = ,E15.8/  ///////////
     $ 5H WITH ,20X,8HDELCA = ,E15.8, 20X, 7HDELC = ,E15.8////)
100   FORMAT (1H1,     3X,1HI,10X,4HX(I), 19X,6HPSI(I), 12X,9HDELTAT(I),
     $ 8X,8HDELTA(I), 14X,4HN(I), 20X,4HP(I)///
     $ (I5,D23.16,D24.16,2D16.8,2D24.16))
      IF (ITER.LT.0) GO TO 400
      IF (IWR.EQ.0) IWR=10
      ELCH=1.60206E-19
      NINT=2.5E13
      PERM=8.85434E-14*16.
      JNORM=ELCH*NINT/SQRT (PERM/ELCH*VT/NINT)
      J=JN+JP
      JNA=JN*JNORM
      JPA=JP*JNORM
      JA =J *JNORM
      VAA=VA*VT
      WRITE (6,25) VAA,VA,ITER,DELTAM,ERRPS, JNA,JN,JPA,JP,JA,J
      CALL PSITRL (PSITR,VA)
      X(1)=0.
      DO 110 I=2,IL
110   X(I)=X(I-1)+STEP(I-1)
      DO 120 I=1,IL
120   DELTAT(I)=PSI(I)-PSITR (I)
      IWRM=IWR*50
      NPAGES=IL/IWRM
```

```
      IF(MOD(IL,IWRM).NE.0) NPAGES=NPAGES+1
      DO 200 K=1,NPAGES
      ILMD=IWRM*K
      IF (ILMD.GT.IL) ILMD=IL
      IIN=IWRM*(K-1) +1
200   WRITE (6,100) (I,X(I),PSI(I) ,DELTAT(I),DELTA(I),N(I),P(I),I=IIN,
     $ ILMD,IWR)
      RETURN
C*****************PRINTOUT OF RESULTS CONCERNING      TOTAL INCREMENTAL CAPA-  *
C*  CITANCE CALCULATIONS.       CHECK ON THE IDENTITY                          *
C*                            DELC  =  DELCA                                   *
C*  IS PERFORMED.  WHERE                                                       *
C*       DELC = DERIVATIVE OF THE DIFFERENCE BETWEEN THE ELECTRIC FIELD AT     *
C*              THE EXTERNAL CONTACTS WITH RESPECT TO THE APPLIED VOLTAGE      *
C*       DELCA= INTEGRAL OF THE DIFFERENCE BETWEEN HOLE AND ELECTRON INCRE-    *
C*              MENTS FOR AN INCREMENT OF APPLIED VOLTAGE         **************
400   CONTINUE
      CAPNR=1./CAPN**2
      CAPPR=1./CAPP**2
      DELCA=CAPP-CAPN
      WRITE (6,30) DELVAR,DELVA,CAPN,CAPP,CAPNR,CAPPR,DELCA,DELC
      RETURN
      END
```

```
***********************    DECKS    'SP2'  TO  'SP5'    ***********************
```

APPENDIX E

COMPUTER PROGRAM FOR THE REVERSE STEADY-STATE PROBLEM

In this Appendix the computer program (in Fortran IV, version 4) for the solution of the reverse steady-state problem is reported. The method of solution is described in Section 3.3 and in Fig. 3.1. Successive solutions of the direct problem are required.

The program consists of a main program (deck 'PNR'), a first set of subprograms (decks 'S01' to 'S15' of Appendix C, and 'S16R'), and a second set of subprograms (decks 'SP1' to 'SP4' or 'SP5' of Appendix C), organized with the same criteria of Appendix C.

Main program.

Deck 'PNR'. The main program drives the subprograms actually performing the required calculations.

Decks 'S01' to 'S15'. As in Appendix C.

Subroutine 'VOLTIN'.

Deck 'S16R'. Furnishes the voltage at the terminals of the device approximately corresponding to a specified total current. This is performed initially by an estimation on the basis of the first-order theory (Appendix A) and subsequently by a Lagrangian interpolation on the exact current-voltage characteristic.

Decks 'SP1' to 'SP5'. As in Appendix C.

```
$IBFTC PNR      DECK
C*****************************************************************************
C*                M A I N     P R O G R A M       (REVERSE PROBLEM)          *
C*****************************************************************************
C*                                                                           *
C*****************************************************************************
C*                THIS PROGRAM SOLVES THE BASIC TWO-CARRIER TRANSPORT EQUA-  *
C*  TIONS, GOVERNING THE BEHAVIOR OF SEMICONDUCTOR DEVICES, APPLIED TO AN N-P *
C*  JUNCTION UNDER THE FOLLOWING ASSUMPTIONS                                 *
C*  (A)  NON DEGENERATE CONDITIONS                                           *
C*  (B)  CONSTANT TEMPERATURE                                                *
C*  (C)  TIME INDEPENDENT IMPURITY DISTRIBUTION                              *
C*  (D)  FULL IONIZATION OF THE IMPURITIES                                   *
C*  (E)  ONE-DIMENSIONAL STRUCTURE                                           *
C*  (F)  STEADY-STATE CONDITIONS ONLY                                        *
C*  (G)  OHMIC CONTACTS                                                      *
C*  (H)  ABSENCE OF GENERATION-RECOMBINATION IN THE INTERIOR                 *
C*  (I)  CONSTANT MOBILITIES                                                 *
C*  (J)  REVERSE PROBLEM.   GIVEN   A TOTAL CURRENT, THE VOLTAGE AT THE TER- *
C*       MINALS IS OBTAINED (TOGETHER WITH ALL THE PARAMETERS AND DISTRIBU-  *
C*       TIONS OF INTEREST)                                                  *
C*  NO APPROXIMATIONS IN THE SET OF EQUATIONS HAVE BEEN INTRODUCED.          *
C*  THE  N-REGION IS ASSUMED LOCATED ON THE LEFT SIDE OF THE METALLURGICAL   *
C*  INTERFACE  M.                                                            *
C*                                                                           *
C*                THIS PROGRAM USES A SUCCESSIVE APPROXIMATION SCHEME BASED  *
C*  ON  AN INTERPOLATION PROCEDURE ON THE FUNCTION 'VOLTAGE VERSUS CURRENT'  *
C*  AND ON THE USE OF THE BASIC PROGRAM FOR THE DIRECT PROBLEM.   ESTIMATION *
C*  (BY FIRST ORDER THEORY, IF APPLICABLE)  OF THE FIRST FEW POINTS ON THE   *
C*  CURVE  'VOLTAGE VERSUS CURRENT'  IS NECESSARY.  (SEE SUBROUTINE 'VOLTIN'). *
C*  THE WHOLE PROGRAM IS BUILT IN A HIGHLY MODULAR FASHION, FEATURING A MAIN *
C*  PROGRAM CALLING SEVERAL SUBPROGRAMS, IN FAVOR OF  A GREATER FLEXIBILITY  *
C*  AND SIMPLICITY OF LOGIC ORGANIZATION.                                    *
C*  SUBPROGRAMS EXPLICITLY CALLED BY THIS MAIN PROGRAM ARE                   *
C*                SUBROUTINE  'STRUCT'  (DEFINES THE STRUCTURE PARAMETERS)   *
C*                SUBROUTINE  'FSTORD'  (COMPUTES FIRST-ORDER THEORY PARAME- *
C*                                       TERS)                               *
C*                SUBROUTINE  'STPSEL'  (SELECTS THE STEP DISTRIBUTION)      *
C*                SUBROUTINE  'DOPING'  (FURNISHES THE IMPURITY DISTRIBUTION) *
C*                SUBROUTINE  'PSITRL'  (FURNISHES THE TRIAL POTENTIAL FUNC- *
C*                                       TION)                               *
C*                SUBROUTINE  'MOBCAR'  (YIELDS THE MOBILE CARRIER CONCEN-   *
C*                                       TRATIONS FOR A GIVEN POTENTIAL )    *
C*                SUBROUTINE  'POISSN'  (FURNISHES AN IMPROVED POTENTIAL DI- *
C*                                       STRIBUTION BY SOLVING POISSON'S     *
C*                                       EQUATION FOR GIVEN MOBILE CARRIERS) *
C*                SUBROUTINE  'VOLTIN'  (ESTIMATES THE VOLTAGE AT THE TERMI- *
C*                                       NALS CORRESPONDING TO A SPECIFIED   *
C*                                       VALUE OF TOTAL CURRENT)             *
C*                SUBROUTINE  'PRINT'   (WRITES OUTPUT DATA ON PRINTOUT      *
C*                                       SHEET)                              *
C*                SUBROUTINE  'PLOT'    (EXECUTES PLOTS OF RELEVANT QUANTI-  *
C*                                       TIES)                               *
C*                SUBROUTINE  'PUNCH'   (PUNCHES ON OUTPUT CARDS RELEVANT    *
C*                                       QUANTITIES)                         *
C*                SUBROUTINE  'TAPE'    (RECORDS ON MAGNETIC TAPE RELEVANT   *
C*                                       QUANTITIES)                         *
C*  OTHER SUBPROGRAMS MAY BE CALLED BY THE ABOVE SUBROUTINES.                *
C*  DOUBLE PRECISION ARITHMETIC IS USED.                                     *
C*                                                                           *
C*                                                                           *
```

```
C*                INPUT PARAMETERS ARE                                       *
C*                                                                           *
C*  DATA CARD   1. PARAMETERS CONCERNING THE STRUCTURE ARE READ IN THE SUB-  *
C*                 ROUTINE  'STRUCT'  (SEE SUBROUTINE  'STRUCT'  )           *
C*                                                                           *
C*  DATA CARD   2. PARAMETERS CONCERNING THE MATERIAL PROPERTIES ARE READ  IN *
C*                 THE SUBROUTINE  'STRUCT'  (SEE SUBROUTINE  'STRUCT'  )    *
C*                                                                           *
C*  DATA CARD   3. PARAMETERS CONCERNING THE ACTUAL SPECIFIED CURRENT ARE    *
C*                 READ IN THIS MAIN PROGRAM AS FOLLOWS                      *
C*  JS    = SPECIFIED TOTAL CURRENT    (NORMALIZED)                          *
C*  FXP   = (OPTIONAL) MULTIPLICATIVE CORRECTION FACTOR TO THE FIRST-ORDER   *
C*          WIDTH OF THE DEPLETED REGION IN THE LOW-CONDUCTIVITY SIDE (IF OMIT- *
C*          TED, NO CORRECTION IS PERFORMED)                                 *
C*  ERRJ  = TOLERANCE PARAMETER FOR THE SPECIFIED CURRENT                    *
C*  ITMAX= MAXIMUM NUMBER OF POISSON'S ITERATIONS                            *
C*  ERRPS= MAXIMUM ERROR ALLOWED ON THE FINAL POTENTIAL FUNCTION.   THE NUM- *
C*          BER OF POISSON'S ITERATIONS IS DETERMINED EITHER BY  ITMAX  OR BY *
C*          ERRPS  WHICHEVER APPLIES FIRST.                                  *
C*  PSIMPR=(REQUIRED AT EXTREMELY HIGH INJECTION LEVELS, OPTIONAL OTHERWISE) *
C*          PARAMETER THAT DETERMINES THE VALUE OF THE FIRST-ORDER TRIAL ELEC- *
C*          TROSTATIC POTENTIAL AT THE INTERFACE BETWEEN THE DEPLETED AND NEU- *
C*          TRAL REGION IN THE LOW-CONDUCTIVITY SIDE.(IF OMITTED, NO CORRECTION *
C*          IS PERFORMED).                                                   *
C*  IWR   = PARAMETER THAT CONTROLS THE PRINTOUT IN THE SUBROUTINE  'PRINT'  *
C*          (SEE SUBROUTINE  'PRINT' )                                       *
C*  INTAPE=PARAMETER THAT CONTROLS THE PROCEDURE OF RECORDING DATA ON MAGNE- *
C*          TIC TAPE  (SEE SUBROUTINE  'TAPE'  )                             *
C*  ISTOP= PARAMETER THAT CONTROLS THE REPETITION OF THE SOLUTION FOR SEVERAL *
C*          SPECIFIED CURRENTS AS FOLLOWS                                    *
C*                ISTOP = 0     THE STRUCTURE AND MATERIAL PARAMETERS ARE NOT *
C*                              CHANGED FOR THE FOLLOWING SPECIFIED CURRENT  *
C*                              (NEW STRUCTURE AND MATERIAL DATA CARDS  1. AND *
C*                              2.  MUST NOT BE INSERTED FOR THE FOLLOWING SPE- *
C*                              CIFIED CURRENT)                              *
C*                ISTOP = 1     LAST SPECIFIED CURRENT OF THE SET            *
C*                ISTOP = 2     THE STRUCTURE AND MATERIAL PARAMETERS ARE CHAN- *
C*                              GED FOR THE FOLLOWING SPECIFIED CURRENT  (NEW *
C*                              STRUCTURE AND MATERIAL DATA CARDS  1.  AND  2. *
C*                              MUST BE INSERTED FOR THE FOLLOWING SPECIFIED *
C*                              CURRENT)                                     *
C*                                                                           *
C*  DATA CARD   4. PARAMETERS CONCERNING THE AUTOMATIC STEP SELECTION PROCE- *
C*                 DURE, INCLUDING THE TOTAL NUMBER OF POINTS DESIRED, ARE   *
C*                 READ IN THE SUBROUTINE  'STPSEL'  (SEE SUBROUTINE 'STPSEL') *
C*                 ONE DATA CARD FOR EACH SPECIFIED CURRENT MUST BE FURNISHED *
C*                 IN THE APPROPRIATE ORDER.                                 *
C*                                                                           *
C*                                                                           *
C*                OUTPUT PARAMETERS ARE                                      *
C*                                                                           *
C*  PSI   = ONE-DIMENSIONAL ARRAY, EXACT POTENTIAL DISTRIBUTION              *
C*  N     = ONE-DIMENSIONAL ARRAY, EXACT ELECTRON DISTRIBUTION               *
C*  P     = ONE-DIMENSIONAL ARRAY, EXACT HOLE DISTRIBUTION                   *
C*  X     = ONE-DIMENSIONAL ARRAY, ABSCISSA OF EACH POINT THROUGHOUT THE JUNC- *
C*          TION                                                             *
C*  STEP  = ONE-DIMENSIONAL ARRAY, NON UNIFORM STEP MAGNITUDE AT EACH POINT  *
C*  JN    = ELECTRON CURRENT                                                 *
C*  JP    = HOLE CURRENT                                                     *
C*  VA    = VOLTAGE AT THE TERMINALS          (NORMALIZED)                   *
C*  VAA   = VOLTAGE AT THE TERMINALS        (UNNORMALIZED)                   *
```

```
C*                                                                          *
C*                  ALLOWANCE FOR  SEVEN DOUBLE PRECISION ARRAYS  (STEP,PSI,  *
C*  N,P,DELTA  +  TWO WORKING ARRAYS IN THE LABELED  COMMON  /WORK/ ) AND      *
C*  ONE SINGLE PRECISION ARRAY  (NIM), ALL OF DIMENSION  1000, HAS BEEN MADE.  *
C*****************************************************************************
      DOUBLE PRECISION STEP(1000),PSI(1000),VA
     $,N(1000),P(1000),DELTA(1000),DUMMY(2000)
     $,             ND,NA,NN,PP,NP,PN,VD,M,L
      REAL NIM(1000),JN,JP,J,JI(10),VAI(11),HI(10),JS
      COMMON /STRC/ ND,NA,NN,PP,NP,PN,VD,M,L,IM,IL,VT,GAMN,GAMP
     $         /MCAR/ N,P,JN,JP
     $         /XST / STEP
     $         /WORK/ DUMMY
     $         /TRDG/ DELTA
     $         /PSNM/ PSI,NIM
     $         /VTIN/ HI,VAI,HMAX,IBR,DELHI,ITV1
10    FORMAT (3E10.0,I10,2E10.0,2I5,5X,I5)
15    FORMAT (1H1,32H FOR A SPECIFIED CURRENT     JS = ,E16.8//7H ERRJ =,
     $E12.3/ 7H FXP  =,F10.5/ 7H ERRPS=, E12.3/ 7H ITMAX=, I4//////)
20    FORMAT (1H1, 32H CURRENT VOLTAGE ITERATION DATA    //////
     $5X,1H1,15X,5HJI(I),20X,6HVAI(I) //  (I6,2E25.8))
30    FORMAT (1H0,////////////////27H SPECIFIED CURRENT     JS = ,E16.8,
     $3X,13H(NORMALIZED)  /  27H EXTERNAL  VOLTAGE     VA = ,D16.8,3X,
     $ 13H(NORMALIZED)    ,30X, 4HVAA=   ,E16.8,3X,7H(VOLTS)    ////
     $ 46H RELATIVE TOLERANCE FOR THE SPECIFIED CURRENT // 20H OBTAINED
     $  ERRJA = ,E12.5, 20X, 20H SPECIFIED   ERRJ = , E12.5//////)
90    FORMAT (1H1,47H ERROR IN THE SIGN OF THE SPECIFIED CURRENT JS  ,
     $E16.8 /32H ONLY POSITIVE CURRENTS ALLOWED  )

C*****************STRUCTURE AND MATERIAL PROPERTIES DEFINITIONS***************
100   CALL STRUCT

C*****************READING OF THE SPECIFIED CURRENT AND CONTROL PARAMETERS     *
C*  FROM DATA CARD    3  ,****************************************************
120   READ (5,10) JS,FXP,ERRJ,ITMAX,ERRPS,PSIMPR,IWR,INTAPE,ISTOP
      WRITE (6,15) JS,ERRJ,FXP,ERRPS,ITMAX
      IF (JS.LE.0.)WRITE (6,90) JS
      ITV=0
      IREAD=1
      IPRINT=1
      IBR=1
      HS=ALOG(JS)
      J=JS
130   CALL VOLTIN (J,VA,HS,ITV)
      IF (ITV.LT.0) GO TO 9999
C*****************************************************************************
C*                    BASIC PROGRAM FOR THE DIRECT PROBLEM                    *
C*****************************************************************************
      KW=1
      CALL FSTORD (VA,FXP,KW,PSIMPR)
      IF (KW.LT.0) GO TO 9999
      IF (ITV.GT.3) GO TO 150
      CALL STPSEL (JRET,IREAD,IPRINT)
      IF (JRET.EQ.1) GO TO 9999
      CALL DOPING (NIM)
150   CALL PSITRL (PSI,VA)
      DELTAM=1.E20
      ITER=0
170   CALL MOBCAR (PSI,VA)
      IF (ITER.EQ.ITMAX.OR. DELTAM.LE.ERRPS ) GO TO 300
      CALL POISSN (DELTAM,IL)
      ITER=ITER+1
      GO TO 170
300   CONTINUE
      J=JN+JP
      IF (ITV.EQ.0) GO TO 400
      IREAD=0
      IPRINT=0
C*****************ACCURACY TEST ***********************************************
      IF (ABS((JS-J)/JS).GT.ERRJ) GO TO 130

C*****************DISPLAYING AND RECORDING RESULTS*****************************
400   ERRJA=(JS-J)/JS
      DO 410 I=1,ITV1
      VAI(I)=VT*VAI(I)
410   JI(I)= EXP(HI(I))
      VAA=VA*VT
      ITV=ITV1+1
      VAI(ITV)=VAA
      JI(ITV)=J
      WRITE (6,20) (I,JI(I),VAI(I),I=1,ITV)
      WRITE (6,30) JS,VA,VAA,ERRJA,ERRJ
      CALL FSTORD (VA,FXP, 1,PSIMPR)
      CALL FSTORD (VA,FXP, 2,PSIMPR)
      CALL PRINT (IWR,ITER,VA,DELTAM,ERRPS)
      CALL PUNCH (VA,DELTAM,FXP,ITER)
      CALL PLOT (VA,IL)
      CALL TAPE (VA,DELTAM,ITER,IDTP,INTAPE)
9999  IF (ISTOP.EQ.2) GO TO 100
      IF (ISTOP.EQ.0) GO TO 120
      CALL TAPE (VA,DELTAM,ITER,  0,  4)
      STOP
      END


**********************   DECKS    'S01'  TO  'S15'    **********************


$IBFTC S16R    DECK
      SUBROUTINE VOLTIN (J,VA,HS,ITV)
C*****************************************************************************
C*                  THE SUBROUTINE  'VOLTIN'  COMPUTES THE VOLTAGE AT THE EX-  *
C*  TERNAL CONTACTS APPROXIMATELY CORRESPONDING TO A SPECIFIED TOTAL CURRENT  *
C*  THROUGH THE JUNCTION.    SUCCESSIVE APPLICATIONS OF THIS ROUTINE LEAD TO  *
C*  THE EXACT VALUE OF VOLTAGE AT THE TERMINALS FOR THE SPECIFIED CURRENT.    *
C*                                                                            *
C*                  THIS ROUTINE USES A LAGRANGIAN INTERPOLATION SCHEME ON THE *
C*  FUNCTION  'VOLTAGE VERSUS LOGARITHM OF CURRENT'  ,AFTER HAVING SURROUNDED *
C*  THE VALUE OF SPECIFIED CURRENT BY TWO VALUES OF CURRENT, OBTAINED THROUGH *
C*  ESTIMATION OF THE CORRESPONDING VOLTAGES WITH THE AID OF THE FIRST ORDER  *
C*  THEORY FOR AN ABRUPT JUNCTION.                                            *
C*  THE BASIC PROGRAM FOR THE DIRECT PROBLEM IS USED TO COMPUTE THE EXACT CUR- *
C*  RENTS CORRESPONDING TO THE VOLTAGES OBTAINED EITHER BY ESTIMATION OR BY   *
C*  INTERPOLATION.                                                            *
C*  THIS ROUTINE IS RESTRICTED TO POSITIVE CURRENTS ONLY.                     *
C*                                                                            *
C*                  SUBPROGRAMS NEEDED ARE                                    *
C*                            SUBROUTINE  'FSTORD'                            *
C*                            SUBROUTINE  'SLAGR'                             *
C*                                                                            *
```

```
C*                  INPUT PARAMETERS ARE                                     *
C*  HS    = NATURAL LOGARITHM OF THE SPECIFIED CURRENT                       *
C*  HI    = ONE-DIMENSIONAL ARRAY, VARIABLE REPRESENTING THE NATURAL LOGARITHM *
C*          OF THE CURRENT ON THE EXACT CURRENT - VOLTAGE CHARACTERISTIC     *
C*  VAI   = ONE-DIMENSIONAL ARRAY, VARIABLE REPRESENTING THE VOLTAGE AT THE  *
C*          TERMINALS ON THE EXACT CURRENT - VOLTAGE CHARACTERISTIC          *
C*  J     = EXACT CURRENT COMPUTED WITH THE BASIC PROGRAM FOR THE DIRECT PROB- *
C*          LEM  CORRESPONDING TO THE VOLTAGE OBTAINED BY THE PREVIOUS CALL  *
C*          OF THIS ROUTINE                                                  *
C*  ITV   = ITERATION TALLY.    MUST BE SET TO ZERO BEFORE THE FIRST CALL OF *
C*          THIS ROUTINE.   THE MAXIMUM ALLOWED VALUE IS      ITV = 10  .    *
C*                                                                           *
C*                  OUTPUT PARAMETERS ARE                                    *
C*  VA    = VOLTAGE AT THE TERMINALS                                         *
C*  ITV   = ITERATION TALLY.    AS AN OUTPUT PARAMETER  IT ALSO REPRESENTS AN *
C*          INDEX  OF PERFORMANCE OF THIS ROUTINE,  AS FOLLOWS               *
C*                    ITV  .GT.  ZERO   GOOD PERFORMANCE OF THE ROUTINE      *
C*                    ITV  .EQ.  ZERO   THE SPECIFIED TOLERANCE ON THE SPECIFIED *
C*                                      CURRENT  HS  HAS NOT BEEN REACHED.   *
C*                                      PRINTOUT OF AN ERROR MESSAGE INDICATES *
C*                                      THE CAUSE.  THE BEST SOLUTION OBTAINED *
C*                                      IS FURNISHED.                        *
C*                    ITV  .LT.  ZERO   EXECUTION OF THE ROUTINE IS ABORTED. *
C*                                      PRINTOUT OF AN ERROR MESSAGE INDICATES *
C*                                      THE CAUSE.  NO SOLUTION IS FURNISHED. *
C****************************************************************************
      DIMENSION VAI(11),VAFSO(20),HFSO(20),HI(10),DUMMY(6)
      DOUBLE PRECISION VA
     $,               ND,NA,NN,PP,NP,PN,VD,M,L
      REAL JNFSOR,J
      COMMON /FSO / DUMMY,JNFSOR
     $       /SIRC/ ND,NA,NN,PP,NP,PN,VD,M,L,IM,IL,VT,GAMN,GAMP
     $       /VTIN/ HI,VAI,HMAX,IBR,DELHI,ITV1
      ITV=ITV+1
      ITV1=ITV-1
      H=ALOG(J)
      IF (ITV.NE.1) HI(ITV1)=H
      GO TO (120,10,200),IBR
10    IF (ITV.LT.3) GO TO 20
15    IF ((HI(ITV1).GE.HS.AND.HI(ITV-2).LE.HS).OR.
     $    (HI(ITV1).LE.HS.AND.HI(ITV-2).GE.HS) )  GO TO 190
20    IF (ITV.GT.6) GO TO 920
      H=(HS-HI(1))*FLOAT(ITV)+HS
      IF (H.GT.HMAX) H=HMAX

C******************FIRST-ORDER  THEORY ESTIMATION OF THE VOLTAGE AT THE TER-   *
C*  MINALS FOR A GIVEN CURRENT  J=EXP(H).    A SUCCESSIVE APPROXIMATION SCHEME *
C*  IS USED TO SOLVE THE RELEVANT IMPLICIT RELATIONS. *************************
120   IBR=2
      R=1.
      VAMAX=1.98*(VD-DLOG(PP))
      KL=1
      VAFSO(1)=0.
      HFSO(1)=-1.E 37
      VAFSO(2)=VAMAX
      DO 150 K=2,20
      VA=VAFSO(K)
      CALL FSTORD (VA,1.,3,0.)
      HFSO(K)=ALOG(JNFSOR)
      IF (K.GT.2) GO TO 122
      IF (HS.GT.HFSO(2)) GO TO 900
122   IF(ABS((HFSO(K)-H)/H).LT.1.E-6) GO TO 155
      R=R+R
      IF (HFSO(K).LT.H) GO TO 125
      VAFSO(K+1)=VAFSO(K)-VAMAX/R
      KU=K
      GO TO 135
125   VAFSO(K+1)=VAFSO(K)+VAMAX/R
      KL=K
135   IF (K.GT.6) VAFSO (K+1)=(H-HFSO(KL))* (VAFSO(KU)-VAFSO(KL))/(HFSO
     $ (KU)-HFSO(KL))+VAFSO(KL)
150   CONTINUE
155   HMAX=HFSO(2)
      GO TO 400
190   IBR=3
C*******************TEST ON THE PERFORMANCE OF THIS ROUTINE. *******************
200   IF (ITV.LT.5) GO TO 230
      IF (ABS(HI(ITV1)-HS).LT.DELHI) GO TO 220
      VA=VAI(ITV-2)
      J=EXP(HI(ITV-2))
      WRITE (6,960)
210   ITV=0
      RETURN
220   IF (ITV.LE.11) GO TO 230
      WRITE (6,950)
      GO TO 210

C*****************EXECUTE LAGRANGIAN INTERPOLATION ****************************
230   DELHI=ABS (HI(ITV1)-HS)
      CALL SLAGR (HI,VAI,HS,ITV1,VASP)
      VA=VASP
400   VAI(ITV)=VA
      RETURN
C*****************PRINTOUT OF ERROR MESSAGES **********************************
900   WRITE (6,910)
910    FORMAT (1H0,//////28H ERROR IN SUBROUTINE VOLTIN  /
     $86H THE SPECIFIED CURRENT JS EXCEEDS THE MAXIMUM VALUE ALLOWED BY
     $THE FIRST-ORDER THEORY./
     $122H IF A HIGHER VALUE OF CURRENT IS SPECIFIED, THE FIRST-ORDER TH
     $EORY ESTIMATION IN THE SUBROUTINE  'VOLTIN' MUST BE MODIFIED/
     $22H NO SOLUTION IS GIVEN    )
915    ITV=-10
       RETURN
920    WRITE (6,930)
930    FORMAT (1H0,//////28H ERROR IN SUBROUTINE VOLTIN  /
     $86H THE CONDITION OF STATEMENT 15 IS NOT REACHED WITHIN THE ALLOWE
     $D NUMBER OF ITERATIONS        /
     $22H NO SOLUTION IS GIVEN    )
       GO TO 915
950    FORMAT (1H0,//////28H ERROR IN SUBROUTINE VOLTIN  /
     $96H THE SPECIFIED TOLERANCE PARAMETER HAS NOT BEEN REACHED WITHIN
     $THE ALLOWED NUMBER OF ITERATIONS  /
     $36H THE BEST SOLUTION ACHIEVED IS GIVEN    )
960    FORMAT (1H0,//////28H ERROR IN SUBROUTINE VOLTIN  /
     $73H AN ILL-CONDITIONED MATRIX PREVENTS ANY FURTHER REFINING OF THE
     $ SOLUTION    /
     $36H THE BEST SOLUTION ACHIEVED IS GIVEN    )
       END


************************   DECKS   'SP1'  TO  'SP5'   ************************
```

APPENDIX F

ON THE NUMERICAL SOLUTION OF SECOND ORDER PARTIAL DIFFERENTIAL EQUATIONS OF THE PARABOLIC TYPE.

Terminology, definitions, basic concepts and criteria available from the theory of numerical analysis, concerning the selection of a "sound" discretization scheme for the numerical solution of second-order partial differential equations of the parabolic type, are briefly summarized and references are given.

F-1. Generalities.

A partial differential equation of the second order, linear in the second partial derivatives, in two independent variables x and t, may be written as:

$$A \frac{\partial^2 Y(x,t)}{\partial x^2} + 2B \frac{\partial^2 Y(x,t)}{\partial x \, \partial t} + C \frac{\partial^2 Y(x,t)}{\partial t^2} = \text{known function } f\left(\frac{\partial Y}{\partial x}, \frac{\partial Y}{\partial t}, Y, x, t\right)$$

where A, B and C are known coefficients and $Y(x,t)$ is the unknown function. The equation is called parabolic if $B^2 = AC$. The present interest is for the case $B = C = 0$, in which the parabolic equation may be written in the form:

$$\frac{\partial Y(x,t)}{\partial t} = f\left(\frac{\partial^2 Y}{\partial x^2}, \frac{\partial Y}{\partial x}, Y, x, t\right) \qquad \text{(F-1)}$$

If Eq.(F-1) is taken to represent a physical phenomenon, x represents usually the position coordinate and t the time coordinate.

A typical physical initial value problem specifies boundary

conditions of the open type, i.e. it assigns the function $Y(x,t)$ on an open rectangle defined by

$$\left.\begin{array}{ll} x = x_1 , & \text{any } t \geq 0 \\ x = x_2 , & \text{any } t \geq 0 \\ t = 0 , & x_1 \leq x \leq x_2 \end{array}\right\} \qquad \text{(F-2)}$$

where x_1 and x_2 are two spatial boundaries determining the range of interest of the position coordinate x, and $t = 0$ is taken as the initial time. The known distribution $Y(x,0)$ is then also referred to as the initial condition of the problem. Other types of boundary conditions may be specified, but only the above is here of interest.

The distributions $Y(x,t)$, for $x_1 < x \leq x_2$ and $t \geq 0$, satisfying both Eq.(F-1) and the boundary conditions (F-2), are sought. Two conceptually different techniques may be used to approach the numerical solution of the problem:

(a) the spatial derivatives of Eq.(F-1) are approximated by finite difference schemes to obtain a system of ordinary differential equations, solved numerically by conventional methods;

(b) both spatial and time derivatives are approximated by finite difference schemes to reduce the problem to the solution of a system of algebraic equations.

The former method is particularly suitable for linear partial differential equations [Ref. 29, p. 241], whereas the latter is equally well applicable to more general cases. Also in consideration of the present interest for systems of non-linear partial differential

equations, the attention will be focused on the above technique (b).

A grid or mesh is obtained by discretizing the originally continuous spatial line ($x_1 \le x \le x_2$, constant t) and time line ($t \ge 0$, constant x) in a finite number of points. The distance between consecutive spatial points and time points is referred to as spatial step Δx and time step Δt respectively. Constant (non-constant) values of Δx and Δt throughout the mesh generate a uniform (non-uniform) mesh.

Examples of finite difference formulae are available in Appendix B for the case of non-uniform mesh, and, for instance, in Ref. 30 (p.284) for the simpler case of uniform mesh.

A two-level (multilevel) finite difference scheme is obtained, if a two (three or more)-point finite difference formula is used to approximate the time derivative of Eq.(F-1) at a given point.

An explicit (or implicit) finite difference scheme is obtained depending upon the capability (or lack of capability) of every single algebraic equation, generated by the discretization of Eq.(F-1) at one time point, to yield, independently of the other equations, the value of $Y(x,t)$ at the following time point. The implicit scheme requires in general the solution of a system of simultaneous algebraic equations.

The following nomenclature is adopted:

$D \triangleq$ exact solution of the partial differential equation (F-1)

$\Delta \triangleq$ exact solution of the partial difference equations generated by Eq.(F-1)

$N \triangleq$ numerical solution (actually achieved) of the partial difference equations

<u>discretization error</u> $\triangleq D - \Delta$

<u>numerical error</u> $\triangleq \Delta - N$

The finite distance of the mesh points is responsible for the discretization error. This is often referred to as <u>truncation error</u> since it usually arises from the truncation of a Taylor expansion of the function $Y(x,t)$ at a given point, in the stage of generating finite difference equations. The numerical error is occasionally referred to as <u>round-off</u> error, although this is in general only one of the contributions to the numerical error.

The problem of <u>convergence</u> deals with the conditions under which $\Delta \to D$ for Δx, $\Delta t \to 0$. The problem of numerical <u>stability</u> deals with the conditions under which $(\Delta - N)$ is small throughout the entire region of solution (Ref. 31, p.223).

The knowledge of the conditions of convergence and stability of a particular discretization scheme is a problem of fundamental nature in the numerical solution of partial differential equations of the parabolic type. Attention to this topic is given in the following sections.

<u>F-2. On convergence and stability theories</u>.

The basic concepts of convergence and stability have been described for the first time in Ref. 31 (p.223), based on previous results obtained by Von Neumann regarding a general method to test stability, easily applicable to linear equations with constant coefficients, with possibility of extension to the more general case, in some instances. Von Neumann's method is based on the assumption

that weak* stability (instability) implies strong* stability (instability), and uses a Fourier expansion of a line of error.

A close relationship between convergence and stability is proved in Ref. 32, and it is shown that one implies the other if certain conditions on the original differential equation are satisfied. The evaluation of the convergence is in these cases achieved by examining the behavior of an "amplification factor" (or amplification matrix in the more general case), obtained with the aid of a Fourier expansion of $Y(x,t)$. The theory is limited to linear equations and reduces, in the simplest cases, the analysis of the error to the test on the discretization error, expressed in terms of Δx and Δt. These results are also available in Ref. 20 (pp. 38-73), and the highlights are gathered in Ref. 33 (p. 69). A slightly different approach, based on vector and matrix operators, is given in Ref. 34 (p. 222), and summarized in Ref. 29 (p. 222). A more concise treatment of the above theory is presented in a modern form in Ref. 35 (p. 103).

A different definition of stability, requiring a growth of the numerical error $(\Delta - N)$ not faster than some power of the reciprocals of the step lengths, is presented in Ref. 36 (p. 95). Although different stability criteria are obtained, it may be shown that this definition of stability is closely related to the previous ones.

Ref. 36 (p. 92) and Ref. 32 (p. 13), among others, describe a very elementary method (based on the extreme value principle) to prove

---

* Weak or strong stability (or instability) refers to the effect of a single error introduced at one point of the solution or of the overall error, respectively.

convergence, applicable solely to a limited number of simple cases.

Convergence and stability conditions for specific equations and discretization schemes, resulting from the available theory, are summarized in the following Section.

F-3. Analysis of specific equations and discretization schemes.

F-3.1. Linear equations.

F-3.1.1. Linear equations with constant coefficients.

(a) The heat equation

$$\frac{\partial Y(x,t)}{\partial t} = \sigma \frac{\partial^2 Y(x,t)}{\partial x^2} \quad , \qquad \sigma = \text{constant} > 0 \tag{F-3}$$

is the simplest linear parabolic equation and is treated by most authors [Ref. 29 to 33 and 36]. Ref. 20 (p. 91) gives a collection of finite difference equations approximating Eq.(F-3). Convergence and stability problems are analyzed and the truncation error is given. A few examples are reported below. The following notation is used:

$i \triangleq$ spatial index $(i = 1, 2, 3, \cdots)$

$k \triangleq$ time index $(k = 0, 1, 2, 3, \cdots)$

${}_kY_i \triangleq Y(x_i, {}_kt)$

${}_k(\delta^2 Y)_i \triangleq {}_kY_{i+1} - 2\,{}_kY_i + {}_kY_{i-1}$

$\varepsilon_t \triangleq$ truncation error

In addition, a diagram of the type

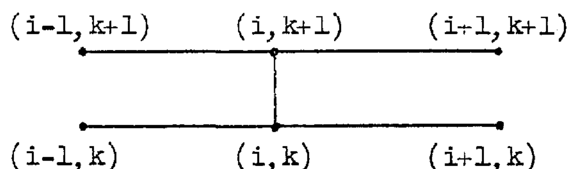

is used to indicate the number and the position of the mesh points involved in each finite difference equation. For conciseness, the indexes identifying the points will be omitted.

1. Explicit:

$$\frac{{}_{k+1}Y_i - {}_kY_i}{\Delta t} = \sigma \frac{{}_k(\delta^2 Y)_i}{(\Delta x)^2}$$

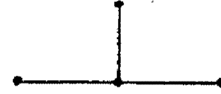

$$\varepsilon_t = O(\Delta t) + O[(\Delta x)^2]$$

Stable if $\frac{\sigma \Delta t}{(\Delta x)^2} = \text{constant} \leq \frac{1}{2}$ as Δt, $\Delta x \rightarrow 0$.

2. Crank-Nicholson (implicit):

$$\frac{{}_{k+1}Y_i - {}_kY_i}{\Delta t} = \sigma \frac{{}_k(\delta^2 Y)_i + {}_{k+1}(\delta^2 Y)_i}{2(\Delta x)^2}$$

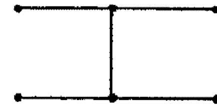

$$\varepsilon_t = O[(\Delta t)^2] + O[(\Delta x)^2]$$

Unconditionally stable.

3. Pure implicit:

$$\frac{{}_{k+1}Y_i - {}_kY_i}{\Delta t} = \sigma \frac{{}_{k+1}(\delta^2 Y)_i}{(\Delta x)^2}$$

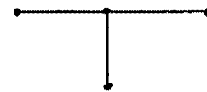

$$\varepsilon_t = O(\Delta t) + O[(\Delta x)^2]$$

Unconditionally stable.

4. Richardson:

$$\frac{{}_{k+1}Y_i - {}_{k-1}Y_i}{2\Delta t} = \sigma \frac{{}_k(\delta^2 Y)_i}{(\Delta x)^2}$$

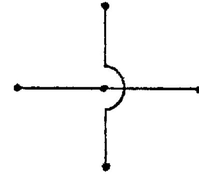

Unconditionally unstable.

5. Du Fort-Frankel (explicit):

$$\frac{{}_{k+1}Y_i - {}_{k-1}Y_i}{2\Delta t} = \sigma \frac{{}_kY_{i+1} - {}_{k+1}Y_i - {}_{k-1}Y_i + {}_kY_{i-1}}{(\Delta x)^2}$$

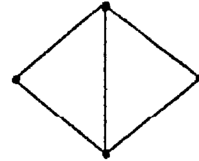

with $\frac{\Delta t}{\Delta x} \to 0$ as Δx, $\Delta t \to 0$

$$\varepsilon_t = O(\Delta t) + O[(\Delta x)^2] + O\left(\frac{\Delta t}{\Delta x}\right)$$

Unconditionally stable.

6. A three-level implicit scheme:

$$(1+\theta)\frac{{}_{k+1}Y_i - {}_kY_i}{\Delta t} - \theta \frac{{}_kY_i - {}_{k-1}Y_i}{\Delta t} = \sigma \frac{{}_{k+1}(\delta Y)_i}{(\Delta x)^2}$$

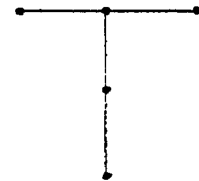

where θ = constant > 0, $\sigma\Delta t/(\Delta x)^2$ = constant

$$\varepsilon_t = O(\Delta t) + O[(\Delta x)^2]$$

Unconditionally stable.

The value $\theta = 0$ generates the two-level implicit scheme 3.

It may be observed that unconditional stability is featured by two-level formulae solely of the implicit type, whereas explicit schemes unconditionally stable are available if a three-level formula is used.

(b) The complete second-order linear equation with constant coefficients

$$\frac{\partial Y(x,t)}{\partial t} = \sigma \frac{\partial^2 Y(x,t)}{\partial x^2} + a \frac{\partial Y(x,t)}{\partial x} + b\ Y(x,t) \quad ,$$

$$\sigma = \text{constant} > 0 \qquad \text{(F-4)}$$

is analyzed in Ref.20[p.98], which shows that stability conditions are not dependent upon the lower order terms, so that the same schemes described in (a) for the heat equation (F-3) are applicable to Eq. (F-4), with a straight forward modification to incorporate the lower order terms in the finite difference equation.

The use of implicit methods leads to the solution of a system of simultaneous finite difference algebraic equations, which may be reduced to the solution of a tridiagonal matrix equation. Since the entries of the tridiagonal matrix are time independent (a consequence of the assumed constancy of the coefficients of Eqs.(F-3) and (F-4)) only one inversion of the matrix during an entire solution is necessary.

3.1.2. Linear equations with non-constant coefficients.

(a) The simplest linear equation with non-constant coefficients

$$\frac{\partial Y(x,t)}{\partial t} = \sigma(x) \frac{\partial^2 Y(x,t)}{\partial x^2} \quad , \quad \sigma(x) > 0 \qquad \text{(F-5)}$$

is analyzed in Ref. 36 (p.107), 20 (p.96), and conclusions are summarized in Ref. 33 (p.74).

It may be shown that discretization schemes of the type

$$\frac{{}_{k+1}Y_i - {}_kY_i}{\Delta t} = \sigma(x_i)\frac{\theta\left[{}_{k+1}(\delta^2 Y)_i\right] + (1-\theta)\left[{}_k(\delta^2 Y)_i\right]}{(\Delta x)^2}, \quad \theta = \text{constant} > 0 \quad \text{(F-6)}$$

are unconditionally stable and convergent for $\frac{1}{2} \le \theta \le 1$, whereas for $0 \le \theta < \frac{1}{2}$ they are stable and convergent if

$$2(1-2\theta)\ \sigma(x)\ \frac{\Delta t}{(\Delta x)^2} \le 1$$

(b) The more general equation (Ref. 20, p. 97)

$$\frac{\partial Y(x,t)}{\partial t} = \mu(x)\ \frac{\partial}{\partial x}\left[\nu(x)\ \frac{\partial Y(x,t)}{\partial x}\right] \quad \text{(F-7)}$$

with $\mu(x)$ and $\nu(x)$ positive and known functions, may be reduced to Eq.(F-5) with the change of variable

$$y(x,t) = \int \frac{1}{\nu(x)}\, dx$$

and therefore may be similarly treated.

An interesting example of numerical computation for this case is shown in Ref. 33 (p.80), including the program in ALGOL. An implicit method of solution is described in Ref. 20 (p.101), with an efficient method of solving a tridiagonal matrix equation.

(c) The complete equation

$$\frac{\partial Y(x,t)}{\partial t} = \sigma(x,t)\ \frac{\partial^2 Y(x,t)}{\partial x^2} + a(x,t)\ \frac{\partial Y(x,t)}{\partial x} + b(x,t)Y(x,t) + c(x,t) \quad \text{(F-8)}$$

with σ, a, b, c known functions, is treated in Ref. 36 (p.107) and Ref. 29 (p.245), among others. For finite difference schemes of the explicit type it is shown that stability (and convergence under certain conditions) is satisfied if

$$\sigma(x,t) > 0 \quad \text{and} \quad 2\,\sigma(x,t)\,\frac{\Delta t}{(\Delta x)^2} < 1$$

For implicit schemes, conditions of stability are not available, with exception of the case of time independent coefficients σ, a, b, c. Stability conditions may then be analyzed with matrix methods. Ref. 29 (p.246) investigates this case, for various types of boundary conditions.

F-3.2. Non-linear equations.

F-3.2.1. Quasi-linear equations.

The quasi-linear partial differential equations represent a particular class of non-linear equations that are linear in the highest derivative of the unknown function $Y(x,t)$.

(a) The simplest type of quasi-linear equation is the semi-linear equation, which is linear in all the derivatives of $Y(x,t)$:

$$\frac{\partial Y(x,t)}{\partial t} = \sigma(x,t)\,\frac{\partial^2 Y(x,t)}{\partial x^2} + a(x,t)\,\frac{\partial Y(x,t)}{\partial x} + b(x,t,Y)\,, \quad \sigma(x,t) > 0 \qquad \text{(F-9)}$$

Under certain restrictions on the known functions σ, a, b, existence, convergence and stability conditions have been investigated in Ref. 37 (p.155) for explicit discretization schemes. For the simplest

explicit scheme, of the type (a)1 described in Subsection 3.1.1, stability is conditioned to the inequality

$$\text{l.u.b.} \quad \sigma(x,t)\,\frac{\Delta t}{(\Delta x)^2} < \frac{1}{2} \qquad \text{(F-10)}$$

This result is consistent with the intuitive extrapolation of the constant coefficients case. Conclusions are also summarized in Ref. 20 (p.109) and Ref. 36 (p.137).

(b) A rather extensive analysis of the more general quasi-linear equation

$$\frac{\partial}{\partial x}\left[p(x,t)\,\frac{\partial Y(x,t)}{\partial x}\right] - q(x,t,Y) = r(x,t,Y)\,\frac{\partial Y}{\partial t} \qquad \text{(F-11)}$$

is given in Ref. 38 (p.484) with proofs of convergence for several explicit and implicit finite difference schemes, under certain conditions on the known functions p, q, r of Eq.(F-11).

An iterative procedure of solution is usually required at each time step to cope with the non-linearities, although special schemes (Ref. 39, p.167) may occasionally be used, based on the solution of tridiagonal matrix equations, to avoid the iterative procedure.

F-3.2.2. Non-linear equations of the general type.

The general non-linear parabolic equation

$$\frac{\partial^2 Y(x,t)}{\partial x^2} = F\left[\frac{\partial Y(x,t)}{\partial t},\ \frac{\partial Y(x,t)}{\partial x},\ Y(x,t),\ x, t\right] \qquad \text{(F-12)}$$

is considered in Ref. 39 (p.167). Convergence is proved under certain conditions of regularity of the coefficients, and the discretization error for a special implicit difference scheme is given. In addition, an example of an iterative procedure is presented and its convergence to the exact solution is proved. Conclusions are also summarized in Ref. 33 (p.98). Remarks of general nature are available in Ref. 36 (p.139) and Ref. 29 (p.249).

A few examples of particular non-linear equations available in the literature are listed below. The equation

$$\frac{\partial Y(x,t)}{\partial t} = \frac{\partial^2}{\partial x^2} [Y(x,t)]^5 \qquad \text{(F-13)}$$

is investigated in Ref. 20 (p.104). A numerical computation is given for a particular difference scheme, together with stability considerations. For the more general equation

$$\frac{\partial Y(x,t)}{\partial t} = \frac{\partial^2}{\partial x^2} [Y(x,t)]^n \qquad \text{(F-14)}$$

an explicit scheme is analyzed in Ref. 29 (p.250), and stability is proved for

$$n \frac{\Delta t}{(\Delta x)^2} [Y(x,t)]^{n-1} \leq \frac{1}{2}$$

Ref. 36 (p.141) gives only suggestions for linearizing the finite difference equations generated by the equation

$$\frac{\partial Y(x,t)}{\partial t} = \sigma \frac{\partial^2 Y(x,t)}{\partial x^2} - \frac{1}{2}\left[\frac{\partial Y(x,t)}{\partial x}\right]^2 + a(x,t) \quad , \quad \sigma = \text{constant} > 0 \tag{F-15}$$

where $a(x,t)$ is a periodic function of x. Stability or convergence considerations are not given. Some attention to the system

$$\begin{cases} \dfrac{\partial Y(x,t)}{\partial t} = \dfrac{\partial^2 Y(x,t)}{\partial x^2} - q\dfrac{\partial Z(x,t)}{\partial t} \\[2ex] \dfrac{\partial Z(x,t)}{\partial t} = - cZ(x,t)\ \exp[- A/Y(x,t)] \quad , \end{cases} \tag{F-16}$$

where q, c, A are constants > 0, is given in Ref. 29 (p.250) and Ref. 36 (p.141) for specific boundary conditions. Only considerations on truncation errors are presented for various methods of solutions.

F-3.3. Conclusion.

A few basic concepts and results of the numerical analysis theory concerning convergence and stability problems for various discretization schemes generated by partial differential equations of the parabolic type have been summarized, and references cited. Whereas the theory is complete for the case of linear equations with constant coefficients, it is rather incomplete for the non-constant coefficient case, and only fragmentary conclusions are available for the non-linear case. The problem of convergence and stability is of fundamental importance, since both features represent a prime requirement for the success of numerical solutions of equations of the parabolic type.

APPENDIX G

COMPUTER PROGRAM FOR THE TRANSIENT PROBLEM

In this Appendix the computer program (in FORTRAN IV, version 4) for the current-driven and voltage-driven transients is reported. The method of solution and the mathematical formulation are described in Chapters VII to IX, and illustrated in Figs. 8.3 and 9.3. The generalized pure implicit discretization scheme has been selected.

The program consists of a main program (deck 'PNT') and a set of subprograms (deck 'T01' to 'T10') each performing logically different operations of the algorithm. This modular organization of the program has the same motivations outlined in Appendix C.

Double precision arithmetic has been mostly used. The size of the vectors and matrices has been chosen according to the memory size of the machine available (32,000 locations). A magnetic "save" tape is required for permanent storage of the initial conditions and of the solutions at each instant of time.

Main program.

Deck 'PNT'. The main program reads the control parameters from a set of DATA cards, and the initial conditions from a magnetic save tape; drives the subprograms actually performing the required calculations and records on peripheral equipment solutions and parameters of interest.

Subroutine 'TAPE'.

Deck 'T01'. Reads from, and records on, magnetic tape distributions of interest.

File definition subprogram.

Deck 'T02'. (Written in Assembler language IBMAP.) Defines the file for one magnetic save tape needed by the deck 'T01'.

Subroutine 'TPRINT'.

Deck 'T03'. Writes on the printout sheet the results of interest.

Subroutine 'TSTEPK'.

Deck 'T04'. Furnishes the time step at the next instant of time, according to the automatic time step adjustment algorithm described in Section 8.4.

Subroutine 'DIFFEQ'.

Deck 'T05'. Furnishes an improved solution of the system of the non-linear partial differential equations 8.15 to 8.17 from trial distributions of the electric field and mobile carrier densities at each instant of time. The mathematical algorithm is described in Subsection 8.2.1.

Subroutine 'SLCV2'.

Computes the spatial slope and curvature of two functions given in discretized form, at each internal point throughout the interior of the device. Two versions are available. Only one must be inserted in the actual program.

Deck 'T06A'. Three point formulae (parabolic interpolation) are used, according to relations (B-11) and (B-12) (Appendix B).

Deck 'T06B'. Five point formulae (Lagrangian interpolation with fourth-order polynomials) are used, according to the formulation of Subsection B-2.3. The relevant matrices are slightly rearranged in this routine in order to achieve a higher efficiency.

Subroutine 'EQUAD'.

Deck 'T07'. Computes the quadrature of the electric field spatial distribution given in discretized form at unevenly spaced points in the interior of the device. The three-point formula (B-3) (parabolic interpolation) is used.

Subroutine 'TRDU1'.

Deck 'T08'. See Deck 'S15' of Appendix C.

Subroutine 'INTERP'.

Deck 'T09'. Furnishes, at a given time, a value of the total current approximately corresponding to a specified value of terminal voltage during the voltage driven transient procedure, according to the algorithm of Section 9.2.

Subroutine 'SLAGR'.

Deck 'T10'. See Deck 'S05' of Appendix C.

```
$IBFTC PNT     DECK
C***********************************************************************
C*                  M A I N    P R O G R A M                          *
C***********************************************************************
C*                                                                     *
C***********************************************************************
C*                 THIS PROGRAM SOLVES THE BASIC TWO-CARRIER TRANSPORT EQUA-   *
C*  TIONS, GOVERNING THE BEHAVIOR OF SEMICONDUCTOR DEVICES, APPLIED TO AN N-P  *
C*  JUNCTION UNDER THE FOLLOWING ASSUMPTIONS                           *
C*  (A)  NON DEGENERATE CONDITIONS                                     *
C*  (B)  CONSTANT TEMPERATURE                                          *
C*  (C)  TIME INDEPENDENT IMPURITY DISTRIBUTION                        *
C*  (D)  FULL IONIZATION OF THE IMPURITIES                             *
C*  (E)  ONE-DIMENSIONAL STRUCTURE                                     *
C*  (F)  ARBITRARY TRANSIENT CONDITIONS                                *
C*  (G)  OHMIC CONTACTS                                                *
C*  (H)  ABSENCE OF GENERATION-RECOMBINATION IN THE INTERIOR           *
C*  (I)  CONSTANT MOBILITIES                                           *
C*                 GIVEN AN APPLIED EXTERNAL EXCITATION OF EITHER CURRENT OR   *
C*  VOLTAGE AS A FUNCTION OF TIME, THE RESPONSE OF THE DEVICE AND THE RELE-    *
C*  VANT INTERNAL DISTRIBUTIONS AS FUNCTIONS OF POSITION AND TIME ARE OBTAINED.*
C*  NO APPROXIMATIONS IN THE SET OF EQUATIONS HAVE BEEN INTRODUCED.    *
C*  THE  N-REGION IS ASSUMED LOCATED ON THE LEFT SIDE OF THE METALLURGICAL     *
C*  INTERFACE  N.                                                      *
C*                                                                     *
C*                 THIS PROGRAM USES AN ITERATIVE SCHEME AT EACH INSTANT OF    *
C*  TIME FOR THE SOLUTION OF A SYSTEM OF THREE NON-LINEAR PARTIAL DIFFEREN-    *
C*  TIAL EQUATIONS IN THREE UNKNOWNS.   THE GENERALIZED PURE IMPLICIT SCHEME   *
C*  IS CHOSEN FOR THE DISCRETIZATION OF THE TWO PARABOLIC EQUATIONS.    A SET  *
C*  OF INITIAL DISTRIBUTIONS FOR THE UNKNOWNS IS REQUIRED.             *
C*  THE WHOLE PROGRAM IS BUILT IN A HIGHLY MODULAR FASHION, FEATURING A MAIN   *
C*  PROGRAM CALLING SEVERAL SUBPROGRAMS, IN FAVOR OF  A GREATER FLEXIBILITY    *
C*  AND SIMPLICITY OF LOGIC ORGANIZATION.                              *
C*  SUBPROGRAMS EXPLICITLY CALLED BY THIS MAIN PROGRAM ARE             *
C*                 SUBROUTINE  'TAPE'     (READS FROM AND RECORDS ON MAGNETIC  *
C*                                         TAPE THE RELEVANT QUANTITIES)      *
C*                 SUBROUTINE  'TPRINT'   (WRITES OUTPUT DATA ON PRINTOUT     *
C*                                         SHEET)                              *
C*                 SUBROUTINE  'TSTEPK'   (DETERMINES THE TIME STEP AT EACH   *
C*                                         INSTANT OF TIME)                    *
C*                 SUBROUTINE  'DIFFEQ'   (FURNISHES AN IMPROVED SOLUTION BY  *
C*                                         SOLVING THE SYSTEM OF DIFFERENTIAL *
C*                                         EQUATIONS FROM A TRIAL SOLUTION)    *
C*                 SUBROUTINE  'INTERP'   (EXECUTES A LINEAR INTERPOLATION ON *
C*                                         THE  I-V  CHARACTERISTIC FOR THE   *
C*                                         VOLTAGE-DRIVEN TRANSIENT)           *
C*  OTHER SUBPROGRAMS MAY BE CALLED BY THE ABOVE SUBROUTINES.          *
C*  DOUBLE PRECISION ARITHMETIC IS USED.                               *
C*                                                                     *
C*                                                                     *
C*                 INPUT PARAMETERS ARE                                *
C*  DATA CARD   1.                                                     *
C*  TSTEP1= MAGNITUDE OF THE INITIAL TIME STEP                         *
C*  TIMEX = INSTANT OF TIME AT WHICH THE TIME STEP IS CHANGED TO   TSTEPX      *
C*  TSTEPX= MAGNITUDE OF THE TIME STEP IMMEDIATELY AFTER THE INSTANT OF TIME   *
C*          TIMEX                                                      *
C*  RMAX  = UPPER BOUND FOR THE RATIO OF CONSECUTIVE TIME STEPS        *
C*  TSTMAX= UPPER BOUND FOR THE TIME STEP                              *
C*  TSTMIN= LOWER BOUND FOR THE TIME STEP                              *
C*  ERRK  = ITERATION RELATIVE ERROR AT EACH INSTANT OF TIME FOR THE TERMI-    *
C*          NAL VOLTAGE                                                *
C*  ERRV  = TOLERANCE ERROR  ON THE TERMINAL VOLTAGE AT EACH INSTANT OF TIME   *
C*          IN A VOLTAGE-DRIVEN TRANSIENT                              *
C*                                                                     *
C*  DATA CARD   2.                                                     *
C*  JITMAX= MAXIMUM NUMBER OF CYCLES IN THE ITERATIVE PROCEDURE AT EACH IN-    *
C*          STANT OF TIME  (MAXIMUM   JITMAX = 100)                    *
C*  KMAX  = INDEX IDENTIFYING THE INSTANT OF TIME AT WHICH THE PROGRAM STOPS   *
C*          (MAXIMUM   KMAX = 200)                                     *
C*  IWR   = PARAMETER THAT CONTROLS THE  PRINTOUT IN THE SUBROUTINE 'TPRINT'   *
C*          (SEE SUBROUTINE 'TPRINT')                                  *
C*  IDTIN = PARAMETER  THAT IDENTIFIES THE POSITION OF THE INITIAL DISTRIBU-   *
C*          TIONS ON THE MAGNETIC TAPE  (SEE SUBROUTINE  'TAPE' )      *
C*  ITAPE = PARAMETER THAT CONTROLS THE PROCEDURE OF RECORDING DATA ON MAGNE-  *
C*          TIC TAPE  (SEE SUBROUTINE  'TAPE')                         *
C*  IPUNCH= PARAMETER THAT CONTROLS THE PROCEDURE OF RECORDING DATA ON PUNCHED *
C*          CARDS AS FOLLOWS                                           *
C*                   IPUNCH.EQ.1  RECORDING ON PUNCHED CARDS OCCURS    *
C*                   IPUNCH.NE.1  RECORDING ON PUNCHED CARDS DOES NOT OCCUR    *
C*  ICURR = PARAMETER THAT SELECTS EITHER THE CURRENT-DRIVEN OR THE VOLTAGE-   *
C*          DRIVEN TRANSIENT PROCEDURE AS FOLLOWS                      *
C*                   ICURR.EQ.1  CURRENT-DRIVEN TRANSIENT              *
C*                   ICURR.NE.1  VOLTAGE-DRIVEN TRANSIENT              *
C*                                                                     *
C*  DATA CARD(S)  3,4,5, ... NN=IFIX((KMAX-1)/8+3) .                   *
C*  J(I),I=1,KMAX = DISCRETIZED EXTERNAL EXCITATION AT THE INSTANTS OF TIME    *
C*                  1  TO  KMAX  INCLUDED                              *
C*                                                                     *
C*  DATA CARD  NN+1.  (ONLY REQUIRED FOR THE VOLTAGE-DRIVEN TRANSIENT).A TRIAL *
C*                    VALUE FOR THE CURRENT IN THE PREDICTION PHASE AT THE     *
C*                    FIRST INSTANT OF TIME IS READ IN THE SUBROUTINE 'INTERP' *
C*  STRUCTURE PARAMETERS AND INITIAL DISTRIBUTIONS  ARE READ FROM MAGNETIC     *
C*  TAPE  (SEE  SUBROUTINE  'TAPE' )                                   *
C*                                                                     *
C*                                                                     *
C*                 OUTPUT PARAMETERS ARE                               *
C*                                                                     *
C*  E   = ONE-DIMENSIONAL ARRAY, EXACT POTENTIAL DISTRIBUTION AT A CERTAIN     *
C*        INSTANT OF TIME                                              *
C*  N   = ONE-DIMENSIONAL ARRAY, EXACT ELECTRON  DISTRIBUTION AT A CERTAIN     *
C*        INSTANT OF TIME                                              *
C*  P   = ONE-DIMENSIONAL ARRAY, EXACT HOLE      DISTRIBUTION AT A CERTAIN     *
C*        INSTANT OF TIME                                              *
C*  VAA (OR   J ) = TERMINAL RESPONSE OF VOLTAGE   (OR  CURRENT )      *
C*  OTHER QUANTITES AS IN SUBROUTINE  'TPRINT'.                        *
C*                                                                     *
C*                 ALLOWANCE FOR TEN DOUBLE PRECISION ARRAYS  ( E,N,P,XSTEP,EK *
C*  + FIVE WORKING ARRAYS IN THE LABELED COMMON  /DWORK/ )  AND TWO SINGLE     *
C*  PRECISON ARRAYS  (DN,DP),ALL OF DIMENSION  810, HAS BEEN MADE.     *
C***********************************************************************
      DOUBLE PRECISION E(810),N(810),P(810),XSTEP(810),EK(810)
     $,ND,NA,VD,VA,DUMMY(4050)
      REAL DN(810),DP(810),J(200),VAA(200),VAAR(200),DELVAA(100)
     $,TIME(200),TSTEP(200)
      COMMON /TSTP/ RMIN,RMAX,  TSTMIN,TSTMAX, ICTST    ,TIME,TSTEP
     $       /EXT / J,VAA
     $       /XST / XSTEP
     $       /TP  / ND,NA,VD,E,N,P,IM,IL,IDI,K,TSTEP1
     $       /TERM/ DELVAA,DVAA,DELVR
     $       /DWORK/ DUMMY, DN,DP
10    FORMAT (8E10.0  /7I10/(8E10.0))
15    FORMAT (6E13.6,2X)
```

```
C******************************************************************************
      GAMP=1./44.
      BGM=93.*GAMP
      ICTST=1
      KRELAX=1
C****************** READING OF THE FIRST   NN= IFIX ((KMAX-1)/8+3)   CARDS     *
      READ(5,10)    TSTEP1,TIMEX,TSTEPX,RMAX,TSTMAX,TSTMIN,ERRK,ERRV
     $,JITMAX,KMAX,IWR,IDTIN,ITAPE,IPUNCH,ICURR
     $, (J(I),I=1,KMAX)
      IF (JITMAX.GT.100) JITMAX=100
      IF (ICURR.EQ.1) GO TO 40
      DO 20 I=1,KMAX
20    VAAR(I)=J(I)
40    IF (IWR.EQ.0) IWR=10
      RMIN=1./RMAX
C****************** READING OF THE STRUCTURE PARAMETERS AND INITIAL DISTRI-   *
C*  BUTIONS FROM A MAGNETIC SAVE TAPE AND WRITING RELEVANT QUANTITIES ON       *
C*  THE PRINTOUT SHEET                                                         *
      CALL TAPE (IDTIN,1)
      CALL TPRINT (IWR,JIT,ICURR,1)
      IL1=IL-1
C*                                                                             *
C****************** INITIATE  K  LOOP                                         *
75    DO 80 I=1,IL
80    EK(I)=E(I)
      IF (TIME(K).LT.TIMEX.OR.KRELAX.NE.1) GO TO 90
      KRELAX=K
      TSTEP1=TSTEPX
90    IF (ICURR.EQ.1) CALL TSTEPK (TSTEP1,K,KRELAX,VAA)
      IF (ICURR.NE.1) CALL TSTEPK (TSTEP1,K,KRELAX,J  )
      GPDT=GAMP/TSTEP1
      GNDT=GPDT/BGM
      K=K+1
      IF (ICURR.EQ.1) GO TO 97
C****************** VOLTAGE-DRIVEN TRANSIENT ONLY                              *
      KT=0
      GO TO 96
92    CONTINUE
      DO 94 I=2,IL1
      N(I)=N(I)-DN(I)
94    P(I)=P(I)-DP(I)
96    CALL INTERP (K,KT,VAA(K),VAAR,J,TIME)
C******************************************************************************
97    DO 98 I=1,IL
      DN(I)=0.
98    DP(I)=0.
      GAMPJ=GAMP*J(K)
      JIT=0
C*                                                                             *
C****************** INITIATE  J  LOOP                                         *
100   JIT=JIT+1
      CALL DIFFEQ(BGM,GPDT,GAMPJ,VAA,VAA1,EK,JIT)
      DELVAA(JIT)=VAA(K)-VAA1
      DVAA=VAA(K)-VAA(K-1)
      DELVR=DELVAA(JIT) /DVAA
      IF (ICURR.NE.1.AND. JIT.LT.JITMAX) GO TO 100
      IF (ABS(DELVR).GT.ERRK.AND.JIT.LT.JITMAX.AND.ICURR.EQ.1) GO TO 100
      IF (ICURR.EQ.1) GO TO 200
      CALL TPRINT (IWR,JIT,ICURR,4)
      IF  ((ABS (VAA(K)-VAAR(K)).GT.ERRV).AND. KT.LT.10) GO TO 92
C*                                                                             *
C****************** RECORDING RELEVANT QUANTITIES AFTER THE TERMINATION OF     *
C*  A  K  LOOP                                                                 *
200   IF (ITAPE.EQ.1) CALL TAPE (0,0)
      CALL TPRINT (IWR,JIT,ICURR,2)
      IF (K.LT.KMAX) GO TO 75
C*                                                                             *
C****************** RECORDING THE EXTERNAL RESPONSE PRIOR THE TERMINATION      *
C*  OF THE PROGRAM                                                             *
      CALL TPRINT (IWR,JIT,ICURR,3)
      IF (IPUNCH.EQ.1) PUNCH 15, (TIME(I),J(I),VAA(I),I=1,K)
      STOP
      END
```

```
$IBFTC T01     DECK
      SUBROUTINE TAPE (IDTIN,IREAD)
C******************************************************************************
C*                 THE SUBROUTINE  'TAPE'   READS FROM AND RECORDS ON MAGNE-  *
C*  TIC  TAPE PARAMETERS AND DISTRIBUTIONS OF INTEREST.                       *
C*  SUBPROGRAM NEEDED                                                          *
C*                 FILE DEFINITION  DECK  'TO2' (IN ASSEMBLER LANGUAGE IBMAP)  *
C*                                                                             *
C*  THE MAGNETIC TAPE IS DEFINED AS  'UNIT 30' .                               *
C*                                                                             *
C*                                                                             *
C*                 AT EACH CALL OF THIS SUBROUTINE THE PROCEDURE IS CONTROLLED *
C*  BY THE PARAMETERS  IREAD,IDTIN,ITAPE  AS FOLLOWS                           *
C*                                                                             *
C*                 IREAD.EQ.1  READING OF THE STRUCTURE PARAMETERS AND INI-    *
C*                             TIAL DISTRIBUTIONS OCCURS                       *
C*                 IREAD.NE.1  READING DOES NOT OCCUR                          *
C*                                                                             *
C*                 IDTIN = PARAMETER THAT IDENTIFIES THE POSITION OF THE INI-  *
C*                         TIAL DISTRIBUTIONS, BY INDICATING THE LOGICAL RE-   *
C*                         CORD OF INTEREST                                    *
C*                                                                             *
C*                 ITAPE.EQ.1  RECORDING OF THE SOLUTIONS AT EACH INSTANT OF   *
C*                             TIME OCCURS                                     *
C*                 ITAPE.NE.1  RECORDING DOES NOT OCCUR                        *
C*                                                                             *
C*                 IN CASE RECORDING AT EACH INSTANT OF TIME OCCURS, A MESSAGE *
C*  IS WRITTEN ON THE PRINTOUT SHEET.                                          *
C*                                                                             *
C*                 THE NUMBER OF WORDS IN THE FIRST LOGICAL RECORD (WHICH ALSO *
C*  CONTAINS THE STRUCTURE PARAMETERS) IS   8*IL + 13 , AND IN EACH OF THE FOL-*
C*  LOWING RECORDS IS  6*IL + 6 .                                              *
C******************************************************************************
      DOUBLE PRECISION  E(810),N(810),P(810),XSTEP(810),ND,NA,VD
      REAL TIME(200),J(200),VAA(200),TSTEP(200)
      COMMON /TSTP/ RMIN,RMAX,  TSTMIN,TSTMAX, ICTST   ,TIME,TSTEP
     $        /EXT /J,VAA
     $        /XST / XSTEP
     $        /TP  / ND,NA,VD,E,N,P,IM,IL,IDT,C,TSTEP1
10    FORMAT (1H0,////////////44H MAGNETIC TAPE RECORDED WITH
     $DT  =, I4 /38X,6HK    =, I4 /38X,6HTIME =,E16.7 /)
      IF (IREAD.NE.1) GO TO 110
C*
```

```
C****************** READING ONLY                                          *
30     READ (30) IDT,K,TIME(K),VAA(K),J(K),ND,NA,VD,IM,IL
      $ ,(XSTEP(I),E(I),N(I),P(I),I=1,IL)
       IF (IDTIN.EQ.1) GO TO 50
       DO 40 II= 2 ,IDTIN
       READ (30) IDT,K,TIME(K),VAA(K),J(K),TSTEP(K-1)
      $, (E(I),N(I),P(I),I=1,IL)
       TSTEP1=TSTEP(K-1)
40     CONTINUE
50     IDT=IDT+1
       RETURN
C*                                                                        *
C****************** WRITING ONLY                                          *
110    WRITE (30) IDT,K,TIME(K),VAA(K),J(K),TSTEP(K-1)
      $, (E(I),N(I),P(I),I=1,IL)
       WRITE (6,10) IDT,K,TIME(K)
       GO TO 50
       END
```

```
$IBMAP T02
**************************************************************************
**               THIS SUBPROGRAM DEFINES THE FILE (AND RELEVANT PARAMETERS) *
**  FOR ONE MAGNETIC SAVE TAPE FOR DATA RECORDING PURPOSES.                 *
**                                                                          *
**               THE TAPE IS DEFINED AS   'UNIT 30'  ON CHANNEL  B(1)       *
**               'DATATR'= TITLE GIVEN TO THE TAPE                          *
**               'BIN'   = OPTION THAT SPECIFIES BINARY RECORDING           *
**               'INOUT' = OPTION THAT SPECIFIES BOTH READING AND WRITING   *
**                         ON THE TAPE                                      *
**               'BLK'   = OPTION THAT SPECIFIES THE LENGTH OF ONE RECORDING *
**                         BLOCK                                            *
**************************************************************************
       ENTRY   .UN30.
.UN30. PZE     UNIT30
UNIT30 FILE    DATATR,B(1),BIN,INOUT,BLK=256,HOLD
       END
```

```
$IBFTC T03     DECK
      SUBROUTINE TPRINT (IWR ,JIT,ICURR,IPR)
C*************************************************************************
C*               THE SUBROUTINE 'TPRINT'  WRITES ON THE PRINTOUT SHEET THE  *
C*  RELEVANT PARAMETERS AND DISTRIBUTIONS  (AT EACH INSTANT OF TIME) , THAT *
C*  REPRESENT THE SOLUTION OF THE PROBLEM.                                  *
C*                                                                          *
C*               THE DISTRIBUTIONS OF INTEREST ARE PRINTED OUT IN A NUMBER  *
C*  OF POINTS CONTROLLED BY THE PARAMETER   IWR  .  (EVERY  (IWR)TH  POINT IS *
C*  PRINTED OUT).   IF THE PARAMETER  IWR  IS OMITTED, A STANDARD VALUE (IWR= *
C*  10) WILL BE CHOSEN BY THIS ROUTINE.                                     *
C*************************************************************************
      DOUBLE PRECISION E(810),N(810),P(810),XSTEP(810), X(810)
     $,DELN(810),DELP(810),DUM1(810),DUM2(810)
     $,M,L,ND,NA,VD
      REAL J(200),VAA(200),TIME(200),TSTEP(200),DN(810),DP(810),DELVAA
     $ (100),DVAAV(200)
      COMMON /TSTP/ RMIN,RMAX,  TSTMIN,TSTMAX, ICTST   ,TIME,TSTEP
     $        /EXT /J,VAA
     $        /TP   / ND,NA,VD,E,N,P,IM,IL,IDT,K,TSTEP1
     $        /XST / XSTEP
     $        /DWORK/ DELN,X,DUM1,DELP,DUM2,DN,DP
     $        /TERM/ DELVAA,DVAA,DELVR
10    FORMAT (1H1, 70HCURRENT-DRIVEN TRANSIENT FOR THE ABRUPT  N-P  STRU
     $CTURE IDENTIFIED BY      ///  )
15    FORMAT (1H1, 70HVOLTAGE-DRIVEN TRANSIENT FOR THE ABRUPT  N-P  STRU
     $CTURE IDENTIFIED BY      ///  )
20    FORMAT (1H0, 5HND = , D24.15/
     $ 6H NA = , D24.15/
     $ 6H M  = , D24.15/
     $ 6H L  = , D24.15/
     $ 6H VD = , D24.15/
     $ 6H IM = , I5     /
     $1H1, 30HTHE INITIAL DISTRIBUTION ARE     ///
     $          1H0, 3HK =,I3,20X,
     $                3HJ =,E15.7,20X, 4HVAA=, F15.8,20X,7HTIME  =,E15.8////
     $ 5X,1HI,11X,1HX,21X,5HXSTEP, 22X,1HE,22X,1HN,22X,1HP///(I6,5D23.12
     $ ))
30    FORMAT (1H1,6H K    =,I4, 29X,12HJ            =, E19.8
     $                               /1X, 6H JIT =,I4,29X,12HVAA          =,F15.8
     $,40X,7HTIME  =,E14.7/40X,12HDVAA         =,F15.8,40X,7HTSTEP =,E14.7
     $/40X,12HDELVAA      =,F15.8,40X,7HR      =, E14.7/
     $                               / 40X,12HDELVAA/DVAA=,F15.8,40X,
     $ 7HRMIN  =, E14.7/107X,7HRMAX  =, E14.7/
     $ 107X,7HTSTMIN=, E14.7/107X, 7HTSTMAX= ,E14.7 ////
     $5X,1HI,11X,1HE,24X,1HN,13X, 2HDN,11X,4HDELN,21X,1HP,14X,2HDP,9 X,
     $4HDELP////  (I6,D20.10,D25.10,E13.5,D13.5,D25.10,E13.5,D13.5  ))
45    FORMAT (1H0,/////)
50    FORMAT (50X,8HDELVAA ( , I3, 4H ) = , F15.8)
60    FORMAT (1H1,46HTHE TERMINAL RESPONSE AS A FUNCTION OF TIME IS////
     $1H0,3X,1HK,10X,7HTIME(K), 10X,6HVAA(K),12X,4HJ(K),20X,8HTSTEP(K),
     $ 10X,7HDVAA(K) /// (I5,E20.7,F15.8,E18.7,E25.7,E20.7))
C*****************************************************************************
      IF (IWR.EQ.0) IWR=10
      GO TO (105,140,170,160), IPR
105   X(1)=0.
      DO 110 I=2,IL
      X(I)=X(I-1)+XSTEP(I-1)
110   IF (I.EQ.IM) M=X(I)
      L=X(IL)
      IF (ICURR.EQ.1) WRITE (6,10)
      IF (ICURR.NE.1) WRITE (6,15)
      WRITE (6,20) ND,NA,M,L,VD,IM,K,J(K),VAA(K),TIME(K)
     $, (I,X(I),XSTEP(I),E(I ),N(I),P(I),I=1,IL,IWR)
      RETURN
140   R=0.
      IF (K.GT.2) R=TSTEP(K-1)/TSTEP(K-2)
      WRITE (6,30) K,J(K),JIT,VAA(K),TIME(K),DVAA,TSTEP1,DELVAA(JIT)
     $,R,DELVR,RMIN,RMAX,TSTMIN,TSTMAX
     $, (I,E(I),N(I),DN(I),DELN(I),P(I),DP(I),DELP(I),I=1,IL,IWR)
160   WRITE (6,45)
      WRITE (6,50) (I,DELVAA(I),I=1,JIT)
      RETURN
170   DVAAV(1)=0.
      DO 180 I=2,K
```

```
180   DVAAV(I)=VAA(I)-VAA(I-1)
      TSTEP(K)=0.
      WRITE (6,60) (I,TIME(I),VAA(I),J(I),TSTEP(I),DVAAV(I),I=1,K)
      RETURN
      END
```

```
$IBFTC T04     DECK
      SUBROUTINE TSTEPK (TSTEP1,K,KRELAX,VAA)
C*************************************************************************
C*                  THE SUBROUTINE  'TSTEPK'  FURNISHES THE TIME STEP AT THE    *
C*   INSTANT OF TIME  K.                                                        *
C*                                                                              *
C*                  AN AUTOMATIC ADJUSTMENT OF THE TIME STEP AT THE INSTANT  K  *
C*   MAY BE EMPLOYED, BASED ON MAINTAINING CONSTANT  TRUNCATION ERROR IN THE    *
C*   TIME DOMAIN OF THE FIRST TIME DERIVATIVE OF THE TERMINAL RESPONSE OF THE   *
C*   DEVICE.                                                                    *
C*                                                                              *
C*                                                                              *
C*                  INPUT PARAMETERS ARE                                        *
C*                                                                              *
C*   K      = INDEX IDENTIFYING THE INSTANT OF TIME                             *
C*   KRELAX = PARAMETER WHICH EXCLUDES THE AUTOMATIC TIME STEP ADJUSTMENT PRO-  *
C*            CEDURE (FOR A FEW INSTANTS OF TIME AFTER AN ARBITRARY TIME STEP   *
C*            SIZE IS IMPOSED BY THE PROGRAMMER) AS FOLLOWS                     *
C*                  IF   K.LT.(KRELAX+3) THE AUTOMATIC STEP SELECTION IS EXLU-  *
C*                  DED AND THE QUANTITY  TSTEP1  IS TAKEN AS THE TIME STEP AT  *
C*                  THE INSTANT K .                                             *
C*   VAA    = ONE-DIMENSIONAL ARRAY, EXTERNAL TIME RESPONSE OF THE DEVICE       *
C*                                                                              *
C*                                                                              *
C*                  OUTPUT PARAMETER                                            *
C*                                                                              *
C*   TSTEP1 = TIME STEP AT THE INSTANT  K                                       *
C*                                                                              *
C*                                                                              *
C*                  A FEATURE THAT PREVENTS OSCILLATIONS ARISING FROM FEEDBACK  *
C*   OF THE ITERATION ERROR AT EACH INSTANT OF TIME IS INCORPORATED,  AND CON-  *
C*   TROLLED BY THE PARAMETER ICTST.                                            *
C*************************************************************************
      DIMENSION VAA(200),TSTEP(200),TIME(200),R(4)
      COMMON /TSTP/ RMIN,RMAX,  TSTMIN,TSTMAX, ICTST   ,TIME,TSTEP
      VAACV=0.
      TSTEP(K)=TSTEP1
      IF (K.LT.(KRELAX+3)) GO TO 200
      IF (ICTST.GT.1.AND.ICTST.LT.4)GO TO 110
      ICTST=1
      ALFA=TSTEP(K-2)/TSTEP(K-3)
      VAACV1=2.*(VAA(K-1)-(ALFA+1.)*VAA(K-2)+ALFA*VAA(K-3))/ (TSTEP(
     $K-2)*TSTEP(K-3))
      ALFA=TSTEP(K-1)/TSTEP(K-2)
      VAACV=2.*(VAA(K)-(ALFA+1.)*VAA(K-1)+ALFA*VAA(K-2))/(TSTEP(
     $K-1)*TSTEP(K-2))
      DVAA=VAA(K)-VAA(K-1)
      DVAA1=VAA(K-1)-VAA(K-2)
      DEN=VAACV*DVAA1
      IF (DEN.EQ.0.) DEN=1.E-20
      RR=SQRT(ABS(VAACV1/DEN*DVAA))
      TSTEP(K)=RR*TSTEP(K-1)
      IF (RR.LT.RMIN) TSTEP(K)=RMIN*TSTEP(K-1)
      IF (RR.GT.RMAX) TSTEP(K)=RMAX*TSTEP(K-1)
      IF (TSTEP(K).LT.TSTMIN) TSTEP(K)=TSTMIN
      IF (TSTEP(K).GT.TSTMAX) TSTEP(K)=TSTMAX
      IF (K.LT.(KRELAX+4)) GO TO 200
      DO 50 I=1,4
      IND=K-I+1
50    R(I)=TSTEP(IND)/TSTEP(IND-1)
      IF (.NOT.((R(1).LT.R(2) .AND. R(2).GT.R(3).AND. R(3).LT.R(4)).OR.
     $ (          R(1).GT.R(2) .AND. R(2).LT.R(3).AND. R(3).GT.R(4))))
     $ GO TO 200
      TSTAV= (TSTEP(K-1)+TSTEP(K-2)+TSTEP(K-3)+TSTEP(K-4))/4.
110   ICTST=ICTST+1
      TSTEP(K)=TSTAV
200   TSTEP1=TSTEP(K)
      TIME(K+1)=TIME(K)+TSTEP(K)
      RETURN
      END
```

```
$IBFTC T05     DECK
      SUBROUTINE DIFFEQ (BGM,GPDT,GAMPJ,VAA,VAA1,EK,JIT)
C*************************************************************************
C*                  THE SUBROUTINE  'DIFFEQ'  IMPROVES THE SOLUTION OF THE      *
C*   SYSTEM OF THREE NON-LINEAR PARTIAL DIFFERENTIAL EQUATIONS FROM A TRIAL     *
C*   FUNCTION, AT EACH  (J)  ITERATION AT EACH INSTANT OF TIME.                 *
C*                                                                              *
C*                  THIS ROUTINE USES A FINITE DIFFERENCE SCHEME BASED ON THE   *
C*   SOLUTION OF TWO TRIPLE-DIAGONAL MATRICES WITH A DIRECT METHOD.             *
C*                                                                              *
C*                  SUBPROGRAMS NEEDED ARE                                      *
C*                            'SLCV2'                                           *
C*                            'EQUAD'                                           *
C*                            'TRDU1'                                           *
C*                                                                              *
C*                                                                              *
C*                  INPUT PARAMETERS ARE                                        *
C*                                                                              *
C*   EK     = ONE-DIMENSIONAL ARRAY, ELECTRIC FIELD SPATIAL DISTRIBUTION AT     *
C*            THE PREVIOUS INSTANT OF TIME  K-1                                 *
C*   E      = ONE-DIMENSIONAL ARRAY, INACCURATE ELECTRIC FIELD SPATIAL DISTRI-  *
C*            BUTION AT THE INSTANT OF TIME  K                                  *
C*   N      = ONE-DIMENSIONAL ARRAY, INACCURATE ELECTRON DENSITY SPATIAL DI-    *
C*            STRIBUTION AT THE INSTANT OF TIME  K                              *
C*   P      = ONE-DIMENSIONAL ARRAY, INACCURATE   HOLE   DENSITY SPATIAL DI-
C*            STRIBUTION AT THE INSTANT OF TIME  K                              *
C*                                                                              *
C*                                                                              *
C*                  OUTPUT PARAMETERS ARE                                       *
C*                                                                              *
C*   E      = ONE-DIMENSIONAL ARRAY, IMPROVED ELECTRIC FIELD SPATIAL DISTRIBU-  *
C*            TION AT THE INSTANT OF TIME  K                                    *
C*   N      = ONE-DIMENSIONAL ARRAY, IMPROVED ELECTRON DENSITY SPATIAL DISTRI-  *
C*            BUTION AT THE INSTANT OF TIME  K                                  *
C*   P      = ONE-DIMENSIONAL ARRAY, IMPROVED   HOLE   DENSITY SPATIAL DISTRI-  *
```

```
C*             BUTION AT THE INSTANT OF TIME  K                              *
C*  DELN    = ONE-DIMENSIONAL ARRAY, CORRECTION FOR THE ELECTRON DENSITY SPA-  *
C*             TIAL DISTRIBUTION AT THE COMPLETION OF EACH  (J)  ITERATION    *
C*  DELP    = ONE-DIMENSIONAL ARRAY, CORRECTION FOR THE , HOLE   DENSITY SPA-  *
C*             TIAL DISTRIBUTION AT THE COMPLETION OF EACH  (J)  ITERATION    *
C*  DN      = ONE-DIMENSIONAL ARRAY, TOTAL CORRECTION FOR THE ELECTRON DENSITY *
C*             SPATIAL DISTRIBUTION AT THE INSTANT  K                        *
C*  DP      = ONE-DIMENSIONAL ARRAY, TOTAL CORRECTION FOR THE   HOLE   DENSITY *
C*             SPATIAL DISTRIBUTION AT THE INSTANT  K                        *
C*  VAA     = ONE-DIMENSIONAL ARRAY, TERMINAL VOLTAGE OF THE DEVICE           *
C*                                                                           *
C*                                                                           *
C*                  THE ARRAYS  EK,E,N,P,DELN,DELP  ARE IN DOUBLE PRECISION  *
C*  AND OF DIMENSION  810.  THE ARRAYS  DN,DP  ARE IN SINGLE PRECISION AND   *
C*  OF DIMENSION  810.  THE ARRAY  VAA  IS IN SINGLE PRECISION AND OF DIMEN- *
C*  SION  200.                                                               *
C****************************************************************************
      DOUBLE PRECISION E(810),N(810),P(810),XSTEP(810),    EK(810)
     $         ,DELN(810),DELP(810),AN(810),AP(810),BN(810),BP(810),NSL
     $(810),PSL(810),VN(810),VP(810),             NCURV(810),PCURV(810)
     $, Z,ZE,ALFA,DOPING,CN,CP,ND,NA,VD,VA
      DIMENSION DN(810),DP(810),VAA(200)
      EQUIVALENCE  (VN,NCURV,DELN),(BN,NSL     ),(BP,PSL),(VP,PCURV,DELP)
     $,(AN,AP)
      COMMON /XST /XSTEP
     $       /TP  / ND,NA,VD,E,N,P,IM,IL,IDT,K,TSTEP1
     $       /DWORK/ NCURV,NSL,PSL,PCURV,AN,DN,DP
      IL1=IL-1
      IMP1=IM+1
      CALL SLCV2 (N,NSL,NCURV,P,PSL,PCURV,IL)
      DO 110 I=1,IL
  110 E(I)=(PSL(I)-BGM*NSL(I)-GAMPJ+EK(I)*GPDT)/(P(I)+N(I)*BGM+GPDT )
      VAA1=VAA(K)
      IF (JIT.EQ.1) VAA1=VAA(K-1)
      CALL EQUAD (E,VD,VA,VAA(K),IL)
      DOPING =ND
      DO 130 I=2,IL1
      ALFA=XSTEP(I)/XSTEP(I-1)
      Z=2.D0/XSTEP(I)
      ZE=E(I)
      IF (I.EQ.IMP1) DOPING =-NA
      RHO=P(I)-N(I)+DOPING
      CN=Z+ZE/ALFA
      VN(I)= - (NCURV(I)+ZE*NSL(I)+N(I)*RHO-GNDT*DN(I))/CN*(XSTEP(I)+
     $XSTEP(I-1))
      BN(I)=((RHO-N(I)-GNDT) * XSTEP(I-1)+ZE-CN) /CN*(ALFA+1.D0)
  130 AN(I)=(Z-ZE)/CN*ALFA
      CALL TRDU1 (AN,BN,VN,IL)
      DO 140 I=2,IL1
      DN(I)=DN(I)+DELN(I)
  140 N(I)=N(I)+DELN(I)
C****************************************************************************
      DOPING =ND
  220 DO 230 I=2,IL1
      ALFA=XSTEP(I)/XSTEP(I-1)
      Z=2.D0/XSTEP(I)
      ZE=E(I)
      IF (I.EQ.IMP1) DOPING =-NA
      RHO=P(I)-N(I)+DOPING
      CP    =Z-ZE/ALFA
      VP(I)= -(PCURV(I)-ZE*PSL(I)-P(I)*RHO-GPDT*DP(I))/CP *(XSTEP(I)
     $+XSTEP(I-1))
      BP(I)=-((RHO+P(I)+GPDT)*XSTEP(I-1) + ZE+CP)/CP *(ALFA+1.D0)
  230 AP(I)=(Z+ZE)/CP*ALFA
      CALL TRDU1 (AP,BP,VP,IL)
      DO 240 I=2,IL1
      DP(I)=DP(I)+DELP(I)
  240 P(I)=P(I)+DELP(I)
      RETURN
      END
```

```
$IBFTC T06A    DECK
      SUBROUTINE SLCV2 (Y,YSL,YCV,T,TSL,TCV,IL)
C****************************************************************************
C*                 THE SUBROUTINE  'SLCV2'  COMPUTES THE SPATIAL SLOPE AND   *
C*  CURVATURE OF TWO FUNCTIONS GIVEN IN DISCRETIZED FORM THROUGHOUT THE POINT *
C*  INTERVAL  1 - IL .                                                       *
C*                                                                           *
C*                 THIS ROUTINE USES A PARABOLIC INTERPOLATION SCHEME AT EACH *
C*  SPATIAL POINT (THREE-POINT  FORMULA)  SUITABLE FOR NON-UNIFORM STEPS.    *
C*  THE SLOPE AND CURVATURE AT EACH POINT ARE THAT OF THE PARABOLA TRACED    *
C*  THROUGH THE POINT ITSELF AND THE TWO ADJACENT POINTS.                    *
C*  DOUBLE PRECISION ARITHMETIC IS USED.                                     *
C*                                                                           *
C*                                                                           *
C*                 INPUT PARAMETERS ARE                                      *
C*                                                                           *
C*  Y       = ONE-DIMENSIONAL ARRAY WHOSE SPATIAL SLOPE AND CURVATURE ARE SOUGHT*
C*  T       = ONE-DIMENSIONAL ARRAY WHOSE SPATIAL SLOPE AND CURVATURE ARE SOUGHT*
C*  IL      = TOTAL NUMBER OF SPATIAL POINTS                                 *
C*  XSTEP   = ONE-DIMENSIONAL ARRAY, NON-UNIFORM SPATIAL STEP SIZE AT EACH   *
C*            SPATIAL POINT                                                  *
C*                                                                           *
C*                                                                           *
C*                 OUTPUT PARAMETERS ARE                                     *
C*                                                                           *
C*  YSL     = ONE-DIMENSIONAL ARRAY, FIRST SPATIAL DERIVATIVE AT EACH SPATIAL *
C*            POINT OF THE GIVEN ARRAY  Y                                    *
C*  TSL     = ONE-DIMENSIONAL ARRAY, FIRST SPATIAL DERIVATIVE AT EACH SPATIAL *
C*            POINT OF THE GIVEN ARRAY  T                                    *
C*  YCV     = ONE-DIMENSIONAL ARRAY, SECOND SPATIAL DERIVATIVE AT EACH SPATIAL *
C*            POINT OF THE GIVEN ARRAY  Y                                    *
C*  TCV     = ONE-DIMENSIONAL ARRAY, SECOND SPATIAL DERIVATIVE AT EACH SPATIAL *
C*            POINT OF THE GIVEN ARRAY  T                                    *
C*                                                                           *
C*                                                                           *
C*                 ALL THE ARRAYS ARE OF DIMENSION  810  AND IN DOUBLE PRE-  *
C*  CISION.                                                                  *
C****************************************************************************
      DOUBLE PRECISION XSTEP(1),YSL(1),YCV(1),Y(1)
     $,ALFA,ALFAF,ALFAP1,XZ,ALFA1
     $,T(1),TSL(1),TCV(1)
      COMMON /XST / XSTEP
      IL1=IL-1
      DO 400 I=2,IL1
      ALFA=XSTEP(I)/XSTEP(I-1)
      ALFAP1=ALFA+1.D0
      ALFA1=ALFA-1.D0
```

```
      ALFAF=ALFA/ALFAP1*ALFA
      XZ=2.D0/(XSTEP(I)*(XSTEP(I)+XSTEP(I-1)))
      TSL(I)= (T(I+1)/ALFAP1   +ALFA)*T(I)-ALFAF   *T(I-1))/XSTEP(I)
      YSL(I)= (Y(I+1)/ALFAP1   +ALFA)*Y(I)-ALFAF   *Y(I-1))/XSTEP(I)
      TCV(I)=(T(I+1)-ALFAP1   *T(I)+ALFA   *T(I-1))*XZ
      YCV(I)=(Y(I+1)-ALFAP1   *Y(I)+ALFA   *Y(I-1))*XZ
400   CONTINUE
      YSL(1)= (Y(2)-Y(1))/XSTEP(1)
      TSL(1)= (T(2)-T(1))/XSTEP(1)
      YSL(IL)=(Y(IL)-Y(IL1 ))/XSTEP(IL1 )
      TSL(IL)=(T(IL)-T(IL1 ))/XSTEP(IL1 )
      RETURN
      END



$IBFTC T06B    DECK
      SUBROUTINE SLCV2 (Y,YSL,YCV,T,TSL,TCV,IL)
C***********************************************************************
C*                 THE SUBROUTINE  'SLCV2'  COMPUTES THE SPATIAL SLOPE AND     *
C*  CURVATURE OF TWO FUNCTIONS GIVEN IN DISCRETIZED FORM THROUGHOUT THE POINT  *
C*  INTERVAL  1 - IL .                                                         *
C*                                                                             *
C*                 THIS ROUTINE USES A LAGRANGIAN INTERPOLATION SCHEME AT      *
C*  EACH SPATIAL POINT ( FIVE POINT FORMULA) SUITABLE FOR NON-UNIFORM STEPS.   *
C*  THE SLOPE AND THE CURVATURE AT EACH POINT ARE THAT OF THE FOURTH ORDER     *
C*  POLYNOMIAL TRACED THROUGH THE POINT ITSELF AND THE FOUR ADJACENT POINTS.   *
C*  DOUBLE PRECISION ARITHMETIC IS USED.                                       *
C*                                                                             *
C*                                                                             *
C*                 INPUT PARAMETERS ARE                                        *
C*                                                                             *
C*  Y      = ONE-DIMENSIONAL ARRAY WHOSE SPATIAL SLOPE AND CURVATURE ARE SOUGHT*
C*  T      = ONE-DIMENSIONAL ARRAY WHOSE SPATIAL SLOPE AND CURVATURE ARE SOUGHT*
C*  IL     = TOTAL NUMBER OF SPATIAL POINTS                                    *
C*  XSTEP  = ONE-DIMENSIONAL ARRAY, NON-UNIFORM SPATIAL STEP SIZE AT EACH      *
C*           SPATIAL POINT                                                     *
C*                                                                             *
C*                                                                             *
C*                 OUTPUT PARAMETERS ARE                                       *
C*                                                                             *
C*  YSL    = ONE-DIMENSIONAL ARRAY, FIRST SPATIAL DERIVATIVE AT EACH SPATIAL   *
C*           POINT OF THE GIVEN ARRAY  Y                                       *
C*  TSL    = ONE-DIMENSIONAL ARRAY, FIRST SPATIAL DERIVATIVE AT EACH SPATIAL   *
C*           POINT OF THE GIVEN ARRAY  T                                       *
C*  YCV    = ONE-DIMENSIONAL ARRAY, SECOND SPATIAL DERIVATIVE AT EACH SPATIAL  *
C*           POINT OF THE GIVEN ARRAY  Y                                       *
C*  TCV    = ONE-DIMENSIONAL ARRAY, SECOND SPATIAL DERIVATIVE AT EACH SPATIAL  *
C*           POINT OF THE GIVEN ARRAY  T                                       *
C*                                                                             *
C*                                                                             *
C*                 ALL THE ARRAYS ARE OF DIMENSION  810  AND IN DOUBLE PRE-    *
C*  CISION.                                                                    *
C***********************************************************************
      DOUBLE PRECISION XSTEP(1),YSL(1),YCV(1),Y(1)
     $,WB,WC,BC,W ,ALFA  ,YI
     $,T(1),TSL(1),TCV(1),TI,BCT
     $, R11,R12,R13,R14,R15,    U11,U12,U13,U14
     $, R21,R22,R23,R24,R25,    U21,U22,U23,U24
     $, R31,R32,R33,R34,R35,    U31,U32,U33,U34
     $, R41,R42,R43,R44,R45
     $     ,R52,R53,R54,R55
     $, S11,S21,S31,S41,    V11,V21,V31
      COMMON /XST / XSTEP
C***********************************************************************
      IL2=IL-2
      IL3=IL-3
      R12=-XSTEP(1)-XSTEP(2)
      R13=1.D0/R12
      R22=-XSTEP(2)
      R23=1.D0/R22
      R52=-XSTEP(2)-XSTEP(3)
      R53=1.D0/R52
      R14=R13*R13
      R24=R23*R23
      R54=R53*R53
      R15=R14*R13
      R25=R24*R23
      R55=R54*R53
C***********************************************************************
      DO 300 I=3,IL2
      R32=XSTEP(I)
      R42=R32+XSTEP(I+1)
      R33=1.D0/R32
      R43=1.D0/R42
      R34=R33*R33
      R44=R43*R43
      R35=R34*R33
      R45=R44*R43
      YI=Y(I)
      R11=(Y(I-2)-YI)*R15
      R21=(Y(I-1)-YI)*R25
      R31=(Y(I+1)-YI)*R35
      R41=(Y(I+2)-YI)*R45
      U11=R11-R41
      U12=R12-R42
      U13=R13-R43
      U14=R14-R44
      U21=R21-R41
      U22=R22-R42
      U23=R23-R43
      U24=R24-R44
      U31=R31-R41
      U32=R32-R42
      U33=R33-R43
      U34=R34-R44
      WB=U22*U33-U32*U23
      WC=U22*U34-U32*U24
      BC=U21*U32-U31*U22
      W=U12*(U23*U34-U33*U24) - U13*WC + U14*WB
      YSL(I)= (U11*WB-U12* (U21*U33-U31*U23) + U13*BC) / W
      YCV(I)= -2.D0*(U11*WC-U12* (U21*U34-U31*U24) + U14*BC) / W
      TI=T(I)
      S11=(T(I-2)-TI)*R15
      S21=(T(I-1)-TI)*R25
      S31=(T(I+1)-TI)*R35
      S41=(T(I+2)-TI)*R45
      V11=S11-S41
      V21=S21-S41
      V31=S31-S41
```

```
      BCT=V21*U32-V31*U22
      TSL(I)=(V11*WB-U12*(V21*U33-V31*U23) + U13*BCT) / W
      TCV(I)= -2.D0*(V11*WC-U12*(V21*U34-V31*U24)+ U14*BCT ) / W
      R12=R52
      R13=R53
      R14=R54
      R15=R55
      R22=-R32
      R23=-R33
      R24= R34
      R25=-R35
      R52=-R42
      R53=-R43
      R54= R44
      R55=-R45
300   CONTINUE
C*****************************************************************************
      DO 400 I=2,IL,IL3
      ALFA=XSTEP(I)/XSTEP(I-1)
      TSL(I)= (T(I+1)/(ALFA+1.D0)+(ALFA-1.D0)* T(I)- ALFA**2/(ALFA+1.D0)
     $ *T(I-1))/ XSTEP(I)
      TCV  (I)=2.D0*( T(I+1)-(ALFA+1.D0)*T(I)+ALFA*T(I-1))/(XSTEP(I)*
     $(XSTEP(I-1)+XSTEP(I)))
      YSL(I)= (Y(I+1)/(ALFA+1.D0)+(ALFA-1.D0)* Y(I)- ALFA**2/(ALFA+1.D0)
     $ *Y(I-1))/ XSTEP(I)
400   YCV  (I)=2.D0*( Y(I+1)-(ALFA+1.D0)*Y(I)+ALFA*Y(I-1))/(XSTEP(I)*
     $(XSTEP(I-1)+XSTEP(I)))
      YSL(1)=(Y(2)-Y(1))/XSTEP(1)
      TSL(1)=(T(2)-T(1))/XSTEP(1)
      YSL(IL)=(Y(IL)-Y(IL-1))/XSTEP(IL-1)
      TSL(IL)=(T(IL)-T(IL-1))/XSTEP(IL-1)
      RETURN
      END
```

```
$IBFTC T07     DECK
      SUBROUTINE EQUAD (    E,VD,VA,VAA,IL)
C*****************************************************************************
C*                 THE SUBROUTINE  'EQUAD'  COMPUTES THE QUADRATURE OF THE    *
C*  ELECTRIC FIELD SPATIAL DISTRIBUTION, LIMITS OF INTEGRATION BEING THE      *
C*  POINT BOUNDARIES  1 - IL.                                                 *
C*                                                                            *
C*                 THIS ROUTINE USES A PARABOLIC INTERPOLATION AT EVERY OTHER *
C*  SPATIAL POINT, SUITABLE FOR NON-UNIFORM SPATIAL STEP DISTRIBUTION. SPE-   *
C*  CIALIZED FOR THE CASE OF UNIFORM STEP THE SCHEME REDUCES TO SIMPSON'S     *
C*  RULE.                                                                     *
C*                                                                            *
C*                                                                            *
C*                 INPUT PARAMETERS ARE                                       *
C*                                                                            *
C*  E       = ONE-DIMENSIONAL ARRAY, ELECTRIC FIELD SPATIAL DISTRIBUTION TO   *
C*            BE INTEGRATED                                                   *
C*  IL      = TOTAL NUMBER OF SPATIAL POINTS                                  *
C*  XSTEP   = ONE-DIMENSIONAL ARRAY, NON-UNIFORM SPATIAL STEP SIZE AT EACH    *
C*            SPATIAL POINT                                                   *
C*  VD      = DIFFUSION POTENTIAL                                             *
C*                                                                            *
C*                                                                            *
C*                 OUTPUT PARAMETERS ARE                                      *
C*                                                                            *
C*  VA      = TERMINAL VOLTAGE  (NORMALIZED)                                  *
C*  VAA     = TERMINAL VOLTAGE  (UNNORMALIZED)                                *
C*                                                                            *
C*                                                                            *
C*                 ALL THE ARRAYS ARE OF DIMENSION  810  AND IN DOUBLE PRECI- *
C*  SION.                                                                     *
C*****************************************************************************
      DOUBLE PRECISION XSTEP(1) ,E(1),VD,VA,ALFA,Q1,Q3,DV
      COMMON /XST / XSTEP
      IL2=IL-2
      DV=0.
      DO 410 I=1,IL2,2
      K=IL-I
      ALFA=XSTEP(K)/XSTEP(K-1)
      Q1=2.D0-ALFA
      Q3=2.D0-1.D0/ALFA
410   DV= (Q1*E(K-1)+(6.D0-Q1-Q3)*E(K)+Q3*E(K+1))/6.D0*(XSTEP(K)+XSTEP
     *(K-1))+DV
      VA=VD-DV
      VAA=VA*.025875
      RETURN
      END
```

```
$IBFTC T08     DECK
      SUBROUTINE TRDU1 (A,B,D,IL)
C*****************************************************************************
C*                 THE SUBROUTINE  'TRDU1'   SOLVES A TRIPLE-DIAGONAL SYSTEM  *
C*  OF THE FORM    T * DELTA  =  D   ,WHERE  T  IS A GIVEN TRIPLE-DIAGONAL    *
C*  MATRIX WITH UPPER DIAGONAL ENTRIES EQUAL TO UNITY,  DELTA  IS THE UNKNOWN *
C*  VECTOR,  D  IS THE KNOWN VECTOR.                                          *
C*                                                                            *
C*                 THIS ROUTINE USES A DIRECT METHOD BASED ESSENTIALLY ON     *
C*  GAUSSIAN ELIMINATION AND BACKSUBSTITUTION WHICH REDUCES IN THE CASE CON-  *
C*  SIDERED TO A SET OF RECURSION RELATIONS.                                  *
C*  DOUBLE PRECISION ARITHMETIC IS USED.                                      *
C*                                                                            *
C*                 INPUT PARAMETERS ARE                                       *
C*  A      = ONE-DIMENSIONAL ARRAY, LOWER DIAGONAL OF THE TRIPLE-DIAGONAL MATRIX *
C*  B      = ONE-DIMENSIONAL ARRAY, DIAGONAL OF THE TRIPLE-DIAGONAL MATRIX    *
C*  D      = ONE-DIMENSIONAL ARRAY, KNOWN VECTOR                              *
C*  (IL-2) = NUMBER OF EQUATIONS (SIZE OF THE TRIPLE-DIAGONAL MATRIX )        *
C*                                                                            *
C*                 OUTPUT PARAMETERS ARE                                      *
C*  D      = ONE-DIMENSIONAL ARRAY, ORIGINALLY THE   KNOWN VECTOR             *
C*                                                                            *
C*                 ALL THE ARRAYS ARE OF DIMENSION  1000  AND IN DOUBLE PRE-  *
C*  CISION                                                                    *
C*                                                                            *
C*                 NO WORKING ARRAYS ARE NEEDED.  THIS IS ACHIEVED THROUGH    *
C*  USE OF INTRINSIC EQUIVALENCE.   DURING THE EXECUTION OF THIS ROUTINE THE  *
C*  ARRAYS  B  AND  D  ARE ERASED.                                            *
C*****************************************************************************
      DOUBLE PRECISION A(1),B(1),D(1)
      IL1=IL-1
      IL2=IL-2
```

```
      D(2)=D(2)/B(2)
      DO 20 I=3,IL1
      B(I)=B(I)-A(I)/B(I-1)
20    D(I)=(D(I)-A(I)*D(I -1))/B(I)
      DO 30 I=2,IL2
      K=IL-I
30    D(K)=D(K)-D(K+1)/B(K)
      D(1)=0.
      D(IL)=0.
      RETURN
      END
```

```
$IBFTC T09     DECK
      SUBROUTINE INTERP (K,KT,VAA,VAAR,J,TIME)
C***********************************************************************
C*                  THE SUBROUTINE  'INTERP'  FURNISHES AT THE TIME  K  A VALUE *
C*  OF TOTAL CURRENT APPROXIMATELY CORRESPONDING TO A SPECIFIED VALUE OF TER-  *
C*  MINAL  VOLTAGE, DURING THE VOLTAGE-DRIVEN TRANSIENT PROCEDURE.             *
C*                                                                             *
C*                  THIS ROUTINE USES EITHER A PREDICTION SCHEME ON THE AVAIL- *
C*  ABLE CURRENT VERSUS TIME RESPONSE (J VERSUS TIME), OR AN INTERPOLATION     *
C*  SCHEME ON THE CURRENT-VOLTAGE CHARACTERISTIC FROZEN AT THE INSTANT OF      *
C*  TIME  K  (JTR VERSUS VTR).                                                 *
C*                  SUBPROGRAM NEEDED                                          *
C*                         'SLAGR'                                             *
C*                                                                             *
C*                                                                             *
C*                  INPUT PARAMETERS ARE                                       *
C*                                                                             *
C*  K       = INDEX IDENTIFYING THE INSTANT OF TIME                            *
C*  J       = ONE-DIMENSIONAL ARRAY, TOTAL CURRENT AVAILABLE AT THE INSTANTS   *
C*            1,2,3 ... K-1                                                    *
C*  TIME    = ONE-DIMENSIONAL ARRAY, INSTANTS OF TIME                          *
C*  VAAR(K)= SPECIFIED VALUE OF TERMINAL VOLTAGE AT THE INSTANT  K             *
C*  JTR(1) = INITIAL GUESS FOR THE TOTAL CURRENT AT THE INSTANT  K=2, READ IN  *
C*            FROM A  DATA  CARD                                               *
C*                                                                             *
C*                                                                             *
C*                  OUTPUT PARAMETER                                           *
C*                                                                             *
C*  J(K)    = TOTAL CURRENT AT THE INSTANT  K, CORRESPONDING TO THE SPECIFIED  *
C*            TERMINAL VOLTAGE  VAAR(K)                                        *
C***********************************************************************
      REAL JTR(10),VTR(10),J(200),VAAR(200),TIME(200) ,X(3),Y(3)
      COMMON /INTP/ JTR,VTR
2     FORMAT (E10.0)
      KT=KT+1
      IF (KT.NE.1) VTR(KT-1)=VAA
      IF (K .EQ.3.AND.KT.EQ.1) GO TO 60
      IF (K .GE.4) GO TO 100
      IF (KT.EQ.1) GO TO 10
      IF (KT.EQ.2) GO TO 20
      IF (KT.EQ.3) GO TO 130
      GO TO 140
10    READ (5,2) JTR(1)
      GO TO 500
20    FCT=2.
      IF ( ABS(VTR(1)).GT.ABS(VAAR(K  ))) FCT=.5
      JTR(2)=JTR(1)*FCT
      GO TO 500
60    JTR(1)=J (K-1)
      GO TO 500
100   IF (KT.EQ.1) GO TO 110
      VTR(KT-1)=VAA
      IF (KT.EQ.2) GO TO 120
      IF (KT.EQ.3) GO TO 130
      GO TO 140
110   JTR(1)= (TIME(K  )-TIME(K-2)) / (TIME(K-1)-TIME(K-2))*((J(K-1))-
     $    (J(K-2))) +    (J(K-2))
      GO TO 500
120   DO 125 I=1,3
      INDX=K-I
      X(I)=TIME(INDX)
      IF (J(INDX).EQ.0.) J(INDX)=1.E-7
125   Y(I)=    (J(INDX))
      CALL SLAGR (X,Y,TIME(K  ),3,JTR(2))
      RAT=JTR(2)/JTR(1)
      IF (RAT.LT.1.001 .AND.RAT.GT..999 ) JTR(2)=JTR(1)*1.2
      GO TO 500
130   JTR(3)= (VAAR(K  )-VTR(1)) /(VTR(2)-VTR(1))*( JTR(2)-JTR(1)) +
     $ JTR(1)
      GO TO 500
140   IF (KT.EQ.4) GO TO 160
      I=1
      IF (ABS(VTR(2)-VAAR(K  )) .GT. ABS (VTR(1)-VAAR(K  )))  I=2
      IF (ABS(VTR(3)-VAAR(K  )) .GT. ABS (VTR(I)-VAAR(K  )))  I=3
      VTR(I)=VTR(KT-1)
      JTR(I)=JTR(KT-1)
160   DO 170 I=1,3
      X(I)=VTR(I)
170   Y(I)=JTR(I)
      CALL SLAGR (X,Y,VAAR(K  ),3,JTR(KT))
500   J(K  )=JTR(KT)
      KT1=KT-1
      KP=K
      IF (KT.EQ.1) WRITE (6,505)KP,KT,KT,JTR(KT)
505   FORMAT (1H1, 4H  K=, I4,//4H KT=,I4///5X,1HI,19X,3HJTR //I6,E25.8)
      IF (KT.NE.1)
     $WRITE (6,510)KP,KT, (I,JTR(I),VTR(I),I=1,KT1), KT,JTR(KT)
510   FORMAT (1X,////////
     $                 4H  K=,I4,//4H KT=, I4//5X, 1HI,19X,3HJTR,22X,3HV
     $TR //(I6,2E25.8))
      RETURN
      END
```

```
$IBFTC T10     DECK
      SUBROUTINE SLAGR (JT,VAIT,JTW,MM,DP)
C***********************************************************************
C*                  THE SUBROUTINE  'SLAGR' EXECUTES A LAGRANGIAN INTERPOLA-   *
C*  TION ON TWO ONE-DIMENSIONAL ARRAYS NOT UNIFORMLY SPACED.                   *
C*                                                                             *
C*                  THIS ROUTINE CONSTRUCTS THE PERTINENT MATRIX,TRIANGULARI-  *
C*  ZES IT WITH THE GAUSSIAN ELIMINATION PROCESS, SOLVES THE SYSTEM BY BACK-   *
C*  SUBSTITUTION TO OBTAIN THE COEFFICIENTS OF THE INTERPOLATING POLYNOMIAL,   *
```

```
C*  AND COMPUTES THE VALUE OF SUCH POLYNOMIAL AT THE DESIRED POINT.             *
C*  DOUBLE PRECISION ARITHMETIC IS USED.                                          *
C*                                                                                *
C*                     INPUT PARAMETERS ARE                                       *
C*  JT    = ONE-DIMENSIONAL ARRAY, ABSCISSA OF THE GIVEN POINTS (DIMENSION=10)    *
C*  VAIT  = ONE-DIMENSIONAL ARRAY, ORDINATE OF THE GIVEN POINTS (DIMENSION=10)    *
C*  JTW   = ABSCISSA OF THE DESIRED POINT                                         *
C*  MM    = NUMBER OF POINTS GIVEN  (THE ORDER OF THE INTERPOLATING POLYNOMIAL    *
C*          IS MM-1).    MAXIMUM  MM VALUE  =  10.                                *
C*                                                                                *
C*                     OUTPUT PARAMETERS ARE                                      *
C*  DP    = ORDINATE OF THE DESIRED POINT                                         *
C*                                                                                *
C*                     ALL THE INPUT AND OUTPUT QUANTITIES ARE IN SINGLE PRECISION *
C**********************************************************************************
      REAL JT(10),VAIT(10),JTW
      DOUBLE PRECISION JTM(10,11),ZZ,SUM,CF(10)
1     FORMAT (1X,//1X,8D16.8)
      IF(MM.LE.10) GO TO 100
      WRITE (6,10) MM
10    FORMAT (49H ERROR IN SUBROUTINE 'SLAGR'.   THE PARAMETER MM=, I6,
     $ 30HEXCEEDS THE MAXIMUM PERMITTED   ///)

C*****************BUILD THE PERTINENT MATRIX***************************************
100   MIT=MM+1
200   DO 205 I=1,MM
      JTM(I,1)=1.
205   JTM(I,MIT)=VAIT(I)
      DO 210 I=1,MM
      DO 210 K=2,MM
210   JTM(I,K)=JTM(I,K-1)*JT(I)

C*****************TRIANGULARIZE THE MATRIX BY GAUSSIAN ELIMINATION*****************
      M1=MM-1
      DO 300 KK=1,M1
      IL=1+KK
      DO 300 IR=IL,MM
      ZZ=JTM(IR,KK)/JTM(KK,KK)
      DO 300 K=IL,MIT
300   JTM(IR,K)=JTM(IR,K)-ZZ*JTM(KK,K)

C*****************SOLVE THE MATRIX BY BACK-SUBSTITUTION****************************
      CF(MM)=JTM(MM,MIT)/JTM(MM,MM)
      DO 320 I=2,MM
      IR=MIT-I
      IRP1=IR+1
      SUM=0.
      DO 310 J=IRP1,MM
310   SUM=JTM(IR,J)*CF(J)+SUM
320   CF(IR)=(JTM(IR,MIT)-SUM)/JTM(IR,IR)

C*****************COMPUTE THE VALUE OF THE INTERPOLATING POLYNOMIAL AT THE*****
C*  DESIRED POINT*****************************************************************
      DP=CF(MM)
      DO 350 I=2,MM
      IR=MIT-I
350   DP= JTW*DP+CF(IR)
      RETURN
      END
```

LIST OF PRINCIPAL SYMBOLS

Symbol	Description	FORTRAN notation
A	Cross-sectional area of the device	A
B	external contact of the base of a transistor	B
C	total incremental capacitance per unit area	CAP
C_d	incremental diffusion capacitance per unit area	CAPDF
C_t	incremental transition region capacitance per unit area	CAPSK
i	spatial index (integer)	I
I'	external current	IEXT
j	iteration index (integer)	ITER
J, J_n, J_p, J_D	total, electron, hole, displacement current densities	J,JN,JP,JD
J_B, J_C, J_E	base, collector, emitter total current densities	JB,JC,JE
J_{Sat}	saturation current density	JSAT
k	time index (integer)	K
ℓ	total number of spatial points (integer) [index identifying the point L]	IL
L	external contact on the right side of the device	L
$M(M_C)$	metallurgical interface between the N-material and P-material (at the collector junction of a transistor)	M (MC)
$M_N(M_P)$	interface between the neutral and depleted N-region (P-region)	MN (MP)
n	electron density	N
$n_N(n_P)$	electron density in the N-material (P-material) in thermal equilibrium	NN(NP)

N, N_A, N_D	net impurity, acceptor, donor densities	NIM, NA, ND
O	external contact on the left side of the device	O
p	hole density	P
$p_N(p_P)$	hole density in the N-material (P-material) in thermal equilibrium	PN (PP)
Q	electric charge of one polarity per unit area	
R	external resistor	R
RATMX	upper bound for the ratio of consecutive steps	RATMX
$s_L(s_O)$	surface recombination velocity at the external contact L (O)	SL (SO)
S (or Δx)	spatial step	STEP (or XSTEP)
S_{Mx}	upper bound for the spatial step	SMX
t	time coordinate	TIME
U	generation-recombination rate	
$V(V_A)$	general (specific) applied voltage	V (VA)
V_d	diffusion (or barrier) potential	VD
$V_{dC}(V_{dE})$	diffusion potential at the collector (emitter) junction in a transistor	VDC(VDE)
$V_{BC}(V_{BE})$	base-to-collector (base-to-emitter) voltage in a transistor	VBC(VBE)
$V_S(V_B)$	external voltage source (battery)	VS(VB)
$w_N(w_P)$	neutral region width in the N-region (P-region)	WN(WP)
x	spatial coordinate	X
$x_N(x_P)$	transition region width in the N-region (P-region)	XN(XP)
α	ratio between consecutive spatial steps	ALFA
$\gamma_n(\gamma_p)$	reciprocal of the electron (hole) mobility	GAMN(GAMP)

δ	correction for the electrostatic potential in the iterative scheme	DELTA
$\Delta n(\Delta p)$	in Part I: increment of electron (hole) density for a small increment of applied voltage	DELTAN(DELTAP)
	in Part II: correction for the electron (hole) density in the time-dependent iterative scheme	DELN(DELP)
Δt	time step	TSTEP
Δx (or S)	spatial step	STEP (or XSTEP)
ε_t	truncation error	
ρ	net electric charge density	RHO
σ	conductivity of the material	COND
$\sigma_L(\sigma_0)$	surface charge density at the external contact L(O)	
τ_r	dielectric relaxation constant	TR
τ_t	steady-state transit time of minority carriers	TT
$\varphi_n(\varphi_p)$	electron (hole) quasi-Fermi level	FERMIN(FERMIP)
χ	injection parameter	INJPAR
ψ	electrostatic potential	PSI

Dimensioned quantities

D_o	unit of carrier diffusion constant	
$D_n(D_p)$	electron (hole) diffusion constant	
$-e$ $(e>0)$	electronic charge	- ELCH
k	Boltzmann's constant	
L_D	intrinsic Debye length	LD
n_I	intrinsic carrier density	NINT
T	absolute temperature	

V_t	thermal voltage	VT
ε	permittivity of the material	PERM
$\mu_n(\mu_p)$	electron (hole) mobilities	MOBN, MOBP

<u>Special Symbol</u>

$\triangleq$	defined as

REFERENCES

[1] W. Shockley, "The Theory of p-n Junctions in Semiconductors and p-n Junction Transistors", Bell Syst. Tech. J., vol. 28, pp. 435-489; July 1949.

[2] J. L. Moll, "The Evolution of the Theory for the Voltage-Current Characteristic of P-N Junctions", IRE Proc., vol. 46, pp. 1076-1082; June 1958.

[3] R. L. Pritchard, "Advances in the Understanding of the P-N Junction Triode", IRE Proc., vol. 46, pp. 1130-1141; June 1958.

[4] A. W. Matz, "A One-Dimensional Transistor Model Based Strictly on the Space-Charge Neutrality Approximation", Solid-St. Phys. Electron. Telecomm. (Internat. Conf. Proc., Brussels 6/1958), pp. 1000-1023; 1960.

[5] R. D. Middlebrook, "Conditions at a p-n Junction in the Presence of Collected Current", Solid-St. Electron., vol. 6, pp. 555-571; November 1963.

[6] K. M. Van Vliet, "High Injection Theories of the p-n Junction in the Charge-Neutrality Approximation", Solid-St. Electron., vol. 9, pp. 185-201; March 1966.

[7] C. T. Sah, "The Spatial Variation of the Quasi-Fermi Potentials in p-n Junctions", IEEE Trans. on Electron Devices, vol. ED-13, pp. 839-846; December 1966.

[8] J. R. Macdonald, "Accurate Solution of an Idealized One-Carrier Metal-Semiconductor Junction Problem", Solid St. Electron., vol. 5, pp. 11-37; January 1962.

[9] H. Lawrence and R. M. Warner, Jr., "Diffused Junction Depletion Layer Calculations", Bell Syst. Tech. J., vol. 39, pp. 389-403; March 1960.

[10] K. G. Breitschwerdt, "Characteristics of Diffused P-N Junctions in Epitaxial Layers", IEEE Trans. on Electron Devices, vol. ED-12, pp. 13-19; January 1965.

[11] J. J. Sparkes, "A Reappraisal of Certain Aspects of Transistor Theory", J. Electronics and Control, vol. 16, pp. 153-168; February 1964.

[12] F. van der Maesen et al., "Steady-State Injection in Semiconductors", Philips Res. Rep., vol. 17, pp. 479-512; October 1962.

[13] D. P. Lieb et al., "Abrupt Junction Diode Theory", IRE Trans. on Electron Devices, vol. ED-9, pp. 143-153; March 1962.

[14] K. Kano and H. J. Reich, "Forward Transient Behavior of P-N Junction Diodes at High Injection Levels", IEEE Trans. on Electron Devices, vol. ED-11, pp. 515-523; November 1964.

[15] Y. F. Chang, "The Conduction-Diffusion Theory of Semiconductor Junctions", J. Appl. Phys., vol. 38, pp. 534-544; February 1967.

[16] D. E. Fulkerson and A. Nussbaum, "A Computer Solution for the Steady-State Behavior of a P-N Junction Diode", Solid-St. Electron., vol. 9, pp. 709-719; July 1966.

[17] M. Sanchez, "Hole and Electron Concentrations in a p-n-Abrupt-Junction Diode as Obtained by Exact Computer Solutions of the Differential Equations", Electronics Letters, vol. 3, pp. 117-119; March 1967. Also, "Electric Field in a p-n-Abrupt-Junction Diode as Obtained by Exact Computer Solution of the Differential Equations", Electronics Letters, vol. 3, pp. 160-162; April 1967. Also, "Electron Current Density and Electrostatic Potential in a p-n-Abrupt-Junction Diode as Obtained by Exact Computer Solution of the Differential Equations", Electronics Letters, vol. 3, pp. 223-224; May 1967.

[18] H. K. Gummel, "A Self-Consistent Iterative Scheme for One-Dimensional Steady-State Transistor Calculations", IEEE Trans. on Electron Devices, vol. ED-11, pp. 455-465; October 1964.

[19] J. L. Moll, "Physics of Semiconductors", McGraw-Hill Inc.; 1964.

[20] R. D. Richtmyer, "Difference Methods for Initial Value Problems", Interscience, New York, N.Y.; 1957.

[21] H. K. Gummel, "Hole-Electron Product of pn Junctions", Solid-St. Electron., vol. 10, pp. 209-212; March 1967.

[22] Y. F. Chang, "The Capacitance of p-n Junctions", Solid-St. Electron., vol. 10, pp. 281-287; April 1967.

[23] C. T. Kirk, Jr., "A theory of Transistor Cutoff Frequency (f_T) Falloff at High Current Densities", IEEE Trans. on Electron Devices, vol. ED-9, pp. 164-174; March 1962.

[24] D. P. Kennedy, "Reverse Transient Characteristics of a P-N Junction Diode Due to Minority Carrier Storage", IRE Trans. on Electron Devices, vol. ED-9, pp. 174-182; March 1962.

[25] W. Ko, "The Forward Transient Behavior of Semiconductor Junction Diodes", Solid-St. Electron., vol. 3, pp. 59-69; January 1961.

[26] E. L. Steele, "Charge Storage in Junction Diodes", J. Appl. Phys., vol. 25, pp. 916-918; July 1954.

[27] M. Byczkowski and J.R. Madigan, "Minority Carrier Lifetime in p-n Junction Devices", J. Appl. Phys., vol. 28, pp. 878-881; August 1957.

[28] A. S. Grove and C. T. Sah, "Simple Analytical Approximations to the Switching Times in Narrow Base Diodes", Solid St. Electron., vol. 7, pp. 107-110; January 1964.

[29] L. Fox, "Numerical Solution of Ordinary and Partial Differential Equations", Pergamon Press; 1962.

[30] K. S. Kunz, "Numerical Analysis", McGraw Hill; 1957.

[31] G. C. O'Brien et al., "A Study of the Numerical Solution of Partial Differential Equations", J. Math. and Phys., vol. 29, pp. 223-251; 1950.

[32] P. Lax and R. Richtmyer, "Survey of the Stability of Linear Finite Difference Equations", Comm. Pure Appl. Math., vol. 9, pp. 267-293; May 1956.

[33] C. Gram, "Selected Numerical Methods", Regnecentralen, Copenhagen; 1962.

[34] A. N. Lowan, "On the Convergence of Various Iteration Processes", Scripta Mathematica, vol. 22, pp. 222-227; 1956.

[35] R. E. Esch, "A Necessary and Sufficient Condition for Stability of Partial Difference Equation Problems", J. Assoc. for Computing Machinery, vol. 7, pp. 163-175; April 1960.

[36] E. Forsythe and W. Wasow, "Finite Difference Methods for Partial Differential Equations", Wiley; 1960.

[37] F. John, "On Integration of Parabolic Equations by Difference Methods", Comm. Pure Appl. Math., vol. 5, pp. 155-211; May 1952.

[38] J. Douglas, Jr., "The Application of Stability Analysis in the Numerical Solution of Quasi-Linear Parabolic Differential Equations", Trans. Amer. Math. Soc., vol. 89, pp. 484-518; September 1958.

[39] M. Lees, "Approximate Solutions of Parabolic Equations", J. Soc. Indust. Appl. Math., vol. 7, pp. 167-183; June 1959.